



Tectonic and Isotopic evolution of the Dharwar Craton, India.

Venkata Pavan Katuru

Department of Earth Sciences
School of Physical Sciences
The University of Adelaide

January 2021

Table of Contents

Thesis Summary	iii
Declaration	iv
Acknowledgements	v
Introduction and background Geology	1
1. Introduction	1
2. Geological background	1
3. Thesis outline	8
Archaean crustal evolution of the Dharwar Craton, India: Insights from magmatic and meta-igneous zircon U–Pb, REE and Hf isotopes	13
1. Introduction	14
2. Methods	19
3. Results	21
4. Discussion	40
5. Conclusions	52
Detrital record of the Mesoarchean and lower Neoproterozoic meta-quartzites in Dharwar Craton, India: Evidence of Eoarchean to Mesoarchean crustal evolution from detrital zircon U–Pb, Hf isotopes and REE compositions	58
1. Introduction	59
2. Geological Background	61
3. Methods	66
4. Results	67
5. Discussion	75
6. Conclusions	93
Detrital zircon record of the Kaladgi-Badami basin: Correlation with Paleoproterozoic basins across India and Madagascar	99
1. Introduction	100
2. Geological Background	101
3. Methods	105
4. Results	106
5. Discussion	109
6. Conclusions	119

Thermal history of the Dharwar Craton, India: Implications from multiple accessory mineral U–Pb geochronology, REE compositions from the western margin of the Dharwar Craton, Karwar Block and Coorg Block	126
1. Introduction.....	128
2. Geological Background	129
3. Methods.....	132
4. Results	133
5. Discussion	147
6. Conclusions.....	155
Key outcomes and conclusions of the thesis	160
1. Crustal evolution model of Dharwar Craton from meta-igneous lithologies.....	161
2. Detrital record of the Mesoarchean and lower Neoproterozoic meta-quartzites.....	162
3. Proterozoic intracratonic sedimentary basin.....	163
4. Thermal Record of the Dharwar Craton.....	163
5. Implications for the crustal and isotopic evolution of Dharwar Craton.....	164
Appendices	165
Appendix 2.1 Granitoids of the Dharwar Craton: U–Pb zircon data	166
Appendix 2.2 Granitoids of the Dharwar Craton: REE zircon data	190
Appendix 2.3 Granitoids of the Dharwar Craton: Lu–Hf zircon data.....	220
Appendix 3.1 Detrital Record of the Dharwar Craton: U–Pb zircon data.....	228
Appendix 3.2 Detrital Record of the Dharwar Craton: Lu–Hf zircon data	247
Appendix 3.3 Detrital Record of the Dharwar Craton: REE zircon data.....	249
Appendix 4.1 Detrital Record of the Kaladgi-Badami basin: U–Pb zircon data	267
Appendix 4.2 Detrital Record of the Kaladgi-Badami basin: REE zircon data	280
Appendix 5.1 Thermal history of the Dharwar Craton: U–Pb zircon data	300
Appendix 5.2 Thermal history of the Dharwar Craton: REE zircon data	315
Appendix 5.3 Thermal history of the Dharwar Craton: U–Pb apatite data	326
Appendix 5.4 Thermal history of the Dharwar Craton: REE apatite data	341
Appendix 5.5 Thermal history of the Dharwar Craton: U–Pb monazite data.....	355
Appendix 5.6 Thermal history of the Dharwar Craton: REE monazite data.....	359

Thesis Summary

The crustal evolution of a craton could be studied from analysing its zircon U-Pb record and associated isotopic and elemental composition. The Dharwar Craton in southern India is one such craton on which several independent studies have been conducted on isolated domains within the craton. In this thesis, we have attempted to create a robust tectonic and isotopic evolution model of the Dharwar Craton which also includes previously published data. This thesis is divided into four chapters spanning from the Archean origins of the craton to the latest thermal events affecting various domains within the craton.

Chapter 1 deals with zircon U-Pb dating, rare earth element (REE) composition and Lu-Hf isotopic analysis from granitoids sampled across the various domains within the Dharwar Craton to evaluate the crustal evolution episodes from individual domains and compare them to build a robust crustal architecture model for the Dharwar Craton including previously published data.

Chapter 2 deals with the detrital record of the Dharwar Craton deposited within the various volcano-sedimentary greenstone belts that unconformably overly the basement granitoid gneisses and igneous batholiths through detrital zircon U-Pb dating, REE compositions. The detrital sequences sampled from the Western Dharwar Craton have been analysed for detrital zircon Lu-Hf isotopes to further constrain the crustal evolution processes within the Western Dharwar Craton.

Chapter 3 deals with the detrital record of the Kaladgi-Badami basin, an east-west trending intracratonic Paleoproterozoic basin that unconformably overlies the northern part of Dharwar Craton, which formed as part of the widespread Proterozoic sedimentation across India termed as Purana basins. The detrital zircon U-Pb dating, REE compositional data from various stratigraphic units has been used to infer potential source regions and to compare with sedimentary records across other Paleoproterozoic basins across India and Madagascar to understand the post-assembly tectonic process within the Dharwar Craton which led to the formation of the Kaladgi-Badami basin.

Chapter 4 deals with the thermal record of the Western Dharwar Craton by magmatic and meta-igneous zircon, apatite and monazite: U-Pb dating, REE composition sampled along the western margin along the Dharwar Craton including the adjacent Coorg block and Karwar block. The difference between ages obtained using high-temperature zircon ($>800^{\circ}\text{C}$) U-Pb dating and medium temperature ($450\text{--}550^{\circ}\text{C}$) apatite U-Pb dating was used to infer the timing and spatial extent of the last thermal event experienced across the Dharwar Craton and correlate with contemporaneous tectonic events.

Declaration

I certify that this work contains no material which has been accepted for the award of any other degree or diploma in my name in any university or other tertiary institution and, to the best of my knowledge and belief, contains no material previously published or written by another person, except where due reference has been made in the text. In addition, I certify that no part of this work will, in the future, be used in a submission in my name for any other degree or diploma in any university or other tertiary institution without the prior approval of the University of Adelaide and where applicable, any partner institution responsible for the joint award of this degree.

I give permission for the digital version of my thesis to be made available on the web, via the University's digital research repository, the Library Search and also through web search engines, unless permission has been granted by the University to restrict access for a period of time.

VENKATA PAVAN KATURU

26/01/2021

Acknowledgements

This has been one hell of a journey for me personally, starting life in a new country and finishing thesis in the middle of a pandemic has taught me new things about myself and I am proud finally draw the curtain over another phase of my life.

I would like to acknowledge my excellent supervisors for their supervision over the years and motivating me to finish my PhD. I would like to acknowledge all the PhD student cohort of the Earth Sciences department, of present and past, at the University of Adelaide who have created a welcoming atmosphere and making my stay in Adelaide memorable, especially during the days of having a beer over a zoom call in the middle of a lockdown.

I would also like to acknowledge the friends I have made outside of the university who have supported me in many ways to successfully finish my thesis.

Lastly, I would like to dedicate this work to my parents whose unwavering love and affection made it possible for me to chase my dreams.

Statement of Authorship 1

Title of Paper	Archaean crustal evolution of the Dharwar Craton, India: Insights from magmatic and meta-igneous zircon U–Pb, REE and Hf isotopes
Publication Status	<input type="checkbox"/> Published <input type="checkbox"/> Accepted for Publication <input type="checkbox"/> Submitted for Publication <input checked="" type="checkbox"/> Unpublished and Unsubmitted work written in manuscript style
Publication Details	Pavan, K., Collins, A.S., Santosh, M., Foden, J.D., Sajeev, K., In prep. Archaean crustal evolution of the Dharwar Craton, India: Insights from magmatic and meta-igneous zircon U–Pb, REE and Hf isotopes

Principal Author

Name of Principal Author (Candidate)	Venkata Pavan Katuru		
Contribution to the Paper	Conceptualisation of the work, development of ideas and conclusions, carried out fieldwork, sample preparation and analytical work, interpretation of the data, wrote the manuscript.		
Overall percentage (%)	80%		
Certification:	This paper reports on original research I conducted during the period of my Higher Degree by Research candidature and is not subject to any obligations or contractual agreements with a third party that would constrain its inclusion in this thesis. I am the primary author of this paper.		
Signature		Date	26/1/2020

Co-Author Contributions

By signing the Statement of Authorship, each author certifies that:

- the candidate's stated contribution to the publication is accurate (as detailed above);
- permission is granted for the candidate to include the publication in the thesis; and
- the sum of all co-author contributions is equal to 100% less the candidate's stated contribution.

Name of Co-Author	Alan Collins		
Contribution to the Paper	Supervised work, helped with data interpretation, fieldwork and manuscript revision		
Signature		Date	25/1/2020

Name of Co-Author	M Santosh		
Contribution to the Paper	Supervised work, helped with data interpretation, and planning fieldwork		
Signature		Date	23/1/2020

Name of Co-Author	John Foden		
Contribution to the Paper	Helped with data interpretation and manuscript revisions		
Signature		Date	24/1/2020

Name of Co-Author	Sajeev Krishnan		
Contribution to the Paper	Helped with the organisation and logistics of fieldwork. Facilitated initial sample preparation and storage facilities		
Signature		Date	24/1/2020

Statement of Authorship 2

Title of Paper	Detrital record of the Mesoarchean and lower Neoarchean meta-quartzites in Dharwar Craton, India: Evidence of Eoarchean to Mesoarchean crustal evolution from detrital zircon U–Pb, Hf isotopes and REE compositions		
Publication Status	<input type="checkbox"/> Published <input type="checkbox"/> Accepted for Publication <input type="checkbox"/> Submitted for Publication <input checked="" type="checkbox"/> Unpublished and Unsubmitted work written in manuscript style		
Publication Details	Pavan, K., Collins A, S., Santosh, M., Foden, J.D., Sajeev, K., in prep. Detrital record of the Mesoarchean and lower Neoarchean meta-quartzites in Dharwar Craton, India: Evidence of Eoarchean to Mesoarchean crustal evolution from detrital zircon U–Pb, Hf isotopes and REE compositions		

Principal Author

Name of Principal Author (Candidate)	Venkata Pavan Katuru		
Contribution to the Paper	Conceptualisation of the work, development of ideas and conclusions, carried out fieldwork, sample preparation and analytical work, interpretation of the data, wrote the manuscript.		
Overall percentage (%)	80%		
Certification:	This paper reports on original research I conducted during the period of my Higher Degree by Research candidature and is not subject to any obligations or contractual agreements with a third party that would constrain its inclusion in this thesis. I am the primary author of this paper.		
Signature		Date	26/1/2020

Co-Author Contributions

By signing the Statement of Authorship, each author certifies that:

- iv. the candidate's stated contribution to the publication is accurate (as detailed above);
- v. permission is granted for the candidate to include the publication in the thesis; and
- vi. the sum of all co-author contributions is equal to 100% less the candidate's stated contribution.

Name of Co-Author	Alan Collins		
Contribution to the Paper	Supervised work, helped with data interpretation, fieldwork and manuscript revision		
Signature		Date	25/1/2020

Name of Co-Author	M Santosh		
Contribution to the Paper	Supervised work, helped with data interpretation, and planning fieldwork		
Signature		Date	23/1/2020

Name of Co-Author	John Foden		
Contribution to the Paper	Helped with data interpretation and manuscript revisions		
Signature		Date	24/1/2020

Name of Co-Author	Sajeev Krishnan		
Contribution to the Paper	Helped with the organisation and logistics of fieldwork. Facilitated initial sample preparation and storage facilities		
Signature		Date	24/1/2020

Statement of Authorship 3

Title of Paper	Detrital zircon record of the Kaladgi-Badami basin: Correlation with Paleoproterozoic basins across India and Madagascar		
Publication Status	<input type="checkbox"/> Published <input type="checkbox"/> Accepted for Publication <input type="checkbox"/> Submitted for Publication <input checked="" type="checkbox"/> Unpublished and Unsubmitted work written in manuscript style		
Publication Details	Pavan, K., Collins A, S., Santosh, M., Sarbani Patranabis-Deb, Saha, D., Foden, J,D., Sajeev, K., in prep. Detrital zircon record of the Kaladgi-Badami basin: Correlation with Paleoproterozoic basins across India and Madagascar		

Principal Author

Name of Principal Author (Candidate)	Venkata Pavan Katuru		
Contribution to the Paper	Conceptualisation of the work, development of ideas and conclusions, carried out fieldwork, sample preparation and analytical work, interpretation of the data, wrote the manuscript.		
Overall percentage (%)	80%		
Certification:	This paper reports on original research I conducted during the period of my Higher Degree by Research candidature and is not subject to any obligations or contractual agreements with a third party that would constrain its inclusion in this thesis. I am the primary author of this paper.		
Signature		Date	26/1/2021

Co-Author Contributions

By signing the Statement of Authorship, each author certifies that:

- the candidate's stated contribution to the publication is accurate (as detailed above);
- permission is granted for the candidate to include the publication in the thesis; and
- the sum of all co-author contributions is equal to 100% less the candidate's stated contribution.

Name of Co-Author	Alan Collins		
Contribution to the Paper	Supervised work, helped with data interpretation, fieldwork and manuscript revision		
Signature		Date	25/1/2020

Name of Co-Author	M Santosh		
Contribution to the Paper	Supervised work, helped with data interpretation, and planning fieldwork		
Signature		Date	23/1/2020

Name of Co-Author	John Foden		
Contribution to the Paper	Helped with data interpretation and manuscript revisions		
Signature		Date	24/1/2020

Name of Co-Author	Sajeev Krishnan		
Contribution to the Paper	Helped with the organisation and logistics of fieldwork. Facilitated initial sample preparation and storage facilities		
Signature		Date	24/1/2020

Name of Co-Author	Sarbani Patranabis-Deb		
Contribution to the Paper	Helped with the organisation and assisted with identifying key sample locations during fieldwork.		
Signature		Date	23/1/2020

Name of Co-Author	Dilip Saha		
Contribution to the Paper	Helped with the organisation and assisted with identifying key sample locations and in obtaining structural information during fieldwork.		
Signature		Date	23/1/2020

Statement of Authorship 4

Title of Paper	Thermal history of the Dharwar Craton, India: Implications from multiple accessory mineral U–Pb geochronology, REE compositions from the western margin of the Dharwar Craton, Karwar Block and Coorg Block
Publication Status	<input type="checkbox"/> Published <input type="checkbox"/> Accepted for Publication <input type="checkbox"/> Submitted for Publication <input checked="" type="checkbox"/> Unpublished and Unsubmitted work written in manuscript style
Publication Details	Pavan, K., Collins A, S., Santosh, M., Foden, J.D., in prep. Thermal history of the Dharwar Craton, India: Implications from multiple accessory mineral U–Pb geochronology, REE compositions from the western margin of the Dharwar Craton, Karwar Block and Coorg Block

Principal Author

Name of Principal Author (Candidate)	Venkata Pavan Katuru		
Contribution to the Paper	Conceptualisation of the work, development of ideas and conclusions, carried out sample preparation and analytical work, interpretation of the data, wrote the manuscript.		
Overall percentage (%)	80%		
Certification:	This paper reports on original research I conducted during the period of my Higher Degree by Research candidature and is not subject to any obligations or contractual agreements with a third party that would constrain its inclusion in this thesis. I am the primary author of this paper.		
Signature		Date	26/1/2020

Co-Author Contributions

By signing the Statement of Authorship, each author certifies that:

- iv. the candidate's stated contribution to the publication is accurate (as detailed above);
- v. permission is granted for the candidate to include the publication in the thesis; and
- vi. the sum of all co-author contributions is equal to 100% less the candidate's stated contribution.

Name of Co-Author	Alan Collins		
Contribution to the Paper	Supervised work, helped with data interpretation, collection of samples		
Signature		Date	25/1/2020

Name of Co-Author	M Santosh		
Contribution to the Paper	Supervised work, helped with data interpretation		
Signature		Date	23/1/2020

Name of Co-Author	John Foden		
Contribution to the Paper	Helped with data interpretation		
Signature		Date	24/1/2020

1

Introduction and Geological background to Dharwar Craton, India

1. Introduction:

The Archaean era acts as the bridge between the nascent Hadean earth to the proterozoic era. Continental growth models have converged that the majority of the preserved crust had formed already in the Neoarchean before ca. 2.5 Ga (Dhuime et al., 2012; Condie et al., 2014). Evidence for remelting of older crust have been preserved in much of the Archean crust suggesting active tectonic processes that recycled older crust. The features of these tectonic processes have been disputed and include from modern style horizontal tectonic processes to more vertical style tectonic accretion involving plumes and stagnant lid-drip style tectonic recycling (Jayananda et al., 2000, 2018, 2020; Li et al., 2018; Nebel et al., 2018; Cawood et al., 2018). More recent models predict the secular cooling of the mantle took place during the Archaean era (Spencer et al., 2017; Huang et al., 2020). The Archaean cratons display distinct magmatism events, suggesting that the magmatic events during this period were not globally contemporaneous and different proto-continents shared similar histories. These proto-plates have amalgamated and broke up with each other suggesting the development of tectonic processes that would eventually evolve into modern-style plate tectonics during the Mesoarchean era (Jayananda et al., 2018; Manikyamba et al., 2017; Pehrrson et al., 2013). The Dharwar Craton in India is one such craton formed during the Archean era with limited geochronological and isotopic data available (e.g. Jayananda et al., 2015, 2020; Lancaster et al., 2015; Yang and Santosh, 2015; Dey, 2013) and contains Paleoproterozoic to Neoarchean granite-greenstone terranes which display distinct magmatic pulses and crust building episodes which include both vertical and lateral accretion of juvenile crustal protoliths and crustal recycling (Manikyamba and Kerrich, 2012; Manikyamba et al., 2015, 2017; Rogers and Santosh, 2004).

2. Geological Background:

The Dharwar Craton in southern India is one of the major archean cratons in Peninsular India and is considered to be a tilted oblique crustal section that ranges from the Paleoproterozoic to Neoarchean in age and an amalgamation of microcontinents that preserve the evidence of continental growth and recycling during this period. The Dharwar Craton is bound by the Deccan Traps flood basalt on the north along with the Paleoproterozoic basin called the Kaladgi-Badami Basin (Chapter 4) and the Neoarchean amalgamation of micro blocks towards the south which include the Nilgiri Block, Biligirirangan, Shevaroy and Madras Block from west to east (Ishwar-Kumar et al., 2016; Peucat et al.,

2013) and the Coorg Block in the south-west separated by a Mesoarchean suture zone called the Mercara Shear Zone (MCSZ). On the north-west, the Karwar Block is separated from the Dharwar Craton by a proposed suture zone called the Kumta Shear Zone (KSZ). The Dharwar Craton primarily comprises of basement granitoid suites particularly Tonalite–Trondhjemite–Granodiorite (TTG) suites traditionally known as Peninsular Gneisses along with bimodal volcano-sedimentary greenstone belts, ranging from ages ca. 3.6–2.5 Ga, that overly the basement gneisses (Peucat et al., 1995; Chadwick et al., 2000; Jayananda et al., 2008; Manikyamba et al., 2017). These greenstone belts have been categorised into the older Sargur Group greenstone belts (older than 3.0 Ga) and younger Dharwar supergroup (2.9–2.6 Ga) further classified into the lower Bababudan Group and the upper Chitradurga Group greenstone belts (Hokada et al., 2013). A progressive increase in the grade of metamorphism is reported from the north, showing upper greenschist – lower amphibolite grade rocks, to the south of Dharwar Craton exposing high-grade granulite facies rocks (Chadwick et al., 2000; Ramakrishnan and Vaidyanadhan, 2008).

Previously, the Dharwar Craton was subdivided into the Western Dharwar Craton (WDC) and Eastern Dharwar Craton (EDC) separated by an N-S strike 500 km long granitic batholith called the Closepet Granite (Naqvi, 2005; Jayananda et al., 2006; Chardon et al., 2011). Subsequent studies proposed a high strain mylonitic shear zone named as Chitradurga Shear Zone (CSZ) to act as the boundary between WDC and EDC (Jayananda et al., 2008, 2013; Chardon et al., 2011). The contact between WDC and EDC was later proposed to be a transitional zone extending between the CSZ and Closepet Granite and has been termed as the Central Dharwar Province (CDP) (Peucat et al., 2013) based on U–Pb zircon ages and Sm–Nd isotopic studies (Dey, 2013). Further studies have renamed it to the Central Dharwar Craton and proposed the eastern boundary to be the Kadiri–Kolar greenstone belt in the southern region of the CDC (Santosh and Li, 2018; Jayananda et al., 2018,2020).

2.1 Meta-igneous record of the Dharwar Craton

The Western Dharwar Craton, bound by the Arabian Sea in the west and by the Chitradurga Shear Zone (CSZ) on the east, contains abundant TTG gneisses – comprising of dark grey tonalitic to granodioritic banded gneisses (Jayananda et al., 2015); and two generations of volcano-sedimentary greenstone detrital sequences which include both the older Sargur Group and younger Dharwar Supergroup. The U–Pb zircon ages coupled with Nd and Hf isotopic data reveal TTG accretion during distinct major episodes at ca. 3.45–3.3 Ga and 3.2 Ga (Jayananda et al., 2015,2018; Guitreau et al., 2017). The TTG ages are closer to the detrital ages associated with the Sargur group volcanic sequences (Jayananda et al., 2008) and the detrital zircon record from the area (Sarma et al., 2012; Hokada et al., 2013; Lancaster et al., 2015; Maibam et al., 2016; Wang and Santosh, 2019). The TTGs are intruded by

two generations of potassic granites around ca. 3.0 Ga and ca. 2.6 Ga (Jayananda et al., 2006, 2018; Chadwick et al., 2011). Sm—Nd garnet-whole-rock isochron dating of mafic rocks, gneisses and pelitic rocks reveal major thermal event at ca. 2.52 Ga with cooling until ca. 2.45 Ga (Jayananda et al., 2013) and metamorphic titanite dated near the Holenarsipur Schist Belt in the south has been linked to the emplacement of trondhjemite plutons at ca. 3.1 Ga (Jayananda et al., 2013, 2015).

The Central Dharwar Craton contains older weakly foliated migmatitic TTGs and younger foliated dark grey banded gneisses (Jayananda et al., 2018). The abundance of older TTGs decreases from the Chitradurga Shear Zone towards the Kolar—Kadiri greenstone belt (Chardon et al., 2011; Jayananda et al., 2013; Peucat et al., 2013). U—Pb zircon ages reveal TTG accretion during ca. 3.37—3.23 Ga and ca. 3.15 — 2.96 Ga and the transitional TTGs towards the east forming at ca. 2.7—2.56 Ga followed by sanukitoid emplacement during ca. 2.56—2.52 Ga (Jayananda et al., 2018). The anatectic granites from the southern Closepet granite have been dated at ca. 2.52 Ga (Jayananda et al., 2013; Friend and Nutman, 1991) and calc-alkaline intrusions between the Closepet Granite and the Kolar greenstone belt have been reported for zircon ages around ca. 2.55 Ga (Krogstad et al., 1991; Jayananda et al., 2000; Chardon et al., 2002).

The basement rocks in the Eastern Dharwar Craton consist of minor dark grey banded to weakly migmatitic gneisses and light pink to whitish grey diatexitic gneisses (Jayananda et al., 2018). The granodiorites along the eastern margin of the Kolar greenstone belt have been reported for U—Pb zircon ages at ca. 2.55—2.53 Ma with remnants of ca. 2.7 Ga transitional TTG enclaves (Krogstad et al., 1991; Chardon et al., 2002). TTGs to the south of the EDC are proposed to have accreted at ca. 2.56 — 2.53 Ga and the granitoids in the northern part of EDC adjacent to the Hutti greenstone belt provide zircon U—Pb ages ranging from ca. 2.57—2.52 Ga (Sarma et al., 2008; Anand et al., 2014).

2.2 Volcano-sedimentary record of the Dharwar Craton

The volcano-sedimentary greenstone belts overlying the Dharwar Craton are divided into the older Sargur group and younger Dharwar Supergroup (Swami Nath and Ramakrishnan, 1981). The Dharwar Supergroup is further classified into the lower Bababudan Group and the upper Chitradurga Group greenstone belts (Hokada et al., 2013). The Sargur group has been proposed to be associated with komatiite volcanism around ca. 3.35 Ga representing melt extraction from the mantle (Jayananda et al., 2008). Based on the geochronology of the Sargur Group, the WDC was inferred to be older than ca. 3.5 Ga and deposited before ca. 3.0 Ga. (Nutman et al., 1992). The older TTG gneisses across the WDC and CDC are overlain by younger Dharwar Supergroup which is also considered to stratigraphically overlie the Sargur Group with the lower units from the Bababudan Group revealing an Sm—Nd age at ca. 2911 Ma (Kumar et al., 1996). Monazite electron microprobe age at 3082 Ma was

reported from Holenarsipur Greenstone belt from the Sargur Group (Hokada et al., 2013). Secondary ion mass spectrometer (SIMS) U–Pb age from detrital zircon from the basal unit from the Bababudan group at 3162 Ma has been reported as the maximum depositional age for the Dharwar Supergroup (Krapez et al., 2020). The overlap of ages between the basal units of Sargur Group and the Bababudan Group has rendered the stratigraphic relationship between Sargur Group and Dharwar Supergroup inconclusive (K. Patra et al., 2020). Supracrustal rocks of the Dharwar Craton younger than ca. 2.8 Ga have been placed in the Dharwar Supergroup, however, stratigraphic correlations between the distinct units have been difficult due to lack of spatial connection between each other and lack of regional lithostratigraphy has rendered some units with precise U–Pb ages (Sarma et al., 2012) without stratigraphic context (Krapez et al., 2020). The Chitradurga Group was defined to unconformably overlie the Bababudan Group along with the basement gneisses (Chadwick et al., 1989). The supracrustals from the Eastern Dharwar Craton have not been formally correlated with the western/central Dharwar supracrustals and very few attempts have been done to establish regional correlations among the supracrustal units.

2.3 Existing crustal evolution theories on the Dharwar Craton

Previous studies have explained the current configuration of the Dharwar Craton by proposing various crustal evolution models. Initial accretionary models considered the WDC and EDC as separate continents that formed separately, then collided with each other. The greenstone belts were envisaged as plate margin volcanism and/or marginal basins in these models (Krogstad et al., 1989; Chadwick et al., 2000; Santosh and Li, 2018). Alternative models consider the Dharwar Craton as one entity through the Archaean, where the craton evolved by “sagduction”, which involves the gravitational sinking of the greenstone belts that were overlying the basement gneisses along with tectonic sliding at the margins (Chardon and Jayananda, 2008). Mantle plume driven mantle-derived magmatic-diapir accretion (Jayananda et al., 2000), and combination of plume-arc processes (Jayananda et al., 2008, 2013, 2018; Manikyamba and Kerrich, 2012) have also been proposed to explain the formation of the Dharwar Craton.

These initial models led to the use of more analyses that included studying Lu–Hf and Sm–Nd systematics in the rocks that give information about the timing of when the original melt has been separated from the depleted mantle, giving more insight into the episodes of crustal growth and talking about the origin of the rocks before they reach the surface. This led to the development of Lu–Hf datasets of Dharwar craton including works on Gadag greenstone belt (Sarma et al., 2012), Hutti Greenstone belt (Anand et al., 2014) and regional detrital studies across the Dharwar craton (e.g Lancaster et al., 2015; Maibam et al., 2016). The Lu–Hf datasets reveal that the crustal growth in both

EDC and WDC was contemporaneous with continuous crustal recycling till ca. 3.0 Ga, cratonisation in WDC took place in two episodes at 3.3 Ga and 2.7 Ga and the younger EDC had its crustal extraction from 3.0–2.5 Ga (Lancaster et al., 2015). The Nd isotope analysis datasets for the Dharwar (e.g. Dey, 2013) suggests that both EDC and WDC hold Nd isotopic signatures leading to depleted mantle ages at 3.5 Ga. The major period of juvenile crust formation in WDC was during 3.35–3.0 Ga accompanied by crustal recycling. The data interpretation from Dey, (2013) suggests that a) the mantle was re-fertilized during the Mesoarchaeon which contributed to the extensive mafic volcanism in 2.9–2.6 Ga in WDC, accompanied with crustal recycling during 2.7–2.6 Ga, b) the EDC remnant gneisses were already derived from a recycled Palaeoarchaeon crust that was destroyed by late Neoarchaeon juvenile crustal addition during 2.7–2.5 Ga along with recycling of the older crust. Dey (2013), however, has the lacunae involving the timing of earliest crustal extraction and spatial coverage of the Nd-isotope record especially involving the felsic and intermediate lithologies.

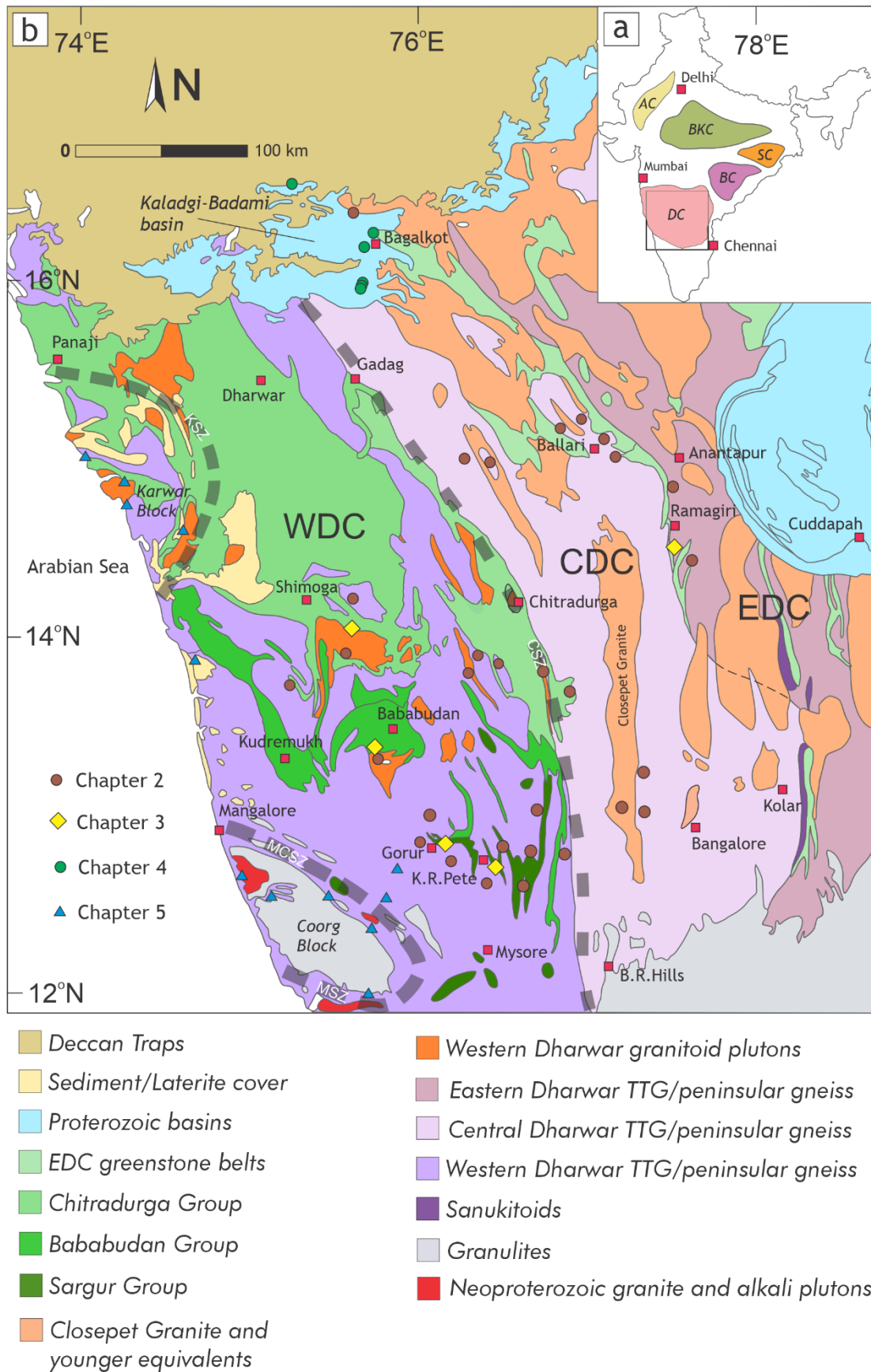


Figure 1: The geological map of the Dharwar Craton (adapted from Jayananda et al., 2013a). a) Map of India outlining major cratons across peninsular India. DC: Dharwar Craton, BC: Bastar Craton, SC:

Singhbhum Craton, BKC: Bundelkhand Craton, AC: Aravalli Craton. b) Geological map of the Dharwar Craton with sample locations denoted by symbols representing each chapter outlined in this thesis. The major suture zones are marked by dashed lines and are named as KSZ — Kumta Shear Zone, MCSZ — Mercara Shear Zone, MSZ — Moyar Shear Zone. The individual domains of the Dharwar Craton have been labelled as WDC — Western Dharwar Craton, CDC — Central Dharwar Craton, EDC — Eastern Dharwar Craton.

3. Thesis Outline:

The Dharwar Craton records suites of rocks that span the majority of the Archean period and records the transition in tectonic processes from the Paleoarchean to the Neoarchean followed by post-assembly events that led to the formation of intracratonic sedimentary basins, in this case, the Kaladgi-Badami basin. In this thesis, we have attempted to create a robust tectonic and isotopic evolution model of the Dharwar Craton which also includes previously published data. Various fields of geoscience are currently exploring efficient ways to manage and quantify large data sets as part of reporting and citing. This PhD research also explores ways to statistically compare large isotopic datasets in addition to the collection of new data in key regions. This PhD research has been driven by a multi-disciplinary approach to interpreting isotopic and geochemical datasets to understand the evolution of the Dharwar Craton and surrounding formations.

This thesis is divided into four chapters spanning from the Archean origins of the craton to the latest thermal events affecting various domains within the craton. The following chapters constitute unpublished and unsubmitted original work written in manuscript style. There is some repetition in the introduction, geological background, methodology and discussion sections of each chapter.

Chapter 2 deals with zircon U-Pb dating, rare earth element (REE) composition and Lu-Hf isotopic analysis from granitoids sampled across the various domains within the Dharwar Craton to evaluate the crustal evolution episodes from individual domains and compare them to build a robust crustal architecture model for the Dharwar Craton, from the Paleo- to Neoarchean, including previously published data in turn updating the existing crustal evolution histories to include the recent domain of Central Dharwar Craton as a separate entity from the Eastern Dharwar Craton. The new U-Pb age data from the granitoids have been used to identify the spatial extent of the previously reported crustal accretion episodes from the Meso- to Neoarchean. The rare earth element (REE) compositions have been used to infer the depth of crystallization of the zircons within the lithology. We compare the crustal domains within the Dharwar Craton with each other and their crustal evolution history to differentiate and identify similar/distinct suites within the Dharwar Craton. We also compare the entire Lu-Hf data set of the Dharwar Craton (published + new data) with Lu-Hf data sets of other major cratons to test the hypothesis for the existence of Neoarchean supercontinental amalgamation.

Chapter 3 deals with the detrital record of the Dharwar Craton deposited within the various volcano-sedimentary greenstone belts that unconformably overlie the basement granitoid gneisses and igneous batholiths through detrital zircon U-Pb dating, REE compositions. We attempt to improve upon the existing spatial correlations proposed by Krapez et al. (2020) and K. Patra et al. (2020) among the Western Dharwar Craton supracrustals. We compare the detrital record of the reported samples, in this study, belonging to the various groups of greenstone belts overlying the Dharwar Craton with previously published data to compare source regions. We compare the REE compositions from the detrital zircons against their crystallization ages to infer periods of deeper crystallization. The detrital sequences sampled from the Western Dharwar Craton have been analysed for detrital zircon Lu-Hf isotopes and compared against previous published detrital Lu-Hf data sets to further constrain the Paleo-Mesoarchean crustal evolution processes within the Western Dharwar Craton.

Chapter 4 deals with the detrital record of the Kaladgi-Badami basin, an east-west trending intracratonic Paleoproterozoic basin that unconformably overlies the northern part of Dharwar Craton, which formed as part of the widespread Proterozoic sedimentation across India termed as Purana basins. The detrital zircon U-Pb dating, REE compositional data from various stratigraphic units has been used to infer potential source regions and to compare with sedimentary records across other Paleoproterozoic basins across India and Madagascar, using multi-dimensional scaling, to check for similarities in the sedimentary environments and potential source regions. We test the hypothesis of the “Greater Dharwar Craton” model by Tucker et al. (2011) to learn if the Kaladgi-Badami basin forms a missing link between the Itremo Group in Madagascar and the Cuddapah Basin in India. The correlations were used to hypothesize post-assembly tectonic processes within the Dharwar Craton which led to the formation of the Paleoproterozoic Kaladgi-Badami basin.

Chapter 5 deals with the thermal record of the western margin of Dharwar Craton by magmatic and meta-igneous zircon, apatite and monazite: U-Pb dating, REE composition sampled along the western margin along the Dharwar Craton including the adjacent Coorg block and Karwar block. We interpret the apatite U-Pb ages to investigate the cooling and reactivation histories along the active margins between the Dharwar Craton—Coorg Block and Dharwar Craton—Karwar Block. We interpret the REE compositions from the zircons to infer the depth of crystallization and the REE compositions from apatites to infer exhumation history versus hydrothermal alteration of the protolith. The apatite U-Pb ages coupled with zircon and monazite U-Pb ages have been used infer the timing and spatial extent of thermal events experienced by the lithologies.

4. References:

- 1) Anand, R., S. Balakrishnan, E. Koojiman and K. Mezger (2014). "Neoarchean crustal growth by accretionary processes: Evidence from combined zircon–titanite U–Pb isotope studies on granitoid rocks around the Hutti greenstone belt, eastern Dharwar Craton, India." *Journal of Asian Earth Sciences* 79: 72–85.
- 2) Cawood, P.A., Hawkesworth, C.J., Pisarevsky, S.A., Dhuime, B., Capitanio, F.A., Nebel, O., 2018. Geological archive of the onset of plate tectonics. *Phil. Trans. Royal Soc. A* 376, 20170405.
- 3) Chadwick, B., V. N. Vasudev and G. V. Hegde (2000). "The Dharwar craton, southern India, interpreted as the result of Late Archaean oblique convergence." *Precambrian Research* 99: 91–111.
- 4) Chadwick, B. R., M.; Viswanatha, M. N. (1981). "Structural and Metamorphic Relations between Sargur and Dharwar Supracrustal Rocks and Peninsular Gneiss in Central Karnataka." *Journal of Geological Society of India* 22(12).
- 5) Chardon, D., Peucat, J.-J., Jayananda, M., Choukroune, P., Fanning, C.M., 2002. Archaean granite–greenstone tectonics at Kolar (south India): interplay of diapirism and bulk homogenous contraction during juvenile magmatic accretion. *Tectonics* 21, 1016, doi:10.1029/2001TC901032.
- 6) Chardon, D., M. Jayananda and J.-J. Peucat (2011). "Lateral constrictional flow of hot orogenic crust: Insights from the Neoarchean of south India, geological and geophysical implications for orogenic plateaux." *Geochemistry, Geophysics, Geosystems* 12(2): n/a–n/a.
- 7) Condie, K.C., 2014. Growth of continental crust: a balance between preservation and recycling. *Mineral. Mag.* 78, 623–637.
- 8) Dey, S. (2013). "Evolution of Archaean crust in the Dharwar craton: The Nd isotope record." *Precambrian Research* 227: 227–246.
- 9) Dhuime, B., Hawkesworth, C.J., Cawood, P.A., Storey, C.D., 2012. A change in the geodynamics of continental growth 3 billion years ago. *Science* 335, 1334e1336.
- 10) Friend, C. and A. Nutman (1991). "SHRIMP U–Pb geochronology of the Closepet granite and Peninsular gneiss, Karnataka, South India." *Journal of the Geological Society of India* 38(4): 357–368.
- 11) Guitreau, M., S. B. Mukasa, L. Loudin and S. Krishnan (2017). "New constraints on the early formation of the Western Dharwar Craton (India) from igneous zircon U–Pb and Lu–Hf isotopes." *Precambrian Research* 302(Supplement C): 33–49.
- 12) Hokada, T., K. Horie, M. Satish-Kumar, Y. Ueno, A. Nasheeth, K. Mishima and K. Shiraishi (2013). "An appraisal of Archaean supracrustal sequences in Chitradurga Schist Belt, Western Dharwar Craton, Southern India." *Precambrian Research* 227: 99–119.
- 13) Huang, G., Palin, R., Wang, D. et al. Open-system fractional melting of Archean basalts: implications for tonalite–trondhjemite–granodiorite (TTG) magma genesis. *Contrib Mineral Petrol* 175, 102 (2020). <https://doi.org/10.1007/s00410-020-01742-9>
- 14) Ishwar-Kumar, C., M. Santosh, S. A. Wilde, T. Tsunogae, T. Itaya, B. F. Windley and K. Sajeew (2016). "Mesoproterozoic suturing of Archean crustal blocks in western peninsular India: Implications for India–Madagascar correlations." *Lithos* 263: 143–160.
- 15) Jayananda, M., J. F. Moyen, H. Martin, J. J. Peucat, B. Auvray and B. Mahabaleswar (2000). "Late Archaean (2550–2520 Ma) juvenile magmatism in the Eastern Dharwar craton, southern India: constraints from geochronology, Nd–Sr isotopes and whole rock geochemistry." *Precambrian Research* 99: 225–254.
- 16) Jayananda, M., D. Chardon, J. J. Peucat and R. Capdevila (2006). "2.61 Ga potassic granites and crustal reworking in the western Dharwar craton, southern India: Tectonic, geochronologic and geochemical constraints." *Precambrian Research* 150: 1–26.
- 17) Jayananda, M., J. J. Peucat, D. Chardon, B. K. Rao, C. M. Fanning and F. Corfu (2013). "Neoarchean greenstone volcanism and continental growth, Dharwar craton, southern India: Constraints from SIMS U–Pb zircon geochronology and Nd isotopes." *Precambrian Research* 227(Supplement C): 55–76.
- 18) Jayananda, M. T., Y., T. Miyazaki, R. V. Gireesh, K.-u. Kapfo, Tushipokla, H. Hiroshi and T. Kano (2013). "Geochronological constraints on Meso- and Neoarchean regional metamorphism and magmatism in the Dharwar craton, southern India." *Journal of Asian Earth Sciences* 78: 18–38.
- 19) Jayananda, M., Santosh, M., Aadhiseshan, K.R., 2018. Formation of Archean (3600–2500 Ma) continental crust in the Dharwar craton, southern India. *Earth Sci.Rev.* 181, 12–42.
- 20) Jayananda, M., D. Chardon, J. J. Peucat, Tushipokla and C. M. Fanning (2015). "Paleo- to Mesoarchean TTG accretion and continental growth in the western Dharwar craton, Southern India: Constraints from

- SHRIMP U–Pb zircon geochronology, whole-rock geochemistry and Nd–Sr isotopes." *Precambrian Research* 268: 295–322.
- 21) Jayananda, M., K. R. Aadhiseshan, M. A. Kusiak, S. A. Wilde, K.-u. Sekhmo, M. Guitreau, M. Santosh and R. V. Gireesh (2020). "Multi-stage crustal growth and Neoproterozoic geodynamics in the Eastern Dharwar Craton, southern India." *Gondwana Research* 78: 228–260.
 - 22) Krapez, B., Srinivasa Sarma, D., Ram Mohan, M., McNaughton, N.J., Rasmussen, B., and Wilde, S.A. 2020, Tectonostratigraphy of the Late Archean Dharwar Supergroup, Dharwar Craton, India: Defining a tectonic history from spatially linked but temporally distinct intracontinental and arc-related basins *Earth-Science Reviews*, 201: 102966. doi:10.1016/j.earscirev.2019.102966.
 - 23) Krogstad, E. J., S. Balakrishnan, D. K. Mukhopadhyay, V. Rajamani and G. N. Hanson (1989). "Plate Tectonics 2.5 Billion Years Ago: Evidence at Kolar, South India." *Science* 243(4896): 1337–1340.
 - 24) Krogstad, E. J., G. N. Hanson and V. Rajamani (1991). "U–Pb Ages of Zircon and Sphene for Two Gneiss Terranes Adjacent to the Kolar Schist Belt, South India: Evidence for Separate Crustal Evolution Histories." *The Journal of Geology* 99(6): 801–815.
 - 25) Kumar, A., Bhaskar Rao, Y.J., Sivaraman, T.V., and Gopalan, K. 1996, Sm–Nd ages of Archean metavolcanics of the Dharwar craton, south India: *Precambrian Research*, 80: 205–216. doi:10.1016/S0301-9268(96)00015-0.
 - 26) Lancaster, P.J., Dey, S., Storey, C.D., Mitra, A.M., and Bhunia, R.K. 2015, Contrasting crustal evolution processes in the Dharwar craton: Insights from detrital zircon U–Pb and Hf isotopes *Gondwana Research*, 28: 1361–1372. doi:10.1016/j.gr.2014.10.010.
 - 27) Li, S.-S., M. Santosh and R. M. Palin (2018). "Metamorphism during the Archean–Paleoproterozoic transition associated with microblock amalgamation in the Dharwar Craton, India." *Journal of Petrology*: epy102–egy102.
 - 28) Maibam, B., A. Gerdes and J. N. Goswami (2016). "U–Pb and Hf isotope records in detrital and magmatic zircon from eastern and western Dharwar craton, southern India: Evidence for coeval Archean crustal evolution." *Precambrian Research* 275: 496–512.
 - 29) Manikyamba, C., S. Ganguly, M. Santosh and K. S. V. Subramanyam (2017). "Volcano-sedimentary and metallogenic records of the Dharwar greenstone terranes, India: Window to Archean plate tectonics, continent growth, and mineral endowment." *Gondwana Research* 50: 38–66.
 - 30) Manikyamba, C. and R. Kerrich (2012). "Eastern Dharwar Craton, India: Continental lithosphere growth by accretion of diverse plume and arc terranes." *Geoscience Frontiers* 3(3): 225–240.
 - 31) Manikyamba, C., A. Saha, M. Santosh, S. Ganguly, M. Rajanikanta Singh, D. V. Subba Rao and M. Lingadevaru (2014). "Neoproterozoic felsic volcanic rocks from the Shimoga greenstone belt, Dharwar Craton, India: Geochemical fingerprints of crustal growth at an active continental margin." *Precambrian Research* 252: 1–21.
 - 32) Manikyamba, C., S. Ganguly, M. Santosh, A. Saha, A. Chatterjee and A. C. Khelen (2015). "Neoproterozoic arc–juvenile back-arc magmatism in eastern Dharwar Craton, India: Geochemical fingerprints from the basalts of Kadiri greenstone belt." *Precambrian Research* 258: 1–23.
 - 33) Naqvi, S. M., R. M. K. Khan, C. Manikyamba, M. R. Mohan and T. C. Khanna (2006). "Geochemistry of the Neoproterozoic high-Mg basalts, boninites and adakites from the Kushtagi–Hungund greenstone belt of the Eastern Dharwar Craton (EDC); implications for the tectonic setting." *Journal of Asian Earth Sciences* 27(1): 25–44.
 - 34) Nutman A P, Chadwick B, Ramakrishnan M and Viswanatha M N 1992 SHRIMP U–Pb ages of detrital zircons in Sargur supracrustal rocks in western Karnataka, southern India; *J. Geol. Soc. India* 39 367–374
 - 35) O. Nebel, F. A. C., J.-F. Moyen, R. F. Weinberg, F. Clos, Y. J. Nebel-Jacobsen and P. A. Cawood (2018). "When crust comes of age: on the chemical evolution of Archean, felsic continental crust by crustal drip tectonics." *Philosophical Transactions of the Royal Society A* 376: 20180103.
 - 36) Patra, K., A. Giri, R. Anand, S. Balakrishnan and J. K. Dash (2020). "Dharwar stratigraphy revisited: new age constraints on the 'oldest' supracrustal rocks of western Dharwar craton, southern India." *International Geology Review*: 1–21.
 - 37) Pehrsson, S. J., R. G. Berman, B. Eglington and R. Rainbird (2013). "Two Neoproterozoic supercontinents revisited: The case for a Rae family of cratons." *Precambrian Research* 232: 27–43.

- 38) Peucat, J. J., Bouhallier, H., Fanning, C. M., & Jayananda, M. (1995). Age of the Holenarsipur greenstone belt, relationships with the surrounding gneisses (Karnataka, South India). *The Journal of Geology*, 103(6), 701-710.
- 39) Peucat, J.-J., M. Jayananda, D. Chardon, R. Capdevila, C. M. Fanning and J.-L. Paquette (2013). "The lower crust of the Dharwar Craton, Southern India: Patchwork of Archean granulitic domains." *Precambrian Research* 227(Supplement C): 4-28.
- 40) Rogers, John JW, and M. Santosh. *Continents and supercontinents*. Oxford University Press, 2004.
- 41) Ramakrishnan, M., R. Vaidyanadhan and G. S. o. India (2008). *Geology of India*, Geological Society of India.
- 42) Srinivasa Sarma, D. M., N J, E. Belusova, M. Ram Mohan and I. R. Fletcher (2012). "Detrital zircon U–Pb ages and Hf-isotope systematics from the Gadag Greenstone Belt: Archean crustal growth in the western Dharwar Craton, India." *Gondwana Research* 22: 843-854.
- 43) Santosh, M. and S.-S. Li (2018). "Anorthosites from an Archean continental arc in the Dharwar Craton, southern India: Implications for terrane assembly and cratonization." *Precambrian Research* 308: 126-147.
- 44) Sarma, D. & McNaughton, Neal & Fletcher, Ian & Groves, D. & Mekala, Ram & Balaram, V.. (2008). Timing of gold mineralization in the Hutti gold deposit, Dharwar Craton, South India. *Economic Geology*. 103. 1715-1727. 10.2113/gsecongeo.103.8.1715.
- 45) Swami Nath, J. and M. Ramakrishnan (1981). Early Precambrian Supracrustals of Southern Karnataka 112: 350.
- 46) Spencer, C. J., C. L. Kirkland and R. J. M. Taylor (2016). "Strategies towards statistically robust interpretations of in situ U–Pb zircon geochronology." *Geoscience Frontiers* 7(4): 581-589.
- 47) Tucker, R. D., J. Y. Roig, C. Delor, Y. Amelin, P. Goncalves, M. H. Rabarimanana, A. V. Ralison and R. W. Belcher (2011). "Neoproterozoic extension in the Greater Dharwar Craton: a reevaluation of the "Betsimisaraka suture" in Madagascar This article is one of a series of papers published in this Special Issue on the theme of Geochronology in honour of Tom Krogh." *Canadian Journal of Earth Sciences* 48(2): 389-417.
- 48) Yang, Q.-Y. and M. Santosh (2015). "Zircon U–Pb geochronology and Lu–Hf isotopes from the Kolar greenstone belt, Dharwar Craton, India: Implications for crustal evolution in an ocean-trench-continent transect." *Journal of Asian Earth Sciences* 113: 797-811.

2

Archaean crustal evolution of the Dharwar craton,
south India: Insights from magmatic and meta-
igneous zircon U–Pb, REE and Hf isotopes

Abstract:

Various tectonic models explaining the continental growth and accretion history for terrane formation within the Archean Dharwar Craton of south India have been proposed. These commonly subdivide the craton into a western, eastern and sometimes a central domain (WDC, EDC and CDC, respectively), based on the age and chemistry of an, as yet, relatively limited zircon database. In this study, we present U–Pb, rare earth element (REE) and Hf isotopic data from zircons collected from magmatic and meta-igneous suites across the breadth of Dharwar Craton, to create a more robust Archean crustal evolution model integrating previous data.

The U–Pb data captures stages of tonalite-trondhjemite-granodiorite (TTG) magmatism in the WDC at ca. 3.4 Ga and ca. 3.2 Ga, in the CDC at ca. 3.3 Ga and ca. 3.0 Ga and then later transitional type TTGs in the EDC from 2.7–2.6 Ga—these are now deformed into orthogneisses and are what are conflated in the literature as the Peninsular Gneiss. Relatively undeformed granites within the WDC were dated at ca. 3.0 Ga, ca. 2.6 Ga, and in the CDC at ca. 2.6 Ga and ca. 2.55 Ga. The REE compositions from the same zircons were used to infer the depth of crystallisation compared to the plagioclase stability field. The $(La/Yb)_N$, $(Gd/Yb)_N$ ratios in zircon were cumulatively used to reveal the timing of crustal thickening associated with deeper partial melting (and/or crystallisation) of the source to produce the TTG domains around 3.2 Ga and 2.6 Ga. The combined ϵ_{Hf} plot from all the terranes reveals that crustal growth and crustal melting/recycling was continuous and coeval within the WDC and CDC until ca. 3.0 Ga. Magmatism, involving considerable crustal recycling, continued in the CDC until ca. 2.55 Ga. The 2.6 Ga potassic granites arise from a juvenile source contaminated with pre-existing crust with $\epsilon_{Hf}(t)$ values between +2.2 to -2.06. The $\epsilon_{Hf}(t)$ values from the transitional TTG gneisses in the northern Dharwar craton lie between +4.5 to +1.46 and show that crustal growth in the EDC originated from a juvenile source.

The WDC and CDC appear to share similar antiquity and are linked through their history. The EDC, however, is interpreted to have formed away from the rest of the Dharwar Craton and accreted to the CDC at ca. 2.6–2.55 Ga along a suture that is represented by the Ramagiri Greenstone Belt.

1. Introduction:

The Archaeon links the nascent earth of the Hadean to the more recognisable planet of the Proterozoic. Recent continental growth models converge on models where the majority of the preserved continental crust had already formed before the end of the Neoarchaeon, before 2.5 Ga (Dhuime et al., 2012; Condie et al., 2014). Much of this Archaeon crust preserves evidence of remelting of older crust, suggesting that tectonic processes were active that recycled pre-existing crust. However,

the nature of these tectonic processes are disputed and include stagnant lid drip type tectonics, vertical tectonic accretion involving plumes and modern horizontal tectonic processes. (Cawood et al., 2018; Jayananda et al., 2000, 2018, 2020; Li et al., 2018; Nebel et al., 2018). Pulses of magmatism have been recognised in all Archaean cratons, but the timing of magmatism varies, suggesting that magmatic pulses were not globally synchronous, and that different proto-continentals existed that shared similar histories. These entities broke up and collided with each other in ways that suggest that at least by the Mesoarchaean that some-sort of horizontal proto-plate tectonics was operating (Jayananda 2000, 2018; Li et al., 2018; Manikyamba et al., 2017; Wyman and Kerrich, 2009, Pehrsson et al., 2013). Recent palaeomagnetic data also support modern-like horizontal plate velocities by 3.2 Ga (Brenner et al. 2020). The Dharwar craton in South India is one such craton that formed during the Archaean. It is a major terrain where limited geochronological and geochemical data are available (e.g. Jayananda et al., 2015, 2019, 2020; Guitreau et al., 2017; J.Y. Wang et al., 2020; Santosh and Li, 2018; Lancaster et al., 2015, Dey 2013). Yet, what is available has been used to suggest that by the Neoarchaean, at least, it formed a member of a continental-consortium with the Rae and Sask cratons of North America, the Mawson Craton of Australia/Antarctica, Siberia, West Africa, North China and the Congo/São Francisco Craton—a configuration called Nunavutia (Pehrsson et al., 2013).

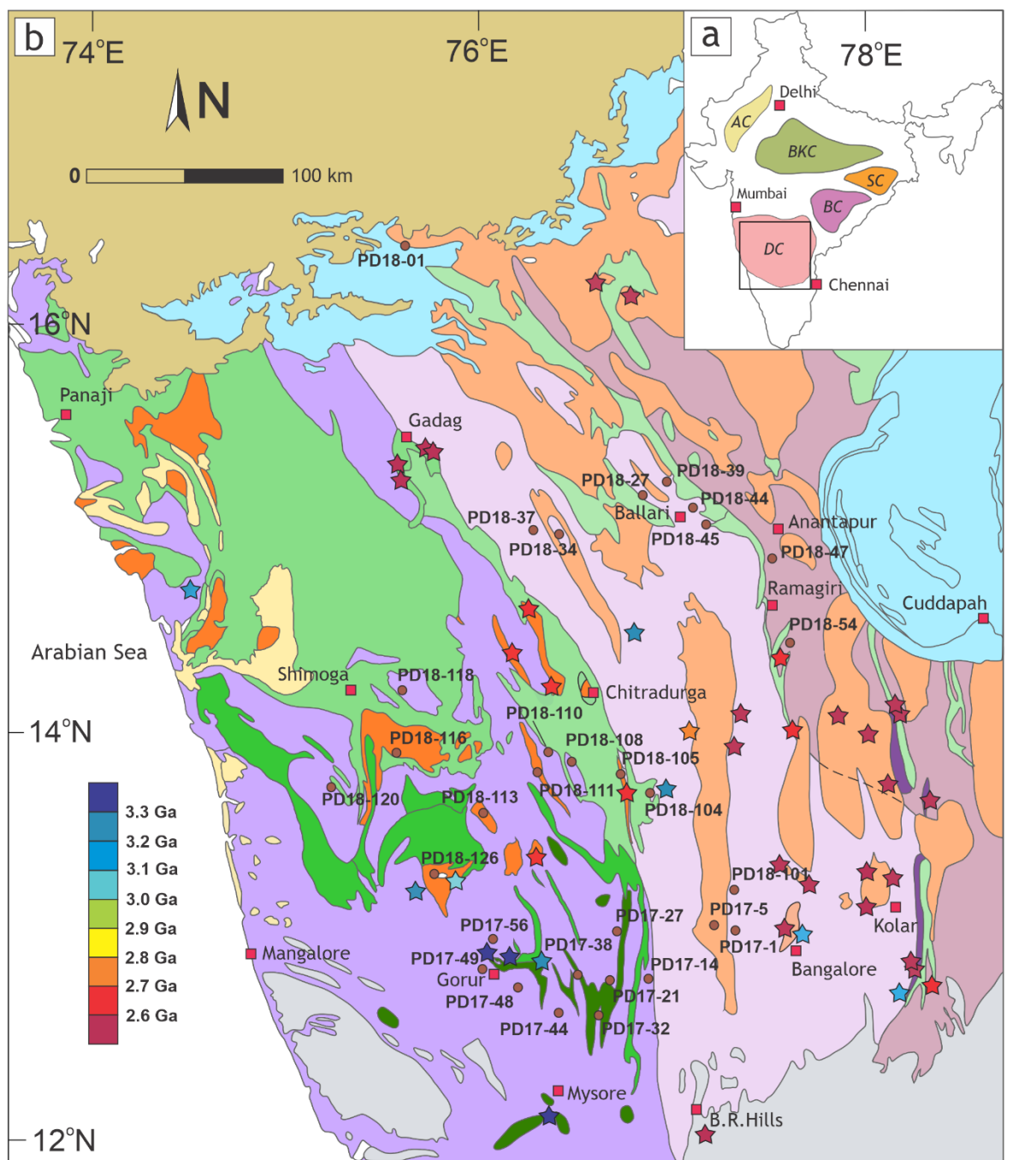
In this study, we have collected rock samples from magmatic and meta-igneous suites across the Dharwar Craton targeting the ubiquitous tonalite-trondhjemite-granodiorite (TTG) gneisses and potassic granitoids that occur across the whole craton. We have collected zircon U–Pb isotopic data from these samples to ascertain the timing of magmatism across the different domains of the Dharwar Craton. REE data from zircons were also collected and interpreted to infer the effective depth of source and/or crystallisation using REE elemental ratios and Lu–Hf isotopes were analysed to study the nature and composition of the source from which the magmatic suites evolved. Together, these data, with published comparable data, are used to establish a crustal evolution model for the Dharwar Craton. The data are then compared with contemporary cratons from around the world to examine whether the age ‘barcode’ preserved in the Dharwar Craton is consistent with the Nunavutia hypothesis, or with other palaeogeographic reconstructions.

2. Geological Background:

The Dharwar Craton forms a significant part of the continental shield of southern India. It is a tilted oblique crustal section that ranges from Paleoarchaean to Neoarchaean in age and comprises granitoids basement with structurally overlying metamorphosed volcanic, volcanoclastic, and sedimentary rocks that make up the greenstone belts and record a range of metamorphic grades (Jayananda et al., 2013a,b, 2015; Chardon et al., 2008, 2011). A notable, and unusual feature of the Dharwar Craton is that

metamorphic grade increases, progressively from north to south, from greenschist facies to granulite facies, at a high angle to the structural strike (Ramakrishnan and Vaidyanadhan, 2008).

The various lithologies within the craton include common tonalite-trondhjemite-granodiorite suites (3.36–2.7 Ga), which have been traditionally known as the Peninsular Gneiss (Smeeth, 1915), as well as bimodal volcanic and sedimentary greenstone belts. The latter are split into two groups. The older Sargur Group (>3.0 Ga), and the younger Dharwar Supergroup (2.9 – 2.6 Ga). All of these are intruded by potassic granitoids (Maibam et al., 2016, Jayananda et al., 2000, 2006; Chadwick et al., 2007). The Dharwar Craton has been divided into two zones, the Western Dharwar Craton (WDC) and the Eastern Dharwar craton (EDC), demarcated by a broadly north-south granite batholith (called the Closepet granite) that has been dated at ca. 2.55 Ga (Manikyamba et al., 2012, Jayananda et al., 2000; Moya et al., 2003; Ramakrishnan and Vaidyanadhan, 2008). The transitional zone between the Chitradurga Schist Belt and the Closepet Batholith has been referred to as Central Dharwar Craton in recent years (Peucat et al., 2013, Dey et al., 2013; Jayananda et al., 2015; 2018; Li and Santosh, 2018), forming a third subdivision of the craton.



- Deccan Traps
- Sediment/Laterite cover
- Proterozoic basins
- EDC greenstone belts
- Chitradurga Group
- Bababudan Group
- Sargur Group
- Closepet Granite and younger equivalents
- Western Dharwar granitoid plutons
- Eastern Dharwar TTG/peninsular gneiss
- Central Dharwar TTG/peninsular gneiss
- Western Dharwar TTG/peninsular gneiss
- Sanukitoids
- Granulites
- U-Pb age data - This study
- ☆ Published U-Pb zircon ages for TTG & related granitoids

Figure 1: (a) Geological framework of India representing the distribution of major Archean cratons (after Rogers, 1986), DC: Dharwar Craton, BC: Bastar Craton, SC: Singhbhum Craton, BKC: Bundelkhand Craton, AC: Aravalli Craton. (b) Geological map of the Dharwar Craton, South India (modified after Jayananda, 2013a). Previously published meta-igneous zircon U-Pb ages are indicated by a star with colours representing ages from the scale shown. The locations sampled for this study are indicated by brown circles.

The oldest parts of the Western Dharwar Craton are the protoliths of the Peninsular Gneiss in the Gorur area (Fig. 1), where crystallisation ages have been interpreted to stretch back to ca. 3.41 Ga (Guitreau et al., 2017). These are overlain by metavolcanic and metasedimentary rocks of the Sargur Group (ca. 3.35–3.00 Ga) that consist of metamorphosed komatiites, tholeiitic basalts and rare felsic lava flows as well as sedimentary quartzites, pelites, conglomerates and banded iron formations. The younger Dharwar Supergroup at ca. 2.9 – 2.6 Ga unconformably overlies the Peninsular Gneiss and Sargur Group. It is divided into two subgroups; the Bababudan Group, comprising metabasalts, gabbros, ultramafic schists, quartzites, phyllites and conglomerates, and the Chitradurga Group, which includes mafic and felsic volcanic rocks, iron and manganese formations, quartzites and pelites that are intruded by calc-alkaline to potassic granites (Swami Nath and Ramakrishnan, 1981, Ramakrishnan and Vaidhyadathan, 2008, Chadwick 2000, Chardon et al 2011; Tushipokla and Jayananda, 2013; Jayananda 2000, 2006, 2008, 2013a, 2013b; Manikyamba et al., 2017). Several workers have suggested that the shear zone along the eastern margin of the Chitradurga Schist Belt marks the eastern boundary of the WDC (Peucat et al 2013, Jayananda et al 2008, 2013a, 2013b, Chardon et al., 2011). High-K plutons intruded the Western Dharwar craton at 3.0 Ga (Chardon et al., 2011, Jayananda et al., 2020).

The contact between the EDC and the WDC is considered as a diffuse transitional zone between the Shimoga Schist Belt and the Gadag Greenstone Belt in the northeast, and bound by the Closepet Granite (Chadwick et al. 2007). This region is characterised by WDC-like TTG rocks, but with crystallisation ages between 2.7–2.5 Ga, similar to the crystallisation ages of granitoids in the EDC (Ramakrishnan and Vaidyanadhan, 2008). The transitional zone has been termed the Central Dharwar Craton (CDC) in recent studies (Peucat et al., 2013, Jayananda et al., 2018, 2020). Ca. 3.0 Ga orthogneisses near the Kolar Schist Belt form the oldest known component of the CDC. Neoarchean (ca. 2.7 Ga) banded gneisses are much more voluminous and form the basement to a series of greenstone belts that are characterized by volcanics that include major gold deposits.

The EDC is dominated by voluminous Neoarchean (ca. 2630–2530 Ma) TTG gneisses and calc-alkaline granites (Peucat et al., 1993, Peucat et al., 2013). These are structurally interlayered with ca. 2.7 Ga greenstone belts that preserve relics of Mesoarchean crust (ca. 3.14–3.00 Ga; Chadwick et al., 2000; Jayananda et al., 2000).

Detrital zircon Lu–Hf datasets include works on Gadag greenstone belt (Sarma et al., 2012), Hutti Greenstone belt (Anand et al., 2014), some detrital records from the metasedimentary domains scattered across the Dharwar craton (e.g Lancaster et al., 2015; Maibam et al., 2016) have been used to interpret that the crustal growth in both EDC and WDC was contemporaneous and agreed upon that cratonisation in WDC took place in two episodes at 3.3 Ga and 2.7 Ga and the younger EDC had its crustal extraction from 3.0 Ga to 2.5 Ga (Lancaster et al., 2015).

The Nd isotope record for the Dharwar Craton (Dey, 2013) suggests the EDC and WDC reveal Nd isotopic signatures leading to depleted mantle ages at ca. 3.5 Ga. The major period of juvenile crust formation in WDC was during 3.35 – 3.0 Ga accompanied by crustal recycling. The data interpretation from Dey (2013) suggests that a) the mantle was re-fertilized during the Mesoarchaeon which contributed to the extensive mafic volcanism in 2.9 – 2.6 Ga in WDC, accompanied with crustal recycling during 2.7 – 2.6 Ga, b) the EDC remnant gneisses were already derived from a recycled PalaeoArchaean crust that was destroyed by late Neoarchaeon juvenile crustal addition during 2.7–2.5 Ga along with recycling of the older crust. The study (Dey 2013), however, could not constrain the initiation of the juvenile magmatic TTG accretion in the Dharwar Craton.

The comparisons of crustal evolution histories of the WDC and EDC using these methods are considered incomplete and biased towards data from studies on the volcano-sedimentary greenstone belts and associated granitoids (Manikyamba and Kerrich, 2012; Yang et al., 2015; Jayananda et al., 2013; Dey et al., 2013, 2015). Recent isotopic studies have been published on the basement gneisses of the Dharwar Craton which are confined to localised domains (Guitreau et al., 2017, Ranjan et al., 2020., Jayananda et al., 2015, 2020; J.Y. Wang et al., 2020; Li and Santosh, 2018). The need for spatially extensive isotopic studies for the basement granitoid gneisses would provide a better understanding for the comparison and studying the evolution of the Dharwar Craton as a whole, clarifying the accretion of individual crustal domains if they resulted from coeval crustal growth or retaining different formation histories.

3. Methods:

3.1 Zircon U–Pb geochronology and REE composition:

Thirty-one rock samples were crushed and sieved for a zircon fraction (<500 μm) at the petrology lab facility at the Indian Institute of Science, Bangalore. The fractions were panned for heavy minerals. Magnetic minerals were removed using a neodymium. The resulting fractions were handpicked for zircons, mounted in epoxy resin, ground and polished to half thickness of the zircons. These zircon mounts were carbon-coated and imaged by a Gatan cathodoluminescence (CL) detector

attached to Quanta 600 MLA Scanning Electron Microscope to identify various domains within the zircons suitable for analysis. U–Pb geochronology was performed at Adelaide Microscopy, The University of Adelaide, using an Agilent 7900 ICP-MS. This was attached to a New Wave 213 nm laser (NWR-213) and an ASI RESOLution 193 nm excimer laser during different sessions. Both laser used a spot size of 30 μm and a frequency of 5 Hz. The isotopes ^{204}Pb , ^{206}Pb , ^{207}Pb , ^{208}Pb , ^{232}Th , ^{238}U were measured for U–Pb geochronology. GEMOC GJ-1 zircon (TIMS ages $^{207}\text{Pb}/^{206}\text{Pb} = 602 \pm 4.3 \text{ Ma}$, $^{206}\text{Pb}/^{238}\text{U} = 600.7 \pm 1.1 \text{ Ma}$ and $^{207}\text{Pb}/^{235}\text{U} = 602.0 \pm 1.0 \text{ Ma}$; Jackson et al., 2004) was used for the correction of U–Pb fractionation for laser sessions. The Plesovice zircon (ID-TIMS $^{206}\text{Pb}/^{238}\text{U}$ age = $337.13 \pm 0.37 \text{ Ma}$) was used as an internal standard to test the accuracy of the laser sessions. A total of 167 Plesovice zircon analyses yielding a weighted average $^{206}\text{Pb}/^{238}\text{U}$ age of $338.23 \pm 0.86 \text{ Ma}$ (2SD, MSWD = 2.3), which was within the uncertainty of the ID-TIMS age of Sláma et al. (2008). Rare Earth Elements: ^{139}La , ^{140}Ce , ^{141}Pr , ^{146}Nd , ^{147}Sm , ^{153}Eu , ^{157}Gd , ^{159}Tb , ^{163}Dy , ^{165}Ho , ^{166}Er , ^{169}Tm , ^{172}Yb , ^{175}Lu ; also ^{49}Ti , ^{89}Y , ^{178}Hf were simultaneously measured over the same spots on the zircons along with U–Pb isotopes using 50 μm spot size analyses over NIST SRM 610 glass as reference material (Norman et al., 1996, Norman et al., 1998, Jochum et al., 2011). The U–Pb data and REE data were separately processed using Iolite (Paton et al., 2011).

3.2 Zircon Lu–Hf analysis:

Zircon grains with less than 10% discordance were targeted for Hf isotope analysis, which was carried out using a New Wave UP-193 Eximer laser (193 nm), attached to a Thermo-Scientific Neptune multicollector ICP-MS following methods described on Payne et al. (2013). CL images were used as a guide to target zircons within the same domain as the U–Pb ablation spot. Beam diameters of 35 μm or 50 μm were used depending on the grain size. Zircons were typically ablated for $\sim 80 \text{ s}$ using a 5 Hz repetition rate with a 4 ns pulse rate and an intensity of $\sim 4.4 \text{ J/cm}^2$ in a helium atmosphere that was mixed with argon upstream of the ablation cell. HfTRAX, a Microsoft Excel macro (Payne et al., 2013) was used to carry out zircon data reduction. Data was normalised to $^{179}\text{Hf}/^{177}\text{Hf} = 0.7325$ using an exponential correction for mass bias. The Yb and Lu isobaric interferences on ^{176}Hf were corrected following the methodology of Woodhead et al. (2004). Zircon standards were analysed before and during analysis to assess the performance and stability of the instrument. Mudtank zircon was used as primary standard and 13 analyses yielded a mean $^{176}\text{Hf}/^{177}\text{Hf}$ ratio of 0.282489 ± 0.000018 (2 SD), which was within the uncertainty of the published value of 0.282507 ± 0.000006 (Woodhead and Hergt, 2005). The initial $^{176}\text{Hf}/^{177}\text{Hf}_{\text{CHUR}(t)}$ was calculated using a ^{176}Lu decay constant of $1.865 \times 10^{-11} \text{ year}^{-1}$ (Scherer et al., 2001) with modern $^{176}\text{Hf}/^{177}\text{Hf}$ and $^{176}\text{Lu}/^{177}\text{Hf}$ values of 0.282785 and 0.0336, respectively (Bouvier et al., 2008). The values of crustal model ages (T_{DMC}) were calculated using a ^{176}Lu decay constant of $1.865 \times 10^{-11} \text{ year}^{-1}$ (Scherer et al., 2001), modern $^{176}\text{Hf}/^{177}\text{Hf} = 0.28325$, modern $^{176}\text{Lu}/^{177}\text{Hf} = 0.0384$ (Griffin et

al., 2000), and a bulk crust value of $^{176}\text{Lu}/^{177}\text{Hf} = 0.015$ (Griffin et al., 2002). The reported uncertainties for $\varepsilon_{\text{Hf}}(t)$ were calculated as $^{176}\text{Hf}/^{177}\text{Hf}_{\text{sample}}$ uncertainty converted to epsilon notation and reported at 2σ level.

Concordia diagrams ($^{207}\text{Pb}/^{235}\text{U}$ vs $^{206}\text{Pb}/^{238}\text{U}$) were generated to represent the data using the Isoplot 4.15 plugin on Microsoft Excel (Ludwig, 2003) and an online version of IsoplotR (Vermeesch, 2018) was used to calculate the upper intercepts of the discordant lines and mean ages. The analytical ellipses have been coloured to represent Th/U ratios. The thickness of the data ellipses represent two standard deviations in error. The mean standard weighted deviation (MSWD) has been calculated along the discordant lines drawn following the strategies mentioned in Spencer et al. (2016). The number of ellipses used to calculate the MSWD and upper intercept of the discordant lines is indicated. The REE compositions have been normalised against chondrite values from Boynton et al. (1984), using the Geochemical Data Toolkit for R (GCDkit6.0) (Janousek et al., 2006) to calculate REE ratios. In particular, Eu anomalies, $\text{La}_\text{N}/\text{Yb}_\text{N}$ ratios (light rare earth element, LREE, vs heavy rare earth element, HREE), and $\text{Gd}_\text{N}/\text{Yb}_\text{N}$ ratios (middle rare earth element, MREE, vs HREE) were calculated.

Lu–Hf analyses on near concordant (>85% concordance) zircons were obtained from the same domains from which the U–Pb data were collected. The results are presented in Fig. 9 and are plotted as ratios against $^{207}\text{Pb}/^{206}\text{Pb}$ ages.

4. Results:

4.1 Sample descriptions:

Thirty granitoid samples were used for zircon U–Pb analysis, of twenty-eight samples, were analysed for Lu–Hf isotopes. The samples were collected in a series of transects that includes the WDC, CDC and EDC, mostly within the state territory of Karnataka, to ensure a significant spatial coverage over the whole craton. The northernmost sample is from the Closepet Granite equivalent near Bagalkote; the southernmost sample was collected near Akkihebbalu village. The longitudinal spread extends from Ramagiri Greenstone Belt in the EDC to Sringeri town in the WDC (Figure 1).

Sample	Lithology	Region	Latitude	Longitude	Elevation
PD17-1	Bt Granite	Closepet Granite	12.93823	77.35293	804
PD17-5	Granite	Closepet Granite	12.94583	77.26208	850
PD17-14	Pegmatoidal Granitoid Gneiss	Transitional Central zone	12.81692	76.86365	690
PD17-21	Granitoid Gneiss	Western Dharwar	12.78800	76.71220	854
PD17-27	Granitoid Gneiss	Western Dharwar	12.92885	76.75573	824
PD17-32	Granitic Gneiss	Western Dharwar	12.62553	76.63278	841
PD17-38	Tonalite Thronhjemetite Granodiorite Gneiss	Western Dharwar	12.73630	76.48962	869

PD17-44	Tonalite Thronthjemite Granodiorite Gneiss	Western Dharwar	12.59772	76.37252	757
PD17-48	Tonalite Thronthjemite Granodiorite Gneiss	Western Dharwar	12.77307	76.15093	907
PD17-49	Tonalite Thronthjemite Granodiorite Gneiss	Western Dharwar	12.83033	76.06583	885
PD17-56	Tonalite Thronthjemite Granodiorite Gneiss	Western Dharwar	12.92985	76.08125	994
PD18-01	Bt Granite	Closepet Granite	16.33885	75.61198	525
PD18-27	Tonalite Thronthjemite Granodiorite Gneiss	Central Dharwar	15.13743	76.84401	488
PD18-34	Bt Granite	Central Dharwar	14.97457	76.44863	690
PD18-37	Bt Granite	Central Dharwar	14.98212	76.36622	645
PD18-39	Granodiorite	Central Dharwar	15.13962	76.98873	415
PD18-44	Granitoid gneiss	Central Dharwar	14.97192	77.22908	497
PD18-45	Granitoid gneiss	Central Dharwar	14.893	77.27879	493
PD18-47	Tonalite Thronthjemite Granodiorite Gneiss	Eastern Dharwar	14.72877	77.51852	371
PD18-54	Tonalite Thronthjemite Granodiorite Gneiss	Eastern Dharwar	14.32158	77.56143	461
PD18-101	Porphyritic Kfs Granite	Closepet Granite	13.17818	77.28368	922
PD18-104	Tonalite Thronthjemite Granodiorite Gneiss	Central Dharwar	13.54972	76.99198	760
PD18-105	Tonalite Thronthjemite Granodiorite Gneiss	Central Dharwar	13.72904	76.88171	660
PD18-108	Tonalite Thronthjemite Granodiorite Gneiss	Western Dharwar	13.89725	76.43247	679
PD18-110	Weakly foliated Granodiorite	Western Dharwar	13.86205	76.35491	689
PD18-111	Granitic Gneiss	Western Dharwar	13.77185	76.32336	670
PD18-116	Granite	Western Dharwar	13.90487	75.57293	593
PD18-118	Tonalite Thronthjemite Granodiorite Gneiss	Western Dharwar	14.20827	75.61265	569
PD18-120	Granodioritic Gneiss	Western Dharwar	13.67886	75.24567	613
PD18-126	Granite	Western Dharwar	13.30347	75.82401	1035

Table 1: Table representing the lithologies sampled for this study categorised into Western, Central and Eastern Dharwar Cratons along with Closepet Batholith and their locations.

4.2 Zircon U–Pb geochronology, REE compositions and Lu–Hf isotopic data:

4.2.1 TTG gneisses of the Western Dharwar Craton:

WDC Gneisses

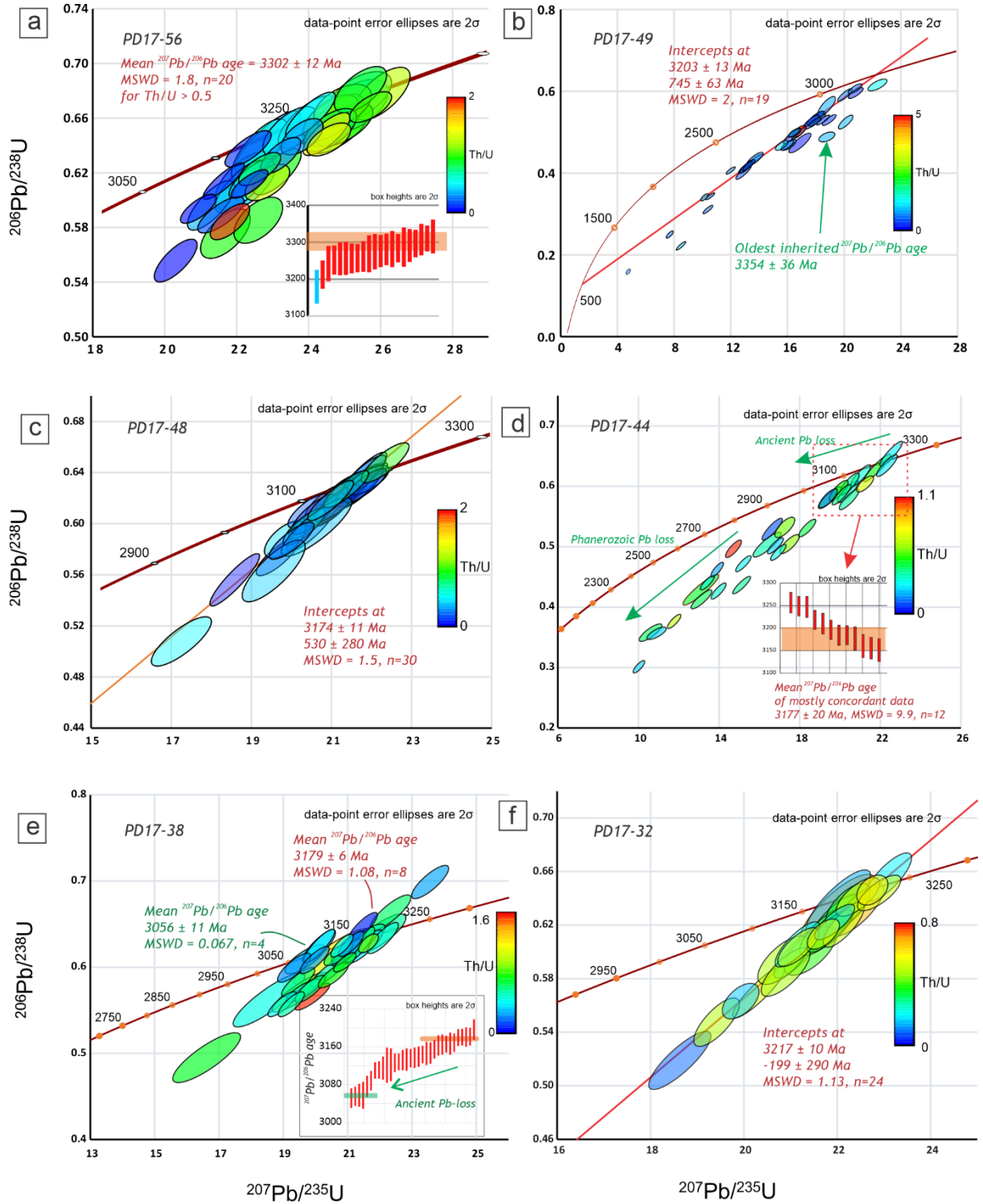


Figure 2 representing the U–Pb data from older gneisses of the Western Dharwar Craton.

PD17-56 is collected from a quarry in Javenahalli village, which lies in the vicinity of the oldest rocks so far reported from the Western Dharwar craton — the Gorur gneiss (Figure 2 (a)). The sample collected is a TTG gneiss that yielded mostly concordant zircons with $^{207}\text{Pb}/^{206}\text{Pb}$ ages ranging from 3334

± 37 Ma to 3176 ± 30 Ma. The Th/U ratios of analysed volumes decrease with age. Zircons younger than 3.25 Ga yield Th/U ratios < 0.2 . Zircons with Th/U > 0.5 yield a mean $^{207}\text{Pb}/^{206}\text{Pb}$ age of 3302 ± 12 Ma (MSWD = 1.8, $n=20$). The age data are interpreted to indicate magmatic crystallisation at 3302 ± 12 Ma, followed by deformation and metamorphism with preferential expulsion of Th from the zircon lattice (Williams and Claesson, 1987) at ca. 3.2 Ga. (Figure This is further supported by the presence of bright rims around the zircons seen under CL (Figure 8). Seven spots yield initial $^{176}\text{Hf}/^{177}\text{Hf}$ values of 0.280627–0.280720 with $\epsilon\text{Hf}(t)$ values in a range of +0.08 to +3.82. The zircons yielded Eu/Eu* values between 0.33–0.88, $\text{La}_\text{N}/\text{Yb}_\text{N}$ ratios varied from 0.00001–0.1; $\text{Gd}_\text{N}/\text{Yb}_\text{N}$ ranged between 0.0068–0.1224.

PD17-49 is from a homogenous granodioritic gneiss collected in Gorur town along the Gorur-Hassan road. The zircons are short and thick (Figure 8) with vague oscillatory zoning. The data are quite discordant, however, we have used nineteen of the youngest, and most concordant, grains to define an indicative discordia, marking the younger boundary of array. This has an upper intercept of 3203 ± 13 Ma (MSWD = 2, $n=19$). Older, possibly inherited grains, yield $^{207}\text{Pb}/^{206}\text{Pb}$ ages up to 3354 ± 36 Ma. We interpret 3203 ± 13 Ma as the best estimate of the time of crystallisation of the gneiss protolith supported by zircons showing mostly oscillatory zoning within the CL images (Figure 8). The zircons yielded Eu/Eu* values between 0.47–0.87, $\text{La}_\text{N}/\text{Yb}_\text{N}$ ratios varied from 0.0085–0.8676; $\text{Gd}_\text{N}/\text{Yb}_\text{N}$ ranged between 0.0447–1.1574. Four spots yield initial $^{176}\text{Hf}/^{177}\text{Hf}$ values of 0.280683–0.280775 with $\epsilon\text{Hf}(t)$ values in a narrow range of -3.84 to +1.43.

PD17-48 is from a TTG gneiss collected from the west of Holenarsipur town. The zircons are elongated with clear oscillatory zoning in the CL images (Figure 8). It has yielded mostly near-concordant data ($>90\%$), with a few highly discordant grains that align along a discordia line with an upper intercept of 3174 ± 11 Ma (MSWD = 1.5, $n = 30$). A weighted mean of $^{207}\text{Pb}/^{206}\text{Pb}$ ages from the near concordant grains ($>90\%$) yielded a mean of 3153 ± 6 Ma (MSWD = 1.02, $n = 29$). This is interpreted as the best estimate of the age of crystallization of the TTG protolith. The zircons yielded Eu/Eu* values between 0.61–3.38, $\text{La}_\text{N}/\text{Yb}_\text{N}$ ratios varied from 0.0085–0.8676 and $\text{Gd}_\text{N}/\text{Yb}_\text{N}$ ranged between 0.0447–1.1574. Seven spots yield initial $^{176}\text{Hf}/^{177}\text{Hf}$ values of 0.280733–0.280751 with $\epsilon\text{Hf}(t)$ values in a narrow range of -1.00 to +1.25.

PD17-44 is a granodioritic mesosome, collected from a migmatitic TTG gneiss. The zircons are short and commonly display metamict textures, with a few that preserve oscillatory-zoning. The oldest zircons are used to define a discordia line that marks to old margin of the array (Figure 2(d)). This has an upper intercept age of 3209 ± 11 Ma (MSWD = 2.5, $n=10$). The $^{207}\text{Pb}/^{206}\text{Pb}$ ages of near concordant ($>90\%$) zircons define a weighted mean of 3177 ± 20 Ma (MSWD = 9.9, $n=12$). The zircons yielded Eu/Eu* values between 0.11–1.11. $\text{La}_\text{N}/\text{Yb}_\text{N}$ ratios varied from 0.00004–0.3548 and $\text{Gd}_\text{N}/\text{Yb}_\text{N}$ ranged between

0.01–0.3487. Six spots yield initial $^{176}\text{Hf}/^{177}\text{Hf}$ values of 0.280719–0.280770 with $\epsilon\text{Hf}(t)$ values in a narrow range of -2.25 to -0.23.

PD17-38 is from a TTG gneiss collected from a quarry named Singanahalli Gate. The outcrop has veins of aplite and pegmatite cutting through segregated leucosome and melanosome that are uniformly distributed. The zircons appear thick elongated (Figure 8) and mostly display imperfect oscillatory zoning in CL, with a few exceptions displaying ideal magmatic zoning. The zircons from this sample have yielded mostly near-concordant grains (>90% concordant) with $^{207}\text{Pb}/^{206}\text{Pb}$ ages from 3182 ± 17 Ma to 3052 ± 20 Ma. A mean of the eight oldest near-concordant ages yielded a $^{207}\text{Pb}/^{206}\text{Pb}$ age of 3179 ± 7 Ma, which is interpreted as the age of crystallisation of the protolith of this gneiss. The four youngest near concordant $^{207}\text{Pb}/^{206}\text{Pb}$ ages, which also have Th/U ratios <0.2, are interpreted to provide the best estimate of the timing of metamorphism and deformation at 3056 ± 11 Ma. The zircons yielded Eu/Eu* values between 0.39–0.68, $\text{La}_\text{N}/\text{Yb}_\text{N}$ ratios from 0–0.0697 and $\text{Gd}_\text{N}/\text{Yb}_\text{N}$ ratios between 0.0189–0.1375. Seven spots yield initial $^{176}\text{Hf}/^{177}\text{Hf}$ values of 0.280739–0.280817 with $\epsilon\text{Hf}(t)$ values in a narrow range of -1.39 to +1.85.

PD17-32 is a uniformly banded granodioritic gneiss collected on the west margin of Melukote Hill. The zircons are mostly short and rounded and display magmatic oscillatory zoning. This sample yielded ages that have an upper intercept of 3217 ± 9.4 Ma (MSWD = 1.13, n=24) and appear to have suffered modern Pb loss with a zero lower intercept. The upper intercept is interpreted to represent the best estimate for crystallization of the protolith of the gneiss. The zircons yielded Eu/Eu* values between 0.13–0.43, $\text{La}_\text{N}/\text{Yb}_\text{N}$ ratios varied from 0–0.62 and $\text{Gd}_\text{N}/\text{Yb}_\text{N}$ ranged between 0.0229–0.1087. Six spots yield initial $^{176}\text{Hf}/^{177}\text{Hf}$ values of 0.280709–0.280824 with $\epsilon\text{Hf}(t)$ values widely ranging from -0.59 to +6.23.

PD18-118 is a TTG gneiss acquired at a contact zone with amphibole bearing schists of the Chitradurga Group, near the town of Honnali (Figure 1). The sample contained large pristine zircons that preserve magmatic oscillatory zoning in CL. The zircons are near concordant and yield a weighted mean $^{207}\text{Pb}/^{206}\text{Pb}$ age of 3284 ± 9 Ma (MSWD = 0.94, n=32), which is interpreted as the crystallization age of the protolith of the gneiss. The zircons yielded Eu/Eu* values between 0.25–0.39, $\text{La}_\text{N}/\text{Yb}_\text{N}$ ratios from 0–0.0008 and $\text{Gd}_\text{N}/\text{Yb}_\text{N}$ between 0.041–0.0871. Seven spots yield initial $^{176}\text{Hf}/^{177}\text{Hf}$ values of 0.280633–0.280676 with $\epsilon\text{Hf}(t)$ values in a narrow range of +2.33 to +4.68.

PD18-108 is from a uniform banded TTG gneiss obtained from an outcrop structurally enclosed within the western segment of the Chitradurga Greenstone Belt. The gneisses are thought to represent a basement to the greenstone belt. Most U–Pb data are discordant. A group of near concordant (>85%) zircons were used to calculate a weighted mean $^{207}\text{Pb}/^{206}\text{Pb}$ age of 3232 ± 32 Ma (MSWD = 2.5, n=7). This

is interpreted as the best approximation for the age of crystallization of the gneiss protolith as CL images of these zircons preserve good magmatic oscillatory zoning. The zircons yielded Eu/Eu* values between 0.32–1.67, La_N/Yb_N varied from 0.0033–0.3876 and Gd_N/Yb_N ranged between 0.0589–0.8603. Six spots yield initial ¹⁷⁶Hf/¹⁷⁷Hf values of 0.280662–0.280739 with εHf(t) values in a wider range of +1.51 to +4.29.

PD18-110 is a weakly foliated TTG gneiss on the western side of the Chitradurga Greenstone Belt. It yielded zircons with ages that align along a broad discordant array with a Mesoproterozoic upper intercept. The CL images show two groups of zircons—long elongated grains with good oscillatory zoning, and long elongated subhedral grains with a dark CL response. Two concordant zircons have similar ²⁰⁷Pb/²⁰⁶Pb ages of 3235 ± 37 Ma and 3203 ± 35 Ma, whilst a younger grain is dated at 3073 ± 35 Ma. The discordant analyses form an array from these concordant data towards the origin. The zircons yielded Eu/Eu* values between 0.18–1.36, La_N/Yb_N ratios varied from 0.0002–0.7127 and Gd_N/Yb_N ranged between 0.0795–0.9937. Four spots yield initial ¹⁷⁶Hf/¹⁷⁷Hf values of 0.280721–0.280819 with εHf(t) values in a wider range of -1.36 to +4.94.

PD18-120 is a weakly foliated granitic gneiss sampled from a cliff face at Thirthahalli village (Figure 1). The zircons are mostly subhedral and thick with uneven oscillatory zoning combined with partially metamict cores in some grains (Figure 8). This sample has yielded zircons that range from slightly reversely discordant to highly normally discordant. Thirteen near concordant (95–105%) analyses form a linear array and are used to calculate a discordia with an upper intercept of 3154 ± 9 Ma (MSWD = 1.6, n = 13), which is interpreted as the best estimate of crystallisation of the granite. A sole concordant analysis at 2935 ± 6 Ma may represent a later thermal event. The zircons yielded Eu/Eu* values between 0.21–0.79, REE ratios—La_N/Yb_N varied from 0–0.0871; Gd_N/Yb_N ranged between 0.0086–0.5216. Six spots yield an initial ¹⁷⁶Hf/¹⁷⁷Hf values of 0.280662–0.280739 with εHf(t) values in a wider range of +1.51 to +4.29.

PD17-21 is a banded gneiss on the western margin of the Nagamangala Greenstone Belt. The zircons from this sample are mostly elongated with clear magmatic oscillatory zoning and a few subhedral grains that appear to have an unclear/metamict CL response. The zircons broadly define a triangular array of data, with the concordia maximum and minimum ages of 3048 ± 24 Ma and 2924 ± 23 Ma, with a lower intercept at ca 624 ± 89 Ma. There is a spread in ²⁰⁷Pb/²⁰⁶Pb grain ages of the near concordant (>85%) zircons with general decrease in Th/U ratio with decreasing age. These data are interpreted to represent crystallization of the gneiss protolith at, or before, 3048 ± 24 Ma and Pb-loss during metamorphism at ca 2924 ± 23 Ma. The zircons yielded Eu/Eu* values between 0.32–1.27,

La_N/Yb_N ratios varied from 0.0028–0.0872 and Gd_N/Yb_N ranged between 0.0151–0.0791. Six spots yield initial ¹⁷⁶Hf/¹⁷⁷Hf values of 0.280831–0.280914 with εHf(t) values ranging from -2.04 to +0.54.

PD18-111 was collected west of the Chitradurga Greenstone Belt from a uniformly banded migmatitic granitic gneissic body. All data define a linear discordia array. The >85% concordant zircons have Th/U ratios greater than 0.2 and yielded a weighted mean ²⁰⁷Pb/²⁰⁶Pb age of 3216 ± 17 Ma (MSWD = 12, n=13). This is interpreted as the best estimate of the crystallization age of the gneissic protolith from the oscillatory zoning visible in the CL images. The zircons yielded Eu/Eu* values between 0.39–0.59, La_N/Yb_N varied from 0.006 – 0.06 and Gd_N/Yb_N ranged between 0.05–0.29. Four spots yielded initial ¹⁷⁶Hf/¹⁷⁷Hf values of 0.280685–0.280734 with εHf(t) values in a narrow range of +1.48 to +3.33.

WDC Gneisses (continued)

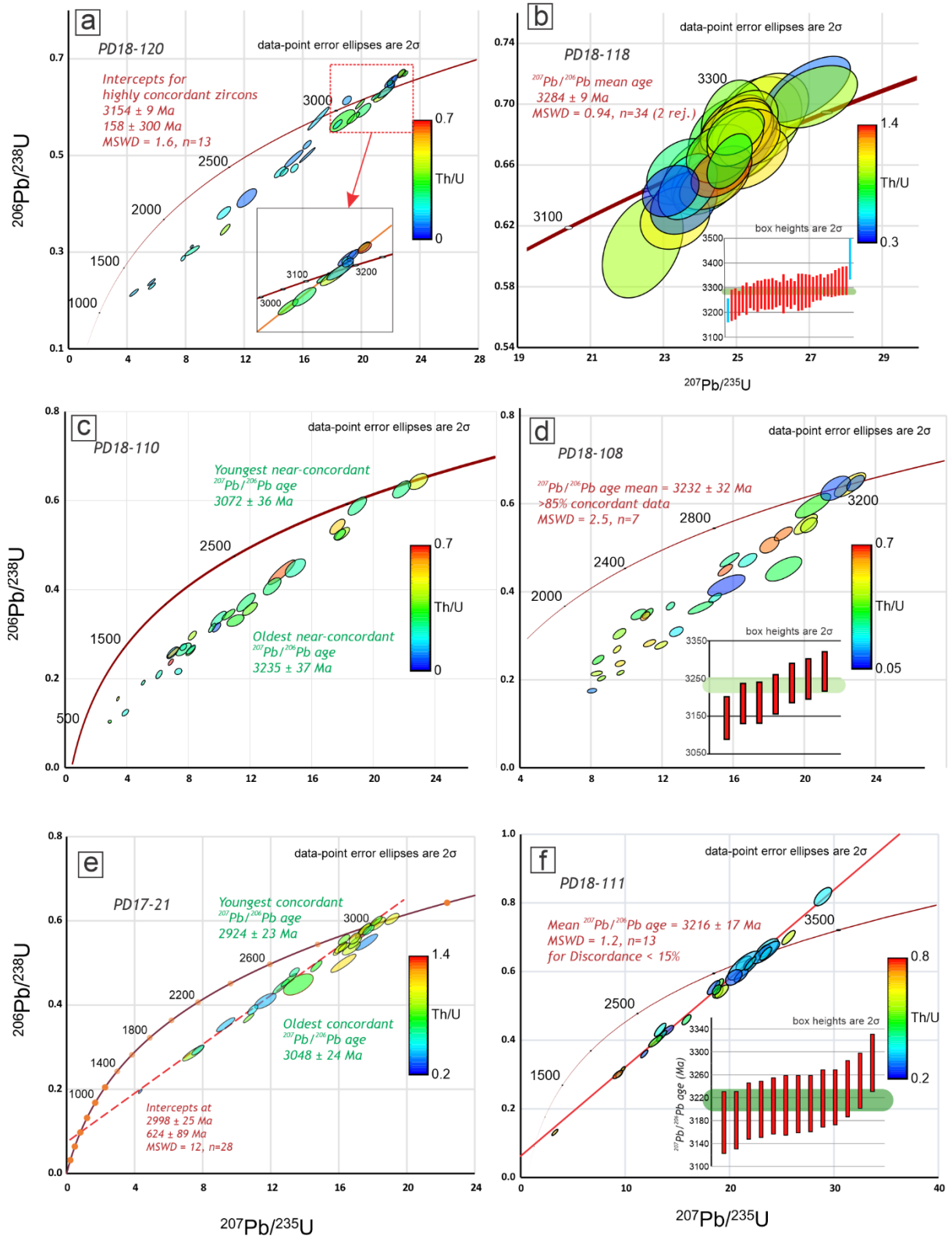


Figure 3 representing the U–Pb data from older gneisses of the Western Dharwar Craton

4.2.2 Undeformed granitoids of the Western Dharwar Craton:

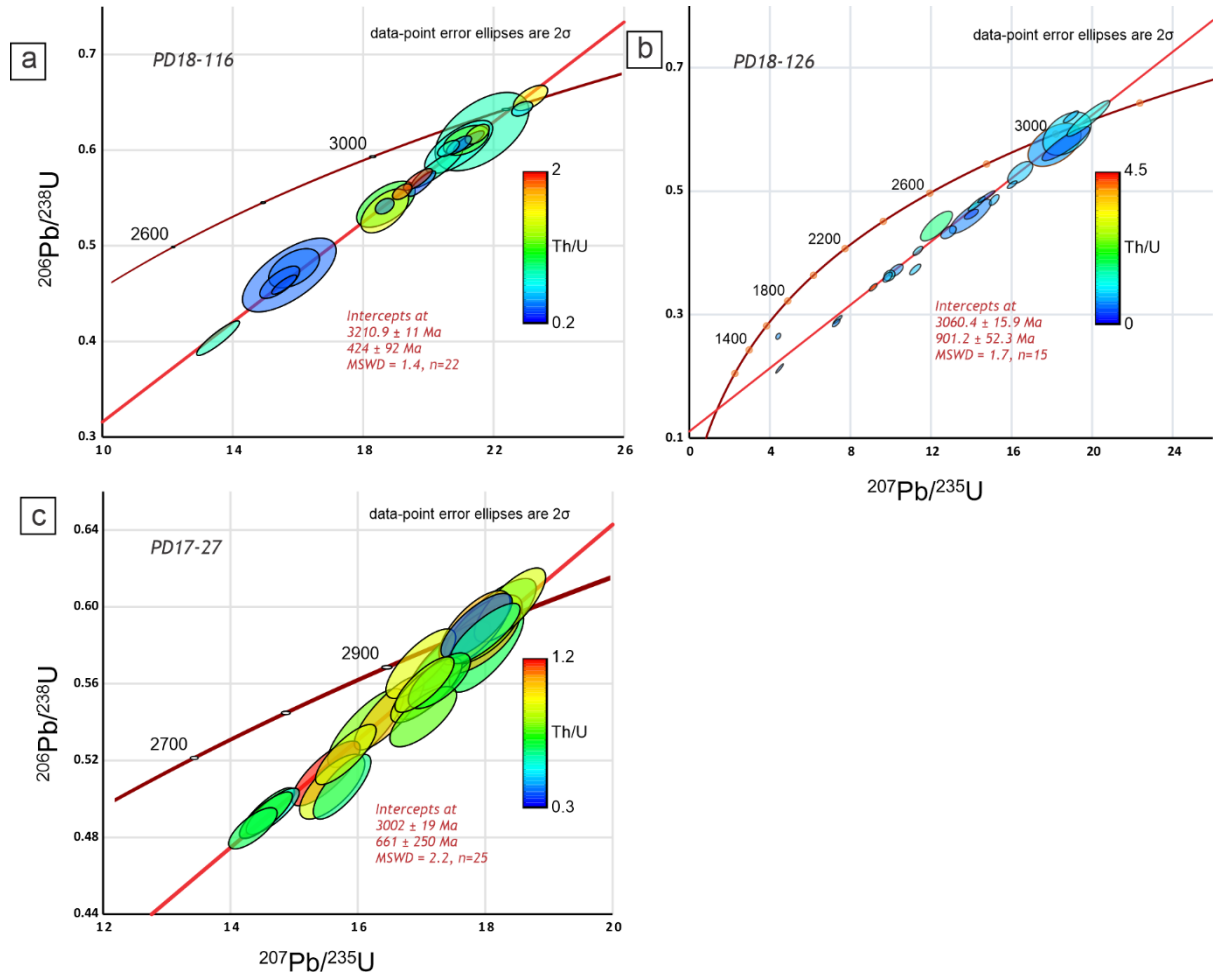


Figure 4 representing the U–Pb data from undeformed granitoids of the Western Dharwar Craton.

PD18-116 was sampled from a massive granite quarry in the town of Shimoga (Figure 1). It yielded zircons that define a discordia line with an upper intercept of 3211 ± 11 Ma and a lower intercept of 424 ± 92 Ma (MSWD = 1.4, n=22). The more discordant grains are generally lower in Th/U ratio. The age of 3211 ± 11 Ma is interpreted as the crystallization age of this granite as the zircons display clear magmatic oscillatory zoning in CL. The zircons yielded Eu/Eu* values between 0.16–0.87, $\text{La}_\text{N}/\text{Yb}_\text{N}$ ratios varied from 0.0002–0.0478 and $\text{Gd}_\text{N}/\text{Yb}_\text{N}$ ranged between 0.0472–0.3247. Eight spots yield initial $^{176}\text{Hf}/^{177}\text{Hf}$ values of 0.280713–0.280769 with $\epsilon\text{Hf}(t)$ values in a narrow range of +0.12 to +3.58.

PD18-126 was acquired from a massive granite body towards the south-east of Chikamagalur town (Figure 1). The zircons from this sample are slightly elongated and show subtle oscillatory zoning. Zircon U–Pb data align along a discordia line with an upper intercept of 3060 ± 16 Ma and a lower intercept of 901 ± 52 Ma (MSWD = 1.7, n=15). The upper intercept is interpreted as the best estimate of the age of crystallization of this granite. The zircons yielded Eu/Eu* values between 0.43–2.4, $\text{La}_\text{N}/\text{Yb}_\text{N}$

ratios varied from 0.0004–0.14 and Gd_N/Yb_N ranged between 0.0219–0.5593. Six spots yield initial $^{176}Hf/^{177}Hf$ values of 0.280796–0.280885 with $\epsilon Hf(t)$ values in a wider range of -4.75 to -1.05.

PD17-27 is a slightly foliated granite body collected towards the north of Nagamangala town (Figure 1). The zircons are slightly elongated and mostly display oscillatory zoning. This sample yielded mostly near concordant zircons that align along a discordia line with an upper intercept age of 3002 ± 19 Ma and an imprecise lower intercept age of 661 ± 250 Ma (MSWD = 2.2, n=25). The upper intercept is taken as the best estimate for the crystallization age of the granite. Five spots yield initial $^{176}Hf/^{177}Hf$ values of 0.280859 – 0.280868 with $\epsilon Hf(t)$ values ranging from -1.87 to +0.77. The zircons yielded Eu/Eu^* values between 0.25–0.46, La_N/Yb_N ratios varied from 0.004–0.18 and Gd_N/Yb_N ranged between 0.0498–0.101.

4.2.3 Foliated gneisses of the Central Dharwar Craton:

PD18-104 was collected from a banded gneiss sandwiched by two greenstone belts belonging to the Sargur Group on the eastern margin of the Chitradurga Greenstone Belt (Figure 1). The zircons display cores and very thin rims in CL. The cores define a discordia line with an upper intercept of 3301 ± 22 Ma (MSWD = 0.81, n=25). This is interpreted as the age of crystallization of the gneiss protolith. Ancient isotopic disturbance is recorded by eight analyses that lie to the left of this discordia. A discordia constructed through these eight analyses has an upper intercept of 3184 ± 35 Ma (MSWD = 1.5, n=8). We interpret this to indicate the time of metamorphism and partial melting. The zircons yielded Eu/Eu^* values between 0.25–0.38, La_N/Yb_N ratios varied from 0.0022–0.5102 and Gd_N/Yb_N ranged between 0.0736–0.529. Five laser spots yield initial $^{176}Hf/^{177}Hf$ values of 0.280624–0.280654 with $\epsilon Hf(t)$ values in a narrow range of +1.72 to +3.04.

PD18-34 was collected from a granodioritic TTG gneiss structurally enclosed within a granitic body to the north-west of the Closepet granite batholith (Figure 1). The zircons are short and thick and display an overall dark CL response with a few grains displaying subtle oscillatory zonation. Most zircons were highly discordant with only five analyses near-concordance. These consist of four analyses between 3067 ± 41 Ma and 2927 ± 33 Ma and a lone concordant analysis with a $^{207}Pb/^{206}Pb$ age of 3368 ± 35 Ma. The zircons yielded Eu/Eu^* values between 0.15–2.26, La_N/Yb_N varied from 0.0001–0.8357 and Gd_N/Yb_N ranged between 0.0257–0.8082. Three spots yielded initial $^{176}Hf/^{177}Hf$ values of 0.280854–0.280901 with $\epsilon Hf(t)$ values in a narrow range of -2.52 to -0.68.

PD17-14 is a pegmatite-bearing uniformly banded gneiss, collected on the eastern fringe of the southern extension of the Chitradurga Greenstone Belt (Figure 1). Most of the zircon grains are small and elongated with metamict cores and preserved oscillatory zoning towards the rims. The analyses

with the youngest $^{207}\text{Pb}/^{206}\text{Pb}$ ages define a discordia line with an upper intercept of 3014 ± 24 Ma (MSWD = 1.5, n=12). Two concordant older grains have ages of 3142 ± 35 Ma and 3062 ± 25 Ma. The zircons yielded Eu/Eu* values between 0.35–0.76, $\text{La}_\text{N}/\text{Yb}_\text{N}$ ratios varied from 0.0061–1.6371 and $\text{Gd}_\text{N}/\text{Yb}_\text{N}$ ranged between 0.0437–0.4786. No grains were selected for Hf isotopic analysis as the zircons were not big enough for the spot size of 50 μm .

PD18-27 is a melanosome collected from a quarry to the west of Ballari (Bellary) city (Figure 1) and the gneiss was intruded by granitic and pegmatitic dykes. The zircons vary in shape and appear to have an overall dark CL response, with a few grains showing subtle oscillatory zoning. The zircons are highly discordant. Twelve grains can be used to form a discordia line marking the upper boundary of the data array in the concordia plot. This discordia has an upper intercept of 2722 ± 20 Ma (MSWD = 1.3, n=12) and a lower intercept of 546 ± 17 Ma. We tentatively use the upper intercept as an estimate of crystallisation of the protolith of the gneiss. The discordant analyses also appear to have lost variable amounts of Pb in the modern environment, drawing them down from the discordia towards the origin. The zircons yielded Eu/Eu* values between 0.16–0.87, $\text{La}_\text{N}/\text{Yb}_\text{N}$ ratios varied from 0.0002–0.0478 and $\text{Gd}_\text{N}/\text{Yb}_\text{N}$ ranged between 0.0472–0.3247. Two spots yielded initial $^{176}\text{Hf}/^{177}\text{Hf}$ values of 0.281039 and 0.281056 with $\epsilon\text{Hf}(t)$ values of -0.73 and -0.69.

PD18-44 was from a TTG gneiss containing porphyritic mafic enclaves collected from the east of Ballari city (Figure 1). The zircons yielded many discordant data. The grains are short and thick and mostly preserve oscillatory zoning in CL. Some of the grains contain inclusions. Five near-concordant data define a mean weighted mean $^{207}\text{Pb}/^{206}\text{Pb}$ age of 2670 ± 23 Ma (MSWD = 0.52, n=5). This is interpreted as the best estimate of the crystallisation age of the gneiss protolith. The zircons yielded Eu/Eu* values between 0.13–2.23, $\text{La}_\text{N}/\text{Yb}_\text{N}$ ratios varied from 0.0017–0.3334 and $\text{Gd}_\text{N}/\text{Yb}_\text{N}$ ranged between 0.0533–0.3841. Five spots yield initial $^{176}\text{Hf}/^{177}\text{Hf}$ values of 0.281057–0.281089 with $\epsilon\text{Hf}(t)$ values in a narrow range of -6.96 to -5.32.

PD18-39 was collected from a weakly foliated granodioritic gneiss north of Ballari city (Figure 1). Sixteen zircons define a discordia line with an upper intercept of 2677 ± 22 Ma (MSWD = 1.5, n=16) with a modern lower intercept. This is interpreted as the best estimate of the crystallization age of the gneiss protolith since the zircons show oscillatory zoning and have an elongated euhedral shape. The discordant zircons below this line are interpreted to reflect older, possibly inherited zircons. The zircons yielded Eu/Eu* values between 0.38–0.56, $\text{La}_\text{N}/\text{Yb}_\text{N}$ ratios varied from 0.0031–0.2783 and $\text{Gd}_\text{N}/\text{Yb}_\text{N}$ ranged between 0.0344–0.5108. Three spots yield initial $^{176}\text{Hf}/^{177}\text{Hf}$ values of 0.281064–0.281072 with $\epsilon\text{Hf}(t)$ values in a narrow range of -3.66 to -1.83.

PD18-37 was collected from a weakly foliated granite to the west of the Closepet Granite that intruded into older basement gneiss. Eighteen of the twenty-eight analyses define a discordia line with an upper intercept of 2566 ± 16 Ma (MSWD = 1.3, n=18), which is interpreted as the best estimate of the age of crystallization of the granite. One concordant zircon yielded a $^{207}\text{Pb}/^{206}\text{Pb}$ age of 2748 ± 49 Ma that is interpreted as an inherited grain as it had a darker CL response compared to the other grains that preserved weak oscillatory zoning. The zircons yielded Eu/Eu* values between 0.39–1.04, $\text{La}_\text{N}/\text{Yb}_\text{N}$ ratios varied from 0.0008–1.5921 and $\text{Gd}_\text{N}/\text{Yb}_\text{N}$ ranged between 0.0674–1.4508. Seven spots yield initial $^{176}\text{Hf}/^{177}\text{Hf}$ values of 0.281126–0.281166 with $\epsilon\text{Hf}(t)$ values in a narrow range of -4.01 to -0.76.

CDC Gneisses

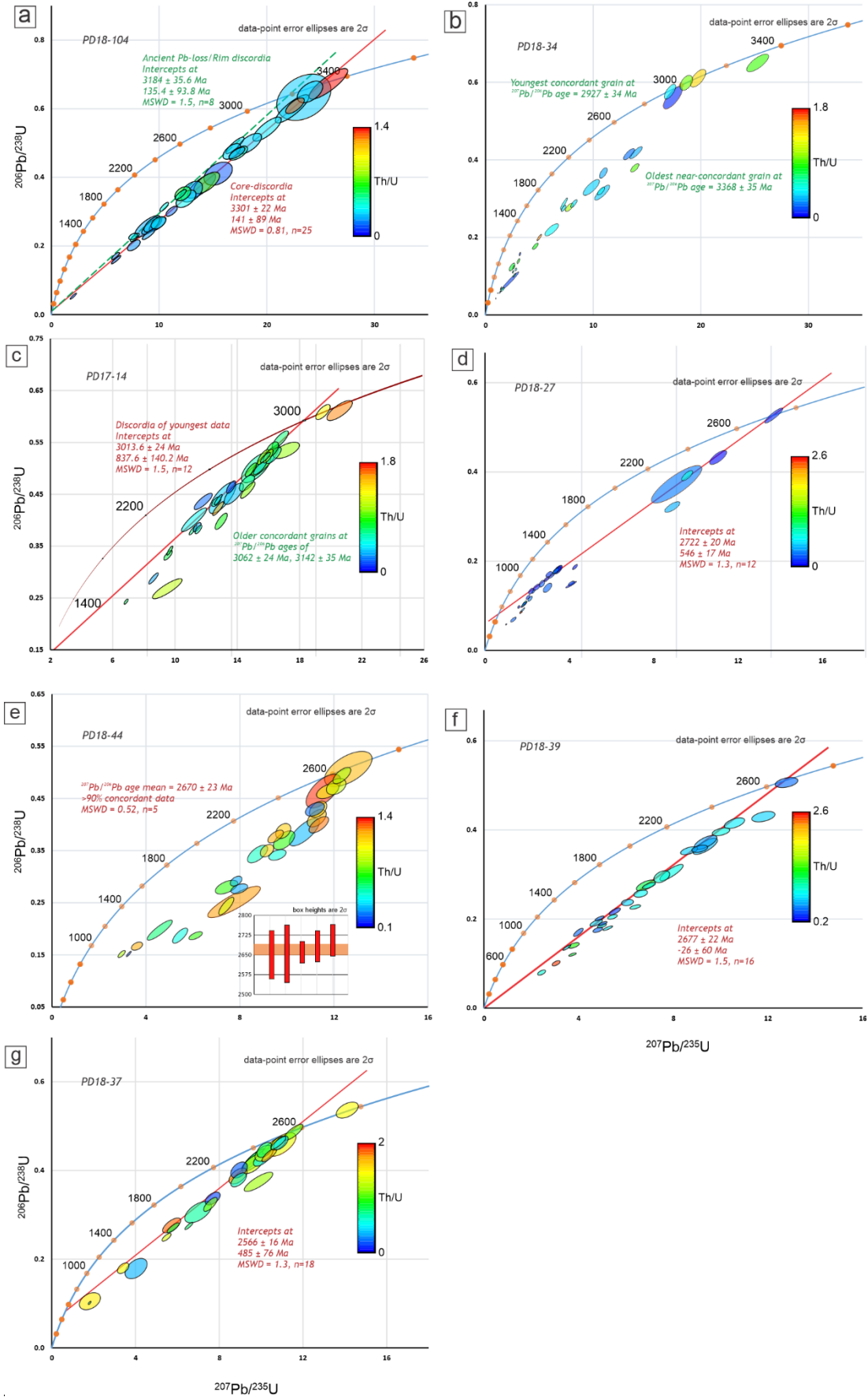


Figure 5 showing U–Pb data from the gneisses across the Central Dharwar Craton with the older gneiss to west in (a) to the younger gneiss towards the east of Central Dharwar.

4.2.4 Felsic batholiths of the Central Dharwar Craton:

PD18-45 was from a homogenous granodiorite body a few kilometres south-east from PD18-44. Zircon U–Pb data define a discordia line with an upper intercept of 2676 ± 17 Ma and a lower intercept of 467 ± 47 Ma (MSWD = 0.81, n=25). The upper intercept is interpreted as the time of granite crystallization. The lower intercept is interpreted to represent Palaeozoic isotopic disturbance. The zircons appear thick and slightly elongated and display subtle oscillatory zoning, but overall have a dark CL response. The zircons yielded Eu/Eu* values between 0.12–7.54, LaN/YbN ratios varied from 0.0011–0.2942 and GdN/YbN ranged between 0.0258–0.1575. Five spots yield initial $^{176}\text{Hf}/^{177}\text{Hf}$ values of 0.281098–0.281179 with $\epsilon\text{Hf}(t)$ values in a narrow range of +1.46 to +3.66.

PD18-105 was collected from a banded gneiss with mafic enclaves that was intruded by metre-thick granite veins within a quarry near the town Sira, which lies between the Chitradurga Greenstone Belt and the Sargur Group (Figure 1). The sample was taken from the granite vein. The zircons are mostly euhedral and majority of the CL response of the zircons appear to be in a stage between magmatic oscillatory zoning and metamictization. Sixteen of the zircons are used to define a discordia line that marks the upper boundary of the data array. This discordia has an upper intercept of 2604 ± 16 Ma and a lower intercept of 504 ± 33 Ma (MSWD = 1.2, n=16). The upper intercept is interpreted as marking the best estimate of crystallisation of the granite. The lower intercept is likely to represent isotopic disturbance associated with the orogenesis preserved south of the Dharwar Craton (Plavsa et al. 2015). Analyses that plot below this discordia are suggested to represent discordant inherited grains. The zircons yielded Eu/Eu* values between 0.05–0.78, LaN/YbN ratios varied from 0.0002–0.5024 and GdN/YbN ranged between 0.0486–0.3590. Five spots yield initial $^{176}\text{Hf}/^{177}\text{Hf}$ values of 0.281057–0.281164 with $\epsilon\text{Hf}(t)$ values in a narrow range of -2.06 to +2.2.

CDC Granitoids

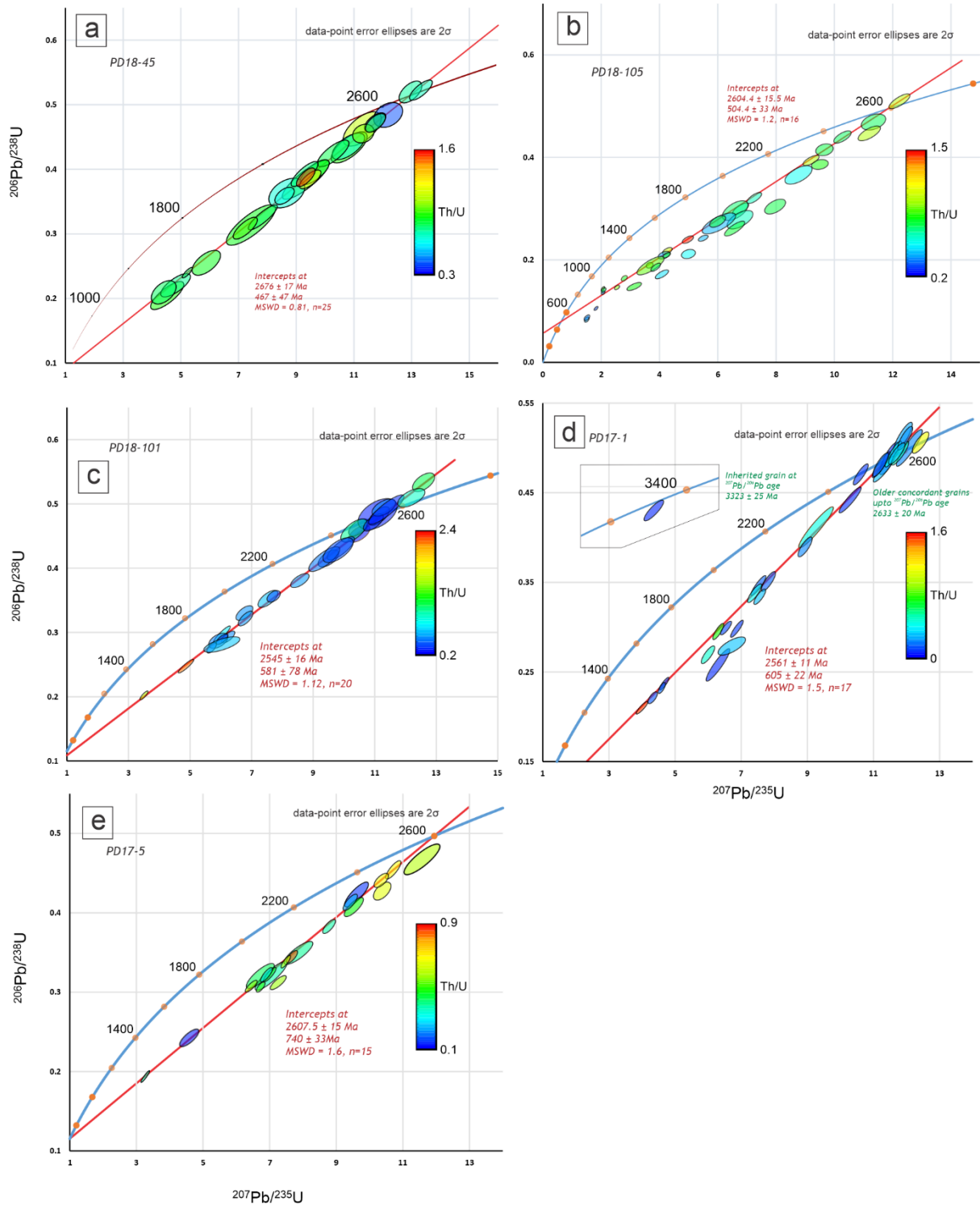


Figure 6 represents the U–Pb data from felsic batholiths across the Central Dharwar Craton.

PD17-1 is a granite collected from the eastern periphery of the southern part of the Closepet granite. The zircons are crystalline and elongated in shape and mostly preserve subtle oscillatory zoning. Eighteen zircon grains define a discordia line that bounds the data array and has an upper intercept age of 2561 ± 11 Ma and a lower intercept of 605 ± 22 Ma (MSWD = 1.5, n=17). The upper

intercept is interpreted as the best estimate of crystallization of the granite. Concordant zircons form a spread back to 2633 ± 20 Ma, with one discrete concordant analysis at 3323 ± 25 Ma. These are interpreted as inherited zircons. One younger analysis at 2486 ± 17 Ma may suggest hydrothermal zircon growth post crystallization. The zircons yielded Eu/Eu* values between 0.12–6.06, La_N/Yb_N ratios varied from 0.0001–0.4855 and Gd_N/Yb_N ranged between 0.0063–0.079. Seven spots yield initial $^{176}\text{Hf}/^{177}\text{Hf}$ values of 0.281104–0.281165 and the $\epsilon\text{Hf}(t)$ values range from -6.77 to -3.87.

PD18-101 was collected from the eastern boundary of the Closepet Granite, 40 kilometres north of PD17-1, from a porphyritic granite with orthoclase phenocrysts up to 2 cm long. The zircons have Th/U ratios > 0.2 and align along a discordia line with upper intercept of 2545 ± 16 Ma and a lower intercept of 581 ± 78 Ma (MSWD = 1.12, n=20). The upper intercept is interpreted as the best estimate of the age of crystallization of this sample. The zircons preserve oscillatory zoning in CL and yielded Eu/Eu* values between 0.38–0.98, La_N/Yb_N ratios between 0.0–4.427 and Gd_N/Yb_N between 0.0268–0.16. Five spots yield initial $^{176}\text{Hf}/^{177}\text{Hf}$ values of 0.281130–0.281182 with $\epsilon\text{Hf}(t)$ values in a narrow range of -7.24 to -6.03.

PD17-5 is a calc-alkaline sample in the Closepet Granite batholith containing dark biotite-rich veins near Thagachaguppe village between Bangalore and Mandya. The zircon analyses define a broad discordant array with fifteen of them used to define a discordia line that bounds the young margin of the array and yields an upper intercept of 2607.5 ± 15 Ma and a lower intercept of 740 ± 33 Ma (MSWD = 1.6, n=15). The zircons have Eu/Eu* values between 0.32–0.63, La_N/Yb_N ratios between 0.0095–0.3590 and Gd_N/Yb_N between 0.0540–0.2078. This sample was not selected for Hf-isotopic analysis due to presence of numerous apatite inclusions within the oscillatory zoned zircons.

4.2.5 Transitional TTGs and granites of the Eastern Dharwar craton:

PD18-01 is a granite collected at the northern periphery of the Closepet Granite adjacent to the Kaladgi-Badami basin, in the north of the Dharwar Craton. Zircon U–Pb data are quite spread and many are discordant. Eight of the analyses are used to define a discordia line that bounds the young boundary of the array, with an upper intercept of 2613 ± 24 Ma and an imprecise lower intercept of 446 ± 110 Ma (MSWD = 0.97, n=8). The upper intercept is taken as the best estimate of the age of crystallisation of the granite, as the zircons display faint, yet well-defined, oscillatory zoning in CL. The other discordant data are interpreted as an unresolved mix of older inheritance, Phanerozoic Pb loss and possible common Pb. The zircons yielded Eu/Eu* values between 0.5–1.52, La_N/Yb_N ratios between

0.0009–0.6940 and Gd_N/Yb_N ratios between 0.0420–0.4136. Four spots yield initial $^{176}Hf/^{177}Hf$ values of 0.281060–0.281148, with $\epsilon Hf(t)$ values in a narrow range of -0.03 to +2.26.

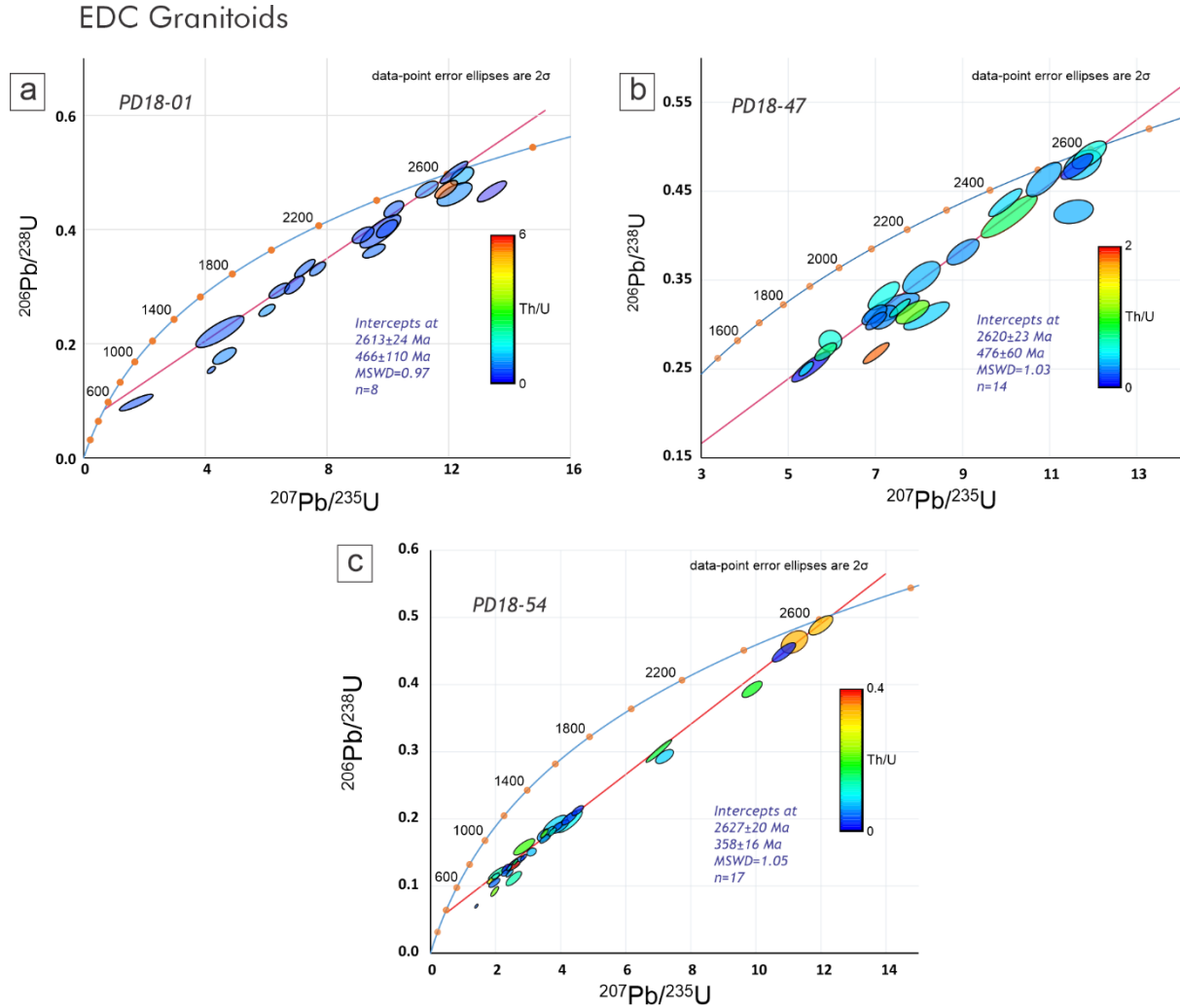


Figure 7 showing the U–Pb data from the zircons from Eastern Dharwar Granitoids.

PD18-47 is the melanosome from a banded TTG gneiss that is cross-cut with aplite veins. It was collected from south of Anantpur town (Figure 1). Fourteen of the youngest analyses define a discordia line with an upper intercept age of 2620 ± 23 Ma and a lower intercept of 476 ± 60 Ma ($MSWD = 1.03$, $n=14$). The upper intercept is taken as the best estimate of the age of crystallisation, which is supported by the recognition that these zircons are elongated and preserve oscillatory zoning in CL. Older discordant grains are interpreted to be a combination of common Pb, Phanerozoic Pb loss and or/inheritance. The zircons yielded Eu/Eu^* values between 0.24–1.94, La_N/Yb_N ratios varied from

0.0036–12.9218 and Gd_N/Yb_N ranged between 0.0081–2.0731. Four spots yield initial $^{176}Hf/^{177}Hf$ values of 0.281098–0.281179 with $\epsilon Hf(t)$ values in a narrow range of +1.46 to +3.66.

PD18-54 was from a uniformly banded migmatitic gneiss on the eastern boundary of the Ramagiri Greenstone Belt. Zircons are mostly discordant with low Th/U ratios < 0.1. Seventeen of the youngest $^{207}Pb/^{206}Pb$ ages are used to define a discordia line with an upper intercept at 2627 ± 20 Ma and a lower intercept of 358 ± 16 Ma (MSWD = 1.05, n=17). An array of highly discordant data spreading from this discordia line towards the origin are interpreted to reflect a second Pb loss phase in the modern environment. We interpret the unusual lower intercept age to also reflect modern isotopic disturbance that has offset all the discordant data towards the origin. The zircons yielded Eu/Eu* values between 0.36–0.87, La_N/Yb_N ratios varied from 0.0278–1.1240 and Gd_N/Yb_N ranged between 0.0448–1.451. Three spots yield initial $^{176}Hf/^{177}Hf$ values of 0.281085–0.281118 with $\epsilon Hf(t)$ values in a narrow range of +2.75 to +4.50.

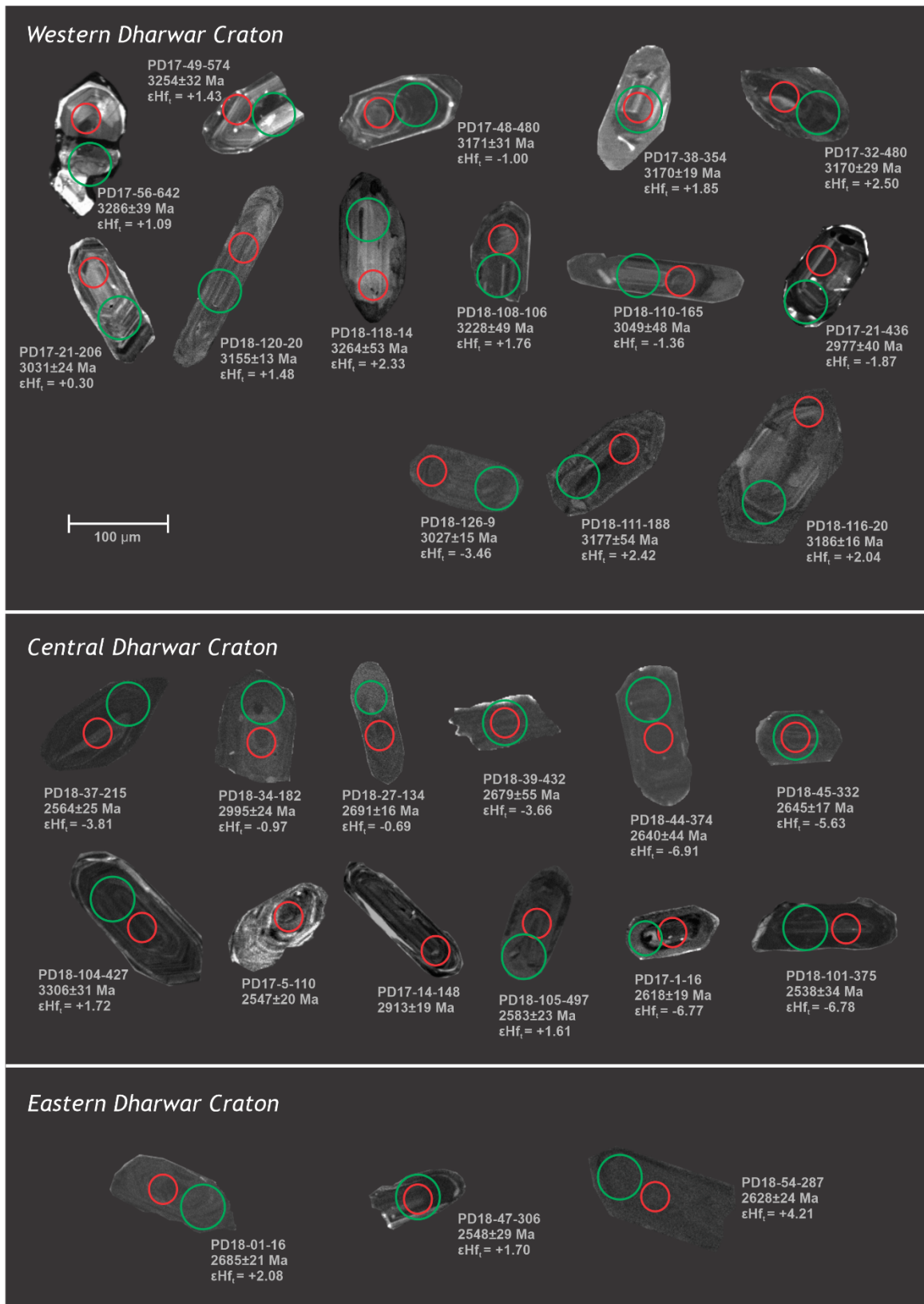


Figure 8: Representative cathodoluminescence (CL) images of zircons from each sample analyzed in this study labelled with constrained U–Pb age and corresponding $\epsilon Hf(t)$ value. The red and green circles represent the ablated portion of the zircon for U–Pb age and Lu–Hf isotopes respectively.

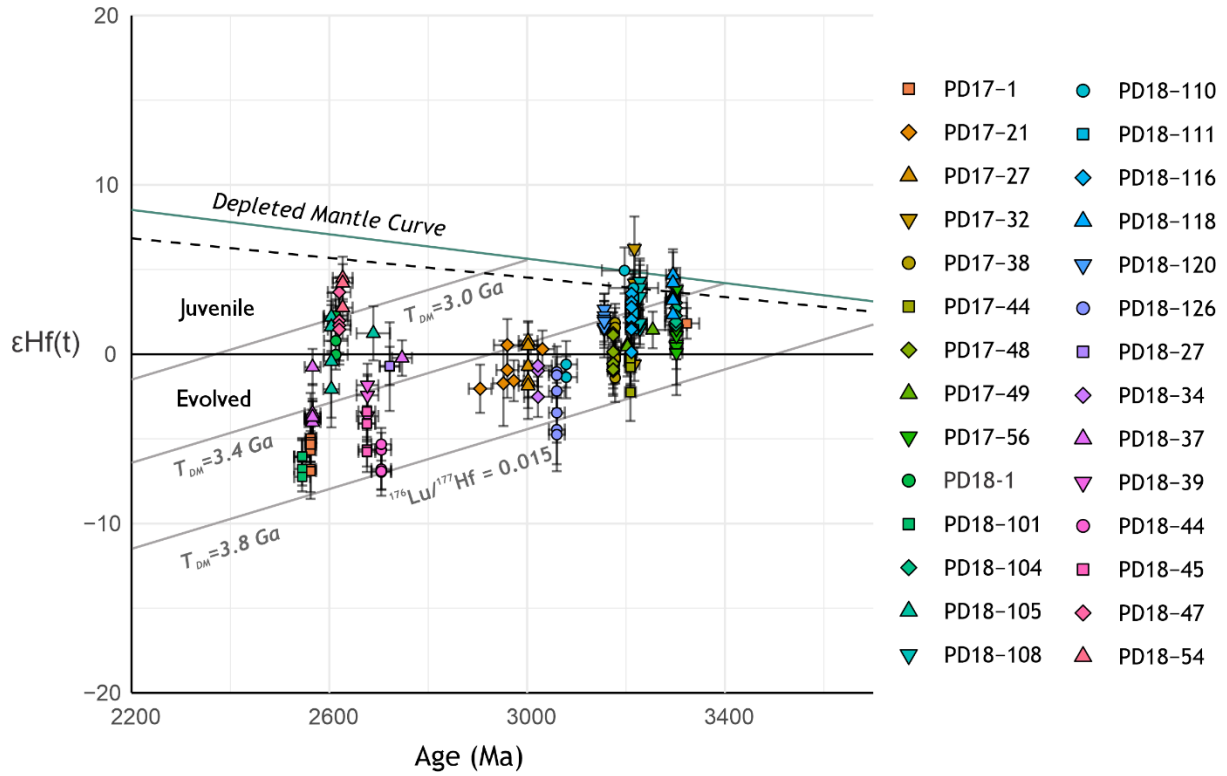


Figure 9: $\epsilon\text{Hf}(t)$ versus interpreted magmatic ages obtained in this study for each sample. The uncertainties plotted are at 2σ . The horizontal line at $\epsilon\text{Hf}(t) = 0$ represents CHUR – Chondritic Uniform Reservoir, representing the bulk Earth. The depleted mantle line is calculated by using the $\epsilon\text{Hf}(t)$ equation with the values: modern $^{176}\text{Hf}/^{177}\text{Hf}_{\text{DM}} = 0.28325$ (Griffin et al., 2000) and modern $^{176}\text{Hf}/^{177}\text{Hf}_{\text{CHUR}} = 0.282785$ (Bouvier et al., 2008). The new crust line has been adapted from Dhuime et al. (2011). The values of crustal model ages (T_{DM}^{C}) and crustal evolution lines were calculated using a ^{176}Lu decay constant of $1.865 \times 10^{-11} \text{ year}^{-1}$ (Scherer et al., 2001), modern $^{176}\text{Hf}/^{177}\text{Hf} = 0.28325$, modern $^{176}\text{Lu}/^{177}\text{Hf} = 0.0384$ (Griffin et al., 2000), and a bulk crust value of $^{176}\text{Lu}/^{177}\text{Hf} = 0.015$ (Griffin et al., 2002).

5. Discussion:

5.1 Magmatic/accretionary episodes of Dharwar craton from zircon U–Pb data:

5.1.1 Western Dharwar Craton

The WDC is regarded as the oldest part of the Dharwar Craton and has a nucleus of TTG gneisses, whose protoliths crystallised at 3.4–3.0 Ga (Lancaster et al., 2015; Peucat et al., 2013). The protolith to sample PD17-56 crystallised at ca. 3300 Ma and forms a part of the oldest kernel of the WDC. The decreasing Th/U ratios with age, shown by zircons from this sample, are interpreted to reflect ancient Pb-loss during ca. 3.2 Ga metamorphism and partial melting. This magmatic and metamorphic event is recorded throughout the WDC, and is recorded in the protolith crystallisation ages of samples PD17-38, PD17-44, PD17-48, PD17-49, PD18-108, PD18-111, PD18-116, PD18-118, PD18-120 that range from ca. 3.28–3.15 Ga. The next tectonic event in the WDC is at about 3.07–3.00 Ga when potassic granites intrude through the area (Jayananda et al., 2006, Chadwick et al., 2007, Chardon et al., 2011), which was observed in the crystallisation ages of the samples PD18-126 and PD17-27 (and

arguably PD18-110). PD17-38 also experienced zircon growth and isotopic disturbance at this time. These two magmatic events are separated by Mesoarchaeon upper-amphibolite facies metamorphism of the Holenarsipur greenstone belt (3.14-3.10 Ga). The WDC is bound on the east by the Chitradurga greenstone belt/shear zone (Chadwick et al., 1981) that preserves two volcano-sedimentary groups—the older Sargur Group (3.22–2.92 Ga) and the younger Dharwar Supergroup (2.68–2.63 Ga) (Hokada et al., 2013, Nasheeth et al., 2015). The crystallisation ages for the magmatic and meta igneous samples within the WDC are reflected in the detrital zircon record of metasandstones within the Chitradurga Greenstone Belt. To the north of the Chitradurga Greenstone Belt, magmatic ages have been reported from felsic volcanics and granites of ca. 2.59 Ga and ca. 2.56 Ga (Sarma et al., 2011; Mohan et al., 2014), demonstrating the presence of K-feldspar rich intrusions in the late Neoarchaeon (Li Shanshan et al., 2018).

5.1.2 Central Dharwar Craton

The recently defined Central Dharwar Craton (CDC) has evolved through two stages of TTG magmatism (3.38–3.23 Ga and 3.15–2.96 Ga), these are followed by the intrusion of transitional TTGs between 2.70–2.56 Ga and sanukitoids at ca. 2.56–2.52 Ga (Chardon et al., 2011, Jayananda et al., 2013a, 2018). To the south, the high-grade gneisses and granulites in Biligiri-Rangan Hills (Figure 1) preserve protolith crystallisation ages 3.36–3.31 Ga, 3.2–3.1 Ga and 2.99–2.97 Ga (Peucat et al., 2013; Ratheesh Kumar et al., 2016). The Biligiri-Rangan Hills area, in particular, preserves a magmatic history very similar to that of the WDC.

Sample PD18-104 represents the earlier phase of TTG accretion in the central block and has experienced a thermal overprint that is coeval with metamorphism in the Biligiri-Rangan Hills region at ca. 3.21–3.16 Ga. Samples PD17-14, PD17-21, PD17-27, along with the vestigial remnant of the basement in the CDC (i.e., PD18-34), represent the second stage of TTG magmatism that may be associated with reworking of the existing crust during the same thermal event. PD18-27, PD18-39, PD18-44, PD18-45, PD18-47, PD18-01 and PD18-54 represent the younger phase of TTG magmatism (Krogstad et al., 1991, Balakrishnan et al., 1999), here ranging between 2.72–2.61 Ga. The Chitradurga Shear Zone acts as the western boundary of CDC and is bound by the Kolar-Kadiri Greenstone Belt on its east. The CDC has experienced three major thermal events at 3.2 Ga, 2.6 Ga and 2.5 Ga hypothesized from textural garnet Lu–Hf isochrons from Biligiri Rangan hills on the southern fringe (Jayananda et al., 2013; Yang and Santosh, 2015). The CDC is made up of older gneisses to the west which have experienced similar histories as the older gneisses in the WDC. Concordia diagram of PD17-32 captures the 3.2 Ga thermal event with samples from southern region of WDC crystallizing following the event. PD18-105 appears to have witnessed the local 2.6 Ga thermal event near the Chitradurga greenstone

belt, emplaced as high-K granitic pluton derived from reworking Archaean basement (Jayananda et al., 2006) and is formed contemporaneously with the transitional TTGs that span between CDC and EDC.

The Closepet Granite batholith cuts older rocks in the CDC, is roughly N-S oriented and stretches for over 500 km. It formed around 2.52–2.50 Ga (Chardon et al., 2011; Jayananda et al., 2013) from deep crustal melting associated with crustal thickening through underplating from mantle-generated magmas (Moyen et al., 2001). The intrusion of this vast batholith caused partial melting of the older gneisses through contact metamorphism along its periphery. PD17-1 and PD18-101 are from the south east periphery of the Closepet Granite and mark this late ca. 2.55 Ga magmatism/thermal event. PD17-37 was sampled from the north western periphery of the Closepet Granite and preserves a similar crystallisation age. PD17-5 is from a K-rich gneiss that may represent a ca. 2.62 Ga vestigial basement to the Closepet Granite.

5.1.3 Eastern Dharwar Craton

The samples PD18-47, PD18-54, PD18-01, were sampled close to the western margin of the EDC, the first two samples from east of the Ramagiri Greenstone Belt (Figure 1). PD18-01 is a granodioritic member of the transitional TTGs that are found in both the CDC (ca. 2670-2600 Ma) and the EDC (ca. 2590-2580 Ma; Jayananda et al 2019). These rocks have been explained as the products of melting of mafic lower crust, or melting of composite sources within an arc setting (Jayananda et al., 2006, Jayananda et al., 2018). These transitional TTGs were preceded by bimodal greenstone volcanism at ca. 2745 – 2670 Ma and form much of the basement of the EDC. The gneisses PD18-47, PD18-54, also crystallised at this time (ca. 2.62 Ga) during this phase of continental growth.

Figure 10 provides a summary of all the meta-igneous suites that were sampled across the Dharwar Craton. The ages have been combined and plotted as a kernel density estimate which has been filtered for <10% discordance. The heights of the peaks are based on the quantity of near-concordant zircons yet broadly summarize the crustal growth episodes across the entire Dharwar Craton. The U–Pb ages of individual samples have been chronologically arranged as per spatial distribution from WDC towards EDC shows distinct episodes of crustal growth during ca 3.4 – 3.2 Ga, 3.2 – 3.0 Ga, 2.7 – 2.6 Ga, 2.6 – 2.55 Ga which also coincides with the major detrital signatures of the corresponding volcano-sedimentary greenstone sequences across the Dharwar Craton.

5.2 Nature and composition of source from Zircon Lu-Hf isotopic data:

Previous craton-wide Nd isotope data from mafic rocks were used to propose that the WDC formed by accretion of juvenile felsic and mafic components between 3.36 and 3.0 Ga, which was followed by dominant mafic crust addition from ca. 2.9 Ga to 2.6 Ga (Dey 2013). Dey (2013), also argued

that the craton experienced major crustal reworking between 2.6–2.5 Ga that was associated with only minor mantle-derived input. Much of this was corroborated by Lancaster et al. (2015), who presented a large study of detrital zircon U–Pb and Lu–Hf isotopic data from throughout the Dharwar Craton. They suggested that significant juvenile crustal extraction occurred between 3.3–2.7 Ga, with cratonization of the WDC occurring around 3.0 Ga and the initiation of continuous crustal extraction as far back as ca. 3.7 Ga, from the existence of detrital zircons of this antiquity.

Guitreau et al. (2017) focussed on the oldest part of the WDC and studied the igneous zircon record of the Gorur gneiss and its surroundings to infer the initiation of crustal extraction. Their data revealed multiple zircon signatures that included inherited pre-3.4 Ga zircons. Although none of our samples are that old, Sample PD17-56 contains ca. 3.3 Ga zircon with varying ϵ_{Hf} values that suggest the presence of older crustal material in the magmatic source, with model ages between 3.63–3.44 Ga. The CDC gneisses of the eastern flank of the Chitradurga Greenschist Belt (PD18-104) also have ca. 3.3 Ga protolith ages and preserve ϵ_{Hf} values that approach chondritic values suggesting the presence of older Palaeoarchaeoan crust. Inherited zircon in sample PD17-01 also suggests the presence of crust of similar age. Our data support earlier studies that conclude that the WDC and CDC share a late Eoarchaeoan–Palaeoarchaeoan history between 3.63–3.3 Ga, with 3.3 Ga magmatism in both sourced from juvenile depleted mantle sources with very short crustal residence times (Dey et al., 2013, Lancaster et al., 2015, Guitreau et al., 2017).

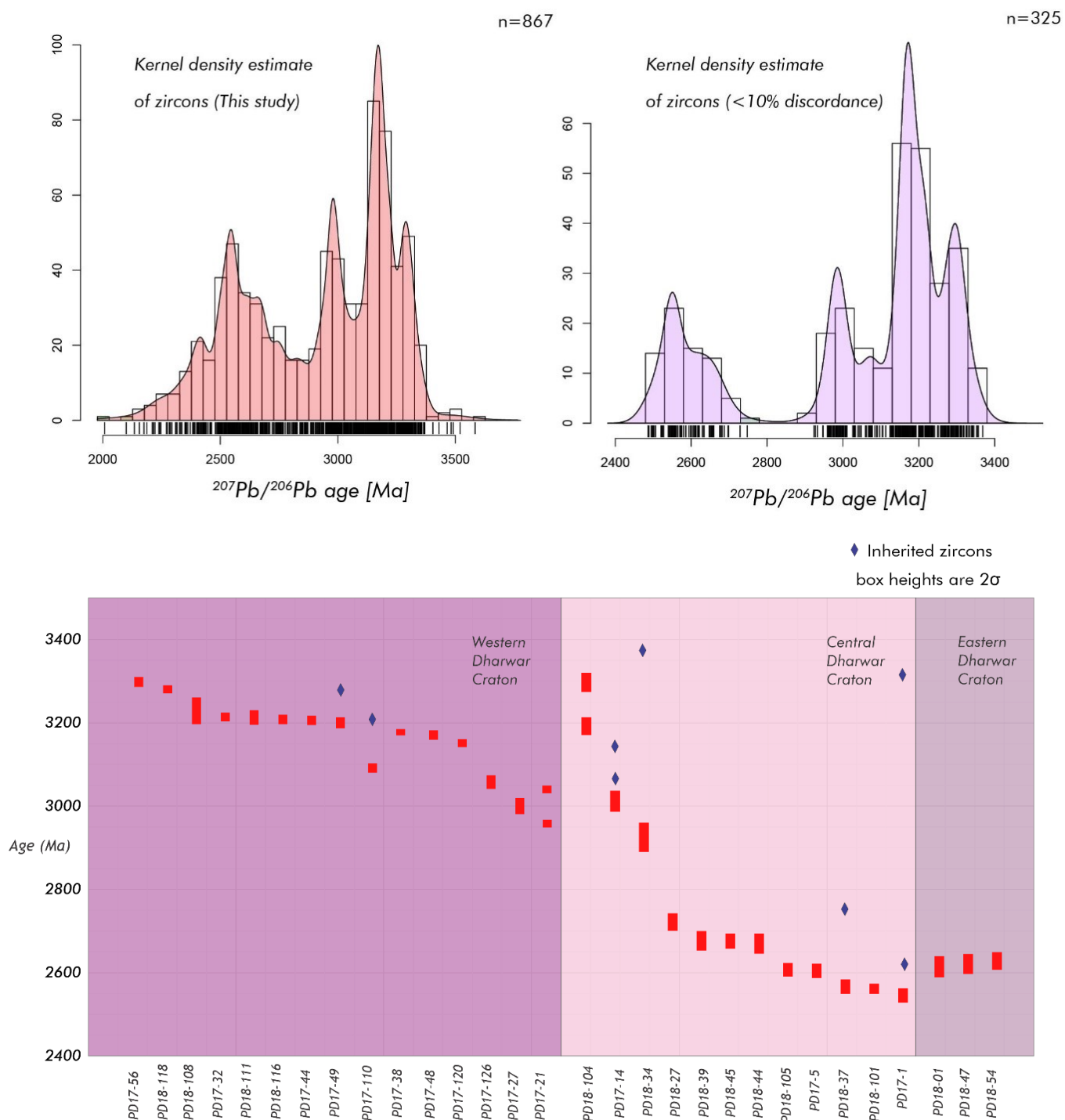


Figure 10: Summary of zircon age data from this study to highlight Archaean crustal growth episodes in the Dharwar craton. The constrained U–Pb ages of each sample along with inherited zircons are plotted chronologically to reflect general trend of crustal growth from Western Dharwar Craton towards the Eastern Dharwar Craton.

Latest Palaeoarchean (3.3–3.2 Ga) rocks from the WDC record a period of depleted-mantle derived magmatism that is best shown in the juvenile hafnium isotopes of sample PD18-118, but also is shown by the variable ϵ_{Hf} values of PD18-108, PD18-116, PD18-111 and PD17-32 that trend towards the depleted mantle.

After 3.2 Ga, $\epsilon_{\text{Hf}}(t)$ values in WDC zircons shift negatively, towards near-chondritic values, which is interpreted to show increasing reworking of pre-existing crust (samples PD17-49, PD17-48, PD17-44, PD18-120 and in inherited zircons from sample PD17-32). Magmatism of this age is coeval with metamorphism in the Biligiri-Rangan Hills (ca. 3.21–3.16 Ga.) (Jayananda et al., 2013a, 2015, Peucat et al., 2013). After a short magmatic gap at ca. 3.15–3.10 Ga, that is represented by metamorphism in Holenarsipur Greenstone Belt at ca. 3.14–3.10 Ga (Peucat et al., 1995), the negative ϵ_{Hf} shift continues in ca. 3.10–2.90 Ga zircon, where WDC and CDC protolith zircon preserve mostly negative values (PD17-27, PD17-21, PD18-126). Previous workers have suggested that this tectonism may be explained by plume triggered near-edge subduction in multiple short-lived oceanic arcs from tectonic overburden of the greenstone volcanism (Guitreau et al., 2017, Jayanada et al., 2008). Alternatively, Amaldev et al. (2016) invoked a hypothesis involving the accretion of the Coorg Block with the WDC at around 3.1 Ga to cause magmatism and metamorphism over this broad timeframe. The exposed basement in the CDC, PD18-34, has slightly negative ϵ_{Hf} values with similar T_{DM} ages as PD18-104 and other coeval samples from WDC implying that it has crystallised from a slightly enriched protolith with a longer crustal residence time, which is consistent with the Paleoarchean inherited grain present in this sample.

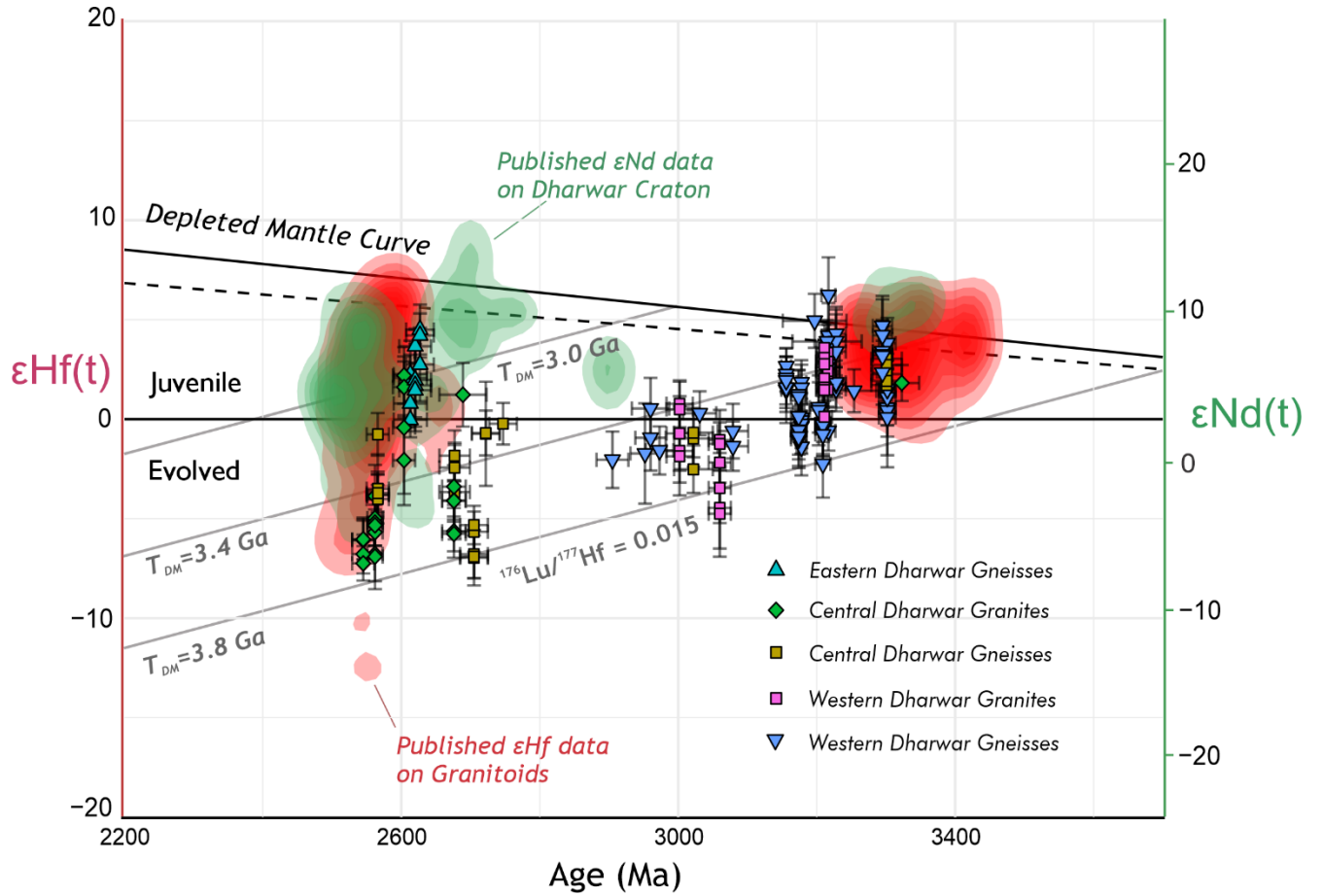


Figure 11: $\epsilon\text{Hf}(t)$ versus interpreted protolith ages obtained in this study grouped into categories. $^{207}\text{Pb}/^{206}\text{Pb}$ zircon U-Pb ages have been used for samples without clear interpreted protolith ages. Previously published $\epsilon\text{Hf}(t)$ values from the granitoids across Dharwar Craton have been plotted as a contour plot in red. Previously published $\epsilon\text{Nd}(t)$ data across the mafic and felsic magmatic suites in Dharwar Craton have been combined and converted into $\epsilon\text{Hf}(t)$ values using the equation, $\epsilon\text{Hf}(t) = [(\epsilon\text{Nd}(t) * 1.36) + 2.89]$ (Vervoort and Blichert-Toft, 1999) and plotted as contours in green. Data for Hf-Nd systematics gathered from Jayananda et al., 2018 (and references therein), 2020, Dey, 2013, J.Y.Wang et al., 2020; Ranjan et al., 2020

Two phases of Neoarchaean volcanism are recorded in the Dharwar Craton. In the WDC, the younger greenstone group in the Chitradurga Greenstone Belt formed at ca. 2.76–2.67 Ga, whereas the supracrustal sequences in the EDC represent the youngest greenstone belts at ca. 2.58–2.54 Ga (Jayananda et al., 2013). The ca. 2.76–2.67 Ga magmatism at the border between the WDC and the CDC preserves notably juvenile Nd isotope values (Dey, 2013), which is in marked contrast to the near contemporaneous felsic magmatism in the CDC around ca. 2.7–2.6 Ga (samples PD18-39, PD18-44, PD18-45; Fig. 13), which preserves ϵHf values down to -8. This bimodal nature suggests a process where depleted mantle sourced mafic volcanism instigated crustal melting and the production of voluminous felsic magmatism. The samples PD18-101, PD17-1, PD18-37 show further evolved signature, with crystallization ages between ca. 2.6–2.55 Ga, in their ϵHf values inferring they could have been reworked from the above terrain through interaction with a plume related to the juvenile calc-alkaline

sanukitoid volcanism at ca. 2.57 - 2.52 Ga resulted in emplacement of anatectic granitic batholiths such as the Closepet granite.

Samples PD18-01, PD18-45, PD18-54 lie with ages between ca. 2.6–2.55 Ga to the east of the Ramagiri Greenstone Belt and its northern equivalent, Hungund-Maski Schist Belt, within the EDC. They preserve juvenile ϵ_{Hf} values, suggesting that they form by melting of the contemporaneous depleted mantle and, therefore, represent a different source from that of granites in both the WDC and CDC. These rocks formed after the transitional TTGs and before the extensive calc-alkaline sanukitoid magmatism seen throughout the Eastern Dharwar Craton. The near depleted mantle values suggest very low crustal contamination, and/or the absence of any older crust in the EDC. The Ramagiri Greenstone Belt marks a well-defined isotopic boundary between the combined older Archaean WDC/CDC and the Neoarchean EDC.

5.3 Depth of melting/crystallization:

Previous work on the depth of crystallisation of the Dharwar Craton granitoids has focussed on whole rock major and trace element compositions (especially heavy rare earth elements—HREE—Y, Nb, Ta and Sr) to deduce the nature and depth of the melts and the residual mineralogy of the source (Jayananda et al., 2018, S. Ranjan et al., 2020., J.-Y. Wang et al., 2020). The elements partition into amphibolite or eclogite residue dependant on the depth of melting, evaluated based on the Sr/Y vs Y plot and $(\text{La/Yb})_{\text{N}}$ vs $(\text{Yb})_{\text{N}}$ diagram (Martin, 1986; Defant and Drummond, 1990; Moyen 2011). The TTGs of the Dharwar Craton have been grouped into low-Al TTGs, which indicate shallow depth melting of a mafic source, and high-Al TTGs with low Y, Yb, high Sr/Y and $(\text{La/Yb})_{\text{N}}$ values suggesting deeper melting with garnet alongside clinopyroxene/hornblende in the residue. Jayananda et al. (2018) suggested that the transitional TTGs around ca. 2.7–2.6 Ga, which bear moderate to high Sr/Y and $(\text{La/Yb})_{\text{N}}$ ratios coupled with variable HREE depletion, formed from partial melting of mafic sources at variable depths. The EDC sanukitoids had moderate to high fractionated REE patterns with varying Y values and Sr/Y ratios that were inadequate to measure the depth of melting. The anatectic granites have moderate to poorly fractionated REE patterns with low Sr/Y ratios and moderate to low $(\text{La/Yb})_{\text{N}}$ vs Yb_{N} , which suggest a lower to mid-crustal source (Jayananda et al., 2018).

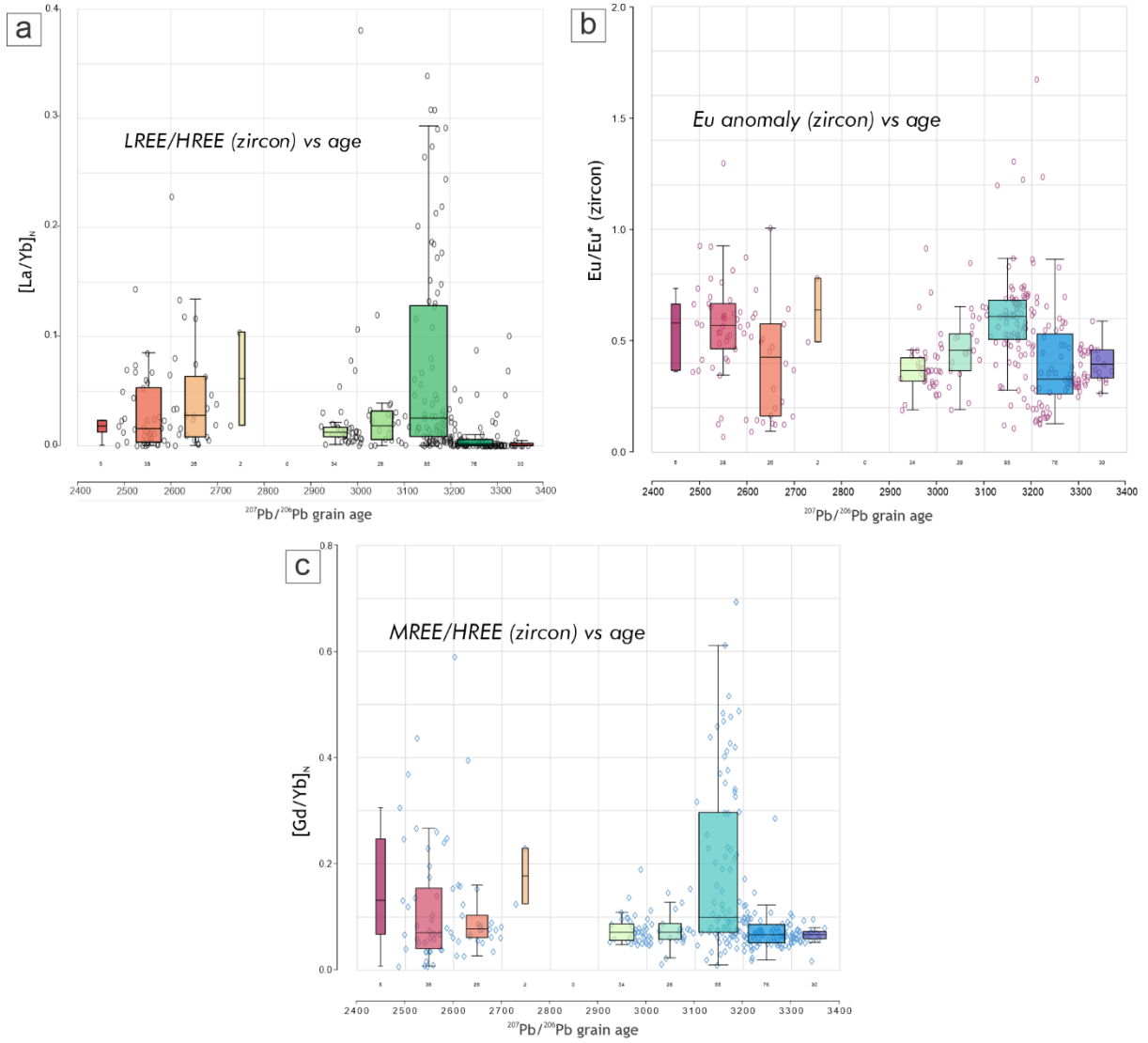


Figure 12: Rare earth element data from >90% concordant zircons of the Dharwar Craton, plotted as various REE ratios vs $^{207}\text{Pb}/^{206}\text{Pb}$ grain age of individual zircons. Boxplots have been drawn at intervals of every 100 Ma and has been centred inside the intervals. The thickness of the boxplot represents the number of analyses within the age interval and is denoted by the number below it. The horizontal line inside the box plot represents the median of the ratios that have been represented within the age bracket. The error bars represent the maximum and minimum values of the box plot distribution with any data points beyond the error bars as potential outliers. The lower and upper bounds of the boxplot is defined by the lower and upper quartile of zircon ratios.

In this study, we have inferred the depth of melting (and/or crystallisation) of the source, based on REE compositions of the zircons that were measured simultaneously during the collection of U–Pb data (McKenzie et al., 2018). Igneous zircons tend to sequester HREEs compared to LREE and MREEs (Speer and Cooper, 1982; Hanchar and van Westrenen, 2007) when the zircon grows in an REE saturated melt and where there is no other REE-compatible phase competing for the elements. The diffusion of REEs in zircon is minimal after crystallisation (Cherniak et al., 1997), hence the zircon

preserves the REE composition it incorporated from the source melt. However, to ensure the reliability of the interpretations, we have only plotted >90% concordant zircon data. Magma sources with melt residual compositions that include HREE phases such as garnet and amphibole influence the MREE/HREE ratios in the analysed zircons (McKenzie et al., 2018). A similar influence will occur with garnet crystallising from a magma as it will compete with zircon for the HREEs. Higher MREE/HREE ratios in zircons represent flatter HREE trends in the $REE_{(N)zircon}$ spider plots that could infer high-pressure assemblages or the presence of garnet or amphibole in the source melt, or in the magma, which signifies relatively deep magma generation and/or crystallisation where garnet is stable.

The REE compositions from zircons have been collectively plotted as LREE/HREE, MREE/HREE and Eu/Eu^* with time, to infer crustal thickness and depth of crystallisation/crustal differentiation (McKenzie et al., 2018). The zircons were selected using a near-concordance filter as a correlation between degree of concordance and REE composition was seen, suggesting REE open system behaviour in when Pb is lost. The data are illustrated as La_N/Yb_N versus age to represent the LREE/HREE ratio and Gd_N/Yb_N versus age, to focus on the MREE/HREE ratio. Eu/Eu^* has been calculated as $Eu/Eu^* = Eu_N / \sqrt{Sm_N * Gd_N}$ and is used to infer the presence or absence of plagioclase crystallisation during deep crustal differentiation. Boxplots are used to look at the trends within the data.

Europium anomalies vary considerably through the Archaean, but are consistently negative ($Eu/Eu^* < 1$), indicating the common presence of plagioclase in the source, or crystallising early in the magma. There is a notable decrease in the anomaly (Eu/Eu^* rises towards 1) from the Palaeoarchean to 3.2–3.1 Ga, which can be interpreted as Eu-saturation occurring before plagioclase/feldspar fractionation which can happen during a non-equilibrium process such as metamorphism (Trail et al., 2012).

The La_N/Yb_N ratios show that there is an increase in the average LREE/HREE ratio around 2.6 Ga – 2.7 Ga and again after 3.15Ga. According to McKenzie et al., 2018 the La_N/Yb_N ratios trend along average crustal thickness which could be inferred as potential crustal thickening events around 3.15–3.2 Ga and 2.6–2.7 Ga. The $(Gd/Yb)_N$ versus age plot shows higher ratios towards 2.6–2.7 Ga and 3.1–3.2 Ga which agree with the inferences from LREE/HREE ratios. The higher Gd_N/Yb_N ratios (> 0.1) represent deeper crystallisation of zircons alongside deep crystallising minerals such as garnet and amphibole which accurately describe the formation ages of the TTG gneisses in the Dharwar.

5.4 Comparison with other Archaean terranes: implications for global Archaean crustal processes

The Archaean crustal record of the Dharwar Craton has been correlated with other Archaean domains like Bundelkhand Craton in central India, North China Craton, Pilbara and Yilgarn Cratons in Australia, Kaapval and Tanzania Cratons in southern Africa, Antongil Craton in Madagascar, Superior craton and Rae family of cratons in North America (Pehrsson et al 2013, Lancaster et al., 2015, Jayananda et al., 2018). The above Archaean cratons comprise similar lithologies bearing TTGs, volcano-sedimentary greenstone sequences and Archaean progeny granitoids such as anatectic granites and calc-alkaline granitoids (Cawood et al., 2018, Nebel et al., 2018).

The crust building events in the Dharwar Cratons at ca 3.4 – 3.2 Ga have been involved with crustal components from upto ca. 3.8 Ga (Lancaster et al., 2015). This coincides and correlates with older TTG crustal building events in various Archaean cratons such as Bundelkhand craton at ca. 3.33 – 3.27 Ga; Kaapval craton at ca. 3.45 Ga, 3.32 Ga, 2.9 Ga; Pilbara craton at ca 3.5 – 3.2 Ga; Tanzania craton at ca 3.2 – 3.14 Ga; Antongil Craton at ca 3.32 – 3.18 Ga respectively. (Lancaster et al., 2015, Jayananda et al., 2018 and references therein)

The paleoarchaeo to mesoarchaeo crustal growth in Dharwar Craton could have experienced transitional type tectonics from asymmetrical drip-type gravitational sinking, due to tectonic overburden of the overlying greenstone volcanism, as proposed in Nebel et al., 2018. The partial melting of the sinking lithosphere resulted in an accretion of transitional TTG type melts crystallizing in the CDC around ca 2.7 – 2.6 Ga. This coincides with documented crustal growth episodes during 2.7 Ga in Bundelkhand craton; ca. 2.72 – 2.6 Ga in North China Craton; ca. 2.75 – 2.6 Ga in Kaapval Craton; ca 2.72 – 2.63 Ga in the Yilgarn Craton, ca 2.72 – 2.64 Ga in the Tanzania Craton. (Jayananda et al., 2018 and references therein)

The further differentiation of the partial melted delaminated crust evolved to create Archaean progeny granites such as the Closepet Granite in the CDC at ca 2.55 Ga. In WDC, the sinking/subducting plate was proposed to have undergone shallow – mid-crustal partial melting (Jayananda 2018) which resulted in the formation of granitic batholiths such as the Shimoga and Chikamagalur granite at ca. 3.0 Ga which could be associated with the Holenarsipur greenstone volcanism around 3.1 Ga.

The deep-sinking crustal material has been proposed to cause aesthenosphere upwelling resulting in juvenile high potassic calc-alkaline sanukitoid melts that were preceded by the transitional type TTG melts. (Jayananda et al., 2018, 2020). The sanukitoid volcanism in the EDC has been proposed to have occurred in an episode ca. 2.57 – 2.52 Ga, as part of bimodal volcanism, preceded by the

crystallization of transitional type TTG gneisses during 2.7 – 2.6 Ga (J.Y. Wang et al., 2020). Similar bimodal volcanic episode has been reported from the Woodburn Lake group in the Rae Craton in North America, associated with the formation of the neoarchaeon Rae greenstone belt during 2.72 – 2.65 Ga (Pehrsson et al 2013). Correlations with accretionary episodes from other Archean cratons include ca. 2.57 – 2.54 Ga in Bundelkhand Craton; ca. 2.55 – 2.5 Ga in North China Craton; ca. 2.61 – 2.59 Ga in central Limpopo belt. (Lancaster et al., 2015, Jayananda et al., 2018 and references therein)

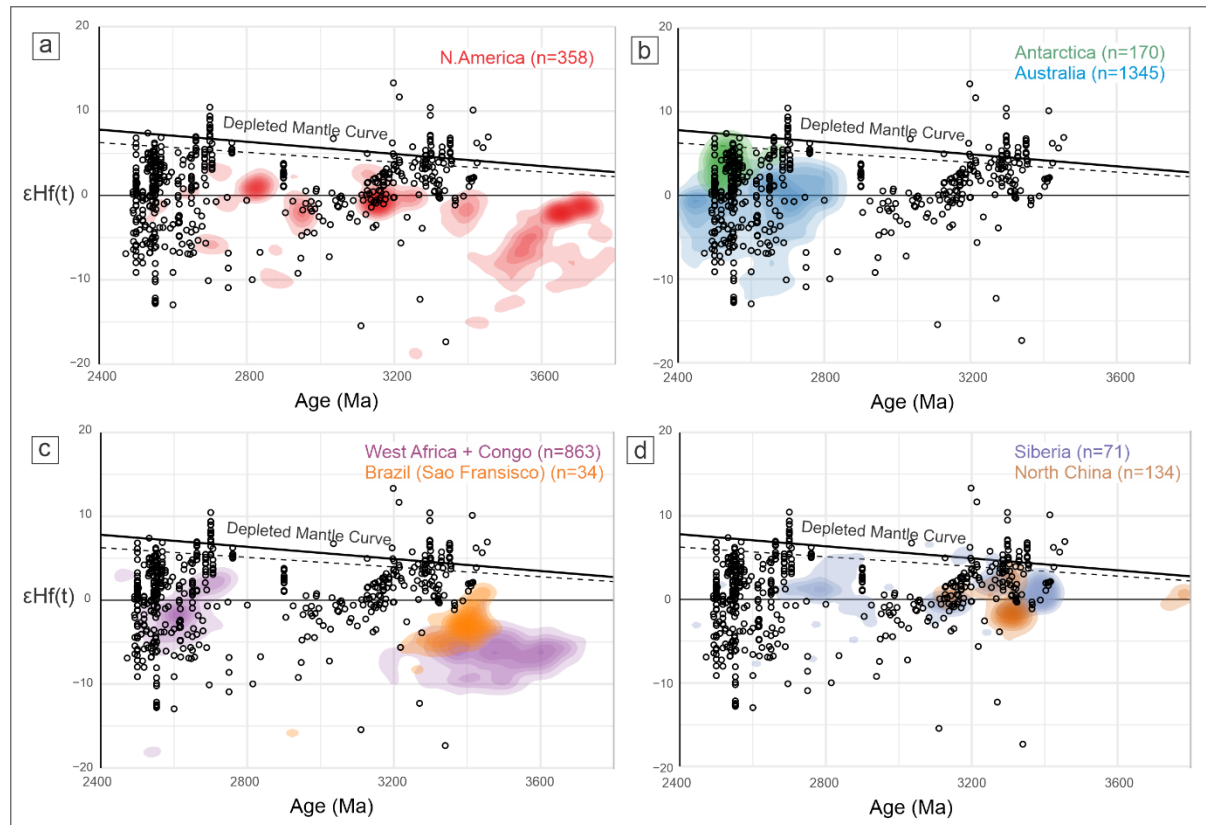


Figure 13: The $\epsilon\text{Hf}(t)$ values of the Dharwar Craton represented in circles (data from this study and including published Nd-Hf isotopic data) plotted against various Archean domains across the world using the global zircon database published in Spencer et al., 2017 to test out the Nunavutia hypothesis.

The crustal evolution of the Dharwar Craton plotted in $\epsilon\text{Hf}(t)$ space has been compared with the crustal evolution histories of other major Archean cratons mainly discussed in Pehrsson et al. (2013) to belong the clan of Nunavutia, a major continental amalgamation proposed to have existed between ca. 2.55 – 2.45 Ga, consisting mainly the cratons of Rae, Sask, Siberia, West Africa, Congo, Sao Fransisco, Mawson, Gawler, Siberia and North China Cratons. We have used a global zircon database from Roberts and Spencer, (2015) to compare and test the Nunavutia hypothesis. We have observed that the younger CDC and EDC correlate with the Archean cratons in North America (Rae + Sask), Australia (Gawler), Antarctica (Mawson), West African cratons and partially correlate with the Siberian craton.

The older Mesoarchean components in WDC and CDC correlate with North America, Siberia and North China cratons and we have deemed the Nunavutia hypothesis inconclusive due to lack of enough data points from the Dharwar Craton around the period of proposed existence of Nunavutia, between ca. 2.54 – 2.45 Ga used for the correlation.

6. Conclusions:

- 1) The Dharwar Craton has evolved through various phases including juvenile accretion of TTG suites at ca. 3.4– 3.2 Ga with crustal components extracted up to ca 3.8 Ga in the WDC. Continuous reworking of the existing ancient crust towards the east through localised island arc-like tectonic activity until ca. 3.0 Ga leading to the formation of potassic felsic plutons and younger TTG domains. The interaction of these younger domains with greenstone volcanism at 2.7 – 2.6 Ga created transitional type tectonics creating transitional type TTG domains that are prevalent to the east of CDC. This was followed by extensive juvenile magmatism at ca. 2.57 – 2.52 Ga in the EDC which could have been the thermal trigger to cause further differentiation/crustal reworking in the CDC to create Archaean progeny granites such as the Closepet granite batholith at 2.55 Ga.
- 2) WDC and CDC appear to have evolved contemporaneously until 3.0 Ga which was evident with similar aged 3.4 Ga zircon bearing gneisses in both domains and presence of inherited zircon at 3.3 Ga in Closepet granite. The thermal disturbance at 3.0 Ga observed in the zircon U–Pb could be attributed to the formation of localised high potassic plutons in WDC and younger TTG domains that form the basement of the CDC. The CDC experienced further recycling until 2.55 Ga attributed to bimodal volcanism which accreted transitional type TTGs at ca. 2.7 – 2.6 Ga and juvenile magmatism in the EDC at ca. 2.58 – 2.52 Ga.
- 3) The $\epsilon\text{Hf}(t)$ dataset from this study, combined with published $\epsilon\text{Hf}(t)$ values on granitoids and $\epsilon\text{Nd}(t)$ values from greenstone belts and associated granitoids show the influence of juvenile greenstone magmas around at ca. 2.7 – 2.6 Ga on reworking of ancient existing crust to produce the transitional TTG around the same time period.
- 4) Combined Eu/Eu^* , LREE/HREE , MREE/HREE ratios from analysed zircons across the Dharwar craton have been used as markers to infer timing of crustal growth/thickening events at ca. 3.2 Ga and 2.7 – 2.6 Ga.
- 5) The Ramagiri greenstone belt has been proposed to be the isotopic boundary separating the crustal reworked transitional type TTG suites and Archaean progeny granites in the CDC from juvenile sanukitoid magmatism on the EDC.

- 6) The documented crustal accretion events in the Dharwar craton can be compared to major cratons in the world including Bundelkhand Craton in central India, North China Craton, Pilbara and Yilgarn Cratons in Australia, Kaapval and Tanzania Cratons in southern Africa, Antongil Craton in Madagascar, Superior craton and Rae family of cratons in North America. These cratons record extensive crustal growth and major accretionary episodes equivalent to the times of crustal growth in the Dharwar Craton around ca. 3.45– 3.3 Ga, 3.23 - 3.15 Ga, 3.0 – 2.9 Ga and 2.7 – 2.55 Ga.
- 7) The Dharwar Craton lacks enough data points in $\epsilon\text{Hf}(t)$ space around the proposed time of existence of the Nunavutia amalgamation of cratons, hence the correlation with the global zircon database Spencer et al. (2017) has been regarded inconclusive and would have to be tested using an updated database.

7. Acknowledgements:

We acknowledge the support of Dr David Kelsey and Dr Sarah Gilbert for their support at Adelaide Microscopy in the acquisition of the zircon cathode-luminescence imaging (CL) and U–Pb and REE data using LA–ICPMS respectively during 2017 and 2018. Dr. Morgan Blades and Dr. Justin Payne are acknowledged for their help obtaining Lu–Hf data from the zircons. The Petrology lab team at Indian Institute of Science, India are acknowledged for their assistance during fieldwork logistics and sample preparation. Mr. Kiran Sasidharan and Mr. Thamam Mubarish are acknowledged for the assistance in fieldwork. Pavan Katuru is supported during his PhD by the scholarship provided by the University of Adelaide.

8. Appendix:

The zircon U–Pb data are provided in Appendix 2.1. The zircon REE concentrations are provided in Appendix 2.2. The Lu–Hf isotopic data from the zircons analysed in this study are provided in Appendix 2.3.

9. References:

- 1) Amaldev, T., M. Santosh, L. Tang, K. R. Baiju, T. Tsunogae and M. Satyanarayanan (2016). "MesoArchaean convergent margin processes and crustal evolution: Petrologic, geochemical and zircon U–Pb and Lu–Hf data from the Mercara Suture Zone, southern India." *Gondwana Research* 37(Supplement C): 182-204.
- 2) Anand, R., S. Balakrishnan, E. Koojiman and K. Mezger (2014). "Neoproterozoic crustal growth by accretionary processes: Evidence from combined zircon–titanite U–Pb isotope studies on granitoid rocks around the Hutti greenstone belt, eastern Dharwar Craton, India." *Journal of Asian Earth Sciences* 79: 72-85.

- 3) Balakrishnan, S., G. Hanson and V. Rajamani (1991). "Pb and Nd isotope constraints on the origin of high Mg and tholeiitic amphibolites, Kolar schist belt, South India." *Contributions to Mineralogy and Petrology* 107(3): 279-292.
- 4) Bouvier, A., J. D. Vervoort and P. J. Patchett (2008). "The Lu–Hf and Sm–Nd isotopic composition of CHUR: constraints from unequilibrated chondrites and implications for the bulk composition of terrestrial planets." *Earth and Planetary Science Letters* 273(1-2): 48-57.
- 5) Boynton, W. V. (1984). Cosmochemistry of the rare earth elements: meteorite studies. In *Developments in geochemistry* (Vol. 2, pp. 63-114): Elsevier.
- 6) Brenner, A.R., Fu, R.R., Evans, D.A.D., Smirnov, A.V., Trubko, R., Rose, I.R., 2020. Paleomagnetic evidence for modern-like plate motion velocities at 3.2 Ga. *Sci Adv* 6, eaaz8670.
- 7) Cawood, P.A., Hawkesworth, C.J., Pisarevsky, S.A., Dhuime, B., Capitanio, F.A., Nebel, O., 2018. Geological archive of the onset of plate tectonics. *Phil. Trans. Royal Soc. A* 376, 20170405.
- 8) Chadwick, B., V. N. Vasudev and G. V. Hegde (2000). "The Dharwar craton, southern India, interpreted as the result of Late Archaean oblique convergence." *Precambrian Research* 99: 91-111.
- 9) Chadwick, B. R., M.; Viswanatha, M. N. (1981). "Structural and Metamorphic Relations between Sargur and Dharwar Supracrustal Rocks and Peninsular Gneiss in Central Karnataka." *Journal of Geological Society of India* 22(12).
- 10) Chadwick, B. V., V; Hegde, G; Nutman, A (2007). "Structure and SHRIMP U/Pb zircon ages of granites adjacent to the Chitradurga Schist belt: implications for neoproterozoic convergence in the Dharwar Craton, Southern India." *Journal of the Geological Society of India* 69 (1): 5-24.
- 11) Chardon, D. and M. Jayananda (2008). "Three-dimensional field perspective on deformation, flow, and growth of the lower continental crust (Dharwar craton, India)." *Tectonics* 27(TC1014).
- 12) Chardon, D., M. Jayananda and J.-J. Peucat (2011). "Lateral constrictional flow of hot orogenic crust: Insights from the NeoArchaean of south India, geological and geophysical implications for orogenic plateaux." *Geochemistry, Geophysics, Geosystems* 12(2): n/a-n/a.
- 13) Cherniak, D.J., Hanchar, J.M., and Watson, E.B., 1997, Rare-earth diffusion in zircon: *Chemical Geology*, v. 134, p. 289–301, [https://doi.org/10.1016/S0009-2541\(96\)00098-8](https://doi.org/10.1016/S0009-2541(96)00098-8).
- 14) Condie, K.C., 2014. Growth of continental crust: a balance between preservation and recycling. *Mineral. Mag.* 78, 623–637.
- 15) Dhuime, B., Hawkesworth, C.J., Cawood, P.A., Storey, C.D., 2012. A change in the geodynamics of continental growth 3 billion years ago. *Science* 335, 1334e1336.
- 16) Dey, S. (2013). "Evolution of Archaean crust in the Dharwar craton: The Nd isotope record." *Precambrian Research* 227: 227-246.
- 17) Griffin, W., N. Pearson, E. Belousova, S. v. Jackson, E. Van Acherbergh, S. Y. O'Reilly and S. Shee (2000). "The Hf isotope composition of cratonic mantle: LAM-MC-ICPMS analysis of zircon megacrysts in kimberlites." *Geochimica et Cosmochimica Acta* 64(1): 133-147.
- 18) Griffin, W. L., X. Wang, S. E. Jackson, N. J. Pearson, S. Y. O'Reilly, X. Xu and X. Zhou (2002). "Zircon chemistry and magma mixing, SE China: In-situ analysis of Hf isotopes, Tonglu and Pingtan igneous complexes." *Lithos* 61(3): 237-269.
- 19) Guitreau, M., S. B. Mukasa, L. Loudin and S. Krishnan (2017). "New constraints on the early formation of the Western Dharwar Craton (India) from igneous zircon U–Pb and Lu–Hf isotopes." *Precambrian Research* 302: 33-49.
- 20) Hanchar, J.M., and van Westrenen, W., 2007, Rare earth element behavior in zircon-melt systems: *Elements*, v. 3, p. 37-42, <https://doi.org/10.2113/gselements.3.1.37>.
- 21) Hokada, T., K. Horie, M. Satish-Kumar, Y. Ueno, A. Nasheeth, K. Mishima and K. Shiraishi (2013). "An appraisal of Archaean supracrustal sequences in Chitradurga Schist Belt, Western Dharwar Craton, Southern India." *Precambrian Research* 227: 99-119.
- 22) Jackson, S. E., N. J. Pearson, W. L. Griffin and E. A. Belousova (2004). "The application of laser ablation-inductively coupled plasma-mass spectrometry to in situ U–Pb zircon geochronology." *Chemical Geology* 211(1): 47-69.

- 23) Jayananda, M., D. Chardon, J. J. Peucat and R. Capdevila (2006). "2.61 Ga potassic granites and crustal reworking in the western Dharwar craton, southern India: Tectonic, geochronologic and geochemical constraints." *Precambrian Research* 150: 1-26.
- 24) Jayananda, M., D. Chardon, J. J. Peucat, Tushipokla and C. M. Fanning (2015). "Paleo- to MesoArchaean TTG accretion and continental growth in the western Dharwar craton, Southern India: Constraints from SHRIMP U–Pb zircon geochronology, whole-rock geochemistry and Nd–Sr isotopes." *Precambrian Research* 268: 295-322.
- 25) Chardon, Dominique & Jayananda, Mudlappa & Chetty, talari & Peucat, Jean-Jacques. (2008). Precambrian continental strain and shear zone patterns: South Indian case. *Journal of Geophysical Research*. 113. 10.1029/2007JB005299.
- 26) Janoušek, V., Farrow, C. M. & Erban, V. 2006. Interpretation of whole-rock geochemical data in igneous geochemistry: introducing Geochemical Data Toolkit (GCDkit). *Journal of Petrology* 47(6):1255-1259
- 27) Jayananda, M., J. F. Moyen, H. Martin, J. J. Peucat, B. Auvray and B. Mahabaleswar (2000). "Late Archaean (2550–2520 Ma) juvenile magmatism in the Eastern Dharwar craton, southern India: constraints from geochronology, Nd–Sr isotopes and whole rock geochemistry." *Precambrian Research* 99: 225-254.
- 28) Jayananda, M., J. J. Peucat, D. Chardon, B. K. Rao, C. M. Fanning and F. Corfu (2013). "NeoArchaean greenstone volcanism and continental growth, Dharwar craton, southern India: Constraints from SIMS U–Pb zircon geochronology and Nd isotopes." *Precambrian Research* 227(Supplement C): 55-76.
- 29) Jayananda, M. T., Y., T. Miyazaki, R. V. Gireesh, K.-u. Kapfo, Tushipokla, H. Hiroshi and T. Kano (2013). "Geochronological constraints on Meso- and NeoArchaean regional metamorphism and magmatism in the Dharwar craton, southern India." *Journal of Asian Earth Sciences* 78: 18-38.
- 30) Wang, J.-Y., M. Santosh, M. Jayananda and K. R. Aadhiseshan (2020). "Bimodal magmatism in the Eastern Dharwar Craton, southern India: Implications for Neoproterozoic crustal evolution." *Lithos* 354-355: 105336.
- 31) Jochum, K. P., U. Weis, B. Stoll, D. Kuzmin, Q. Yang, I. Raczek, D. E. Jacob, A. Stracke, K. Birbaum, D. A. Frick, D. Günther and J. Enzweiler (2011). "Determination of Reference Values for NIST SRM 610–617 Glasses Following ISO Guidelines." *Geostandards and Geoanalytical Research* 35(4): 397-429.
- 32) Krogstad, E. J., G. N. Hanson and V. Rajamani (1991). "U–Pb Ages of Zircon and Sphene for Two Gneiss Terranes Adjacent to the Kolar Schist Belt, South India: Evidence for Separate Crustal Evolution Histories." *The Journal of Geology* 99(6): 801-815.
- 33) Lancaster, P. J., S. Dey, C. D. Storey, A. Mitra and R. K. Bhunia (2015). "Contrasting crustal evolution processes in the Dharwar craton: Insights from detrital zircon U–Pb and Hf isotopes." *Gondwana Research* 28(4): 1361-1372.
- 34) Li, S.-S., M. Santosh and R. M. Palin (2018). "Metamorphism during the Archean–Paleoproterozoic transition associated with microblock amalgamation in the Dharwar Craton, India." *Journal of Petrology*: epy102-egy102.
- 35) Ludwig, K. (2003). "User's manual for IsoPlot 3.0." A Geochronological Toolkit for Microsoft Excel 71.
- 36) M, Jayandanda., Santosh. M and Adhisekharan. K.R (2018). "Formation of Archaean (3600–2500 Ma) continental crust in the Dharwar Craton, southern India." *Earth-Science Reviews* 181: 12-42.
- 37) Maibam, B., A. Gerdes and J. N. Goswami (2016). "U–Pb and Hf isotope records in detrital and magmatic zircon from eastern and western Dharwar craton, southern India: Evidence for coeval Archaean crustal evolution." *Precambrian Research* 275: 496-512.
- 38) Manikyamba, C., S. Ganguly, M. Santosh and K. S. V. Subramanyam (2017). "Volcano-sedimentary and metallogenic records of the Dharwar greenstone terranes, India: Window to Archaean plate tectonics, continent growth, and mineral endowment." *Gondwana Research* 50: 38-66.
- 39) Manikyamba, C. and R. Kerrich (2012). "Eastern Dharwar Craton, India: Continental lithosphere growth by accretion of diverse plume and arc terranes." *Geoscience Frontiers* 3(3): 225-240.
- 40) McKenzie, N. R., A. J. Smye, V. S. Hegde and D. F. Stockli (2018). "Continental growth histories revealed by detrital zircon trace elements: A case study from India." *Geology* 46(3): 275-278.
- 41) Moyen, J. F., H. Martin, M. Jayananda and B. Auvray (2003). "Late Archaean granites: a typology based on the Dharwar Craton (India)." *Precambrian Research* 127(1): 103-123.

- 42) Moyen, J. F., Martin, H., & Jayananda, M. (2001). Multi-element geochemical modelling of crust–mantle interactions during late-Archaean crustal growth: the Closepet granite (South India). *Precambrian Research*, 112(1-2), 87-105.
- 43) O. Nebel, F. A. C., J.-F. Moyen, R. F. Weinberg, F. Clos, Y. J. Nebel-Jacobsen and P. A. Cawood (2018). "When crust comes of age: on the chemical evolution of Archaean, felsic continental crust by crustal drip tectonics." *Philosophical Transactions of the Royal Society A* 376: 20180103.
- 44) Nasheeth, A., T. Okudaira, K. Horie, T. Hokada and M. Satish–Kumar (2015). "SHRIMP U–Pb zircon ages of granitoids adjacent to Chitradurga shear zone, Dharwar craton, South India and its tectonic implications." *Journal of Mineralogical and Petrological Sciences* 110(5): 224-234.
- 45) Norman, M. D., W. L. Griffin, N. J. Pearson, M. O. Garcia and S. Y. O'Reilly (1998). "Quantitative analysis of trace element abundances in glasses and minerals: A comparison of laser ablation inductively coupled plasma mass spectrometry, solution inductively coupled plasma mass spectrometry, proton microprobe and electron microprobe data." *Journal of Analytical Atomic Spectrometry* 13(5): 477-482.
- 46) NORMAN, M. D., N. J. PEARSON, A. SHARMA and W. L. GRIFFIN (1996). "QUANTITATIVE ANALYSIS OF TRACE ELEMENTS IN GEOLOGICAL MATERIALS BY LASER ABLATION ICPMS: INSTRUMENTAL OPERATING CONDITIONS AND CALIBRATION VALUES OF NIST GLASSES." *Geostandards Newsletter* 20(2): 247-261.
- 47) Paton, C., J. Hellstrom, B. Paul, J. Woodhead and J. Hergt (2011). "Lolite: Freeware for the visualisation and processing of mass spectrometric data." *Journal of Analytical Atomic Spectrometry* 26(12): 2508-2518.
- 48) Payne, J. L., N. J. Pearson, K. J. Grant and G. P. Halverson (2013). "Reassessment of relative oxide formation rates and molecular interferences on in situ lutetium–hafnium analysis with laser ablation MC-ICP-MS." *Journal of Analytical Atomic Spectrometry* 28(7): 1068-1079.
- 49) Pehrsson, S. J., R. G. Berman, B. Eglington and R. Rainbird (2013). "Two Neoproterozoic supercontinents revisited: The case for a Rae family of cratons." *Precambrian Research* 232: 27-43.
- 50) Peucat, J.-J., M. Jayananda, D. Chardon, R. Capdevila, C. M. Fanning and J.-L. Paquette (2013). "The lower crust of the Dharwar Craton, Southern India: Patchwork of Archaean granulitic domains." *Precambrian Research* 227(Supplement C): 4-28.
- 51) Peucat, J. J., H. Bouhallier, C. M. Fanning, and M. Jayananda (1995), Age of the Holenarsipur greenstone belt, relationships with the surrounding gneisses (Karnataka, South India), *J. Geol.*, 103, 701 – 710.
- 52) Peucat, J.-J.; Mahabaleswar, B.; and Jayananda, M., 1993, Age of younger tonalitic magmatism and granulitic metamorphism in the south Indian transition zone (Krishnagiri area): comparison with older Peninsular gneisses from the Gorur-Hassan area: *Jour. Metamor. Geol.*, v. 11, p. 879-888.
- 53) Ramakrishnan, M., R. Vaidyanadhan and G. S. o. India (2008). *Geology of India*, Geological Society of India.
- 54) Ranjan, S., D. Upadhyay, K. Abhinay and C. Srikanthappa (2020). "Paleoarchean and Neoproterozoic Tonalite–Trondhjemite–Granodiorite (TTG) and granite magmatism in the Western Dharwar Craton, southern India: Implications for Archean continental growth and geodynamics." *Precambrian Research* 340.
- 55) Roberts, Nick M. W. and Christopher J. Spencer. "The Zircon Archive of Continent Formation through Time." *Geological Society, London, Special Publications* 389, no. 1 (2015): 197-225. <http://dx.doi.org/10.1144/sp389.14>.
- 56) R.T, Ratheesh Kumar, M. Santosh, Qiong-Yan Yang, Ishwar-Kumar C, Neng-Song Chen, and Krishnan Sajeev. "Archean Tectonics and Crustal Evolution of the Biligiri Rangan Block, Southern India." *Precambrian Research* 275 (01/23 2016): 406–28. <http://dx.doi.org/10.1016/j.precamres.2016.01.022>.
- 57) Santosh, M. and S.-S. Li (2018). "Anorthosites from an Archaean continental arc in the Dharwar Craton, southern India: Implications for terrane assembly and cratonization." *Precambrian Research* 308: 126-147.
- 58) Srinivasa Sarma, D. M., N J, E. Belusova, M. Ram Mohan and I. R. Fletcher (2012). "Detrital zircon U–Pb ages and Hf-isotope systematics from the Gadag Greenstone Belt: Archean crustal growth in the western Dharwar Craton, India." *Gondwana Research* 22: 843-854.
- 59) Sarma, D., I. Fletcher, B. Rasmussen, N. McNaughton, R. Mekala and D. Groves (2011). "Archaean gold mineralization synchronous with late cratonization of the Western Dharwar Craton, India: 2.52 Ga U–Pb ages of hydrothermal monazite and xenotime in gold deposits." *Mineralium Deposita* 46: 273-288.

- 60) Scherer, E., C. Münker and K. Mezger (2001). "Calibration of the lutetium-hafnium clock." *Science* 293(5530): 683-687.
- 61) Sláma, J., J. Košler, D. J. Condon, J. L. Crowley, A. Gerdes, J. M. Hanchar, M. S. A. Horstwood, G. A. Morris, L. Nasdala, N. Norberg, U. Schaltegger, B. Schoene, M. N. Tubrett and M. J. Whitehouse (2008). "Plešovice zircon — A new natural reference material for U–Pb and Hf isotopic microanalysis." *Chemical Geology* 249(1): 1-35.
- 62) Swami Nath, J. and M. Ramakrishnan (1981). Early Precambrian Supracrustals of Southern Karnataka 112: 350.
- 63) Smeeth, W.F. 1915. Outline of the Geological History of Mysore, Government of India, 21 pp.
- 64) Speer, J.A., and Cooper, B.J., 1982, Crystal-structure of synthetic hafnon, HfSiO_4 , comparison with zircon and the actinide orthosilicates: *American Mineralogist*, v. 67, p. 804–808.
- 65) Spencer, C. J., C. L. Kirkland and R. J. M. Taylor (2016). "Strategies towards statistically robust interpretations of in situ U–Pb zircon geochronology." *Geoscience Frontiers* 7(4): 581-589.
- 66) Trail, D., Watson, E.B., and Tailby, N.D., 2012, Ce and Eu anomalies in zircon as proxies for the oxidation state of magmas: *Geochimica et Cosmochimica Acta*, v. 97, p. 70–87, [https:// doi.org/10 .1016 /j .gca .2012 .08 .032](https://doi.org/10.1016/j.gca.2012.08.032).
- 67) Tushipokla and M. Jayananda (2013). "Geochemical constraints on komatiite volcanism from Sargur Group Nagamangala greenstone belt, western Dharwar craton, southern India: Implications for MesoArchaean mantle evolution and continental growth." *Geoscience Frontiers* 4(3): 321-340.
- 68) Vermeesch, P., 2018, IsoplotR: a free and open toolbox for geochronology. *Geoscience Frontiers*, v.9, p.1479-1493, doi: 10.1016/j.gsf.2018.04.001.
- 69) Williams, I.S., Claesson, S., 1987. Isotopic evidence for the Precambrian provenance and Caledonian metamorphism of high grade paragneisses from the Seve Nappes, Scandinavian Caledonides. *Contributions to Mineralogy and Petrology* 97, 205-217.
- 70) Woodhead, J., J. Hergt, M. Shelley, S. Eggins and R. Kemp (2004). "Zircon Hf-isotope analysis with an excimer laser, depth profiling, ablation of complex geometries, and concomitant age estimation." *Chemical Geology* 209(1): 121-135.
- 71) Woodhead, J. D. and J. M. Hergt (2005). "A preliminary appraisal of seven natural zircon reference materials for in situ Hf isotope determination." *Geostandards and Geoanalytical Research* 29(2): 183-195.
- 72) Wyman, D. and R. Kerrich (2009). "Plume and arc magmatism in the Abitibi subprovince: Implications for the origin of Archean continental lithospheric mantle." *Precambrian Research* 168: 4-22.
- 73) Yang, Q.-Y. and M. Santosh (2015). "Zircon U–Pb geochronology and Lu–Hf isotopes from the Kolar greenstone belt, Dharwar Craton, India: Implications for crustal evolution in an ocean-trench-continent transect." *Journal of Asian Earth Sciences* 113: 797-811.

3

Detrital record of Mesoarchean and lower Neoarchean meta-quartzites in Dharwar Craton, India: Evidence of Eoarchean to Mesoarchean crustal evolution from detrital zircon U–Pb, Hf isotopes and REE compositions

Abstract

Archean cratons act as windows to understand the early Earth as some of them preserve Eoarchean to Mesoarchean tectono-thermal signatures, which, in turn, can be inherited by subsequent detrital formations. In this study, we analyse detrital zircons from various detrital sequences overlying the Archean Dharwar Craton in southern India for U–Pb, Lu–Hf isotopic data and REE compositions to construct and compare the tectono-sedimentary processes prevalent during the Meso- to Neoarchean across the Dharwar Craton. The U–Pb age data show that the sedimentary sources for the detrital suites coincide with the timing of major crustal accretion/growth events across the Dharwar Craton. The stratigraphic correlations between various subgroups have been revisited combining current study with previously published data. Lu–Hf isotope data reveal the involvement of the neighbouring Coorg Block during the sedimentation of the lower Sargur Group greenstone belts; the upper Dharwar Supergroup reveal sources with mostly Paleoarchean crustal extraction ages that have been previously reported for the crustal accretion episodes of the Dharwar Craton. The REE compositions from the detrital zircons plotted as $(\text{Gd}/\text{Yb})_N$ ratios infer a localised subduction zone near the Holenarsipur Schist Belt (HSB); timing of granitoid emplacement which contributed to the formation of the Bababudan Group greenstone belts. We conclude that the Dharwar Craton had limited sedimentation during the Mesoarchean evident from the presence of narrow linear belts and involved detrital material from the adjacent Coorg Block and widespread sedimentation took place during the Neoarchean possibly initiated by the extensive mafic volcanism.

1. Introduction:

The formation and evolution of the continental crust, their incorporation into cratons and supercontinents, combined with their destruction at convergent margins account for the major themes in understanding the evolution of the Earth. (Nance et al., 2014; Spencer et al., 2017; Hawkesworth et al., 2018). The initiation of modern-style subduction like plate tectonics and the emergence of continental crust above the sea level is still debated (Palin et al., 2020). Recent geological models and numerical models mark the Archean era as a crucial period that experienced the secular cooling of the mantle (Spencer et al., 2017; Huang et al., 2020). The Archean cratons provide essential windows to understand the history and nature of the continental growth and its emergence in the early Earth as some of them preserve Eoarchean to Mesoarchean tectonic imprints (Roberts and Santosh, 2018; J.Y.Wang and Santosh, 2019). Paleoarchean to Neoarchean granite-greenstone terranes display distinct magmatic pulses and crust building episodes which include vertical and lateral accretion of juvenile

crustal protoliths and crustal recycling (Smithies et al., 2009; Manikyamba and Kerrich, 2012; Manikyamba et al., 2015, 2017; Santosh et al., 2005).

The Dharwar Craton in southern India is considered an amalgamation of microcontinents that preserve the records of continental growth and recycling during distinct thermal and tectonic events from ca. 3.8–2.5 Ga (Jayananda et al., 2018; Santosh and Li, 2018). Volcano-sedimentary successions of Archean greenstone belts ranging from ages ca. 3.6–2.5 Ga overly the basement gneisses (Peucat et al., 1995; Chadwick et al., 2000; Jayananda et al., 2008; Manikyamba et al., 2017). Several previous studies have focused on the basement Tonalite–Trondhjemite–Granodiorite (TTG) gneisses with associated granitoid plutons and greenstone belts, and proposed various crustal evolution models ranging from plume-arc accretions to modern style subduction-accretion collision (Dey et al., 2013; Jayananda et al., 2018 and references therein; Santosh and Li, 2018; Jayananda et al., 2020). However, the pre-3.4 Ga record of the Dharwar Craton has not been reported yet from meta-igneous sampling. A few studies have attempted to study the detrital zircon record of the metasediments in the Dharwar Craton (Lancaster et al., 2015; Hokada et al., 2013; Maibam et al., 2016; Krapež et al., 2020; Gao and Santosh, 2020), but the focus has mainly been the upper Neoproterozoic detrital sequences which host gold and various metallogenic deposits (Manikyamba et al., 2017). The older metasediments have been reported in very few studies, which do not provide a comprehensive review of the older volcano-sedimentary greenstone belts that record the initial episodes of the crustal evolution of the Dharwar Craton, and their stratigraphic correlation with other greenstone belts is still uncertain.

In this study, we have presented detrital zircon U-Pb data from the older (older than 2.7 Ga) metasedimentary greenstone belts across the Dharwar Craton and compare with previous correlative interpretations (Patra et al., 2020; Krapež et al., 2020; Chadwick et al., 1991).

The detrital zircon investigations carried out by Lancaster et al. (2015) report significant crustal extraction events at ca. 3.3 Ga and 2.7 Ga with crustal reworking in the Eastern Dharwar Craton until ca. 2.55–2.50 Ga. Maibam et al. (2016) reported contemporaneous crust formation in the Western and Eastern Dharwar Cratons between ca. 3.6–3.2 Ga. The samples reported in this study with proximity to the oldest nucleus of the Dharwar Craton, the Gorur Gneiss aged at ca. 3.4 Ga (Guitreau et al., 2017) are reported for detrital zircon Lu–Hf isotopic data and Rare Earth Element (REE) compositions to interpret the source regions for the sediments that suggest major crustal events during ca. 3.35–3.2 Ga and continuous crustal recycling trend observed in the Western Dharwar Craton and potentially in the Coorg Block in the Paleoproterozoic. The REE compositions show potential implications for the existence of localised modern-style tectonics in the Mesoproterozoic era.

2. Geological Background:

The basement of the Indian shield is composed of Archean cratonic nuclei such as the Dharwar Craton, Bastar Craton and Singhbhum craton that have amalgamated through Archean—Proterozoic collisional sutures (J.Y. Wang and Santosh, 2019). The boundaries of the Dharwar Craton include the Deccan Traps basalts on the north and the Southern Granulite Terrane to the south. The dominant makeup of the Dharwar Craton comprises of Archean granitoid–gneiss and greenstone sequences. The Dharwar Craton is subdivided into three major domains: the Western Dharwar Craton (WDC), the Eastern Dharwar Craton (EDC) and the Central Dharwar Craton (CDC) based mainly on the age and nature of the greenstone belts, the grade of metamorphism and interpreted crustal thickness (Swaminath and Ramakrishnan, 1981; Jayananda et al., 2000) combined with the usage of isotope geochronological data (Peucat et al., 2013; Dey et al., 2013). A progressive increase in the grade of metamorphism is reported from north to south of the Dharwar Craton with the northern parts showing upper greenschist to lower amphibolite grade of rocks and the southern parts exposing high-grade granulite rocks (Chadwick et al., 2000). The metamorphic grade progression is attributed to the northward tilt of the craton exposing the lower crust, experiencing higher grade metamorphism, in the south (Chardon et al., 2008; Moyen et al., 2003; Jayananda et al., 2013).

Previously, the WDC and the EDC were considered as the subdivisions of the Dharwar Craton with the Closepet Granite marking the boundary (Naqvi, 2005; Jayananda et al., 2006; Chardon et al., 2011). The subsequent studies proposed a steep high-strain mylonitic Gadag-Mandya shear zone, later renamed as the Chitradurga Shear Zone (CSZ), on the eastern margin of the Chitradurga Greenstone Belt (CGB) to act as the boundary between the two domains (Jayananda et al., 2008; 2013; Chardon et al., 2011). The contact between the WDC and EDC was later proposed to be a transitional zone extending from the Chitradurga Shear Zone (CSZ) to the Closepet Granite and demarcated as the Central Dharwar Province (CDP) (Peucat et al., 2013) based on U-Pb zircon ages and Nd isotopic studies. The CDP has been referred to as Central Dharwar Craton (CDC) in more recent studies (Santosh and Li, 2018; Jayananda et al., 2018; 2020).

2.1 Western Dharwar Craton Greenstone belts:

The WDC is predominantly comprised of Tonalite—Trondhjemite—Granodiorite (TTG) gneisses ranging in ages from ca. 3.4—3.2 Ga (Guitreau et al., 2017; Jayananda et al., 2015, 2018) with crustal inheritance up to ca. 3.8 Ga (Beckinsale et al., 1980; Bhaskar Rao et al., 1992; Meen et al., 1992; Peucat et al., 1993). These gneisses were accreted mainly during the Mesoarchean (Peucat et al., 1993) along with Neoarchean (ca. 2.6 Ga) potassic granitoid plutons (Jayananda et al., 2006). These gneisses are

interlayered with the Sargur Group (> 3.0 Ga) greenstone belts, which are unconformably overlain by the Dharwar Supergroup Greenstones (ca. 2.9–2.5 Ga), in turn, subdivided into the Bababudan Group and the Chitradurga Group greenstones (Hokada et al., 2013).

2.1.1 Sargur Group:

The Sargur Group greenstones occur within the TTG gneisses of WDC and show ages of ca. 3.4 Ga and have been described as small and linear greenstone belts in the southern part of WDC (Manikyamba et al., 2017). The Sargur type belts are grouped based on their location (Manikyamba et al., 2017) and include schist belts occurring at Holenarsipur (HSB), Nuggihalli, Krishnarajapete (K.R. Pete) (KSB), Mayasandra, Nagamangala, Melukote, Kalyadi, Banavara, Hadanur. These are estimated to have formed alongside the komatiite flows at ca. 3.35 Ga (Jayananda et al., 2008) and associated felsic flows at ca. 3.30 Ga (Peucat et al., 1995; Tushipokla and Jayananda, 2013). These older greenstone belts are intruded by Gorur Gneiss of ca. 3.4 Ga near the Holenarsipur belt. The Sargur Group is notable for the presence of ca. 3.6–3.5 Ga SHRIMP zircon U-Pb ages (Ramakrishnan and Vaidyanathan, 2008). The Sargur Group tapers out towards the north of the WDC, which is overlain by the larger greenstone belts of the Dharwar Supergroup Greenstone belts. The most precise age reported for the Sargur Group comes from SHRIMP $^{207}\text{Pb}/^{206}\text{Pb}$ ages from a rhyolitic flow from Holenarsipur Greenstone Belt at 3298 ± 7 Ma (Peucat et al., 1993).

2.1.2 Dharwar Supergroup:

The Dharwar Supergroup was earlier divided into younger greenstone belts that were deposited on the quartz pebble conglomerate (QPC) as Bababudan and Chitradurga Groups (Ramakrishnan et al., 1978; Swami Nath and Ramakrishnan, 1981). The Bababudan Group starts with the QPC, interpreted as a paleosol (Srinivasan and Ojakangas, 1986), as a basal unit and is followed by a quartzite (Manikyamba et al., 2017). These quartzites are interbedded with MORB and within-plate type volcanic rocks (Bhaskar Rao et al., 1992), which are overlain by a sequence of conglomerates, BIFs, schistose rocks and greywackes across the Kudremukh, Shimoga, Bababudan and Chitradurga greenstone/schist belts. In the Bababudan Group, Sm-Nd whole-rock isochron ages reveal basalt in the lower stratigraphy at ca. 2.91 Ga and ca. 2.84 Ga in the higher stratigraphic levels (Kumar et al., 1996), while tuffs reveal zircons with SHRIMP U-Pb ages at ca. 2.72 Ga (Trendall et al., 1997). The lower Bababudan Group exposed in the Bababudan, and Kudremukh Greenstone (KGB) belts are considered to have developed in an intra-cratonic setting. The Bababudan Group Greenstone belts and Chitradurga Group Greenstone belts are not to be confused with individual greenstone belts such as the Bababudan Greenstone Belt (BBG) and Chitradurga Greenstone Belt (CGB) which belong to their respective groups.

The Chitradurga Group consists of conglomerates with a disrupted framework, greywackes, phyllites, BIFs, cherts, shales, volcanic basalts and rhyolites. The Chitradurga Group is characterised by three horizons of BIFs, three horizons of conglomerate, and four lithostratigraphic units, of which one of them is the Bababudan Group (Krapež et al., 2020). Lateral stratigraphic variations in the Chitradurga Group include lithological changes and also loss or gain of strata on syn- and post-folding structures (Chadwick et al., 1983; Krapež et al., 2020). Mafic and felsic volcanics from the Chitradurga Group were dated using Sm–Nd whole-rock isochron method to reveal magmatism at ca. 2.74 Ga. The ca. 2.6 Ga orogeny in the Chitradurga Greenstone Belt (Jayananda et al., 2006, 2013) is proposed to have erased the signatures of the undeformed volcanic sequences except for isolated amphibolitic enclaves within the Peninsular Gneiss (Manikyamba et al., 2017).

The Shimoga and Chitradurga greenstone belts were proposed to have formed in convergent setting resulting in the exposure of the rocks belonging to the Chitradurga Group (Manikyamba et al., 2014). The Shimoga Greenstone Belt (SGB) appears to represent an intervention between the Bababudan Group and the Chitradurga Group (Krapež et al., 2020) from past lithostratigraphic correlations with the lower groups of the SGB correlating with the Bababudan Group and the upper groups of the SGB with the Chitradurga Group (Chadwick et al., 1988; Chadwick et al., 1991). The Chitradurga group extends to the far north, forming a structurally dismembered lithotectonic complex named as the Gadag Duplex (Chadwick et al., 2003). The detrital zircons from the Gadag Greenstone Belt (GGB) report several age populations ranging from ca. 3.4–2.55 Ga with major crust forming events at ca. 3.6 and 3.36 Ga with juvenile addition at ca. 2.6 Ga (Sarma et al., 2012; J.Y. Wang et al., 2019).

The relationship between the Bababudan Group and the Chitradurga Group has not been thoroughly explored, but recent works have explained the current state of play for the comprehensive comparison of lithostratigraphy and geochronology of the Dharwar Supergroup (Manikyamba et al., 2017; Krapež et al., 2020). Krapež et al. (2020) proposed that the basal units of the Chitradurga Group and Bababudan Group are identical and only differ by a spatial unconformity. In a recent study, the youngest whole-rock Sm–Nd isochron age (2934 ± 88 Ma) from the Holenarsipur Schist belt, from the Sargur Group, has been compared to the oldest ages reported from the lowest stratigraphic units belonging to the Bababudan Group, interpreting the Sargur Group to represent lower stratigraphic ultramafic units of the Dharwar Supergroup with no clear temporal distinction to separate these two groups (Patra et al., 2020). However, Hokada et al. (2013) showed the distinction between the Sargur Group and Dharwar Supergroup with the presence of kyanite and monazite grains in the muscovite quartzite schists dated from the Holenarsipur Schist Belt interpreting the quartzite undergoing high-grade metamorphism to form kyanite and monazite at monazite U–Pb age of 3082 ± 66 Ma. Combining

these existing theories, the greenstone belts occurring across the WDC represent complex volcano-sedimentary processes through the Mesoarchean to the Neoarchean.

2.2 Central Dharwar and Eastern Dharwar Craton Greenstone Belts:

The Central Dharwar Craton is comprised by a mix of ca. 3.4–3.0 Ga and ca. 2.7–2.5 Ga crust that that was affected by thermal events during ca. 3.20 and 2.62 Ga (Jayananda et al., 2011; 2013a). The Eastern Dharwar Craton is comprised of juvenile accreted granitoids ranging from ca. 2.6–2.52 Ga (Jayananda et al., 2020). The greenstone belts associated with the CDC and EDC are represented by Neoarchean supra-crustal sequences linked into groups such as a) Sandur Schist belt occurring between the Closepet Granite; b) Ramagiri–Penakacherla–Hungund greenstone belts; c) Kolar–Kadiri–Hutti greenstone belts and several smaller greenstone belts (Manikyamba et al., 2017; Manikyamba and Kerrich, 2011). The presence of komatiites similar to the WDC, but in lower volume, have been reported from only the Sandur and Ramagiri greenstone belts (Zachariah et al., 1995; Manikyamba et al., 2008). The prominent feature of the greenstone belts is the preservation of various subduction zone volcanic rocks with associated gold mineralisation (Manikyamba et al., 2017) of which, the Hutti Greenstone Belt is still mined for gold. While formal correlations with greenstone belts across the WDC have not been made, U–Pb ages of felsic volcanism across CDC and WDC have been used to compare the formation periods of the Eastern Dharwar Greenstone belts with the Neoarchean supra-crustals in the WDC. Krapež et al. (2020) have drawn comparisons between the lower groups of the Bababudan Group and the Sandur Group with Mesoarchean maximum depositional ages, the upper Chitradurga Group with the Hutti Greenstone Belt. Granodiorites aged at ca. 2.62 Ga (Balakrishnan et al., 1999) intruding the pillow basalts associated with the ca. 2.7 Ga felsic volcanism near Ramagiri, has been linked to the formation of the Bababudan Group (Krapež et al., 2020) through the tuff zircon U–Pb ages at ca. 2.72 Ga (Trendall et al., 1997).

The Kolar Schist Belt in the Eastern Dharwar Craton is comprised of BIFs, amphibolite, quartz mica schist and porphyritic granite with mafic enclaves representing accreted relicts of an ocean–trench–continent transitional zone within a Neoarchean convergent margin (Yang and Santosh, 2015). Komatiitic amphibolites have been reported for Sm–Nd isochron ages of ca. 2.69 Ga and ca. 2.73 Ga (Balakrishnan et al., 1988). Zircon records reveal emplacement ages in the Kolar Schist Belt at ca. 2.63 Ga and 2.53 Ga, followed by metamorphism at ca. 2.41 Ga (Krogstad et al., 1989). Detrital zircons from the BIFs reveal zircons representing two significant events of crustal growth at ca. 2.7 and 2.5 Ga.

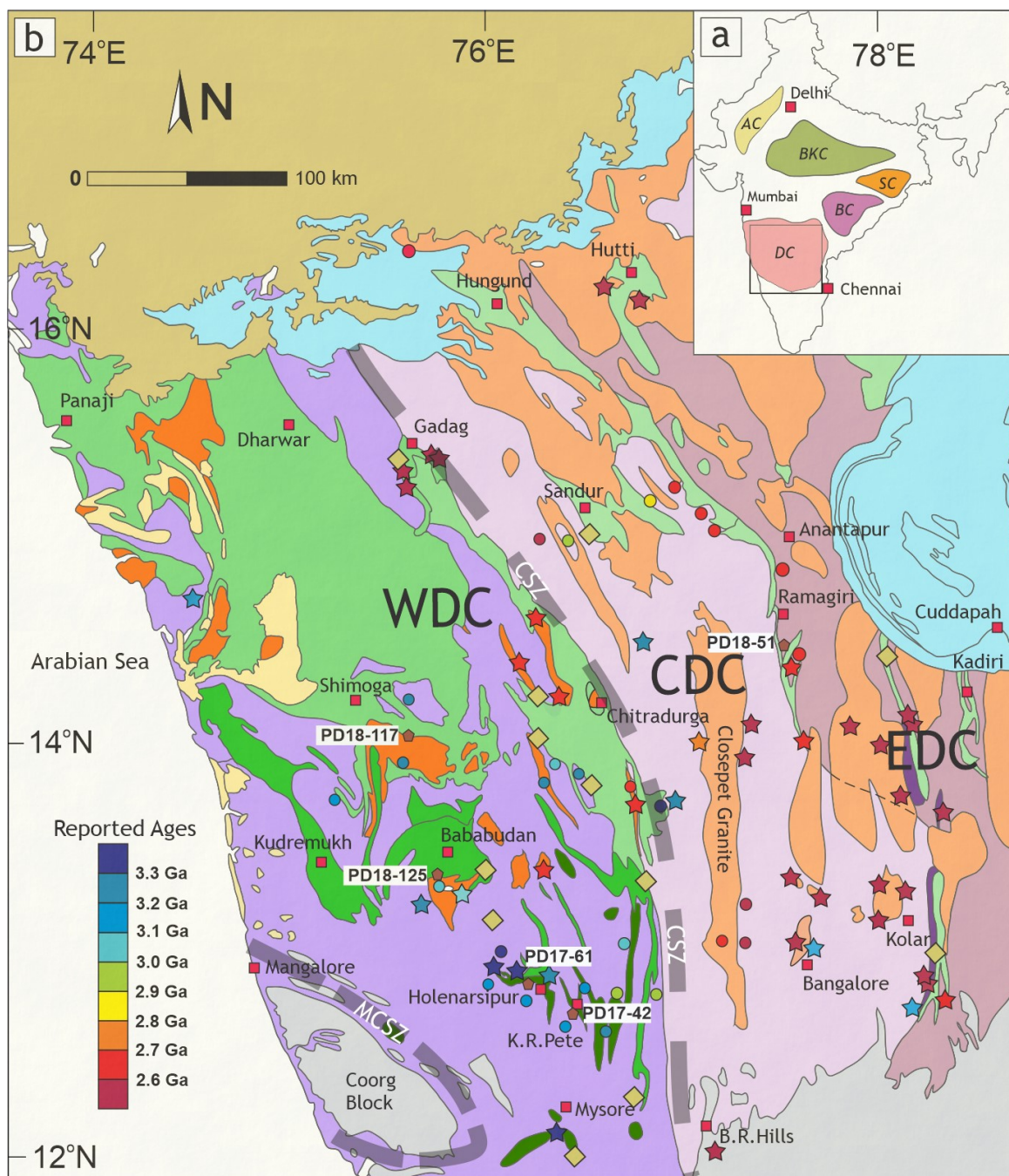


Figure 1: (a) Geological framework of India showing the location of major Archean cratons: DC – Dharwar Craton, AC – Aravalli Craton, BKC – Bundhelkhand Craton, BC – Bastar Craton, SC – Singbhum Craton. (b) Geological map of the Dharwar Craton with dashed lines representing major shear zones discussed in this study; CSZ – Chitradurga Shear Zone, MCSZ – Mercara Shear Zone. The three main domains within the Dharwar Craton, namely Western Dharwar Craton (WDC), Central Dharwar Craton (CDC) and Eastern Dharwar Craton (EDC). Individual published magmatic and meta-igneous zircon ages represented using 'Reported Ages' legend on the left represented by star symbols. The reported magmatic ages from Chapter 2 have been shown in circles coloured using the same legend. Previously published detrital studies with zircon Lu-Hf datasets have been displayed in the map marked by gold coloured diamonds. Brown pentagon shapes marked sample locations in this study, and major towns have been drawn in red squares.

3. Methods:

3.1 Zircon U–Pb dating:

The quartzite samples were crushed and sieved for a zircon fraction ($<500\text{ }\mu\text{m}$) at the petrology lab facility at the Indian Institute of Science, Bangalore. The fractions were panned for heavy minerals. Magnetic minerals were removed, and resulting fractions were handpicked for zircons, mounted in epoxy resin and polished at the University of Adelaide. The grain mounts were carbon-coated and imaged by a Gatan cathodoluminescence (CL) detector attached to Quanta 600 MLA Scanning Electron Microscope to identify various domains within the zircons suitable for analysis. U–Pb geochronology was performed at Adelaide Microscopy, The University of Adelaide, using an Agilent 7900 ICP-MS attached to a New Wave 213 nm laser (NWR-213). The laser used a spot size of $30\text{ }\mu\text{m}$ and a frequency of 5 Hz. The isotopes ^{204}Pb , ^{206}Pb , ^{207}Pb , ^{208}Pb , ^{232}Th and ^{238}U were measured for U–Pb geochronology. GEMOC GJ-1 zircon (TIMS ages $^{207}\text{Pb}/^{206}\text{Pb} = 602 \pm 4.3\text{ Ma}$, $^{206}\text{Pb}/^{238}\text{U} = 600.7 \pm 1.1\text{ Ma}$ and $^{207}\text{Pb}/^{235}\text{U} = 602.0 \pm 1.0\text{ Ma}$; Jackson et al., 2004) was used for the correction of U–Pb fractionation for laser sessions. The Plesovice zircon (ID-TIMS $^{206}\text{Pb}/^{238}\text{U}$ age = $337.13 \pm 0.37\text{ Ma}$) was used as an internal standard to test the accuracy of the laser sessions. Rare Earth Elements – ^{139}La , ^{140}Ce , ^{141}Pr , ^{146}Nd , ^{147}Sm , ^{153}Eu , ^{157}Gd , ^{159}Tb , ^{163}Dy , ^{165}Ho , ^{166}Er , ^{169}Tm , ^{172}Yb , ^{175}Lu , ^{89}Y , ^{178}Hf were simultaneously measured from the zircons along with U–Pb isotopes using $50\text{ }\mu\text{m}$ spot size analyses over NIST-SRM 610 glass as reference material (Norman et al., 1996, Norman et al., 1998, Jochum et al., 2011). The U–Pb and REE data were separately processed using Iolite™ (Paton et al., 2011). Concordia diagrams ($^{207}\text{Pb}/^{235}\text{U}$ vs $^{206}\text{Pb}/^{238}\text{U}$) were generated to represent the data using the Isoplot 4.15 plugin on Microsoft Excel (Ludwig, 2003) and an online version of IsoplotR (Vermeesch, 2018) was used to calculate the upper intercepts of the discordant lines and mean ages. The analytical ellipses have been coloured to represent Th/U ratios. The mean standard weighted deviation (MSWD) has been calculated for $^{207}\text{Pb}/^{206}\text{Pb}$ ages to represent the peaks of detrital distribution in the Kernel Density Estimates (KDE), for zircons greater than 85%

concordance, shown in figure 4. The U–Pb age data has been represented as a top-down view of the probability density estimate (PDE) in figure 6. The REE compositions have been normalised against chondrite values from Boynton et al. (1984), using the Geochemical Data Toolkit for R (GCDkit6.0) (Janousen et al., 2006) to calculate REE ratios. In particular, Eu anomalies represented by Eu/Eu^* (where $\text{Eu}^* = \sqrt{(\text{Sm}_N \times \text{Gd}_N)}$), La_N/Yb_N ratios (light rare earth element (LREE) vs heavy rare earth element (HREE)), and Gd_N/Yb_N ratios (middle rare earth element (MREE) vs HREE) were calculated and plotted against individual zircon $^{207}\text{Pb}/^{206}\text{Pb}$ ages.

3.2 Zircon Lu–Hf analysis:

Zircon grains from the Holenarsipur Schist Belt (HSB) (PD17-61) and K.R.Pete Schist Belt (KSB) (PD17-42) with less than 15% discordance in U–Pb ages were targeted for Hf isotope analysis, which was carried out using a Nu Plasma II multi-collector inductively coupled plasma mass spectrometer at the John De Laeter Centre at Curtin University, Australia. CL images were used as a guide to target zircons within the same domain as the U–Pb ablation spot. ^{180}Hf , ^{179}Hf , ^{178}Hf , ^{177}Hf , ^{176}Hf , ^{175}Lu , ^{174}Hf , ^{173}Yb , ^{172}Yb and ^{171}Yb were counted on the Faraday collector array. The time-resolved data was reduced using Iolite™ from data reduction scheme after Woodhead et al. (2004). Data was normalised to $^{179}\text{Hf}/^{177}\text{Hf} = 0.7325$ using an exponential correction for mass bias (Patchett and Tatsumoto, 1980). The Yb and Lu isobaric interferences on ^{176}Hf were corrected following the methodology of Woodhead et al. (2004). Zircon standards GEMOC GJ-1, Plesovice, 91500, R33 were analysed before and during analysis to assess the performance and stability of the instrument (reported in the appendix). Mudtank zircon was used as the primary standard, and 17 analyses yielded a mean $^{176}\text{Hf}/^{177}\text{Hf}$ ratio of 0.282507 ± 0.0000094 (2σ), which was slightly over the uncertainty of the published value of 0.282507 ± 0.000006 (Woodhead and Hergt, 2005). The initial $^{176}\text{Hf}/^{177}\text{Hf}_{\text{CHUR}(t)}$ was calculated using a ^{176}Lu decay constant of $1.865 \times 10^{-11}/\text{year}$ (Scherer et al., 2001) with modern $^{176}\text{Hf}/^{177}\text{Hf}$ and $^{176}\text{Lu}/^{177}\text{Hf}$ values of 0.282785 and 0.0336, respectively (Bouvier et al., 2008). The values of crustal model ages (T_{DM^C}) were calculated using a ^{176}Lu decay constant of $1.865 \times 10^{-11}/\text{year}$ (Scherer et al., 2001), modern $^{176}\text{Hf}/^{177}\text{Hf} = 0.28325$, modern $^{176}\text{Lu}/^{177}\text{Hf} = 0.0384$ (Griffin et al., 2000), and a bulk crust value of $^{176}\text{Lu}/^{177}\text{Hf} = 0.015$ (Griffin et al., 2002). The reported uncertainties for $\epsilon\text{Hf}(t)$ were calculated as $^{176}\text{Hf}/^{177}\text{Hf}_{\text{sample}}$ uncertainty converted to epsilon notation and reported at 2σ level.

4. Results:

Four metasedimentary quartzites have been chosen to represent various detrital groups across the stratigraphy of the greenstone successions over the Western Dharwar Craton. One muscovite bearing

quartzite has been collected near the Ramagiri Greenstone Belt as a lithostratigraphic unit with limited detrital zircon data. The locations and details of the samples are summarised in the table below.

Sample	Latitude	Longitude	Location	Lithology	Detrital unit	Category
<i>PD17-42</i>	12.6357	76.4639	Krishnarajapete	Fuchsite Quartzite	K.R. Pete Schist Belt (KSB)	Bababudan Group Greenstone belt (?)
<i>PD17-61</i>	12.7935	76.2866	Holenarsipur	Kyanite bearing Fuchsite Quartzite	Holenarsipur Schist Belt (HSB)	Sargur Group Greenstone belt
<i>PD18-51</i>	14.2972	77.4890	Ramagiri	Muscovite bearing Quartzite	Ramagiri Greenstone Belt (RGB)	Eastern Dharwar Craton Greenstone
<i>PD18-117</i>	14.0573	75.6876	Shimoga	Fuchsite Quartzite	Shimoga Schist Belt (SSB)	Chitradurga Group Greenstone (?)
<i>PD18-125</i>	13.3440	75.7692	Chikamagaluru	Quartzite	Bababudan Group Greenstone belt	Bababudan Group Greenstone belt

Table 1: Table showing coordinates and nearest landmark to sample locations, along with lithology, name of the detrital units and expected stratigraphic category among the detrital units in Dharwar Craton.

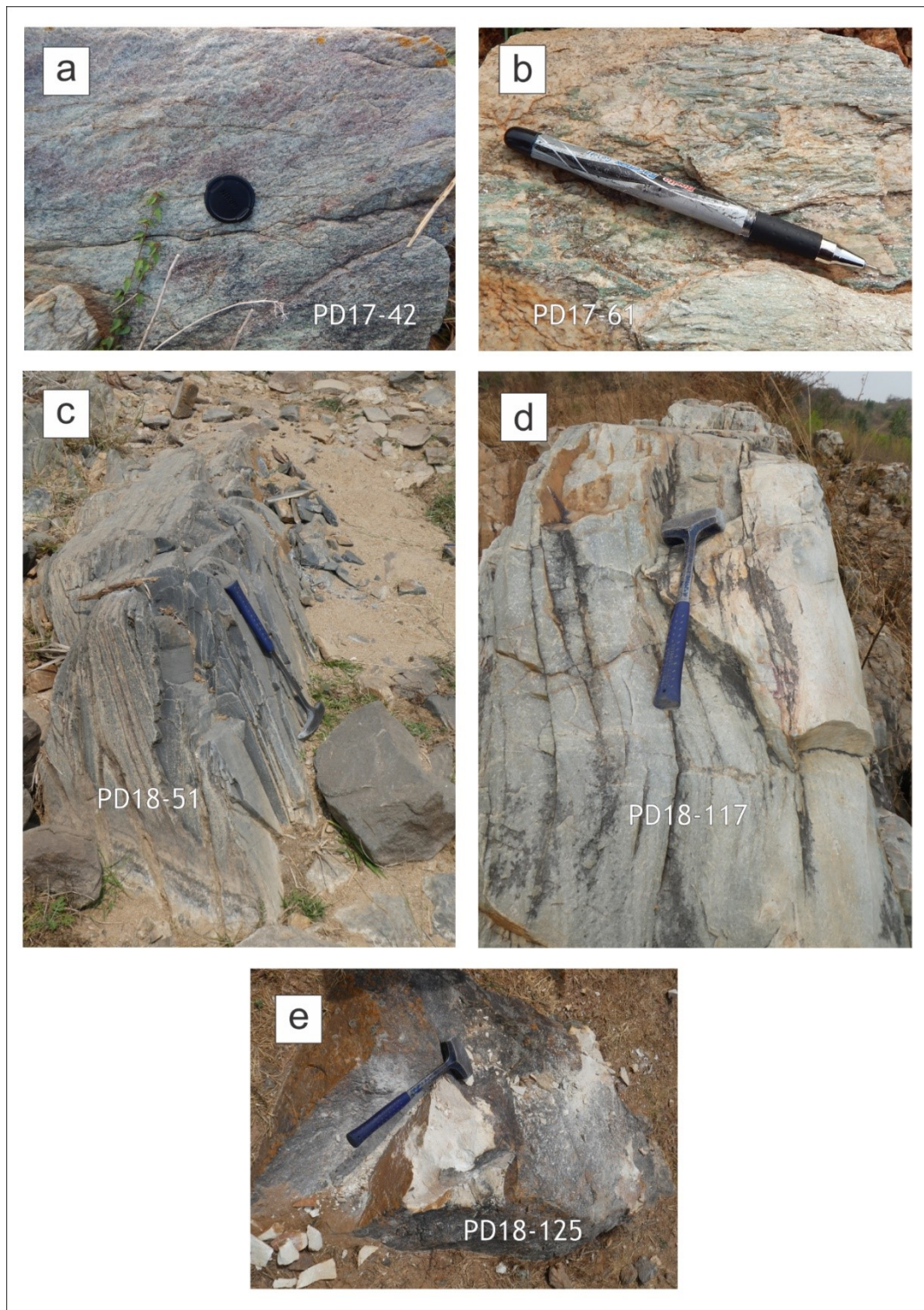


Figure 2: Field photographs showing various sample locations. (a) Fuchsite-Quartzite (PD17-42) collected near K.R.Pete town showing reddish-brown weathering. (b) Kyanite bearing Fuchsite-Quartzite (PD17-61) collected near Holenarsipur town, the sample contained Kyanite needles. (c) Muscovite bearing Quartzite (PD18-51) collected south of Ramagiri town. (d) Fuchsite-Quartzite (PD18-117) collected south of Shimoga town occurring as deformed beds. (e) Quartzite sample (PD18-125) collected north of Chikamagalur town.

4.1 Zircon U–Pb dating and REE composition:

PD17-42 was a fuchsite bearing quartzite collected towards the southwest of Krishnarajpete (K.R. Pete) town. The fuchsite quartzite showed weathering in reddish-brown colouring. One hundred fifteen zircons have been analysed for U–Pb dating of which 57 zircons reveal near-concordant (concordance greater than 85% in this case) ages. The zircons appear irregularly shaped with broken and rounded edges. The morphology of the zircons ranged from elongated zircons with aspect ratio 3:1 to 3:2 with a thickness between 40 – 100 μm . The cathode luminescence (CL) images reveal a majority of the zircons showing igneous oscillatory zoning with internal cracks and occasional metamict textures. The kernel density estimate (KDE) calculated using the near-concordant ages filtered using discordance less than fifteen percentage reveal major age peaks converging at mean $^{207}\text{Pb}/^{206}\text{Pb}$ ages at 3178 ± 12 Ma (MSWD = 2.2, $n = 20$), 3307 ± 15 Ma (MSWD = 1.8, $n = 12$) and 3420 ± 22 Ma (MSWD = 2.1, $n = 7$) along with minor detrital contribution at 3105 ± 18 Ma (MSWD = 0.8, $n = 4$) and ca. 2.85 Ga. The measured Th/U ratios for the near-concordant zircons range from 0.036 to 1.68. The youngest near concordant zircon had $^{207}\text{Pb}/^{206}\text{Pb}$ age of 2737 ± 54 Ma. The REE compositions from the near concordant zircons reveal Eu/Eu* values ranging from 0.11 to 0.86, $\text{La}_\text{N}/\text{Yb}_\text{N}$ values ranging from 0.00002 to 0.22 and $\text{Gd}_\text{N}/\text{Yb}_\text{N}$ values ranging from 0.0288 to 0.7822.

PD18-117 is a quartzite collected to the south of Shimoga town. Ninety-three zircons have been analysed for U–Pb and REE analysis of which 28 analyses are less than fifteen per cent discordance. The zircons appear well-rounded in shape with broken edges with aspect ratios of 1:3 to 1:1 and thickness ranging from 30 – 90 μm . The CL imaging of the zircons reveals a majority of the grains showing magmatic oscillatory zoning with a minor fraction showing thin (up to 10 μm) bright rims. The near-concordant zircons were used to calculate the KDE which revealed major detrital contribution converging at mean $^{207}\text{Pb}/^{206}\text{Pb}$ ages, 2991 ± 16 Ma (MSWD = 1.3, $n = 11$), 3224 ± 18 Ma (MSWD = 0.95, $n = 4$) and minor contributions at ca. 3.15 – 3.05 Ga and ca. 3.3 Ga. The youngest near-concordant zircon had $^{207}\text{Pb}/^{206}\text{Pb}$ age of 2925 ± 41 Ma. The measured Th/U ratios for the near-concordant zircons range from 0.052 to 1.1. The REE compositions from the near concordant zircons reveal Eu/Eu* values ranging from 0.13 to 1.02, $\text{La}_\text{N}/\text{Yb}_\text{N}$ values ranging from 0.0001 to 0.02 and $\text{Gd}_\text{N}/\text{Yb}_\text{N}$ values ranging from 0.045 to 0.5.

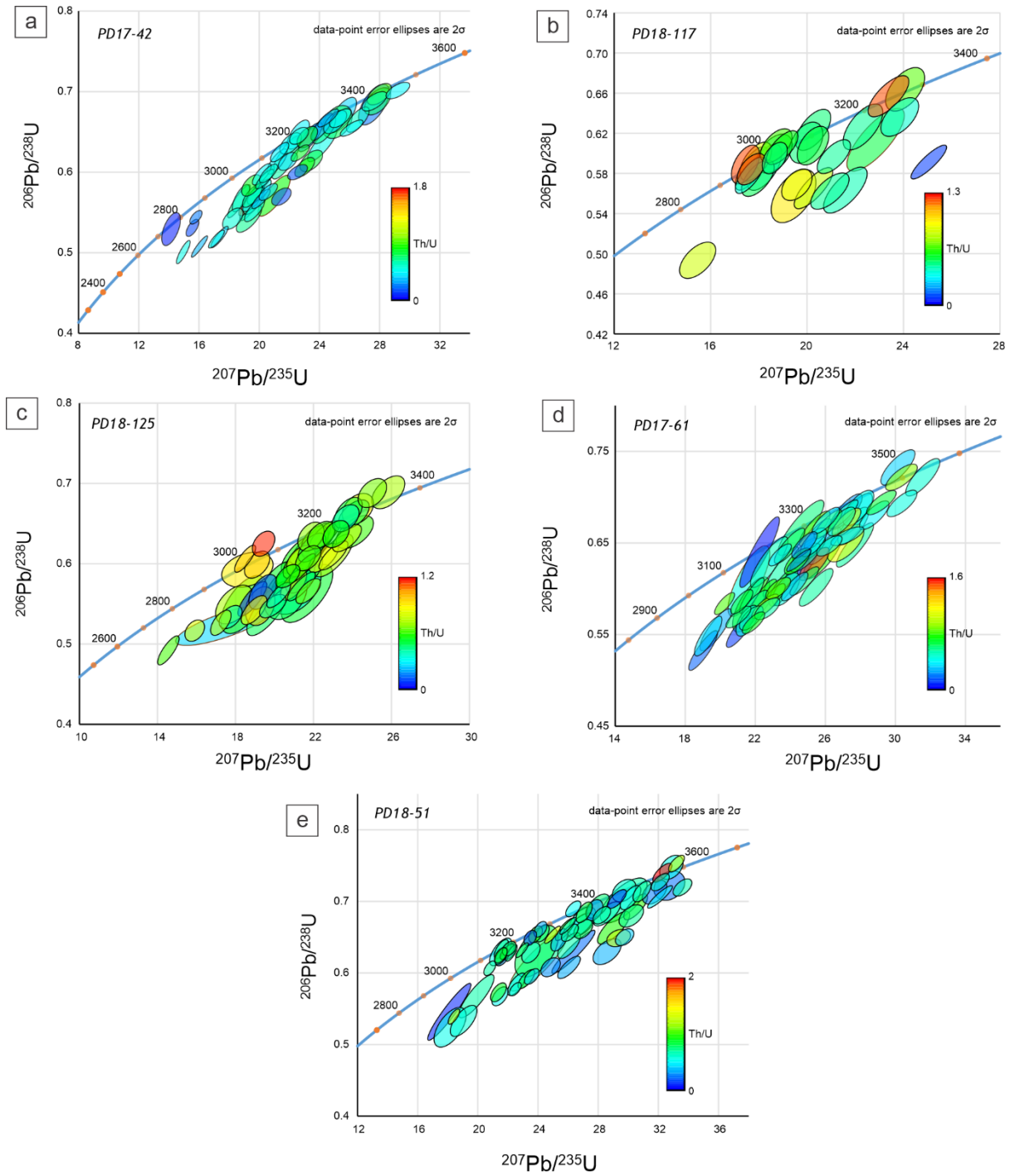


Figure 3: U-Pb Concordia diagrams for the detrital zircons analysed in this study. The ellipses represent the 2σ error in age determination of each grain and are coloured using Th/U ratio as the colour scale shown next to each plot. Zircons with concordance greater than 85% shown in the figure. (a) Fuchsite-Quartzite (PD17-42) collected from near K.R.Pete town, (b) Fuchsite-Quartzite (PD18-117) collected south of Shimoga town, (c) Quartzite sample (PD18-125) collected from Chikamagalur town, (d) Kyanite bearing Fuchsite-Quartzite (PD17-61) collected from Mangalapura village near Holenarsipur town, (e) Muscovite bearing Quartzite (PD18-51) collected south of Ramagiri town.

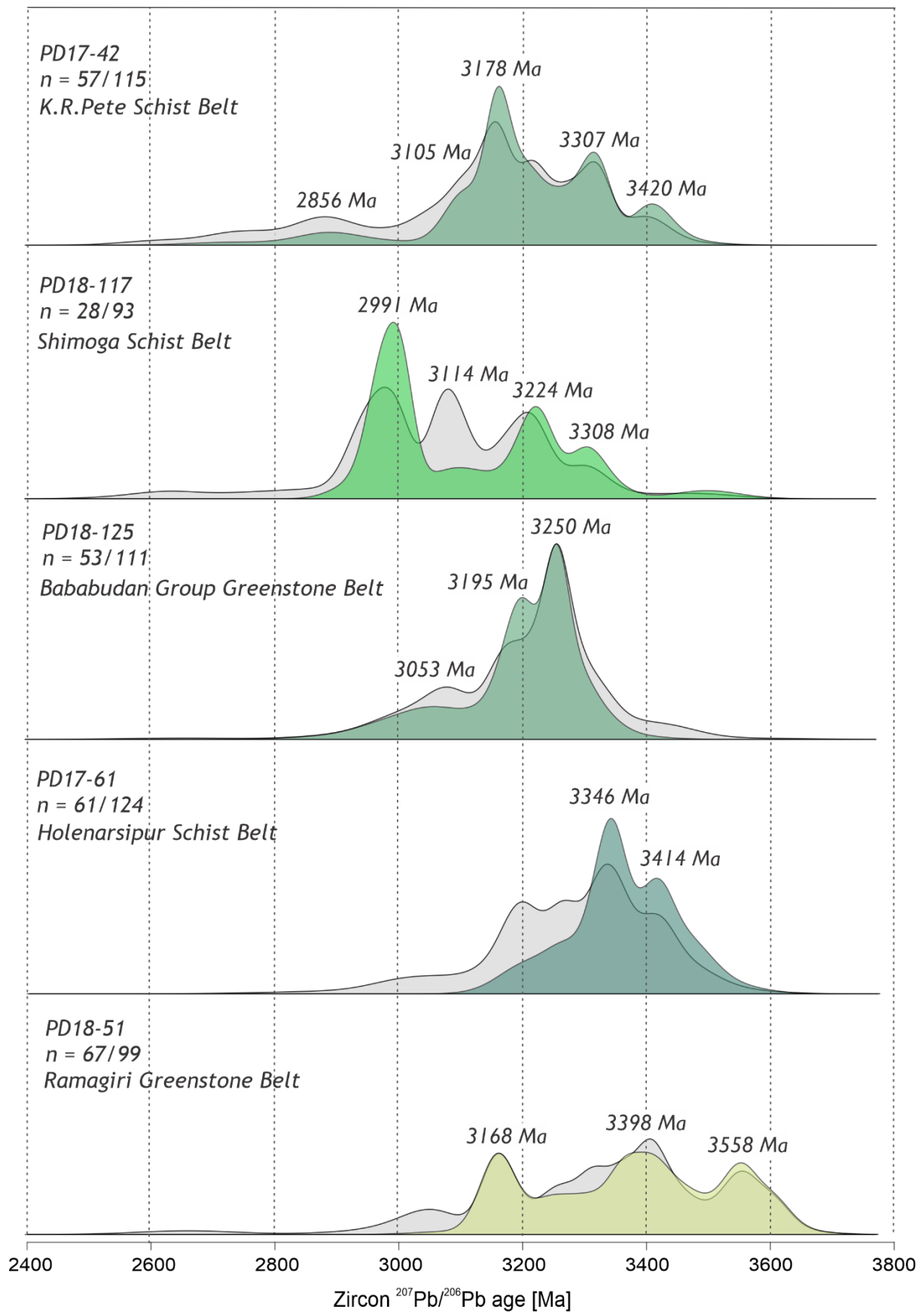
PD18-125 was collected from a quartzite formation in Chikamagalur town. One hundred eleven zircons have been analysed for U–Pb and REE data from which 53 analyses were filtered for U–Pb ages that are greater than 85 percentage concordance. The morphology of the analysed zircons included a significant fraction of elongated near-euhedral zircons with aspect ratios of 1:2 to 1:4 with a thickness of 40 – 60 μm . The remaining fraction contained rounded grains with broken edges with aspect ratios of 1:2 to 4:5 and thickness of 60 – 100 μm . The zircon grains reveal oscillatory zoning in response to CL imaging with no metamict textures. The KDE calculated using the near concordant zircons revealed major age peaks converging at mean $^{207}\text{Pb}/^{206}\text{Pb}$ age at 3250 ± 10 Ma (MSWD = 0.57, $n = 10$) and 3194 ± 10 Ma (MSWD = 0.76, $n = 12$) with minor contributions at ca. 3.15 – 2.95 Ga and ca. 3.33 – 3.27 Ga. The youngest near-concordant zircon had $^{207}\text{Pb}/^{206}\text{Pb}$ age of 2965 ± 33 Ma. The measured Th/U ratios for the near-concordant zircons range from 0.051 to 1.16. The REE compositions from the near concordant zircons reveal Eu/Eu* values ranging from 0.06 to 0.86, $\text{La}_\text{N}/\text{Yb}_\text{N}$ values ranging from 0.0001 to 0.04 and $\text{Gd}_\text{N}/\text{Yb}_\text{N}$ values ranging from 0.02 to 0.307.

PD17-61 was collected from a kyanite bearing fuchsite-quartzite formation along the road from Holenarsipur town towards Mangalapura village. This sample was collected to represent the Sargur Group Greenstone detrital suite as the mineral assemblage of kyanite-muscovite quartzite was previously published to represent the regional metamorphism in Sargur Group supracrustal rocks (Hokada et al., 2013). The zircon grains were mostly rounded and imperfect shapes with broken edges with aspect ratios ranging from 1:4 to 3:2 with a thickness of 35 – 100 μm . The zircon grains mostly preserved oscillatory zoning with some grains showing metamict textures in response to CL imaging. One hundred twenty-four zircons were analysed for U–Pb data and REE compositions, of which 61 analyses were filtered for greater than 85 percentage concordance. The KDE for near concordant zircons revealed major detrital age peaks converging at mean $^{207}\text{Pb}/^{206}\text{Pb}$ age at 3414 ± 12 Ma (MSWD = 1.2, $n = 11$) and 3346 ± 9 Ma (MSWD = 1.02, $n = 13$) with decreasing contribution at ca. 3.3 – 3.17 Ga and ca. 3.55 – 3.45 Ga. The youngest near-concordant zircon had $^{207}\text{Pb}/^{206}\text{Pb}$ age of 3174 ± 46 Ma. The measured Th/U ratios for the near-concordant zircons range from 0.022 to 1.5. The REE compositions from the near concordant zircons reveal Eu/Eu* values ranging from 0.19 to 0.75, $\text{La}_\text{N}/\text{Yb}_\text{N}$ values ranging from 0.0018 to 0.471 and $\text{Gd}_\text{N}/\text{Yb}_\text{N}$ values ranging from 0.036 to 1.176.

PD18-51 was collected from a muscovite bearing quartzite bed within the Ramagiri greenstone belt in the Eastern Dharwar Craton near Ramagiri town. Ninety-nine zircons were analysed for U–Pb data and REE analysis of which 67 analyses were filtered for greater than 85 per cent concordance. The zircons were rounded with broken edges with aspect ratios of 1:3 to 1:1 and thickness of 30 – 90 μm . The zircon grains show typical darker CL imaging response with subtle oscillatory zoning and occasional metamict zones within the grains. The calculated KDE plot revealed major detrital

contributions converging at broad age peaks with mean $^{207}\text{Pb}/^{206}\text{Pb}$ age of 3558 ± 17 Ma (MSWD = 5.8, n = 13), 3398 ± 25 Ma (MSWD = 18, n = 23) and 3168 ± 13 Ma (MSWD = 2.1, n = 11) with minor contributions at ca. 3.3 – 3.2 Ga and ca. 3.65 Ga. The youngest near-concordant zircon had $^{207}\text{Pb}/^{206}\text{Pb}$ age of 3089 ± 25 Ma. The measured Th/U ratios for the near-concordant zircons range from 0.056 to 1.35 with one grain with high Th/U ratio of 13.3. The REE compositions from the near concordant zircons reveal Eu/Eu* values ranging from 0.07 to 1.19, La_N/Yb_N values ranging from 0.0001 to 0.47 and Gd_N/Yb_N values ranging from 0.015 to 0.99.

Figure 4: Kernel Density Estimates (KDE) created using detrital zircon $^{207}\text{Pb}/^{206}\text{Pb}$ age. The KDE for zircons with near-concordant ages (> 85% concordance) has been represented with colour overlain on KDE created using $^{207}\text{Pb}/^{206}\text{Pb}$ ages from all analysed zircons from each detrital sample, here represented with a grey coloured KDE. The number of zircons used in calculating the KDE has been shown on the left with $n = x/y$ format, where x and y represent the number of near-concordant zircons and total analysed zircons respectively. Major detrital age peaks for the coloured KDEs have been calculated using mean $^{207}\text{Pb}/^{206}\text{Pb}$ ages and the age representing the detrital peak is shown in the figure.



4.2 Lu-Hf isotopic analysis:

Lu-Hf isotopic analysis was carried out in situ, on zircons directly adjacent to where the U-Pb, REE data was obtained. Analyses were targeted in the same CL domain as the other analyses. A total of 49 zircons were analysed for Lu-Hf analysis which, shown in figure 5, includes two samples, PD17-42 and PD17-61, to focus on the Paleoproterozoic–Mesoproterozoic crustal processes within the Western Dharwar Craton.

Twenty-six zircons were analysed from the sample PD17-61 representing Holenarsipur Schist Belt (HSB) for Lu-Hf analysis, and the results show initial $^{176}\text{Hf}/^{177}\text{Hf}$ ratios between 0.280521–0.280949. $\epsilon\text{Hf}(t)$ values range between -6.3 to +2.59 for zircons aged between ca. 3.35–3.2 Ga; -0.12 to +8.92 for zircons aged between ca. 3.55–3.35 Ga. The data indicate the involvement of Eoarchean to Paleoproterozoic juvenile sources until 3.35 Ga and a mixture of juvenile Paleoproterozoic and reworked Eoarchean crustal components as sources for the zircons from ca. 3.35–3.2 Ga.

Twenty-three zircons were analysed from the sample PD17-42 representing K.R.Pete Schist Belt (KSB) for Lu-Hf analysis, and the results show initial $^{176}\text{Hf}/^{177}\text{Hf}$ ratios between 0.280683–0.281042. $\epsilon\text{Hf}(t)$ values range between -7.13 to +6.84 for zircons aged between ca. 3.6–3.4 Ga; -5.24 to +4.26 for zircons aged between ca. 3.35–3.1 Ga and -19.61 to -8.79 for zircons younger than ca. 2.9 Ga. The data indicates juvenile Paleoproterozoic sources until ca. 3.4 Ga with a minor contribution from older reworked sources, a mixture of juvenile Paleoproterozoic, and reworked Eoarchean sources.

5. Discussion:

5.1 Detrital zircon U-Pb age constraints, potential source regions and correlations:

The detrital greenstone sequences in the Dharwar craton have been categorised into lithostratigraphic groups namely the Sargur group, and the younger Dharwar supergroup involving Bababudan group, Chitradurga group in the Western Dharwar Craton. The Yeshwantnagar formation is proposed to be analogous to the Bababudan group and the Kolar group greenstone belt is equivalent to the Chitradurga group in the Eastern Dharwar Craton (Ramakrishna and Vaidyanathan, 2008).

The oldest detrital zircons occur in the muscovite bearing quartzite from the Ramagiri greenstone belt, sample PD18-51 (Figure 4). These zircons define a $^{207}\text{Pb}/^{206}\text{Pb}$ age range of ca. 3649 Ma to 3457 Ma clustering at 3558 ± 17 Ma (MSWD = 5.8, $n=13$) in the kernel density estimate. These ages coincide with the presence of similarly-aged detritus from the metasedimentary sequences near the Kolar greenstone belt (Maibam et al., 2016) and Sargur Group (Lancaster et al., 2015). Limited detrital $^{207}\text{Pb}/^{206}\text{Pb}$ ages older than 3.5 Ga also occur in the fuchsite quartzite of the Holenarsipur Schist Belt within the Sargur

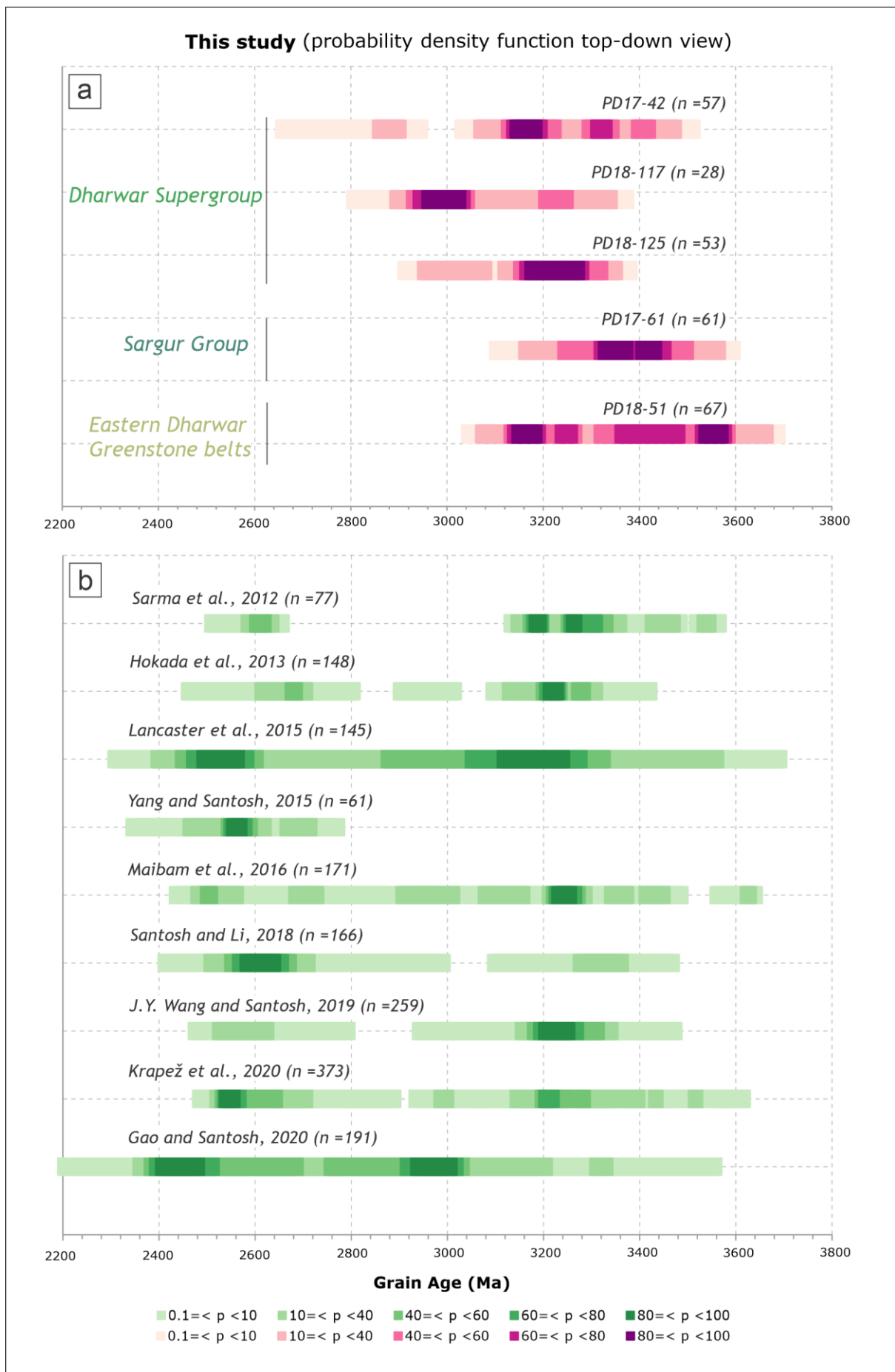
Group (sample PD17-61, Figure 4). The sources for the older Palaeoarchean zircons in PD18-51 are expected to be occurring as relicts within the Mesoarchean basement of the northern part of Eastern Dharwar Craton (Rajamanickam et al., 2014), which are yet to be explored (Maibam et al., 2016). The older TTG gneisses around the Gorur gneiss contain inherited zircons with ages older than 3.5 Ga are interpreted as potential sources for older Palaeoarchean detrital zircons within PD17-61. The occurrence of detrital U–Pb ages older than ~3.5 Ga in the basal detrital sequences of both WDC and EDC suggests the involvement of coeval Palaeoarchean sources in the nucleation of the Dharwar Craton as a whole.

The subsequent crustal building episode within the Dharwar Craton around ca. 3.45 – 3.3 Ga was explained as formed by melting of hydrated basalts at differential crustal depths (Jayandanda et al., 2015; Jayananda et al., 2018). This has been observed from the detrital record of the Ramagiri greenstone belt quartzite (PD18-51) that has a group of zircons that range in $^{207}\text{Pb}/^{206}\text{Pb}$ age from ca. 3457 – 3357 Ma broadly clustering at 3398 ± 25 Ma (MSWD = 18, n = 23); the Holenarsipur greenstone belt (PD17-61) at mean $^{207}\text{Pb}/^{206}\text{Pb}$ age of 3414 ± 12 Ma (MSWD = 1.2, n = 11) until 3346 ± 9 Ma (MSWD = 1.02, n = 13) and fuchsite quartzite near Krishnarajpete (PD17-42) with mean $^{207}\text{Pb}/^{206}\text{Pb}$ age of 3420 ± 22 Ma (MSWD = 2.1, n = 7). In the Western Dharwar Craton, the gneisses to the west of the Holenarsipur schist belt were reported previously for zircons, both inherited and magmatic, at U–Pb age of ca. 3.4 Ga (Guitreau et al., 2017; S. Ranjan et al., 2020). This crustal building episode continued till ca. 3.3 Ga. This is reflected in detrital zircons from the Holenarsipur schist belt (PD17-61) with $^{207}\text{Pb}/^{206}\text{Pb}$ mean age of 3346 ± 9 Ma (MSWD = 1.02, n = 13), the K.R.Pet schist belt (PD17-42) with a mean $^{207}\text{Pb}/^{206}\text{Pb}$ age of 3307 ± 15 Ma (MSWD = 1.8, n = 12) and the fuchsite quartzite to the south of Shimoga (PD18-117) with $^{207}\text{Pb}/^{206}\text{Pb}$ grain ages close to ca. 3.3 Ga. The ca. 3.3 Ga age signature has been reported in the detrital zircon U–Pb age data from several detrital studies across the supra-crustal sequences within the Dharwar Craton as shown in Figure 6 (Sarma et al., 2012; Hokada et al., 2013; Lancaster et al., 2015; Maibam et al., 2016; Santosh and Li, 2018; J.Y. Wang and Santosh, 2020; Krapez et al., 2020; Gao and Santosh, 2020). The sources for the ca. 3.3 Ga zircons in the WDC supra-crustals are proposed to be the older TTG gneisses towards the west of the Holenarsipur schist belt surrounding the Sargur Group greenstone belts (Guitreau et al., 2017; S. Ranjan et al., 2020; Jayananda et al., 2018, Santosh and Li, 2018) and also the reported magmatic U–Pb ages from the gneisses within the WDC from Chapter 2 from the west of Holenarsipur town at constrained protolith ages at 3302 ± 12 Ma (sample PD17-56 in Chapter 2) and 3284 ± 9 Ma (sample PD18-118 in Chapter 2). The Sargur group is proposed to have received primary detritus from the surrounding TTG gneisses, and the overlying detrital groups could have potentially received detritus aged at ca. 3.3 Ga from the combination of surrounding TTG gneisses and the eroding Sargur group greenstone belt. The presence of ca. 3.3 Ga detritus in the KDE of the Ramagiri greenstone belt has been explained to be sourced from the older crustal basement (>3.2 Ga) towards the western

margin of the Central Dharwar Craton (CDC) (Nasheeth et al., 2015; Jayananda et al., 2020), supported by the presence of zircon cores aged at 3301 ± 22 Ma (sample PD18-104 in Chapter 2). Relicts of Paleoproterozoic basement in the CDC interpreted from the inherited zircon with a $^{207}\text{Pb}/^{206}\text{Pb}$ age of 3323 ± 25 Ma, reported from the Closepet Granite in chapter 2 (sample PD17-1) supports the existence of relicts of Meso- to Paleoproterozoic crust in the CDC.

The following crustal building episode in the Dharwar Craton was explained as the two-stage accretion of the oceanic island arc crust resulting in the formation of TTG gneisses between ca. 3.25–3.2 Ga and ca. 3.15–3.0 Ga (Jayananda et al., 2020). The timing of the first stage of accretion has been observed as a significant detrital population in the KDEs of Bababudan Group at detrital age peaks at mean $^{207}\text{Pb}/^{206}\text{Pb}$ ages 3250 ± 10 Ma (MSWD = 0.57, n = 10) and 3194 ± 10 Ma (MSWD = 0.76, n = 12) for the quartzite sample (PD18-125), and at 3224 ± 18 Ma (MSWD = 0.95, n = 4) for the fuchsite quartzite north of Shimoga (PD18-117). This period coincides within the reported ages of detrital zircons between the ages of ca. 3.25–3.2 Ga on the Dharwar Craton (Sarma et al., 2012; Hokada et al., 2013; Lancaster et al., 2015; Maibam et al., 2016; J.Y. Wang and Santosh, 2020; Krapež et al., 2020) shown in Figure 6. In the WDC, the TTG gneisses surrounding the Sargur group and Dharwar Supergroup (which includes the Bababudan Group and the Chitradurga group greenstone belts) form the primary detrital sources for the zircons aged between ca. 3.25–3.2 Ga (Jayananda et al., 2015), whereas the supra-crustal sequences of CDC and EDC are expected to have sourced detrital zircons of this period sourced from the west of Closepet Granite where meta-igneous zircon ages older than ca. 3.2 Ga have been reported (Jayananda et al., 2020).

Figure 5: Top-down view of Probability Density Estimates (PDE) of the samples used in this study compared with published detrital studies used in this study to compare the most probable $^{207}\text{Pb}/^{206}\text{Pb}$ age peaks. The PDE for zircons with near-concordant ages (> 85% concordance) has been plotted with the intensity of the colour representing higher probability shown by the legend below. In figure (a), the sample name is written next to the PDE with n representing the number of zircons used in the creation of the PDE. Figure (b) shows the PDEs representing various detrital studies used to reflect prevalent periods of crustal accretion and magmatism reflected in the detrital record across the craton. The number of zircons used in calculating the PDE is represented by n, and individual $^{207}\text{Pb}/^{206}\text{Pb}$ ages have been used to calculate the PDE.



The timing of the second stage crustal accretion at ca. 3.15–3.0 Ga has been regarded as the time of predominant crustal recycling and metamorphism of the existing crustal components as a consequence of thickening of the crust (Nutman et al., 1992; Jayananda et al., 2013a, 2015, 2018) and intrusion of surrounding granitoids (Nutman et al., 1992; Lancaster et al., 2015). Detrital zircons representing this period have been identified in the detrital record across the meta-quartzites over Dharwar Craton (Maibam et al., 2016; Lancaster et al., 2015; Hokada et al., 2013; Gao and Santosh, 2020; J.Y. Wang and Santosh, 2019; Krapež et al., 2020). In this study except for the kyanite bearing fuchsite quartzite from Holenarsipur Greenstone Belt (PD17-61), this period has been represented as major age peaks among the KDE of the quartzites analysed in the WDC, in the fuchsite quartzite in Shimoga Schist Belt (SSB) (PD18-117) at 2991 ± 16 Ma (MSWD = 1.3, $n = 11$), K.R.Pete Schist Belt (KSB) (PD17-42) at 3105 ± 18 Ma (MSWD = 0.8, $n = 4$) and as a minor population within the KDE representing the detrital zircon record of Ramagiri greenstone belt (PD18-51) and the quartzite near Chikamaguluru, i.e. PD18-125. The potential sources have been noticed as surrounding TTG gneisses experiencing regional metamorphism (Jayananda et al., 2013). The regional metamorphism has been observed in the zircon U–Pb data reported in Chapter 2 from the gneisses to the west of the Chitradurga Greenstone Belt (CGB) (see sample PD18-110 in Chapter 2), and within the exposed basement to the east of CGB (Chardon et al., 2011) and sample PD18-34 in Chapter 2. The sources for the detrital zircons between ages of ca. 3.0–2.9 Ga include a) granitoid batholiths around ca. 3.06–2.94 Ga observed near the Kudremukh formation within the Western Ghat belt (Pahari et al., 2019), b) the Chikamaguluru granitoid pluton reported in Chapter 2 at 3060 ± 16 Ga (see sample PD18-126 in Chapter 2), and c) the pegmatoid bearing gneisses and granites in the vicinity of the CGB (reported in U–Pb data for samples PD17-14, PD17-21, PD17-27 in Chapter 2). The significant population of zircons in the detrital record of the Shimoga Schist Belt at ca. 3.0 Ga can be correlated with the Chitradurga Group greenstone sequences presuming that the zircons from this period have been sourced from the western margin of Chitradurga Greenstone Belt (CGB). However, Krapež et al. (2020) proposed that the Chitradurga Group and the Bababudan Group are spatially linked but temporally unrelated successions.

The youngest near-concordant $^{207}\text{Pb}/^{206}\text{Pb}$ age from the kyanite bearing fuchsite quartzite of Holenarsipur belt within the Sargur Group (PD17-61) is 3174 ± 46 Ma. Monazite U–Th–Pb age data from the kyanite bearing muscovite schists in the Sargur Group were reported at 3082 ± 66 Ma (Hokada et al., 2013) to represent the timing of the metamorphism to kyanite-muscovite grade. The possibility of the monazites being detrital persists lowering the MDA of the Holenarsipur belt towards ca. 3.0 Ga. Recent Sm–Nd isotopic data on layered intrusive ultramafic rocks from Holenarsipur and Nuggihalli greenstone belts within the Sargur Group have produced the youngest reported Sm–Nd isochron age of 2934 ± 88 Ma (Patra et al., 2020) which interpreted to have triggered the intrusive granitoid batholiths

around ca. 3.0–2.9 Ga in the WDC contributing detritus to quartzites belonging to the Bababudan group with MDA of 2925 ± 41 Ma for sample PD18-125 and 2965 ± 33 Ma for sample PD18-117 which coincides with the MDA reported from the basal quartzite of the Deogiri Formation, within the Sandur Group in Central Dharwar Craton, at 2958 ± 20 Ma (Krapež et al., 2020). Sm-Nd isochron age for the Kalasapura formation of the Bababudan group has been reported as 2911 ± 49 Ma (Kumar et al., 1996) which is coeval with the recently proposed MDA for the basal groups of Bababudan Group Greenstone Belt at 2934 ± 88 Ma. Patra et al. (2020) suggested that the Sargur Group rocks represent older ultramafic equivalents of the Dharwar Supergroup, which includes the Bababudan Group.

The fuchsite quartzite near Krishnarajpete (PD17-42) contains detrital zircons younger than ca. 2.9 Ga with the youngest near-concordant (>85% concordance) $^{207}\text{Pb}/^{206}\text{Pb}$ age at 2737 ± 54 Ma with a Th/U ratio of 0.036 which is usually attributed to the zircon experiencing open-system behaviour or metamorphism (Rubatto, 2017; Yakymchuk et al., 2018). This low Th/U ratio has been interpreted as potential Pb-loss event trending towards ca. 2.7 Ga which can be attributed to the formation of the intracontinental rift basin, the Bababudan basin, previously proposed to have initiated from ca. 2765 Ma (Krapež et al., 2020) and followed by the formation of the Chitradurga Group volcano-sedimentary sequences which intervened with simultaneous formation of the Bababudan Group supra-crustal sequences that continued until 2719 ± 7 Ma reported from zircon U–Pb ages from ash-fall tuffs (Trendall et al., 1997; Krapež et al., 2020). Hence, the fuchsite quartzite formation near Krishnarajpete (PD17-42) has been interpreted to be a part of the Bababudan Group stratigraphy. The claims of MDA for the Bababudan Group at two different periods – in the Mesoarchean at 2911 ± 49 Ma (Kumar et al., 1996; Patra et al., 2020) and the Neoarchean at 2719 ± 7 Ma (Trendall et al., 1997; Krapež et al., 2020), show the need for further investigation into the stratigraphic chronology of the Dharwar Supergroup as mentioned by Hokada et al. (2013). This discrepancy in the MDA can be explained by considering the formation of the Bababudan Group occurring in two-stages. The first stage initiated during the 3.0 Ga mafic volcanism and regional metamorphism in the WDC (Jayananda et al., 2013); the second stage of sedimentation happening as a result of Neoarchean mafic volcanism which has been reported across the Dharwar Craton. The alternate explanation for the Bababudan Group is continuous sedimentation across the Bababudan Basin from the Mesoarchean to Neoarchean with the above-contested ages (Trendall et al., 1997; Kumar et al., 1996) acting as the constraints for the opening and closure of the Bababudan basin, but requires further investigation due to lack of zircon populations between ca. 2.9 – 2.72 Ga.

The youngest detrital zircon $^{207}\text{Pb}/^{206}\text{Pb}$ age from the muscovite bearing quartzite from Ramagiri greenstone belt in the CDC is 3089 ± 25 Ma. The metabasalts from Ramagiri greenstone belt have been dated using Sm-Nd isochron at 2746 ± 64 Ma (Zachariah et al., 1995) and associated felsic volcanic

lithologies at 2707 ± 18 Ma (Balakrishnan et al., 1999). The surrounding granitoid rocks were dated using zircon U–Pb dating yielding ages ranging from ca. 2.65 – 2.52 Ga (Jayananda et al., 2020; Balakrishnan et al., 1999). The absence of Neoarchean ages within the detrital record of the sample PD18-51 has been interpreted as the formation of the quartzite occurring as a result of the mafic volcanism across the Hungund-Penakacherla-Ramagiri greenstone belts in the Neoarchean (Zachariah et al., 1995; Balakrishnan, 1990; Nutman et al., 1996) from eroding nearby Meso- to Paleoarchean granitoids and basement gneisses prevalent in the CDC. The sources for the zircons representing the older $^{207}\text{Pb}/^{206}\text{Pb}$ ages at ca. 3.7–3.5 Ga are yet to be reported (Maibam et al., 2016). This interpretation makes the Ramagiri greenstone belt analogous to the formation of the Bababudan Basin within the WDC through ca. 2765 – 2720 Ma (Krapež et al., 2020).

5.2 Interpretation of detrital Lu-Hf isotopic data

The samples PD17-61 and PD17-42 were selected for detrital Lu-Hf isotopic analysis representative of the detrital record of the Dharwar Craton during the period of Paleoarchean until the widespread Neoarchean magmatism around ca. 2.7 Ga. Metasedimentary sequences analysed for Lu-Hf isotopic data are the Holenarsipur Greenstone Belt (PD17-61) within the Sargur Group and the fuchsite quartzite near Krishnarajpete (PD17-42), which has been interpreted to represent the upper stratigraphic unit within the Bababudan Group. Figure 4 shows the Lu-Hf data from this study described as epsilon Hf notation at the timing of crystallisation for the zircon, denoted as $\epsilon\text{Hf}(t)$, to reveal the crustal extraction ages of the source protoliths.

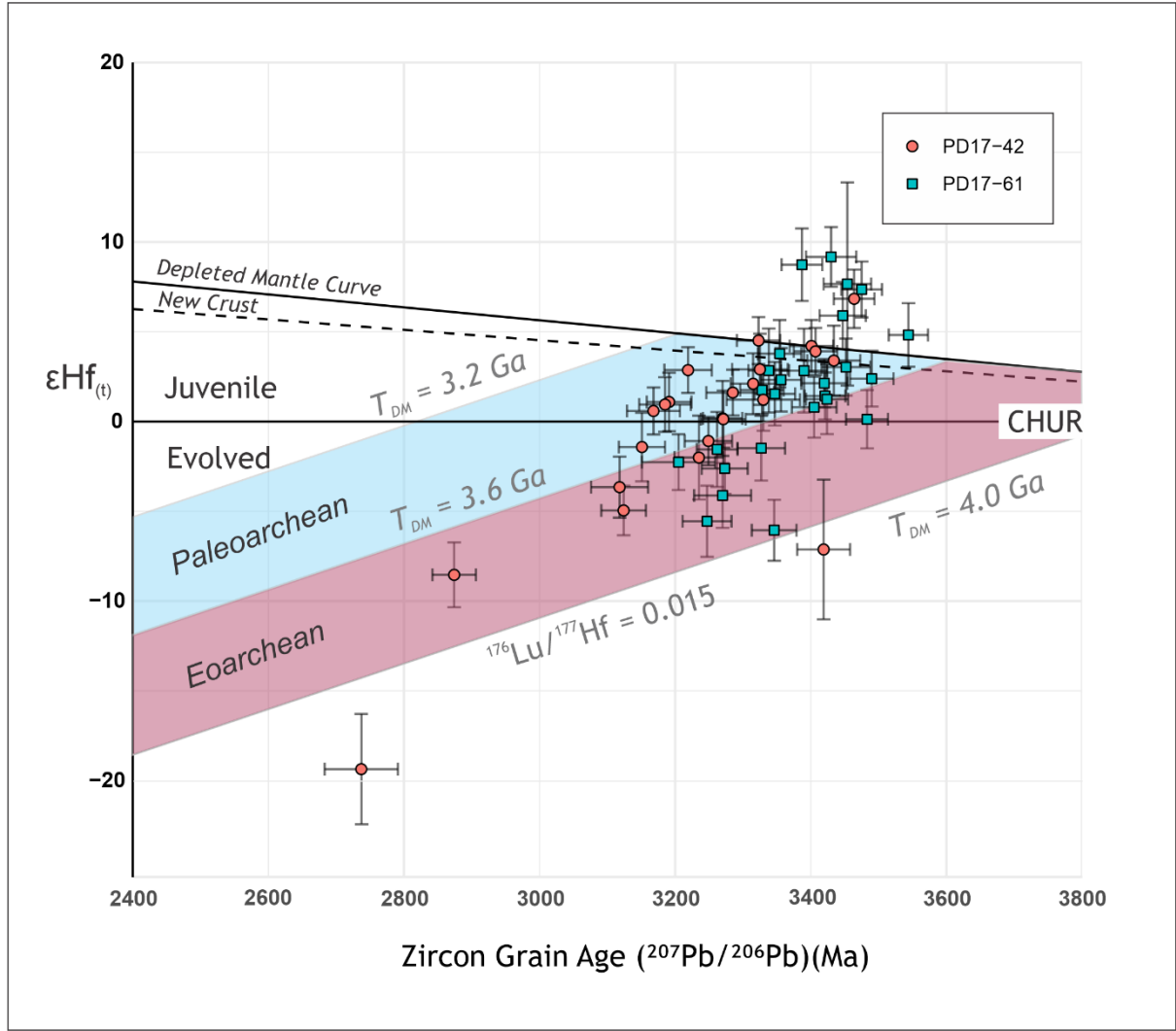


Figure 6: The plot of $\epsilon\text{Hf}(t)$ vs. $^{207}\text{Pb}/^{206}\text{Pb}$ ages for the zircon grains analysed for Lu–Hf isotopic analysis in this study. The uncertainties plotted are at 2σ . CHUR – Chondritic Uniform Reservoir, representing the bulk Earth. The depleted mantle line is calculated by using the $\epsilon\text{Hf}(t)$ equation with the values: modern $^{176}\text{Hf}/^{177}\text{Hf}_{\text{DM}} = 0.28325$ (Griffin et al., 2000) and modern $^{176}\text{Hf}/^{177}\text{Hf}_{\text{CHUR}} = 0.282785$ (Bouvier et al., 2008). The new crust line has been adapted from Dhuime et al. (2011). The values of crustal model ages (T_{DM}^{C}) and crustal evolution lines were calculated using a ^{176}Lu decay constant of $1.865 \times 10^{-11} \text{ year}^{-1}$ (Scherer et al., 2001), modern $^{176}\text{Hf}/^{177}\text{Hf} = 0.28325$, modern $^{176}\text{Lu}/^{177}\text{Hf} = 0.0384$ (Griffin et al., 2000), and a bulk crust value of $^{176}\text{Lu}/^{177}\text{Hf} = 0.015$ (Griffin et al., 2002).

The $\epsilon\text{Hf}(t)$ data in figure 6 for the sample PD17-61 is represented by two clusters zircons. Zircons in the Holenarsipur schist belt with $^{207}\text{Pb}/^{206}\text{Pb}$ ages ranging from ca. 3544 – 3328 Ma define the first cluster with positive $\epsilon\text{Hf}(t)$ values that are interpreted to be derived from juvenile Paleoarchean sources with crustal extraction ages ranging from $T_{\text{DM}} = 3.6\text{--}3.4$ Ga. The zircons with $^{207}\text{Pb}/^{206}\text{Pb}$ ages

ranging from ca. 3346—3205 Ma define the second cluster with negative $\epsilon\text{Hf}(t)$ values interpreted to be derived from evolved Eoarchean sources. This can be explained as the period of juvenile magmatic crust building episodes spanning from ca. 3.6—3.32 Ga has caused pre-existing Eoarchean protoliths to undergo crustal recycling around ca. 3.35—3.2 Ga which had eroded into the Holenarsipur schist belt. The komatiites dated from the vicinity of the Sargur Group, reported to have erupted at Sm-Nd isochron age of ca. 3352 ± 110 Ma (Jayananda et al., 2008), but this age was discounted for its poor precision by Patra et al. (2020) and suggested the usage of SHRIMP $^{207}\text{Pb}/^{206}\text{Pb}$ ages from zircons in a rhyolitic flow from the Holenarsipur greenstone belt at 3298 ± 7 Ma (Peucat et al., 1995) to precisely represent the Sargur supra-crustal rocks. The juvenile mafic, ultramafic magmatism and associated felsic lithologies around ca. 3.35—3.3 Ga could have been the cause for the recycling of the pre-existing Eoarchean protoliths after ca. 3346 Ma that continued till ca. 3205 Ma in the source regions for the Holenarsipur schist belt.

The $\epsilon\text{Hf}(t)$ values for PD17-42 revealed sources that form a linear array interpreted to be a result of continuous continental recycling through ca. 3.4—3.15 Ga with crustal extraction ages ranging from $T_{\text{DM}} = 3.6\text{—}3.4$ Ga, also previously reported by Lu-Hf isotopic studies across the Dharwar Craton (Jayananda et al., 2018; Guitreau et al., 2017; Lancaster et al., 2015). One zircon grain aged at $^{207}\text{Pb}/^{206}\text{Pb}$ age of 3419 ± 39 Ma with an $\epsilon\text{Hf}(t)$ value of -7.12 ± 3.89 with a large error is interpreted to be derived from an evolved Eoarchean source protolith. The zircons younger with $^{207}\text{Pb}/^{206}\text{Pb}$ ages younger than ca. 3150 Ma in this sample reveal negative $\epsilon\text{Hf}(t)$ values that show a continuous recycling trend until ca. 2874 ± 32 Ma interpreted to derived from sources with crustal extraction ages in the Eoarchean which is interpreted to be sourced from further reworking of source protoliths for the Sargur Group supra-crustal rocks with crustal extraction ages in the Eoarchean. A highly negative $\epsilon\text{Hf}(t)$ value of -19.36 ± 3.07 at ca. 2737 ± 54 Ma has been regarded as an anomaly and excluded from interpretation due to low Th/U ratio, $\text{Th}/\text{U} = 0.036$, measured during the collection of U-Pb age data with suspected open-system behaviour for the zircon grain.

5.3 Comparison with published detrital and magmatic Lu-Hf isotopic studies on the Dharwar Craton

Craton-wide isotopic studies have played a substantial role in the understanding of the crustal evolution and architecture of the Dharwar Craton. The detrital zircon Lu-Hf isotopic datasets have put forth the crustal evolution history of the Dharwar Craton as explained by comparing the $\epsilon\text{Hf}(t)$ values from detrital sequences across the western and eastern domains of the craton (WDC and EDC) (Lancaster et al., 2015; Maibam et al., 2016; Krapež et al., 2020). The detrital record of the Chitradurga Greenstone Belt (CGB) and Gadag Greenstone Belt (GGB) (Hokada et al., 2013; Sarma et al., 2012; Krapež et al., 2020) have contributed in understanding the process of mafic volcanism and

sedimentation during the Archean between WDC and CDC. The published Lu-Hf data from the detrital sequences across Dharwar Craton, compiled into a comprehensive database in this study, aids in further constraining the relationship between the evolutionary histories of crustal domains within the Dharwar Craton, now divided into Western Dharwar Craton (WDC), Central Dharwar Craton (CDC) and Eastern Dharwar Craton (EDC) (Peucat et al., 2013; Jayananda et al., 2018, 2020; Santosh and Li, 2018).

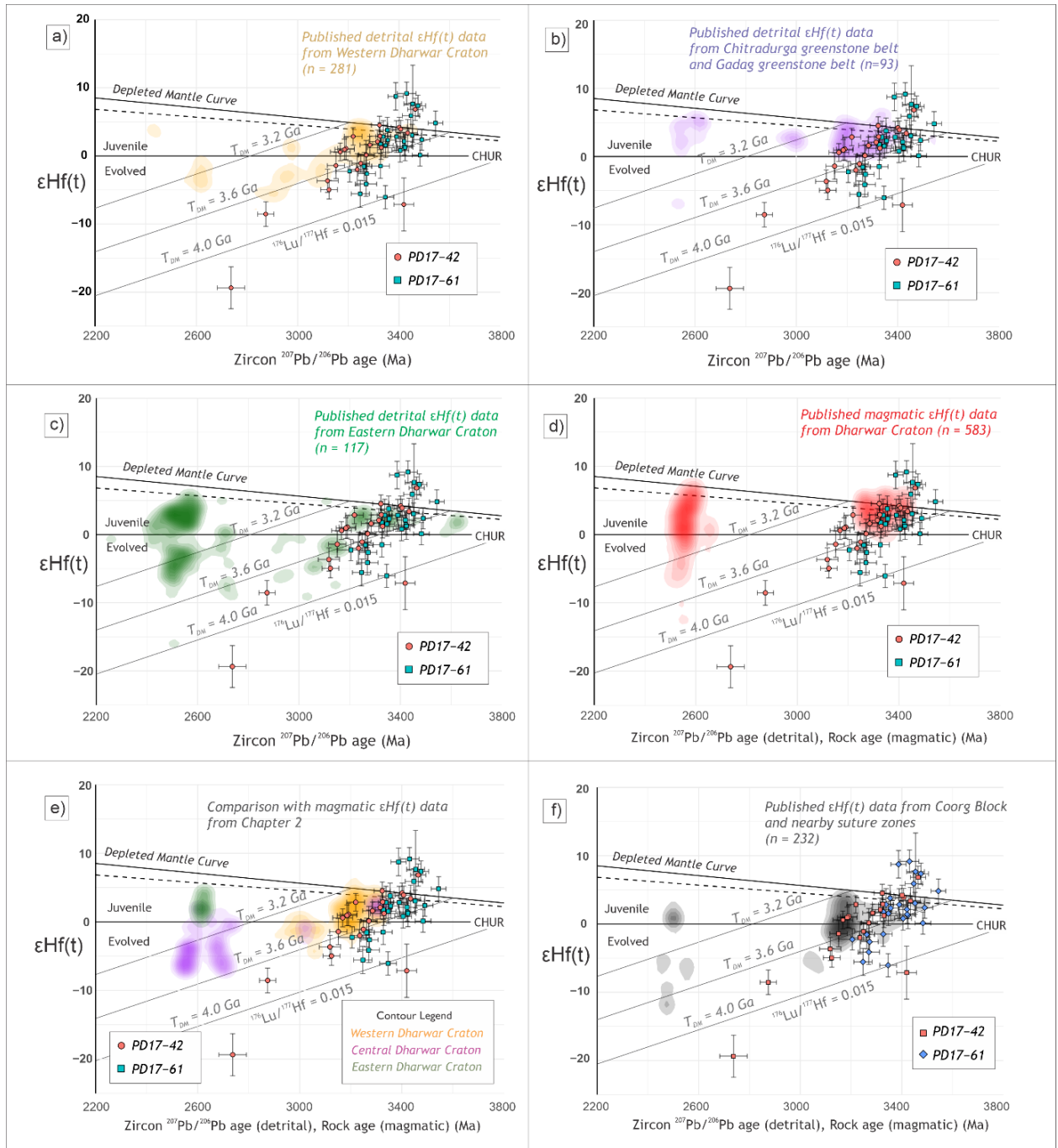


Figure 7: The plot of $\epsilon\text{Hf}(t)$ vs. $^{207}\text{Pb}/^{206}\text{Pb}$ ages for the zircon grains analysed for Lu–Hf isotopic analysis in this study compared to published detrital and magmatic zircon Lu–Hf data across the Dharwar Craton and Coorg Block plotted as density contour plot. The number of analyses used to create the density plot is shown on the top right (n). (a) The $\epsilon\text{Hf}(t)$ values compared against published detrital zircon $\epsilon\text{Hf}(t)$ data from the detrital units associated with the WDC plotted here as density plot in $\epsilon\text{Hf}(t)$ space; (b) The $\epsilon\text{Hf}(t)$ values compared against published detrital zircon $\epsilon\text{Hf}(t)$ data from the detrital units associated with detrital studies along the Chitradurga Shear Zone, which marks the boundary between WDC and CDC, plotted as density plot; (c) $\epsilon\text{Hf}(t)$ values compared against published detrital zircon $\epsilon\text{Hf}(t)$ data from the detrital units associated with the former Eastern Dharwar Craton (includes CDC and EDC); (d) $\epsilon\text{Hf}(t)$ values compared against published zircon $\epsilon\text{Hf}(t)$ data from magmatic and meta-igneous lithologies within the Dharwar Craton (references mentioned in Chapter 2); (e) $\epsilon\text{Hf}(t)$ values compared against reported zircon $\epsilon\text{Hf}(t)$ data from the meta-igneous lithologies from Chapter 2; (f) $\epsilon\text{Hf}(t)$ values compared against published detrital zircon $\epsilon\text{Hf}(t)$ data from the detrital and meta-igneous units associated with the Coorg Block, Mercara Shear Zone.

In this chapter, we compare our results with published detrital and magmatic Lu–Hf isotopic data from the Dharwar Craton (Sarma et al., 2012; Hokada et al., 2013; Lancaster et al., 2015; Yang and Santosh, 2015; Maibam et al., 2016; Santosh and Li, 2018; J.Y. Wang and Santosh, 2019; Krapež et al., 2020; Gao and Santosh, 2020) categorising based on their association with the western and eastern domains within the Dharwar Craton in Figure 7. The published Lu–Hf data have been expressed as $\epsilon\text{Hf}(t)$ data plotted against the reported zircon $^{207}\text{Pb}/^{206}\text{Pb}$ age as a density plot. The detrital sequences occurring to the west of the Chitradurga Greenstone belt (CGB) have been regarded as being associated with the Western Dharwar Craton (WDC). The detrital sequences to the east of CGB have been categorised to be associated with the former Eastern Dharwar Craton, which is divided further into the CDC and EDC (Peucat et al., 2013; Jayananda et al., 2020; Santosh and Li, 2018). The detrital Lu–Hf data from the Chitradurga Greenstone Belt (CGB) and Gadag Greenstone Belt have been compared separately due to their occurrence along the Chitradurga Shear Zone (CSZ), which acts as the dividing boundary between WDC and CDC (Ramakrishnan and Vaidhyanathan, 2008). The $\epsilon\text{Hf}(t)$ data published on the magmatic and meta-igneous granitoids (references in Chapter 2) across the entire Dharwar Craton has also been compared to the detrital data from this study to compare potential source regions. The reported magmatic and meta-igneous $\epsilon\text{Hf}(t)$ data from Chapter 2 has also been used to compare likely source regions and the continental evolution trend in $\epsilon\text{Hf}(t)$ plot.

The figure 7 (a) shows the published detrital $\epsilon\text{Hf}(t)$ for WDC detrital units plotted as density plot, which reveals the evolution trend of the source regions that show progressive crustal growth and recycling initiating around ca. 3.3 Ga from juvenile protoliths that were extracted at $T_{\text{DM}} = 3.7\text{--}3.2$ Ga and continued till 2.8 Ga. The WDC was intruded at 2.6 Ga, by reworked magma from a combination of Meso- to Neoarchean sources. The $\epsilon\text{Hf}(t)$ data for the K.R.Pet schist belt (PD17-42) correlates effectively with the evolution trend formed by the published detrital Lu–Hf record of the WDC until ca

3.15 Ga with Paleoproterozoic crustal extraction ages. The negative $\epsilon_{\text{Hf}}(t)$ values from 3.35 Ga in the detrital history of the Holenarsipur schist belt (PD17-61) show different sources extracted from the mantle during the Eoarchean. The presence of monazite and kyanite in the quartzites in Holenarsipur schist belt (HSB) with the age of monazite at 3082 ± 66 Ma (Hokada et al., 2013) along with the proposed maximum depositional age (MDA) for the HSB at 2934 ± 88 Ma (Patra et al., 2020), interpreted as detrital monazite and kyanite being deposited in the HSB after 2934 Ma. The collision of the Coorg Block with the WDC creating kyanite, sillimanite bearing assemblages in the Mercara Shear Zone around 3.0 Ga (Amaldev et al., 2016) supports this interpretation. Lu-Hf isotopic data from the Coorg block and Mercara Shear Zone (Santosh et al., 2014, 2015; Amaldev et al., 2016) reveal negative $\epsilon_{\text{Hf}}(t)$ values around ca. 3.35–3.1 Ga with crustal extraction ages dating back to the Eoarchean (see Figure 7(f)). These $\epsilon_{\text{Hf}}(t)$ values correlate with the presence of similar zircons in the detrital record of HSB and KSB. This correlation suggests that the Coorg Block along with Mercara Shear Zone is a likely detrital source to the HSB for the zircons crystallising from an evolving Eoarchean protolith. The $\epsilon_{\text{Hf}}(t)$ data from the southern part of the Coorg Block also correlate with the negative $\epsilon_{\text{Hf}}(t)$ values reported from the K.R.Pet Schist Belt (KSB) from ca. 3.15–2.85 Ga with Eoarchean crustal extraction ages suggesting the involvement of the Coorg Block in the detrital record of the KSB.

The Lu-Hf data zircons from the detrital record of Chitradurga Greenstone Belt (CGB) and the Gadag Greenstone Belt (GGB) represented as $\epsilon_{\text{Hf}}(t)$ in figure 7(b), reveal that the detrital sources for the zircons aged between $^{207}\text{Pb}/^{206}\text{Pb}$ ages of ca. 3.3–3.15 Ga to be derived from juvenile depleted-mantle sources with short crustal residence times with crustal extraction ages in the Paleoproterozoic. The CGB and GGB share similar origins as the for detrital zircons with $^{207}\text{Pb}/^{206}\text{Pb}$ ages between ca. 3.3–3.1 Ga with the KSB, ca. 3.3 Ga with the HSB.

Figure 7(c) shows the $\epsilon_{\text{Hf}}(t)$ values reported from the detrital record of the former Eastern Dharwar Craton (CDC and EDC) represented as a density plot. Positive $\epsilon_{\text{Hf}}(t)$ values around ca. 3.65–3.55 Ga are interpreted to infer sources with shorter crustal residence time and have crustal extraction ages in the Paleoproterozoic (Maibam et al., 2016). These sources are proposed to have acted as the pre-cursors for the protoliths derived from evolved Paleoproterozoic sources, reported in the detrital record of the HSB (PD17-61). This interpretation provides an alternative explanation the zircons younger than 3.25 Ga with Paleoproterozoic crustal extraction ages in the detrital history of the HSB and KSB are derived from identical sources that have deposited similar zircons into the detrital record of the former Eastern Dharwar Craton. The similarity between the crustal extraction ages of the Paleoproterozoic zircons in the detrital histories of the Coorg Block and the Central, Eastern Dharwar blocks, from the density plots in figures 7(c) and 7(f), requires further investigation. This hypothesis is justified by considering similar sources contributing detritus to the detrital sequences within Coorg Block and the Central and Eastern

domains of Dharwar Craton. The most likely sources would be the basement gneisses and granitoid plutons occurring within the Western Dharwar Craton weathering on a large scale as observed by the spatial coverage of detrital sequences within the Western Dharwar Craton (e.g. Sirsi Shelf and greywacke formations north of Shimoga).

The $\epsilon\text{Hf}(t)$ values from this study have been compared to the published Lu-Hf data from Dharwar Craton to correlate the source regions with the reported detrital ages, as shown in figure 7(d). The older detrital zircons within the HSB and KSB between ca. 3.4–3.2 Ga with positive $\epsilon\text{Hf}(t)$ values correspond to be sourced from coeval juvenile lithologies in the Dharwar Craton. The $\epsilon\text{Hf}(t)$ values representing the published magmatic and meta-igneous granitoids across Dharwar Craton shows a gap in the record of the evolution of the craton between ca. 3.1–2.7 Ga due to lack of sampling or the localised nature of the studies published, and also does not represent the episodes of mafic volcanism across the Dharwar Craton. To complement the published magmatic Lu-Hf record of the Dharwar Craton, we compare the $\epsilon\text{Hf}(t)$ values from this study against the Lu-Hf data reported from Chapter 2 which includes magmatic and meta-igneous lithologies which also represent cratonisation episodes during ca. 3.0–2.9 Ga and categorised based on the sampled domain with the Dharwar Craton shown in figure 7(e). Similar to the correlation shown in figure 7(d), the juvenile $\epsilon\text{Hf}(t)$ values in the Paleoproterozoic detrital zircons correspond to the juvenile signatures from the oldest units dated in the Western Dharwar Craton and Central Dharwar Craton in Chapter 2. The Mesoproterozoic $\epsilon\text{Hf}(t)$ values from the KSB correlate with the evolution trend of the Western Dharwar Craton (WDC) (Lancaster et al., 2015; Jayananda et al., 2018) inferring the Mesoproterozoic lithologies in the WDC as the source regions for the KSB.

In conclusion, the detrital record of the Sargur Group and the lower Bababudan Group have been sourced from relicts of different pre-cursors for the Dharwar Craton until ca. 3.3 Ga. The Sargur Group has received detritus from juvenile to evolved crustal lithologies with crustal extraction ages in the Eoproterozoic possibly from the Coorg Block or other similar Archean cratons existing during that period (e.g. North China Craton (Lancaster et al., 2015)). The detrital zircons of Sargur Group with crustal extraction ages in the Paleoproterozoic are sourced from the surrounding TTGs and related granitoids in the WDC. The K.R.Pete Schist Belt (KSB) potentially representing the Bababudan Group received detritus mostly from the lithologies preserved in the WDC and CDC that formed during the Paleo- to Mesoproterozoic from the correlation between the $\epsilon\text{Hf}(t)$ values of the KSB, and the meta-igneous record of the Dharwar Craton reported in Chapter 2.

5.4 Detrital Zircon Rare Earth Element data and depth of crystallisation of source protoliths:

The zircons analysed for U–Pb data were simultaneously measured for rare earth element (REE) concentrations. The europium anomalies in the zircons represented by Eu/Eu^* values ($\text{Eu}/\text{Eu}^* = \text{Eu}/\sqrt{(\text{Sm}_N \times \text{Gd}_N)}$) are measured to infer the changes in the amount of feldspar over time. Zircon Eu/Eu^* reflects the ratios of $\text{Eu}^{3+}/\text{Eu}^{\text{total}}$ for the crystallising melt hosting the zircons which can be used qualitatively to estimate the fraction of plagioclase or alkali feldspar (Trail et al., 2012; Holder et al., 2020). The Eu/Eu^* in zircon can be influenced by the growth and breakdown of feldspars and plagioclase (Holder et al., 2015, 2020; Rubatto et al., 2006, 2013) which is sensitive to changes in pressure and temperatures because of processes like high-pressure metamorphism and partial melting (Holder et al., 2020). The ratios between light rare earth elements (LREE) and middle rare earth elements (MREE) against the heavy rare earth elements (HREE) in zircon have been used to correlate with regional-scale trends in the depth of crystallisation and magma diversification (Chapman et al., 2015; Profeta et al., 2015; Farner and Lee, 2017; McKenzie et al., 2018). Elevated LREE/HREE and MREE/HREE ratios in zircons are predicted to occur in rocks experiencing fractionation in the presence of garnet and amphibole, which both require pressures greater than 1 GPa (Rapp and Watson, 1995; Rubatto, 2002). The temperatures needed for the formation of such residual phases could not be easily translated into geodynamic regimes due to the early Earth's mantle being generally hotter with higher thermal gradients that are compared to be equivalent to the metamorphism at the base of thickened Archean mafic crust (Huang et al., 2020). The MREE/HREE ratio is more resistant to open system and thermal diffusion behaviour in zircon that has the propensity to sequester heavy rare earth elements (HREE) into its crystal lattice relative to light rare earth elements (LREE). Oceanic crust melting during subduction resulting in intermediate magmas with low LREE/HREE ratios, due to LREE depleted nature of mid-oceanic ridge basalts (MORB) (Defant and Drummond, 1990), which could affect the LREE/HREE ratios in the zircons crystallising in the melt. The caveat for using these trace-element ratios to infer the depth of crystallisation of sources is the assumption that the fractionation of REEs into the zircons occurs during crystallisation alone and not by other processes that involve partitioning of REEs from the crystallising melt (McKenzie et al., 2018; Holder et al., 2020). This assumption includes that the petrogenesis of the tonalite-trondhjemite-granodiorite (TTG) lithologies has occurred majorly by partial melting of thickened tholeiitic crust (Condie et al., 1994; McKenzie et al., 2018) as the TTGs form the primary detrital sources for the Neoarchean and Mesoarchean detrital sequences reported in this study. We have plotted, in figure 8, the REE compositions from the near-concordant (> 85% concordance) against the measured $^{207}\text{Pb}/^{206}\text{Pb}$ age as the discordant zircons were suspected of displaying open-system behaviour.

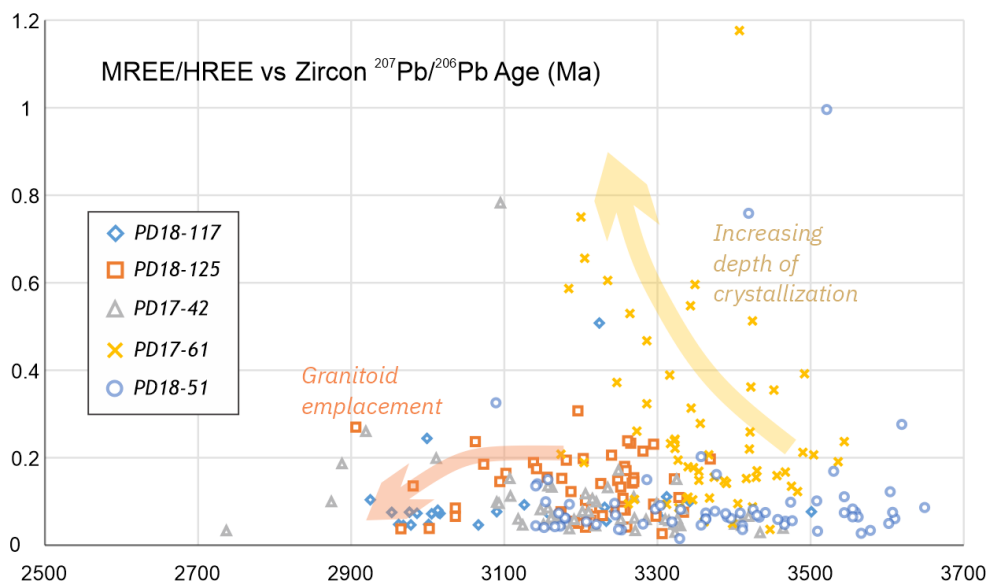
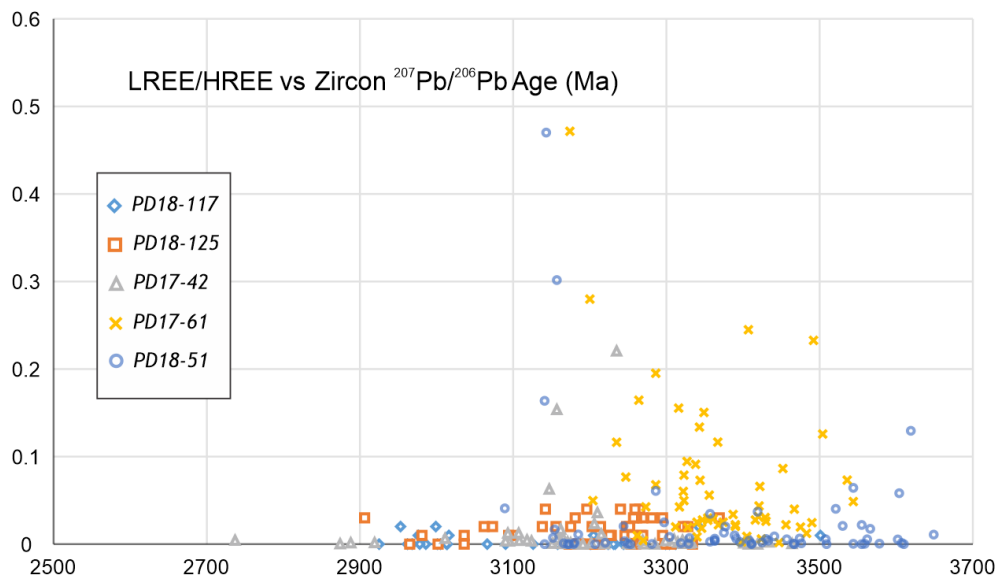
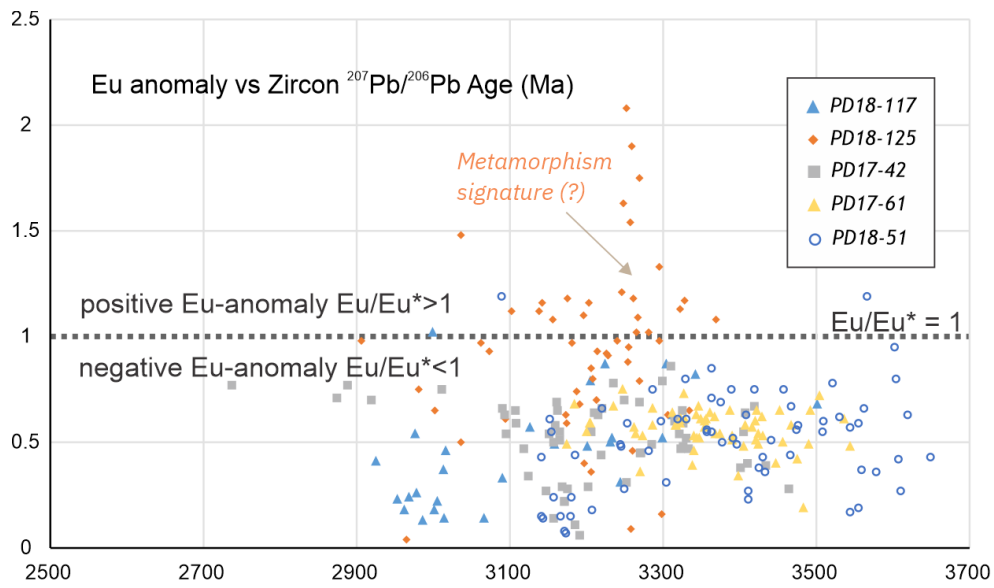


Figure 8: The Rare Earth Element composition from analysed zircons plotted against $^{207}\text{Pb}/^{206}\text{Pb}$ ages with concordance greater than 85%. The concentrations of REE have been normalised to chondritic values from Bonython et al., 1984. (a) Eu-anomaly represented by $(\text{Eu}/\text{Eu}^)_N$ plotted against $^{207}\text{Pb}/^{206}\text{Pb}$ ages for near-concordant zones. The dotted line represents $\text{Eu}/\text{Eu}^* = 1$ interpreted as zircons exhibiting no Eu-anomaly. (b) LREE/HREE ratio represented by La_N/Yb_N plotted against $^{207}\text{Pb}/^{206}\text{Pb}$ ages with individual zircons coloured using the legend in the inset. (c) MREE/HREE ratio represented by Gd_N/Yb_N plotted against $^{207}\text{Pb}/^{206}\text{Pb}$ ages with individual zircons coloured using the legend in the inset. Arrows represent the trends observed in the REE plots to infer the depth of crystallisation of the protolith.*

Figure 8(a) shows the Eu-anomalies in zircon plotted against the measured $^{207}\text{Pb}/^{206}\text{Pb}$ age. The values of Eu/Eu^* show negative Eu-anomalies ($\text{Eu}/\text{Eu}^* < 1$) varying between 0.3–0.7 during the period ca. 3.55–3.25 Ga in the zircons representing the detrital record of the Ramagiri Greenstone Belt (RGB), Holenarsipur Schist Belt (HSB) and the K.R.Pet Schist Belt (KSB). The varying negative Eu-anomalies represent the variable amount of plagioclase or alkali feldspars within the crystallising melt which could be explained by the variance in partial melting of the tholeiitic basalt (Nagel et al., 2012) involved in the generation of TTG magmas. The quartzite near the Chikamagalur pluton (PD17-125) revealed zircons that display highly positive Eu-anomaly ($\text{Eu}/\text{Eu}^* > 1$) around ca. 3.25 Ga, which continued until ca. 3.1 Ga with slightly positive Eu-anomalies. The positive Eu-anomalies could be related to zircon saturation occurring before plagioclase/feldspar fractionation (Trail et al., 2012) as a result of non-equilibrium processes such as metamorphism or alteration. Hence the zircons around ca. 3.2–3.1 Ga reported from PD18-125 possibly represent the beginning of metamorphic processes that occurred during the crustal building episodes involving metamorphism and reworking in the Dharwar Craton about ca. 3.15–3.0 Ga (Jayananda et al., 2018). The melts generated as a result of such reworking processes, like the melting of subducted basalts, would be depleted in LREE (Martin et al., 2014). These in turn, would crystallise high fractions of feldspars/plagioclase and zircons with highly negative Eu-anomalies. Zircons with highly negative Eu-anomalies are observed (figure 8 (a)) around ca. 3.2–3.1 Ga in the samples from the KSB (PD17-42) and the RGB (PD18-51) inferring that the reworking was craton-wide during this period. The zircons around ca. 3.0 Ga from the fuchsite quartzite near Shimoga town (PD18-117) show similar highly negative Eu-anomalies and could have been sourced from the granitoid plutons, with high feldspar fraction, emplaced in the WDC around 3.1–3.0 Ga that formed as a result of the previous craton-wide reworking. One such Mesoarchean granitoid pluton was reported in Chapter 2 from the Chikamagalur granite (PD18-126 in chapter 2) at 3060 ± 16 Ma. The zircons with $^{207}\text{Pb}/^{206}\text{Pb}$ ages between ca. 3.05–2.85 Ga from the KSB and sample PD18-125 exhibit Eu-anomaly values closer to 1 ($\text{Eu}/\text{Eu}^* = 1$) suggesting the presence of residual garnet in the source, but requires further evidence to confirm.

$\text{La}_\text{N}/\text{Yb}_\text{N}$ and $\text{Gd}_\text{N}/\text{Yb}_\text{N}$ values from zircons represent the LREE/HREE and MREE/HREE ratios, plotted against $^{207}\text{Pb}/^{206}\text{Pb}$ ages in figure 8(b), 8(c) respectively. The lower LREE/HREE and MREE/HREE ratios in zircons represent the source magmas being generated at lower levels of thickened crust or a volcanic plateau (Huang et al., 2020) which was observed throughout the detrital record of all the detrital units reported in this study. The LREE/HREE and MREE/HREE ratios in zircons from the Holenarsipur Schist Belt (HSB) reveal an increasing trend in $\text{La}_\text{N}/\text{Yb}_\text{N}$, $\text{Gd}_\text{N}/\text{Yb}_\text{N}$ ratios from ca. 3.5–3.2 Ga. These zircons could have been sourced from TTG magmas that have crystallised from sources with increasing residual garnet and amphibole (Huang et al., 2020) which require high pressures (> 1 GPa) (Rapp and Watson, 1995). This high-pressure signature in the geochemistry of TTGs, produced before the Neoproterozoic, has been explained as evidence for the beginning of localised subduction in the early Earth in the process of a secular change in the global tectonic regime (Huang et al., 2020). Hence, we conclude that the zircons showing an increasing trend of LREE/HREE and MREE/HREE ratios in the HSB are likely to be sourced from a localised subduction-like regime forming small island arcs, which accreted together until ca. 3.2 Ga across the Dharwar Craton, as previously proposed by Guitreau et al. (2017). Subduction-accretion processes could have been prevalent in the Mesoproterozoic previously reported by trace-element systematics in greenstone belts in the Yilgarn and Pilbara cratons in Australia (Smithies et al., 2018). The Sargur Group, to which the HSB belongs to, is interpreted to represent an example of a Mesoproterozoic greenstone belt preserving oceanic crust due to subduction-accretion processes (Patra et al., 2020). Elevated LREE/HREE ratios are also observed in the zircons from the Ramagiri Greenstone Belt (RGB) and K.R. Pete Schist Belt (KSB) aged between ca. 3.2–3.1 Ga, inferring similar source regions as the HSB for zircons of this period. The quartzite (PD18-125) near Chikamagalur also revealed zircons with relatively high LREE/HREE ($\text{La}_\text{N}/\text{Yb}_\text{N} > 0.04$) and MREE/HREE ($\text{Gd}_\text{N}/\text{Yb}_\text{N} > 0.15$) ratios during the periods of ca. 3.25–3.1 Ga, which could have been sourced from reworked magmas through localised subduction occurring near the HSB, with lower fractions of residual garnet and amphiboles. The lower MREE/HREE and LREE/HREE ratios in zircons aged between ca. 3.05–2.95 Ga in the detrital record of samples PD18-125 and PD18-117 reveal identical sources which could have formed at lower levels of thickened crust. The MREE/HREE ratios at ca. 2.9 Ga, in figure 8(c), are relatively higher, possibly representing the thickening of the crust, marking the end of Mesoproterozoic cratonisation of the Dharwar Craton (Lancaster et al., 2015). The initiation of subduction style tectonics in the Dharwar Craton has been extended to the Neoproterozoic where it was explained as the preservation of oceanic crust as an Archean analogue of melange formation in the Paleozoic era (Gao and Santosh, 2020).

The Eu-anomalies, LREE/HREE and MREE/HREE ratios reported from the detrital sequences are consistent with the interpretations from the magmatic and meta-igneous granitoids detailed in

Chapter 2 (figure 12, Chapter 2). The meta-igneous zircon record from Chapter 2 reveals elevated LREE/HREE and MREE/HREE ratios from zircons around ca. 3.2–3.1 Ga which were collected from the TTGs and granitoids concentrated in the Western Dharwar Craton and to the east of Chitradurga Greenstone Belt (CGB) in the Central Dharwar Craton, interpreted to have crystallised under thickened crust with residual garnet and amphibole. Meta-igneous zircons, crystallising between ca. 3.1–2.95 Ga (Chapter 2), show lower LREE/HREE and MREE/HREE which could be interpreted as potential source regions for zircons reported in PD18-117, PD18-125 and the KSB (PD17-42) with similar $^{207}\text{Pb}/^{206}\text{Pb}$ ages.

5.5 Stratigraphic and Tectonic implications:

The WDC experienced limited sedimentation in the Mesoarchean which was confined in the form of narrow linear belts that could be explained by submarine sedimentation. Widespread distribution of the upper Neoarchean greenstone and detrital units suggest the emergence of the Western Dharwar Craton above the sea-level between the Mesoarchean–Neoarchean, with sedimentation happening northward towards the Shimoga Schist Belt followed by the formation of the Gadag Duplex. The basal units from the Shimoga Schist Belt have comparable MDA with the Bababudan Group but regarded as a basal group belonging to the Chitradurga Group, inferring the correlation of the basal units of Chitradurga Group and Bababudan Group. We suggest the Dharwar Supergroup consisting of the similar basal units and lower groups which branched out into different sub-groups based on the spatial occurrence of the upper Neoarchean detrital units into Chitradurga and Bababudan Groups. The Chitradurga Group has detrital groups that are younger than the upper groups of the Bababudan Group greenstone belts. The K.R.Pete Schist Belt is correlated with the lower groups within the Dharwar Supergroup instead of its previous association with the Sargur Group. The Ramagiri Greenstone Belt can be considered an equivalent to the upper groups of the Bababudan Group that is estimated to have formed around ca. 2.7 Ga and proposed to have formed with limited deep-water sedimentation resulting in narrow linear belts.

The positive $\epsilon\text{Hf}(t)$ values from ca. 3.4 Ga, in this study, reveal episodes of juvenile crustal extraction from ca. 3.4 Ga (Guitreau et al., 2017) and reworking of inherited Eoarchean–Paleoarchean pre-cursors which we propose to have been inherited from the same pre-cursors for the Coorg Block. The Coorg Block contributed to the detrital units forming in the Western Dharwar Craton observed in the similarities in $\epsilon\text{Hf}(t)$ values of detrital zircons reported in this study with the density plot of $\epsilon\text{Hf}(t)$ values reported from the Coorg Block and Mercara Shear Zone (Santosh et al., 2015, 2016; Amaldev et al., 2016). This supports the collisional accretion between the Coorg Block and Western Dharwar Craton occurring around ca. 3.1 Ga (Amaldev et al., 2016). The MREE/HREE ratios plotted against $^{207}\text{Pb}/^{206}\text{Pb}$ age reveal an increasing depth of crystallisation between ca. 3.5–3.2 Ga, coupled with the positive Eu-

anomalies around ca. 3.25 Ga suggest localised subduction style reworking (Huang et al., 2020) in the WDC during the Paleoproterozoic resulting in the emplacement of protoliths which show a positive Eu-anomaly in their zircons. This reworking is supported by negative $\epsilon_{\text{Hf}}(t)$ values from zircons crystallising after ca. 3.25 Ga in the detrital record reported from the Holenarsipur Schist Belt (HSB) and the K.R.Pete Schist Belt (KSB).

6. Conclusion:

- 1) Comparison with ~1300 previously published Lu-Hf isotopic data from detrital zircons in a categorical manner reveal similarities in provenance to each other and also correlate with our data.
- 2) The WDC had multiple episodes of sedimentation that coincide with the episodes of crustal accretion from multiple sources witnessed by similar Eoarchean crustal extraction ages between the detrital zircon record of the WDC and the crustal extraction ages in Mercara shear zone, Coorg Block, WDC, CDC, EDC sequences.
- 3) The WDC experienced limited sedimentation in the Mesoproterozoic in form of linear narrow belts that could have occurred through submarine sedimentation. During the Neoproterozoic, there was extensive sedimentation of the Neoproterozoic greenstone sequences leading to widespread upper greenschist detrital sequences.
- 4) The basal group within the Shimoga Schist Belt has comparable maximum depositional age (MDA) with the Bababudan Group. From the detrital zircon record, these groups are correlated to the basal groups of the Chitradurga Group. The lithostratigraphic correlation of the K.R. Pete Schist Belt with the Dharwar Supergroup is at the basal groups of the Bababudan Group, instead of the Sargur Group as previously mapped, and is also proposed here to be an equivalent to the basal groups of the Chitradurga Group. The Ramagiri Group in the EDC can be considered an equivalent to the upper groups of the Bababudan group which formed at ca. 2.7 Ga with the assumption that the Bababudan group has formed during two episodes of sedimentation.
- 5) The +ve $\epsilon_{\text{Hf}}(t)$ values from ca. 3.4 Ga detrital zircons reveal juvenile crustal extraction from ca. 3.5 Ga onwards with a potential reworking of Eoarchean precursors inherited alongside the crustal evolution of the CDC, EDC and the Coorg Block.
- 6) The Coorg Block and the Dharwar Craton could have shared similar pre-cursors which evolved during juvenile accretionary events across the Coorg Block and WDC. This leads to the conclusion that the Coorg Block contributed detritus to the Mesoproterozoic detrital sequences across WDC and shared similar crustal evolution history with the WDC until the Neoproterozoic.

- 7) The MREE/HREE ratios from the detrital zircons in the HSB reveal an increasing depth of crystallization with time inferring a localised subduction zone near the Holenarsipur greenstone belt around ca. 3.2 Ga and the decreasing MREE/HREE ratios in the detrital sequences near the Bababudan Group reveal the decreasing depth of crystallization which could infer granitoid emplacement such as the Chikamagalur pluton.

7. Acknowledgements:

We acknowledge the support of Dr Sarah Gilbert for support at Adelaide Microscopy who has been instrumental in the acquisition of the zircon U–Pb and REE data using LA–ICPMS respectively during 2017 and 2018. We acknowledge the John De Laeter Centre at Curtin University, Western Australia for facilitating the detrital zircon Lu–Hf isotopic analysis. The Petrology lab team at Indian Institute of Science, India are acknowledged for their assistance during fieldwork logistics and sample preparation. Mr Kiran Sasidharan and Mr Thamam Mubarish are acknowledged for the assistance in fieldwork. Pavan Katuru is supported during his PhD by the scholarship provided by the University of Adelaide.

8. Appendix:

Zircon U–Pb data provided in appendix 3.1. The REE compositions of the detrital zircons provided in appendix 3.2. Detrital zircon Lu–Hf isotope data provided in appendix 3.3.

9. References:

- 1) Amaldev, T., M. Santosh, L. Tang, K. R. Baiju, T. Tsunogae and M. Satyanarayanan (2016). "Mesoarchean convergent margin processes and crustal evolution: Petrologic, geochemical and zircon U–Pb and Lu–Hf data from the Mercara Suture Zone, southern India." *Gondwana Research* 37(Supplement C): 182-204.
- 2) Balakrishnan, S. , Rajamani, V. , and Hanson, G.N. 1999, U–Pb Ages for Zircon and Titanite from the Ramagiri Area, Southern India: evidence for accretionary origin of the Eastern Dharwar Craton during the late Archean: *The Journal of Geology*, 107 1, 69–86. doi:10.1086/314331
- 3) Beckinsale, R. D., S. A. Drury and R. W. Holt (1980). "3,360-Myr old gneisses from the South Indian Craton." *Nature* 283: 469.
- 4) Bouvier, A., J. D. Vervoort and P. J. Patchett (2008). "The Lu–Hf and Sm–Nd isotopic composition of CHUR: constraints from unequilibrated chondrites and implications for the bulk composition of terrestrial planets." *Earth and Planetary Science Letters* 273(1-2): 48-57.
- 5) Boynton, W. V. (1984). *Cosmochemistry of the rare earth elements: meteorite studies*. Developments in geochemistry, Elsevier. 2: 63-114.
- 6) Chadwick, B. , Vasudev, V.N. , and Hegde, G.V. 2000, The Dharwar craton, southern India, interpreted as the result of late Archaean oblique convergence *Precambrian Research*, 99 1–2, 91–111. doi:10.1016/S0301-9268(99)00055-8
- 7) Chadwick, B. V., V; Hegde, G; Nutman, A (2007). "Structure and SHRIMP U/Pb zircon ages of granites adjacent to the Chitradurga Schist belt: implications for neoproterozoic convergence in the Dharwar Craton, Southern India." *Journal of the Geological Society of India* 69 (1): 5-24.

- 8) Chapman, J. B., G. E. Gehrels, M. N. Ducea, N. Giesler and A. Pullen (2016). "A new method for estimating parent rock trace element concentrations from zircon." *Chemical Geology* 439: 59-70.
- 9) Chardon, D. and M. Jayananda (2008). "Three-dimensional field perspective on deformation, flow, and growth of the lower continental crust (Dharwar craton, India)." *Tectonics* 27(TC1014).
- 10) Chardon, D., M. Jayananda and J.-J. Peucat (2011). "Lateral constrictional flow of hot orogenic crust: Insights from the Neoarchean of south India, geological and geophysical implications for orogenic plateaux." *Geochemistry, Geophysics, Geosystems* 12(2).
- 11) Condie, K.C., 1994, *Archean crustal evolution: Developments in Precambrian geology Volume 11*: Amsterdam, Elsevier, 527 p.
- 12) Defant, M.J., and Drummond, M.S., 1990, Derivation of some modern arc magmas by melting of young subducted lithosphere: *Nature*, v. 347, p. 662–665, <https://doi.org/10.1038/347662a0>.
- 13) Farner, M.J., and Lee, C.T.A., 2017, Effects of crustal thickness on magmatic differentiation in subduction zone volcanism: A global study: *Earth and Planetary Science Letters*, v. 470, p. 96–107, <https://doi.org/10.1016/j.epsl.2017.04.025>.
- 14) Friend, C. and A. Nutman (1991). "SHRIMP U-Pb geochronology of the Closepet granite and Peninsular gneiss, Karnataka, South India." *Journal of the Geological Society of India* 38(4): 357-368.
- 15) Gao, P. and M. Santosh (2020). "Mesoarchean accretionary mélange and tectonic erosion in the Archean Dharwar Craton, southern India: Plate tectonics in the early Earth." *Gondwana Research* 85: 291-305.
- 16) Griffin, W., N. Pearson, E. Belousova, S. v. Jackson, E. Van Achterbergh, S. Y. O'Reilly and S. Shee (2000). "The Hf isotope composition of cratonic mantle: LAM-MC-ICPMS analysis of zircon megacrysts in kimberlites." *Geochimica et Cosmochimica Acta* 64(1): 133-147.
- 17) Guitreau, M., Mukasa, S.B., Loudin, L., and Sajeev, K. 2017, New constraints on the early formation of the Western Dharwar Craton (India) from igneous zircon U-Pb and Lu-Hf isotopes *Precambrian Research*, 302: 33–49.
- 18) Hokada, T., Horie, K., Satish-Kumar, M., Ueno, Y., Nasheeth, A., Mishima, K., and Shiraishi, K. 2013, An appraisal of Archaean supracrustal sequences in Chitradurga Schist Belt, Western Dharwar Craton, Southern India *Precambrian Research*, 227: 99–119. [doi:10.1016/j.precamres.2012.04.006](https://doi.org/10.1016/j.precamres.2012.04.006).
- 19) Holder, R. M., Hacker, B. R., Kylander-Clark, A. R. C., & Cottle, J. M. (2015). Monazite trace-element and isotopic signatures of (ultra)high-pressure metamorphism: Examples from the Western Gneiss region, Norway. *Chemical Geology*, 409, 99–111. <https://doi.org/10.1016/j.chemgeo.2015.04.021>
- 20) Holder, R. M., Yakymchuk, C., & Viete, D. R. (2020). Accessory mineral Eu anomalies in suprasolidus rocks: Beyond feldspar. *Geochemistry, Geophysics, Geosystems*, 21, e2020GC009052. <https://doi.org/10.1029/2020GC009052>
- 21) Huang, G., Palin, R., Wang, D. et al. Open-system fractional melting of Archean basalts: implications for tonalite–trondhjemite–granodiorite (TTG) magma genesis. *Contrib Mineral Petrol* 175, 102 (2020). <https://doi.org/10.1007/s00410-020-01742-9>
- 22) Jayananda, M., J. F. Moyen, H. Martin, J. J. Peucat, B. Auvray and B. Mahabaleswar (2000). "Late Archaean (2550–2520 Ma) juvenile magmatism in the Eastern Dharwar craton, southern India: constraints from geochronology, Nd–Sr isotopes and whole rock geochemistry." *Precambrian Research* 99: 225-254.
- 23) Jayananda, M., Chardon, D., Capdevila, R., Kano, T., Peucat, -J.-J., and Channabasappa, S. 2008, 3.35 Ga komatiite volcanism in the western Dharwar craton, southern India: constraints from Nd isotopes and whole rock geochemistry *Precambrian Research*, 162, 160–179. 1–2 [doi:10.1016/j.precamres.2007.07.010](https://doi.org/10.1016/j.precamres.2007.07.010)
- 24) Jayananda, M., Chardon, D., Peucat, -J.-J., Tushipokla, and Fanning, C.M. 2015, Paleo- to Mesoarchean TTG accretion and continental growth in the western Dharwar craton, Southern India: constraints from SHRIMP U-Pb zircon geochronology, whole-rock geochemistry and Nd-Sr isotopes *Precambrian Research*, 268: 295–322. [doi:10.1016/j.precamres.2015.07.015](https://doi.org/10.1016/j.precamres.2015.07.015).

- 25) Jayananda, M. , Peucat, J.J. , Chardon, D. , Rao, B.K. , Fanning, C.M. , and Corfu, F. 2013, Neoarchean greenstone volcanism and continental growth, Dharwar craton, southern India: constraints from SIMS U–Pb zircon geochronology and Nd isotopes *Precambrian Research*, 227: 55–76.
doi:10.1016/j.precamres.2012.05.002.
- 26) Jayananda, M. , Santosh, M. , and Adiseshan, K.R. 2018, Formation of Archaean (3600-2500 Ma) continental crust in the Dharwar Craton, southern India: *Earth-Science Reviews*,
doi:10.1016/j.earscirev.2018.03.013.
- 27) Jayananda, M., K. R. Aadhiseshan, M. A. Kusiak, S. A. Wilde, K.-u. Sekhamo, M. Guitreau, M. Santosh and R. V. Gireesh (2020). "Multi-stage crustal growth and Neoarchean geodynamics in the Eastern Dharwar Craton, southern India." *Gondwana Research* 78: 228-260.
- 28) Jochum, K. P., U. Weis, B. Stoll, D. Kuzmin, Q. Yang, I. Raczek, D. E. Jacob, A. Stracke, K. Birbaum, D. A. Frick, D. Günther and J. Enzweiler (2011). "Determination of Reference Values for NIST SRM 610–617 Glasses Following ISO Guidelines." *Geostandards and Geoanalytical Research* 35(4): 397-429.
- 29) Krapez, B. , Srinivasa Sarma, D. , Ram Mohan, M. , McNaughton, N.J. , Rasmussen, B. , and Wilde, S.A. 2020, Tectonostratigraphy of the Late Archean Dharwar Supergroup, Dharwar Craton, India: Defining a tectonic history from spatially linked but temporally distinct intracontinental and arc-related basins *Earth-Science Reviews*, 201: 102966. doi:10.1016/j.earscirev.2019.102966.
- 30) Lancaster, P.J. , Dey, S. , Storey, C.D. , Mitra, A.M. , and Bhunia, R.K. 2015, Contrasting crustal evolution processes in the Dharwar craton: Insights from detrital zircon U–Pb and Hf isotopes *Gondwana Research*, 28: 1361–1372. doi:10.1016/j.gr.2014.10.010.
- 31) Ludwig, K.R. , 2003, User's manual for Isoplot 3.00. A geochronological toolkit for microsoft excel. Berkeley CA: Berkeley Geochronology Centre Special Publication no Vol. 4, 21–22.
- 32) Maibam, B., A. Gerdes and J. N. Goswami (2016). "U–Pb and Hf isotope records in detrital and magmatic zircon from eastern and western Dharwar craton, southern India: Evidence for coeval Archaean crustal evolution." *Precambrian Research* 275: 496-512.
- 33) Manikyamba, C., Kerrich, R., Khanna, T.C., Krishna, A.K., Satyanarayanan, M., 2008. Geochemical systematics of komatiite-tholeiite and adakitic-arc basalt associations: the role of a mantle plume and convergent margin in formation of the Sandur Superterrane, Dharwar craton, India. *Lithos* 106, 155–172.
- 34) Manikyamba, C. and R. Kerrich (2012). "Eastern Dharwar Craton, India: Continental lithosphere growth by accretion of diverse plume and arc terranes." *Geoscience Frontiers* 3(3): 225-240.
- 35) Manikyamba, C. and R. Kerrich (2011). "Geochemistry of alkaline basalts and associated high-Mg basalts from the 2.7Ga Penakacherla Terrane, Dharwar craton, India: An Archean depleted mantle-OIB array." *Precambrian Research* 188(1): 104-122.
- 36) Manikyamba, C., A. Saha, M. Santosh, S. Ganguly, M. Rajanikanta Singh, D. V. Subba Rao and M. Lingadevaru (2014). "Neoarchean felsic volcanic rocks from the Shimoga greenstone belt, Dharwar Craton, India: Geochemical fingerprints of crustal growth at an active continental margin." *Precambrian Research* 252: 1-21.
- 37) Martin, H., J.-F. Moyen, M. Guitreau, J. Blichert-Toft and J.-L. Le Pennec (2014). "Why Archaean TTG cannot be generated by MORB melting in subduction zones." *Lithos* 198-199: 1-13.
- 38) McKenzie, N. R., A. J. Smye, V. S. Hegde and D. F. Stockli (2018). "Continental growth histories revealed by detrital zircon trace elements: A case study from India." *Geology* 46(3): 275-278.
- 39) Nagel, T. J., J. E. Hoffmann and C. Münker (2012). "Generation of Eoarchean tonalite-trondhjemite-granodiorite series from thickened mafic arc crust." *Geology* 40(4): 375-378.
- 40) Nasheeth, A., T. Okudaira, K. Horie, T. Hokada and M. Satish–Kumar (2015). "SHRIMP U–Pb zircon ages of granitoids adjacent to Chitradurga shear zone, Dharwar craton, South India and its tectonic implications." *Journal of Mineralogical and Petrological Sciences* 110(5): 224-234.
- 41) Naqvi, S. M., R. M. K. Khan, C. Manikyamba, M. R. Mohan and T. C. Khanna (2006). "Geochemistry of the NeoArchaean high-Mg basalts, boninites and adakites from the Kushtagi–Hungund greenstone belt of the Eastern Dharwar Craton (EDC); implications for the tectonic setting." *Journal of Asian Earth Sciences* 27(1): 25-44.

- 42) Naqvi, S. M. and J. G. Rana Prathap (2007). "Geochemistry of adakites from Neoarchean active continental margin of Shimoga schist belt, Western Dharwar Craton, India: Implications for the genesis of TTG." *Precambrian Research* 156(1): 32-54.
- 43) Norman, M. D., N. J. Pearson, A. Sharma and W. L. Griffin (1996). "Quantitative Analysis of Trace Elements in Geological Materials by Laser Ablation ICPMS: Instrumental Operating Conditions and calibration values of NIST Glasses." *Geostandards Newsletter* 20(2): 247-261.
- 44) Nutman, A.P. , Chadwick, B. , Ramakrishnan, M. , and Viswanatha, M.N. 1992, SHRIMP U–Pb ages of detrital zircon in Sargur supracrustal rocks in western Karnataka, southern India. *Journal of Geological Society of India*, 39, 367–374
- 45) Pahari, A., L. Tang, C. Manikyamba, M. Santosh, K. S. V. Subramanyam and S. Ganguly (2019). "Meso-Neoarchean magmatism and episodic crustal growth in the Kudremukh-Agumbe granite-greenstone belt, western Dharwar Craton, India." *Precambrian Research* 323: 16-54.
- 46) Paton, C., J. Hellstrom, B. Paul, J. Woodhead and J. Hergt (2011). "Iolite: Freeware for the visualisation and processing of mass spectrometric data." *Journal of Analytical Atomic Spectrometry* 26(12): 2508-2518.
- 47) Patra, Kiranmala, Anshuman Giri, R. Anand, S. Balakrishnan, and Jitendra K. Dash. "Dharwar Stratigraphy Revisited: New Age Constraints on the 'Oldest' Supracrustal Rocks of Western Dharwar Craton, Southern India." *International Geology Review* (2020): 1-21.
- 48) Peucat, -J.-J. , Bouhallier, H. , Fanning, C.M. , and Jayananda, M. 1995, Age of Holenarsipur schist belt, relationships with the surrounding gneisses (Karnataka, South India). *Journal of Geology*, 103, 701–710
- 49) Peucat, J. J., Jayananda, M., Chardon, D., Capdevila, R., Fanning, C. M., & Paquette, J. L. (2013). The lower crust of the Dharwar Craton, Southern India: Patchwork of Archean granulitic domains. *Precambrian Research*, 227, 4–28. <https://doi.org/10.1016/j.precamres.2012.06.009>
- 50) Profeta, L., Ducea, M.N., Chapman, J.B., Paterson, S.R., Gonzales, S.M.H., Kirsch, M., Petrescu, L. and DeCelles, P.G., 2015, Quantifying crustal thickness over time in magmatic arcs: *Scientific Reports*, v. 5, 17786, <https://doi.org/10.1038/srep17786>.
- 51) Ramakrishnan, M., and Vaidyanathan, R. , 2008, *Geology of India: Geological Society of India Bangalore*, v. I 556.
- 52) Rapp, R.P., and Watson, E.B., 1995, Dehydration melting of metabasalt at 8–32 kbar Implications for continental growth and crust-mantle recycling: *Journal of Petrology*, v. 36, p. 891–931, <https://doi.org/10.1093/petrology/36.4.891>.
- 53) Rubatto, D. (2002). "Zircon trace element geochemistry: partitioning with garnet and the link between U–Pb ages and metamorphism." *Chemical Geology* 184(1): 123-138.
- 54) Rubatto, D., Hermann, J., & Buick, I. S. (2006). Temperature and bulk composition control on the growth of monazite and zircon during low-pressure Anatexis (Mount Stafford, Central Australia). *Journal of Petrology*, 47(10), 1973–1996. <https://doi.org/10.1093/petrology/egl033>
- 55) Rubatto, D., & Hermann, J. (2007). Experimental zircon/melt and zircon/garnet trace element partitioning and implications for the geochronology of crustal rocks. *Chemical Geology*, 241(1–2), 38–61.
- 56) Rubatto, D., Chakraborty, S., & Dasgupta, S. (2013). Timescales of crustal melting in the higher Himalayan crystallines (Sikkim, Eastern Himalaya) inferred from trace element-constrained monazite and zircon chronology. *Contributions to Mineralogy and Petrology*, 165(2), 349–372.
- 57) Rubatto, D. (2017). "Zircon: The Metamorphic Mineral." *Reviews in Mineralogy and Geochemistry* 83(1): 261-295.
- 58) Santosh, M. and S.-S. Li (2018). "Anorthosites from an Archean continental arc in the Dharwar Craton, southern India: Implications for terrane assembly and cratonization." *Precambrian Research* 308: 126-147.
- 59) Santosh, M., Q.-Y. Yang, E. Shaji, T. Tsunogae, M. R. Mohan and M. Satyanarayanan (2015). "An exotic Mesoarchean microcontinent: The Coorg Block, southern India." *Gondwana Research* 27(1): 165-195.

- 60) Santosh, M., Q.-Y. Yang, E. Shaji, M. R. Mohan, T. Tsunogae and M. Satyanarayanan (2016). "Oldest rocks from Peninsular India: Evidence for Hadean to Neoproterozoic crustal evolution." *Gondwana Research* 29(1): 105-135.
- 61) Scherer, E., C. Münker and K. Mezger (2001). "Calibration of the lutetium-hafnium clock." *Science* 293(5530): 683-687.
- 62) Sláma, J., J. Košler, D. J. Condon, J. L. Crowley, A. Gerdes, J. M. Hancher, M. S. A. Horstwood, G. A. Morris, L. Nasdala, N. Norberg, U. Schaltegger, B. Schoene, M. N. Tubrett and M. J. Whitehouse (2008). "Plešovice zircon — A new natural reference material for U–Pb and Hf isotopic microanalysis." *Chemical Geology* 249(1): 1-35.
- 63) Smithies, R.H., Ivanic, T.J., Lowrey, J.R., Morris, P.A., Barnes, S.J., Wyche, S., and Lu, Y.-J. 2018, Two distinct origins for Archean greenstone belts. *Earth and Planetary Science Letters*, 487, 106–116
- 64) Spencer, C. J., C. Yakymchuk and M. Ghaznavi (2017). "Visualising data distributions with kernel density estimation and reduced chi-squared statistic." *Geoscience Frontiers* 8(6): 1247-1252.
- 65) Srinivasa Sarma, D. M., N J, E. Belusova, M. Ram Mohan and I. R. Fletcher (2012). "Detrital zircon U–Pb ages and Hf-isotope systematics from the Gadag Greenstone Belt: Archean crustal growth in the western Dharwar Craton, India." *Gondwana Research* 22: 843-854.
- 66) Trail, D., Watson, E.B., and Tailby, N.D., 2012, Ce and Eu anomalies in zircon as proxies for the oxidation state of magmas: *Geochimica et Cosmochimica Acta*, v. 97, p. 70–87, <https://doi.org/10.1016/j.gca.2012.08.032>.
- 67) Trendall, A.F., de Laeter, J.R., Nelson, D.R., and Mukhopadhyay, D. 1997, A precise U–Pb age for the base of Mulaingiri formation (Bababudan Group, Dharwar Super-group) of the Karnataka craton. *Journal of Geological Society of India*, 50, 161–170.
- 68) Tushipokla and M. Jayananda (2013). "Geochemical constraints on komatiite volcanism from Sargur Group Nagamangala greenstone belt, western Dharwar craton, southern India: Implications for Mesoarchean mantle evolution and continental growth." *Geoscience Frontiers* 4(3): 321-340.
- 69) Vermeesch, P., 2018, IsoplotR: a free and open toolbox for geochronology. *Geoscience Frontiers*, v.9, p.1479-1493, doi: 10.1016/j.gsf.2018.04.001.
- 70) Wang, J.-Y. and M. Santosh (2019). "Eoarchean to Mesoarchean crustal evolution in the Dharwar craton, India: Evidence from detrital zircon U–Pb and Hf isotopes." *Gondwana Research* 72: 1-14.
- 71) Woodhead, J., J. Hergt, M. Shelley, S. Eggins and R. Kemp (2004). "Zircon Hf-isotope analysis with an excimer laser, depth profiling, ablation of complex geometries, and concomitant age estimation." *Chemical Geology* 209(1): 121-135.
- 72) Woodhead, J. D. and J. M. Hergt (2005). "A preliminary appraisal of seven natural zircon reference materials for in situ Hf isotope determination." *Geostandards and Geoanalytical Research* 29(2): 183-195.
- 73) Yang, Q.-Y. and M. Santosh (2015). "Zircon U–Pb geochronology and Lu–Hf isotopes from the Kolar greenstone belt, Dharwar Craton, India: Implications for crustal evolution in an ocean-trench-continent transect." *Journal of Asian Earth Sciences* 113: 797-811.

4

Detrital zircon record of the Kaladgi-Badami basin:
Correlation with Paleoproterozoic basins across India and
Madagascar

Abstract:

Peninsular India is comprised of a collage of Archean cratons separated by Proterozoic mobile-belts and intracratonic basins, collectively termed as 'Purana basins', that formed across the Indian peninsula during extensional tectonic events. In this chapter, we present detrital zircon U–Pb geochronological data from the Kaladgi-Badami basin and then compare it against previously reported detrital record of Paleoproterozoic sequences across southern India and Madagascar. The rare earth element (REE) compositions from the analyzed zircons have been interpreted to fingerprint the depth of crystallization of the sources, which is coupled with published zircon U–Pb ages from the Dharwar Craton and paleocurrent data to interpret source regions. The detrital formations analyzed here preserve major detrital age peaks at 2.6–2.5 Ga, which are interpreted to be sourced from the adjacent Eastern Dharwar Craton and Hungund Schist Belt. The maximum depositional age of the older Lokapur Group is constrained at 2332 ± 65 Ma. The younger Badami Group contains a near-concordant zircon that has a $^{207}\text{Pb}/^{206}\text{Pb}$ age of 1820 ± 26 Ma that we interpret to constrain the maximum age of its deposition. Multidimensional scaling (MDS) analysis comparing the Kaladgi-Badami Basin, with other Paleoproterozoic sequences across southern India and Madagascar, demonstrate the provenance similarity between the lower groups of the Kaladgi-Badami basin with the greenstone sequences of the Dharwar Craton. The younger Badami Group, however, shares similar age provenance to the Papagni Formation in the Cuddapah Basin. Dyke swarms across the northern Dharwar Craton are interpreted to reflect rifting that created the basin for the Lokapur Group. The younger Badami Group arenites are suggested to have formed similarly to the Papagni Group in the Cuddapah Basin when the Dharwar Craton was surrounded by a shallow sea.

1. Introduction:

Peninsula India hosts a series of large intra-continental basins that are known as the 'Purana basins' (Holland, 1909). These cover up to twenty per cent area of peninsular India and, although they are recognized as Proterozoic (Kale and Phansalkar, 1991), their detailed geochronology and correlation are only now being revealed (Saha et al. 2016). The disparities in the ages and tectonic settings between the individual basins have been previously explored and earlier correlations were mostly based on lithostratigraphy (Basu and Bickford, 2014; Meert and Pandit, 2014). Existing geochronological data from the Purana basins largely consists of older Rb–Sr, Sm–Nd isochrons, and Pb–Pb model ages that have large uncertainties (Padmakumari et al. 1998, Joy et al. 2019). More recently, detrital zircon U–Pb geochronological data has begun to allow correlation between the basins (e.g. Saha et al. 2016). However, to date, the enigmatic Kaladgi-Badami and Bhima basins have very limited geochronological data, hindering the correlation of Proterozoic basins (Saha et al., 2016).

The significance of these basins has been highlighted in the recent controversy as to the origin and configuration of the supercontinents Columbia/Nuna and Rodinia that in part rely on correlations between Palaeoproterozoic basins in Africa, Madagascar and India (Collins and Windley 2002; Collins and Pisarevsky, 2005; Cox et al. 2004; Fitzsimons and Hulscher, 2005; Tucker et al. 2011; Armistead et al. in review). Specifically, the Greater Dharwar Craton model (Tucker et al. 2011) suggests that the Kaladgi-Badami and Bhima basins form a potential missing link between the Itremo Group of Madagascar and the Cuddapah Basin of SE India—linking central Madagascar to the Dharwar Craton in the late Palaeoproterozoic/early Mesoproterozoic. Alternatively, central Madagascar is depositionally linked to eastern Africa and was separate from India at the time (Cox et al. 1998; 2004; Collins and Windley 2002; Collins and Pisarevsky 2005; Armistead et al, 2020).

In this study, detrital zircon U–Pb geochronological data from the Kaladgi-Badami basin are presented and correlated with existing published detrital zircon sedimentary records of Paleoproterozoic formations across southern India and Madagascar to address these hypotheses. The source regions contributing to the sedimentation of the Kaladgi-Badami basin also have been fingerprinted using the rare earth element (REE) composition of the zircons analysed to qualitatively estimate the depth of crystallization of the source protolith and compared against zircon U–Pb ages reported from the Dharwar Craton (Jayananda et al. 2015, 2020; Wang J.Y. et al., 2020; new data Chapter 2).

2. Geological Background:

The Kaladgi-Badami basin is thought to contain rocks deposited in the late Palaeoproterozoic/Mesoproterozoic to Neoproterozoic (Dey 2015). The basin lies in the northern part of Karnataka state and has an east-west trend. It overlies the Peninsular Gneiss of the Dharwar Craton and is covered by the volcanic Deccan traps (Jayaprakash et al., 1987). The basin sequence is subdivided into the older Bagalkot Group, which is overlain by the Badami Group. These are divided by an angular unconformity. The rocks of the Bagalkot Group include arenite, shale, and carbonate rocks along with their associated cherts and conglomerates. The Bagalkot Group is further divided into Simikeri and Lokapur groups by the presence of a disconformity. The basement of the Bagalkot Group is made up of the peninsular gneisses and greenstone belts of the Dharwar craton and the closepet Granite, which provided the detritus to Kaladgi – Badami basin (Joy et al. 2019). The Bagalkot Group was deformed and eroded before deposition of the Badami Group (Viswanathaiah, 1977).

The Badami Group comprises undeformed, horizontally bedded arenites, shales and limestones unconformably overlying both the Bagalkot Group and Archean rocks of the Dharwar Craton.

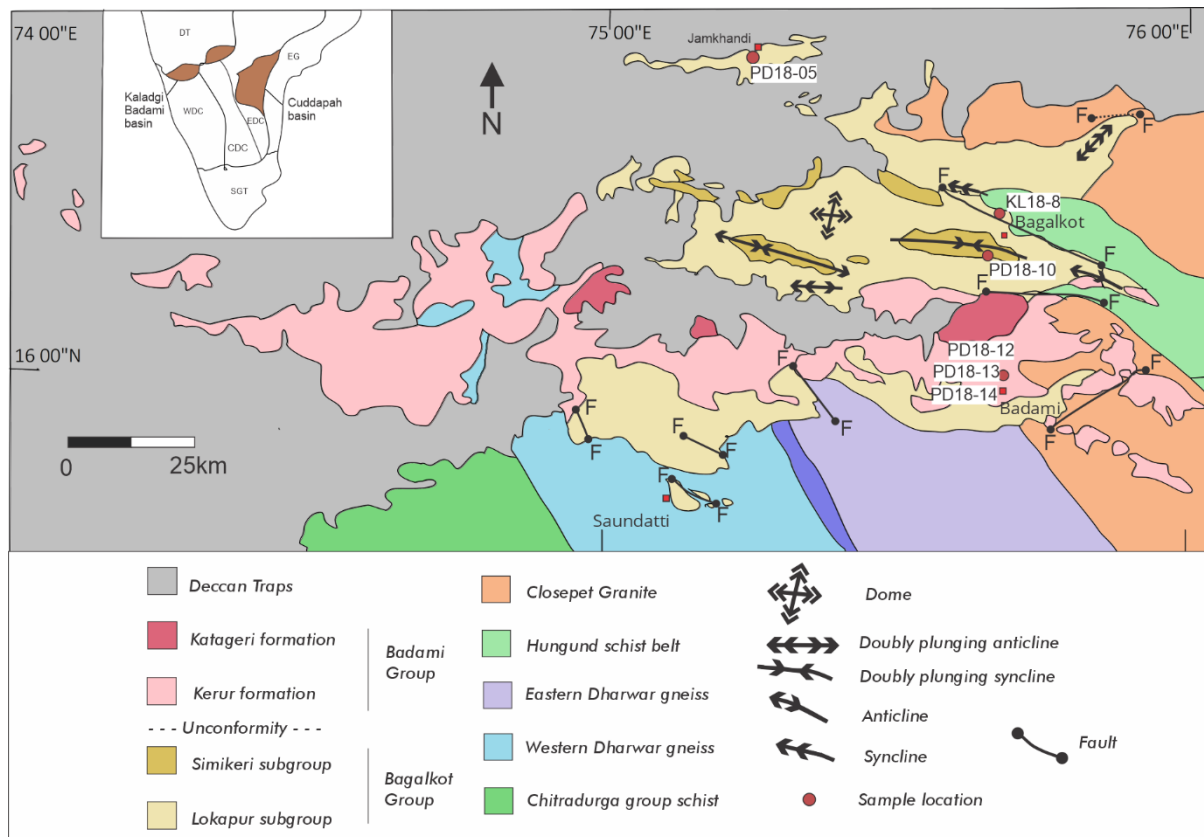


Figure 1: Geological map of the Kaladgi-Badami basin (modified after Jayaprakash et al., 1987, Dey et al., 2009), the inset showing the placement of major Proterozoic basins across southern India with major tectono-stratigraphic domains outlined as DT – Deccan Traps; WDC – Western Dharwar Craton; EDC – Eastern Dharwar Craton; CDC – Central Dharwar Craton; EG – Eastern Ghats domain; SGT – Southern Granulite Terrane.

The evolution of deposition in the basin has been explained by initial sedimentation limited to detritus eroded only from the basement gneisses, followed by sediments derived from mixed sources of basement gneisses and greenstone belts, as well as the Closepet Batholith. (Dey et al. 2008b, 2009b, 2015). The Peninsular Gneiss basement is mainly composed of tonalite-trondjemite-granodiorite (TTG) in NNW trending belts, ranging in age from Mesoarchaeon to Neoarchaeon. The Closepet Granite comprises of K- and LREE rich granodiorites and granites (Dey et al., 2003, 2006, 2009b). The volcano-sedimentary sequences underlying the Bagalkot Group (greenstone belts) form the Hungund-Kushtagi Belt, located on the SE fringe of the basin, and the Chitradurga Group (Dharwar Supergroup) to the SW. They are both dominated by metagreywackes, metapelites, and metabasalts.

The cyclic nature of sedimentation was explained through repeated phases of marine transgression caused by episodes of foundering of the cratonic basin (Kale and Phansalkar, 1991). Depositional environments for the two subgroups of the Bagalkot Group are explained with the Lokapur Subgroup deposited in a transgressive beach environment along with basal minor fluvial

deposits leading to cycles of alternating muddy tidal flat deposits and carbonates (Kale and Phansalkar, 1991; Kale et al., 1996; Bose et al., 2008; Dey et al., 2009b). The overlying Simikeri Subgroup is thought to reflect high energy beach deposits grading up to tidal flat deposits (Kale and Phansalkar, 1991). The Badami Group reflects a major transgressive of shallow marine/estuarine environments (Kale and Phansalkar, 1991; Sathyanarayana, 1994).

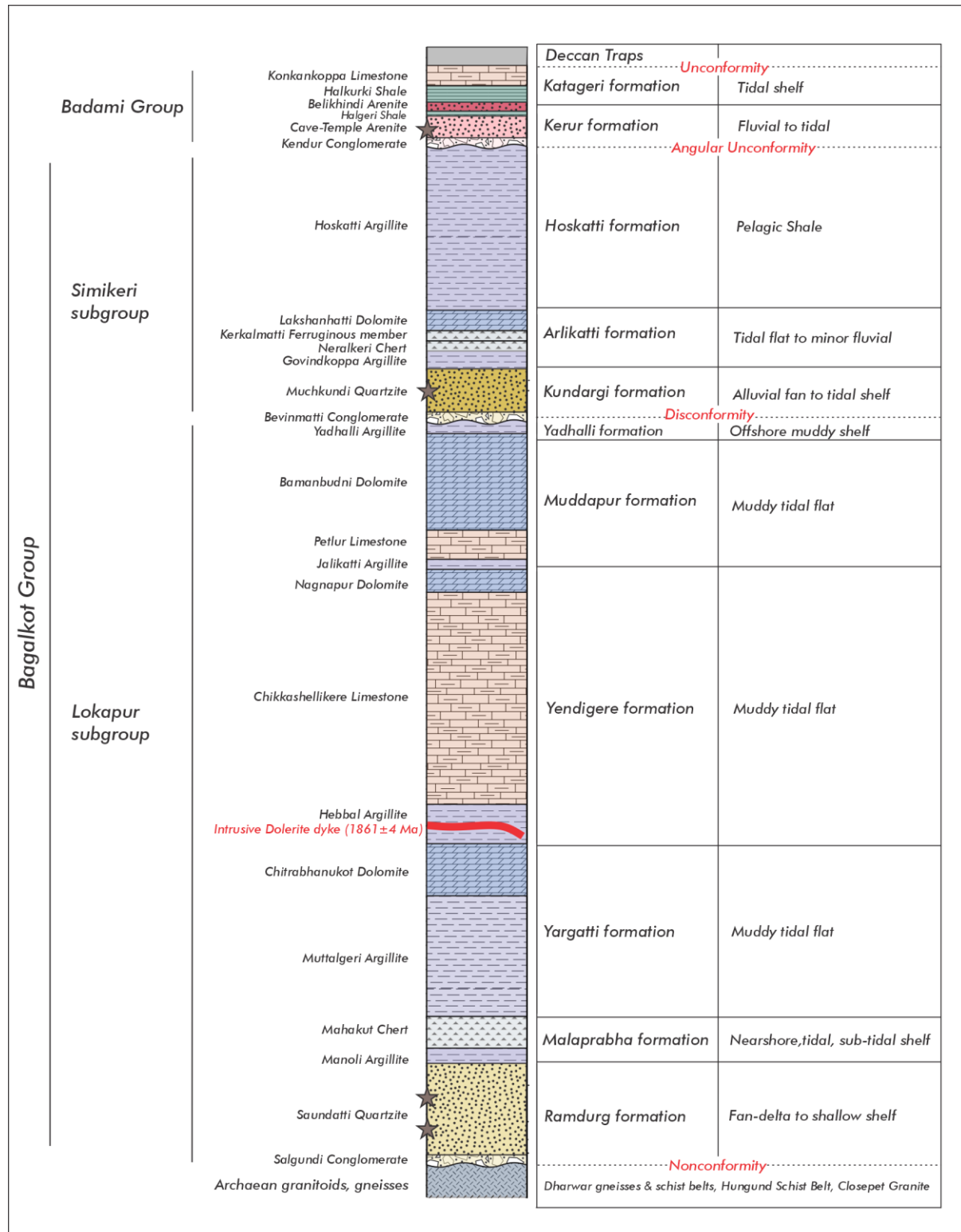


Figure 2: The stratigraphy of the Kaladgi-Badami basin. Sedimentary structures are not drawn to scale. The relative thickness of each layer was adapted from Jayaprakash et al., 2007. Individual formations have been marked on the right of the stratigraphic column. Sedimentary environments of each formation and reported intrusive dyke age has been adapted from Joy et al., 2019. The star symbols represent the stratigraphic units sampled for this study.

Isotopic age data are rare for the Kaladgi basin sediments. A Nd depleted mantle model age (T_{DM}) of ~2540 Ma was published (Padmakumari et al., 1998) for the Govindkoppa Argillite from the Kundargi Formation, which was interpreted as the age of the source. In the absence of absolute age data, Kale and Phansalkar (1991), correlated the Bagalkot and Badami Groups, based on lithostratigraphy, with unmetamorphosed Neoproterozoic and Mesoproterozoic successions of other supercratonic basins of Peninsular India (collectively termed the 'Purana basins'). Joy et al. (2019) recently constrained the formation of the lower Lokapur Group to $>1861 \pm 4$ Ma, by obtaining a U–Pb baddeleyite age from an intrusive dolerite dyke. Limestones from the Katageri Formation (upper Badami Group) have also been analyzed for U–Th–Pb isotopes, which yielded an imprecise isochron age of 0.96 Ga (Joy et al., 2019). These authors proposed that the two Badami Group represented a return to deposition after an almost billion year Ma gap.

The quartzite and arenite members of the Kaladgi Basin succession have been targeted in this study shown in Figure 1 and Figure 2, to understand the detrital record and to isotopically constrain the depositional time period of the subgroups. The Saundatti Quartzite occurs along the margin of the basin, hosting the Bagalkot Group and varies in composition. The Muchkundi Quartzite, is present higher in the succession, is a highly mature quartz arenite of which the lower portion of the formation contains altered feldspar clasts. The Cave-Temple Arenite is a 200 km continuous formation overlaying a variety of Archaean basement and Bagalkot Group in an irregular E–W trend and contains fragments of Bagalkot Group rocks, signifying that a component of it is recycled from lower in the basin (Dey et al., 2006, 2009b).

The provenance, tectonics, and basin evolution of the Kaladgi Basin was discussed by Dey et al. (2009b, 2015). These authors proposed that the intracratonic Kaladgi Basin initiated by faulting along the northern margin that uplifted a granitic source and transported immature detritus to the northern margin (Dickinson et al., 1983), explaining the presence of fresh potassic feldspars within the northern margins of Saundatti Quartzite and Salgundi Conglomerate. Predominant exposure of Na-rich granitoids (TTG gneisses) along the northern margin today led to speculation that K-rich granites lie beneath the Deccan traps (Dey, 2006). The southern Saundatti Quartzite is more mature than its northern counterpart as the feldspar grains are highly altered inferring a more stable tectonic condition characterized by low relief in the source. The Muchkundi Quartzite is a quartz arenite belonging to the

Simikeri Subgroup. It also contains altered feldspars inferring that the Simikeri Subgroup deposited over the whole source area under stable tectonic setting (Dey et al., 2009b). The Simikeri Subgroup deposition was followed by the closure of the marine basin, and deformation and uplift of the Bagalkot Group sediments. The Badami Group sediments were deposited in an E–W trending basin on top of the Bagalkot Group and Archean basement. The northern border of the Badami Group involving the Cave Temple arenite is marked by an E–W trending fault called Sirur-Katageri fault. The southern side of the fault was downthrown, which acted as the depositional basement for the Badami Group (Dey, 2006).

3. Methods:

Six samples of arenites were crushed for zircons at the Indian Institute of Science, Bangalore, India. They were created into grain bearing epoxy mounts at the University of Adelaide. The polished zircon mounts were carbon-coated and imaged by a Gatan cathodoluminescence (CL) detector attached to Quanta 600 MLA Scanning Electron Microscope to identify various domains within the zircons suitable for analysis. U–Pb geochronology from the zircon was performed at the Adelaide Microscopy facility at the University of Adelaide using the Agilent 7900 ICP-MS attached to New Wave (NWR-213) 213nm laser ablation system with a spot size of 30 μm and frequency of 5 Hz. The isotopes ^{204}Pb , ^{206}Pb , ^{207}Pb , ^{208}Pb , ^{232}Th , ^{238}U have been measured for U–Pb zircon geochronology. GEMOC GJ-1 zircon (Thermal Ionization Mass Spectrometry (TIMS) ages $^{207}\text{Pb}/^{206}\text{Pb} = 602 \pm 4.3$ Ma, $^{206}\text{Pb}/^{238}\text{U} = 600.7 \pm 1.1$ Ma and $^{207}\text{Pb}/^{235}\text{U} = 602.0 \pm 1.0$ Ma; Jackson et al., 2004) was used for the correction of U–Pb fractionation for the analysis. The Plesovice zircon (ID-TIMS $^{206}\text{Pb}/^{238}\text{U}$ age = 337.13 ± 0.37 Ma) was used as a secondary standard. Seventy two Plesovice standard zircon grains were analyzed yielding $^{206}\text{Pb}/^{238}\text{U}$ age of 331 ± 1 Ma (2SD, MSWD = 1.3), which was within the acceptable uncertainty compared to the ID-TIMS age of Slama et al. (2008). Rare Earth Elements ^{139}La , ^{140}Ce , ^{141}Pr , ^{146}Nd , ^{147}Sm , ^{153}Eu , ^{157}Gd , ^{159}Tb , ^{163}Dy , ^{165}Ho , ^{166}Er , ^{169}Tm , ^{172}Yb , ^{175}Lu , ^{49}Ti , ^{89}Y , ^{178}Hf were simultaneously measured over the same spots on the zircons along with U–Pb isotopes using 50 μm spot size analyses over NIST SRM 610 glass as reference material (Norman et al., 1996, Norman et al., 1998, Jochum et al., 2011). The U–Pb and REE data were separately processed using Iolite (Paton et al., 2011). The processed U–Pb data were plotted using IsoplotR (Vermeesch, 2018) and the Isoplot 4.15 plugin in Microsoft Excel (Ludwig, 2003). The rare earth elemental concentrations and ratios were calculated using the Geochemical data toolkit for R (GCDkit 6.0) (Janousek et al., 2006) and were normalized to the uniform reservoir published in Boynton (1984).

4. Results:

Sample No	Lithology	Stratigraphy	Latitude	Longitude	Elevation
KL 18/8	Pink felspathic Arenite	Saundatti Quartzite	16.25322 N	75.69061 E	-
PD18-05	Pink felspathic Arenite	Saundatti Quartzite	16.49388 N	75.28836 E	520 m
PD18-10	Quartz Arenite	Muchkundi Quartzite	16.14263 N	75.66629 E	524 m
PD18-12	Quartz Arenite	Cave Temple Arenite	15.93813 N	75.67631 E	575 m
PD18-13	Quartz Arenite	Cave Temple Arenite	15.93813 N	75.67631 E	590 m
PD18-14	Quartz Arenite	Cave Temple Arenite	15.93813 N	75.67631 E	610 m

Table 1: Lithology and location of the detrital quartzites sampled for this study.

PD18-05 has been collected from the exposed felspathic arenite beds exposed at the Jamkundi tree-park near Jamkhandi town. The sample collected was a pink feldspar rich arenite with well-rounded grains of quartz and feldspar within a siliciclastic cement implying a mature sandstone member of the Saundatti Quartzite litho-stratigraphic unit. The quartzite beds are along a North 20 degree towards West strike with 200 degree dip direction, show symmetrical ripple patterns on the exposed surface, was interpreted as a marine transgressive regime. 107 analyzed zircon grains yielded 34 results that passed a <10% discordance filter to reveal broadly clustered $^{207}\text{Pb}/^{206}\text{Pb}$ age peak with a maxima at ~2550 Ma in a probability density plot. The youngest $^{207}\text{Pb}/^{206}\text{Pb}$ age from the population is 2332 ± 65 Ma. Few grains reveal older Archean components around ca. 2.77 Ga. The rare earth element ratios for the near concordant zircons range from 0.13 – 0.9 for Eu/Eu^* , 0.00005 – 0.0327 for $\text{La}_\text{N}/\text{Yb}_\text{N}$ and 0.0228 – 0.5881 for $\text{Gd}_\text{N}/\text{Yb}_\text{N}$.

KL18-8 is a pink felspathic arenite collected towards north of Bagalkot town to the western periphery of the Hungund schist belt. The location lies in a trough and is cross-stratified with the thickly bedded felspathic pink arenite which also belongs to the Saundatti Quartzite in Ramdurg Formation member of the Lokapur Subgroup. 90 analyzed zircons yielded 14 results that passed the <10% discordance filter, reveal a bimodal distribution in the probability density plot at ~2.55 Ga and ~2.6 Ga. One grain shows older inheritance at $^{207}\text{Pb}/^{206}\text{Pb}$ age at 3043 ± 55 Ma. The rare earth element ratios for

the near concordant zircons range from 0.36 – 1.11 for Eu/Eu*, 0.0105 – 0.0551 for $\text{La}_\text{N}/\text{Yb}_\text{N}$ and 0.1725 – 0.8035 for $\text{Gd}_\text{N}/\text{Yb}_\text{N}$.

PD18-10 is from a quartz rich arenite interbedded with well-rounded feldspar rich conglomerate, collected near Muchkundi temple, known as the Muchkundi quartzite from the Kundargi formation that forms the base of the Simikeri subgroup. 83 analyzed zircons yielded only 11 results that passed <10% discordance filter, revealed probability peaks at ca. ~2.55 Ga, 2.64 Ga and 2.7 Ga. One zircon reveals older Archean inheritance at $^{207}\text{Pb}/^{206}\text{Pb}$ age of 3104 ± 70 Ma. The rare earth element ratios for the near concordant zircons range from 0.08 – 0.82 for Eu/Eu*, 0.00001 – 0.0428 for $\text{La}_\text{N}/\text{Yb}_\text{N}$ and 0.0361 – 0.5741 for $\text{Gd}_\text{N}/\text{Yb}_\text{N}$.

PD18-12 is collected at the bottom section of a channel cross stratified sandstone containing quartz arenite in mostly horizontal undeformed beds. The location appears to have experienced extensive large scale weathering and contains undeformed layers of sandstone with occasional conglomerate beds which is believed to be part of the Kerur Formation in the lower Badami Group. 104 analyzed zircons yielded 20 results that passed <10% discordance filter. The resultant ages cluster at ca. 2.55 Ga, 2.6 Ga with older inheritance around 2.9 – 3.0 Ga and 3.35 Ga. Three analysed zircons cluster at younger $^{207}\text{Pb}/^{206}\text{Pb}$ age peak of 1.8 Ga, with the youngest near-concordant detrital zircon having a $^{207}\text{Pb}/^{206}\text{Pb}$ age at 1820 ± 26 Ma. The rare earth element ratios for the near concordant zircons range from 0.09 – 0.84 for Eu/Eu*, 0.0001 – 0.3148 for $\text{La}_\text{N}/\text{Yb}_\text{N}$ and 0.0363 – 0.1447 for $\text{Gd}_\text{N}/\text{Yb}_\text{N}$.

PD18-13 is collected fifty meters above from PD18-12 representing a stratigraphically younger mostly horizontal surface. The distribution of interlayered conglomerate beds was sparse and the sample was taken from a quartz rich arenite bed. 90 analyzed zircons yielded only two results that passed the <10% discordance filter at $^{207}\text{Pb}/^{206}\text{Pb}$ ages of 2537 ± 40 Ma and 3291 ± 20 Ma. The rare earth element ratios for the near concordant zircons range from 0.3 – 0.67 for Eu/Eu*, 0.00036 – 0.0019 for $\text{La}_\text{N}/\text{Yb}_\text{N}$ and 0.0607 – 0.0479 for $\text{Gd}_\text{N}/\text{Yb}_\text{N}$.

PD18-14 has been collected from a horizontal ferrogenuous quartz arenite bed lying approximately 100 metres above PD18-12. 60 analyzed zircons yielded five results that passed the <10% discordance filter which revealed minor probability density peaks at $^{207}\text{Pb}/^{206}\text{Pb}$ ages of 2580 Ma, 2630 Ma with the youngest $^{207}\text{Pb}/^{206}\text{Pb}$ age at 2539 ± 34 Ma. The rare earth element ratios for the near concordant zircons range from 0.3 – 0.67 for Eu/Eu*, 0 – 0.0005 for $\text{La}_\text{N}/\text{Yb}_\text{N}$ and 0.0481 – 0.0842 for $\text{Gd}_\text{N}/\text{Yb}_\text{N}$.

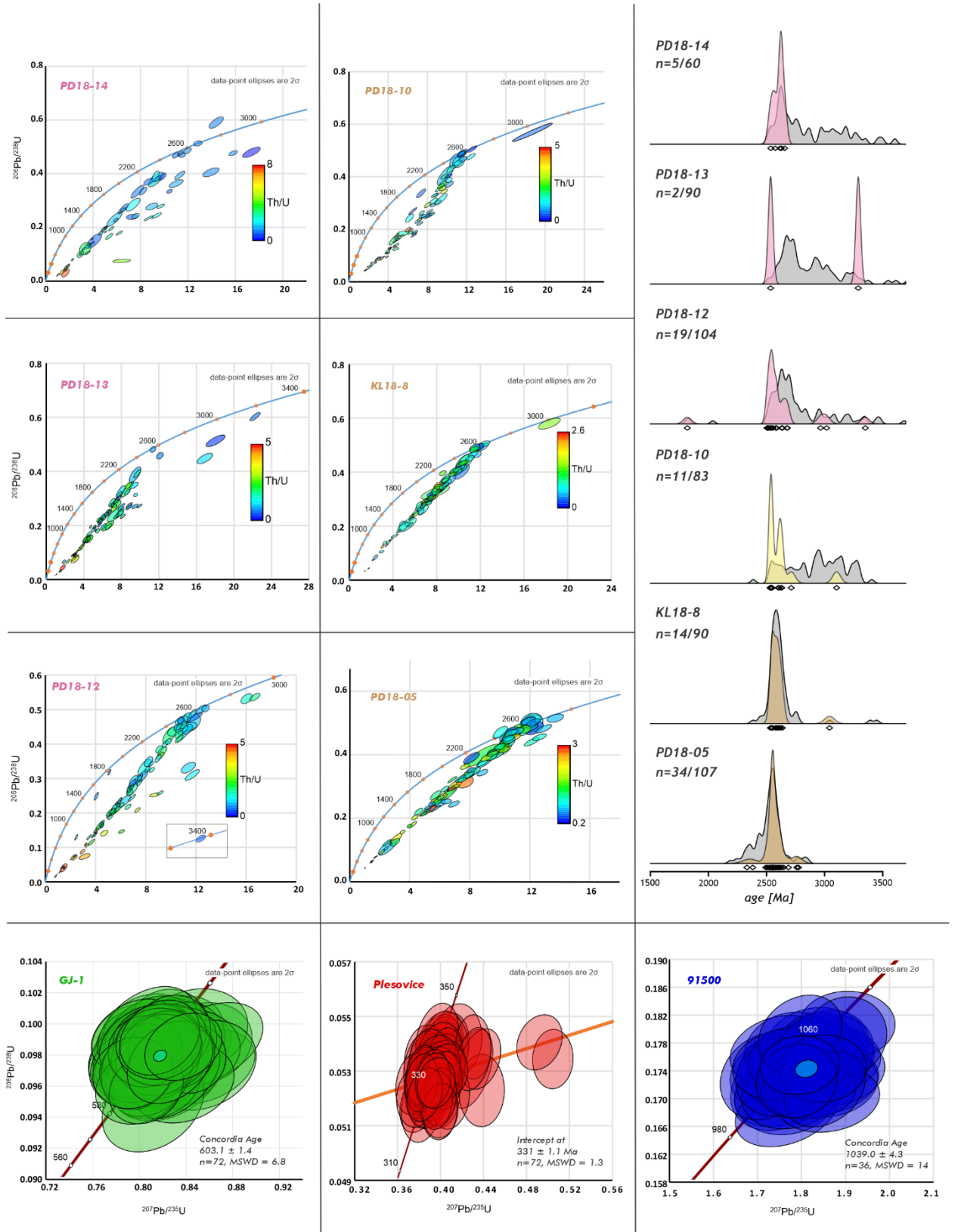


Figure 3: a) The U-Pb zircon concordia plot showing the detrital record of samples labelled on the top left in each Concordia plot. b) The detrital KDE plotted relative to stratigraphy, the coloured plot defining the KDE based on <10% discordant zircons, the grey KDE reflecting all the grains analyzed. The number n =

x/y representing x as the number of near concordant zircons with < 10% discordance, y as the total number of zircons analyzed.

5. Discussion:

5.1 U–Pb data and potential source regions

The zircon populations analyzed display high amounts of discordance within the U–Pb isotopic data plots. The physical transport of sediments involved in the formation of sandstones are expected to favour the least isotopically disturbed zircon grains resulting in concordant U–Pb ages. However, high amount of discordant ages were previously reported from the Kaladgi-Badami basin (Joy et al., 2019). This could be explained by Pb-loss happening to the detrital zircons post-deposition. The detrital populations in the Concordia diagrams appear to form broad discordant arrays that converge towards modern near zero aged Pb-loss which is interpreted as postdepositional Pb-loss in the Phanerozoic. Moreover, the immature nature of the arenitic members of the Kaladgi-Basin has been speculated to the poor sorting on the quality of zircons (Joy et al., 2019). Hence only near-concordant U–Pb ages have been filtered and used for discussing the provenance of the detrital zircon populations.

The samples KL18-8 and PD18-05 are collected from the Ramdurg Formation that forms the base of the lower Lokapur Group. KL18-8 recorded detrital components predominantly at ca. ~ 2.55 Ga, 2.6 Ga and older Archean component from ca 3.0 Ga. Previously published paleocurrent directions in Joy et al., 2019, infer N- to NW-directed transport implying the source regions occurring to the S- to SE of the basin. In these southern areas, the Closepet Granite formed at ca. 2.55 Ga (Friend and Nutman, 1991) and the Eastern Dharwar Craton contains bimodal volcanism that occurred in episodes of 2.7 - 2.6 Ga and 2.57 – 2.52 Ga (Wang J.Y. et al. 2020, Chapter 2 this thesis). The older Archean age could have resulted from detrital material transported from the weathering of the Hungund schist-belt underlying the base of the lower group. The younger detrital age zircon at ca. 2332 ± 65 Ma is inferred to have derived from zircons affected by nearby dyke swarms which have intruded the Dharwar Craton post-assembly (Soderlund et al., 2019). The presence of post-Archean sources underlying the Deccan traps could be a possible explanation for the detrital zircons younger than the ages correlating to the Closepet Granite.

Sample PD18-10 is collected from Muchkundi Quartzite from the Kundargi Formation, that forms the base of the Simikeri Group that overlies the lower Lokapur Group. The detrital U–Pb data mostly record ages of ca. 2.55 Ga and 2.6 Ga with slightly older components dated at ca. 2.75 Ga and ca. 3.1 Ga. These ages are representative of the transitional type gneisses occurring in the Central Dharwar Craton and younger TTGs towards the Eastern Dharwar Craton (Jayananda et al., 2020;

Chapter 2 in this thesis). The older age peaks at 2.75 Ga and 3.1 Ga could have been sourced from the Hungund Schist belt that underlies the basin and older basement gneisses of the Dharwar Craton.

Sample PD18-12 was collected from the base of undeformed horizontal arenite beds from the Cave-temple arenite member of the Kerur Subgroup within the Badami Group. The major age peaks occur at ca. 2.55 Ga, 2.6 Ga with older detrital signatures from ca. 3.1 – 2.9 Ga and ca. ~ 3.35 Ga. The published paleocurrents of the lower Kerur Group (Joy et al., 2019) record a strong SW direction implying the sources occurring to the NE to E of the basin. The Eastern Dharwar Craton and associated volcano-sedimentary schist belts including the nearby Hungund Schist belt are inferred to be potential source regions. The younger peak of 1.8 Ga in the detrital record can be vaguely attributed to affect of the ca. 1.8 Ga dolerite dyke that intruded the lower Lokapur Group. The SW-directed paleocurrent also allows contributions from far away sources beyond the Dharwar Craton, including possibly the Cuddapah basin.

5.2 Depth of crystallization of detrital source protoliths:

Zircon is known to incorporate rare earth elements (REEs) into its structure. In this study, we have adapted a previously published strategy from McKenzie et al. (2018), using various REE normalized ratios to obtain the crystallization conditions of the source protoliths to potentially fingerprint the source regions contributing to the detrital record of the Kaladgi-Badami basin. The ratios of Eu/Eu^* , $(\text{La}/\text{Yb})_N$ and $(\text{Gd}/\text{Yb})_N$ from the zircons were used to represent Eu-anomaly (+ve when >1 , -ve when <1), light REE versus heavy REE (LREE/HREE typically ranging from 0 – 0.1) and middle REE versus heavy REE (MREE/HREE typically ranging from 0 – 1) to infer potential source protoliths.

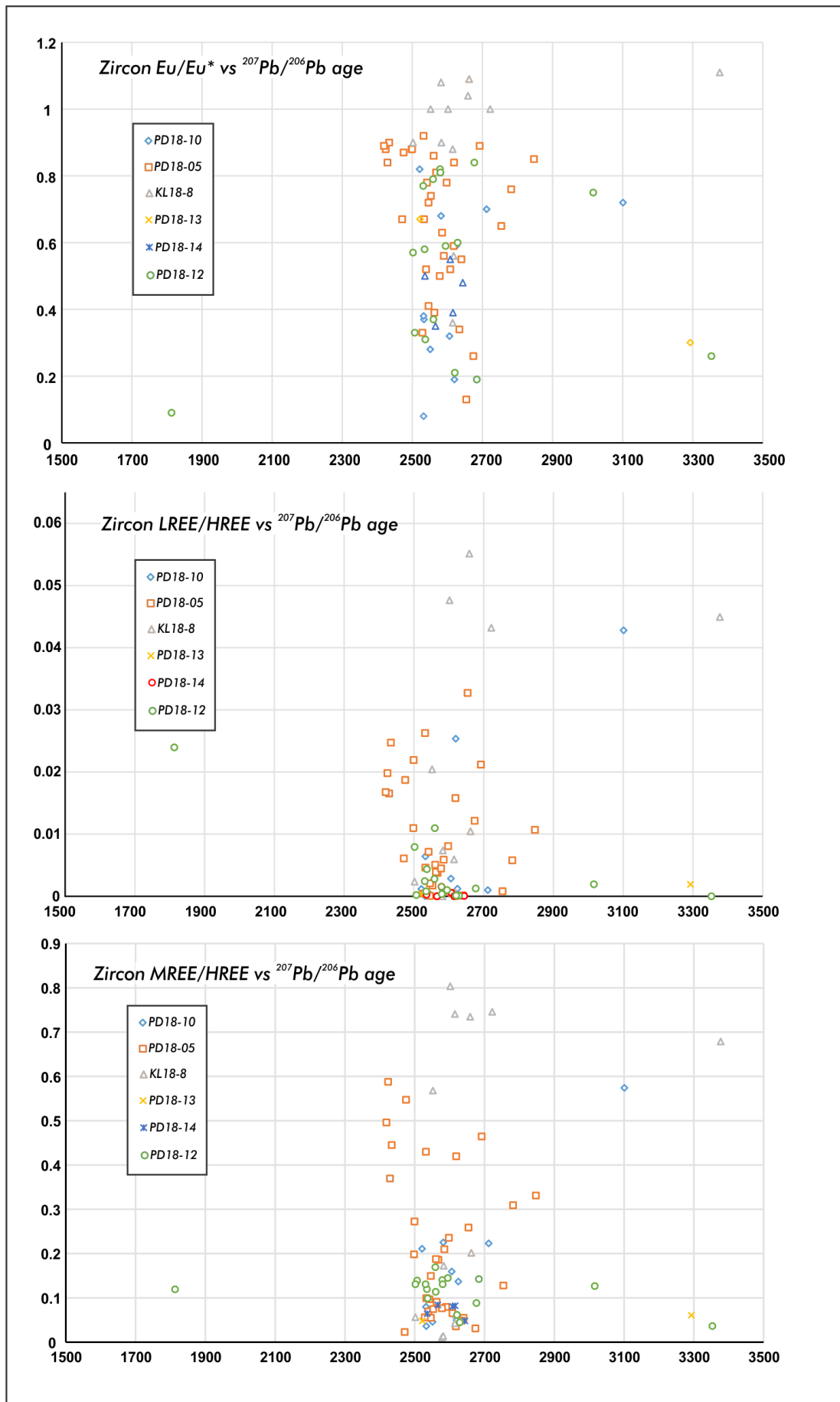


Figure 4: The rare earth elements (REE) ratios plotted for < 10% discordance zircons from each sample. The inset legend shows each sample associated with the plotted symbol. a) The Eu-anomaly, $(Eu/Eu^*)_N$ where $Eu^* = \sqrt{Sm \cdot Gd}$, versus $^{207}Pb/^{206}Pb$ age; b) (La_N/Yb_N) representing LREE/HREE versus $^{207}Pb/^{206}Pb$ age; c) (Gd_N/Yb_N) representing the MREE/HREE versus $^{207}Pb/^{206}Pb$ age.

In the upper Badami Group, the samples collected at the Kerur Formation, PD18-12, PD18-13, PD18-14 exhibit highly varied Eu/Eu^* but negative Eu anomalies ($Eu/Eu^* < 1$) infer the crystallization of the zircons in the source protolith was in presence of plagioclase which incorporates Eu into its crystal lattice. The ratios of $(La/Yb)_N$ and $(Gd/Yb)_N$, however, were consistent and low signifying zircon originated from magmatic protoliths crystallizing at relatively shallow depths. We hypothesize that the TTG gneisses from the Eastern Dharwar Craton, which records bimodal magmatism in episodes spanning 2.7–2.6 Ga and 2.6–2.54 Ga (Jayananda et al, 2020; J.Y. Wang et al., 2020) as probable source regions as the lithologies contain plagioclase that formed during their formation through crustal anatexis leading to varied negative Eu-anomaly values in the associated crystallizing zircons. Older zircons (>3.0 Ga) show highly negative Eu-anomalies and low and consistent LREE/HREE, MREE/HREE values signifying an older Archean source which can be correlated with the Western Dharwar Craton (WDC) (Jayananda et al., 2018). The detrital zircon at 1820 ± 26 Ma shows large negative Eu-anomaly signifying highly differentiated source.

In the Simikeri Group, the detrital zircons from the sample PD18-10 show varied negative Eu-anomaly values similar to the above Badami Group. The detrital zircons with ages of 2.7–2.5 Ga show consistently low LREE/HREE and MREE/HREE ratios showing shallow crystallization compared to the stability field of minerals like garnet and amphibole which incorporate the HREE into their crystal structure increasing the LREE/HREE and MREE/HREE values in the zircons. The detrital zircon at 3104 ± 70 Ma shows higher LREE/HREE and MREE/HREE signifying deeper crystallization of the protolith, which might be correlated to crustal thickening events which are previously reported across the Dharwar Craton. (Jayanada et al., 2015).

In the lower Lokapur Group, samples PD18-05 and KL18-8 show varied REE compositions in their detrital zircon record. The sample KL18-8 contains zircons that show a positive Eu-anomaly between the ages of 2.7–2.5 Ga and slightly negative Eu-anomalies for the majority of remaining zircons. The Eu/Eu^* values from the sample KL18-8 show positive Eu-anomalies ($Eu/Eu^* > 1$) which signifies the europium saturating into the zircon before differentiation into plagioclase/feldspar, which can happen in a non-equilibrium process like metamorphism or alteration (Trail et al., 2012). The sample KL18-8 was collected at the margin of the Hungund-Kushtagi Neoproterozoic greenstone sequence, which explains the alteration or metamorphism of adjacent protoliths probably during the Neoproterozoic

bimodal volcanism previously reported across the Eastern and Central Dharwar Craton during the same period. The LREE/HREE and MREE/HREE ratios range from low to moderately high signifying input from deeper crystallizing protoliths. The Closepet batholith and coeval granitic intrusions across the Dharwar Craton are inferred to be major source regions for the detritus along with a minor contribution from older components from the older TTG gneisses or the adjacent Hungund Schist belt. Sample PD18-05, collected from the same stratigraphic unit, reflects varied negative Eu-anomaly inferring presence of plagioclase in the source which was previously proposed to be underlying the Deccan Traps (Dey et al., 2015). The LREE/HREE and MREE/HREE ratios increase after 2.55 Ga signifying increasing crystallization depth, which can be associated with the crustal thickening due to the final assembly of Dharwar Craton.

5.3 Comparison of detrital ages across Kaladgi-Badami basin and other Paleoproterozoic basins across India and Madagascar using Multidimensional scaling (MDS)

An extensive database of published detrital data from India and Madagascar has been adapted from Armistead et al. (in review), to test possible correlations between the Paleoproterozoic sediments within the Kaladgi-Badami basin with Paleoproterozoic basins across Madagascar and India. Regions from India that are compared are, the lower groups of the Cuddapah Basin and the Southern Granulite Terrane. From Madagascar, the datasets from the Ambatolampy Group, the Itremo Group along with other associated groups pooled into the Greater Itremo Group, which include the Maha Group, the Sahantaha Group and Southern Madagascar (Armistead et al., in review). These are all thought to be part of the Greater Dharwar Craton of Tucker et al. (2011a), but to have been part of Africa in the alternative models of Collins and Windley (2002; Collins and Pisarevsky, 2005; Armistead et al. in review). Previously published U–Pb detrital ages from the Kaladgi-Badami basin (Joy et al., 2019) have been added to our data to increase the database. The Kernel Density Estimates (KDEs) of the samples from the Kaladgi-Badami basin (this study) have been plotted against the database of the combined data from each domain with a top-down view in Figure 5. The U–Pb detrital ages from the datasets have been filtered for ten per cent discordance to remove discordant peaks from the age spectra.

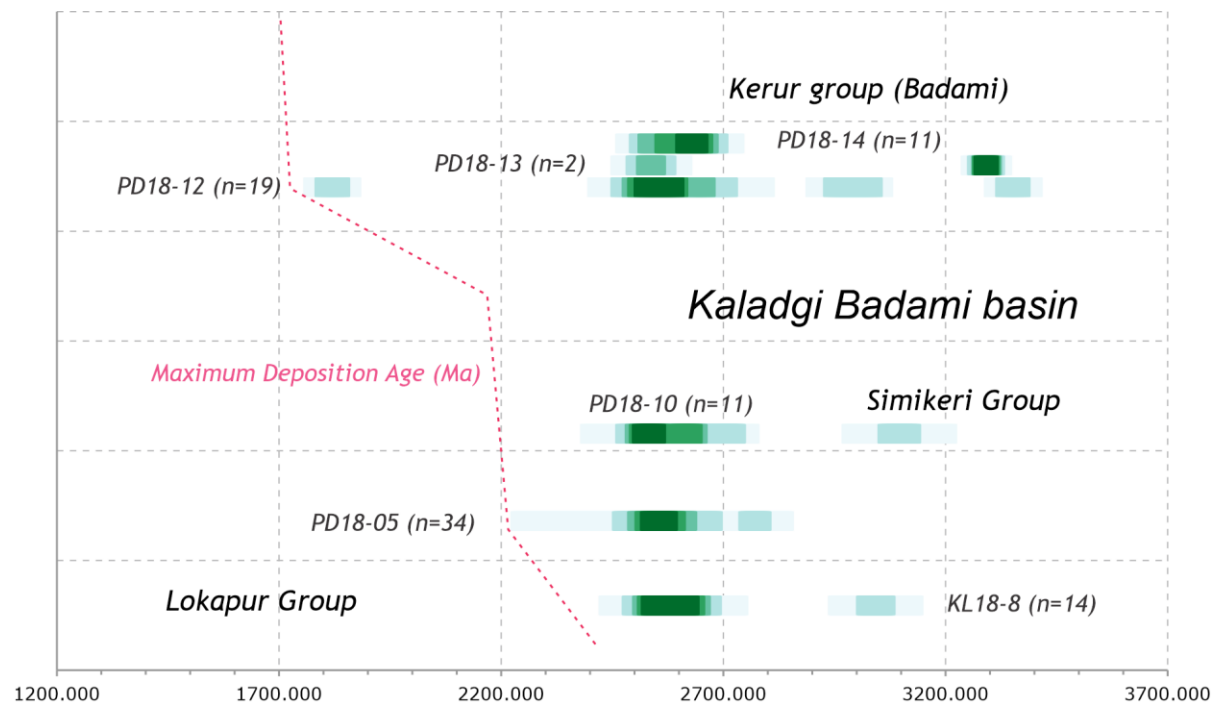


Figure 5: Top down view of probability density estimates of detrital U–Pb zircon data from (a) The samples dated from various formations of Kaladgi-Badami basin. (b) The published data used for correlation with the detrital data from sedimentary formations in India: Cuddapah basin, Southern Granulite Terrain (SGT), Dharwar Craton; in Madagascar: Sahantaha Group, Maha Group, Itremo Group, Ambatolampy Group, Southern Madagascar detritals.

The Lokapur Subgroup shows major detrital signatures at 2.6–2.5 Ga is interpreted as to have sourced from the basement gneisses and granite domains from the Central Dharwar Craton and Eastern Dharwar Craton. The younger detrital age at 2.3 Ga is comparable to the previously published study on the Kaladgi-Badami basin. The Simikeri Subgroup has similar detrital peak at 2.55 Ga, which is attributed to the Closepet Granite, but the depositional age is previously constrained by an intrusive dolerite dyke with U–Pb baddeleyite age at 1861 ± 4 Ma (Joy et al., 2019). The upper Badami Group has similar age peaks slightly shifting from 2.55 Ga to 2.6 Ga, but the sample at the base of the Cave-Temple Arenite has a near concordant zircon dated at 1820 ± 26 Ma, which forms the maximum depositional age of the Kerur Group. The lower bound on the depositional age is poorly constrained with an imprecise U–Th–Pb isochron at ca. 0.96 Ga (Joy et al., 2019).

The detrital age peaks at ca. 2.6–2.5 Ga in the Kaladgi-Badami basin along with the minor 1.8 Ga contributions are well correlated with the presence of similar-aged peaks within the lower groups of the Cuddapah basin (Collins et al. 2015). The older ages correlate well with the published detrital record of the Dharwar Craton confirming its contribution. The Southern Granulite Terrane combined detrital record has slightly younger depositional ages, but has major detrital peaks around ca. 2.55 Ga and ca. 2.1–1.9 Ga, which appears to have a different depositional history compared to the Kaladgi-Badami basin after 2.5 Ga.

The Paleoproterozoic sequences in Madagascar contain detritus with significant age peaks at 2.5 Ga and 1.8 Ga. While low volume older (pre 2.5 Ga) detrital contributions in the Itremo Domain could be explained to be sourced from the Greater Dharwar Craton (Tucker et al., 2011), the significant contribution at 1.8 Ga in the Itremo is hard to attribute to Palaeoproterozoic southern India, and contrasts with the Kaladgi-Badami basin and corollaries in the Cuddapah Basin (Collins et al. 2015). The Malagasy Palaeoproterozoic sedimentary rocks have been interpreted to be sourced from African rocks (Cox et al., 1998; Cox et al., 2004; Fitzsimons and Hulscher, 2005) and recently revised to be Tanzania Craton in east Africa (Armistead et al., in review). The detrital record of the Ambatolampy Group (Archibald et al. 2015) does overlap with the detrital record of the lower groups of the Cuddapah basin and the ages prevalent in Kaladgi-Badami basin. However, the Ambatolampy Group samples do still show numerous ca. 1.8 Ga detritus, it is just that much of this is discordant and therefore not counted in this data treatment. The detrital KDE peaks from Southern Madagascar have age peaks at

1.8 Ga which is present in the upper Badami basin, and 2.2 Ga which is not reflected in any of the groups of the Kaladgi-Badami basin.

To compare the sedimentary environment of the Kaladgi-Badami basin, we have compared the detrital record of each sample within the domains against each other using an MDS (multidimensional scaling) plot. Similar sedimentary records will plot closer on the graph and are enveloped by a contour to represent their domain. Each sample has been marked on the map with India together with Madagascar in the Paleoproterozoic (Ishwar Kumar et al., 2013). The samples are represented by a pie-diagram representing their detrital record within specified intervals to reflect the sedimentary contributions from source regions. The table below summarizes the studies used to create the data set for the MDS plot.

Type	Country	References
Detrital	Madagascar	Archibald et al. (2015); Armistead et al. (2020); BGS-USGS-GLW (2008); Boger et al. (2014); Collins et al. (2012); Collins et al. (2003b); Costa et al. (2019); Cox et al. (1998); Cox et al. (2004); De Waele et al. (2011); Fitzsimons and Hulscher (2005); Tucker et al. (2011a); Tucker et al. (2011b).
Detrital	India	Armistead et al. (2017); Collins et al. (2007a); Collins et al. (2015); Henderson et al. (2014); Ishwar-Kumar et al. (2013); Joy et al. (2015); Kooijman et al. (2011); Kumar et al. (2016); Lancaster et al. (2015); Li et al. (2017); Maibam et al. (2016); Maibam et al. (2011); Plavsa et al. (2014); Prakash and Sharma (2011); Raith et al. (2010); Sarma et al. (2012); Teale et al. (2011); Upadhyay et al. (2009)

For this comparison, the detrital data sets with maximum depositional ages between 2700 – 1500 Ma have been used to omit older detrital sequences that are related to the older greenstone sequences on the Antongil–Dharwar Craton and other younger Mesoproterozoic sequences. The ages from each sample have been filtered for concordance between 85% and 105%. The samples with less than 5 grains after filtering have been removed to minimize overweighting of fewer ages. The detrital data used from the Itremo Group have been consolidated into three age groups that have been represented by their respective KDE in piechart form.

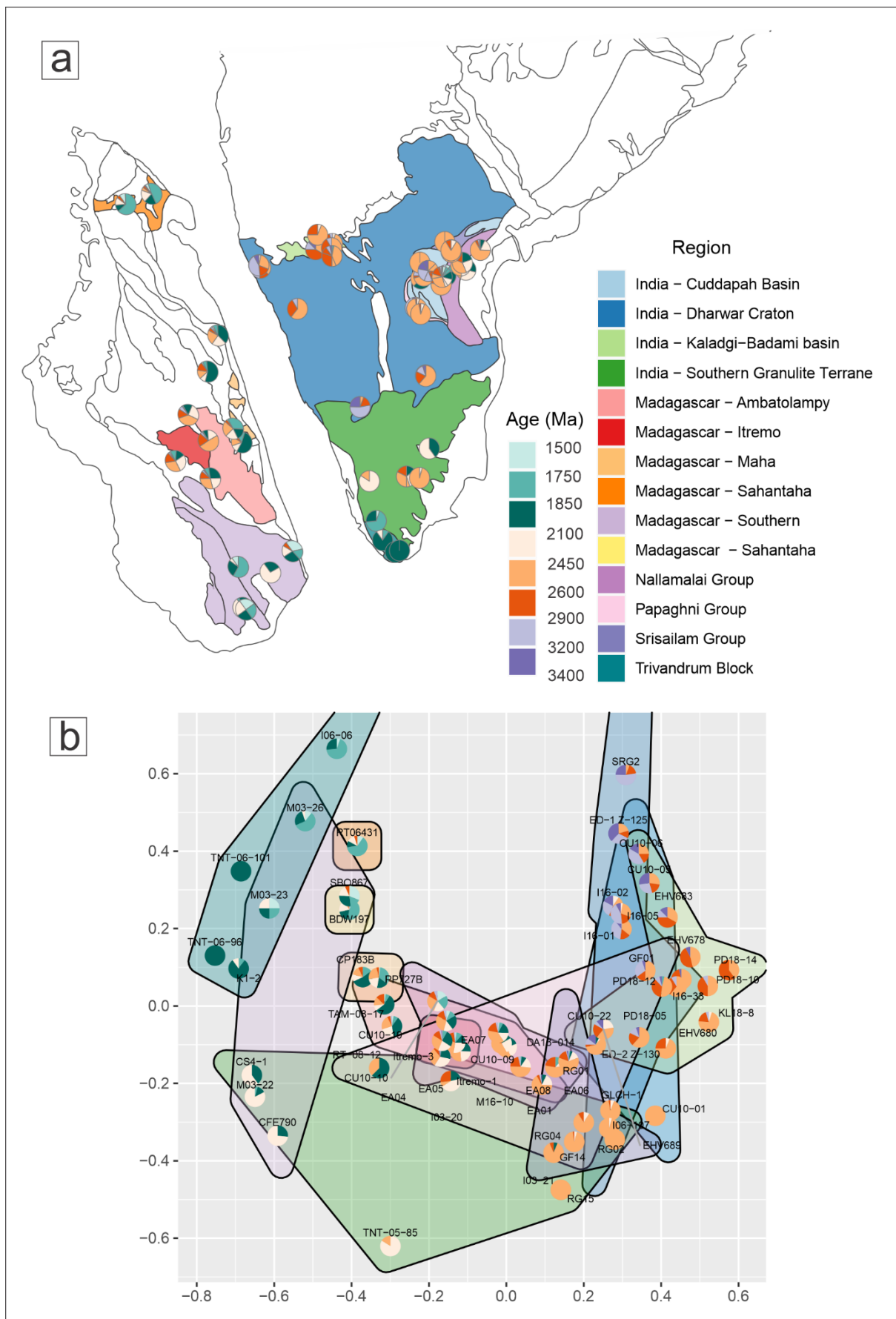


Figure 6: a) Geographical locations of detrital zircon U–Pb data from Paleoproterozoic basins across southern India and Madagascar (including this study) represented by piecharts depicting the fractions of age data using the age brackets shown in the legend. The sedimentary formations have been coloured using the legend over the map. b) Multidimensional scaling analysis of the detrital samples filtered by maximum depositional ages between 2700—1500 Ma to include only Paleoproterozoic detrital sequences. The samples have been grouped based on sedimentary formations and coloured using the same colour scheme as the map in (a).

From the MDS plot, the provenance record of the Kaladgi-Badami basin, including the published data, plot closer to the detrital record of the lower formations in the Cuddapah basin and the Dharwar Craton, and show significant dissimilarity to the provenance record of basins in Madagascar, which in turn are closely related. This implies a similar sedimentary system across the Madagascar Paleoproterozoic basins. The Ambatolampy Group, which contained similar ages to that of the Kaladgi-Basin, plots far from its contour representing the dissimilarity in sedimentary environments.

The southern regions of Madagascar plot in similar positions to some of the detrital records of those belonging to the Southern Granulite Terrane, with the possibility of being related sedimentary systems (Plavsa et al. 2014). The Maha and Sahantaha groups appear to be closely related in sedimentary environments to the Itremo Group which has been reported by Armistead et al. (2020).

The formations of the Cuddapah Basin share some similarities to the Itremo Group with some formations preserving significant ca. 1.8 Ga detritus. The Nallamalai Group, in particular, shares similar detrital zircon age record to that of the Itremo Group. Collins et al. (2015), interpreted the Nallamalai Group to represent a foreland basin sequence deposited proximal to the evolving Krishna Orogen. These authors demonstrated how coeval sediments deposited in a platform setting to the west (the Srisalam Group) did not contain much Krishna Orogen-derived detritus. The Kaladgi-Badami Basin continues this trend of decreasing Palaeoproterozoic zircon seen progressively in the Cuddapah Basin. This questions the idea that Malagasy Palaeoproterozoic basins were sourced from India as the dominant ca. 1.8–2.0 Ga detritus in these rocks are not reflected in the Indian basins found between a possible Madagascan-extension to the Palaeoproterozoic Dharwar Craton and the possible source in the SE Indian Krishna Orogen. Instead, Palaeoproterozoic zircon in the Itremo and other Paleoproterozoic groups across Madagascar has been proposed to be sourced from Tanzania Craton in east Africa.

The Kaladgi-Badami basin is now proposed to have shared similar sedimentary environment as the lower groups of the Cuddapah basin such as the Papagni Group and was part of wide-spread sedimentation across the Indian subcontinent during the Paleoproterozoic. After the deposition of the Lokapur Group, it was intruded by a dolerite dyke at ca. 1860 Ma, which may be part of an extensive

mafic intrusive event that includes mafic sills within the Cuddapah Basin Tadipatri Formation (Joy et al., 2019). The paleocurrent flow in the lower groups has been reported to be towards NW-N direction implying the contribution of Eastern Dharwar Craton which is in agreement with our findings. Paleocurrents are then reported to have changed towards an SW direction during the sedimentation of the upper Badami Group, which may have brought the rare ca. 1.8 Ga zircons from far sources such as the Cuddapah Basin.

5.4 Formation of the Kaladgi-Badami basin post-assembly of Dharwar Craton

The Kaladgi-Badami basin formed as an intra-cratonic basin after the final assembly of the Dharwar Craton. Its formation may have been initiated by the dyke swarm activity across the craton (Soderlund et al., 2019), weakening the crust. Dyke intrusions occur throughout the eastern Dharwar Craton at ca. 1.86 Ga (Sarma et al., 2020), and these may correlate with the formation of the basin. The lower groups formed due to the contribution from the Dharwar Craton with paleocurrent flows occurring in NW-N directions (Joy et al., 2019). The presence of 1861 ± 4 Ma dolerite dyke intruding through the lower Lokapur Subgroup provides evidence that sedimentation was deposited before ca. 1.86 Ga. The Simikeri Group may post-date ca 1.86 Ga, as no dykes are reported to intrude it. The Badami Group contains zircons aged at ca 1.8 Ga is interpreted to have been deposited by river systems, with unidirectional paleocurrents trending to the SW. The significance of a U–Th–Pb isochron from the

Katagiri limestone formation at ca 0.96 Ga (Joy et al., 2019) has been questioned (Patil Pillai et al. 2019), however, it has been interpreted to suggest that the Bhima Formation was deposited in the Neoproterozoic, and may correlate with lithologically similar quartz arenites of the Kurnool Group of the Cuddapah basin (Collins et al., 2015). This would suggest a major transgression across the northern Dharwar Craton at this time.

6. Conclusions:

- 1) The lower groups of the Kaladgi-Badami basin within the Bagalkot Group have a maximum depositional age of 2332 ± 65 Ma. Whereas the youngest detrital zircon in the Badami Group is 1820 ± 26 Ma.
- 2) The major peaks in the detrital record of the lower Lokapur subgroup coincide with the crystallization ages of major lithologies in the region around ca. 2.6–2.55 Ga. The felspathic arenite collected at the margin of the Hungund-Kushtagi greenschist belt revealed detrital zircons with distinct geochemical signatures inferring alteration of the source protoliths.

- 3) The multidimensional scaling (MDS) revealed that the upper Badami Group has deposited from similar sources as the Papagni Group within the Cuddapah basin and does not bear similarities to the Itremo Group, hence not in agreement with the Greater Dharwar Craton hypothesis proposed by Tucker et al., (2011).
- 4) The initiation of sedimentation in the Kaladgi-Badami basin is proposed to have occurred after the assembly of the Dharwar Craton around ca. 2.3 Ga, and constrained between ca. 2.3 Ga and 1.86 Ga, due to dyke swarm activity weakening the crust and causing asymmetry from extensional tectonics within the northern and southern margins of the current basin.

7. Acknowledgements:

We acknowledge the support of Dr Sarah Gilbert for support at Adelaide Microscopy, the University of Adelaide in performing the detrital zircon U–Pb isotope and REE compositional analysis. We thank Dr Amlan Banerjee for assistance during fieldwork along with the PhD students from the Geological Studies Unit (GSU) at the Indian Statistical Institute, India. The Petrology lab team at Indian Institute of Science, India are acknowledged for their assistance during fieldwork logistics and sample preparation. We thank Dr Sheree Armistead for discussions related to R programming to create multidimensional scaling plots and pie-charts during her PhD at the University of Adelaide. Venkata Pavan Katuru is supported during his PhD by the scholarship provided by the University of Adelaide.

8. Appendix

The U–Pb data from the detrital zircons have been provided in appendix 4.1. The REE compositions of the detrital zircons from the Kaladgi-Badami basin have been provided in appendix 4.2.

9. References:

- 1) Archibald, Donnelly B., Alan S. Collins, John D. Foden, Justin L. Payne, Richard Taylor, Peter Holden, Théodore Razakamanana, and Christopher Clark. "Towards Unravelling the Mozambique Ocean Conundrum Using a Triumvirate of Zircon Isotopic Proxies on the Ambatolampy Group, Central Madagascar." *Tectonophysics* 662 (2015/11/01/ 2015): 167-82.
<http://dx.doi.org/https://doi.org/10.1016/j.tecto.2015.02.018>.
- 2) Armistead, Sheree E., Alan S. Collins, Justin L. Payne, John D. Foden, Bert De Waele, E. Shaji, and M. Santosh. "A Re-Evaluation of the Kumta Suture in Western Peninsular India and Its Extension into Madagascar." *Journal of Asian Earth Sciences* (2017/08/18/ 2017).
<http://dx.doi.org/https://doi.org/10.1016/j.jseaes.2017.08.020>.

- 3) Armistead, Sheree Ellen, Alan S Collins, Renata da Silva Schmitt, Raiza Costa, Bert De Waele, Théodore Razakamanana, Justin Payne, and John Foden. *Proterozoic Basin Evolution and Tectonic Geography of Madagascar During the Nuna/Columbia Supercontinent*.
- 4) Basu, A., & Bickford, M. (2014). Contributions of zircon U–Pb geochronology to understanding the volcanic and sedimentary history of some Purāna basins, India. *Journal of Asian Earth Sciences*, 91, 252–262. doi:10.1016/j.jseae.2013.06.018
- 5) Basu, Abhijit and M. Bickford. "An Alternate Perspective on the Opening and Closing of the Intracratonic Purana Basins in Peninsular India." *Journal of the Geological Society of India* 85 (05/01 2015): 5-25. <http://dx.doi.org/10.1007/s12594-015-0190-y>.
- 6) Bradley, D. C. (2008). Passive margins through earth history. *Earth-Science Reviews*, 91(1), 1-26. doi:<https://doi.org/10.1016/j.earscirev.2008.08.001>
- 7) Bradley, D. C. (2011). Secular trends in the geologic record and the supercontinent cycle. *Earth-Science Reviews*, 108(1), 16-33. doi:<https://doi.org/10.1016/j.earscirev.2011.05.003>
- 8) BGS-USGS-GLW. "Revision De La Cartographie Géologique Et Minière Des Zones Nord Et Centre De Madagascar." *British Geological Survey Research Report CR/08/078. Republique de Madagascar Ministère de L'energie et des Mines*, (2008): 1-1049.
- 9) Boger, S. D., W. Hirdes, C. A. M. Ferreira, Bernd Schulte, T. Jenett, and Christopher Fanning. "From Passive Margin to Volcano–Sedimentary Forearc: The Tonian to Cryogenian Evolution of the Anosyen Domain of Southeastern Madagascar." *Precambrian Research* 247 (07/01 2014): 159–86. <http://dx.doi.org/10.1016/j.precamres.2014.04.004>.
- 10) Bose, Pradip K., Subir Sarkar, Soumik Mukhopadhyay, Bikas Saha, and Patrick Eriksson. "Precambrian Basin-Margin Fan Deposits: Mesoproterozoic Bagalkot Group, India." *Precambrian Research* 162, no. 1 (2008/04/05/ 2008): 264-83. <http://dx.doi.org/https://doi.org/10.1016/j.precamres.2007.07.022>.
- 11) Boynton, William V. "Cosmochemistry of the Rare Earth Elements: Meteorite Studies." In *Developments in Geochemistry*, vol 2, 63-114: Elsevier, 1984.
- 12) Bradley, Dwight C. "Passive Margins through Earth History." *Earth-Science Reviews* 91, no. 1 (2008/12/01/ 2008): 1-26. <http://dx.doi.org/https://doi.org/10.1016/j.earscirev.2008.08.001>.
- 13) Chakraborty, Partha Pratim, Sukanta Dey, and Sarada Prasad Mohanty. "Proterozoic Platform Sequences of Peninsular India: Implications Towards Basin Evolution and Supercontinent Assembly." *Journal of Asian Earth Sciences* 39, no. 6 (2010/11/09/ 2010): 589-607. <http://dx.doi.org/https://doi.org/10.1016/j.jseae.2010.04.030>.
- 14) Collins, Alan, P. Kinny, and Razakamanana Théodore. "Depositional Age, Provenance and Metamorphic Age of Metasedimentary Rocks from Southern Madagascar." *Gondwana Research* 21 (01/01 2012): 353-61. <http://dx.doi.org/10.1016/j.gr.2010.12.00>.
- 15) Collins, Alan S., Sarbani Patranabis-Deb, Emma Alexander, Cari N. Bertram, Georgina M. Falster, Ryan J. Gore, Julie Mackintosh, Pratap C. Dhang, Dilip Saha, Justin L. Payne, Fred Jourdan, Guillaume Backé, Galen P. Halverson, and Benjamin P. Wade. "Detrital Mineral Age, Radiogenic Isotopic Stratigraphy and Tectonic Significance of the Cuddapah Basin, India." *Gondwana Research* 28, no. 4 (2015/12/01/ 2015): 1294-309. <http://dx.doi.org/https://doi.org/10.1016/j.gr.2014.10.013>.
- 16) Collins, Alan S, M Santosh, I Braun, and C Clark. "Age and Sedimentary Provenance of the Southern Granulites, South India: U-Th-Pb Shrimp Secondary Ion Mass Spectrometry." *Precambrian Research* 155, no. 1-2 (2007): 125-38.

- 17) Cox, Rónadh, Richard A Armstrong, and Lewis D Ashwal. "Sedimentology, Geochronology and Provenance of the Proterozoic Itremo Group, Central Madagascar, and Implications for Pre-Gondwana Palaeogeography." *Journal of the Geological Society* 155, no. 6 (1998): 1009-24.
- 18) Cox, Ronadh, Drew S Coleman, Carla B Chokel, Stephen B DeOreo, Joseph L Wooden, Alan S Collins, Bert De Waele, and Alfred Kröner. "Proterozoic Tectonostratigraphy and Paleogeography of Central Madagascar Derived from Detrital Zircon U-Pb Age Populations." *The Journal of Geology* 112, no. 4 (2004): 379-99.
- 19) De Waele, B., R. J. Thomas, P. H. Macey, M. S. A. Horstwood, R. D. Tucker, P. E. J. Pitfield, D. I. Schofield, K. M. Goodenough, W. Bauer, R. M. Key, C. J. Potter, R. A. Armstrong, J. A. Miller, T. Randriamananjara, V. Ralison, J. M. Rafahatelo, M. Rabarimanana, and M. Bejoma. "Provenance and Tectonic Significance of the Palaeoproterozoic Metasedimentary Successions of Central and Northern Madagascar." *Precambrian Research* 189, no. 1 (2011/08/01/ 2011): 18-42.
<http://dx.doi.org/https://doi.org/10.1016/j.precamres.2011.04.004>.
- 20) Dewashish Upadhyay, Axel Gerdes, and Michael M. Raith. "Unraveling Sedimentary Provenance and Tectonothermal History of High-Temperature Metapelites, Using Zircon and Monazite Chemistry: A Case Study from the Eastern Ghats Belt, India." *The Journal of Geology* 117, no. 6 (2009): 665-83.
<http://dx.doi.org/10.1086/606036>.
- 21) Dey, SUKANTA, Rao, R Gajapathi, Gorikhan, RA, Veerabhaskar, D, Kumar, Sunil, Kumar, MARY K. "Geochemistry and Origin of Northern Closepet Granite from Gudur-Guledagudda Area, Bagalkot District, Karnataka." (2003).
- 22) Dey, Sukanta. "Geological History of the Kaladgi–Badami and Bhima Basins, South India: Sedimentation in a Proterozoic Intracratonic Setup." *Geological Society, London, Memoirs* 43, no. 1 (2015): 283-96.
- 23) Dey, Sukanta, A. K. Rai, and Anjan Chaki. *Widespread Arkose Along the Northern Margin of the Proterozoic Kaladgi Basin, Karnataka: Product of Uplifted Granitic Source or K-Metasomatism?* Vol. 71, 2008.
- 24) Dey, Sukanta, A. K. Rai, and Anjan Chaki. "Palaeoweathering, Composition and Tectonics of Provenance of the Proterozoic Intracratonic Kaladgi–Badami Basin, Karnataka, Southern India: Evidence from Sandstone Petrography and Geochemistry." *Journal of Asian Earth Sciences* 34, no. 6 (2009/05/20/ 2009): 703-15. <http://dx.doi.org/https://doi.org/10.1016/j.jseaes.2008.10.003>.
- 25) Dickinson, William R, L Sue Beard, G Robert Brakenridge, James L Erjavec, Robert C Ferguson, Kerry F Inman, Rex A Knepp, F Alan Lindberg, and Paul T Ryberg. "Provenance of North American Phanerozoic Sandstones in Relation to Tectonic Setting." *Geological Society of America Bulletin* 94, no. 2 (1983): 222-35.
- 26) Fitzsimons, ICW and B Hulscher. "Out of Africa: Detrital Zircon Provenance of Central Madagascar and Neoproterozoic Terrane Transfer across the Mozambique Ocean." *Terra Nova* 17, no. 3 (2005): 224-35.
- 27) Henderson, Bonnie, Alan S. Collins, Justin Payne, Caroline Forbes, and Dilip Saha. "Geologically Constraining India in Columbia: The Age, Isotopic Provenance and Geochemistry of the Protoliths of the Ongole Domain, Southern Eastern Ghats, India." *Gondwana Research* 26, no. 3 (2014/11/01/ 2014): 888-906. <http://dx.doi.org/https://doi.org/10.1016/j.gr.2013.09.002>.
- 28) Ishwar-Kumar, C., M. Santosh, S. A. Wilde, T. Tsunogae, T. Itaya, B. F. Windley, and K. Sajeew. "Mesoproterozoic Suturing of Archean Crustal Blocks in Western Peninsular India: Implications for India–Madagascar Correlations." *Lithos* 263 (2016/10/15/ 2016): 143-60.
<http://dx.doi.org/https://doi.org/10.1016/j.lithos.2016.01.016>.
- 29) Jackson, Simon E., Norman J. Pearson, William L. Griffin, and Elena A. Belousova. "The Application of Laser Ablation-Inductively Coupled Plasma-Mass Spectrometry to in Situ U–Pb Zircon Geochronology." *Chemical Geology* 211, no. 1 (2004/11/08/ 2004): 47-69.
<http://dx.doi.org/https://doi.org/10.1016/j.chemgeo.2004.06.017>.

- 30) Janoušek, V., Farrow, C. M. & Erban, V. 2006. Interpretation of whole-rock geochemical data in igneous geochemistry: introducing Geochemical Data Toolkit (GCDkit). *Journal of Petrology* 47(6):1255-1259
- 31) Jayananda, M., D. Chardon, J. J. Peucat, Tushipokla, and C. M. Fanning. "Paleo- to Mesoproterozoic Tectonic Accretion and Continental Growth in the Western Dharwar Craton, Southern India: Constraints from Shrimp U–Pb Zircon Geochronology, Whole-Rock Geochemistry and Nd–Sr Isotopes." *Precambrian Research* 268 (2015): 295-322. <http://dx.doi.org/10.1016/j.precamres.2015.07.015>.
- 32) Jayaprakash, A.V., ; Sundaram, V.,; Hans, S.K.,; Mishra, R.N.,. "Geology of the Kaladgi-Badami Basin: Purana Basins of Peninsular India (Middle to Late Proterozoic)." *Memoir Geological Society of India* 6 (1987): 201-26.
- 33) Jochum, Klaus Peter, Ulrike Weis, Brigitte Stoll, Dmitry Kuzmin, Qichao Yang, Ingrid Raczek, Dorrit E. Jacob, Andreas Stracke, Karin Birbaum, Daniel A. Frick, Detlef Günther, and Jacinta Enzweiler. "Determination of Reference Values for NIST SRM 610–617 Glasses Following ISO Guidelines." *Geostandards and Geoanalytical Research* 35, no. 4 (2011): 397-429. <http://dx.doi.org/doi:10.1111/j.1751-908X.2011.00120.x>.
- 34) Joy, Sojen, Sarbani Patranabis-Deb, Dilip Saha, Hielke Jelsma, Roland Maas, Ulf Söderlund, Sebastian Tappe, Gert van der Linde, Amlan Banerjee, and Unni Krishnan. "Depositional History and Provenance of Cratonic "Purana" Basins in Southern India: A Multipronged Geochronology Approach to the Proterozoic Kaladgi and Bhima Basins." *Geological Journal* 54, no. 5 (2019): 2957-79. <http://dx.doi.org/10.1002/gj.3415>.
- 35) Kale, V. S., Vaishali Ghunakikar, P. P. Thomas, and V. V. Peshwa. *Macrofacies Architecture of the First Transgressive Suite Along the Southern Margin of the Kaladgi Basin*. 1996.
- 36) Kale, Vivek S. and V. G. Phansalkar. "Purana Basins of Peninsular India: A Review." *Basin Research* 3, no. 1 (1991): 1-36. <http://dx.doi.org/https://doi.org/10.1111/j.1365-2117.1991.tb00133.x>.
- 37) Kooijman, Ellen, Dewashish Upadhyay, Klaus Mezger, Michael M. Raith, Jasper Berndt, and C. Srikantappa. "Response of the U–Pb Chronometer and Trace Elements in Zircon to Ultrahigh-Temperature Metamorphism: The Kadavur Anorthosite Complex, Southern India." *Chemical Geology* 290, no. 3 (2011/11/24/ 2011): 177-88. <http://dx.doi.org/https://doi.org/10.1016/j.chemgeo.2011.09.013>.
- 38) Kumar, T. Vijaya, Y.J. Bhaskar Rao, Diana Plavsa, Alan S. Collins, J.K. Tomson, B. Vijaya Gopal, and E.V.S.S.K. Babu. "Zircon U–Pb Ages and Hf Isotopic Systematics of Charnockite Gneisses from the Ediacaran–Cambrian High-Grade Metamorphic Terranes, Southern India: Constraints on Crust Formation, Recycling, and Gondwana Correlations." *GSA Bulletin* 129, no. 5-6 (2017): 625-48. Accessed 9/7/2020. <http://dx.doi.org/10.1130/b31474.1>.
- 39) Lancaster, Penelope J., Sukanta Dey, Craig D. Storey, Anirban Mitra, and Rakesh K. Bhunia. "Contrasting Crustal Evolution Processes in the Dharwar Craton: Insights from Detrital Zircon U–Pb and Hf Isotopes." *Gondwana Research* 28, no. 4 (2015): 1361-72. <http://dx.doi.org/10.1016/j.gr.2014.10.010>.
- 40) Li, Shan-Shan, M. Santosh, G. Indu, E. Shaji, and T. Tsunogae. "Detrital Zircon Geochronology of Quartzites from the Southern Madurai Block, India: Implications for Gondwana Reconstruction." *Geoscience Frontiers* 8, no. 4 (2017/07/01/ 2017): 851-67. <http://dx.doi.org/https://doi.org/10.1016/j.gsf.2016.07.002>.
- 41) Ludwig, K.R. "User's Manual for Isoplot 3.0." *A Geochronological Toolkit for Microsoft Excel* 71 (2003).
- 42) Maibam, B., A. Gerdes, and J. N. Goswami. "U–Pb and Hf Isotope Records in Detrital and Magmatic Zircon from Eastern and Western Dharwar Craton, Southern India: Evidence for Coeval Archaean Crustal Evolution." *Precambrian Research* 275 (2016): 496-512. <http://dx.doi.org/10.1016/j.precamres.2016.01.009>.

- 43) Maibam, B, JN Goswami, and R Srinivasan. "Pb–Pb Zircon Ages of Archaean Metasediments and Gneisses from the Dharwar Craton, Southern India: Implications for the Antiquity of the Eastern Dharwar Craton." *Journal of Earth System Science* 120, no. 4 (2011): 643–61.
- 44) McKenzie, N. Ryan, Andrew J. Smye, Venkatraman S. Hegde, and Daniel F. Stockli. "Continental Growth Histories Revealed by Detrital Zircon Trace Elements: A Case Study from India." *Geology* 46, no. 3 (2018): 275–78. <http://dx.doi.org/10.1130/G39973.1>.
- 45) Norman, M. D., W. L. Griffin, N. J. Pearson, M. O. Garcia, and S. Y. O'Reilly. "Quantitative Analysis of Trace Element Abundances in Glasses and Minerals: A Comparison of Laser Ablation Inductively Coupled Plasma Mass Spectrometry, Solution Inductively Coupled Plasma Mass Spectrometry, Proton Microprobe and Electron Microprobe Data." *Journal of Analytical Atomic Spectrometry* 13, no. 5 (1998): 477–82. <https://www.scopus.com/inward/record.uri?eid=2-s2.0-0032072961&partnerID=40&md5=f2c15cb5cd919f458c7151f2045b68ec>.
- 46) NORMAN, M.D., N.J. PEARSON, A. SHARMA, and W.L. GRIFFIN. "Quantitative Analysis of Trace Elements in Geological Materials by Laser Ablation Icpms: Instrumental Operating Conditions and Calibration Values of Nist Glasses." *Geostandards Newsletter* 20, no. 2 (1996): 247–61. <http://dx.doi.org/doi:10.1111/j.1751-908X.1996.tb00186.x>.
- 47) Padmakumari, VM, VV Sambasiva Rao, and R Srinivasan. *Model Nd and Rb–Sr Ages of Shales of the Bagalkot Group, Kaladgi Supergroup, Karnataka*. Abstracts, National symposium on Late Quaternary geology and sea level changes, 1998.
- 48) Paton, Chad, John Hellstrom, Bence Paul, Jon Woodhead, and Janet Hergt. "Iolite: Freeware for the Visualisation and Processing of Mass Spectrometric Data." *Journal of Analytical Atomic Spectrometry* 26, no. 12 (2011): 2508–18.
- 49) Plavsa, Diana, Alan Collins, Justin Payne, John Foden, Chris Clark, and M. Santosh. "Detrital Zircons in Basement Metasedimentary Protoliths Unveil the Origins of Southern India." *Geological Society of America Bulletin* 126 (05/02 2014). <http://dx.doi.org/10.1130/B30977.1>.
- 50) Prakash, D. "New Shrimp U–Pb Zircon Ages of the Metapelitic Granulites from Nw of Madurai, Southern India." *Journal of the Geological Society of India* 76, no. 4 (2010): 371–83.
- 51) Saha, D., S. Patranabis-Deb, and A. S. Collins. "Chapter One - Proterozoic Stratigraphy of Southern Indian Cratons and Global Context." In *Stratigraphy & Timescales*, edited by Michael Montenari, vol 1, 1–59: Academic Press, 2016.
- 52) Sathyanarayan, S, Ravindra, B. M, Ranganathan, N. "The Younger Proterozoic Badami Group, Northern Karnataka." *Geo Karnataka* (1994): 227–33.
- 53) Sláma, Jiří, Jan Košler, Daniel J. Condon, James L. Crowley, Axel Gerdes, John M. Hanchar, Matthew S. A. Horstwood, George A. Morris, Lutz Nasdala, Nicholas Norberg, Urs Schaltegger, Blair Schoene, Michael N. Tubrett, and Martin J. Whitehouse. "Plešovice Zircon — a New Natural Reference Material for U–Pb and Hf Isotopic Microanalysis." *Chemical Geology* 249, no. 1 (2008/03/30/ 2008): 1–35. <http://dx.doi.org/https://doi.org/10.1016/j.chemgeo.2007.11.005>.
- 54) Söderlund, Ulf, Wouter Bleeker, Kursad Demirer, Rajesh K. Srivastava, Michael Hamilton, Mimmi Nilsson, Lauri J. Pesonen, Amiya K. Samal, Mudlappa Jayananda, Richard E. Ernst, and Madabhooshi Srinivas. "Emplacement Ages of Paleoproterozoic Mafic Dyke Swarms in Eastern Dharwar Craton, India: Implications for Paleoreconstructions and Support for a ~30° Change in Dyke Trends from South to North." *Precambrian Research* 329 (2019/08/01/ 2019): 26–43. <http://dx.doi.org/https://doi.org/10.1016/j.precamres.2018.12.017>.
- 55) Srinivasa Sarma, D McNaughton, N J, Elena Belusova, M Ram Mohan, and I R Fletcher. "Detrital Zircon U–Pb Ages and Hf–Isotope Systematics from the Gadag Greenstone Belt: Archean Crustal Growth in the

Western Dharwar Craton, India." *Gondwana Research* 22 (2012): 843-54.
<http://dx.doi.org/10.1016/j.gr.2012.04.001>.

- 56) Teale, William, Alan S. Collins, John Foden, Justin L. Payne, Diana Plavsa, T. R. K. Chetty, M. Santosh, and Mark Fanning. "Cryogenian (~830ma) Mafic Magmatism and Metamorphism in the Northern Madurai Block, Southern India: A Magmatic Link between Sri Lanka and Madagascar?" *Journal of Asian Earth Sciences* 42, no. 3 (2011/08/10/ 2011): 223-33.
<http://dx.doi.org/https://doi.org/10.1016/j.jseaes.2011.04.006>.
- 57) Tucker, R. D., J. Y. Roig, C. Delor, Y. Amelin, P. Goncalves, M. H. Rabarimanana, A. V. Ralison, and R. W. Belcher. "Neoproterozoic Extension in the Greater Dharwar Craton: A Reevaluation of the "Betsimisaraka Suture" in Madagascar" This Article Is One of a Series of Papers Published in This Special Issue on the Theme of Geochronology in Honour of Tom Krogh." *Canadian Journal of Earth Sciences* 48, no. 2 (2011/02/01 2011): 389-417. Accessed 2020/09/07. <http://dx.doi.org/10.1139/E10-034>.
- 58) Viswanathaiah, M. N. "Lithostratigraphy of the Kaladgi and Badami Groups, Karnataka." *Indian Mineralogist* 18 (1977): 122-32.
- 59) Wang, Jing-Yi, M. Santosh, M. Jayananda, and K. R. Aadhiseshan. "Bimodal Magmatism in the Eastern Dharwar Craton, Southern India: Implications for Neoproterozoic Crustal Evolution." *Lithos* 354-355 (2020/02/01/ 2020): 105336. <http://dx.doi.org/https://doi.org/10.1016/j.lithos.2019.105336>.

5

Thermal history of the Dharwar Craton, India:
Implications from multiple accessory mineral U–
Pb geochronology, REE compositions from the
western margin of the Dharwar Craton, Karwar
Block and Coorg Block

Abstract:

Zircon U–Pb and Lu–Hf isotopic studies have been widely used to infer major geological and magmatic events from rocks in the continental crust. Recently, low temperature ($> 350^{\circ}\text{C}$) geochronology has been employed coupled with zircon U–Pb isotopic data to infer the exhumation history of the lower crust or reactivation history in lithologies across active margins. In this study, we have sampled granitoid lithologies along the western margin of the Dharwar Craton in India, in the vicinity of shear zones, to the west of Dharwar, namely – the Kumta Shear Zone (KSZ) in the north which separates the Dharwar Craton from the Karwar Block; the Mercara (MCSZ) which acts as a boundary between the Coorg Block and the southern domain of the Dharwar Craton and Moyar Shear Zone (MSZ) that forms the southern boundary of the Coorg Block. We obtained U–Pb isotopic data and REE compositions from zircon, apatite and monazite (2 samples) to understand the timing of crystallization, metamorphism, nature of exhumation across the western margin of the Dharwar Craton. The zircon U–Pb ages from the Karwar Block coincide with major widespread crustal growth and metamorphism episodes previously reported across the Dharwar Craton with apatite cooling ages slightly younger than the zircon U–Pb ages. The Mesoarchean gneisses to the east of the MCSZ reveal apatite cooling ages around ca. 2.4 Ga and inferred to have been reactivated by the Neoproterozoic amalgamation of microblocks to the south of Dharwar Craton and Coorg Block around ca. 2.5 Ga. The Mesoarchean gneisses on the northern margin of the Coorg Block near MCSZ show apatite cooling ages closer to the crystallization ages of the Neoproterozoic granite and alkali plutons that have intruded the suture zones around the Coorg Block and the apatites show LREE depletion inferring hydrothermal alteration in the Neoproterozoic. In conclusion, we support the previous studies that proposed the Karwar Block as a N-W extension of the Dharwar Craton. The gneisses on the western margin of western Dharwar Craton to the east of MCSZ have experienced their last thermal reactivation around ca. 2.4 Ga and the apatite cooling ages in the Neoproterozoic volcanics within the Mercara – Moyar Shear Zone have been resultant of crustal accretion events on the northern margin of the Southern Granulite Terrane.

1. Introduction:

The continental evolution history of the rocks that make up the continental crust and the timing of major geological events have been traced from the zircon record of the respective protoliths (Corfu et al., 2003). The mineral zircon, occurs as a common accessory mineral within silica-rich rocks and has been widely used to infer magmatic, hydrothermal and metamorphic events (Li et al., 2019) along with the crustal and mantle evolution history (Dhuime et al., 2011). One such craton where extensive zircon U–Pb and Lu–Hf systematics have been studied is the Dharwar Craton in India. However, recent low (> 500 °C) temperature thermochronology techniques such as Rb–Sr isotopic dating on K-rich minerals, to interpret the timing of orogenic events, uplift and exhumation histories (Hogmalm et al., 2017; Tillberg et al., 2020), have been applied to the western margin of the Dharwar Craton and the Karwar Block (Li et al., 2020) to supplement the zircon isotopic data (U–Pb, Lu–Hf) as a new approach to gain better insights into history of crustal evolution and major orogenic, crystallization and metamorphic events (Armistead et al., 2020).

In this study, we have followed an alternative approach to address the low-medium temperature (> 350 °C) chronology, which has been established within the last few years, by analyzing apatites for U–Pb isotopes using Laser Ablation—Inductively Coupled Plasma Mass Spectrometer (LA-ICPMS) (Cochrane et al., 2014). The apatites, sensitive to temperatures greater than 350 °C (Blackburn et al., 2011) have been used to understand a) exhumation processes within lower crustal rocks, b) tectonic stability of cratons and lower crust, c) tectonic history of active margins which have experienced multiple collisions and orogenic events resulting in significant exhumation (Cochrane et al., 2014). Alternatively, the apatite ages can also reflect interaction with aqueous fluids during retrograde metamorphism or growth of apatites during prograde metamorphism (Nutman et al., 2007) however, caution has to be exercised in attempting to infer thermal histories from apatite U–Pb dates. The apatite U–Pb ages can be used to understand ancient Pb-loss events reflected in the Concordia diagrams from the zircon U–Pb isotopic data and the exhumation histories of lithologies in the vicinity of active margins.

In this study, we have sampled across the active margins to the western margin of the Dharwar Craton, near the Kumta Shear Zone which acts as a boundary between the Karwar Block and the Western Dharwar Craton; along the Mercara Shear Zone which acts as a suture zone between the Coorg Block and the southern region of the Western Dharwar Craton; and the southern margin of the Coorg Block separated from the Nilgiri Block by the Moyar Shear Zone. We have separated and analysed the accessory minerals for U–Pb mainly zircon and apatite, also monazite for two samples, to understand the timing and spatial extent of the thermal record of the Dharwar Craton from north to south. We have

also studied the rare earth element (REE) compositions of these accessory phases to infer about depth of protolith crystallization and role of fluids in the cooling ages from apatite U–Pb data.

2. Geological Background:

The Dharwar Craton is one of the major cratonic nuclei in Peninsular India and has been further divided into three crustal domains namely the western, eastern and the central Dharwar Craton. The Western Dharwar Craton (WDC) and the Central Dharwar Craton (CDC) are separated by the Chitradurga greenstone belt; and the CDC and the Eastern Dharwar Craton have amalgamated along the Kolar–Kadiri greenstone belt to the south (Jayananda et al., 2018; Li et al., 2018a; Wang and Santosh, 2019; Santosh and Li, 2018) and along the Ramagiri–Penakacherla greenstone sequences in the north (see discussion in Chapter 2 this thesis). The Dharwar Craton was amalgamated with a number of microblocks in the southern margin which include the Coorg Block accreting in the Mesoarchean (Amaldev et al., 2016), and the meso- to Neoarchean accreting Nilgiri, Biligirirangan, Shevaroy and Madras Blocks from west to east (Li et al., 2018b; Ishwar Kumar et al., 2016; Peucat et al., 2013). The western margin of the WDC has been defined by the presence of a discrete block called the Karwar Block separated by the Kumta Shear Zone. The Karwar Block's tectonic history and its correlation with the Dharwar Craton is still controversial, with studies correlating the Kumta Shear Zone to Betsimisaraka Shear Zone in Madagascar (Ishwar-Kumar et al., 2016) and another classification considering Karwar Block to be a northwestern extension of the Dharwar Craton (Rekha et al., 2013, 2014; Armistead et al., 2017).

The continental crust of the Dharwar Craton comprises of different types of Tonalite-Trondhjemite-Granodiorite (TTG) gneisses, anatectic granites and sanukitoids which have formed over major magmatic crustal accretion events during ca. 3.45 – 3.3 Ga, 3.23 – 3.15 Ga, 3.0 – 2.96 Ga, 2.7 – 2.6 Ga and 2.56 – 2.5 Ga (Jayananda et al., 2015, 2018, Chapter 2 in this thesis). The WDC contains older protoliths with ages ca. 3.45 – 3.2 Ga adjacent to the gneisses in the CDC forming at ca. 3.23 – 2.96 Ga. The Dharwar Craton is overlain by sequences of greenstone belts that have been categorised into the older Sargur Group and the younger Dharwar Supergroup which was further divided into the Bababudan Group and the Chitradurga Group, detailed further in Chapter 3.

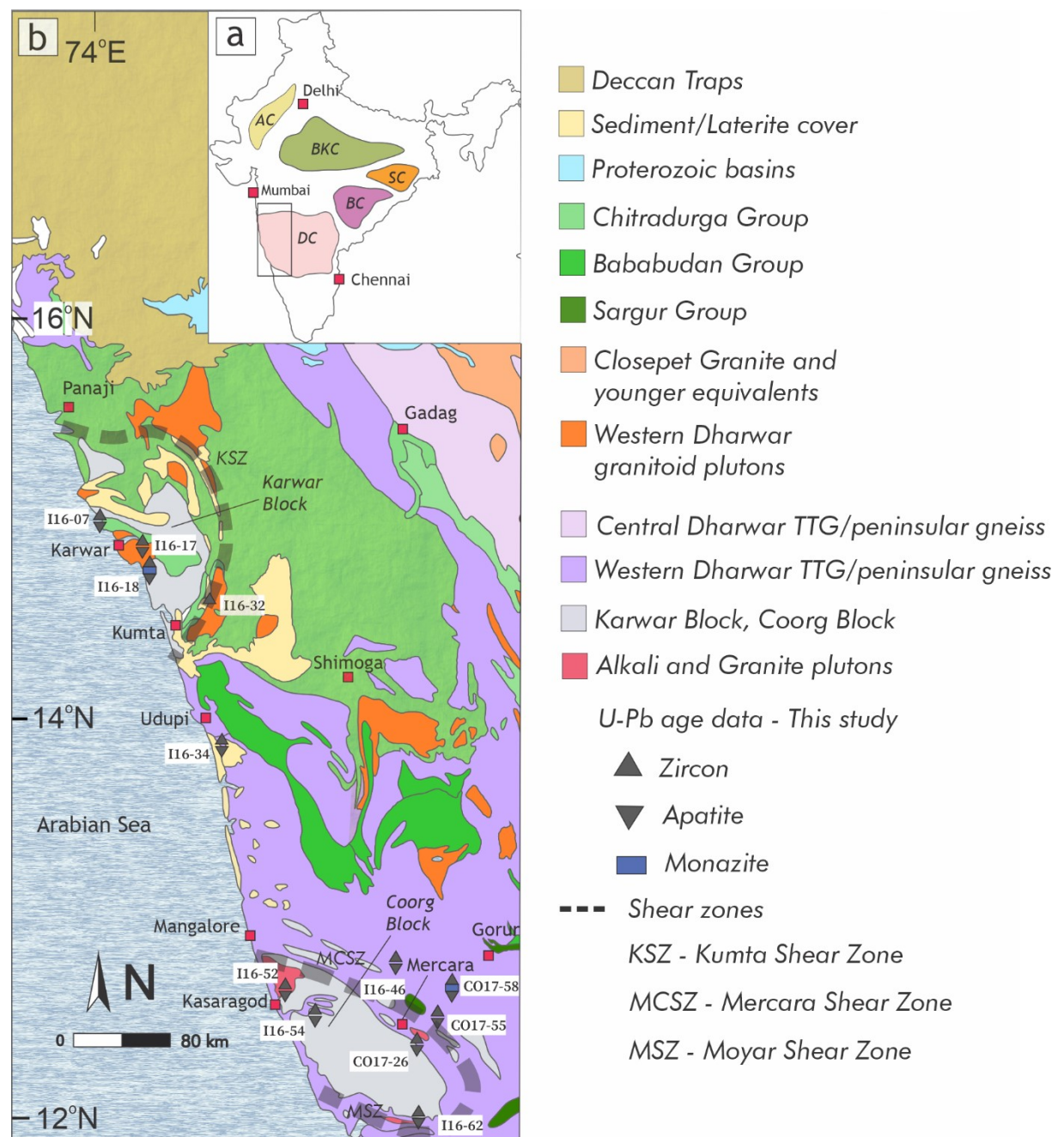


Figure 1: a) The distribution of major cratons across the Indian peninsula (after Rogers, 1986). DC: Dharwar Craton, BC: Bastar Craton, SC: Singhbhum Craton, BKC: Bundelkhand Craton, AC: Aravalli Craton. b) Geological map of the Western Dharwar Craton with adjacent Karwar Block and Coorg Block showing sample locations with major towns marked in red squares. The symbols in the legend indicate the accessory minerals analysed for U-Pb data.

The Karwar block on the west of WDC has been studied primarily with focus on models for India-Madagascar correlations (Ishwar-Kumar et al., 2013, 2016; Rekha et al., 2013, 2014; Armistead et al., 2017). The basement has been initially dated for Rb-Sr whole rock dating for 3400 ± 140 Ma with migmatites between ca. 2.65–2.4 Ma and Goa group sedimentary sequences which have been correlated to extend towards the younger groups within the Chitradurga Group (Dhondial et al., 1987). Metamorphism in the Karwar block was broadly contemporaneous with major metamorphic events reported in the Dharwar Craton (Armistead et al., 2017; Jayananda et al., 2013) around ca. 3.1–3.0 Ga and ca. 2.55–2.52 Ga (Jayananda et al., 2013; Peucat et al., 2013). The younger monazite U-Pb ages reported by Rekha et al. (2013) have been explained to represent the closure of the Goa Basin by Armistead et al., (2017) also discounting the correlation by Ishwar-Kumar et al., (2013) between the Kumta Shear Zone and the Betsimisaraka Shear Zone in Madagascar due to lack of lithostratigraphic correlation.

The Coorg Block lies to the west of the Dharwar Craton separated by the Mercara Shear Zone and has been explained to have distinct structure, chronology and metamorphic P–T conditions (Ishwar-Kumar et al., 2013, 2016; Santosh et al., 2015). The Coorg Block is characterised by hornblende gabbro, charnockite and layered hornblende anorthosite interpreted as rocks forming in a magmatic arc (Santosh et al., 2015). The Mercara Shear Zone (MCSZ) contains highly sheared and deformed gneisses and it terminates in the south against the Moyar Shear Zone (MSZ) which forms the southern boundary of the Coorg Block and the northern boundary of the Nilgiri Block (Ishwar-Kumar et al., 2016). Both the MCSZ and MSZ are intruded by younger granite and alkali plutons which have been explained as a part of widespread Cryogenian magmatism across the network of suture zones between the Dharwar Craton and the Southern Granulite Terrane (SGT) (Santosh et al., 2014). A number of metamorphic ages have been proposed for the MCSZ portraying complex tectonic history. Mesoproterozoic suturing ages of ca. 1.2 Ga and 1.5 Ga have been proposed (Ishwar-Kumar et al., 2016; Santosh et al., 2015). Textural dating of monazite grains revealed chemical ages between ca. 2.5–2.2 Ga to the west of the MCSZ and were correlated to the metamorphic ages in the Betsimisaraka Shear Zone in Madagascar (Rekha et al., 2013). Metamorphic overgrowths on zircon dated at ca. 3.0 Ga have been identified by Amaldev et al. (2016) and constrained the peak P–T conditions for mafic granulites to 10–12 kbar at 700–900 °C. Santosh et al. (2015) reported P–T conditions of 6 kbar at 820–870 °C for the hornblende in charnockites and Ishwar-Kumar et al. (2013) reported 15–20 kbar at 1000 °C peak P–T conditions for the mafic granulites in MCSZ.

3. Methods:

The samples were processed and panned for heavy minerals. Magnetic minerals were removed, and resulting fractions were handpicked for zircons, apatite and monazite, mounted in epoxy resin and polished at the University of Adelaide. The grain mounts were carbon-coated and imaged by a Gatan cathode luminescence (CL) detector attached to Quanta 600 MLA Scanning Electron Microscope to identify various domains within the zircons suitable for analysis. U–Pb geochronology was performed at Adelaide Microscopy, The University of Adelaide, using an Agilent 7900 ICP-MS attached with a RESOLUTION LR 193nm Excimer laser system. The laser used a spot size of 31 μm and a frequency of 5 Hz for zircon. The isotopes ^{204}Pb , ^{206}Pb , ^{207}Pb , ^{208}Pb , ^{232}Th and ^{238}U were measured for U–Pb geochronology. GEMOC GJ-1 zircon (Isotope dilution TIMS ages $^{207}\text{Pb}/^{206}\text{Pb} = 602 \pm 4.3$ Ma, $^{206}\text{Pb}/^{238}\text{U} = 600.7 \pm 1.1$ Ma and $^{207}\text{Pb}/^{235}\text{U} = 602.0 \pm 1.0$ Ma; Jackson et al., 2004) was used for the correction of U–Pb fractionation for zircon laser sessions. The Plesovice zircon (ID-TIMS $^{206}\text{Pb}/^{238}\text{U}$ age = 337.13 ± 0.37 Ma; Sláma et al., 2008) and 91500 zircon (aged at ca. 1065 Ma; Wiedenback et al., 1995) were analysed alongside the samples as an internal standard to test the accuracy of the laser sessions. The secondary standards yielded a calculated ages of 340.5 ± 1.5 Ma (2σ , MSWD = 3.5, $n = 36$) for Plesovice, and 1035 ± 32 Ma (2σ , MSWD = 0.97, $n = 36$) for 91500 zircon.

McClure Mountain apatite (Isotope dilution $^{207}\text{Pb}/^{235}\text{U}$ age = 523.5 ± 2 Ma, LA-ICPMS age = 516 ± 9 Ma; Schoene and Bowring, 2006; Thompson, 2016) was used as the primary standard for U–Pb fractionation correction in apatite dating along with OD306 (Isotope dilution age = 1596.7 ± 7.1 Ma, LA-ICPMS age = 1544.8 ± 23.5), 401-apatite (Isotope dilution age = 530.3 ± 1.5 Ma, LA-ICPMS age = 506.2 ± 8.1 Ma; Thompson et al., 2016) which were used as internal standards to test the laser accuracy. The data reduction was performed using “VisualAge_UcomPbine” data reduction scheme (DRS) (Chew et al., 2014) in the Iolite software package (Paton et al., 2011). This DRS was selected as it could account for variable common Pb in the standards and analysed samples and apply it for the baseline, downhole fractionation and drift corrections in the ICP-MS data. The McClure Mountain apatite analysed for this study revealed a lower intercept age of 537 ± 11 Ma (2σ , MSWD = 1.2, $n = 19$), the secondary standards show lower intercept ages of 1628 ± 11 Ma (2σ , MSWD = 1.8, $n = 38$) for OD306 and 530.2 ± 2.6 Ma (2σ , MSWD = 0.67, $n = 38$) for 401-Apatite.

An internal monazite standard, MAdel ($^{206}\text{Pb}/^{238}\text{U}$ age = 520–510 Ma; Payne et al., 2008) was used as a primary standard for the U–Pb fractionation correction in monazite U–Pb dating along with secondary standard Ambat ($^{206}\text{Pb}/^{238}\text{U}$ age at ca. 520 Ma) and 94-222/Bruna-NW (aged at ca. 450 Ma, Payne et al., 2008) to check the accuracy of the laser. The ages calculated from this study for the

standards are 518.2 ± 2.7 Ma (2σ , MSWD = 0.046, $n = 15$) for MAdeI, 450 ± 2.9 Ma (2σ , MSWD = 0.102, $n = 10$) for 94-222/Bruna-NW apatite and 517.8 ± 3.9 Ma (2σ , MSWD = 0.91, $n = 10$) for the Ambat standard.

Rare Earth Elements (REE) – ^{139}La , ^{140}Ce , ^{141}Pr , ^{146}Nd , ^{147}Sm , ^{153}Eu , ^{157}Gd , ^{159}Tb , ^{163}Dy , ^{165}Ho , ^{166}Er , ^{169}Tm , ^{172}Yb , ^{175}Lu , ^{178}Hf , and ^{89}Y were simultaneously measured from the zircons and monazite along with U–Pb isotopes using 50 μm spot size analyses over NIST-SRM 610 glass as reference material (Jochum et al., 2011). The analysed apatite grains were measured for ^{88}Sr and ^{90}Zr along with REE and ^{89}Y against NIST-SRM 612 glass as reference material. The U–Pb and REE data were separately processed using Iolite™ (Paton et al., 2011). The REE concentrations in monazite grains were calculated normalised to an internal standard assuming thirty per cent weight per volume (30% w/v) of cerium (Ce) compared to the sum of the REEs ($\sum\text{REE}$) during data reduction against NIST-SRM 610 standard in Iolite.

Concordia diagrams ($^{207}\text{Pb}/^{235}\text{U}$ vs $^{206}\text{Pb}/^{238}\text{U}$) were generated to represent the data using the Isoplot 4.15 plugin on Microsoft Excel (Ludwig, 2003) and an online version of IsoplotR (Vermeesch, 2018) was used to calculate the intercepts of the discordia lines and mean ages. The analytical ellipses have been coloured to represent Th/U ratios for zircons and monazites. The Sr/Y ratios were used to discriminate the apatites analysed, with higher Sr/Y ratios attributed to more mafic melts (Belousava et al., 2002). The REE compositions have been normalised against chondrite values from Boynton et al. (1984), using the Geochemical Data Toolkit for R (GCDkit6.0) (Janousen et al., 2006) to calculate REE ratios. In particular, Eu anomalies represented by Eu/Eu^* (where $\text{Eu}^* = \sqrt{(\text{Sm}_N \times \text{Gd}_N)}$), La_N/Sm_N ratios (light rare earth element (LREE) vs middle rare earth element (MREE)), and Gd_N/Yb_N ratios (middle rare earth element (MREE) vs HREE) were calculated and plotted against individual zircon $^{207}\text{Pb}/^{206}\text{Pb}$ ages and isochron corrected ages for apatites.

4. Results:

Eleven samples were chosen to represent felsic to intermediate granitoids occurring at the western margin of the Western Dharwar Craton, Karwar Block and Coorg Block. The locations are summarised in the table below.

Sample	Latitude	Longitude	Rock type	Category	Zircon Ages	Inherited Zircons	Apatite Ages	Monazite Ages
I16-07	15.018	74.034	Porphyritic granite	Karwar Block	3000 ± 32 Ma	n/a	3015 ± 80 Ma	n/a
I16-17	14.847	74.258	Bt-rich granite	Karwar Block	3210 ± 37 Ma	n/a	3127 ± 219 Ma	n/a
I16-18	14.749	74.251	Bt-rich granitic gneiss	Karwar Block	2971 ± 14 Ma	n/a	2781 ± 71 Ma	2962 ± 17 Ma
I16-32	14.621	74.604	Kfs-rich Syenite	Karwar Block	3000 ± 31 Ma	3270 ± 23 Ma	n/a	n/a

I16-34	13.848	74.668	Granodioritic Gneiss	Western Dharwar Craton	3266 ± 5 Ma, 3206 ± 10 Ma	n/a	3169 ± 44 Ma	n/a
I16-46	12.520	75.478	Granodioritic Gneiss	Coorg Block	3299 – 3087 Ma	n/a	755 ± 23 Ma	n/a
I16-52	12.635	75.028	Syenite	Coorg Block	842 ± 20 Ma	3257 ± 18 Ma, 3197 ± 21 Ma	837 ± 12 Ma	n/a
I16-54	12.527	75.071	TTG melanosome	Coorg Block	3187 ± 9 Ma	3357 ± 34 Ma	838 ± 34 Ma, 646 ± 43 Ma	n/a
I16-62	12.062	75.761	Biotite-microgranite	Coorg Block	856 ± 20 Ma	n/a	622 ± 52 Ma	n/a
CO17-26	12.373	75.704	Granite	Coorg Block	812 ± 29 Ma	3235 ± 18 Ma	711 ± 37 Ma	n/a
CO17-55	12.501	75.802	Felsic gneiss	Western Dharwar Craton	3476 – 3112 Ma	n/a	2414 ± 74 Ma	n/a
CO17-58	12.597	75.845	TTG Gneiss	Western Dharwar Craton	3412 – 2897 Ma	n/a	2382 ± 62 Ma	3045 ± 29 Ma

Table 5.1 Summary of samples and accessory mineral U–Pb ages from this study. The zircon ages shown as single ages are upper intercepts of discordia lines or calculated mean $^{207}\text{Pb}/^{206}\text{Pb}$ age, the spread in $^{207}\text{Pb}/^{206}\text{Pb}$ ages in archean samples are shown here as $x - y$ where x, y are the maximum and minimum $^{207}\text{Pb}/^{206}\text{Pb}$ ages. The reported inherited zircons are older zircons with greater than 90% concordance. The apatite ages shown are lower intercepts calculated in the Tera-Wasserburg plots. The monazite ages reported are upper intercepts of discordia lines calculated in the Concordia diagram.

4.1 Accessory mineral U–Pb dating and REE compositions

I16-07 is collected from a porphyritic granite collected near Karwar town on the west coast of the Karwar Block. The zircons appear euhedral and elongated with aspect ratios of 1:5 to 2:3 and width ranging from 50–100 μm . Zircon U–Pb dating revealed only two concordant zircons with a mean $^{207}\text{Pb}/^{206}\text{Pb}$ age of 3000 ± 32 Ma with Th/U ratios ranging from 0.09–1.49, Eu/Eu* values ranging from 0.22–0.8 and $\text{La}_\text{N}/\text{Sm}_\text{N}$ values ranging from 0.004 to 1.895, $\text{Gd}_\text{N}/\text{Yb}_\text{N}$ values between 0.028–0.173. The Apatite U–Pb dating data plotted on a Tera-Wasserburg plot revealed a discordia line with a lower intercept at 3015 ± 80 Ma (MSWD = 1.1, $n = 30$) with Eu/Eu* values ranging from 0.14–0.23 and $\text{La}_\text{N}/\text{Sm}_\text{N}$ values ranging from 0.283–0.58 and Sr/Y ratios between 0.04–0.11.

I16-17 is collected from a biotite rich granitoid near the east of Karwar town within the Karwar Block. The sample yielded a low fraction of zircons, and the apatite grains contained zircon inclusions which appear to be exsolving from the apatite grains. Zircons appear euhedral with aspect ratios between 1:5 to 2:3 with width ranging from 50 – 150 μm . Near-concordant zircons were used to define a mean $^{207}\text{Pb}/^{206}\text{Pb}$ age of 3210 ± 37 Ma (MSWD = 3.4, $n = 6$) interpreted as the age of the protolith. The analysed zircons reveal Th/U ratios ranging from 0.17–0.65, Eu/Eu* values ranging from 0.53–0.97 and $\text{La}_\text{N}/\text{Sm}_\text{N}$ values ranging from 0.082–1.258, $\text{Gd}_\text{N}/\text{Yb}_\text{N}$ values between 0.09–0.568. Apatite U–Pb

data plotted on Tera-Wasserburg plot define an imprecise discordia line with a lower intercept of 3127 ± 219 Ma (MSWD = 3.8, $n = 29$) with Eu/Eu* values ranging from 0.27–1.08 and La_N/Sm_N values ranging from 0.12–0.563 and Sr/Y ratios between 0.17–0.34.

I16-18 is medium-grained biotite rich granitoid gneiss collected towards the south-east of Karwar town. The zircons are mostly euhedral with aspect ratios 1:5 to 1:3 with width ranging from 50–100 μm . The zircons mostly display oscillatory zoning in response to CL imaging with occasional metamict textures and presence of core and rim textures in a few rounded zircons which were interpreted to be inherited zircons. The zircon U–Pb dating revealed four near concordant zircons which were used to calculate a mean $^{207}\text{Pb}/^{206}\text{Pb}$ age of 2971 ± 14 Ma (MSWD = 0.15, $n = 4$) and an inherited zircon with $^{207}\text{Pb}/^{206}\text{Pb}$ age of 3115 ± 44 Ma. Analysed zircons show Th/U ratios between 0.07–0.86, Eu/Eu* values ranging from 0.14–0.81 and La_N/Sm_N values ranging from 0.02–3.69 and Gd_N/Yb_N values between 0.023–0.286. Apatite U–Pb dating reveals a discordia line in Tera-Wasserburg plot, defined by 30 apatite grains with a lower intercept of 2781 ± 71 Ma (MSWD = 1.5, $n = 30$) with Eu/Eu* values ranging from 0.24–0.34 and La_N/Sm_N values ranging from 0.332–0.48. Monazite grains appear to be euhedral in shape and analysed for U–Pb data which reveal a mean $^{207}\text{Pb}/^{206}\text{Pb}$ age of 2962 ± 17 Ma (MSWD = 0.01, $n = 31$) with Th/U ratios ranging between 15.99–37.82 and La_N/Sm_N values ranging from 3.50–6.649 and Sr/Y ratios between 0.024–0.089.

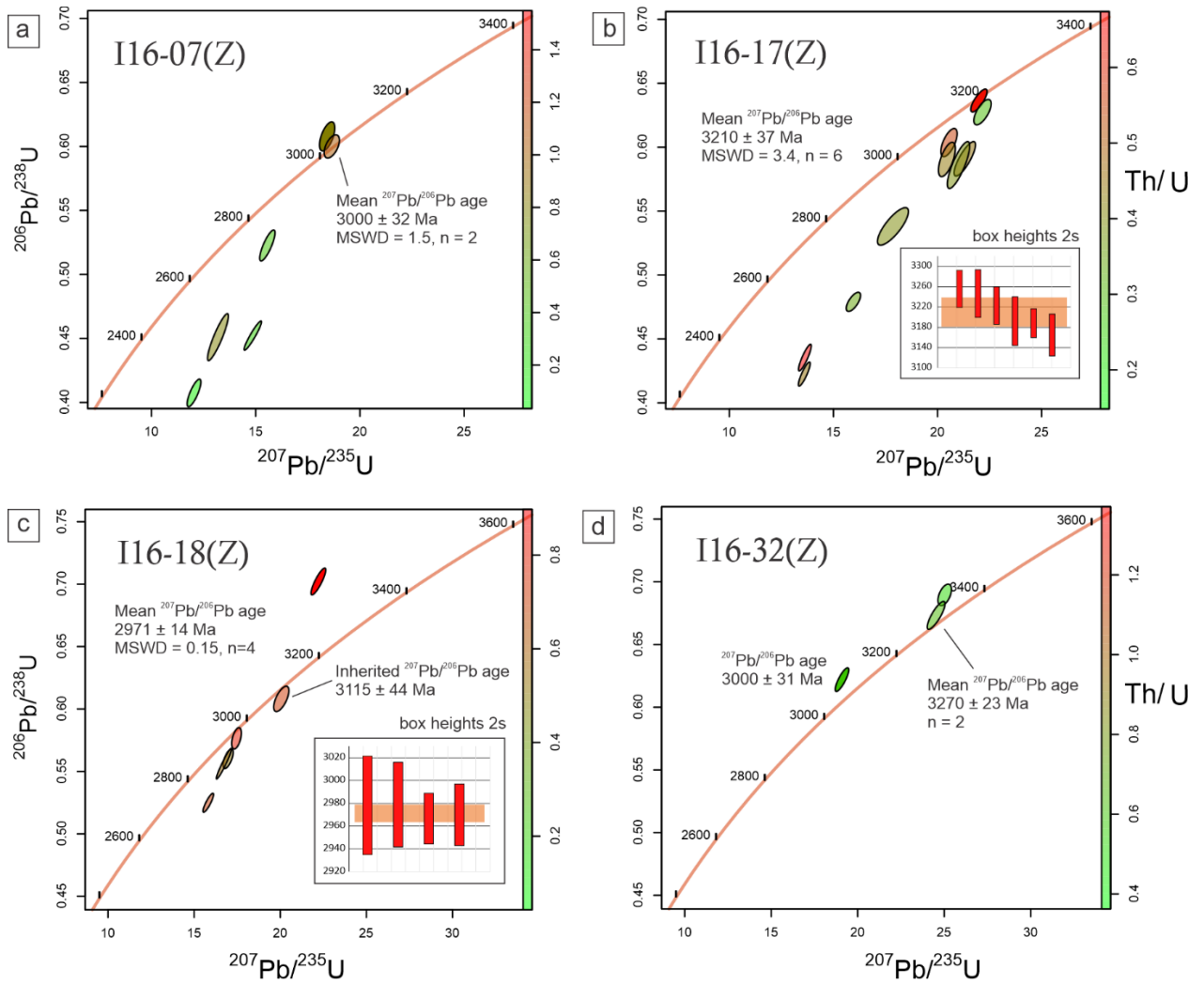


Figure 2: The zircon U–Pb age data from the basement granitoids within Karwar Block and vicinity of proposed Kumta Shear Zone (Ishwar-Kumar et al., 2013) plotted as Concordia diagrams using IsoplotR (Vermeesch et al., 2018). The zircon U–Pb data ellipses are coloured using the Th/U ratios from the analysed zircons. The mean $^{207}\text{Pb}/^{206}\text{Pb}$ ages have been calculated for zircons that show greater than 85% concordance.

I16-32 is a K-felspar rich syenite collected from a granitoid pluton along the Kumta Shear Zone. The zircons appear to be euhedral with several cracks and inclusions with aspect ratios between 1:3 to 2:3, and width ranging from 50–100 μm . The zircons display subtle oscillatory zoning in response to CL imaging with visible cracks and inclusions in the majority of the zircons. Zircon U–Pb dating revealed only three near concordant zircons with two older zircons with mean $^{207}\text{Pb}/^{206}\text{Pb}$ age of 3270 ± 23 Ma and a younger zircon with $^{207}\text{Pb}/^{206}\text{Pb}$ age of 3000 ± 31 Ma with Th/U ratios between 0.4–1.33. The analysed zircons exhibit Eu/Eu* values between 0.15–1.58; La_N/Sm_N values between 0.025–3.784 and Gd_N/Yb_N values between 0.04–0.163. The sample contained a low fraction of apatite grains which were reverse discordant, interpreted to contain large amounts of common Pb, could not be constrained to reveal a U–Pb age, however, exhibit Eu/Eu* values between 0.18–0.46 and La_N/Sm_N values between 0.062–2.32 and Sr/Y ratios between 0.01–1.5.

I16-34 is a granodioritic gneiss collected near the town of Udupi on the western margin of the Western Dharwar Craton. The zircons appear to be partial to well-rounded with aspect ratios between 1:1 to 1:4 and width ranging from 45–120 μm . Most zircons reveal uneven shaped cores with preserved oscillatory zones surrounded by bright thin (15–20 μm) rims in response to CL imaging. Zircon U–Pb dating was targeted into the zircon cores and revealed two groups of zircons in the concordia plot. The older cluster of zircon analyses clustered around a mean $^{207}\text{Pb}/^{206}\text{Pb}$ age of 3266 ± 5 Ma (MSWD = 1; n = 26) and a younger group of zircons which define a discordia line with an upper intercept age of 3206 ± 10 Ma (MSWD = 0.5, n = 3) interpreted to represent the interference from the rims of the zircons. The Th/U ratios range between 0.287–0.698. The REE concentrations from the analysed zircons reveal Eu/Eu* ratios range between 0.1–0.66, $\text{La}_\text{N}/\text{Sm}_\text{N}$ values between 0.002–1.146 and $\text{Gd}_\text{N}/\text{Yb}_\text{N}$ values between 0.028–0.073. Apatite U–Pb dating revealed mostly reverse discordant data and the younger grains on the Tera-Wasserburg plot were constrained with a mean $^{207}\text{Pb}/^{206}\text{Pb}$ age of 3169 ± 44 Ma (MSWD = 4, n = 11). The apatite grains analysed reveal Eu/Eu* ratios between 0.41–0.95 and $\text{La}_\text{N}/\text{Sm}_\text{N}$ values between 0.295–1.057 and Sr/Y ratios between 0.11 – 1.77.

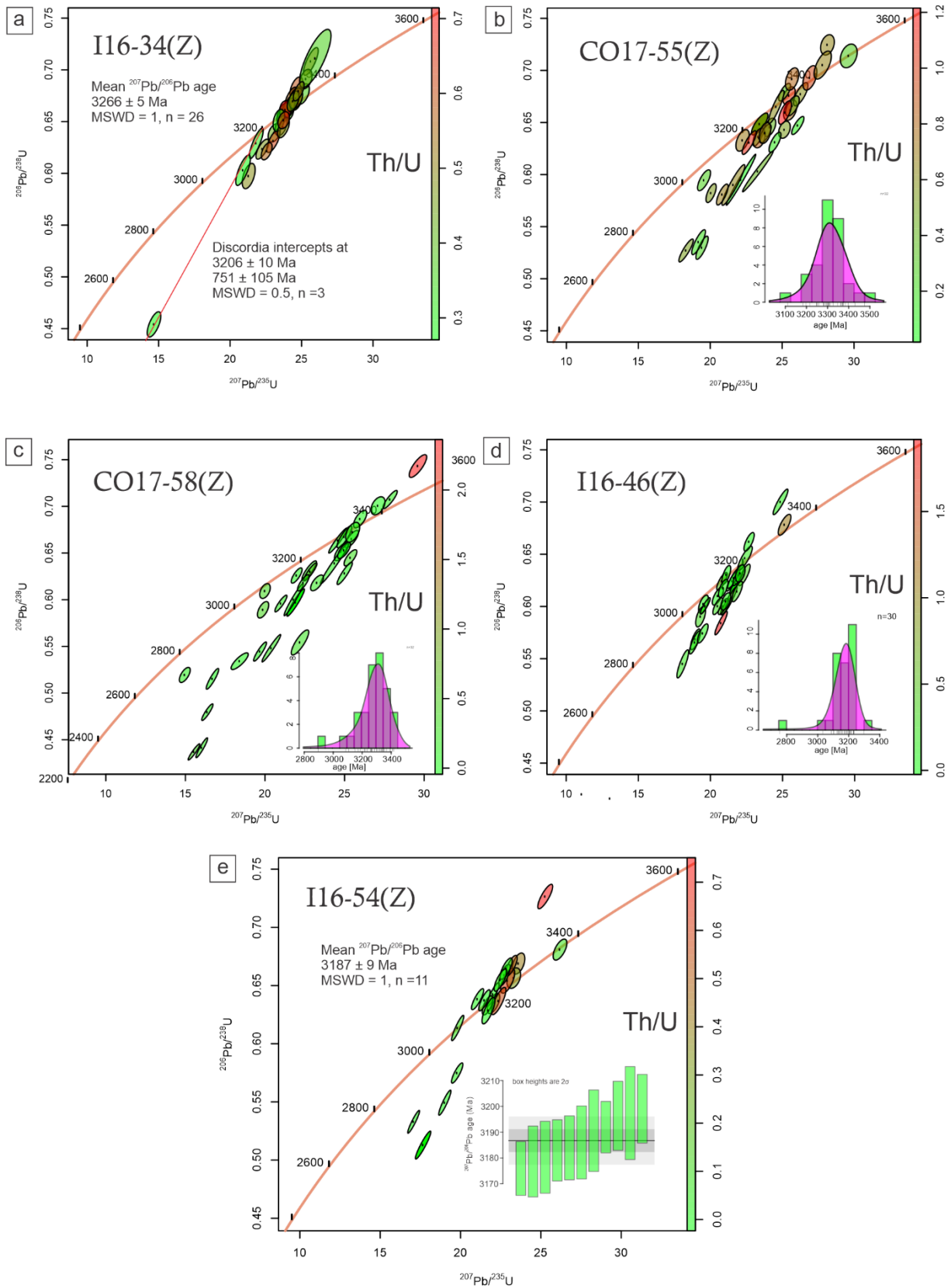


Figure 3: The zircon U–Pb data from Mesoarchean granitoid gneisses along (a) the western margin of the Dharwar Craton near Udipi town, (b),(c) the western boundary of the Western Dharwar Craton east of the Mercara Shear Zone, (d),(e) from the northern margin within the interior of the Coorg Block. The samples with a spread in $^{207}\text{Pb}/^{206}\text{Pb}$ ages have been represented by Kernel density estimate in the bottom right of

figures (b),(c) and (d). For figures (a),(e) the mean $^{207}\text{Pb}/^{206}\text{Pb}$ age has been calculated to interpret the protolith ages.

I16-46 is a granodioritic gneiss collected towards the north-west of Madikeri town (also known as Mercara) at the boundary of the Coorg Block. The zircons were elongated with rounded edges with several grains containing inclusions, in aspect ratios from 1:4 to 2:3 with width ranging between 75–200 μm . The zircons in response to CL imaging display oscillatory zoning along with metamict textures occurring in zones. Zircon U–Pb data plotted on the concordia diagram show near concordant (>85% concordance) $^{207}\text{Pb}/^{206}\text{Pb}$ ages ranging from ca. 3299 – 3087 Ma. The zircons show Th/U ratios between 0.04–1.84, Eu/Eu* ratios between 0.02–0.63, $\text{La}_\text{N}/\text{Sm}_\text{N}$ values between 0.007–12.77 and $\text{Gd}_\text{N}/\text{Yb}_\text{N}$ values between 0.013–0.372. Apatite U–Pb data plotted on Tera-Wasserburg plot reveal a discordia line with lower intercept age of 755 ± 23 Ma (MSWD = 2, n = 29) with Eu/Eu* values ranging from 0.54–3.07 and $\text{La}_\text{N}/\text{Sm}_\text{N}$ values between 0.116–0.371 and Sr/Y ratios between 0.02 – 0.89.

I16-52 is a syenite collected from the western margin of the Coorg Block south of Mangalore town. The zircons appear euhedral and crystalline in elongated and angular shapes with aspect ratios from 1:3 to 2:3 with width ranging between 50–150 μm . The CL imaging revealed two fractions of zircons, the first group with oscillatory zoning and the second group with dark cores surrounded by thick oscillatory zoned rims. Zircon U–Pb data show inherited zircons with near-concordant (> 85% concordance) $^{207}\text{Pb}/^{206}\text{Pb}$ ages of 3129 ± 40 Ma, 3121 ± 26 Ma, 3257 ± 36 Ma, 3197 ± 42 Ma. The zircons were estimated to have crystallised at a mean $^{207}\text{Pb}/^{206}\text{Pb}$ age at 842 ± 20 Ma (MSWD = 3, n = 27). The analysed zircons reveal Th/U ratios between 0.04–1.45, Eu/Eu* ratios between 0.29–0.76, $\text{La}_\text{N}/\text{Sm}_\text{N}$ ratios between 0.003–0.503, $\text{Gd}_\text{N}/\text{Yb}_\text{N}$ ratios between 0.02–0.244. Apatite U–Pb data plotted on Tera-Wasserburg plot reveals a discordia line with a lower intercept age of 837 ± 12 Ma (MSWD = 0.8, n = 30) with Eu/Eu* ratios between 0.23–1.22 and $\text{La}_\text{N}/\text{Sm}_\text{N}$ ratios between 0.163–3.18 and Sr/Y ratios between 0.25 – 4.07.

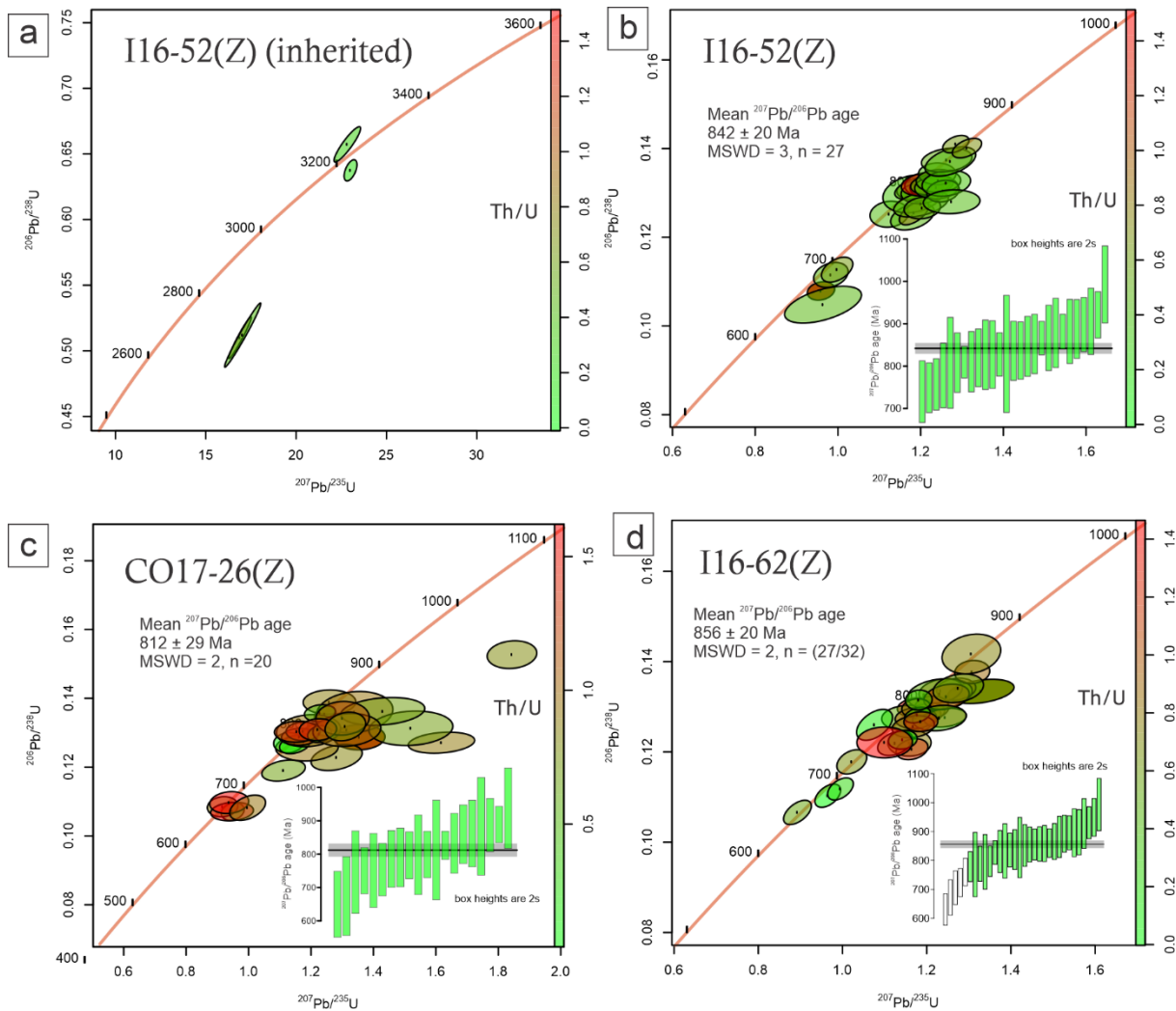


Figure 4: Zircon U–Pb data plotted as Concordia for the Neoproterozoic volcanics around the Coorg Block. (a),(b) show the zircon U–Pb data from the syenite sampled from the alkali complex north of the Coorg Block. (c) shows the zircon U–Pb data from the granite sampled from within the Mercara Shear Zone, (d) shows the zircon U–Pb data from the alkali pluton sampled from the vicinity of the Moyar Shear Zone south of the Coorg Block. Mean $^{207}\text{Pb}/^{206}\text{Pb}$ ages were used to constrain protolith crystallisation ages due to high variability in $^{206}\text{Pb}/^{238}\text{U}$ ages.

I16-54 is from a granodioritic melanosome from a granitoid gneiss near Kasaragod town in Kerala state. The zircons are elongated with rounded edges with aspect ratios from 1:3 to 4:5 with width ranging between 75–200 μm . The analysed zircons exhibit oscillatory zoning with a few grains containing cracks running through laterally. Zircon U–Pb data plotted on Wetherill concordia diagram show inherited zircon at $^{207}\text{Pb}/^{206}\text{Pb}$ age of 3357 ± 34 Ma and a cluster with mean $^{207}\text{Pb}/^{206}\text{Pb}$ age 3187 ± 9 Ma (MSWD = 1, n = 11) and a younger concordant zircon with $^{207}\text{Pb}/^{206}\text{Pb}$ age of 3082 ± 20 Ma. The analysed zircons reveal Th/U ratios between 0.005–0.72, Eu/Eu* ratios between 0.2–2.67, La_N/Sm_N ratios between 0.007–1.723, Gd_N/Yb_N ratios between 0.004–0.272. Apatite U–Pb dating revealed two groups of apatite analyses that define two distinct discordia lines with lower intercept ages of 838 ± 34

Ma (MSWD = 0.9, n = 8) and 646 ± 43 Ma (MSWD = 1, n = 8) with Eu/Eu* ratios between 0.21 – 1.44 and La_N/Sm_N ratios between 0.012 – 0.194 and Sr/Y ratios between 0.06 – 0.5.

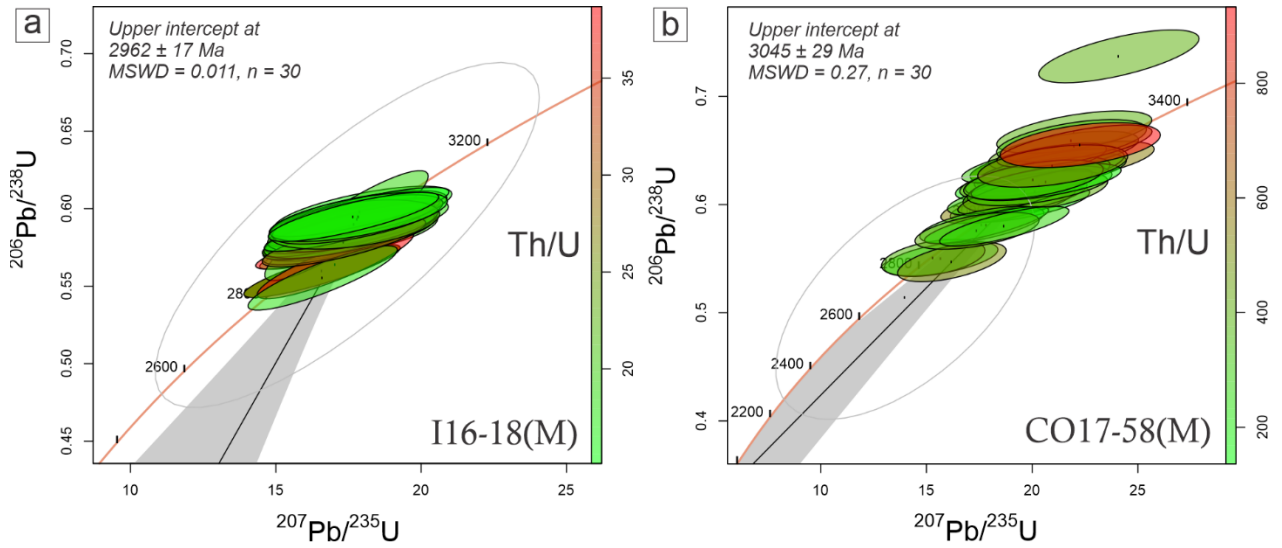


Figure 5: Monazite U–Pb age data plotted on Concordia diagram using IsoplotR and the data-ellipses have been coloured using Th/U ratios. (a) is the monazite dated from the biotite-rich granitic gneiss collected within the Karwar Region. (b) The monazites dated from the Tonalite–Trondhjemite–Granodiorite gneiss collected to the east of the Mercara Shear Zone at the boundary of the Dharwar Craton.

I16-62 is collected from a biotite-rich microgranite from the southern margin of the Coorg Block. The zircons appear elongated, mostly euhedral with a low fraction of grains displaying curved edges and aspect ratios ranging from 1:5 to 1:3 with the width between 50–120 μm . Zircon CL imaging revealed most zircons exhibiting euhedral crystalline shapes and oscillatory zoning. Zircon U–Pb dating plotted on the Wetherill Concordia diagram show the zircons constrained to a mean $^{207}\text{Pb}/^{206}\text{Pb}$ age of 856 ± 20 Ma (MSWD = 2, n = 27). Zircon analyses exhibit Th/U ratios between 0.05 – 1.41, Eu/Eu* ratios between 0.42 – 0.76, La_N/Sm_N ratios between 0.001 – 4.976, Gd_N/Yb_N ratios between 0.027 – 0.121. Apatite U–Pb data plotted on Tera–Wasserburg plot reveal a discordia line with a lower intercept age of 622 ± 52 Ma (MSWD = 2, n = 27) with Eu/Eu* ratios between 0.37 – 1.26 and La_N/Sm_N ratios between 0.137 – 2.143 and Sr/Y ratios between 0.28 – 0.8.

CO17-26 has been collected from a granite body near Madikeri (Mercara) town. The zircons appear elongated and euhedral with aspect ratios of 1:5 to 1:3 and width between 50–120 μm . Zircons display clear oscillatory zoning in response to CL imaging. Zircon U–Pb data have been constrained to a mean $^{207}\text{Pb}/^{206}\text{Pb}$ age of 843 ± 41 Ma (MSWD = 1.3, n = 26) as they have high variability in $^{206}\text{Pb}/^{238}\text{U}$ ages ranging from 916 ± 37 Ma to 666 ± 26 Ma. An inherited zircon at $^{207}\text{Pb}/^{206}\text{Pb}$ age of 3234 ± 36 Ma has been identified. The analysed zircons reveal Th/U ratios between 0.1 – 1.56, Eu/Eu* ratios between 0.52 – 0.92, La_N/Sm_N ratios between 0.001 – 0.197, Gd_N/Yb_N ratios between 0.022 – 0.142. Apatite U–Pb

dating revealed a discordia constrained to a lower intercept age of 711 ± 37 Ma (MSWD = 2, $n = 30$) with Eu/Eu* ratios between 0.91–3.17, La_N/Sm_N ratios between 0.231–0.608 and Sr/Y ratios between 0.21 – 0.59.

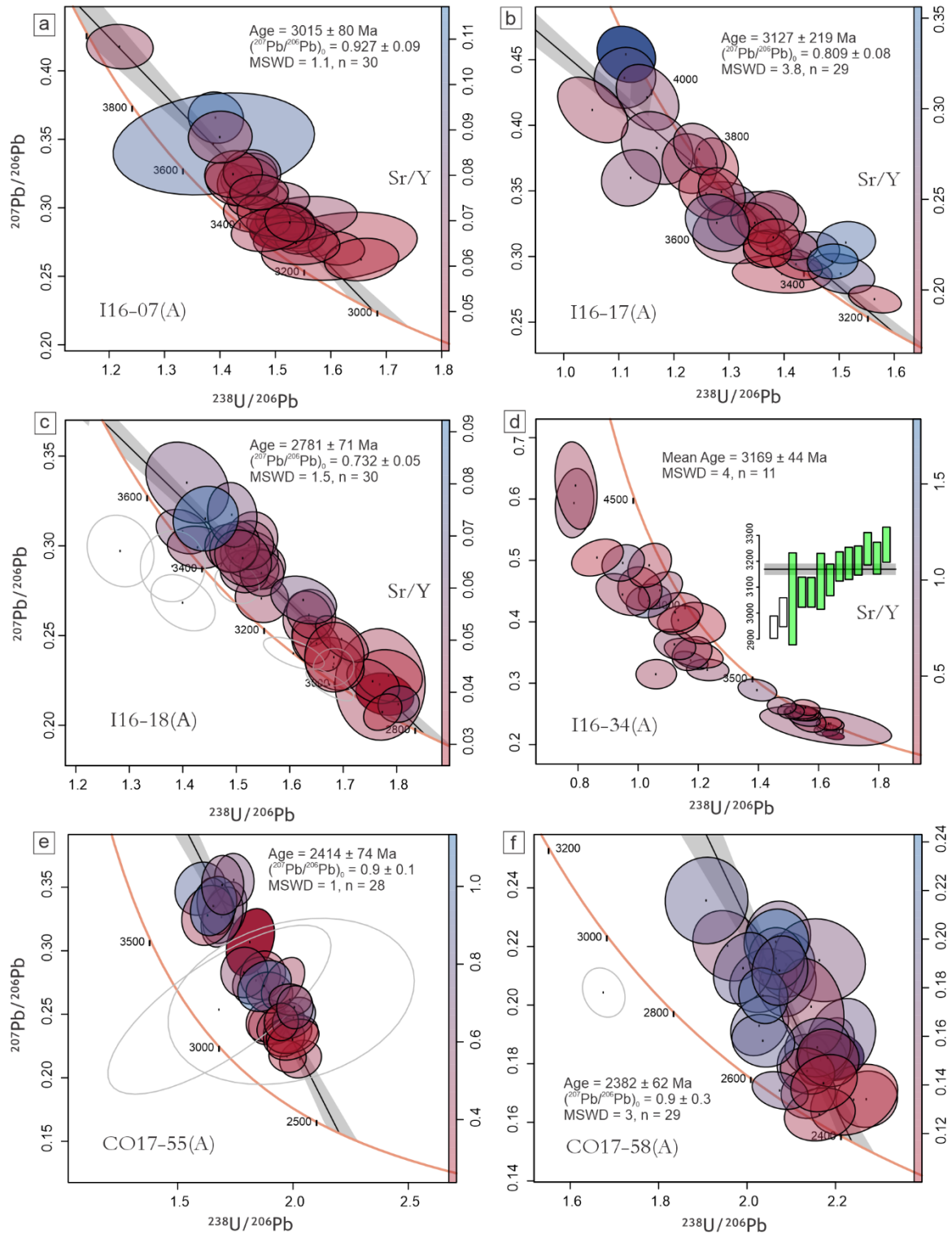


Figure 6, Apatite U–Pb age data represented on Tera-Wasserburg plot. The data ellipses have been coloured using Sr/Y ratios to differentiate felsic/mafic characteristic of source material (Belousava et al.,

2002). The sample names have been written in the bottom left and denoted with (A) to represent apatite age data. The hollow ellipses were not used in the calculation of the regression lines using IsoplotR (Vermeesch et al., 2018). (a),(b),(c) are lithologies sampled in and around the Karwar Block. (d) has been sampled at the western margin of the Western Dharwar Craton. (e),(f) have been sampled northeast from the Mercara Shear Zone towards the Western Dharwar Craton.

CO17-55 has been collected from a felsic granitoid gneiss with visible leucosomes and melanosomes, towards the north-east of Madikeri town in the vicinity of the Mercara Shear Zone (MSZ). The zircons appear elongated with well-rounded edges with aspect ratios from 1:4 to 2:3 with the width between 50–150 μm . The zircons show visible cores with magmatic oscillatory zoning along with bright overgrowths with a thickness between 10–30 μm . Zircon U–Pb dating revealed near concordant $^{207}\text{Pb}/^{206}\text{Pb}$ ages between 3476 ± 53 Ma and 3112 ± 42 Ma with Th/U ratios between 0.062–1.17, Eu/Eu* ratios between 0.17–0.99, $\text{La}_\text{N}/\text{Sm}_\text{N}$ ratios between 0.003–3.11, $\text{Gd}_\text{N}/\text{Yb}_\text{N}$ ratios between 0.02–0.086. Apatite U–Pb dating reveals a discordia line with a lower intercept age of 2414 ± 74 Ma (MSWD = 1, n = 28) with Eu/Eu* ratios between 0.24–0.72, $\text{La}_\text{N}/\text{Sm}_\text{N}$ ratios between 0.199–5.088 and Sr/Y ratios between 0.27 – 1.1.

CO17-58 has been collected from a TTG granitoid gneiss with leucosomes and melanosomes present within the sample collected from the western margin of the Western Dharwar Craton. The zircons appear elongated to well-rounded in shape with the width between 40–150 μm . The zircons display dark CL response with oscillatory zoning and a fraction of zircons showing cores and thin rims (5–10 μm). Zircon U–Pb dating reveals the zircons with near-concordant (> 85% concordance) $^{207}\text{Pb}/^{206}\text{Pb}$ ages between 3412 ± 31 Ma to 2897 ± 46 Ma. The Th/U ratios from the zircons range between 0.04–2.27 with Eu/Eu* ratios between 0.09–0.97, $\text{La}_\text{N}/\text{Sm}_\text{N}$ ratios between 0.119–6.564, $\text{Gd}_\text{N}/\text{Yb}_\text{N}$ ratios between 0.047–0.767. Monazite grains separated from powdered sample appear to be rounded in shape, and a few monazite grains contain apatite inclusions. Monazite U–Pb dating revealed a constrained discordia line on the Concordia diagram with the upper intercept of 3050 ± 35 Ma (MSWD = 0.18, n = 29) with Th/U ratios between 91–903, $\text{La}_\text{N}/\text{Sm}_\text{N}$ values between 5.513–10.747. Apatite U–Pb dating revealed a discordia line on Tera-Wasserburg plot defined with a lower intercept age of 2382 ± 62 Ma (MSWD = 3, n = 29) with Eu/Eu* ratios between 0.07–0.18 and $\text{La}_\text{N}/\text{Sm}_\text{N}$ ratios between 0.134–2.895 and Sr/Y ratios between 0.07 – 0.23.

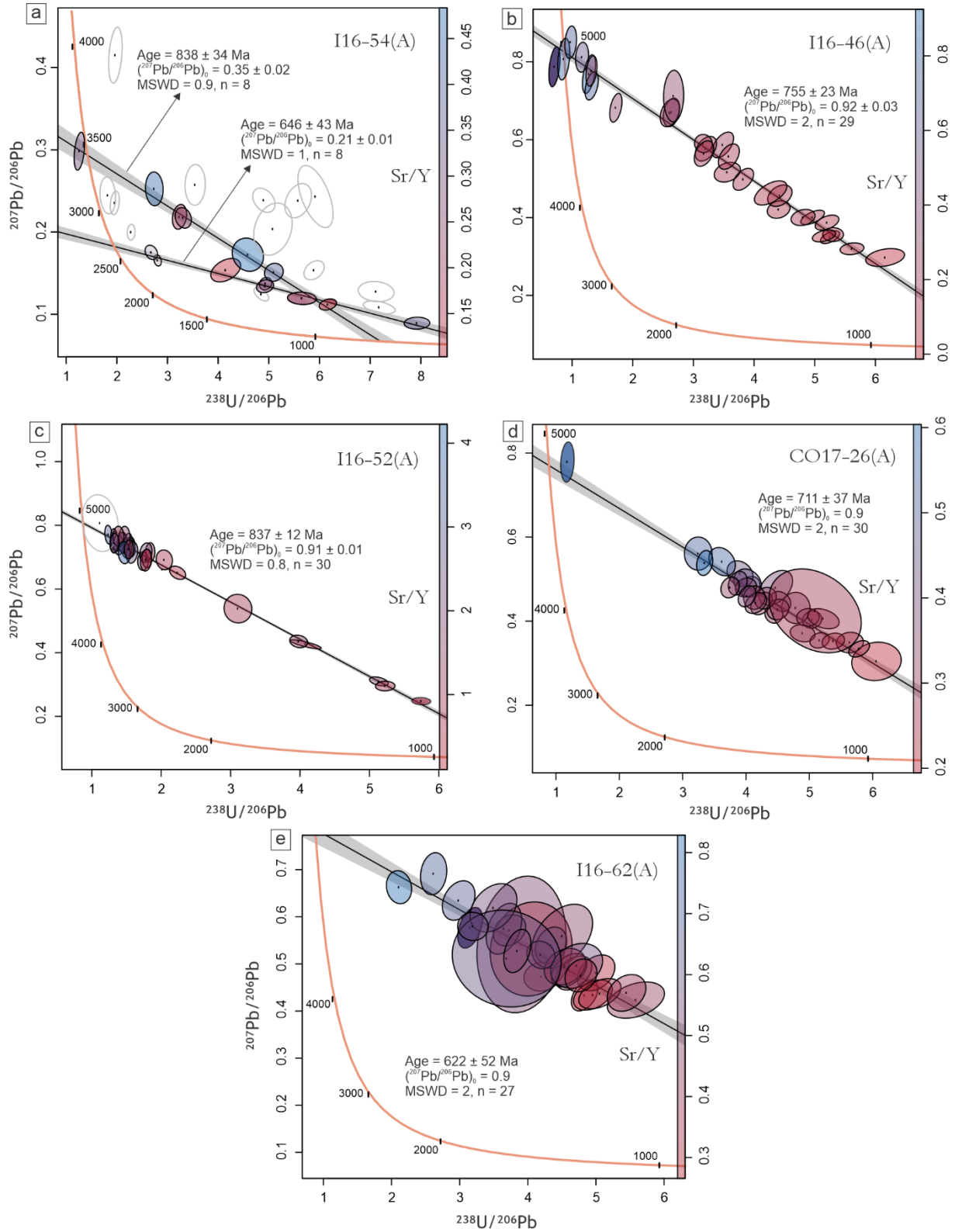


Figure 7: Apatite U-Pb age data represented on Tera-Wasserburg plot. The data ellipses have been coloured using Sr/Y ratios to differentiate felsic/mafic characteristic of source material (Belousava et al., 2002). The sample names have been written in the bottom left and denoted with (A) to represent apatite age data. The hollow ellipses were not used in the calculation of the regression lines using IsoplotR (Vermeesch et al., 2018). (a),(b) represent apatites analysed from gneisses collected at the northern margin

of the Coorg Block. (c),(d),(e) represent the Neoproterozoic alkali and granitic plutons that intrude the suture zones surrounding the Coorg Block.

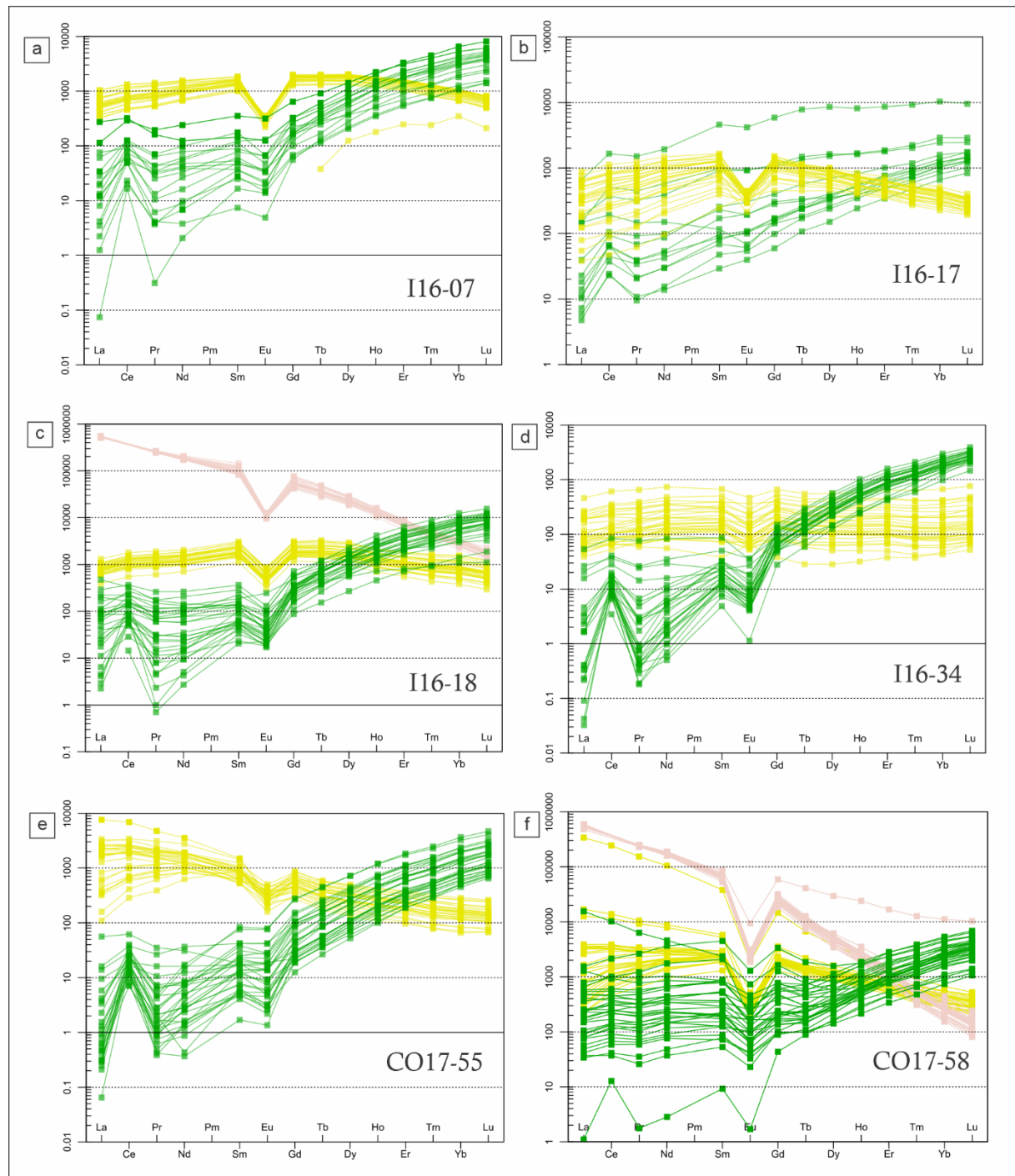


Figure 8: The rare earth element (REE) spider plots for accessory minerals from each sample analysed in this study. The green curves represent zircon REE compositions, yellow curves represent the apatite REE composition and orange curves reflect the REE concentrations in Monazite grains. The REE concentrations have been normalised to chondritic values from Boynton et al., 1984 using the R package GCDkit 6.0 (Janousek et al., 2006). The sample names are denoted in the bottom right of each plot. (a),(b),(c) are lithologies sampled in and around the Karwar Block. (d) has been sampled at the western margin of the Western Dharwar Craton. (e),(f) have been sampled northeast from the Mercara Shear Zone towards the Western Dharwar Craton.

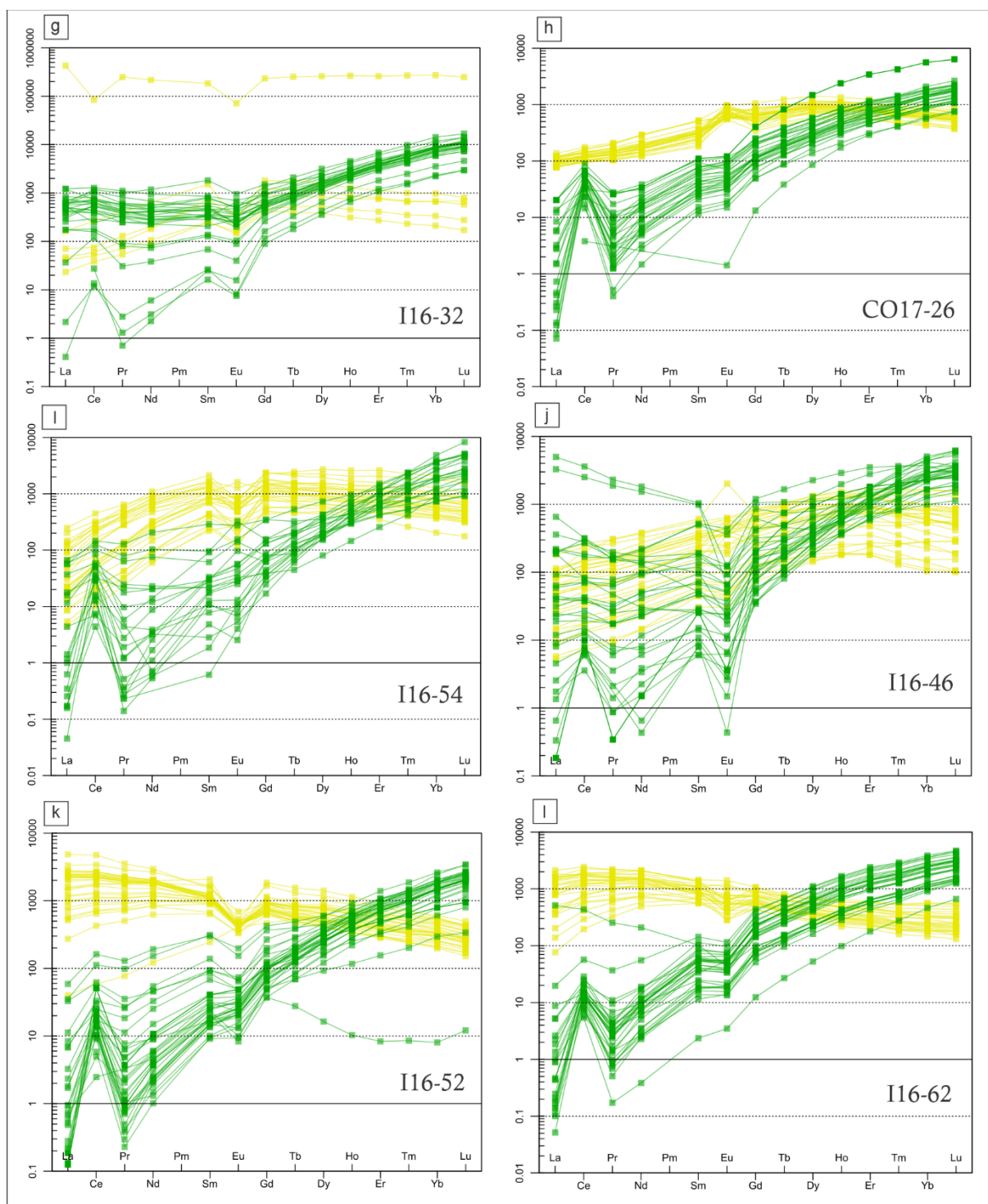


Figure 8 (continued) (g) has been collected from a syenite in the vicinity of the Kumta Shear Zone. (i),(j) represent apatites analysed from gneisses collected at the northern margin of the Coorg Block. (k),(l),(h) represents the Neoproterozoic alkali and granitic plutons that intrude the suture zones surrounding the Coorg Block.

5. Discussion:

5.1 Accessory Mineral Geochronology:

The U-Pb ages dated around the Karwar region show zircon U-Pb ages at 3000 ± 32 Ma in the northern Karwar region and 2971 ± 14 Ma in the southern Karwar region. The prevalence of ages around ca. 3.2 Ga within the Karwar region and nearby the recently proposed Kumta shear zone (Ishwar et al., 2013) suggest the presence of protoliths initially crystallizing around ca. 3.2 Ga and experiencing ancient Pb-loss at 3.0 Ga. This feature has been prominently observed from previous studies on the crustal evolution history of the Western Dharwar Craton (Jayananda et al., 2018 and Chapter 2 in this thesis) which supports the hypothesis put forth by Armistead et al. (2017) that the Karwar Block is an extension of the WDC to the north-west. Similar ages have been reported in a recent study (Li et al., 2020) from the Karwar Block with reported zircon U-Pb ages for amphibolite at ca. 3147 Ma and a porphyritic granite aged at ca. 2966 Ma, also reported by published monazite ages from the Karwar porphyritic granite around ca. 2.95 Ga (Rekha et al., 2013) which was interpreted to represent the age of anatectic amphibolite facies metamorphism in the region. One of the monazites dated in this study, I16-18, is from a sample collected from the periphery of the granitic domain within the Karwar which revealed an upper intercept age of 2962 ± 17 Ma which coincides with the previously reported monazite ages for the Karwar and Chauri blastoporphyratic granitoids (Rekha et al., 2013). The U-Pb ages from the zircons and monazites from the biotite-rich granitic gneiss, I16-18, reveal that the crystallization of the accessory phases was contemporaneous from the short cooling period as evident from the apatite U-Pb age at ca. 2781 ± 71 Ma which is closer to the reported zircon and monazite age for this sample.

Previous works have explored crystallization and cooling ages near the Karwar to correlate the Kumta shear zone with Betsimisaraka shear zone in Madagascar (Ishwar Kumar et al., 2016; Rekha et al., 2014) and to trace the archean to proterozoic evolution of the Dharwar Craton (Li et al., 2020). In this study, we have chosen the apatite grains to represent the cooling ages for temperatures between 375–550 °C from the Karwar block as attempted in previous studies (Cochrane et al., 2014). Ishwar Kumar et al. (2013) have proposed the phengite and biotite K–Ar cooling ages at ca. 1326 Ma and 1385 Ma to represent a cooling age from the P-T conditions of a quartz phengite schist from the Kumta shear zone reaching up to to 18 kbar pressure at 550 °C and K–Ar cooling age for the surrounding TTGs at ca. 1746 and 1796 Ma. Li et al. (2020) have used the Rb–Sr dating for biotite and plagioclase within the Karwar region to construct isochrons at ca. 3050 ± 130 Ma for the amphibolite, ca. 2973 ± 38 Ma for hornblende-gneiss and ca. 2706 ± 28 Ma for a trondhjemite. The apatite cooling ages reported in this study for the Karwar region represent the magmatic protoliths and are closer to their zircon crystallization ages inferring faster cooling rates or near-surface protolith emplacement; and agree with

the Rb–Sr ages reported from the Karwar region (Li et al., 2020). The Karwar block is presumably a north-west extension of the Dharwar Craton with cooling ages closer to the crystallization age in the Mesoarchean. The younger cooling ages reported by Ishwar et al. (2013) and the textural monazite U–Pb ages younger than ca. 2.9 Ga previously reported by Rekha et al., (2013, 2014) relate to the deformation of the sedimentary units overlying the Karwar region such as the Goa schist belt which was compared to the Chitradurga group of greenstone belts overlying the Dharwar Craton. The syenite sample (I16-32) dated to the west of the proposed Kumta shear zone yielded a low amount of apatite fraction which were highly reverse discordant data which can be explained by metasomatic activity related to the alteration of monazites into fluorapatite near the schistose localities near the N-W edge of the Dharwar Craton (Rekha et al., 2013b).

The granodioritic gneiss sampled near the Udupi town on the west coast of the Dharwar Craton revealed zircon U–Pb age constrained to mean $^{207}\text{Pb}/^{206}\text{Pb}$ age at ca. 3266 ± 5 Ma with younger zircons forming a discordia line with upper intercept age at 3206 ± 10 Ma. The apatite U–Pb lower intercept age in the Tera-Wasserburg plot at 3169 ± 44 Ma suggest the protolith had crystallized at ca. 3266 Ma and experienced probable Pb-loss at ca. 3.2 Ga with faster cooling rates (less than 50 Ma in this case). This correlates with the crustal accretion episode in the Western Dharwar Craton between ca. 3.35 – 3.2 Ga (Jayananda et al., 2015, 2018, 2020) which was also reported from the zircon U–Pb ages from the TTG gneisses from WDC from Chapter 2 in this thesis.

The granitoid gneisses collected at the western margin of the WDC in the vicinity of the Mercara Shear Zone reveal zircon $^{207}\text{Pb}/^{206}\text{Pb}$ ages between ca. 3476 – 3112 Ma for the sample closer to the Mercara Shear Zone (CO17-55) and between ca. 3412 – 2897 Ma for the sample (CO17-58) that was further away from the MSZ towards the WDC which could be explained as metapelites recrystallizing while being incorporated into the transitional zone across the MSZ. The ages for CO17-55 agree with previously published ages along the MSZ (Amaldev et al., 2016) explained as magmatic suite constrained between ca. 3.2 – 3.1 Ga, with inherited zircons until ca. 3.5 Ga with a convergent margin between the Coorg Block and the Dharwar Craton around ca. 3.0 Ga from a high-grade metamorphic event using metamorphic overgrowths on zircon rims. The ages reported in this region also correlate with episodes of TTG accretion in the WDC around ca. 3.35–3.28 Ga and ca. 3.23 – 3.2 Ga (Jayananda et al., 2015; data reported in Chapter 2 to the west of WDC) leading to the ambiguity if the Coorg Block represents an older extension of the WDC similar to the Karwar Block. However, the apatite U–Pb ages for the samples CO17-55 and CO17-58, at ca. 2414 ± 74 Ma and 2382 ± 62 Ma respectively, suggest the reactivation of the Mesoarchean suture and supports the previously proposed correlation of the MSZ with the ca. 2.4 Ga Betsimisaraka Suture Zone (Ishwar-Kumar et al., 2013; Rekha et al., 2014). The monazites previously reported from the MSZ (Rekha et al., 2014) with textural dating reveal ca. 2.9 Ga

cores and ca. 2.5 Ga rims which further supports the reactivation of the suture around ca. 2.5 Ga, slightly older than the apatite ages reported in this study. A likely scenario for this reactivation could be caused by the formation of a Neoproterozoic island arc at the boundary of the Coorg Block and Nilgiri Block (Santosh et al., 2013) which also coincides with widespread ca. 2.5 Ga metamorphic event experienced across the southern part of Dharwar Craton (Peucat et al., 2013).

The samples collected from a granodioritic gneiss (I16-46) and a TTG melanosome (I16-54), from the interior boundary of the Coorg Block, reveal $^{207}\text{Pb}/^{206}\text{Pb}$ ages between ca. 3299 — 3087 Ma and ca. 3357 — 3082 Ma respectively, which correlate with the crustal growth episodes in the Coorg Block discussed in Amaldev et al. (2016). The apatite U–Pb ages from the granodioritic gneiss are at 755 ± 23 Ma and the TTG melanosome contained two populations of apatite constrained with distinct discordia lines with intercepts at 838 ± 34 Ma and 646 ± 43 Ma. The apatites from these samples indicate a thermal event which can be correlated to the Syenite magmatism around ca. 0.8 Ga (Santosh et al., 2014) towards the north of the Coorg Block and widespread alkali magmatism towards the south of Dharwar Craton and further Neoproterozoic thermal event arising from the crustal accretion and magmatic events within and beyond the network of shear zones and suture zones that separate the Dharwar Craton from the Southern Granulite Terrane.

The Neoproterozoic volcanics analyzed in this study have been collected around the Coorg Block from the Angadimogar alkaline pluton (Santosh et al., 2014) in the vicinity of Kasargod town (I16-52) and granite near the Mercara town (CO17-26) and to the south of the Coorg Block adjacent to the Peralimala alkaline pluton (Santosh et al., 2014) (I16-62). The Neoproterozoic volcanics display a spread in zircon U–Pb ages along the Concordia diagram from approximately ca. 850 — 660 Ma. The zircon U–Pb ages have been interpreted to have crystallized using mean $^{207}\text{Pb}/^{206}\text{Pb}$ ages to minimise the spread in the data ellipses. The zircon U–Pb crystallization ages are 842 ± 20 Ma for I16-52 with few inherited zircons between ca. 3.2 — 3.1 Ga, 812 ± 29 Ma for CO17-26 with an inherited zircon at $^{207}\text{Pb}/^{206}\text{Pb}$ age of 3235 Ma and 856 ± 20 Ma for I16-62. The apatite U–Pb age for the syenite to the north of Coorg Block, closer to the zircon U–Pb age, is 837 ± 12 Ma and could be responsible for the apatite U–Pb age from the TTG melanosome (I16-54) within the interior of the Coorg Block. The apatite U–Pb ages for the granite near Mercara town (CO17-26) has been constrained at 711 ± 37 Ma and the sample I16-62 has been constrained at 622 ± 52 Ma. These apatite U–Pb ages correlate with the zircon U–Pb ages reported from the Neoproterozoic arc magmatism in the southern Madurai block (Santosh et al., 2017) inferring the spatial extent of the thermal events caused on the lower crust of the Dharwar Craton and the Coorg Block.

5.2 Accessory Mineral REE composition:

The rare earth element (REE) and trace element composition from the accessory phases have been previously used to infer the depth of crystallization and melt characteristic of the source protolith from zircon REE compositions (Grimes et al., 2015, McKenzie et al., 2018). Apatite REE and trace element compositions have been used to categorise detrital apatites (Belousava et al., 2002), fingerprint metasomatic processes that could have affected the protoliths during crystallization/metamorphism (Harlov 2015) and categorize the apatite crystallization between magmatic early cooling and late-stage hydrothermal activity (S. Krneta et al., 2016). In this study, we have used the REE compositions from the accessory phases to supplement the U–Pb age data to infer the depth of crystallization and role of fluids during the closure temperature of these accessory phases within the tectonic settings. The REE compositions have been plotted as spider plots for the accessory phases analysed from each sample in figures 8 and 9 to infer the relative abundances of REE within the accessory phases and understand plausible REE differentiation/mobilisation during initial crystallization or later metasomatic/hydrothermal activity.

The ratios of $[\text{Gd/Yb}]_N$ have been used as a proxy for the ratio of middle rare earth element (MREE) against the heavy rare earth elements (HREE) from the zircons to infer the depth of crystallization from the source magma (McKenzie et al., 2018; Chapter 2,3,4 in this thesis) with higher MREE/HREE ratios inferring deeper crystallization within the stability field of minerals, that have an affinity to sequester middle- to heavy rare earth elements, such as garnet and amphibole. The zircons display variance in light rare earth elements (LREE) compositions likely due to the variability in discordance and growth of other accessory phases such as apatite and monazite. In apatites, the degree of LREE depletion, here represented as decreasing LREE/MREE ratios, can signify the extent of alteration caused due to hydrothermal/metasomatic activity (S. Krneta et al., 2017) and competition with LREE enriched minerals including allanite, epidote and feldspar (K-feldspar) (Wen et al., 2008). The apatites displaying typical granitoid REE patterns (M. Chu et al., 2009) signify the cooling/reactivation age is primarily from thermal re-activation beyond the closure temperature of the apatite, i.e between 375 – 550 °C (Cochrane et al., 2014).

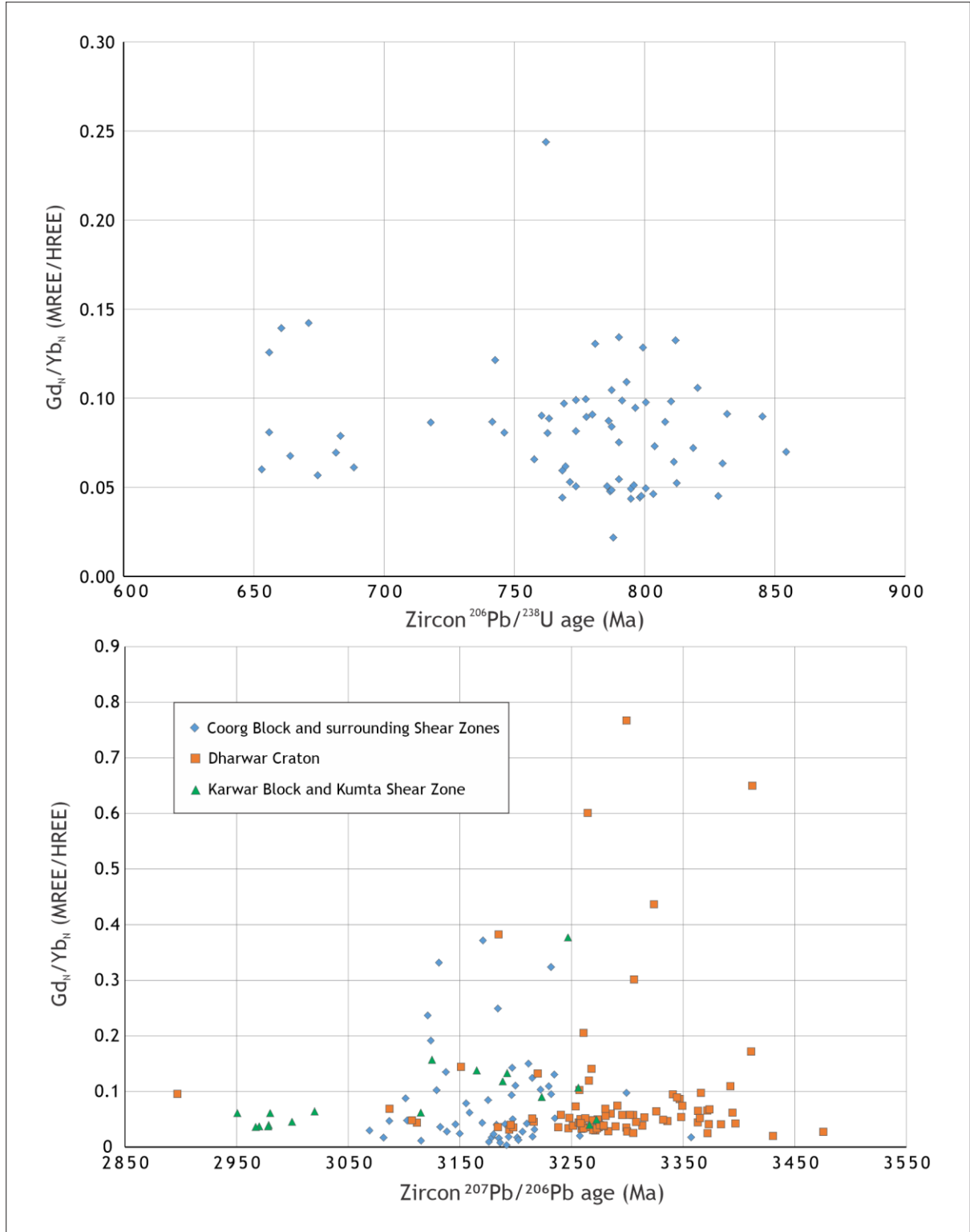


Figure 9: The zircon REE ratios (normalized) here plotted as $[Gd/Yb]_N$ values to represent the MREE/HREE ratios categorized based on location (see legend). The ratios from Mesoarchean aged zircons have been plotted against $^{207}Pb/^{206}Pb$ ages and for the ratios from the Neoproterozoic zircons have been plotted against $^{206}Pb/^{238}U$ ages.

The samples from the Karwar region show an increasing trend in the $[Gd/Yb]_N$ ratios from the zircons analysed from ca. 3.3 – 3.1 Ga as shown in figure 9, signifying the increasing depth of

crystallization/melting of the source magma until ca. 3.1 Ga which was also reported in Chapter 2 from the granitoids within the Dharwar Craton. The apatite cooling ages closer to the zircon U–Pb ages display typical granitoid apatite REE patterns with $[La/Sm]_N$ ratios closer to 1, shown in figure 10, inferring slight alteration in samples I16-07 and I16-17. The $[La/Sm]_N$ ratios in the apatites from sample I16-18 are lower due to the growth of LREE rich phases like monazite during metamorphism (Harlov 2015). The zircons display $[Gd/Yb]_N$ ratios < 0.1 around ca. 3.0 Ga inferring zircon crystallization at lower pressure resulting from possible near-surface protolith emplacement. The Syenite near the Kumta shear zone, I16-32, displays zircon REE patterns with elevated LREE concentrations which could be resulting from discordance or metasomatic activity.

The samples I16-34 and CO17-55 display typical granitoid zircon and apatite REE patterns (M. Chu et al., 2009; Zirner et al., 2015). The sample CO17-58 displays LREE enrichment in the zircon REE patterns with little to no Cerium anomaly, possibly due to the competition with the growth of monazite, and higher $[Gd/Yb]_N$ ratios relative to I16-34 and CO17-55 interpreted here as increased depth of crystallization likely caused due to the crustal accretion between the Coorg Block and the Dharwar Craton (Amaldev et al., 2016, Chapter 3 in this thesis) along with contemporaneous crustal thickening within the Dharwar around ca. 3.2 – 3.1 Ga (discussed in Chapter 2) leading to the crystallization of monazites. The apatites from I16-34 and CO17-55 display typical granitoid REE composition while the apatites from sample CO17-58 display lower $[La/Sm]_N$ values resulting from hydrothermal activity related to later thermal reactivation since the apatite U–Pb age is significantly younger than the monazite U–Pb age to infer that the LREE depletion in these apatites is the growth of monazite.

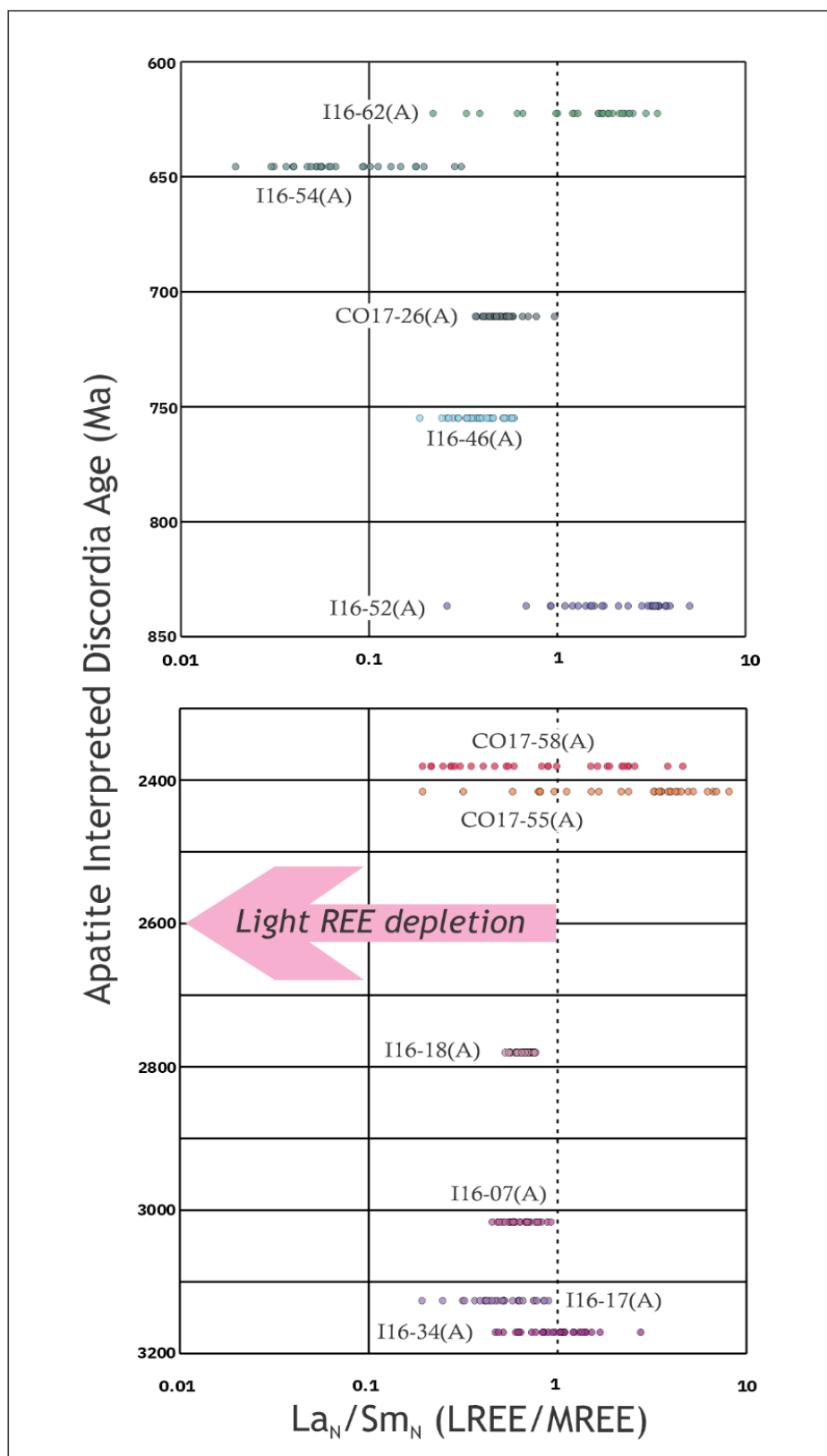


Figure 10: The apatite REE compositions normalized against chondritic values (Boynthon et al., 1984) have been plotted using $[\text{La}/\text{Sm}]_N$ ratios to represent LREE/MREE ratios to infer thermal/hydrothermal reactivation/cooling of the apatites. The lower intercept ages from the apatite U–Pb plots have been used on the y-axis.

The samples I16-46 and I16-54 near the boundary of the Coorg Block reveal variability in the LREE compositions of the zircon REE patterns, however, display $[Gd/Yb]_N$ ratios similar to other granitoids analysed in this study (and also Chapter 2). The apatites in both samples display LREE depletion shown by the low $[La/Sm]_N$ values, shown in figure 11, likely caused by a later hydrothermal alteration (Zirner et al., 2015; S.Krneta et al., 2017) in the Neoproterozoic.

The Neoproterozoic granitic and alkali plutons, CO17-26, I16-52 and I16-62 display typical granitoid pluton $[Gd/Yb]_N$ values, < 0.2 in this study, similar to the Closepet Granite and other magmatic plutons detailed in chapter 2. The apatites from the granite (CO17-26) display LREE depletion likely caused by the same long-lived hydrothermal alteration experienced by the sample I16-46. The apatites in the alkali plutons I16-52 and I16-62 show typical granitoid apatite REE patterns inferring that the emplacement of the Cryogenian Syenite (~840 Ma) to the north of Coorg Block, I16-52, was followed by rapid exhumation and the cooling age of the southern alkali pluton, I16-62 was caused likely due to thermal reactivation during late Cryogenian.

5.3 Tectonic Implications:

The coupled zircon and apatite U–Pb ages from the same protolith have been used in this study to fingerprint the duration between the initial magmatic crystallization and later apatite cooling or thermal/hydrothermal reactivation ages, and the REE compositions from these accessory phases supplement with the depth of source melting and role of fluids in later thermal events. The zircon ages reported in this study represent the crystallization ages of the basement granitoids within the Karwar Block and the Dharwar Craton along with basement gneisses across the Coorg Block and surrounding Neoproterozoic intrusive granitic and alkali plutons. The monazite ages detailed in this study from the Karwar Block and Coorg Block represent monazites crystallizing at ca. 3.0 Ga which correlates with metamorphic monazites crystallizing during the accretion between Coorg Block and WDC at ca. 3045 Ma. However, Rekha et al. (2014) explain that the Karwar Block and Coorg Block have distinct lithologies where the Karwar Block is dominated by blastoporphyritic granitoids which are typical for the WDC; the Coorg Block is dominated by granulite-facies metamorphic lithologies proposing that the Karwar Block is a northwestern extension of the WDC which was also suggested by Armistead et al. (2017). The basement rocks in the Karwar region have experienced the last thermal reactivation event around ca. 2.9 Ga from the monazites that have presumably grown during a metamorphic event. The cooling ages detailed in Ishwar-Kumar et al.(2016) and Rekha et al.(2013), younger than ca. 2.9 Ga are defined by structural deformation of overlying detrital units that deposited over the basement granitoids and the temperatures during these processes were unable to thermally alter the apatite ages within the basement granitoids.

The samples detailed in the vicinity of the Mercara Shear Zone towards the Dharwar Craton, CO17-55 and CO17-58 show apatite cooling ages around ca. 2.4 Ga, younger than the youngest zircon $^{207}\text{Pb}/^{206}\text{Pb}$ ages. The higher $[\text{Gd}/\text{Yb}]_{\text{N}}$ values from the zircons from CO17-58 infer deeper crystallization which correlates with the timing of collision style accretion between the Coorg Block and the Dharwar Craton also evident from the Monazite age at ca. 3045 Ma. The deeper buried lithology is interpreted to have been reactivated during the late Neoproterozoic collision between the Coorg Block and Nilgiri Block (Santosh et al., 2013a) and widespread metamorphic event at ca. 2.5 Ga reported to the south of the Dharwar Craton (Peucat et al., 2013).

The apatites from gneisses from the boundary of the Coorg Block (I16-54 and I16-46) seem to have been affected by thermal aureole caused by adjacent Neoproterozoic granitic and alkali plutons and reveal apatite U–Pb ages younger than the plutons' crystallization age since the closure temperature for apatite U–Pb system is lower than that of zircon U–Pb (Cochrane et al., 2014). The initial crystallization age of the Neoproterozoic plutons have been constrained here using average zircon $^{207}\text{Pb}/^{206}\text{Pb}$ ages in the Cryogenian, around ca. 840 Ma, which coincides with the widespread Cryogenian magmatism reported to the south of the Dharwar Craton (Santosh et al., 2013b, 2014; Plavsa et al., 2012; Collins et al., 2014) and the northern margin of the Southern Granulite Terrane explained to be associated with transcrustal rifting along paleo-suture zones (Santosh et al., 2014). However, the spread in $^{206}\text{Pb}/^{238}\text{U}$ zircon ages is identical in all three plutons surrounding the Coorg Block, from ca. 850 – 650 Ma but they reveal different apatite U–Pb ages at ca. 837 Ma, 711 Ma, 622 Ma across the Mercara Shear Zone — Moyar Shear Zone from NorthWest — SouthEast of the Coorg Block. This is interpreted as the temporally receding thermal aureole of the widespread Cryogenian magmatism in the southeast direction until the Bhavani Shear Zone south of Nilgiri Block with metamorphic ages around ca. 550 Ma (Samuel et al., 2014 and references therein). The subduction of the Southern Granulite Terrain plate (the crustal domains south of Palghat Cauvery Shear Zone) under the Nilgiri Block could have been the cause for the Neoproterozoic volcanics across the suture zones surrounding the Coorg Block which in turn affected the cooling ages of the lithologies at the boundary of the Coorg Block. Hence, we conclude that the combination of zircon, apatite and monazite U–Pb ages can provide vital information about cooling history and the spatial extent of metamorphic and magmatic events across continental boundaries and suture zones surrounding them.

5 Conclusion:

- 1) In the northwestern margin of the Dharwar, within the Karwar Block, the basement granitoids experienced their last thermal event around ca. 3.0 Ga witnessed by metamorphic events which could have crystallized monazite within the melt. The basement rocks appear unaffected by

younger deformation events that have been previously reported to be associated with the overlying detrital units and proposed Kumta Shear Zone suggesting the Karwar Block could be a northwestern extension of the Dharwar Craton.

- 2) The lithologies to the east of the Coorg Block — Dharwar Craton crustal collision zone (Mercara Shear Zone) infer deep crust/high-pressure crystallization from higher MREE/HREE ratios of the zircons and is supported by the metamorphic crystallization of monazite aged at ca. 3.05 Ga and the cooling ages from apatite U–Pb dating reveal reactivation/exhumation during the Neoproterozoic associated with the crustal accretion towards the south of Dharwar Craton and Coorg Block around ca. 2.5 Ga associated with metamorphism.
- 3) The Mesoproterozoic gneisses towards the northern boundary of the Coorg Block have experienced resetting of the apatite U–Pb ages affected by the widespread Cryogenian volcanism within the suture zones surrounding the Coorg Block. The apatites appear to be affected by hydrothermal alteration from lower LREE/MREE ratios; the fluids have been interpreted to have derived from the Neoproterozoic subduction of the crust beneath the Nilgiri Block.
- 4) The Cryogenian granite and alkali plutons reveal a gradient in the apatite U–Pb cooling ages which signify the difference in the rate of cooling as moving closer towards the Moyar–Bhavani Shear Zone and the melange of suture and shear zones occurring to the south of the Coorg Block and the Dharwar Craton. A similar gradient effect could be responsible for the variance in lower intercept ages across the discordant zircons detailed in previous meta-igneous zircon studies across the Dharwar Craton (see Chapter 2).

6 Acknowledgement:

We acknowledge the support of Dr Sarah Gilbert for support at Adelaide Microscopy, the University of Adelaide, who has been instrumental in the acquisition of the zircon, apatite and monazite U–Pb and REE data using LA–ICPMS. We acknowledge the assistance from the University of Adelaide PhD students Angus L. Nixon and Alexander D. Simpson for assistance during apatite U–Pb data reduction and Mitchell J. Bockmann for discussion regarding the Coorg Block. Venkata Pavan Katuru is supported during his PhD by a scholarship provided by the University of Adelaide.

7 Appendix

The zircon U–Pb data has been provided in Appendix 5.1. The zircon REE concentrations in ppm are provided in Appendix 5.2. The Apatite U–Pb data has been provided in Appendix 5.3. The

Apatite REE compositions have been provided in Appendix 5.4. The Monazite U–Pb data has been provided in Appendix 5.5. The Monazite REE concentrations in ppm are provided in Appendix 5.6.

8 References:

- 1) Amaldev, T., M. Santosh, L. Tang, K. R. Baiju, T. Tsunogae and M. Satyanarayanan (2016). "Mesoarchean convergent margin processes and crustal evolution: Petrologic, geochemical and zircon U–Pb and Lu–Hf data from the Mercara Suture Zone, southern India." *Gondwana Research* **37**(Supplement C): 182–204.
- 2) Armistead, S.E., Collins, A.S., Redaa, A., Jepson, G., Gillespie, J., Gilbert, S., Blades, M.L., Foden, J.D., Razakamanana, T., 2020. Structural evolution and medium-temperature thermochronology of central Madagascar: implications for Gondwana amalgamation. *J. Geol. Soc.* <https://doi.org/10.1144/jgs2019-132>.
- 3) Armistead, S.E., Collins, A.S., Payne, J.L., Foden, J.D., De Waele, B., Shaji, E., Santosh, M., 2017. A re-evaluation of the Kumta Suture in western peninsular India and its extension into Madagascar. *J. Asian Earth Sci.* **157**, 317–328.
- 4) Belousova, E. A., W. L. Griffin, S. Y. O'Reilly and N. I. Fisher (2002). "Apatite as an indicator mineral for mineral exploration: trace-element compositions and their relationship to host rock type." *Journal of Geochemical Exploration* **76**(1): 45–69.
- 5) Boynton, W. V. (1984). Cosmochemistry of the rare earth elements: meteorite studies. *Developments in geochemistry*, Elsevier. 2: 63–114.
- 6) Chu, M.-F., K.-L. Wang, W. L. Griffin, S.-L. Chung, S. Y. O'Reilly, N. J. Pearson and Y. Iizuka (2009). "Apatite Composition: Tracing Petrogenetic Processes in Transhimalayan Granitoids." *Journal of Petrology* **50**(10): 1829–1855.
- 7) Chew D. M., Petrus J. A. and Kamber B. S. (2014) U–Pb LAICPMS dating using accessory mineral standards with variable common Pb. *Chem. Geol.* **363C**, 185–199.
- 8) Cochrane, R., R. A. Spikings, D. Chew, J.-F. Wotzlaw, M. Chiaradia, S. Tyrrell, U. Schaltegger and R. Van der Lelij (2014). "High temperature (>350°C) thermochronology and mechanisms of Pb loss in apatite." *Geochimica et Cosmochimica Acta* **127**: 39–56.
- 9) Collins, A.S., Clark, C., Plavsa, D., 2014. Peninsular India in Gondwana: the tectonothermal evolution of the Southern Granulite Terrain and its Gondwanan counterparts. *Gondwana Research* **25**, 190–203.
- 10) Corfu, F., Hanchar, J. M., Hoskin, P. W. Kinny, P., 2003. Atlas of zircon textures. In: Hanchar, J. M. Hoskin, P. W. O. (eds) *Zircon*. Mineralogical Society of America and Geochemical Society, Reviews in Mineralogy and Geochemistry **53**, 469–500.
- 11) Corfu, F., 2013. A century of U–Pb geochronology: the long quest towards concordance. *Bull. Geol. Soc. Am.* **125** (1–2), 33–47.
- 12) Dhoundial, D.P., Paul, D.K., Sarkar, A., Trivedi, J.R., Gopalan, K., Potts, P.J., 1987. Geochronology and geochemistry of Precambrian granitic rocks of Goa. SW India. *Precambrian Res.* **36** (3), 287–302.
- 13) Dhuime, B., Hawkesworth, C., Cawood, P., 2011. When continents formed. *Science* **331**, 154–155.
- 14) Grimes, C.B., Wooden, J.L., Cheadle, M.J. et al. "Fingerprinting" tectono-magmatic provenance using trace elements in igneous zircon. *Contrib Mineral Petrol* **170**, 46 (2015). <https://doi.org/10.1007/s00410-015-1199-3>
- 15) Harlov, D. E. (2015). "Apatite: A Fingerprint for Metasomatic Processes." *Elements* **11**(3): 171–176.
- 16) Hogmalm, K.J., Zack, T., Karlsson, A.K., Sjoqvist, A.S.L., Grabe-Schonberg, D., 2017. In situ Rb–Sr and K–Ca dating by LA–ICP–MS/MS: An evaluation of N₂O and SF₆ as reaction gases. *J. Anal. At. Spectrom.* **32**, 305–313.
- 17) Ishwar-Kumar, C., M. Santosh, S. A. Wilde, T. Tsunogae, T. Itaya, B. F. Windley and K. Sajeew (2016). "Mesoproterozoic suturing of Archean crustal blocks in western peninsular India: Implications for India–Madagascar correlations." *Lithos* **263**: 143–160.
- 18) Ishwar-Kumar, C., B. F. Windley, K. Horie, T. Kato, T. Hokada, T. Itaya, K. Yagi, C. Gouzu and K. Sajeew (2013). "A Rodinian suture in western India: New insights on India–Madagascar correlations." *Precambrian Research* **236**: 227–251.
- 19) Janoušek, V., Farrow, C. M. & Erban, V. 2006. Interpretation of whole-rock geochemical data in igneous geochemistry: introducing Geochemical Data Toolkit (GCDkit). *Journal of Petrology* **47**(6):1255–1259
- 20) Jayananda, M., K. R. Aadhiseshan, M. A. Kusiak, S. A. Wilde, K.-u. Sekhramo, M. Guitreau, M. Santosh and R. V. Gireesh (2020). "Multi-stage crustal growth and Neoproterozoic geodynamics in the Eastern Dharwar Craton, southern India." *Gondwana Research* **78**: 228–260.

- 21) Jayananda, M., D. Chardon, J. J. Peucat, Tushipokla and C. M. Fanning (2015). "Paleo- to Mesoarchean TTG accretion and continental growth in the western Dharwar craton, Southern India: Constraints from SHRIMP U–Pb zircon geochronology, whole-rock geochemistry and Nd–Sr isotopes." *Precambrian Research* **268**: 295–322.
- 22) Jayananda, M. T., Y., T. Miyazaki, R. V. Gireesh, K.-u. Kapfo, Tushipokla, H. Hiroshi and T. Kano (2013). "Geochronological constraints on Meso- and Neoproterozoic regional metamorphism and magmatism in the Dharwar craton, southern India." *Journal of Asian Earth Sciences* **78**: 18–38.
- 23) Jochum, K. P., U. Weis, B. Stoll, D. Kuzmin, Q. Yang, I. Raczek, D. E. Jacob, A. Stracke, K. Birbaum, D. A. Frick, D. Günther and J. Enzweiler (2011). "Determination of Reference Values for NIST SRM 610–617 Glasses Following ISO Guidelines." *Geostandards and Geoanalytical Research* 35(4): 397–429.
- 24) Krneta, S., C. L. Ciobanu, N. J. Cook, K. Ehrig and A. Kontonikas-Charos (2016). "Apatite at Olympic Dam, South Australia: A petrogenetic tool." *Lithos* **262**: 470–485.
- 25) Krneta, S., C. L. Ciobanu, N. J. Cook, K. Ehrig and A. Kontonikas-Charos (2017). "Rare Earth Element Behaviour in Apatite from the Olympic Dam Cu–U–Au–Ag Deposit, South Australia." *Minerals* **7**(8).
- 26) Li, S.S., Palin, R.M., Santosh, M., Shaji, E., Tsunogae, T., 2019. Extreme thermal metamorphism associated with Gondwana assembly: Evidence from sapphirine-bearing granulites of Rajapalayam, southern India. *Geol. Soc. Am. Bull.*, <https://doi.org/10.1130/B35378.1>.
- 27) Li, S.S., Santosh, M., Ganguly, S., Thanooja, P.V., Sajeev, K., Pahari, A., 2018a. Neoproterozoic microblock amalgamation in southern India: evidence from the Nallamalai Suture Zone. *Precambrian Res.* 314, 1–27.
- 28) Li, S.S., Santosh, M., Palin, R.M., 2018b. Metamorphism during the Archean–Proterozoic transition associated with microblock amalgamation in the Dharwar Craton, India. *J. Petrol.* 59 (12), 2435–2462.
- 29) Li, S.-S., M. Santosh, J. Farkaš, A. Redaa, S. Ganguly, S. W. Kim, C. Zhang, S. Gilbert and T. Zack (2020). "Coupled U–Pb and Rb–Sr laser ablation geochronology trace Archean to Proterozoic crustal evolution in the Dharwar Craton, India." *Precambrian Research* **343**: 105709.
- 30) Ludwig, K. (2003). "User's manual for IsoPlot 3.0." A Geochronological Toolkit for Microsoft Excel 71.
- 31) M, Jayananda., Santosh. M and A. K.R (2018). "Formation of Archean (3600–2500 Ma) continental crust in the Dharwar Craton, southern India." *Earth-Science Reviews* **181**: 12–42.
- 32) McKenzie, N. R., A. J. Smye, V. S. Hegde and D. F. Stockli (2018). "Continental growth histories revealed by detrital zircon trace elements: A case study from India." *Geology* 46(3): 275–278.
- 33) Nutman A. P., Friend C. R. L., Horie K. and Hikada H. (2007). The Itsaq Gneiss complex of southern West Greenland and its construction at convergent plate boundaries. *Developments in Precambrian Geology*, Oxford, pp. 15, 187–218.
- 34) O'Reilly, S. Y. and W. L. Griffin (2000). "Apatite in the mantle: implications for metasomatic processes and high heat production in Phanerozoic mantle." *Lithos* **53**(3): 217–232.
- 35) Payne, J. L., Hand, M., Barovich, K., & Wade, B. (2008). Temporal constraints on the timing of high-grade metamorphism in the northern Gawler Craton: implications for assembly of the Australian Proterozoic. *Australian Journal of Earth Sciences*, 55(5), 623–640.
- 36) Paton, C., J. Hellstrom, B. Paul, J. Woodhead and J. Hergt (2011). "Lolite: Freeware for the visualisation and processing of mass spectrometric data." *Journal of Analytical Atomic Spectrometry* **26**(12): 2508–2518.
- 37) Paton, C., J. Hellstrom, B. Paul, J. Woodhead and J. Hergt (2013). *2011 Paton et al JAAS Supp info*.
- 38) Peucat, J.-J., M. Jayananda, D. Chardon, R. Capdevila, C. M. Fanning and J.-L. Paquette (2013). "The lower crust of the Dharwar Craton, Southern India: Patchwork of Archean granulitic domains." *Precambrian Research* **227**(Supplement C): 4–28.
- 39) Plavsa, D., Collins, A.S., Foden, J.F., Kropinski, L., Santosh, M., Chetty, T., Clark, C., 2012. Delineating crustal domains in Peninsular India: age and chemistry of orthopyroxene-bearing felsic gneisses in the Madurai Block. *Precambrian Research* 198, 77–93.
- 40) Plavsa, D., A. Collins, J. Payne, J. Foden, C. Clark and M. Santosh (2014). "Detrital zircons in basement metasedimentary protoliths unveil the origins of southern India." *Geological Society of America Bulletin* **126**.
- 41) Rekha, S. and A. Bhattacharya (2014). "Paleoproterozoic/Mesoproterozoic tectonism in the northern fringe of the Western Dharwar Craton (India): Its relevance to Gondwanaland and Columbia supercontinent reconstructions." *Tectonics* **33**(4): 552–580.
- 42) Rekha, S., A. Bhattacharya and N. Chatterjee (2014). "Tectonic restoration of the Precambrian crystalline rocks along the west coast of India: Correlation with eastern Madagascar in East Gondwana." *Precambrian Research* **252**: 191–208.
- 43) Rekha, S., A. Bhattacharya and T. A. Viswanath (2013). "Microporosity linked fluid focusing and monazite instability in greenschist facies para-conglomerates, western India." *Geochimica et Cosmochimica Acta* **105**: 187–205.

- 44) Rekha, S., T. A. Viswanath, A. Bhattacharya and N. Prabhakar (2013). "Meso/Neoproterozoic crustal domains along the north Konkan coast, western India: The Western Dharwar Craton and the Antongil-Masora Block (NE Madagascar) connection." Precambrian Research **233**: 316-336.
- 45) Samuel, V.O., Santosh, M., Liu, S., Wang, W., Sajeev, K., 2014. Neoproterozoic continental growth through arc magmatism in the Nilgiri Block, southern India. *Precambrian Research*
<http://dx.doi.org/10.1016/j.precamres.2014.1002.1002>.
- 46) Santosh, M. (2020). "The Southern Granulite Terrane: A synopsis." International Union of Geological Sciences **43**(1): 109-123.
- 47) Santosh, M., C.-N. Hu, X.-F. He, S.-S. Li, T. Tsunogae, E. Shaji and G. Indu (2017). "Neoproterozoic arc magmatism in the southern Madurai Block, India: Subduction, relamination, continental outbuilding, and the growth of Gondwana." Gondwana Research **45**: 1-42.
- 48) Santosh, M., Li, S.S., 2018. Anorthosites from an Archean continental arc in the Dharwar Craton, southern India: implications for terrane assembly and cratonization. *Precambrian Research* **308**, 126–147.
- 49) Santosh, M., Q.-Y. Yang, M. Ram Mohan, T. Tsunogae, E. Shaji and M. Satyanarayanan (2014). "Cryogenian alkaline magmatism in the Southern Granulite Terrane, India: Petrology, geochemistry, zircon U–Pb ages and Lu–Hf isotopes." Lithos **208-209**: 430-445.
- 50) Santosh, M., Q.-Y. Yang, E. Shaji, M. R. Mohan, T. Tsunogae and M. Satyanarayanan (2016). "Oldest rocks from Peninsular India: Evidence for Hadean to Neoproterozoic crustal evolution." Gondwana Research **29**(1): 105-135.
- 51) Santosh, M., Q.-Y. Yang, E. Shaji, T. Tsunogae, M. R. Mohan and M. Satyanarayanan (2015). "An exotic Neoproterozoic microcontinent: The Coorg Block, southern India." Gondwana Research **27**(1): 165-195.
- 52) Schoene, B. and S. A. Bowring (2006). "U–Pb systematics of the McClure Mountain syenite: thermochronological constraints on the age of the 40Ar/39Ar standard MMhb." Contributions to Mineralogy and Petrology **151**(5): 615.
- 53) Teale, W., A. S. Collins, J. Foden, J. L. Payne, D. Plavsa, T. R. K. Chetty, M. Santosh and M. Fanning (2011). "Cryogenian (~830Ma) mafic magmatism and metamorphism in the northern Madurai Block, southern India: A magmatic link between Sri Lanka and Madagascar?" Journal of Asian Earth Sciences **42**(3): 223-233.
- 54) Thompson, J. (2016). "Matrix effects in Pb/U measurements during LA-ICP-MS analysis of the mineral apatite." Journal of Analytical Atomic Spectrometry **vol. 31, no. 6**: 1206.
- 55) Tillberg, M., Drake, H., Zack, T., Kooijman, E., Whitehouse, M.J., Åström, M.E., 2020. In situ Rb-Sr dating of slickenfibres in deep crystalline basement faults. *Sci. Rep.* **10**, 562.
- 56) Vermeesch, P., 2018. Isoplot R: A free and open toolbox for geochronology. *Geosci. Front.* **9** (5), 1479–1493.
- 57) Wen, D.-R., Chung, S.-L., Song, B., Izuka, Y., Yang, H.-J., Ji, J., Liu, D. & Gallet, S. (2008a). Late Cretaceous Gangdese intrusions of adakitic geochemical characteristics, SE Tibet: petrogenesis and tectonic implications. *Lithos* doi:10.1016/j.lithos.2008.02.005.
- 58) Zirner, A. L. K., M. A. W. Marks, T. Wenzel, D. E. Jacob and G. Markl (2015). "Rare earth elements in apatite as a monitor of magmatic and metasomatic processes: The Ilímaussaq complex, South Greenland." Lithos **228-229**: 12-22.

6

Key outcomes and Conclusions of the Thesis

Through this multidisciplinary PhD research, we achieved significant progress towards understanding the crustal and isotopic evolution of the Dharwar Craton in India and surrounding geological terranes along with it. The primary aims of this research were:

1. To create a robust crustal evolution model of the Dharwar Craton based on meta-igneous zircon record of the basement granitoids that include previously published meta-igneous Nd-Hf data to create a magmatic Hf map of the Dharwar Craton.
2. To append the existing detrital zircon record of the Dharwar Craton and understand the crustal evolution of the source region. To attempt to improve the spatial and stratigraphic correlation between the various greenstone belts.
3. To study the detrital record of the Paleoproterozoic Kaladgi-Badami basin and test the “Greater Dharwar Craton” theory proposing the Kaladgi-Badami basin as the potential missing link between the Itremo group across Madagascar and the Cuddapah Basin in India.
4. Understand the timing and spatial extent of the last thermal event experienced across the Dharwar Craton and neighbouring crustal domains and correlate it with contemporaneous tectonic events to reveal the thermal record of the Dharwar Craton.

1) Crustal evolution model of the Dharwar Craton from meta-igneous lithologies:

In Chapter 2, we have presented a large dataset comprising of new zircon U–Pb and Lu–Hf data from which we have concluded that the Dharwar Craton has evolved through various phases including juvenile accretion of TTG suites around ca. 3.4–3.2 Ga with crustal components extracted up to ca. 3.8 Ga in the Western Dharwar Craton. Continuous crustal reworking continued contemporaneously in the WDC and CDC until ca. 3.0 Ga. The CDC experienced further recycling until ca. 2.55 Ga attributed to the bimodal volcanism accreting the transitional type TTGs around ca. 2.7–2.6 Ga followed by juvenile magmatism in the EDC at ca. 2.58 – 2.52 Ga. We showed that combining the $\epsilon\text{Hf}(t)$ data from this study when combined with published $\epsilon\text{Hf}(t)$ data from zircon bearing lithologies and $\epsilon\text{Nd}(t)$ data from greenstone belts and associated granitoids form a complete picture filling the gaps in the magmatic zircon record in the $\epsilon\text{Hf}(t)$ data alone. The combined $\epsilon\text{Hf}(t)$ and $\epsilon\text{Nd}(t)$ data in this study reveal the influence of juvenile mafic magmas around ca. 2.7–2.6 Ga initiating reworking of the pre-existing crust to produce transitional type TTGs. The timing of crustal thickening was inferred using zircon REE compositions expressed as LREE/HREE and MREE/HREE ratios plotted against crystallization age. We have also identified that the Ramagiri Greenstone Belt (RGB) acts as a boundary between the reworked transitional type

TTGs across CDC and the Neoarchean juvenile lithologies associated with EDC. Hence we propose the Ramagiri—Penakacherla Greenstone Belt to act as an isotopic boundary between the CDC and EDC in the northern part of the Dharwar Craton similar to the Kadiri—Kolar greenstone belt in the south. We have also tested the Nunavutia hypothesis and compared the $\epsilon\text{Hf}(t) + \epsilon\text{Nd}(t)$ data of the Dharwar Craton with $\epsilon\text{Hf}(t)$ data taken from a global dataset. We report that the younger CDC and EDC correlate with the Archean cratons in North America (Rae + Sask), Australia (Yilgarn + Gawler), Antarctica, West African cratons and partially correlate with the Siberian craton. The older Mesoarchean components in WDC and CDC correlate with North America, Siberia and North China cratons and we have deemed the Nunavutia hypothesis inconclusive due to lack of enough data points from the Dharwar Craton around the period of proposed existence of Nunavutia, between ca. 2.54 — 2.45 Ga used for the correlation.

2) Detrital record of the Mesoarchean and lower Neoarchean meta-quartzites

In Chapter 3, we show that the quartzites analysed in this study reveal maximum depositional ages between Meso- to Neoarchean ages. The ages reported in the detrital record of these sequences coincide with major crustal accretion events reported across the Dharwar Craton (also discussed in Chapter 2). We have compared the $\epsilon\text{Hf}(t)$ data from the detrital sequences in Western Dharwar Craton with published detrital $\epsilon\text{Hf}(t)$ data categorised into greenstone belt within the western, central or eastern block of Dharwar Craton along with published magmatic $\epsilon\text{Hf}(t)$ data and the results from Chapter 2 to correlate the source regions to the detrital units. We show that the older Sargur Group had detrital zircons with similar $\epsilon\text{Hf}(t)$ values from the adjacent Coorg Block which is possible if the Sargur Group had formed after the Mesoarchean amalgamation of the Coorg Block against the western margin of the Dharwar Craton. Another likely scenario for the presence of Eoarchean precursors in $\epsilon\text{Hf}(t)$ data of the Sargur Group could be related to the presence of Eoarchean precursors within the published $\epsilon\text{Hf}(t)$ data from the EDC greenstone belts and identical sources could have provided detrital material to the lower Sargur Group. From the MREE/HREE ratios from the detrital zircons in Holenarsipur we infer that the increase in MREE/HREE ratios of the detrital zircons with time is associated with a high-pressure signature interpreted here as localised subduction like tectonic processes dominating near the Holenarsipur Greenstone Belt in the Sargur Group. The K.R.Pete Schist Belt has detrital $\epsilon\text{Hf}(t)$ data identical to the published $\epsilon\text{Hf}(t)$ data from detrital sequences and meta-igneous lithologies across WDC.

3) Proterozoic intracratonic sedimentary basin

In Chapter 4, we present new detrital zircon age data from the Paleoproterozoic Kaladgi-Badami (KB) basin. We have constrained the deposition of the Kaladgi-Badami basin occurred between ca. 2.3–1.86 Ga likely from weakening of the crust, at the northern margin of the Dharwar Craton, from dyke swarm activity. We compared the sedimentary record across the Kaladgi-Badami against the sedimentary record of Paleoproterozoic basins across southern India and Madagascar using multi-dimensional scaling (MDS) to test the “Greater Dharwar Craton” hypothesis which proposed the KB basin to be the missing link between the Cuddapah basin. Combining the results from the MDS and published paleo-flow directions we have concluded that the sedimentary record of the KB basin is most similar to the Papaghni group within the Cuddapah Basin and share similar sources and not related to the Itremo group contradicting the Greater Dharwar Craton hypothesis. This study provides with the post-tectonic processes that were prevalent at the continental margins in the Paleoproterozoic after the assembly of the Dharwar Craton.

4) Thermal record of the Dharwar Craton

In Chapter 5 we present new U–Pb age data from zircons, apatite and monazites from lithologies along the western margin of the Dharwar Craton. From the apatite U–Pb ages near the Karwar Block, we support the proposal that the Karwar Block is a north western extension of the Dharwar Craton. The Mesoarchean lithologies to the east of Mercara Shear Zone experienced metamorphism around ca. 3.05 Ga from monazite ages, and the exhumation history from apatite U–Pb ages reveal reactivation from widespread metamorphism due to Neoproterozoic amalgamation to the south of Dharwar Craton and Coorg Block. The Mesoarchean gneisses near the Mercara Shear Zone at the northern boundary of Coorg Block were affected by the intrusive Neoproterozoic alkali and granitic plutons experiencing hydrothermal alteration evident from LREE depletion in the apatite REE patterns. The Neoproterozoic volcanics along the suture zones reveal a gradient in their apatite cooling ages signifying the influence of Neoproterozoic subduction to the northern margin of the Bhavani–Palghat–Cauvery Shear Zone.

5) Implications for the crustal and isotopic evolution of the Dharwar Craton

Overall, the research produced in this PhD strongly support:

1. The Western Dharwar Craton and Central Dharwar Craton have experienced continuous contemporaneous crustal growth and recycling until ca. 3.0 Ga and the Central Dharwar Craton continued to further evolve till ca. 2.55 Ga from interaction with Neoproterozoic juvenile mafic magmatism till accretion of juvenile magmas from the Eastern Dharwar Craton. The Ramagiri—Penakacherla greenstone belt acts as the boundary between the Central Dharwar Craton and the Eastern Dharwar Craton.
2. The Coorg Block has accreted to the western margin of the Dharwar Craton during the Mesoproterozoic causing metamorphic assemblages and high-pressure signatures in the REE compositions of the zircons from this collision zone, and identified from the detrital record of the Sargur Group Greenstone belts.
3. The northern margin of the Dharwar Craton was weakened by dyke swarm activity leading to the formation of the Paleoproterozoic intra-cratonic Kaladgi-Badami basin, constrained between ca. 2.3–1.86 Ga, and share similar sedimentary environment to the Papaghni Group in the Cuddapah Basin in India. From the cooling history/thermal record of the western margin of the Dharwar Craton, the Karwar Block is likely to be an extension of the Dharwar Craton to the North-West. The Neoproterozoic micro-block amalgamation along with widespread metamorphism at ca. 2.5 Ga towards the south of the Dharwar Craton and Coorg Block have reactivated the southern and south-western margins of the Dharwar Craton. The gneisses near the Mercara Shear Zone to the northern margin of Coorg Block reveal hydrothermally altered apatite ages closer to the Neoproterozoic volcanics that intrude the margins of the Coorg Block. The apatite U–Pb cooling ages from the Neoproterozoic alkali and granitic plutons reveal longer cooling periods towards the South-East along the Mercara Shear Zone possibly due to the subduction processes near the Palghat–Cauvery Shear Zone.

7

Appendices

Chapter 2:

Appendix 2.1 Granitoids of the Dharwar Craton: U–Pb zircon data	166
Appendix 2.2 Granitoids of the Dharwar Craton: REE zircon data.....	190
Appendix 2.3 Granitoids of the Dharwar Craton: Lu–Hf zircon data.....	220

Chapter 3:

Appendix 3.1 Detrital Record of the Dharwar Craton: U–Pb zircon data	228
Appendix 3.2 Detrital Record of the Dharwar Craton: Lu–Hf zircon data.....	247
Appendix 3.3 Detrital Record of the Dharwar Craton: REE zircon data	249

Chapter 4:

Appendix 4.1 Detrital Record of the Kaladgi-Badami basin: U–Pb zircon data	267
Appendix 4.2 Detrital Record of the Kaladgi-Badami basin: REE zircon data	280

Chapter 5:

Appendix 5.1 Thermal history of the Dharwar Craton: U–Pb zircon data	300
Appendix 5.2 Thermal history of the Dharwar Craton: REE zircon data	315
Appendix 5.3 Thermal history of the Dharwar Craton: U–Pb apatite data.....	326
Appendix 5.4 Thermal history of the Dharwar Craton: REE apatite data	341
Appendix 5.5 Thermal history of the Dharwar Craton: U–Pb monazite data.....	355
Appendix 5.6 Thermal history of the Dharwar Craton: REE monazite data.....	359

Appendix 2.1 Granitoids of the Dharwar Craton: U–Pb zircon data

Comment	$^{207}\text{Pb}/^{235}\text{U}$	2σ	$^{206}\text{Pb}/^{238}\text{U}$	2σ	Error Correlation (ρ)	$^{207}\text{Pb}/^{235}\text{U}$ Age (Ma)	2σ	$^{206}\text{Pb}/^{238}\text{U}$ Age (Ma)	2σ	$^{207}\text{Pb}/^{206}\text{Pb}$ Age (Ma)	Age 2σ	U/Th ratio	Th/U	Concordance
PD18-101-351.d	10.51	0.29	0.453	0.011	0.59493	2481	25	2406	49	2543	39	4.22	0.237	94.61
PD18-101-352.d	10.49	0.27	0.4629	0.011	0.56518	2477	24	2457	47	2499	36	3.76	0.266	98.32
PD18-101-353.d	5.95	0.49	0.278	0.01	0.68156	1967	33	1580	50	2400	45	1.71	0.585	65.83
PD18-101-354.d	12.24	0.37	0.5097	0.012	0.59553	2624	29	2654	53	2578	36	1.15	0.870	102.95
PD18-101-355.d	8.54	0.25	0.379	0.0091	0.64754	2289	27	2071	43	2484	39	2.01	0.498	83.37
PD18-101-356.d	5.957	0.16	0.2865	0.0068	0.71816	1968	22	1624	34	2343	32	2.759	0.362	69.31
PD18-101-357.d	9.81	0.41	0.427	0.016	0.64609	2413	44	2290	74	2516	41	2.854	0.350	91.02
PD18-101-358.d	6.74	0.2	0.319	0.0095	0.70791	2076	27	1784	46	2371	34	2.019	0.495	75.24
PD18-101-359.d	11.12	0.53	0.484	0.02	0.49672	2530	57	2542	93	2540	37	3.97	0.252	100.08
PD18-101-360.d	4.76	0.21	0.2438	0.0088	0.91859	1776	35	1405	45	2220	35	0.452	2.212	63.29
PD18-101-362.d	6.7	0.23	0.3277	0.0095	0.62443	2068	33	1826	47	2348	38	2.096	0.477	77.77
PD18-101-363.d	3.365	0.11	0.1976	0.0057	0.85662	1496	26	1161	31	2007	37	0.653	1.531	57.85
PD18-101-364.d	5.61	0.13	0.2729	0.0069	0.65402	1923	21	1554	35	2335	36	2.489	0.402	66.55
PD18-101-365.d	5.95	0.23	0.2938	0.011	0.91956	1966	38	1659	58	2282	33	1.459	0.685	72.70
PD18-101-373.d	10.7	0.26	0.4559	0.011	0.73715	2496	22	2420	48	2553	32	1.846	0.542	94.79
PD18-101-374.d	11.33	0.32	0.4943	0.011	0.54712	2552	25	2588	50	2514	40	2.171	0.461	102.94
PD18-101-375.d	11.17	0.28	0.481	0.012	0.64554	2536	24	2529	53	2538	34	3.865	0.259	99.65
PD18-101-377.d	9.49	0.28	0.4139	0.011	0.60144	2386	29	2232	53	2507	35	3.2	0.313	89.03
PD18-101-378.d	9.35	0.42	0.413	0.016	0.78556	2370	50	2228	76	2480	37	2.32	0.431	89.84
PD18-101-379.d	10.34	0.36	0.458	0.015	0.64091	2463	36	2428	69	2500	38	1.04	0.962	97.12
PD18-101-380.d	11.41	0.48	0.491	0.019	0.86835	2553	44	2593	88	2546	38	3.58	0.279	101.85
PD18-101-381.d	5.83	0.26	0.2838	0.0097	0.4965	1949	34	1609	48	2306	39	2.23	0.448	69.77
PD18-101-382.d	12.65	0.3	0.5343	0.012	0.55799	2654	23	2758	48	2574	33	0.923	1.083	107.15
PD18-101-383.d	6.16	0.18	0.29	0.0077	0.70801	1994	29	1638	39	2409	39	2.14	0.467	68.00
PD18-101-384.d	7.67	0.18	0.3541	0.0074	0.47724	2192	22	1954	37	2408	34	2.823	0.354	81.15
PD18-101-385.d	10.98	0.27	0.4708	0.011	0.65809	2519	23	2486	46	2552	33	3.56	0.281	97.41
PD18-101-386.d	7.48	0.27	0.3501	0.011	0.67002	2169	31	1934	52	2385	35	1.74	0.575	81.09
PD18-101-387.d	9.9	0.37	0.43	0.015	0.78759	2424	42	2302	71	2503	33	2.93	0.341	91.97
PD18-104-395.d	17.13	0.72	0.468	0.017	0.64962	2940	41	2472	77	3277	33	2.29	0.437	75.43
PD18-104-397.d	5.53	0.37	0.1525	0.01	0.92194	1900	81	914	59	3236	32	7.89	0.127	28.24
PD18-104-398.d	15.22	1.1	0.407	0.028	0.40219	2823	130	2198	150	3283	37	9.9	0.101	66.95
PD18-104-399.d	9.55	0.57	0.262	0.015	0.47466	2390	57	1500	77	3272	34	3.01	0.332	45.84
PD18-104-400.d	7.3	0.34	0.2187	0.01	0.76414	2144	45	1273	55	3128	39	2.23	0.448	40.70
PD18-104-401.d	14.13	1	0.38	0.026	0.65966	2755	81	2075	130	3276	34	1.363	0.734	63.34
PD18-104-402.d	8.91	0.77	0.252	0.02	0.7777	2325	68	1449	100	3231	37	4.29	0.233	44.85

PD18-104-403.d	23.94	0.99	0.649	0.026	0.49156	3263	48	3222	110	3297	35	3.83	0.261	97.73
PD18-104-404.d	10.09	0.34	0.3089	0.011	0.82388	2445	34	1733	55	3101	33	2.895	0.345	55.89
PD18-104-406.d	16.81	0.71	0.491	0.02	0.87267	2923	53	2573	95	3157	33	3.62	0.276	81.50
PD18-104-407.d	12.7	0.85	0.354	0.025	0.44131	2653	110	1950	130	3229	36	4.88	0.205	60.39
PD18-104-408.d	10.8	0.44	0.296	0.012	0.67117	2502	46	1670	62	3255	32	7.35	0.136	51.31
PD18-104-411.d	8.91	0.6	0.2566	0.018	0.65397	2327	66	1472	96	3170	35	3.94	0.254	46.44
PD18-104-419.d	17	0.62	0.468	0.014	0.72512	2930	32	2472	62	3275	34	4.91	0.204	75.48
PD18-104-420.d	1.47	0.25	0.0446	0.0074	0.92229	913	66	281	44	3144	30	13.48	0.074	8.94
PD18-104-421.d	9.48	0.65	0.258	0.017	0.70711	2383	84	1479	92	3260	34	9.9	0.101	45.37
PD18-104-423.d	7.14	0.33	0.2212	0.0079	0.45752	2128	41	1288	41	3053	37	3.27	0.306	42.19
PD18-104-424.d	12.17	0.77	0.3328	0.021	0.54082	2616	85	1851	110	3252	32	3.06	0.327	56.92
PD18-104-425.d	25.68	1.5	0.673	0.037	0.83713	3331	74	3316	160	3342	33	0.718	1.393	99.22
PD18-104-426.d	19.86	1.1	0.539	0.029	0.78782	3083	78	2776	130	3276	30	3.33	0.300	84.74
PD18-104-427.d	22.23	1.3	0.599	0.034	0.83972	3188	75	3020	150	3306	31	3.69	0.271	91.35
PD18-104-428.d	22.51	0.72	0.608	0.019	0.70383	3202	33	3059	77	3303	32	0.76	1.316	92.61
PD18-104-429.d	18.15	0.97	0.496	0.025	0.65247	2992	69	2592	110	3290	40	3.93	0.254	78.78
PD18-104-430.d	11.66	0.43	0.3455	0.012	0.80464	2579	34	1912	56	3132	31	2.47	0.405	61.05
PD18-104-431.d	16.52	0.69	0.473	0.019	0.57698	2905	47	2494	86	3207	37	3.82	0.262	77.77
PD18-104-432.d	11.86	0.62	0.348	0.017	0.39096	2588	68	1920	87	3135	36	1.66	0.602	61.24
PD18-104-434.d	8.52	1	0.2512	0.026	0.75559	2282	98	1443	130	3154	39	4.86	0.206	45.75
PD18-104-442.d	13.64	1.1	0.371	0.03	0.75851	2722	97	2029	150	3313	41	8.27	0.121	61.24
PD18-104-443.d	8.63	0.5	0.228	0.013	0.85305	2288	63	1320	68	3307	37	5.1	0.196	39.92
PD18-104-444.d	7.21	0.5	0.1949	0.013	0.6079	2134	86	1147	73	3268	36	5.7	0.175	35.10
PD18-104-445.d	5.48	0.3	0.1636	0.0087	0.82372	1903	45	976	48	3129	33	5.67	0.176	31.19
PD18-104-447.d	23.04	2.1	0.622	0.056	0.32294	3225	180	3115	270	3310	36	4.02	0.249	94.11
PD18-105-449.d	1.867	0.067	0.1356	0.0037	0.50275	1067	25	819	21	1622	56	1.411	0.709	50.49
PD18-105-450.d	2.59	0.086	0.1589	0.0045	0.46737	1296	24	950	25	1937	44	1.312	0.762	49.04
PD18-105-451.d	5.91	0.48	0.2677	0.017	0.72134	1961	61	1539	79	2416	40	2.46	0.407	63.70
PD18-105-452.d	4.82	0.16	0.2355	0.006	0.62524	1786	31	1363	32	2306	45	0.681	1.468	59.11
PD18-105-453.d	11.33	0.35	0.4685	0.013	0.38576	2549	32	2476	60	2624	33	1.405	0.712	94.36
PD18-105-454.d	6.46	0.29	0.2573	0.012	0.79774	2037	46	1475	61	2642	34	1.334	0.750	55.83
PD18-105-455.d	1.602	0.056	0.0992	0.0033	0.68053	969	23	610	19	1897	46	3.56	0.281	32.16
PD18-105-456.d	4.84	0.2	0.207	0.0074	0.27352	1790	33	1212	39	2535	40	1.951	0.513	47.81
PD18-105-457.d	1.841	0.053	0.1382	0.0035	0.66454	1059	20	834	20	1562	44	1.125	0.889	53.39
PD18-105-459.d	9.61	0.25	0.4135	0.0096	0.23141	2397	24	2230	44	2526	38	1.365	0.733	88.28
PD18-105-460.d	10.24	0.25	0.4388	0.0099	0.68608	2461	23	2344	44	2550	33	1.418	0.705	91.92
PD18-105-461.d	2.336	0.074	0.1407	0.0036	0.50716	1224	21	848	20	1954	48	1.07	0.935	43.40
PD18-105-469.d	8.7	0.39	0.3638	0.015	0.61177	2306	42	2000	71	2561	32	1.892	0.529	78.09
PD18-105-470.d	1.277	0.068	0.0771	0.0042	0.50546	834	32	479	25	1924	46	2.47	0.405	24.90
PD18-105-471.d	1.279	0.083	0.0807	0.0046	0.60436	835	33	500	27	1859	43	2.84	0.352	26.90
PD18-105-472.d	5.864	0.23	0.2715	0.0094	0.58445	1955	40	1548	49	2400	34	1.321	0.757	64.50

PD18-105-473.d	4.12	0.12	0.2053	0.0053	0.80953	1655	25	1203	29	2288	42	1.049	0.953	52.58
PD18-105-474.d	4.077	0.11	0.2046	0.0046	0.61537	1648	22	1199	24	2281	35	1.271	0.787	52.56
PD18-105-475.d	7.88	0.3	0.301	0.012	0.55091	2215	39	1695	60	2743	41	1.36	0.735	61.79
PD18-105-476.d	6.67	0.23	0.2962	0.0096	0.72111	2066	35	1671	49	2486	34	1.689	0.592	67.22
PD18-105-477.d	3.479	0.1	0.1847	0.0045	0.26135	1520	24	1092	25	2162	43	1.125	0.889	50.51
PD18-105-478.d	4.1	0.14	0.2131	0.0055	0.57901	1652	28	1245	30	2189	44	0.963	1.038	56.88
PD18-105-479.d	9.34	0.3	0.3493	0.0096	0.67212	2368	30	1929	46	2755	39	1.154	0.867	70.02
PD18-105-480.d	3.513	0.39	0.184	0.015	0.77662	1529	63	1089	78	2206	43	1.137	0.880	49.37
PD18-105-481.d	3.984	0.17	0.2047	0.0062	0.4536	1630	32	1200	33	2233	47	2.54	0.394	53.74
PD18-105-482.d	6.48	0.37	0.293	0.016	0.56638	2040	64	1655	87	2456	38	1.444	0.693	67.39
PD18-105-483.d	6.65	0.37	0.275	0.015	0.60232	2063	64	1565	79	2601	36	1.658	0.603	60.17
PD18-105-493.d	3.694	0.14	0.1808	0.0066	0.70295	1570	36	1071	37	2305	31	1.427	0.701	46.46
PD18-105-494.d	9.14	0.23	0.3923	0.0083	0.714	2351	23	2132	38	2551	33	1.018	0.982	83.58
PD18-105-495.d	3.91	0.19	0.1667	0.0072	0.7245	1613	34	993	39	2541	35	2.123	0.471	39.08
PD18-105-496.d	2.94	0.21	0.1426	0.0065	0.69826	1391	44	859	36	2323	46	1.262	0.792	36.98
PD18-105-497.d	12.24	0.3	0.5096	0.012	0.771	2622	23	2654	51	2583	29	0.995	1.005	102.75
PD18-105-498.d	5.36	0.14	0.2384	0.005	0.58023	1877	22	1378	26	2475	34	2.461	0.406	55.68
PD18-105-499.d	9.45	0.24	0.3843	0.008	0.24451	2381	23	2095	37	2621	39	1.242	0.805	79.93
PD18-105-500.d	1.85	0.053	0.1306	0.003	0.4534	1065	20	791	17	1680	42	2.52	0.397	47.08
PD18-105-501.d	7.15	0.21	0.318	0.0089	0.72618	2128	28	1781	43	2492	38	1.644	0.608	71.47
PD18-105-503.d	11.18	0.32	0.446	0.012	0.70268	2536	27	2376	55	2689	34	1.016	0.984	88.36
PD18-108-70.d	9.37	0.17	0.2104	0.0045	0.58914	2373	17	1231	24	3561	48	2.365	0.423	34.57
PD18-108-72.d	8.28	0.19	0.1976	0.005	0.59089	2260	20	1162	27	3478	47	2.45	0.408	33.41
PD18-108-73.d	18.75	0.85	0.45	0.023	0.62555	3028	56	2393	110	3485	51	3.11	0.322	68.67
PD18-108-75.d	16.68	0.43	0.47	0.013	0.63175	2920	25	2479	58	3216	51	4.24	0.236	77.08
PD18-108-76.d	20.2	0.39	0.551	0.014	0.47503	3098	19	2828	56	3266	50	2.29	0.437	86.59
PD18-108-77.d	21.74	0.7	0.636	0.023	0.50431	3171	36	3169	95	3169	53	10.68	0.094	100.00
PD18-108-78.d	11.04	0.29	0.2785	0.0068	0.62809	2524	26	1583	35	3390	47	1.776	0.563	46.70
PD18-108-79.d	17.93	0.45	0.505	0.015	0.45806	2984	26	2635	65	3220	49	1.544	0.648	81.83
PD18-108-80.d	22.56	0.74	0.644	0.023	0.73558	3205	28	3203	86	3207	51	1.87	0.535	99.88
PD18-108-81.d	10.41	0.36	0.345	0.0098	0.56539	2474	35	1910	47	2967	50	3.233	0.309	64.37
PD18-108-82.d	6.03	3.1	0.1262	0.058	0.75552	1978	160	766	240	3691	62	5.73	0.175	20.75
PD18-108-83.d	20.44	0.83	0.596	0.023	0.75057	3109	45	3009	94	3285	49	2.81	0.356	91.60
PD18-108-84.d	12.58	0.32	0.3052	0.0091	0.4559	2647	25	1716	43	3452	44	5.19	0.193	49.71
PD18-108-92.d	7.73	0.22	0.1689	0.0043	0.28665	2199	24	1006	24	3615	70	8.24	0.121	27.83
PD18-108-93.d	8.09	0.27	0.2402	0.0086	0.64855	2240	31	1387	44	3123	49	2.945	0.340	44.41
PD18-108-94.d	12.24	0.2	0.3643	0.0075	0.52745	2621	16	2002	35	3136	47	3.619	0.276	63.84
PD18-108-96.d	18.73	0.43	0.531	0.013	0.69112	3026	23	2743	57	3205	50	1.54	0.649	85.59
PD18-108-98.d	10.79	0.22	0.341	0.0083	0.56126	2503	18	1889	39	3033	46	1.6	0.625	62.28
PD18-108-99.d	20.01	0.55	0.553	0.019	0.74894	3089	29	2835	81	3256	49	2.055	0.487	87.07
PD18-108-100.d	9.31	0.3	0.3002	0.01	0.61023	2366	33	1691	53	3002	49	2.46	0.407	56.33

PD18-108-101.d	10.94	0.25	0.3474	0.0094	0.67613	2516	22	1921	46	3019	49	2.989	0.335	63.63
PD18-108-102.d	11.7	0.3	0.274	0.0074	0.65686	2579	26	1560	38	3511	50	2.09	0.478	44.43
PD18-108-103.d	14.81	0.3	0.3832	0.0089	0.68863	2801	19	2089	41	3337	50	4.17	0.240	62.60
PD18-108-104.d	15.46	0.88	0.412	0.02	0.66044	2842	73	2222	100	3298	53	13.19	0.076	67.37
PD18-108-105.d	15.39	0.34	0.4471	0.011	0.74816	2837	22	2381	49	3171	51	1.508	0.663	75.09
PD18-108-106.d	22.88	0.41	0.648	0.015	0.58871	3220	18	3220	60	3228	49	10.38	0.096	99.75
PD18-108-114.d	8	0.27	0.2088	0.0045	0.40775	2226	32	1222	24	3336	63	2.244	0.446	36.63
PD18-108-115.d	9.35	0.23	0.2319	0.0057	0.42481	2372	21	1344	29	3415	51	1.789	0.559	39.36
PD18-108-116.d	9.18	0.18	0.2645	0.007	0.63226	2355	18	1513	36	3185	47	1.965	0.509	47.50
PD18-108-117.d	13.98	0.59	0.3607	0.012	0.80416	2747	50	1985	59	3358	56	3.29	0.304	59.11
PD18-108-118.d	15.64	0.45	0.471	0.013	0.82664	2853	31	2488	58	3109	49	3.59	0.279	80.03
PD18-110-119.d	3.012	0.073	0.1485	0.0041	0.69339	1410	20	892	23	2318	51	2.209	0.453	38.48
PD18-110-121.d	13.87	0.73	0.437	0.023	0.88813	2739	60	2338	110	3051	44	1.517	0.659	76.63
PD18-110-122.d	7.35	0.18	0.2663	0.0063	0.40461	2154	21	1521	32	2831	57	4.69	0.213	53.73
PD18-110-123.d	10.81	0.46	0.3269	0.011	0.49925	2505	49	1823	55	3116	59	3.19	0.313	58.50
PD18-110-124.d	17.72	0.31	0.523	0.01	0.56715	2974	17	2711	44	3151	46	3.38	0.296	86.04
PD18-110-126.d	5.74	0.17	0.2039	0.0078	0.62195	1936	27	1196	43	2851	54	4.73	0.211	41.95
PD18-110-127.d	9.55	0.23	0.3112	0.0087	0.64598	2390	21	1746	42	2972	48	20.4	0.049	58.75
PD18-110-133.d	14.78	0.55	0.447	0.017	0.56281	2804	39	2381	79	3103	51	4.32	0.231	76.73
PD18-110-137.d	10.35	0.35	0.3404	0.01	0.7913	2463	35	1887	50	2981	54	3.14	0.318	63.30
PD18-110-138.d	21.83	0.49	0.626	0.016	0.58214	3173	22	3132	69	3197	46	3.9	0.256	97.97
PD18-110-139.d	6.69	0.31	0.254	0.0098	0.88154	2063	38	1457	51	2733	54	1.63	0.613	53.31
PD18-110-140.d	4.693	0.099	0.1851	0.0047	0.66905	1764	18	1094	25	2670	52	4.49	0.223	40.97
PD18-110-141.d	14.33	1.3	0.377	0.025	0.88285	2765	73	2060	110	3313	53	3.9	0.256	62.18
PD18-110-142.d	11.77	0.4	0.3532	0.012	0.71107	2585	36	1948	58	3117	50	2.738	0.365	62.50
PD18-110-143.d	11.51	0.5	0.3681	0.017	0.76173	2563	49	2019	84	3024	47	3.77	0.265	66.77
PD18-110-144.d	13.24	0.48	0.4049	0.016	0.61843	2699	34	2190	73	3091	50	3.76	0.266	70.85
PD18-110-145.d	7.95	0.22	0.2927	0.0084	0.67139	2228	25	1653	42	2808	55	2.471	0.405	58.87
PD18-110-146.d	7.37	0.41	0.261	0.012	0.68333	2153	63	1494	69	2861	63	3.95	0.253	52.22
PD18-110-147.d	9.69	0.41	0.331	0.014	0.78127	2413	34	1840	66	2920	50	4.22	0.237	63.01
PD18-110-148.d	6.52	0.14	0.2319	0.006	0.71069	2047	19	1343	32	2857	52	1.434	0.697	47.01
PD18-110-149.d	6.64	0.31	0.2534	0.011	0.71202	2060	47	1454	53	2726	59	7.5	0.133	53.34
PD18-110-150.d	7.83	0.25	0.2574	0.0087	0.74441	2213	29	1475	44	2961	54	2.9	0.345	49.81
PD18-110-158.d	2.475	0.089	0.0962	0.0029	0.13946	1262	24	592	17	2699	59	3.227	0.310	21.93
PD18-110-159.d	9.26	0.19	0.3102	0.0085	0.75844	2362	19	1740	42	2933	50	3.84	0.260	59.32
PD18-110-160.d	17.57	0.41	0.541	0.014	0.65292	2964	23	2787	61	3089	49	1.76	0.568	90.22
PD18-110-161.d	17.9	0.39	0.5249	0.012	0.68774	2982	21	2718	53	3160	47	2.4	0.417	86.01
PD18-110-162.d	22.92	0.52	0.644	0.015	0.47628	3221	24	3203	61	3215	50	2.147	0.466	99.63
PD18-110-163.d	3.5	0.18	0.1166	0.0061	0.59588	1525	43	711	35	3074	47	5.33	0.188	23.13
PD18-110-164.d	7.85	0.25	0.2605	0.0084	0.77434	2213	32	1492	44	2951	49	4.73	0.211	50.56
PD18-110-165.d	18.89	0.5	0.588	0.017	0.6793	3031	28	2978	70	3049	48	3.96	0.253	97.67

PD18-110-166.d	7.02	0.19	0.2106	0.0057	0.23715	2113	26	1232	30	3112	52	5.2	0.192	39.59
PD18-111-167.d	2.65	0.24	0.1223	0.0074	0.83482	1310	53	743	42	2401	65	1.465	0.683	30.95
PD18-111-168.d	18.61	0.41	0.537	0.014	0.57763	3019	22	2768	58	3197	49	1.892	0.529	86.58
PD18-111-169.d	15.53	0.36	0.4556	0.012	0.68615	2849	22	2418	54	3164	49	2.3	0.435	76.42
PD18-111-170.d	13.71	0.46	0.424	0.012	0.6989	2726	36	2275	57	3074	50	4.24	0.236	74.01
PD18-111-171.d	18.97	0.54	0.539	0.016	0.6882	3036	29	2773	70	3207	52	1.745	0.573	86.47
PD18-111-172.d	25.51	0.53	0.699	0.017	0.78182	3325	20	3414	65	3250	48	1.709	0.585	105.05
PD18-111-180.d	21.13	0.62	0.622	0.018	0.60514	3142	31	3115	74	3281	50	2.72	0.368	94.94
PD18-111-181.d	8.94	0.27	0.2954	0.0085	0.62401	2328	29	1667	43	2971	54	2.87	0.348	56.11
PD18-111-182.d	21.63	0.43	0.62	0.015	0.57036	3165	20	3106	56	3200	49	4.72	0.212	97.06
PD18-111-184.d	11.4	0.29	0.3546	0.0094	0.79468	2552	23	1955	44	3060	50	3.97	0.252	63.89
PD18-111-185.d	28.88	0.7	0.82	0.022	0.62459	3446	25	3855	78	3212	50	2.98	0.336	120.02
PD18-111-186.d	23.38	0.94	0.664	0.026	0.68161	3239	44	3280	100	3209	50	3.039	0.329	102.21
PD18-111-187.d	9.28	0.2	0.3083	0.0071	0.76611	2362	21	1731	35	2959	49	1.836	0.545	58.50
PD18-111-188.d	21.16	1.3	0.616	0.035	0.74947	3142	83	3090	160	3177	54	3.37	0.297	97.26
PD18-111-189.d	23.18	0.47	0.659	0.015	0.5197	3233	21	3260	56	3206	49	4.02	0.249	101.68
PD18-111-190.d	23.3	1.1	0.655	0.027	0.79058	3233	54	3242	110	3219	50	3.46	0.289	100.71
PD18-111-191.d	20.87	0.55	0.586	0.016	0.70732	3130	27	2970	66	3221	48	3.82	0.262	92.21
PD18-111-192.d	18.72	0.36	0.561	0.013	0.69135	3026	19	2870	55	3138	47	2.046	0.489	91.46
PD18-111-193.d	18.18	0.5	0.551	0.017	0.7565	2995	27	2827	71	3107	51	4.05	0.247	90.99
PD18-111-194.d	13.1	0.41	0.408	0.013	0.83908	2692	27	2206	57	3054	50	2.58	0.388	72.23
PD18-111-202.d	12.49	0.54	0.392	0.014	0.80868	2639	36	2129	64	3067	50	2.07	0.483	69.42
PD18-111-203.d	12.95	0.46	0.426	0.016	0.78759	2671	33	2282	73	3102	51	2.783	0.359	73.57
PD18-111-204.d	23.29	0.47	0.651	0.016	0.75894	3237	19	3228	61	3236	49	3.017	0.331	99.75
PD18-111-205.d	21.77	0.45	0.622	0.016	0.87215	3171	20	3114	63	3210	49	2.851	0.351	97.01
PD18-111-206.d	20.15	0.66	0.581	0.019	0.43501	3097	38	2952	80	3181	50	4.08	0.245	92.80
PD18-111-207.d	8.81	0.39	0.2937	0.01	0.73512	2314	52	1659	52	2947	61	1.322	0.756	56.29
PD18-111-208.d	18.48	0.35	0.5445	0.012	0.54427	3013	19	2800	51	3153	51	2.27	0.441	88.80
PD18-116 - 1.d	19.61	0.37	0.5685	0.0094	0.79352	3071	19	2900	39	3174	14	0.512	1.953	91.37
PD18-116 - 2.d	15.58	1.2	0.467	0.032	0.66382	2850	120	2470	160	3114	47	2.9	0.345	79.32
PD18-116 - 3.d	16.64	0.78	0.5136	0.021	0.62001	2914	59	2671	98	3082	24	0.61	1.639	86.66
PD18-116 - 4.d	18.61	0.75	0.5422	0.02	0.5807	3020	48	2799	87	3169	20	0.985	1.015	88.32
PD18-116 - 5.d	19.74	0.35	0.564	0.011	0.85151	3076	17	2881	44	3199	21	3.11	0.322	90.06
PD18-116 - 6.d	17.24	0.18	0.516	0.0054	0.40215	2947	10	2681	23	3123	17	2.87	0.348	85.85
PD18-116 - 7.d	16.79	0.36	0.5011	0.0089	0.60229	2924	21	2616	38	3127	26	3.04	0.329	83.66
PD18-116 - 8.d	6.28	0.11	0.2464	0.0046	0.8311	2013	16	1419	24	2687	19	2.3	0.435	52.81
PD18-116 - 9.d	20.9	0.32	0.605	0.008	0.67812	3132	15	3047	32	3182	18	2.38	0.420	95.76
PD18-116 - 10.d	15.42	0.32	0.4568	0.0083	0.83596	2838	20	2424	37	3134	19	3.036	0.329	77.35
PD18-116 - 11.d	10.86	0.2	0.3506	0.0055	0.71159	2510	18	1937	26	3006	16	6.52	0.153	64.44
PD18-116 - 12.d	18.57	0.24	0.5401	0.0068	0.37811	3019	13	2783	28	3171	20	2.602	0.384	87.76

PD18-116 - 13.d	13.04	0.44	0.3948	0.011	0.65354	2682	30	2145	49	3102	22	4.152	0.241	69.15
PD18-116 - 14.d	11.11	0.43	0.3584	0.011	0.7894	2532	31	1974	49	3002	22	3.05	0.328	65.76
PD18-116 - 15.d	23.14	0.44	0.655	0.011	0.60663	3230	19	3244	43	3209	26	0.659	1.517	101.09
PD18-116 - 16.d	15.73	0.65	0.4742	0.017	0.48945	2858	48	2501	77	3117	24	2.742	0.365	80.24
PD18-116 - 17.d	19.81	0.52	0.594	0.016	0.61717	3082	28	3005	72	3125	17	0.811	1.233	96.16
PD18-116 - 18.d	15.28	0.51	0.4593	0.014	0.7129	2831	37	2436	64	3120	19	3.01	0.332	78.08
PD18-116 - 19.d	14.07	0.19	0.442	0.0047	0.43436	2753	12	2359	21	3048	19	1.42	0.704	77.40
PD18-116 - 20.d	21.47	0.31	0.6165	0.0086	0.53819	3159	15	3095	35	3186	16	0.775	1.290	97.14
PD18-116 - 21.d	11.42	1	0.3676	0.017	0.88507	2557	66	2018	73	3005	52	0.746	1.340	67.15
PD18-116 - 22.d	18.57	0.61	0.535	0.019	0.5643	3018	38	2759	83	3199	16	0.689	1.451	86.25
PD18-116 - 23.d	21.21	0.39	0.609	0.009	0.822	3146	18	3065	36	3190	16	2.809	0.356	96.08
PD18-116 - 24.d	15.76	0.18	0.4796	0.0046	0.26143	2861	11	2525	20	3099	20	4.81	0.208	81.48
PD18-116 - 25.d	20.2	0.66	0.58	0.017	0.89453	3099	37	2947	70	3188	19	1.25	0.800	92.44
PD18-116 - 26.d	20.89	0.87	0.6031	0.023	0.70279	3132	51	3042	99	3182	16	1.423	0.703	95.60
PD18-116 - 27.d	9.13	0.36	0.2919	0.009	0.92746	2351	32	1651	44	3011	18	2.8	0.357	54.83
PD18-116 - 28.d	21.62	1.2	0.6193	0.034	0.5381	3166	80	3106	150	3198	20	1.263	0.792	97.12
PD18-116 - 29.d	21.12	0.58	0.61	0.013	0.4745	3137	27	3066	53	3170	45	0.865	1.156	96.72
PD18-116 - 30.d	9.35	0.67	0.2966	0.017	0.7902	2371	50	1673	80	3034	22	2.41	0.415	55.14
PD18-116 - 31.d	20.57	0.28	0.6014	0.007	0.59152	3117	13	3035	29	3164	15	1.478	0.677	95.92
PD18-116 - 32.d	10.23	0.42	0.3212	0.012	0.70744	2454	48	1795	61	3051	22	0.728	1.374	58.83
PD18-116 - 33.d	13.2	0.38	0.4462	0.013	0.42276	2693	28	2377	59	3162	22	0.9	1.111	75.17
PD18-116 - 34.d	22.88	0.27	0.6435	0.0063	0.45162	3221	12	3202	25	3221	18	1.7	0.588	99.41
PD18-116 - 35.d	19.12	0.25	0.5555	0.0068	0.53474	3047	13	2847	28	3174	17	0.532	1.880	89.70
PD18-116 - 36.d	8.25	0.29	0.2549	0.009	0.54606	2258	39	1463	48	3086	17	2.399	0.417	47.41
PD18-116 - 37.d	17.84	0.3	0.5382	0.0084	0.17903	2980	17	2775	36	3118	17	1.754	0.570	89.00
PD18-116 - 38.d	13.35	0.55	0.4	0.015	0.9079	2702	47	2167	72	3121	18	1.279	0.782	69.43
PD18-116 - 39.d	11.32	0.27	0.365	0.0073	0.73212	2549	25	2006	35	3003	14	1.299	0.770	66.80
PD18-116 - 40.d	6.348	0.086	0.2541	0.003	0.61018	2024	12	1459	15	2649	20	1.331	0.751	55.08
PD18-118 - 1.d	25.26	0.72	0.677	0.016	0.2893	3312	28	3337	67	3300	48	0.836	1.196	101.12
PD18-118 - 2.d	25.29	0.88	0.664	0.017	0.38855	3309	34	3278	67	3324	53	0.873	1.145	98.62
PD18-118 - 3.d	24.72	0.52	0.662	0.015	0.46365	3294	20	3270	60	3304	36	1.29	0.775	98.97
PD18-118 - 4.d	24.89	0.66	0.682	0.013	0.36273	3298	26	3347	51	3262	42	1.13	0.885	102.61
PD18-118 - 5.d	24.99	0.87	0.666	0.022	0.72579	3305	35	3297	89	3310	43	3.27	0.306	99.61
PD18-118 - 6.d	26.9	1	0.71	0.018	0.61614	3369	35	3452	68	3319	51	2.48	0.403	104.01
PD18-118 - 7.d	24.29	0.8	0.648	0.015	0.44881	3271	33	3214	58	3310	46	0.804	1.244	97.10
PD18-118 - 8.d	24.84	0.81	0.683	0.019	0.42715	3293	31	3348	71	3255	52	0.782	1.279	102.86
PD18-118 - 9.d	25.09	0.71	0.682	0.018	0.3125	3305	28	3347	71	3276	52	0.852	1.174	102.17
PD18-118 - 10.d	24.46	0.73	0.664	0.018	0.29911	3279	29	3276	68	3276	51	0.763	1.311	100.00
PD18-118 - 11.d	25.9	0.91	0.649	0.023	0.6572	3330	31	3217	90	3417	81	2.13	0.469	94.15
PD18-118 - 13.d	24.8	0.84	0.7	0.018	0.61966	3296	33	3436	69	3209	46	1.58	0.633	107.07
PD18-118 - 14.d	23.54	0.68	0.645	0.018	0.36986	3242	29	3201	70	3264	53	1.806	0.554	98.07

PD18-118 - 15.d	24.84	0.75	0.688	0.023	0.18994	3293	29	3366	89	3235	61	1.124	0.890	104.05
PD18-118 - 16.d	24.43	0.76	0.667	0.016	0.24201	3282	32	3289	61	3272	55	1.123	0.890	100.52
PD18-118 - 17.d	24.13	0.86	0.651	0.018	0.44352	3263	35	3224	68	3276	59	1.69	0.592	98.41
PD18-118 - 18.d	24.16	0.84	0.647	0.017	0.4793	3270	34	3211	66	3303	51	1.178	0.849	97.21
PD18-118 - 19.d	24.9	1.1	0.677	0.024	0.2422	3295	43	3323	90	3276	77	1.241	0.806	101.43
PD18-118 - 20.d	24.49	0.7	0.655	0.014	0.41984	3281	29	3254	56	3294	48	0.745	1.342	98.79
PD18-118 - 21.d	25.12	0.79	0.686	0.019	0.34114	3308	33	3358	73	3276	61	0.991	1.009	102.50
PD18-118 - 22.d	22.27	0.93	0.605	0.028	0.3593	3185	44	3045	120	3274	59	1.07	0.935	93.01
PD18-118 - 23.d	23.4	0.83	0.655	0.018	0.30688	3234	35	3239	71	3229	61	1.403	0.713	100.31
PD18-118 - 24.d	23.43	0.77	0.634	0.017	0.29023	3236	33	3160	68	3273	60	2.58	0.388	96.55
PD18-118 - 25.d	27.78	0.88	0.73	0.022	0.35065	3403	32	3526	82	3329	56	0.879	1.138	105.92
PD18-118 - 26.d	23.18	0.8	0.624	0.017	0.17883	3224	34	3119	69	3287	64	0.893	1.120	94.89
PD18-118 - 27.d	23.97	0.91	0.656	0.019	0.42813	3253	38	3245	75	3256	63	1.093	0.915	99.66
PD18-118 - 28.d	15.78	0.23	0.5034	0.0066	0.32968	2862	14	2627	27	3236	27	0.85	1.176	81.18
PD18-118 - 29.d	13.1	0.32	0.4508	0.0079	0.57694	2684	22	2398	35	3233	24	2.84	0.352	74.17
PD18-118 - 30.d	24.63	0.89	0.673	0.022	0.55633	3281	37	3305	84	3266	61	2.2	0.455	101.19
PD18-118 - 31.d	27.1	1	0.705	0.017	0.4055	3384	36	3434	64	3328	56	1.073	0.932	103.19
PD18-118 - 32.d	23.06	0.65	0.642	0.014	0.25257	3223	28	3193	54	3237	48	3.09	0.324	98.64
PD18-118 - 33.d	24.88	0.65	0.677	0.015	0.33229	3298	25	3328	59	3276	45	0.9	1.111	101.59
PD18-118 - 34.d	25.53	1	0.689	0.024	0.25239	3315	40	3368	92	3282	73	1.049	0.953	102.62
PD18-118 - 35.d	25.11	1	0.678	0.024	0.35004	3306	37	3323	91	3287	66	0.9	1.111	101.10
PD18-118 - 36.d	22.4	0.38	0.6615	0.0095	0.58821	3199	17	3271	37	3158	27	18	0.056	103.58
PD18-118 - 37.d	24.9	0.82	0.684	0.015	0.4348	3300	32	3353	57	3279	46	0.954	1.048	102.26
PD18-118 - 38.d	25.76	0.97	0.695	0.021	0.31213	3330	37	3391	79	3283	72	0.924	1.082	103.29
PD18-120 - 1.d	4.087	0.25	0.21	0.0064	0.90437	1650	43	1228	34	2466	38	8.44	0.118	49.80
PD18-120 - 2.d	14.56	0.24	0.4632	0.0068	0.70572	2787	15	2453	29	3028	11	5.24	0.191	81.01
PD18-120 - 3.d	23.01	0.15	0.6701	0.0046	0.67028	3227	6.2	3306	18	3172	8.3	3.17	0.315	104.22
PD18-120 - 4.d	8.15	0.41	0.2982	0.0085	0.87786	2247	38	1682	41	2797	39	4.444	0.225	60.14
PD18-120 - 5.d	22.76	0.25	0.6701	0.0069	0.60496	3216	11	3306	27	3160	13	1.476	0.678	104.62
PD18-120 - 6.d	5.34	0.2	0.224	0.0055	0.85151	1875	32	1303	29	2587	28	6.71	0.149	50.37
PD18-120 - 7.d	21.99	0.33	0.654	0.0099	0.85371	3182	14	3242	38	3134	9.3	23.3	0.043	103.45
PD18-120 - 8.d	11.96	0.56	0.409	0.016	0.6958	2600	65	2208	80	3083	30	16.9	0.059	71.62
PD18-120 - 10.d	14.28	0.33	0.4634	0.0096	0.80423	2768	20	2454	42	3012	9.8	6.07	0.165	81.47
PD18-120 - 11.d	25.34	0.43	0.745	0.013	0.94065	3320	18	3587	50	3162	7.7	7.45	0.134	113.44
PD18-120 - 12.d	21.68	0.48	0.634	0.012	0.85298	3169	23	3165	45	3164.6	8.2	9.04	0.111	100.01
PD18-120 - 14.d	19.39	0.36	0.577	0.01	0.82157	3061	17	2936	42	3149	11	3.03	0.330	93.24
PD18-120 - 15.d	22.24	0.21	0.6585	0.0075	0.72324	3194	9.2	3261	29	3149	10	15.4	0.065	103.56
PD18-120 - 16.d	21.45	0.52	0.6277	0.014	0.86073	3158	27	3140	59	3163	10	2.29	0.437	99.27
PD18-120 - 17.d	19.86	0.26	0.6063	0.0084	0.91712	3084	12	3054	34	3099	12	3.029	0.330	98.55
PD18-120 - 18.d	7.515	0.13	0.2826	0.0047	0.64658	2174	15	1604	23	2756	12	5.87	0.170	58.20
PD18-120 - 19.d	16.18	0.45	0.499	0.013	0.98139	2884	28	2641	59	3088	7	11.16	0.090	85.52

PD18-120 - 20.d	22.75	0.2	0.6718	0.0064	0.68741	3216	8.5	3312	25	3155	13	3.12	0.321	104.98
PD18-120 - 21.d	15.28	0.22	0.4716	0.0073	0.57499	2832.4	13	2490	31	3075	12	5.72	0.175	80.98
PD18-120 - 22.d	10.45	0.28	0.3426	0.0094	0.86206	2475	25	1899	44	2984	11	2.548	0.392	63.64
PD18-120 - 23.d	20.96	0.25	0.6222	0.0061	0.83809	3135	12	3118	24	3144	11	4.1	0.244	99.17
PD18-120 - 24.d	18.3	0.26	0.5638	0.0079	0.78022	3005	14	2882	33	3084	10	5.35	0.187	93.45
PD18-120 - 25.d	10.36	0.39	0.3775	0.011	0.74861	2466	36	2064	52	2822	19	6.264	0.160	73.14
PD18-120 - 26.d	24.78	0.25	0.7251	0.0077	0.87715	3299	9.9	3514	29	3170	7.9	6.25	0.160	110.85
PD18-120 - 27.d	20.1	0.42	0.5931	0.012	0.74318	3095.9	22	3002	48	3149	7.9	3.669	0.273	95.33
PD18-120 - 28.d	18.95	0.25	0.6141	0.0075	0.47158	3038	13	3085	30	3004	19	10.91	0.092	102.70
PD18-120 - 29.d	22.03	0.2	0.6471	0.0056	0.50487	3184	8.6	3217	22	3169	14	13.53	0.074	101.51
PD18-120 - 30.d	18.63	0.72	0.5714	0.019	0.70635	3022	45	2913	83	3101	18	3.134	0.319	93.94
PD18-120 - 31.d	8.119	0.084	0.3069	0.0029	0.69604	2244	9.4	1725	14	2756	11	9.3	0.108	62.59
PD18-120 - 32.d	15.23	0.53	0.4914	0.015	0.92686	2827	34	2576	64	3011	16	12.5	0.080	85.55
PD18-120 - 33.d	5.303	0.22	0.232	0.006	0.92286	1868	31	1345	31	2512	26	10.1	0.099	53.54
PD18-120 - 34.d	16.17	0.24	0.5209	0.0074	0.75738	2886	14	2702	32	3015	14	10.5	0.095	89.62
PD18-120 - 35.d	16.96	0.61	0.576	0.02	0.97162	2929	33	2929	79	2924	9.2	7.62	0.131	100.17
PD18-120 - 36.d	21.95	0.16	0.651	0.0048	0.55544	3181.2	7.2	3232	19	3148	10	4.78	0.209	102.67
PD18-126 - 1.d	10.09	0.18	0.3131	0.0059	-0.06419	2441	16	1755	29	3075	45	2.182	0.458	57.07
PD18-126 - 2.d	7.4	0.16	0.2678	0.0051	0.85489	2158	19	1529	26	2824	18	3.473	0.288	54.14
PD18-126 - 3.d	15.59	0.36	0.399	0.011	-0.2533	2848	22	2162	50	3378	62	37	0.027	64.00
PD18-126 - 4.d	15.38	0.4	0.3956	0.0085	-0.08856	2834	24	2146	40	3375	57	0.562	1.779	63.59
PD18-126 - 5.d	18.91	0.31	0.6208	0.008	0.84247	3038	15	3112	32	2983	14	1.431	0.699	104.32
PD18-126 - 6.d	4.13	0.16	0.2067	0.0062	0.94167	1652	32	1210	33	2274	26	2.249	0.445	53.21
PD18-126 - 7.d	12.7	0.32	0.4308	0.0085	0.50325	2656	27	2309	39	2938	20	1.873	0.534	78.59
PD18-126 - 8.d	10.29	0.21	0.3324	0.0049	0.79172	2459	20	1849	24	3011	27	1.717	0.582	61.41
PD18-126 - 9.d	15.93	0.2	0.5091	0.0051	0.75731	2872	12	2652	22	3027	15	1.463	0.684	87.61
PD18-126 - 10.d	13.21	0.24	0.3856	0.01	0.69398	2693	18	2101	49	3171	30	2.247	0.445	66.26
PD18-126 - 11.d	18.08	1.1	0.5746	0.029	0.47154	2993	84	2926	130	3046	38	1.61	0.621	96.06
PD18-126 - 12.d	8.88	0.16	0.3402	0.0049	0.72457	2324	16	1887	24	2731	16	0.2392	4.181	69.10
PD18-126 - 13.d	14.13	0.35	0.4777	0.0097	0.8882	2757	22	2516	41	2933	16	0.898	1.114	85.78
PD18-126 - 14.d	14.62	0.36	0.4893	0.008	0.92858	2789	24	2567	35	2949	22	2.627	0.381	87.05
PD18-126 - 15.d	10.04	0.29	0.3681	0.0082	0.58133	2438.3	31	2020	40	2811	24	1.738	0.575	71.86
PD18-126 - 16.d	8.65	0.31	0.2615	0.0092	0.76247	2300	34	1497	45	3124	49	0.3074	3.253	47.92
PD18-126 - 17.d	7.08	0.18	0.2872	0.0054	0.88562	2118	24	1627	27	2635	20	1.486	0.673	61.75
PD18-126 - 19.d	19.8	0.89	0.618	0.024	0.9144	3077	53	3100	100	3066	23	0.873	1.145	101.11
PD18-126 - 20.d	12.09	0.66	0.441	0.02	0.7555	2610	70	2352	93	2812	42	0.594	1.684	83.64
PD18-126 - 21.d	13.86	0.29	0.4604	0.0066	0.68413	2739	21	2441	29	2970	20	4.53	0.221	82.19
PD18-126 - 22.d	9.7	0.23	0.3596	0.0072	0.25592	2406	23	1980	35	2784	24	1.056	0.947	71.12
PD18-126 - 23.d	9.18	0.31	0.3006	0.0052	0.50706	2365	34	1693	26	3013	43	2.32	0.431	56.19
PD18-126 - 24.d	9.61	0.19	0.357	0.0067	0.56592	2397	19	1973	32	2775	18	1.507	0.664	71.10
PD18-126 - 25.d	4.06	0.1	0.2596	0.004	0.40497	1644	20	1487	20	1857	34	1.807	0.553	80.08

PD18-126 - 27.d	11.01	0.23	0.3695	0.0071	0.77147	2521	20	2026	34	2950	19	1.276	0.784	68.68
PD18-126 - 28.d	15.02	0.2	0.4839	0.0072	0.643	2815	14	2543	32	3018	21	1.426	0.701	84.26
PD18-126 - 31.d	7	0.16	0.2815	0.0051	0.74388	2110	23	1598	26	2659	20	1.935	0.517	60.10
PD18-126 - 32.d	11.15	0.2	0.4003	0.006	0.69708	2535	17	2170	28	2839	14	1.142	0.876	76.44
PD18-126 - 33.d	18.71	1	0.593	0.029	0.41404	3026	77	3002	130	3050	35	1.063	0.941	98.43
PD18-126 - 34.d	10.32	0.15	0.3548	0.0043	0.76388	2463	13	1957	21	2908	13	4.094	0.244	67.30
PD18-126 - 35.d	18.66	0.99	0.5767	0.023	0.87826	3024	74	2935	100	3083	45	4.61	0.217	95.20
PD18-126 - 36.d	13.81	0.87	0.4569	0.023	0.81359	2735	92	2425	110	2981	56	2.03	0.493	81.35
PD18-126 - 37.d	16.34	0.52	0.5288	0.015	0.59112	2896	36	2736	65	3017	17	1.269	0.788	90.69
PD18-126 - 38.d	10.63	0.22	0.3412	0.0075	0.40406	2491	21	1892	37	3032	20	1.075	0.930	62.40
PD18-01-8.d	1.93	0.12	0.0627	0.0048	0.86489	1090	38	392	28	3042	25	1.567	0.638	12.89
PD18-01-10.d	7.58	0.22	0.3284	0.01	0.67528	2179	28	1830	48	2514	25	1.104	0.906	72.79
PD18-01-11.d	6.22	0.21	0.1469	0.0095	0.5477	2006	27	882	53	3525	63	2.192	0.456	25.02
PD18-01-12.d	4.008	0.11	0.1486	0.0051	0.62283	1634	22	893	28	2780	31	2.271	0.440	32.12
PD18-01-13.d	6.8	0.27	0.2996	0.013	0.6779	2082	33	1688	62	2535	23	2.29	0.437	66.59
PD18-01-14.d	9.69	0.56	0.395	0.024	0.77463	2408	67	2143	120	2623	27	2.88	0.347	81.70
PD18-01-15.d	5.88	0.22	0.2546	0.0087	0.64779	1955	38	1461	46	2522	31	1.899	0.527	57.93
PD18-01-16.d	11.9	0.31	0.4696	0.013	0.70919	2595	24	2480	58	2685	21	1.466	0.682	92.36
PD18-01-17.d	4.674	0.13	0.1518	0.0047	0.59609	1761	24	910	27	2997	25	3.38	0.296	30.36
PD18-01-18.d	3.9	0.1	0.0727	0.002	0.70371	1613	21	452.1	12	3862	18	2.312	0.433	11.71
PD18-01-19.d	5.584	0.15	0.1426	0.0059	0.28474	1915	23	858	32	3387	62	2.96	0.338	25.33
PD18-01-20.d	6.1	0.18	0.1658	0.005	0.71284	1993	27	993	28	3281	23	3.13	0.319	30.27
PD18-01-21.d	13.43	0.4	0.466	0.015	0.81083	2709	29	2463	67	2886	19	0.179	5.587	85.34
PD18-01-22.d	11.25	0.31	0.4696	0.012	0.60829	2542	25	2480	54	2589	24	1.336	0.749	95.79
PD18-01-23.d	3.447	0.1	0.0642	0.0061	0.55475	1514	23	401	36	3862	76	1.51	0.662	10.38
PD18-01-24.d	2.398	0.18	0.0779	0.0042	0.45565	1244	42	484	25	3005	69	2.29	0.437	16.11
PD18-01-25.d	9.11	0.3	0.3884	0.012	0.56153	2353	33	2115	59	2578	28	1.99	0.503	82.04
PD18-01-26.d	12.43	0.32	0.4933	0.013	0.50706	2636	24	2583	58	2675	24	2.27	0.441	96.56
PD18-01-34.d	4.96	0.32	0.1509	0.0054	0.68473	1811	43	906	30	3100	49	2.71	0.369	29.23
PD18-01-35.d	3.145	0.082	0.1009	0.0029	0.60503	1442	20	620	17	3057	26	4.493	0.223	20.28
PD18-01-36.d	1.488	0.46	0.0906	0.012	0.86577	923	110	559	68	1929	110	0.81	1.235	28.98
PD18-01-37.d	4.555	0.24	0.0996	0.0048	0.57027	1740	38	612	28	3608	28	2.99	0.334	16.96
PD18-01-38.d	4.3	0.66	0.2167	0.023	0.80461	1698	83	1264	110	2323	45	1.36	0.735	54.41
PD18-01-39.d	9.47	0.31	0.3601	0.01	0.65721	2382	28	1981	47	2746	30	1.317	0.759	72.14
PD18-01-40.d	12.18	0.48	0.461	0.017	0.61398	2615	38	2442	80	2748	37	1.217	0.822	88.86
PD18-01-41.d	7.15	0.28	0.3294	0.013	0.81199	2127	36	1834	61	2417	23	2.445	0.409	75.88
PD18-01-42.d	6.29	0.26	0.2037	0.015	0.63483	2015	41	1195	85	2997	130	3.43	0.292	39.87
PD18-01-43.d	4.45	0.32	0.1736	0.012	0.65966	1719	48	1031	63	2698	24	3.216	0.311	38.21
PD18-01-44.d	6.29	0.28	0.2895	0.011	0.67457	2015	34	1638	51	2430	24	1.867	0.536	67.41
PD18-01-45.d	10.14	0.27	0.4344	0.012	0.55249	2446	24	2325	53	2551	22	1.982	0.505	91.14
PD18-01-46.d	9.91	0.29	0.3998	0.013	0.61324	2425	27	2167	61	2649	24	1.77	0.565	81.80

PD18-01-47.d	12.16	0.38	0.5	0.016	0.87606	2619	29	2612	73	2628	19	2.33	0.429	99.39
PD18-27-101.d	3.118	0.12	0.1728	0.0058	0.72604	1436	29	1027	31	2100	22	9.26	0.108	48.90
PD18-27-102.d	3.2	0.19	0.176	0.0081	0.78182	1463	49	1045	45	2132	40	4.64	0.216	49.02
PD18-27-103.d	2.72	0.17	0.1348	0.0086	0.60415	1329	54	815	50	2295	33	0.404	2.475	35.51
PD18-27-104.d	1.329	0.041	0.091	0.0026	0.42944	857.9	19	561.3	15	1719	25	2.78	0.360	32.65
PD18-27-105.d	1.777	0.076	0.1132	0.004	0.66193	1036	31	691	24	1894	33	13.2	0.076	36.48
PD18-27-106.d	9.49	0.22	0.3899	0.0094	0.74476	2386	22	2122	44	2613	11	20.2	0.050	81.21
PD18-27-107.d	2.038	0.06	0.1265	0.0035	0.68985	1127	21	767.6	20	1901	22	5.77	0.173	40.38
PD18-27-108.d	1.874	0.089	0.1096	0.0049	0.72323	1071	38	670	29	2011	28	1.454	0.688	33.32
PD18-27-109.d	3.882	0.12	0.1448	0.0043	0.60712	1609	28	872	25	2766	26	3.404	0.294	31.53
PD18-27-110.d	3.208	0.13	0.1759	0.0056	0.66079	1458	35	1044	31	2115	32	8.72	0.115	49.36
PD18-27-111.d	3.86	0.21	0.1418	0.0061	0.94273	1605	43	855	35	2801	26	4.84	0.207	30.52
PD18-27-112.d	2.79	0.12	0.1655	0.0053	0.59016	1346	31	987	29	1966	49	11.75	0.085	50.20
PD18-27-113.d	13.69	0.36	0.5268	0.014	0.89314	2726	25	2733	57	2717	13	4.36	0.229	100.59
PD18-27-114.d	1.924	0.1	0.127	0.0056	0.5182	1089	42	771	33	1787	40	11.5	0.087	43.14
PD18-27-115.d	1.06	0.11	0.0622	0.0047	0.74333	733	44	389	28	1997	40	32.1	0.031	19.48
PD18-27-124.d	2.921	0.11	0.1622	0.0049	0.77637	1386	29	969	27	2094	31	4.63	0.216	46.28
PD18-27-125.d	8.77	0.3	0.3186	0.0099	0.73961	2313	34	1782	49	2822	20	6.62	0.151	63.15
PD18-27-126.d	1.501	0.097	0.0837	0.0047	0.94488	930	50	518	28	2080	57	6.69	0.149	24.90
PD18-27-127.d	0.717	0.024	0.0517	0.0015	0.81194	548	14	325.1	9.9	1665	25	4.43	0.226	19.53
PD18-27-128.d	3.24	0.15	0.1759	0.0077	0.61034	1465	44	1044	41	2136	41	8.91	0.112	48.88
PD18-27-129.d	1.58	0.12	0.0967	0.0056	0.88688	962	45	595	32	1921	40	3.2	0.313	30.97
PD18-27-130.d	1.598	0.089	0.0989	0.0053	0.82205	968	31	608	31	1908	29	14.1	0.071	31.87
PD18-27-131.d	2.678	0.1	0.1546	0.0045	0.68826	1321	31	926	25	2033	48	25.1	0.040	45.55
PD18-27-132.d	2.45	0.11	0.1442	0.0064	0.43718	1249	36	867	34	1992	62	7.92	0.126	43.52
PD18-27-133.d	1.6	0.059	0.0988	0.0026	0.54284	969	24	607	15	1912	48	26.87	0.037	31.75
PD18-27-134.d	10.99	0.34	0.4313	0.013	0.72904	2521	32	2311	60	2691	16	2.53	0.395	85.88
PD18-27-135.d	8.98	1	0.3702	0.035	0.83289	2334	78	2030	160	2602	21	3.67	0.272	78.02
PD18-27-136.d	1.43	0.054	0.0787	0.0023	0.7447	901	24	488.5	14	2125	36	1.399	0.715	22.99
PD18-27-137.d	4.055	0.1	0.1822	0.0049	0.76088	1644	21	1079	26	2471	17	56.3	0.018	43.67
PD18-27-138.d	2.194	0.14	0.136	0.0059	0.60458	1178	40	822	33	1912	44	10.1	0.099	42.99
PD18-34-147.d	13.01	0.43	0.4122	0.012	0.77311	2678	34	2224	56	3044	23	5.73	0.175	73.06
PD18-34-148.d	25.22	0.85	0.651	0.019	0.75327	3315	38	3231	86	3358	32	1.116	0.896	96.22
PD18-34-149.d	10.46	0.58	0.3114	0.016	0.82483	2474	67	1746	83	3131	22	3.19	0.313	55.76
PD18-34-150.d	2.506	0.1	0.132	0.0054	0.74202	1272	32	799	29	2205	21	3.73	0.268	36.24
PD18-34-151.d	0.775	0.076	0.0513	0.003	0.87782	582	36	322.7	18	1776	51	10.24	0.098	18.17
PD18-34-152.d	5.67	0.53	0.2141	0.013	0.7672	1926	59	1251	65	2763	38	2.74	0.365	45.28
PD18-34-153.d	2.066	0.078	0.1161	0.0038	0.74063	1137	23	708	22	2073	25	2.368	0.422	34.15
PD18-34-154.d	2.661	0.065	0.1508	0.0036	0.56426	1317	18	905.6	20	2068	22	17.49	0.057	43.79
PD18-34-155.d	0.863	0.054	0.0615	0.0031	0.89859	630	27	385	19	1687	34	4.11	0.243	22.82

PD18-34-156.d	0.538	0.022	0.04787	0.0013	0.81669	436.5	14	301.4	7.9	1230	36	1.031	0.970	24.50
PD18-34-157.d	4.12	0.22	0.171	0.0069	0.75752	1660	36	1017	37	2607	27	2.48	0.403	39.01
PD18-34-158.d	13.56	0.32	0.3764	0.009	0.70743	2719.2	22	2059	42	3248	11	0.6143	1.628	63.39
PD18-34-159.d	1.903	0.22	0.1166	0.0083	0.67926	1088	66	711	48	1965	55	1.325	0.755	36.18
PD18-34-160.d	2.279	0.063	0.1104	0.0032	0.47938	1205	19	675	19	2340	35	2.636	0.379	28.85
PD18-34-161.d	10.57	0.3	0.3628	0.011	0.62498	2483	26	1994	50	2909	25	1.827	0.547	68.55
PD18-34-169.d	1.739	0.66	0.0807	0.019	0.97126	1019	120	500	100	2444	62	2.47	0.405	20.46
PD18-34-170.d	19.56	0.6	0.611	0.019	0.65114	3069	32	3072	77	3062	15	1.21	0.826	100.33
PD18-34-171.d	6.83	0.27	0.2827	0.012	0.92612	2088	31	1604	58	2600	13	1.268	0.789	61.69
PD18-34-172.d	2.001	0.056	0.104	0.0028	0.66593	1115	20	637.8	16	2253	20	1.967	0.508	28.31
PD18-34-173.d	7.78	0.25	0.2827	0.0085	0.78816	2203	30	1604	43	2818	20	2.38	0.420	56.92
PD18-34-174.d	2.11	0.11	0.0952	0.0042	0.89222	1150	32	586	25	2462	21	3.17	0.315	23.80
PD18-34-175.d	0.994	0.13	0.058	0.0046	0.77297	700	53	363.5	28	2052	57	7.79	0.128	17.71
PD18-34-176.d	6.8	0.18	0.2703	0.0068	0.75134	2084	24	1542	35	2667	20	1.306	0.766	57.82
PD18-34-177.d	9.43	0.63	0.325	0.017	0.78368	2379	94	1814	91	2900	64	3.02	0.331	62.55
PD18-34-178.d	0.354	0.018	0.034	0.0015	0.70645	307.5	13	215.5	9	1109	48	5.29	0.189	19.43
PD18-34-179.d	4.49	0.19	0.1939	0.0071	0.89493	1725	39	1142	38	2520	25	2.15	0.465	45.32
PD18-34-180.d	7.34	0.31	0.2729	0.0089	0.69424	2153	40	1555	46	2780	29	11.4	0.088	55.94
PD18-34-181.d	10.35	0.29	0.3156	0.0084	0.72351	2465	25	1768	41	3101	19	2.381	0.420	57.01
PD18-34-182.d	17.17	0.74	0.56	0.024	0.74286	2942	48	2863	110	2995	24	0.7	1.429	95.59
PD18-34-183.d	18.45	0.48	0.599	0.016	0.46831	3015	24	3023	65	2996	23	0.955	1.047	100.90
PD18-34-191.d	12.75	27	0.376	0.31	0.8809	2655	240	2055	490	3156	120	3.65	0.274	65.11
PD18-34-192.d	16.9	0.44	0.576	0.016	0.70137	2928	25	2931	67	2925	21	1.227	0.815	100.21
PD18-34-193.d	13.67	0.49	0.416	0.013	0.84261	2724	33	2241	63	3104	20	1.079	0.927	72.20
PD18-37-194.d	6.83	0.53	0.303	0.02	0.56651	2087	110	1705	110	2478	67	1.46	0.685	68.81
PD18-37-195.d	8.78	0.36	0.3856	0.015	0.53889	2313	40	2101	71	2523	22	0.811	1.233	83.27
PD18-37-196.d	10.44	0.38	0.4544	0.015	0.81629	2473	38	2414	70	2524	19	0.738	1.355	95.64
PD18-37-197.d	10.01	0.39	0.429	0.017	0.68626	2432	41	2299	80	2546	26	1.92	0.521	90.30
PD18-37-198.d	5.29	0.18	0.2454	0.0074	0.74404	1864	30	1414	39	2405	28	0.753	1.328	58.79
PD18-37-199.d	10.75	0.3	0.4616	0.012	0.84524	2499	26	2445	54	2536	24	1.362	0.734	96.41
PD18-37-200.d	10.05	0.36	0.4378	0.015	0.44142	2438	37	2340	68	2525	22	0.723	1.383	92.67
PD18-37-201.d	9.59	0.47	0.422	0.02	0.76475	2393	62	2269	98	2489	25	1.556	0.643	91.16
PD18-37-202.d	6.379	0.16	0.2713	0.0068	0.86855	2029	22	1547	35	2593	24	2.62	0.382	59.66
PD18-37-203.d	10.92	0.56	0.458	0.022	0.62366	2514	61	2430	100	2573	24	0.765	1.307	94.44
PD18-37-204.d	7.54	0.3	0.3342	0.012	0.51835	2175	41	1858	61	2477	27	1.294	0.773	75.01
PD18-37-205.d	14.11	0.44	0.5367	0.015	0.49118	2756	27	2769	61	2747	20	0.679	1.473	100.80
PD18-37-213.d	1.536	0.057	0.0951	0.003	0.74055	943	24	585	18	1896	34	0.5393	1.854	30.85
PD18-37-214.d	8.81	0.31	0.3769	0.013	0.59042	2316	36	2061	61	2539	28	3.18	0.314	81.17
PD18-37-215.d	10.87	0.29	0.4618	0.013	0.60452	2511	25	2446	56	2564	25	0.655	1.527	95.40
PD18-37-216.d	9.51	0.43	0.4133	0.018	0.61303	2386	49	2229	87	2515	22	6.2	0.161	88.63
PD18-37-217.d	10.07	0.3	0.4455	0.014	0.45968	2439	30	2374	65	2527	27	0.7077	1.413	93.95

PD18-37-218.d	9.78	0.57	0.3724	0.018	0.81799	2413	52	2039	82	2726	32	0.954	1.048	74.80
PD18-37-219.d	10.75	0.3	0.4607	0.013	0.55711	2505	27	2452	58	2533	27	1.082	0.924	96.80
PD18-37-220.d	12.92	0.46	0.3781	0.014	0.80142	2671	37	2066	65	3164	19	1.196	0.836	65.30
PD18-37-221.d	5.54	0.36	0.2725	0.014	0.66728	1904	46	1553	69	2304	29	2.06	0.485	67.40
PD18-37-222.d	3.803	0.44	0.1737	0.019	0.4568	1592	69	1032	96	2430	29	1.856	0.539	42.47
PD18-37-223.d	1.55	0.42	0.099	0.016	0.37697	940	100	608	87	1806	92	8.34	0.120	33.67
PD18-37-224.d	7.43	0.27	0.3207	0.013	0.74617	2162	30	1792	61	2526	21	0.794	1.259	70.94
PD18-37-225.d	5.61	0.24	0.2671	0.0094	0.82105	1916	33	1525	47	2363	21	0.587	1.704	64.54
PD18-37-226.d	8.83	0.33	0.3995	0.015	0.43125	2318	39	2165	71	2488	32	0.87	1.149	87.02
PD18-37-227.d	10.31	0.3	0.434	0.013	0.81622	2461	27	2322	60	2612	17	0.589	1.698	88.90
PD18-37-235.d	3.173	0.23	0.1746	0.01	0.50139	1450	58	1037	55	2153	41	1.314	0.761	48.17
PD18-37-236.d	11.48	0.38	0.486	0.015	0.79501	2558	32	2551	65	2584	23	0.909	1.100	98.72
PD18-37-237.d	9.52	0.47	0.4232	0.021	0.8817	2387	57	2274	99	2488	24	0.688	1.453	91.40
PD18-54-240.d	4.1	0.33	0.1929	0.014	0.78252	1652	62	1136	77	2379	24	13.4	0.075	47.75
PD18-54-241.d	1.785	0.1	0.1099	0.0038	0.62321	1039	32	672	22	1915	46	18.9	0.053	35.09
PD18-54-242.d	11.17	0.34	0.464	0.014	0.35611	2536	32	2456	63	2596	16	69.8	0.014	94.61
PD18-54-243.d	2.214	0.065	0.1225	0.0037	0.71675	1184	20	745	21	2108	33	12.9	0.078	35.34
PD18-54-244.d	3.83	0.21	0.1848	0.0082	0.73643	1598	46	1093	45	2357	45	18.6	0.054	46.37
PD18-54-245.d	3.34	0.14	0.1665	0.0055	0.73611	1487	36	992	31	2278	36	59	0.017	43.55
PD18-54-246.d	1.179	0.041	0.0644	0.0025	0.67564	790	18	402	15	2116	24	136	0.007	19.00
PD18-54-247.d	3.312	0.18	0.172	0.0077	0.49021	1482	37	1023	41	2210	32	3.01	0.332	46.29
PD18-54-248.d	4.101	0.2	0.1976	0.0085	0.76705	1653	49	1162	47	2359	30	9.21	0.109	49.26
PD18-54-249.d	2.091	0.099	0.1147	0.0041	0.53999	1144	38	699	24	2128	47	30	0.033	32.85
PD18-54-250.d	2.355	0.16	0.1256	0.0054	0.71129	1227	43	762	30	2164	47	7.61	0.131	35.21
PD18-54-251.d	7.09	0.23	0.2907	0.0087	0.60374	2121	31	1645	44	2615	25	4.77	0.210	62.91
PD18-54-252.d	3.428	0.17	0.1762	0.0073	0.80908	1509	34	1046	40	2272	31	2.94	0.340	46.04
PD18-54-260.d	2.656	0.08	0.1378	0.0041	0.74749	1315	21	832	23	2257	21	12.9	0.078	36.86
PD18-54-261.d	2.402	0.07	0.1311	0.0036	0.77958	1242	22	794	22	2169	24	104	0.010	36.61
PD18-54-262.d	4.36	0.15	0.209	0.0061	0.69667	1703	26	1223	32	2391	25	26.4	0.038	51.15
PD18-54-263.d	2.915	0.12	0.1463	0.0049	0.31249	1385	29	880	27	2269	32	16.8	0.060	38.78
PD18-54-264.d	1.753	0.099	0.0866	0.006	0.78103	1027	32	535	35	2299	25	12	0.083	23.27
PD18-54-265.d	6.91	0.33	0.299	0.014	0.95403	2087	42	1682	68	2530	16	28.7	0.035	66.48
PD18-54-266.d	1.702	0.15	0.1055	0.006	0.80935	1009	45	647	34	1900	46	16.5	0.061	34.05
PD18-54-267.d	3.311	0.1	0.1743	0.0053	0.76407	1482	24	1035	29	2183	22	10.4	0.096	47.41
PD18-54-268.d	2.127	0.12	0.121	0.0058	0.53631	1156	35	736	33	2034	26	5.59	0.179	36.18
PD18-54-269.d	1.84	0.23	0.1139	0.0084	0.82595	1058	60	695	47	1900	56	29.8	0.034	36.58
PD18-54-270.d	1.745	0.14	0.0996	0.0057	0.68547	1024	41	612	33	2090	32	21.8	0.046	29.28
PD18-54-271.d	10.84	0.3	0.4484	0.012	0.77014	2511	27	2387	56	2646	18	2.539	0.394	90.21
PD18-54-272.d	3.729	0.12	0.1847	0.0052	0.63061	1576	27	1092	28	2294	26	5.04	0.198	47.60
PD18-54-273.d	2.424	0.21	0.1307	0.0077	0.81828	1247	48	791	42	2140	38	6.04	0.166	36.96
PD18-54-274.d	2.68	0.27	0.1541	0.01	0.78399	1321	49	924	52	2043	40	14.95	0.067	45.23

PD18-54-275.d	2.22	0.093	0.1139	0.0044	0.78682	1186	32	695	25	2244	26	49.8	0.020	30.97
PD18-54-276.d	2.352	0.2	0.1061	0.0089	0.74577	1227	46	650	52	2468	30	3.56	0.281	26.34
PD18-54-284.d	3.654	0.31	0.1872	0.012	0.70713	1559	54	1106	59	2275	34	10.4	0.096	48.62
PD18-54-285.d	3.566	0.1	0.1768	0.005	0.71047	1541	24	1049	28	2307	20	6.47	0.155	45.47
PD18-54-286.d	9.84	0.26	0.3924	0.01	0.71016	2421	26	2133	49	2671	20	7.67	0.130	79.86
PD18-54-287.d	12	0.31	0.4892	0.012	0.66128	2603	24	2566	54	2628	19	4.64	0.216	97.64
PD18-47-288.d	7.73	0.32	0.3114	0.011	0.64054	2197	43	1747	55	2644	28	1.938	0.516	66.07
PD18-47-289.d	7.24	0.53	0.316	0.014	0.70165	2139	56	1768	65	2550	44	2.83	0.353	69.33
PD18-47-290.d	7.05	0.3	0.3301	0.013	0.71115	2116	39	1837	62	2395	24	4.16	0.240	76.70
PD18-47-291.d	11.53	0.38	0.4261	0.011	0.24416	2565	29	2287	52	2792	49	1.3	0.769	81.91
PD18-47-292.d	11.74	0.36	0.4797	0.014	0.39115	2580	29	2524	57	2627	38	1.799	0.556	96.08
PD18-47-293.d	9.92	0.32	0.4366	0.013	0.85296	2426	32	2334	62	2503	22	3.37	0.297	93.25
PD18-47-294.d	7.06	0.26	0.3056	0.011	0.43563	2115	35	1718	57	2534	35	3.14	0.318	67.80
PD18-47-295.d	10.01	0.54	0.421	0.02	0.84376	2431	66	2262	99	2563	28	2	0.500	88.26
PD18-47-296.d	5.79	0.22	0.2787	0.0097	0.018339	1944	35	1584	49	2352	30	4.36	0.229	67.35
PD18-47-297.d	7.43	0.2	0.316	0.0085	0.86347	2163	24	1770	42	2558	21	1.846	0.542	69.19
PD18-47-298.d	8.06	0.44	0.3071	0.013	0.77446	2236	62	1725	68	2740	47	0.0872	11.468	62.96
PD18-47-306.d	10.83	0.34	0.463	0.016	0.67275	2506	30	2463	72	2548	29	1.376	0.727	96.66
PD18-47-307.d	7.94	0.36	0.351	0.015	0.57041	2221	53	1940	73	2481	24	2.54	0.394	78.19
PD18-47-308.d	5.221	0.14	0.2467	0.0067	0.75012	1854	24	1421	35	2371	22	3.93	0.254	59.93
PD18-47-309.d	5.33	0.37	0.2488	0.014	0.863	1878	47	1432	69	2404	27	5.41	0.185	59.57
PD18-47-310.d	8.92	0.31	0.3802	0.012	0.62859	2328	35	2076	58	2541	22	15.44	0.065	81.70
PD18-47-311.d	6.83	0.24	0.3083	0.0093	0.63919	2086	34	1732	46	2458	30	1.614	0.620	70.46
PD18-47-312.d	6.87	0.2	0.3014	0.0082	0.71738	2093	27	1698	41	2500	24	3.96	0.253	67.92
PD18-47-313.d	11.61	0.31	0.4778	0.012	0.7499	2571	25	2517	54	2611	21	2.4	0.417	96.40
PD18-47-314.d	6.87	0.25	0.2645	0.0097	0.86691	2098	36	1512	50	2717	16	135.6	0.007	55.65
PD18-47-315.d	11.9	0.33	0.4911	0.013	0.63129	2595	27	2574	56	2612	26	0.957	1.045	98.55
PD18-47-316.d	6.26	3.1	0.2854	0.054	0.88146	2005	180	1616	240	2438	110	3.38	0.296	66.28
PD18-47-317.d	4.72	1.4	0.2201	0.039	0.76711	1766	120	1281	170	2391	63	2.654	0.377	53.58
PD18-47-318.d	5.68	0.21	0.2661	0.0083	0.67318	1926	37	1520	43	2391	32	2.73	0.366	63.57
PD18-47-319.d	7.63	1.7	0.339	0.058	0.91196	2187	110	1878	230	2543	28	0.538	1.859	73.85
PD18-45-320.d	7.11	0.35	0.306	0.014	0.76321	2124	55	1720	74	2575	31	1.294	0.773	66.80
PD18-45-328.d	9.21	0.39	0.3912	0.016	0.80785	2357	47	2128	79	2565	22	1.274	0.785	82.96
PD18-45-329.d	39	92	0.79	1	0.72584	3744	320	3750	1300	3742	88	1.223	0.818	100.21
PD18-45-330.d	5.058	0.15	0.2361	0.0068	0.85848	1828	26	1366	36	2410	19	0.89	1.124	56.68
PD18-45-331.d	1.391	0.14	0.073	0.0057	0.76788	883	47	454	33	2189	36	2.58	0.388	20.74
PD18-45-332.d	11.72	0.29	0.4714	0.012	0.61386	2581	22	2489	52	2645	17	0.643	1.555	94.10
PD18-45-333.d	11.25	0.55	0.462	0.022	0.61245	2543	63	2448	100	2625	26	2.424	0.413	93.26
PD18-45-334.d	12.17	0.42	0.484	0.016	0.32264	2617	37	2545	72	2662	25	1.211	0.826	95.60
PD18-45-335.d	9.25	0.27	0.386	0.012	0.70437	2361	29	2103	53	2584	23	1.242	0.805	81.39

PD18-45-336.d	11.71	0.31	0.4727	0.012	0.60182	2580	26	2500	53	2637	20	1.49	0.671	94.80
PD18-45-337.d	10.22	0.46	0.4235	0.017	0.76885	2459	53	2275	80	2599	29	1.239	0.807	87.53
PD18-45-338.d	7.73	0.42	0.323	0.016	0.86962	2196	62	1805	80	2580	30	0.987	1.013	69.96
PD18-45-339.d	4.344	0.48	0.2001	0.018	0.78326	1701	65	1176	89	2430	31	1.098	0.911	48.40
PD18-45-340.d	10.76	0.47	0.4347	0.017	0.63745	2501	52	2326	80	2635	27	1.347	0.742	88.27
PD18-45-341.d	4.22	0.36	0.2052	0.015	0.47436	1677	62	1203	78	2369	36	1.134	0.882	50.78
PD18-45-342.d	11.29	0.31	0.4547	0.012	0.2167	2546	26	2415	55	2651	24	1.138	0.879	91.10
PD18-45-350.d	13.33	0.33	0.523	0.013	0.76447	2702	24	2711	57	2692	17	1.184	0.845	100.71
PD18-45-351.d	10.79	0.52	0.433	0.02	0.70078	2504	55	2318	95	2646	21	1.137	0.880	87.60
PD18-45-352.d	12.96	0.33	0.5201	0.014	0.56057	2676	25	2698	58	2653	20	1.525	0.656	101.70
PD18-45-353.d	9.25	0.68	0.382	0.025	0.853	2360	110	2082	130	2602	44	1.134	0.882	80.02
PD18-45-354.d	5.73	0.41	0.2516	0.016	0.59329	1934	48	1446	79	2505	23	1.318	0.759	57.72
PD18-45-355.d	2.039	0.43	0.096	0.018	0.75595	1127	89	591	95	2425	34	0.798	1.253	24.37
PD18-45-356.d	3.929	0.25	0.1657	0.01	0.54099	1618	69	987	59	2604	47	1.493	0.670	37.90
PD18-45-357.d	9.57	0.42	0.394	0.016	0.72357	2392	48	2140	78	2616	25	1.028	0.973	81.80
PD18-45-358.d	8.5	0.28	0.3569	0.011	0.52578	2285	28	1967	51	2574	17	1.096	0.912	76.42
PD18-45-359.d	7.31	0.71	0.311	0.026	0.80376	2146	93	1742	130	2548	32	1.41	0.709	68.37
PD18-45-360.d	4.64	0.43	0.2163	0.015	0.74251	1754	57	1262	75	2407	30	1.368	0.731	52.43
PD18-45-361.d	4.61	0.3	0.1823	0.0093	0.71306	1748	63	1078	52	2683	54	1.049	0.953	40.18
PD18-45-362.d	9.41	0.31	0.3827	0.012	0.72561	2378	33	2088	57	2626	23	2.048	0.488	79.51
PD18-45-363.d	13.51	0.37	0.505	0.015	0.78242	2714	27	2632	65	2768	22	0.963	1.038	95.09
PD18-45-364.d	2.65	0.22	0.1228	0.0099	0.81133	1311	67	746	57	2445	27	1.053	0.950	30.51
PD18-45-365.d	8.58	0.52	0.3612	0.019	0.40173	2293	72	1987	97	2631	29	1.73	0.578	75.52
PD18-44-373.d	12.59	0.85	0.507	0.028	0.58026	2648	60	2639	140	2647	52	0.83	1.205	99.70
PD18-44-374.d	11.5	0.62	0.464	0.027	0.63474	2562	72	2453	130	2640	44	0.733	1.364	92.92
PD18-44-375.d	11.27	0.31	0.4285	0.013	0.42659	2543	25	2296	60	2738	28	1.172	0.853	83.86
PD18-44-376.d	12.06	0.35	0.4727	0.013	0.37887	2609	28	2493	58	2689	34	0.968	1.033	92.71
PD18-44-377.d	3.34	0.2	0.1618	0.0065	0.44399	1490	41	967	36	2312	44	1.134	0.882	41.83
PD18-44-378.d	2.982	0.087	0.1466	0.0043	0.89573	1392	23	881	24	2304	18	1.07	0.935	38.24
PD18-44-379.d	9.49	0.31	0.3396	0.0085	0.43245	2384	32	1884	41	2841	39	0.814	1.229	66.31
PD18-44-380.d	9.03	0.24	0.3478	0.01	0.39741	2340	25	1923	49	2725	26	1.368	0.731	70.57
PD18-44-381.d	7.25	0.27	0.24	0.014	0.80047	2139	36	1383	75	3026	63	0.877	1.140	45.70
PD18-44-382.d	12.31	0.32	0.4942	0.013	0.66245	2626	25	2588	56	2656	21	0.861	1.161	97.44
PD18-44-383.d	7.33	1.3	0.242	0.021	0.85466	2150	93	1394	99	2974	81	0.877	1.140	46.87
PD18-44-384.d	9.74	0.27	0.3861	0.012	0.34876	2413	25	2104	55	2674	22	3.327	0.301	78.68
PD18-44-385.d	9.41	0.28	0.3754	0.01	0.62019	2378	29	2054	48	2668	22	4.47	0.224	76.99
PD18-44-386.d	4.34	0.45	0.193	0.016	0.87977	1706	67	1137	82	2485	32	1.7	0.588	45.75
PD18-44-387.d	5.91	0.24	0.1822	0.0064	0.63886	1961	42	1078	36	3076	28	1.8	0.556	35.05
PD18-44-388.d	5.98	4.1	0.2546	0.044	0.55549	1971	200	1462	190	2563	170	1.982	0.505	57.04
PD18-44-396.d	10.67	0.54	0.384	0.022	0.74053	2491	57	2087	100	2813	30	1.138	0.879	74.19
PD18-44-397.d	11.3	0.35	0.3983	0.013	0.63681	2546	31	2160	61	2872	39	0.843	1.186	75.21

PD18-44-398.d	8.62	0.36	0.3413	0.014	0.62869	2297	47	1892	71	2669	19	3.24	0.309	70.89
PD18-44-399.d	11.21	0.34	0.4111	0.014	0.48469	2538	29	2218	64	2805	33	1.372	0.729	79.07
PD18-44-400.d	2.228	3.4	0.0784	0.049	0.6765	1192	260	486	260	2893	130	2.15	0.465	16.80
PD18-44-401.d	7.26	0.4	0.2768	0.011	0.54738	2146	41	1575	54	2749	31	0.774	1.292	57.29
PD18-44-402.d	11.69	0.4	0.4638	0.012	0.50202	2578	31	2455	55	2668	35	0.814	1.229	92.02
PD18-44-403.d	7.68	0.21	0.2885	0.0078	0.44284	2193	25	1633	39	2767	30	3.425	0.292	59.02
PD18-44-404.d	7.82	0.3	0.2736	0.0078	0.45084	2207	32	1558	39	2883	43	2.225	0.449	54.04
PD18-44-405.d	9.78	0.38	0.368	0.015	0.53961	2412	35	2017	73	2760	52	1.04	0.962	73.08
PD18-44-406.d	7.59	0.94	0.2479	0.025	0.86265	2182	77	1427	120	3000	57	5.69	0.176	47.57
PD18-44-407.d	11.13	0.34	0.4285	0.011	0.42788	2531	28	2298	49	2719	32	1.124	0.890	84.52
PD18-44-408.d	5.23	0.27	0.1823	0.012	0.7368	1857	40	1079	64	2921	31	0.799	1.252	36.94
PD18-44-409.d	2.67	0.13	0.1465	0.0057	0.75181	1320	43	881	33	2128	45	1.369	0.730	41.40
PD18-44-410.d	6.15	1.2	0.261	0.017	0.6739	1994	100	1495	81	2548	110	1.75	0.571	58.67
PD18-39-425.d	5.274	0.17	0.2001	0.0044	0.55299	1864	27	1175	24	2752	52	1.232	0.812	42.70
PD18-39-426.d	4.638	0.17	0.1704	0.0048	0.56854	1755	34	1014	27	2777	51	2.435	0.411	36.51
PD18-39-427.d	3.8	0.17	0.1648	0.0076	0.78222	1593	48	983	44	2668	52	2.411	0.415	36.84
PD18-39-428.d	6.49	0.24	0.2532	0.0068	0.34071	2043	33	1455	34	2709	54	1.265	0.791	53.71
PD18-39-429.d	9.29	0.4	0.3699	0.013	0.66411	2364	45	2028	62	2662	57	1.822	0.549	76.18
PD18-39-430.d	4.816	0.16	0.18	0.0039	0.61048	1786	28	1067	21	2777	52	1.274	0.785	38.42
PD18-39-431.d	3.547	0.13	0.1142	0.003	0.73217	1536	28	701	17	3009	53	0.826	1.211	23.30
PD18-39-432.d	10.54	0.36	0.4137	0.01	0.5452	2482	35	2231	47	2679	55	1.378	0.726	83.28
PD18-39-433.d	3.603	0.19	0.135	0.0052	0.59475	1549	38	816	29	2766	51	0.744	1.344	29.50
PD18-39-434.d	12.79	0.4	0.5064	0.0094	0.39865	2663	30	2640	40	2666	53	2.368	0.422	99.02
PD18-39-435.d	9.04	0.28	0.3554	0.0067	0.42562	2340	28	1959	32	2692	53	1.863	0.537	72.77
PD18-39-436.d	3.303	0.14	0.13	0.005	0.87701	1480	37	787	29	2678	52	1.436	0.696	29.39
PD18-39-437.d	6.85	0.23	0.2715	0.0059	0.68458	2090	30	1548	30	2668	53	1.205	0.830	58.02
PD18-39-438.d	9.28	0.43	0.361	0.015	0.74336	2362	50	1984	75	2695	54	1.676	0.597	73.62
PD18-39-439.d	7.82	0.41	0.3013	0.015	0.84156	2207	42	1696	71	2711	55	1.194	0.838	62.56
PD18-39-448.d	5.071	0.17	0.1743	0.0042	0.83012	1829	28	1035	23	2911	54	1.342	0.745	35.55
PD18-39-449.d	11.79	0.41	0.4286	0.0097	0.42873	2585	34	2298	45	2817	53	1.551	0.645	81.58
PD18-39-450.d	4.718	0.16	0.1966	0.0044	0.74998	1769	28	1156	24	2595	53	2.229	0.449	44.55
PD18-39-451.d	2.214	0.14	0.0731	0.0048	0.57878	1184	40	455	28	2963	51	1.145	0.873	15.36
PD18-39-452.d	5.37	0.2	0.2125	0.0064	0.71701	1877	37	1242	35	2666	52	3.072	0.326	46.59
PD18-39-453.d	6.71	0.33	0.2718	0.01	0.63527	2074	44	1550	53	2664	53	0.847	1.181	58.18
PD18-39-454.d	4.571	0.22	0.1864	0.0064	0.6861	1743	35	1102	34	2642	52	1.425	0.702	41.71
PD18-39-455.d	6.256	0.19	0.2227	0.004	0.57961	2011	27	1296	21	2844	51	1.178	0.849	45.57
PD18-39-456.d	2.838	0.14	0.0943	0.0048	0.59397	1365	42	581	29	2953	51	0.4	2.500	19.67
PD18-39-457.d	4.853	0.15	0.1847	0.0038	0.71907	1793	26	1092	21	2744	54	2.33	0.429	39.80
PD18-39-458.d	5.92	0.21	0.2329	0.0059	0.23164	1962	33	1349	31	2698	53	1.53	0.654	50.00
PD18-39-459.d	8.58	0.3	0.351	0.0075	0.54535	2293	31	1939	36	2636	55	1.558	0.642	73.56
PD18-39-460.d	7.4	0.28	0.2918	0.011	0.41275	2160	38	1650	55	2690	53	1.132	0.883	61.34

PD18-39-461.d	9.96	0.31	0.3941	0.0073	0.46138	2430	28	2141	34	2678	54	1.203	0.831	79.95
PD18-39-462.d	6.7	1.9	0.2673	0.07	0.67809	2069	250	1526	280	2653	1.20E+04	1.285	0.778	57.52
PD17-32-245.d	18.16	0.51	0.016	0.016	0.73307	2994	27	2737	70	3157	22	3.348	0.299	86.70
PD17-32-246.d	19.68	0.39	0.014	0.014	0.77847	3072	19	2933	56	3151	24	4.81	0.208	93.08
PD17-32-247.d	21.79	0.41	0.013	0.013	0.80783	3171	18	3084	51	3211	20	3.036	0.329	96.04
PD17-32-248.d	21.1	0.37	0.012	0.012	0.73265	3140	17	3038	50	3191	22	1.87	0.535	95.21
PD17-32-249.d	22.41	0.47	0.016	0.016	0.79161	3200	21	3150	63	3214	25	1.476	0.678	98.01
PD17-32-250.d	19.3	0.41	0.015	0.015	0.7532	3054	21	2806	62	3208	29	2.073	0.482	87.47
PD17-32-251.d	14.7	0.37	0.015	0.015	0.85941	2794	23	2446	64	3041	27	3.7	0.270	80.43
PD17-32-252.d	22.19	0.4	0.014	0.014	0.65858	3190	17	3161	57	3192	29	2.584	0.387	99.03
PD17-32-253.d	23.08	0.42	0.015	0.015	0.79493	3230	17	3247	57	3200	21	5.58	0.179	101.47
PD17-32-254.d	20.77	0.46	0.015	0.015	0.6865	3126	22	2997	62	3193	31	2.112	0.473	93.86
PD17-32-255.d	21.69	0.46	0.015	0.015	0.78129	3165	21	3085	62	3208	24	2.341	0.427	96.17
PD17-32-256.d	21.96	0.69	0.023	0.023	0.79386	3180	31	3147	91	3183	35	1.411	0.709	98.87
PD17-32-256-2.d	14.97	0.61	0.019	0.019	0.81295	2808	38	2254	85	3222	42	1.377	0.726	69.96
PD17-32-266.d	21.87	0.47	0.017	0.017	0.80509	3174	21	3113	68	3200	26	3.382	0.296	97.28
PD17-32-267.d	21.98	0.58	0.02	0.02	0.82581	3179	26	3172	78	3170	29	7.94	0.126	100.06
PD17-32-268.d	20.98	0.53	0.016	0.016	0.80833	3131	25	2980	65	3217	26	2.86	0.350	92.63
PD17-32-269.d	21.08	0.4	0.014	0.014	0.80901	3139	19	3044	54	3189	19	4.97	0.201	95.45
PD17-32-270.d	20.23	0.47	0.016	0.016	0.89613	3098	23	2897	65	3218	20	1.847	0.541	90.02
PD17-32-271.d	21.36	0.47	0.015	0.015	0.65267	3151	21	3026	61	3217	31	2.6	0.385	94.06
PD17-32-272.d	20.82	0.44	0.015	0.015	0.75271	3127	21	2959	61	3222	27	2.147	0.466	91.84
PD17-32-273.d	21.82	0.47	0.015	0.015	0.86866	3172	21	3088	60	3211	20	3.71	0.270	96.17
PD17-32-274.d	22.1	0.37	0.014	0.014	0.78252	3186	17	3106	55	3221	22	1.959	0.510	96.43
PD17-32-275.d	21.11	0.45	0.016	0.016	0.84702	3140	21	3020	64	3204	23	6.47	0.155	94.26
PD17-32-276.d	22.41	0.39	0.012	0.012	0.7064	3199	17	3192	46	3187	22	1.812	0.552	100.16
PD17-32-277.d	22.88	0.39	0.011	0.011	0.74045	3223	16	3201	45	3214	20	1.888	0.530	99.60
PD17-32-287.d	22.05	0.34	0.011	0.011	0.81539	3184	15	3078	46	3238	16	1.775	0.563	95.06
PD17-32-288.d	22.73	0.28	0.0093	0.0093	0.38748	3214	12	3212	36	3195	19	1.66	0.602	100.53
PD17-32-289.d	19.66	0.33	0.012	0.012	0.78406	3073	16	2967	47	3119	21	4.37	0.229	95.13
PD17-32-290.d	21.65	0.29	0.0094	0.0094	0.59459	3166	13	3079	38	3205	21	1.777	0.563	96.07
PD17-32-291.d	21.9	0.36	0.011	0.011	0.79344	3178	16	3117	45	3200	18	6.3	0.159	97.41
PD17-32-292.d	19.83	0.33	0.011	0.011	0.54068	3082	16	2874	46	3202	29	7.14	0.140	89.76
PD17-32-293.d	18.49	0.56	0.018	0.018	0.84445	3012	29	2684	78	3208	30	13.92	0.072	83.67
PD17-32-294.d	16.54	0.25	0.011	0.011	0.65295	2907	14	2774	46	2984	26	2.169	0.461	92.96
PD17-1-10.d	7.71	0.18	0.3496	0.0092	0.83251	2195	20	1931	44	2436	28	8.13	0.123	79.27
PD17-1-11.d	11.89	0.24	0.513	0.014	0.86132	2593	18	2666	57	2523	24	5.57	0.180	105.67
PD17-1-13.d	9.19	0.44	0.411	0.019	0.942	2350	44	2214	86	2460	28	3.65	0.274	90.00
PD17-1-14.d	7.28	0.18	0.3363	0.0086	0.84751	2144	24	1867	42	2407	22	2.503	0.400	77.57
PD17-1-15.d	11.59	0.21	0.494	0.012	0.88216	2570	17	2586	50	2543	19	4.03	0.248	101.69

PD17-1-16.d	12.44	0.21	0.507	0.0099	0.78882	2636	16	2643	42	2618	19	0.876	1.142	100.95
PD17-1-17.d	7.4	0.19	0.345	0.0093	0.90148	2154	22	1907	44	2398	26	7.51	0.133	79.52
PD17-1-18.d	11.96	0.19	0.512	0.011	0.82739	2599	15	2662	46	2536	19	6.4	0.156	104.97
PD17-1-20.d	12.09	0.33	0.501	0.017	0.91464	2605	26	2609	73	2593	22	8.9	0.112	100.62
PD17-1-21.d	6.39	0.14	0.2969	0.0063	0.8243	2029	19	1675	31	2391	18	11.55	0.087	70.05
PD17-1-31.d	6.15	0.14	0.2929	0.0075	0.83938	1997	19	1654	37	2362	25	1.57	0.637	70.03
PD17-1-32.d	4.394	0.092	0.229	0.0051	0.71959	1709	17	1328	27	2200	28	9.1	0.110	60.36
PD17-1-33.d	25.21	0.55	0.662	0.014	0.85826	3315	24	3272	55	3323	25	26.3	0.038	98.47
PD17-1-34.d	4.47	0.12	0.2338	0.0058	0.87494	1722	22	1353	30	2188	21	10.6	0.094	61.84
PD17-1-35.d	5.83	0.17	0.2666	0.0082	0.81015	1953	27	1522	43	2427	26	2.47	0.405	62.71
PD17-1-37.d	8.85	0.18	0.3888	0.0092	0.80884	2319	19	2115	43	2491	21	6.58	0.152	84.91
PD17-1-38.d	4.11	0.12	0.2179	0.0055	0.7047	1656	25	1270	29	2153	32	9.44	0.106	58.99
PD17-1-39.d	6.14	0.3	0.255	0.015	0.91757	1989	39	1462	76	2592	23	18.9	0.053	56.40
PD17-1-41.d	11.8	0.22	0.495	0.011	0.8672	2587	18	2588	48	2572	17	2.21	0.452	100.62
PD17-1-42.d	10.58	0.19	0.471	0.0097	0.86307	2485	17	2483	43	2472	19	14.33	0.070	100.44
PD17-1-51.d	11.7	0.21	0.4946	0.01	0.83237	2578	17	2588	44	2553	19	3.91	0.256	101.37
PD17-1-52.d	10.25	0.28	0.442	0.012	0.92504	2454	27	2355	54	2522	19	17.34	0.058	93.38
PD17-1-53.d	7.44	0.15	0.3323	0.0071	0.81762	2164	19	1848	35	2463	19	3.87	0.258	75.03
PD17-1-54.d	6.57	0.35	0.2764	0.0084	0.71475	2054	52	1572	43	2564	63	3.68	0.272	61.31
PD17-1-55.d	11.2	0.2	0.482	0.011	0.83837	2538	16	2532	48	2529	22	6.91	0.145	100.12
PD17-1-56.d	6.73	0.16	0.296	0.0079	0.88969	2074	20	1670	38	2480	19	13.62	0.073	67.34
PD17-1-58.d	11.46	0.24	0.489	0.015	0.82431	2563	19	2562	68	2542	26	14.74	0.068	100.79
PD17-1-59.d	11.3	0.27	0.477	0.012	0.91238	2546	24	2510	55	2561	39	3.91	0.256	98.01
PD17-1-60.d	11.22	0.23	0.482	0.012	0.90722	2534	17	2530	50	2525	19	15.23	0.066	100.20
PD17-1-61.d	3.78	0.15	0.2066	0.0059	0.90154	1581	29	1210	33	2093	32	0.691	1.447	57.81
PD17-5-70.d	4.44	0.24	0.2396	0.0091	0.76651	1718	37	1384	46	2139	32	8.31	0.120	64.70
PD17-5-71.d	6.81	0.15	0.3204	0.0075	0.81003	2083	20	1790	37	2374	25	3.47	0.288	75.40
PD17-5-72.d	7.28	0.29	0.3042	0.0095	0.67132	2145	32	1711	48	2574	84	1.95	0.513	66.47
PD17-5-73.d	6.63	0.11	0.3046	0.0053	0.71596	2062	15	1713	26	2418	18	2.094	0.478	70.84
PD17-5-75.d	9.64	0.16	0.399	0.0097	0.63514	2399	16	2163	45	2591	36	4.2	0.238	83.48
PD17-5-76.d	11.58	0.45	0.468	0.016	0.84276	2571	37	2488	69	2626	27	1.95	0.513	94.74
PD17-5-77.d	7.17	0.2	0.3103	0.0073	0.80028	2129	26	1741	36	2508	23	1.786	0.560	69.42
PD17-5-78.d	10.36	0.22	0.4274	0.0094	0.56372	2465	20	2292	43	2595	32	1.585	0.631	88.32
PD17-5-79.d	9.57	0.27	0.397	0.0089	0.82144	2388	26	2152	41	2590	28	1.544	0.648	83.09
PD17-5-81.d	6.34	0.15	0.3057	0.0062	0.81958	2021	20	1718	30	2331	21	1.873	0.534	73.70
PD17-5-90.d	8.76	0.19	0.3579	0.008	0.72507	2313	21	1970	38	2616	26	1.355	0.738	75.31
PD17-5-91.d	6.95	0.4	0.319	0.015	0.87716	2098	63	1781	75	2411	42	2.94	0.340	73.87
PD17-5-92.d	9.49	0.24	0.407	0.01	0.78433	2383	24	2198	47	2530	23	2.19	0.457	86.88
PD17-5-93.d	9.38	0.18	0.413	0.0086	0.7663	2374	18	2227	41	2488	23	4.5	0.222	89.51
PD17-5-94.d	3.09	0.11	0.1901	0.0062	0.93762	1422	28	1120	34	1900	24	3.14	0.318	58.95
PD17-5-95.d	11.27	0.16	0.473	0.008	0.7895	2544	13	2495	35	2568	18	1.028	0.973	97.16

PD17-5-96.d	5.87	0.17	0.2635	0.0056	0.82273	1950	26	1506	28	2443	29	2.033	0.492	61.65
PD17-5-97.d	6.31	0.15	0.2606	0.0054	0.62676	2019	19	1492	27	2594	35	1.72	0.581	57.52
PD17-5-98.d	8.73	0.16	0.3822	0.0074	0.75062	2307	17	2085	34	2495	23	2.79	0.358	83.57
PD17-5-99.d	6.91	0.16	0.3206	0.0076	0.86333	2096	20	1791	37	2397	20	2.5	0.400	74.72
PD17-5-100.d	11.86	0.17	0.4398	0.0076	0.78827	2592	14	2348	34	2772	17	2.56	0.391	84.70
PD17-5-101.d	7.23	0.17	0.2728	0.0066	0.57971	2137	21	1554	34	2739	54	2.283	0.438	56.74
PD17-5-110.d	10.7	0.19	0.4546	0.0096	0.81566	2495	16	2413	42	2547	20	1.562	0.640	94.74
PD17-5-111.d	6.62	0.35	0.3189	0.013	0.81969	2060	39	1783	61	2341	25	2.373	0.421	76.16
PD17-5-112.d	9.42	0.82	0.382	0.0095	0.64975	2374	60	2082	44	2620	82	2.08	0.481	79.47
PD17-5-113.d	7.4	0.12	0.3371	0.0066	0.83392	2159	15	1872	32	2430	16	1.76	0.568	77.04
PD17-5-114.d	7.59	0.14	0.3433	0.0066	0.74692	2182	17	1902	32	2441	20	1.164	0.859	77.92
PD17-5-115.d	7.79	0.36	0.3483	0.012	0.82382	2203	46	1925	57	2459	39	2.64	0.379	78.28
PD17-5-116.d	6.6	0.42	0.29	0.0089	0.72196	2054	46	1641	44	2498	64	1.93	0.518	65.69
PD17-5-117.d	9.57	0.3	0.423	0.013	0.82839	2391	32	2271	61	2480	20	7.69	0.130	91.57
PD17-5-118.d	10.33	0.18	0.4411	0.0074	0.65227	2462	16	2354	33	2541	21	1.469	0.681	92.64
PD17-5-119.d	8.27	0.19	0.3375	0.006	0.59027	2258	20	1874	29	2610	33	2.6	0.385	71.80
PD17-14-128.d	14.67	0.31	0.496	0.011	0.81559	2790	21	2595	46	2920	22	1.152	0.868	88.87
PD17-14-129.d	15.64	0.75	0.514	0.025	0.88151	2852	59	2669	110	2968	19	1.145	0.873	89.93
PD17-14-130.d	19.43	0.39	0.609	0.012	0.70508	3066	20	3062	50	3054	22	0.792	1.263	100.26
PD17-14-131.d	15.02	0.8	0.5	0.024	0.69072	2812	68	2611	110	2955	36	1.698	0.589	88.36
PD17-14-132.d	14.47	0.39	0.456	0.013	0.85288	2777	25	2419	57	3041	18	0.993	1.007	79.55
PD17-14-133.d	10.92	0.68	0.398	0.019	0.8933	2511	48	2156	84	2799	27	2.239	0.447	77.03
PD17-14-134.d	20.53	0.69	0.612	0.016	0.75721	3111	36	3075	64	3132	35	0.622	1.608	98.18
PD17-14-135.d	17.01	0.71	0.534	0.013	0.61918	2936	38	2757	52	3045	43	0.977	1.024	90.54
PD17-14-136.d	12.71	0.33	0.395	0.013	0.78456	2656	26	2143	60	3059	22	1.218	0.821	70.06
PD17-14-137.d	12.52	0.21	0.4373	0.0085	0.88022	2642	16	2337	38	2870	15	2.71	0.369	81.43
PD17-14-138.d	21.46	3	0.586	0.044	0.57521	3155	92	2971	160	3259	57	1.288	0.776	91.16
PD17-14-139.d	11.52	0.49	0.434	0.013	0.8309	2568	35	2323	56	2753	24	6.35	0.157	84.38
PD17-14-148.d	15.48	0.31	0.521	0.012	0.78132	2844	20	2699	53	2913	19	0.946	1.057	92.65
PD17-14-149.d	9.15	0.8	0.263	0.016	0.8659	2348	62	1501	78	3199	49	0.893	1.120	46.92
PD17-14-150.d	15.63	0.27	0.52	0.0082	0.84868	2852	16	2711	34	2945	18	1.97	0.508	92.05
PD17-14-151.d	16.08	0.34	0.536	0.012	0.5468	2882	19	2762	49	2945	33	1.284	0.779	93.79
PD17-14-153.d	16.17	0.41	0.524	0.013	0.77533	2885	26	2713	58	2990	17	2.035	0.491	90.74
PD17-14-154.d	15.27	0.35	0.5	0.011	0.80776	2830	25	2612	49	2991	21	3.051	0.328	87.33
PD17-14-155.d	13.36	0.25	0.462	0.01	0.70568	2703	18	2446	46	2908	20	10.71	0.093	84.11
PD17-14-156.d	10.85	0.21	0.3779	0.0078	0.87565	2507	18	2065	37	2874	16	1.592	0.628	71.85
PD17-14-157.d	9.2	0.23	0.3285	0.0079	0.76425	2356	22	1830	38	2841	21	1.354	0.739	64.41
PD17-14-158.d	15.81	0.27	0.523	0.011	0.73895	2863	16	2708	45	2958	24	0.887	1.127	91.55
PD17-14-159.d	11.12	0.21	0.3835	0.0074	0.69287	2531	17	2091	35	2890	26	3.81	0.262	72.35
PD17-14-168.d	14.41	0.41	0.47	0.013	0.64762	2774	27	2480	58	2981	29	1.522	0.657	83.19
PD17-14-169.d	12.79	0.72	0.441	0.025	0.76375	2660	70	2351	120	2888	20	3.37	0.297	81.41

PD17-14-170.d	12.39	0.25	0.4337	0.0077	0.63094	2633	19	2321	35	2865	24	1.718	0.582	81.01
PD17-14-171.d	16.61	0.44	0.555	0.014	0.79952	2910	28	2841	58	2927	27	1.472	0.679	97.06
PD17-14-172.d	12.51	0.3	0.42	0.011	0.86827	2641	23	2258	49	2935	18	0.645	1.550	76.93
PD17-14-173.d	8.24	0.26	0.2831	0.0089	0.87905	2256	32	1606	46	2910	17	3.79	0.264	55.19
PD17-14-174.d	9.32	0.16	0.3378	0.0074	0.86544	2369	17	1875	36	2814	16	1.371	0.729	66.63
PD17-14-175.d	11.21	0.18	0.3791	0.007	0.76154	2539	15	2071	33	2922	19	1.775	0.563	70.88
PD17-14-176.d	13.54	0.52	0.449	0.017	0.7246	2714	38	2402	80	2939	63	3.58	0.279	81.73
PD17-14-177.d	6.43	0.11	0.2377	0.0043	0.77457	2035	15	1374	23	2777	22	1.418	0.705	49.48
PD17-21-186.d	7.18	0.52	0.2807	0.015	0.86826	2127	54	1593	72	2679	33	1.152	0.868	59.46
PD17-21-187.d	18.26	0.39	0.593	0.013	0.74553	3001	22	2999	53	2985	20	1.037	0.964	100.47
PD17-21-188.d	17.35	0.34	0.571	0.012	0.75061	2952	19	2908	52	2966	25	0.721	1.387	98.04
PD17-21-189.d	10.52	0.26	0.3659	0.0092	0.88169	2477	23	2008	43	2875	19	1.21	0.826	69.84
PD17-21-190.d	16.01	0.33	0.533	0.013	0.83986	2874	20	2750	53	2948	23	0.965	1.036	93.28
PD17-21-191.d	16.06	0.3	0.536	0.011	0.75264	2878	18	2762	48	2949	21	1.017	0.983	93.66
PD17-21-192.d	13.51	0.73	0.447	0.021	0.5845	2710	66	2379	98	2963	35	1.329	0.752	80.29
PD17-21-193.d	16.91	0.32	0.548	0.012	0.77579	2927	18	2814	49	2991	22	1.127	0.887	94.08
PD17-21-194.d	19.13	3.6	0.579	0.03	0.73158	3044	90	2939	110	3101	99	0.779	1.284	94.78
PD17-21-195.d	17.07	3.8	0.533	0.033	0.61054	2935	96	2754	120	3039	73	0.953	1.049	90.62
PD17-21-196.d	12.47	0.4	0.442	0.014	0.87949	2636	31	2354	62	2847	21	1.575	0.635	82.68
PD17-21-197.d	17.61	0.54	0.549	0.016	0.85333	2978	31	2816	66	3056	24	2.87	0.348	92.15
PD17-21-206.d	19.14	0.34	0.605	0.011	0.64866	3047	17	3045	44	3031	24	0.963	1.038	100.46
PD17-21-207.d	11.52	0.53	0.407	0.015	0.66514	2553	44	2195	69	2849	27	2.55	0.392	77.04
PD17-21-208.d	6.7	1.2	0.253	0.036	0.97084	2050	110	1450	160	2733	43	1.39	0.719	53.06
PD17-21-209.d	16.21	0.62	0.498	0.018	0.88749	2886	37	2603	76	3073	27	0.902	1.109	84.71
PD17-21-210.d	16.43	1.7	0.534	0.046	0.80766	2896	110	2750	190	2988	45	1.7	0.588	92.03
PD17-21-211.d	9.14	0.45	0.35	0.014	0.87247	2345	53	1949	69	2696	31	2.5	0.400	72.29
PD17-21-212.d	7.47	0.3	0.2889	0.0099	0.80086	2164	40	1634	50	2706	29	2.22	0.450	60.38
PD17-21-213.d	17.48	0.29	0.581	0.012	0.84299	2959	16	2949	48	2952	21	1.13	0.885	99.90
PD17-21-214.d	14.62	15	0.47	0.55	0.92596	2791	190	2478	540	3012	36	1.414	0.707	82.27
PD17-21-215.d	17.51	0.34	0.579	0.011	0.66109	2960	18	2952	42	2960	22	0.947	1.056	99.73
PD17-21-216.d	10.77	0.25	0.3858	0.01	0.65565	2502	21	2102	46	2826	26	2.147	0.466	74.38
PD17-21-217.d	16.23	0.27	0.5367	0.0086	0.77764	2889	16	2768	36	2957	21	1.056	0.947	93.61
PD17-21-218.d	16.89	0.27	0.558	0.011	0.5195	2927	16	2854	46	2960	27	1.082	0.924	96.42
PD17-21-227.d	17.72	0.28	0.578	0.0097	0.69811	2973	15	2948	41	2973	20	1.577	0.634	99.16
PD17-21-228.d	14.59	0.28	0.491	0.011	0.80752	2787	19	2573	47	2929	18	1.315	0.760	87.85
PD17-21-229.d	4.004	0.095	0.1891	0.0043	0.79585	1632	19	1116	23	2364	26	3.54	0.282	47.21
PD17-21-230.d	16.69	0.44	0.534	0.013	0.734	2913	24	2753	53	3010	28	1.015	0.985	91.46
PD17-21-231.d	11.06	93	0.383	2.7	0.94507	2515	420	2084	1900	2870	71	3.702	0.270	72.61
PD17-21-232.d	12.94	0.39	0.458	0.013	0.90963	2669	29	2429	60	2848	19	1.351	0.740	85.29
PD17-21-233.d	18.2	0.28	0.6	0.0097	0.76682	2998	15	3027	39	2962	20	1.222	0.818	102.19
PD17-21-234.d	17.87	3.2	0.565	0.061	0.73734	2986	100	2884	210	3038	53	0.954	1.048	94.93

PD17-21-235.d	13.27	0.24	0.4766	0.0087	0.65694	2697	17	2511	38	2816	24	1.644	0.608	89.17
PD17-21-236.d	16.25	0.28	0.555	0.01	0.67064	2889	17	2843	41	2905	23	1.209	0.827	97.87
PD17-38-303.d	18.87	0.37	0.555	0.012	0.82299	3033	19	2844	52	3145	18	2.63	0.380	90.43
PD17-38-304.d	11.66	0.71	0.372	0.02	0.9023	2571	48	2034	91	3033	27	1.315	0.760	67.06
PD17-38-305.d	22.07	0.4	0.633	0.015	0.83181	3184	18	3157	60	3182	20	2.8	0.357	99.21
PD17-38-306.d	21.33	0.39	0.625	0.017	0.83628	3151	18	3125	66	3147	24	2.51	0.398	99.30
PD17-38-307.d	20.04	0.43	0.623	0.016	0.83171	3090	21	3116	63	3052	20	3.89	0.257	102.10
PD17-38-308.d	19.9	0.38	0.607	0.013	0.82723	3084	18	3055	52	3089	20	4.61	0.217	98.90
PD17-38-309.d	20.98	0.45	0.622	0.016	0.81556	3134	21	3111	63	3134	23	5.7	0.175	99.27
PD17-38-310.d	20.47	1	0.611	0.027	0.87506	3108	60	3068	110	3123	34	1.023	0.978	98.24
PD17-38-311.d	19.38	0.43	0.581	0.014	0.82345	3056	22	2946	58	3116	24	1.73	0.578	94.54
PD17-38-312.d	20.05	0.4	0.624	0.016	0.87035	3091	19	3122	63	3056	20	2.75	0.364	102.16
PD17-38-313.d	19.55	0.45	0.571	0.011	0.80877	3066	23	2918	44	3148	22	2.47	0.405	92.69
PD17-38-314.d	23.57	0.48	0.699	0.016	0.81878	3247	21	3411	63	3133	21	5.02	0.199	108.87
PD17-38-324.d	22.31	0.53	0.663	0.017	0.83607	3194	25	3274	64	3140	21	1.65	0.606	104.27
PD17-38-325.d	18.45	0.93	0.56	0.026	0.87175	3011	64	2865	120	3077	22	2.291	0.436	93.11
PD17-38-326.d	10.49	16	0.338	0.34	0.95099	2467	280	1870	820	3011	66	1.781	0.561	62.11
PD17-38-327.d	20.77	0.29	0.624	0.011	0.78403	3126	14	3122	42	3111	17	2.9	0.345	100.35
PD17-38-328.d	19.42	0.71	0.569	0.019	0.88294	3059	41	2898	82	3166	21	1.215	0.823	91.54
PD17-38-329.d	21.5	0.46	0.623	0.016	0.85775	3158	20	3128	60	3164	21	3.28	0.305	98.86
PD17-38-330.d	21.06	0.33	0.626	0.012	0.80606	3142	14	3129	46	3129	17	7.8	0.128	100.00
PD17-38-331.d	16.47	0.88	0.492	0.024	0.83718	2899	57	2573	110	3122	37	1.493	0.670	82.42
PD17-38-332.d	19.25	0.43	0.598	0.014	0.80549	3051	22	3017	55	3058	24	5.43	0.184	98.66
PD17-38-333.d	19.59	0.52	0.608	0.014	0.79165	3067	27	3057	57	3058	28	4.13	0.242	99.97
PD17-38-334.d	21.43	0.38	0.646	0.014	0.84208	3159	18	3209	53	3112	18	26.8	0.037	103.12
PD17-38-335.d	21.44	0.57	0.631	0.015	0.8152	3155	27	3148	62	3138	21	1.98	0.505	100.32
PD17-38-344.d	20.65	0.37	0.614	0.011	0.74942	3120	17	3082	46	3127	19	1.65	0.606	98.56
PD17-38-345.d	20.86	0.29	0.6043	0.0092	0.76352	3131	13	3045	37	3167	17	1.517	0.659	96.15
PD17-38-346.d	10.54	0.32	0.332	0.012	0.79235	2479	27	1845	57	3036	27	2.83	0.353	60.77
PD17-38-347.d	20.38	0.49	0.594	0.015	0.88303	3106	25	3003	64	3156	19	2.79	0.358	95.15
PD17-38-348.d	19.16	0.34	0.555	0.012	0.80086	3048	18	2845	49	3182	17	1.983	0.504	89.41
PD17-38-349.d	21.98	0.67	0.638	0.019	0.80712	3180	33	3177	77	3168	23	1.842	0.543	100.28
PD17-38-350.d	20.93	0.4	0.616	0.013	0.85373	3133	18	3089	50	3137	19	17.7	0.056	98.47
PD17-38-351.d	19.76	0.39	0.573	0.013	0.80659	3078	20	2915	52	3183	18	1.758	0.569	91.58
PD17-38-352.d	19.83	0.45	0.564	0.013	0.86411	3079	23	2879	54	3198	21	0.638	1.567	90.03
PD17-38-353.d	20.49	0.39	0.589	0.012	0.80265	3112	19	2982	49	3181	17	1.395	0.717	93.74
PD17-38-354.d	21.61	0.26	0.6268	0.009	0.6423	3165	12	3135	36	3170	19	1.157	0.864	98.90
PD17-44-363.d	20.42	0.41	0.578	0.014	0.85927	3109	20	2937	58	3204	21	2.653	0.377	91.67
PD17-44-364.d	10.35	0.47	0.354	0.012	0.82129	2464	34	1950	55	2904	31	2.31	0.433	67.15
PD17-44-365.d	9.76	0.24	0.2966	0.0085	0.81041	2410	23	1673	42	3095	22	4.65	0.215	54.05

PD17-44-366.d	10.66	0.4	0.353	0.0085	0.74484	2490	32	1945	40	2962	50	4.78	0.209	65.67
PD17-44-367.d	17.16	0.41	0.531	0.014	0.72698	2941	23	2742	60	3063	24	1.74	0.575	89.52
PD17-44-369.d	22.55	0.47	0.655	0.017	0.9046	3204	21	3242	66	3162	17	4.037	0.248	102.53
PD17-44-370.d	14.56	0.33	0.495	0.012	0.82183	2783	23	2590	51	2904	21	0.926	1.080	89.19
PD17-44-371.d	16.68	0.33	0.5	0.011	0.84383	2915	19	2609	50	3116	21	4.852	0.206	83.73
PD17-44-372.d	11.55	0.28	0.373	0.0097	0.83017	2565	23	2043	46	2994	22	1.43	0.699	68.24
PD17-44-373.d	8.59	1.4	0.317	0.032	0.78015	2292	94	1773	140	2773	58	2.811	0.356	63.94
PD17-44-382.d	9.38	0.52	0.335	0.017	0.84856	2371	45	1858	80	2837	25	0.179	5.587	65.49
PD17-44-383.d	13.23	0.29	0.438	0.01	0.8469	2693	20	2341	46	2955	23	3.335	0.300	79.22
PD17-44-384.d	17.4	0.4	0.503	0.013	0.79543	2960	22	2623	58	3181	22	1.63	0.613	82.46
PD17-44-385.d	21.84	0.56	0.631	0.019	0.92542	3172	26	3145	74	3176	23	2.04	0.490	99.02
PD17-44-386.d	16.83	0.32	0.489	0.011	0.84275	2923	19	2564	46	3164	20	3.61	0.277	81.04
PD17-44-387.d	12.9	0.74	0.426	0.021	0.92379	2668	75	2285	100	2950	37	2.37	0.422	77.46
PD17-44-388.d	14.68	23	0.469	0.41	0.87883	2792	270	2477	870	3014	73	3.847	0.260	82.18
PD17-44-389.d	13.8	0.31	0.424	0.011	0.83645	2732	21	2277	49	3074	22	3.41	0.293	74.07
PD17-44-390.d	15.06	0.32	0.47	0.011	0.85872	2815	21	2480	50	3049	21	3.691	0.271	81.34
PD17-44-391.d	20.36	0.44	0.591	0.015	0.87193	3105	21	2989	62	3165	20	2.938	0.340	94.44
PD17-44-392.d	22.34	0.43	0.635	0.015	0.86735	3196	19	3163	58	3200	19	4.14	0.242	98.84
PD17-44-393.d	20.04	0.39	0.586	0.014	0.87691	3090	19	2967	57	3155	18	2.57	0.389	94.04
PD17-44-402.d	19.36	0.38	0.58	0.013	0.79754	3058	20	2944	55	3116	20	8.66	0.115	94.48
PD17-44-403.d	16.57	2.7	0.497	0.041	0.79401	2909	70	2599	150	3112	40	2.873	0.348	83.52
PD17-44-404.d	20.44	0.4	0.604	0.015	0.82552	3109	19	3039	59	3140	23	2.658	0.376	96.78
PD17-44-405.d	21	0.42	0.618	0.015	0.8678	3135	20	3095	58	3145	19	3.39	0.295	98.41
PD17-44-406.d	16.2	0.97	0.505	0.027	0.78638	2885	79	2632	130	3088	29	3.19	0.313	85.23
PD17-44-407.d	13.79	3.4	0.434	0.076	0.88392	2731	79	2319	210	3038	44	3.562	0.281	76.33
PD17-44-408.d	12.93	0.43	0.41	0.013	0.85906	2670	29	2213	57	3017	24	2.39	0.418	73.35
PD17-44-409.d	19.44	0.48	0.581	0.015	0.87259	3060	25	2950	63	3116	19	2.18	0.459	94.67
PD17-44-410.d	18.52	1.9	0.522	0.035	0.91944	3019	78	2701	140	3215	37	3.068	0.326	84.01
PD17-44-411.d	16.26	0.58	0.502	0.017	0.86417	2886	39	2616	75	3065	24	2.773	0.361	85.35
PD17-44-412.d	16.52	0.42	0.528	0.015	0.87354	2903	26	2727	63	3013	21	13.78	0.073	90.51
PD17-44-414.d	21.23	0.35	0.604	0.011	0.73562	3147	16	3042	46	3198	21	1.343	0.745	95.12
PD17-44-423.d	19.89	0.39	0.593	0.014	0.80893	3083	19	2998	56	3123	22	1.996	0.501	96.00
PD17-44-425.d	14.97	0.37	0.434	0.012	0.89078	2811	24	2320	55	3168	20	2.586	0.387	73.23
PD17-44-426.d	13.73	0.26	0.46	0.01	0.82218	2729	19	2439	44	2936	20	5.975	0.167	83.07
PD17-44-427.d	18.3	0.35	0.53	0.012	0.83505	3003	19	2737	51	3170	20	2.241	0.446	86.34
PD17-27-429.d	17.81	0.47	0.589	0.016	0.69649	2976	26	2982	64	2962	41	1.113	0.898	100.68
PD17-27-430.d	14.55	0.35	0.492	0.01	0.8044	2784	23	2575	43	2931	33	1.59	0.629	87.85
PD17-27-431.d	14.66	0.57	0.473	0.019	0.82819	2787	37	2490	81	3001	44	0.951	1.052	82.97
PD17-27-432.d	17.84	0.47	0.59	0.014	0.75876	2978	25	2986	58	2961	37	1.448	0.691	100.84
PD17-27-433.d	17.43	0.52	0.574	0.015	0.80275	2955	29	2919	59	2971	37	1.092	0.916	98.25
PD17-27-434.d	14.23	0.32	0.483	0.0089	0.74105	2763	21	2539	39	2923	32	1.5	0.667	86.86

PD17-27-435.d	17.89	0.53	0.583	0.015	0.66875	2980	28	2956	61	2985	42	0.841	1.189	99.03
PD17-27-436.d	17.95	0.51	0.588	0.015	0.67037	2982	28	2978	60	2977	40	1.17	0.855	100.03
PD17-27-437.d	17.24	0.56	0.565	0.02	0.81739	2943	32	2883	82	2977	42	1.306	0.766	96.84
PD17-27-438.d	17	0.39	0.559	0.012	0.78563	2932	22	2857	51	2975	33	1.112	0.899	96.03
PD17-27-439.d	16.06	0.57	0.515	0.017	0.86923	2874	34	2672	74	3010	36	1.691	0.591	88.77
PD17-27-440.d	9.99	0.24	0.3607	0.0099	0.774	2432	23	1983	47	2822	39	0.809	1.236	70.27
PD17-27-441.d	7.57	0.21	0.2807	0.0081	0.83584	2179	25	1593	41	2780	36	0.683	1.464	57.30
PD17-27-450.d	16.05	0.5	0.536	0.017	0.79873	2881	28	2761	71	2947	40	1.508	0.663	93.69
PD17-27-451.d	17.98	0.46	0.586	0.013	0.81222	2985	25	2969	55	2988	33	1.509	0.663	99.36
PD17-27-452.d	16.43	0.46	0.544	0.016	0.81707	2898	27	2796	67	2962	37	1.129	0.886	94.40
PD17-27-452-2.d	11.06	0.37	0.379	0.013	0.81057	2525	32	2069	63	2903	43	8.4	0.119	71.27
PD17-27-453.d	12.84	0.35	0.422	0.012	0.67683	2666	26	2267	54	2977	43	2.1	0.476	76.15
PD17-27-454.d	14.44	0.35	0.49	0.01	0.82457	2779	24	2568	45	2926	32	0.938	1.066	87.76
PD17-27-455.d	15.51	0.43	0.505	0.014	0.70682	2844	26	2630	59	2991	41	1.841	0.543	87.93
PD17-27-456.d	15.67	0.38	0.505	0.014	0.76742	2854	24	2631	58	2989	37	2.701	0.370	88.02
PD17-27-457.d	17.24	0.41	0.561	0.012	0.68847	2945	23	2867	50	2988	36	1.555	0.643	95.95
PD17-27-458.d	16.94	0.46	0.57	0.015	0.75972	2928	26	2906	60	2933	37	1.512	0.661	99.08
PD17-27-459.d	18	0.49	0.577	0.018	0.75298	2986	26	2931	72	3015	41	0.928	1.078	97.21
PD17-27-460.d	15.41	0.45	0.512	0.014	0.78901	2838	29	2661	58	2956	36	1.25	0.800	90.02
PD17-27-461.d	17.03	0.47	0.556	0.014	0.78377	2936	26	2846	57	2982	35	1.57	0.637	95.44
PD17-27-462.d	16.98	0.44	0.542	0.013	0.71588	2930	25	2790	54	3020	38	1.188	0.842	92.38
PD17-27-471.d	18.38	0.47	0.601	0.016	0.75717	3009	25	3027	64	2989	37	1.26	0.794	101.27
PD17-27-472.d	18.08	0.59	0.593	0.018	0.7686	2988	31	2995	73	2977	41	1.643	0.609	100.60
PD17-27-473.d	14.46	0.36	0.491	0.011	0.82635	2776	24	2570	49	2916	31	0.953	1.049	88.13
PD17-27-474.d	15.73	0.4	0.522	0.013	0.80819	2857	25	2703	57	2960	35	1.377	0.726	91.32
PD17-48-475.d	20.4	0.51	0.596	0.015	0.85926	3108	24	3011	62	3159	31	3.85	0.260	95.31
PD17-48-476.d	20.35	0.42	0.6	0.01	0.81244	3106	20	3029	41	3145	29	1.65	0.606	96.31
PD17-48-477.d	21.34	0.42	0.6279	0.0095	0.7127	3152	19	3139	38	3148	30	3.93	0.254	99.71
PD17-48-478.d	21.77	0.49	0.632	0.013	0.89167	3171	22	3153	53	3172	28	4.2	0.238	99.40
PD17-48-479.d	21.75	0.49	0.638	0.015	0.87783	3173	21	3178	57	3151	29	19.3	0.052	100.86
PD17-48-480.d	21.61	0.51	0.628	0.014	0.81652	3164	23	3136	56	3171	31	2.13	0.469	98.90
PD17-48-481.d	19.54	0.44	0.573	0.012	0.81453	3066	22	2915	49	3153	30	2.04	0.490	92.45
PD17-48-482.d	17.08	0.63	0.506	0.016	0.80267	2936	35	2639	71	3136	42	1.094	0.914	84.15
PD17-48-491.d	20.81	0.42	0.611	0.011	0.84111	3130	20	3071	43	3156	28	3.37	0.297	97.31
PD17-48-492.d	20.9	0.45	0.612	0.011	0.77159	3131	21	3074	44	3154	30	2.5	0.400	97.46
PD17-48-493.d	21.07	0.5	0.621	0.013	0.87117	3139	23	3108	52	3144	28	12.5	0.080	98.85
PD17-48-494.d	19.74	0.43	0.587	0.012	0.61981	3077	21	2974	48	3130	30	0.508	1.969	95.02
PD17-48-495.d	21.39	0.46	0.627	0.012	0.74577	3155	21	3135	50	3155	32	5.99	0.167	99.37
PD17-48-496.d	20.85	0.51	0.614	0.014	0.67919	3129	24	3083	55	3150	33	3.13	0.319	97.87
PD17-48-497.d	21.67	0.49	0.63	0.014	0.82005	3168	22	3146	55	3167	30	5.25	0.190	99.34
PD17-48-498.d	21.56	0.43	0.63	0.012	0.87977	3165	19	3148	48	3160	29	6.77	0.148	99.62

PD17-48-499.d	21.77	0.46	0.638	0.013	0.84624	3172	21	3179	50	3152	30	65	0.015	100.86
PD17-48-500.d	20.33	0.42	0.61	0.011	0.79932	3105	20	3069	43	3116	30	8.79	0.114	98.49
PD17-48-501.d	18.45	0.52	0.555	0.017	0.90596	3011	27	2841	70	3114	33	14	0.071	91.23
PD17-48-502.d	20.49	0.48	0.607	0.013	0.80867	3112	23	3054	51	3139	31	2.54	0.394	97.29
PD17-48-503.d	21.07	0.47	0.616	0.012	0.8324	3139	22	3089	47	3161	29	3.42	0.292	97.72
PD17-48-512.d	20.91	0.48	0.618	0.013	0.87037	3133	22	3099	50	3141	29	12.5	0.080	98.66
PD17-48-513.d	21.87	0.44	0.6343	0.0095	0.70496	3176	20	3165	38	3171	30	1.612	0.620	99.81
PD17-48-514.d	21.8	0.45	0.63	0.011	0.83345	3173	20	3145	43	3178	29	2.87	0.348	98.96
PD17-48-515.d	20.23	0.44	0.597	0.012	0.8122	3101	21	3017	48	3146	31	1.056	0.947	95.90
PD17-48-516.d	20.55	0.74	0.597	0.019	0.84756	3115	36	3015	76	3161	37	2.75	0.364	95.38
PD17-48-517.d	22.31	0.5	0.648	0.013	0.81868	3195	22	3218	52	3169	30	7.05	0.142	101.55
PD17-48-518.d	19.45	0.66	0.562	0.02	0.79782	3061	33	2871	81	3174	42	1.446	0.692	90.45
PD17-48-519.d	12.04	0.29	0.3554	0.0073	0.8941	2605	22	1959	35	3145	29	0.545	1.835	62.29
PD17-48-520.d	17.08	0.55	0.49	0.016	0.89268	2937	31	2566	70	3172	34	1.79	0.559	80.90
PD17-48-521.d	19.91	0.47	0.586	0.012	0.81964	3084	23	2968	51	3148	31	4.84	0.207	94.28
PD17-48-522.d	21.31	0.47	0.627	0.012	0.85236	3151	22	3136	47	3146	29	4.34	0.230	99.68
PD17-49-531.d	20.78	0.44	0.596	0.011	0.80069	3126	20	3013	43	3188	29	6.1	0.164	94.51
PD17-49-532.d	10.13	0.29	0.3069	0.0085	0.86846	2444	27	1724	42	3082	34	1.93	0.518	55.94
PD17-49-533.d	17.59	0.44	0.527	0.012	0.87708	2966	24	2728	51	3122	30	2.76	0.362	87.38
PD17-49-534.d	12.71	0.46	0.4	0.015	0.87895	2656	34	2167	70	3041	37	2.81	0.356	71.26
PD17-49-535.d	17.81	0.67	0.528	0.018	0.85731	2977	36	2730	75	3138	36	3.71	0.270	87.00
PD17-49-536.d	16.19	0.51	0.49	0.016	0.87956	2885	30	2570	67	3097	34	3.06	0.327	82.98
PD17-49-537.d	16.35	0.33	0.4977	0.0086	0.74151	2896	20	2602	37	3093	30	1.464	0.683	84.13
PD17-49-538.d	15.85	0.37	0.466	0.01	0.80854	2866	22	2466	44	3146	32	1.799	0.556	78.39
PD17-49-539.d	13.09	0.36	0.417	0.011	0.86325	2684	27	2244	53	3025	33	3.34	0.299	74.18
PD17-49-540.d	11.77	0.27	0.4037	0.0074	0.85309	2584	22	2184	34	2902	30	1.6	0.625	75.26
PD17-49-541.d	4.39	0.14	0.1525	0.0058	0.60227	1708	27	914	33	2865	58	2.237	0.447	31.90
PD17-49-542.d	16.71	0.4	0.501	0.012	0.70728	2917	23	2616	53	3123	39	0.201	4.975	83.77
PD17-49-551.d	18.7	0.47	0.487	0.01	0.50656	3028	24	2556	44	3320	40	1.32	0.758	76.99
PD17-49-552.d	16.76	0.65	0.472	0.02	0.84149	2919	38	2492	90	3197	42	13.68	0.073	77.95
PD17-49-553.d	16.41	0.38	0.4968	0.0084	0.78348	2900	22	2599	36	3119	29	1.476	0.678	83.33
PD17-49-554.d	7.38	0.21	0.2447	0.0073	0.77336	2156	25	1410	38	2957	38	2.247	0.445	47.68
PD17-49-555.d	15.45	0.37	0.466	0.01	0.70687	2842	23	2465	44	3110	35	1.006	0.994	79.26
PD17-49-556.d	13.51	0.49	0.432	0.014	0.81816	2713	35	2311	64	3013	41	2.103	0.476	76.70
PD17-49-557.d	12.85	0.42	0.411	0.012	0.85398	2666	30	2216	56	3018	38	3.01	0.332	73.43
PD17-49-558.d	10.29	0.27	0.3395	0.0071	0.88442	2459	24	1883	34	2966	30	2.41	0.415	63.49
PD17-49-559.d	20.06	0.43	0.524	0.014	0.7975	3093	21	2715	59	3319	36	1.205	0.830	81.80
PD17-49-560.d	20.74	0.41	0.607	0.01	0.79558	3125	19	3054	42	3159	31	1.883	0.531	96.68
PD17-49-561.d	12.86	0.36	0.413	0.013	0.90839	2667	27	2225	60	3014	33	2.302	0.434	73.82
PD17-49-562.d	16.68	0.41	0.496	0.012	0.8773	2914	24	2593	52	3114	30	1.92	0.521	83.27
PD17-49-571.d	17.84	0.36	0.5244	0.0091	0.84764	2980	20	2715	38	3149	28	2.004	0.499	86.22

PD17-49-572.d	8.19	0.28	0.2167	0.0087	0.90172	2249	31	1263	46	3299	37	1.132	0.883	38.28
PD17-49-573.d	13.43	0.54	0.427	0.014	0.92683	2707	39	2288	65	3019	36	0.802	1.247	75.79
PD17-49-574.d	22.35	0.56	0.616	0.012	0.71087	3195	24	3090	49	3254	32	0.802	1.247	94.96
PD17-49-575.d	18.87	0.41	0.529	0.011	0.83024	3033	21	2741	45	3221	30	3.88	0.258	85.10
PD17-49-576.d	15.94	0.44	0.467	0.011	0.72865	2872	26	2468	51	3150	37	1.924	0.520	78.35
PD17-49-577.d	18.68	0.52	0.563	0.02	0.77943	3024	27	2874	84	3116	44	1.371	0.729	92.23
PD17-49-578.d	17.89	0.49	0.534	0.014	0.83651	2981	27	2757	57	3119	32	3.09	0.324	88.39
PD17-49-579.d	20	0.43	0.591	0.013	0.85861	3089	21	2988	51	3143	31	1.8	0.556	95.07
PD17-49-580.d	9.88	0.22	0.3372	0.0073	0.73365	2422	21	1872	35	2910	34	1.011	0.989	64.33
PD17-49-581.d	18.43	0.39	0.529	0.01	0.87533	3011	21	2737	44	3185	28	4.02	0.249	85.93
PD17-56-590.d	22.5	0.65	0.636	0.019	0.74262	3204	29	3169	76	3214	40	1.88	0.532	98.60
PD17-56-591.d	20.11	0.5	0.554	0.013	0.74212	3095	24	2841	52	3231	34	86	0.012	87.93
PD17-56-592.d	24.52	0.62	0.651	0.013	0.61772	3285	25	3235	50	3309	37	1.29	0.775	97.76
PD17-56-593.d	23.61	0.62	0.682	0.016	0.79861	3256	28	3351	64	3181	34	98	0.010	105.34
PD17-56-594.d	20.76	0.42	0.5925	0.0088	0.74126	3126	20	2997	36	3194	29	40.3	0.025	93.83
PD17-56-595.d	24.88	0.67	0.669	0.013	0.48456	3300	26	3300	52	3273	42	0.922	1.085	100.82
PD17-56-596.d	23.37	0.63	0.65	0.015	0.64171	3239	26	3223	60	3241	38	2.21	0.452	99.44
PD17-56-597.d	21.48	0.48	0.613	0.011	0.86536	3159	22	3082	46	3203	30	22.7	0.044	96.22
PD17-56-598.d	22.22	0.43	0.611	0.0086	0.76905	3192	19	3072	35	3254	28	20.7	0.048	94.41
PD17-56-599.d	23.11	0.47	0.632	0.011	0.68989	3232	19	3156	43	3261	31	4.16	0.240	96.78
PD17-56-600.d	24.9	0.69	0.655	0.013	0.58845	3299	28	3245	51	3319	39	1.06	0.943	97.77
PD17-56-601.d	25.68	0.49	0.668	0.0093	0.65709	3333	19	3296	36	3337	30	0.9958	1.004	98.77
PD17-56-610.d	22.47	0.57	0.584	0.014	0.54976	3201	25	2963	55	3342	40	1.1	0.909	88.66
PD17-56-611.d	21.53	0.58	0.574	0.015	0.60532	3159	26	2919	61	3303	42	1.065	0.939	88.37
PD17-56-612.d	25.36	0.75	0.676	0.015	0.54886	3316	29	3324	57	3298	44	1.394	0.717	100.79
PD17-56-613.d	22.27	0.52	0.615	0.012	0.7823	3193	22	3088	46	3245	30	2.52	0.397	95.16
PD17-56-614.d	15.71	0.66	0.422	0.016	0.70934	2854	39	2267	73	3292	53	1.551	0.645	68.86
PD17-56-615.d	23.87	0.68	0.657	0.016	0.72845	3259	28	3252	62	3248	39	2.46	0.407	100.12
PD17-56-616.d	23.01	0.56	0.62	0.014	0.74019	3225	24	3108	58	3282	34	1.087	0.920	94.70
PD17-56-617.d	21.66	0.46	0.583	0.011	0.6782	3166	21	2958	45	3287	33	0.512	1.953	89.99
PD17-56-618.d	22.12	0.72	0.613	0.018	0.59148	3186	31	3078	72	3237	48	3.06	0.327	95.09
PD17-56-619.d	22.18	0.54	0.637	0.011	0.76058	3188	23	3176	45	3176	30	12.4	0.081	100.00
PD17-56-620.d	26	0.66	0.678	0.016	0.66321	3344	25	3334	61	3334	37	0.8	1.250	100.00
PD17-56-621.d	23.96	0.58	0.662	0.014	0.81384	3264	24	3272	53	3243	31	2.1	0.476	100.89
PD17-56-630.d	23.72	0.49	0.646	0.011	0.58238	3255	20	3219	42	3267	33	3.52	0.284	98.53
PD17-56-631.d	22.51	0.49	0.622	0.01	0.69837	3204	21	3115	41	3245	33	1.267	0.789	95.99
PD17-56-632.d	21.4	0.54	0.588	0.011	0.7525	3154	25	2977	44	3248	31	6.93	0.144	91.66
PD17-56-633.d	24.58	0.7	0.658	0.015	0.57653	3287	28	3254	57	3285	39	1.004	0.996	99.06
PD17-56-634.d	22.73	0.52	0.612	0.011	0.58116	3213	22	3082	42	3286	35	0.781	1.280	93.79
PD17-56-635.d	25.25	0.76	0.669	0.016	0.52498	3316	31	3297	63	3315	47	1.59	0.629	99.46
PD17-56-636.d	24.7	0.63	0.658	0.016	0.6614	3293	25	3253	61	3305	38	0.962	1.040	98.43

PD17-56-637.d	25.39	0.61	0.681	0.014	0.62705	3321	23	3346	54	3291	36	1.191	0.840	101.67
PD17-56-638.d	6.96	0.25	0.1884	0.0068	0.47287	2102	32	1112	37	3277	60	5.26	0.190	33.93
PD17-56-639.d	24.42	0.55	0.648	0.013	0.77038	3286	21	3215	53	3312	33	0.651	1.536	97.07
PD17-56-640.d	24.72	0.77	0.653	0.016	0.63946	3292	31	3236	64	3310	43	1	1.000	97.76
PD17-56-641.d	22.74	0.77	0.642	0.019	0.83054	3209	33	3192	75	3198	38	3.7	0.270	99.81
PD17-56-642.d	24.54	0.64	0.66	0.014	0.58364	3286	25	3263	56	3286	39	0.905	1.105	99.30
PD17-56-651.d	21.12	0.55	0.595	0.015	0.75625	3147	23	3008	61	3211	35	3.07	0.326	93.68
PD17-56-652.d	21.99	0.61	0.609	0.016	0.75002	3180	27	3062	64	3241	36	2.077	0.481	94.48
PD17-56-653.d	24.49	0.51	0.644	0.01	0.59434	3289	19	3201	39	3324	32	0.7182	1.392	96.30

Appendix 2.2 Zircon REE compositions (ppm) – Granitoids of the Dharwar Craton

Comments	La139	Ce140	Pr141	Nd146	Sm147	Eu153	Gd157	Tb159	Dy163	Ho165	Er166	Tm169	Yb172	Lu175	Hf178
PD17-44-363	6.49	32.9	2.17	11	12.1	1.57	60.2	20.3	235	81.3	372	80.6	734	139.1	15660
PD17-44-364	34.1	128.6	12.9	68.9	39.6	3.79	129	37.9	374	123.3	552	121.1	1148	220.9	12890
PD17-44-365	48.3	151.3	17.74	103.2	85.8	16.2	261	66.8	493	105.6	331	63	604	129.1	15390
PD17-44-366	36.2	98.5	12.1	68.3	43.7	12.2	136	35.2	301	82.3	346	77.8	802	168.8	15590
PD17-44-367	7.15	40.4	3.59	22.7	18.4	3.03	60.7	17.9	180.6	57	241.1	51.9	513	103.8	12540
PD17-44-369	1.23	17.5	0.403	2.39	3.68	0.313	21.8	8.78	119.1	47.5	231.7	52.5	504	95.8	15480
PD17-44-370	7.96	56.5	3.42	22.9	25	3.5	99.7	30.6	315	104	432	84.5	743	138.1	11760
PD17-44-371	21.9	53.4	6.69	38.6	29.5	3.91	87.9	20.9	184.3	59.8	303	74.8	788	179.1	12100
PD17-44-372	38.7	160.2	16.7	102.8	82.9	10.48	234	58.2	524	151.9	578	110.4	965	172.1	13740
PD17-44-383	10.5	34.8	2.98	17.4	9.2	5.1	30.1	8.9	114.6	54	312	76.1	778	161.8	11230
PD17-44-384	17.2	60.2	7.4	46.3	39	7.7	135	38	341	98	365	64.3	565	104.4	11460
PD17-44-385	280	580	63	202	39.5	4.03	90.8	25.8	276	95.2	402	83.4	773	151.7	10440
PD17-44-386	46.9	115.2	14.12	76.2	59.7	8.59	191	57.2	456	107.8	356	70.1	678	136.3	14750
PD17-44-387	3.84	29	1.43	9.7	10.7	1.19	48.6	16.3	199	80.9	392	90.6	896	184.6	12750
PD17-44-389	32.7	101.3	12.38	72.6	48.9	8.32	143	37.5	310	75	274	56.7	533	107.9	13720
PD17-44-390	54	106	10.8	45.9	21.2	12.53	71.4	20.8	198	61.2	263	56.8	573	114.2	11650
PD17-44-391	10.29	47.1	4.53	26.8	22.6	3.13	70.4	19.9	198.2	63.6	277.8	59.9	581	112.3	12200

PD17-44-392	0.49	11.7	0.249	1.76	3.23	0.312	17.7	7.16	104	50.6	294	73.6	797	175.3	10440
PD17-44-393	47.4	129	14.6	81.4	59.7	9.25	174.6	45.2	409	122	453	86.1	744	144.8	10360
PD17-44-402	11.7	21.7	2.31	11.1	5.5	1.03	20.6	6.5	65.1	25.1	146.7	41.2	491	119.2	16690
PD17-44-404	4.74	38.9	3.05	20.6	15.2	2.2	67.7	21.9	254	95	420	85.2	784	150.1	10630
PD17-44-405	60	158	16.1	68	26.7	7.51	69.5	19.6	179	54.6	242.4	55.5	564	116.4	13780
PD17-44-408	21.4	68.5	7.41	41.8	38.7	15.5	127	36.6	315	85.8	342	72.4	700	141.4	14060
PD17-44-409	57	126	19	90	34.1	5.2	89	24.3	241	80.5	349	72.3	683	135.6	9830
PD17-44-411	12.4	49.4	3.5	20.3	17.8	12.15	63.2	20.3	225	79	366	82.9	823	149.2	19920
PD17-44-412	0.03	4.67	0.038	0.53	0.8	0.145	6.78	3.28	53.2	27.6	168	45.8	510	117.8	14450
PD17-44-414	5.68	33	2.59	19.7	26.2	5.63	137.3	44.3	499	176.9	731	136.1	1142	206.9	10490
PD17-44-423	1.51	31.4	0.779	9.21	17.6	1.72	107.3	37	447	169.2	730	142.9	1254	234.8	10820
PD17-44-425	16.1	75.6	8.9	58.1	39.6	13.1	123.8	33.4	311	90	349	67.8	626	120.2	12930
PD17-44-426	301	630	80	400	86	13.4	105.8	20.9	181	54.4	243.7	54.7	572	125.8	10770
PD17-44-427	11.79	50.2	5.58	35.9	28.3	7.43	103.3	28.2	278	87.9	360	72.5	675	136.7	10040
PD17-38-303	42.8	123.3	12.1	63.4	22.1	7.79	55.5	16.83	190.8	64.6	275	56.2	527	103.6	11000
PD17-38-305	16	43.5	3.31	17.9	11.7	4.16	46.8	15.5	180	62.2	256	47.9	420	78.5	13690
PD17-38-306	40.8	95.1	8.9	43.3	20	6.8	65	21.2	256	84	345	66.8	592	110	11660
PD17-38-307	2.61	15.09	0.559	4.49	4.8	1.91	22.3	7.38	84.4	31.34	145.8	33.28	342.6	73	10540
PD17-38-308	0.314	11.57	0.16	2.24	3.19	1.58	19.3	6.42	75	28.6	137.5	32.3	336	73	10470
PD17-38-309	9.3	25	1.63	7.89	5.43	1.97	24.2	8.8	104	38.6	174	37.6	374	76.3	12700
PD17-38-310	74	199	19.1	102	40.3	13.8	118	35.4	391	123	477	88	746	134	10300
PD17-38-311	10.4	33.3	1.93	11.1	9.83	3.99	41	13.03	143	49.7	217	44.7	412	84.6	9200
PD17-38-312	12.23	39	2.18	12.5	10.75	3.76	43.5	13.6	156.7	55.1	237.6	51.7	508	104	10540
PD17-38-313	12.7	38.6	2.37	11.3	8.1	3.12	37.3	12.9	153	54.1	236	48.5	459	89.5	11150
PD17-38-314	35.9	93.8	7.17	30	9.7	3.25	30.4	9.64	116	39.6	169.6	36	347	71.6	10720
PD17-38-324	15.5	45.6	3.5	18.9	10.7	3.4	38.9	12.5	146	50.6	214	43.7	415	79.6	10950
PD17-38-325	19.6	75	5.46	30.7	14.9	5.32	66.2	22.5	274	97	413	83.8	761	145	12590
PD17-38-327	9.06	42.5	1.98	10.6	8.48	3.39	40	12.72	144.2	51.2	221.4	45.9	449	90	11190
PD17-38-328	25.7	90.6	5.77	28.2	16.5	5.94	72.7	24.4	267	92	376	73.7	644	121	10280

PD17-38-329	6	34	1.73	10.6	7	2.77	30.3	10.4	121	46	202	44.1	428	87.3	12740
PD17-38-330	23.6	51.7	4.04	19	9.2	3.14	29.6	10.5	128	45.3	194	40.4	388	78.6	13530
PD17-38-331	31.1	81	6.8	35.4	15.1	4.95	47.3	14	164	55.5	230	45.9	407	80.4	11060
PD17-38-332	15.1	45.3	3.35	13.9	8.1	2.96	27	8.7	103	36.9	166	37.4	376	79.9	10970
PD17-38-333	17.3	60.1	5.47	31.9	13.9	3.76	45.6	14.5	170	60.7	269	58.7	584	115.5	11090
PD17-38-334	30	22.1	2.26	7.57	1.58	0.45	7.8	3.11	45	19.2	105.1	28.4	333.3	75.6	15110
PD17-38-335	3.07	24.2	0.83	7.41	8.78	3.79	41.1	12.29	132.6	46.7	206.9	43.2	418	87	9570
PD17-38-344	25.3	92	8.5	49.5	21.5	7.67	68	20.4	232	78.4	323	64.6	592	114.9	9720
PD17-38-345	12.5	46.7	3	15.2	9.76	3.67	41.8	14	163.8	57.8	242	48.7	447	89.2	10290
PD17-38-347	5.5	20.9	1.24	7.3	5.5	2.51	27.6	8.8	110	38.6	173	36.4	348	72.5	10520
PD17-38-348	Below LOD	29.3	0.117	2.44	7.69	3.18	50.8	18.9	230	85.3	371	76.1	689	131.5	11800
PD17-38-349	16.3	54.7	4.79	26.4	13.2	4.52	45.6	16.1	186	64.9	276	56.7	526	97.2	11110
PD17-38-350	19.2	49	4.27	22.1	9	3.55	34.9	11	135	48.7	218	46.7	479	99.3	10620
PD17-38-351	10.3	50.9	2.83	16.9	13.8	5.01	62	21.1	252	89.1	385	78.4	720	139.8	11430
PD17-38-352	225	404	44.9	227	121.3	37.2	385	129.3	1509	450	1697	294	2259	348	11350
PD17-38-353	27.2	80.2	7.11	39.3	17.6	6.89	61.4	19.5	221	74.5	301	61.7	547	106.6	9460
PD17-38-354	20.8	44	2.95	14.3	9.42	3.64	42.5	13.85	158.4	55.1	236.2	47	436.9	87.8	9380
PD18-126 - 5	32.8	137.6	20.9	141.7	58.9	14.65	66.3	10.63	90	29.11	131.5	28.64	283.1	61.3	9060
PD18-126 - 6	56.5	270	37.6	229	126.9	56.6	218.8	39.7	316.7	91.6	348.1	71.8	682	134.7	10570
PD18-126 - 7	28.3	132	21.5	147	67.8	12.77	74.3	9.55	63.9	19.63	90.7	20.82	226.8	52.6	9680
PD18-126 - 9	17.9	112	10.3	66	27.1	9.5	51.6	12.52	131.4	47.53	206.1	44	399.9	77.5	9980
PD18-126 - 11	0.101	12.76	0.172	0.8	0.93	0.37	5.21	1.81	26.9	11.69	66.1	16.81	192.2	46.6	10600
PD18-126 - 12	0.395	21.54	0.57	3.14	2.94	0.81	11.3	4.12	54.1	24.85	137	33.4	360	79.6	8980
PD18-126 - 13	39.2	114.9	14.56	74.6	8.86	6.88	8.78	2.03	26.8	13.7	84	23.14	267.2	61.2	11160
PD18-126 - 14	20.7	92.1	12.05	71.7	23.3	9.2	39.9	9.64	96.9	33	145	31.3	316	64.4	10820
PD18-126 - 15	62.8	281	34.9	206	77.3	14.7	77.5	12.12	99.4	33.8	159.4	36.2	375.3	84.3	9640
PD18-126 - 17	8.5	68	6.4	37	18.8	4.2	33.2	9.05	93.3	35.39	160.4	35.72	355.3	71.1	10260
PD18-126 - 19	5.94	65	4.02	19.8	9.43	2.69	34.6	10.93	123.2	44.9	190.8	39.16	357.6	69.3	8100
PD18-126 - 20	4.29	125	3.38	28.5	30.2	10.32	86.7	21.9	203	64.2	267	53.4	491	99.5	7560

PD18-126 - 21	15.2	70.6	10	55.8	26.7	4.19	30	5.57	49	18.31	88.3	21.16	230.2	51.5	10460
PD18-126 - 22	44.6	214.7	37.3	260.9	111.2	49.6	112.6	12.4	76.1	20.83	98.7	25.67	293.8	67.3	9980
PD18-126 - 24	25.5	164	18	100.5	41.9	12.4	53.6	10.4	91.1	31.5	150.2	34.4	355	78.1	10090
PD18-126 - 27	58.1	347	44.2	339	183	73.3	194	20.3	109.2	29.4	123.7	27.3	279.9	60.8	10390
PD18-126 - 28	39.9	202	33.9	211	86.1	28.3	80.4	10.91	65.1	19.28	92.2	23.12	258.7	59.9	10250
PD18-126 - 31	23.5	129.2	17.9	105	41.6	7.66	42.8	7.19	61.8	24.24	116	27.01	294.2	63.5	10630
PD18-126 - 32	5.08	51.7	3.04	20.3	16.2	5.22	61.2	18.78	206.5	69.5	289.3	58.5	514.1	95.9	8430
PD18-126 - 33	56.5	147.2	15.64	91.8	37.2	7.84	57.3	12.46	124.2	42.8	180.6	35.2	318.1	60.3	6640
PD18-126 - 35	10.7	48.4	7.4	40.4	19.9	3.46	22.5	4.75	40.1	15.17	76.8	20.08	235.8	54.6	12520
PD18-126 - 36	14.1	59.3	7.74	48.3	20.2	4.63	24.4	4.15	37.7	15.18	81.1	20.67	244	59.4	10110
PD18-126 - 37	3.36	65.7	1.94	11.6	9.11	2.92	40	12.47	137.7	49.6	206.1	41	374	72.2	8660
PD17-32-247	0.319	26.21	0.267	2.88	6.4	0.836	42.9	16.97	226.8	89.7	415.3	85.8	787	145.6	14590
PD17-32-248	571	1020	110	503	65.5	6.67	83.5	20.7	229	82	353	69.7	620	119.4	9570
PD17-32-249	0.91	50.7	0.52	6.48	12.6	1.72	90.5	34.7	440	166.4	734	144.1	1246	222.3	11500
PD17-32-250	1.55	37.4	1.015	9.43	12.95	2.13	74.2	27	333	126.6	548	108.4	946	171.6	11180
PD17-32-252	0.354	28.37	0.204	3.06	7.83	0.988	55.7	21.66	280.2	111.4	494	101	891	165.6	12340
PD17-32-253	0.0071	17	0.034	1.06	3.29	0.468	27.5	11	148	61.1	289	61.9	591	113.5	14490
PD17-32-254	3.15	39.9	1.94	14.6	15.86	2.39	89	31.2	382	147.1	635	123.6	1080	193.1	12050
PD17-32-255	12.1	58.2	6.2	39.1	19.8	2.44	64.7	21.54	255.4	98.3	436	90.7	825	156.3	12720
PD17-32-256	0.96	46.5	0.67	7.5	12.7	1.99	77	28.2	346	130	567	110.3	994	181.3	12380
PD17-32-266	2.61	33	1.5	10.1	9.92	1.66	53.4	20.78	269.9	105.5	483	105.2	979	190.1	13170
PD17-32-267	3.47	20.6	2.14	12.4	8.25	1.57	24.5	8.69	103.2	40.9	200.8	46.8	483	99.5	12600
PD17-32-269	4.29	26.9	2.36	15.1	12.39	2.24	45.6	16.43	204	84.2	433	102.6	1025	211.1	12840
PD17-32-270	5.65	114.2	3.26	25.1	21.6	3.79	102	35.8	434	163.2	697	140.9	1235	219.1	12690
PD17-32-271	0.922	12.64	0.567	6.24	9.27	2.69	58.3	19.02	227.6	83.4	355.7	70.2	623	118.5	10130
PD17-32-272	3.79	36.6	2.44	15.5	12.53	2.22	50.9	16.02	186.6	68.4	299.2	61.3	556	107.2	12220
PD17-32-274	1.74	29.36	1.015	9.81	15.46	2.12	89.9	31.96	383.5	146.7	634	124.2	1069	192.8	11760
PD17-32-275	3.7	22.2	2.05	14.3	10.3	2.2	34.4	11.1	131.6	53.7	272	65.4	694	149.3	14380
PD17-32-276	0.021	31.3	0.2	4.78	12.87	1.49	86.1	31.8	404	157.1	686	134.4	1156	208.4	11500

PD17-32-277	0.462	26.09	0.577	8.2	17.4	2.78	103.4	35.2	424	155.7	660	127.4	1115	199	11950
PD17-32-288	0.115	37.69	0.183	3.51	11.02	1.22	73.7	28.07	364.8	142.9	622	121.8	1078	194.3	11590
PD17-32-290	2.08	28.58	0.883	8.47	14.21	1.98	88	31.19	376.6	142.2	616	120.4	1016	189.1	11560
PD17-32-291	0.716	9.43	0.367	2.43	1.7	0.192	9.47	3.87	56.5	25.64	134.1	31.63	334.4	73.3	15320
PD17-32-292	2.05	11.15	1.103	6.76	4.1	0.89	15.15	5.56	73.4	30.64	169.2	42.8	483	109.1	14260
PD17-32-293	9.6	61.2	7.81	51.1	23.9	5.09	53.7	14.7	162	57.4	274	65.3	721	152.4	15930
PD17-27-429	9.5	77.5	5.11	30.2	17.2	3.69	59.3	18.85	217.8	82.7	368.7	76.2	678	135.5	10840
PD17-27-430	45.4	194	19.8	101	29.1	5.01	54.9	16.97	187.3	69.1	321.9	68.4	651	133.5	11280
PD17-27-432	9.6	86.2	4.3	22.1	13.36	2.62	41.9	13.85	162.2	61.9	285.4	61.3	574	117.1	11320
PD17-27-433	10.08	104.8	5.28	31.5	20.4	4.39	66.5	20.8	239.1	89.6	402	83.9	751	148	10810
PD17-27-434	37.3	196	23.7	119	56.2	11	105	29.5	296	101.1	437	91	834	165.9	11520
PD17-27-435	15.4	90.5	7.54	41.5	23.6	4.29	74.7	23.12	264.7	97.2	423	87.3	775	146.8	10120
PD17-27-436	11.4	63.8	4.59	28	16.8	3.13	58.5	18.5	211.5	80.1	352	71.9	653	123.3	9930
PD17-27-437	3.84	41.5	1.85	11.7	9.5	2.01	39.6	14.24	170.7	67.4	316	68.9	641	125.9	10770
PD17-27-438	13.3	65.2	2.76	14.8	9.35	1.81	38.6	13.57	162.5	63.6	291	61.3	566	110.6	10290
PD17-27-450	17.5	100.2	11.1	63	34.3	7.09	86	22.7	245	84.6	371	75.7	706	139.6	11110
PD17-27-451	5.45	53.6	2.22	11.68	7.62	1.271	30.9	11.11	136.5	54.4	247.7	53.3	499	101.1	11780
PD17-27-452	8.1	66.1	4.37	23.6	15.15	3	54.9	17.96	207.5	77.9	344.1	70	633	124.1	10270
PD17-27-454	191	359	30.6	108.2	27.6	5.4	69.6	20.98	244.9	89.1	388	78.8	712	139.7	10150
PD17-27-455	58.2	220	24.4	112	41	8	75.1	20.7	219	75.9	334	71.4	680	128.6	11140
PD17-27-456	11.29	63	7.42	36.5	17.6	3.59	33.2	9.5	102.4	36.21	165.9	36.7	363.4	77.9	11340
PD17-27-457	82.9	229	23.2	106.8	32.1	6.24	62.3	17.2	178	61.7	271	56.7	524	105.5	11660
PD17-27-458	17.5	110	11.9	68	30.4	6.85	69.3	18.7	193.6	68.5	304.6	64	586	116.1	10750
PD17-27-459	29.3	90.8	8.4	41.7	20	3.43	64.3	20.91	243.7	89.6	391.5	80	709	134.3	10260
PD17-27-460	26	145	15.1	75.8	34.8	6.72	84.8	25.2	282.5	99.8	434	87.6	798	154.8	10440
PD17-27-461	50	175	14.4	67.5	21.6	4.65	49.8	14.24	155.7	57.2	256	53.5	488	97.6	10540
PD17-27-462	24.3	200	12.4	67	32.1	6.65	78.9	23.8	255	89.3	392	80.5	728	141.1	10550
PD17-27-471	4.34	46.2	3.12	18.5	12.9	2.41	47.4	15.3	186	71.2	321	67	620	119.5	11200
PD17-27-472	12.5	56.2	5.54	29.5	14.5	3.04	44.2	12.7	146.7	53.3	247.9	53	507	100.9	10630

PD17-27-473	8.59	90.7	5.47	28.4	17.67	3.24	59.2	20.28	247.2	93.4	429	89.6	832	160.2	10810
PD17-27-474	14.3	97.3	9.4	54.5	26.5	5.55	75.7	22.38	254.1	91.5	404	83.3	749	147.9	10750
PD18-116 - 1	19.9	145.6	20.2	108.1	80	15.6	147.2	40.3	316	86	323.4	62.3	547	102.7	9200
PD18-116 - 2	4.46	45.3	4.25	36.6	27.2	9.3	69.7	15.7	151	49.6	201	41.8	406	83.2	11090
PD18-116 - 4	14.4	94.2	10.45	60.8	42.8	10	93.4	23.7	213	63.8	248.5	48.28	429.4	83	8970
PD18-116 - 5	6.5	38	6.2	35	25	5.4	43	9.7	88	21.8	92	20.1	208	42.9	11520
PD18-116 - 9	1.86	35.4	2.17	19.9	10.8	4.18	30.2	7.1	80.8	31.2	148	33.5	325	68.4	10680
PD18-116 - 10	10.85	81.6	10	80	53.5	17.5	129.7	22.4	161.6	42.6	162.6	35.28	357	76.5	12590
PD18-116 - 12	7.36	48.2	6.83	44	30.3	10.13	63.4	15.01	136.4	41.3	178.5	39.2	373.8	81.1	12800
PD18-116 - 15	1.76	44.3	2.04	17.9	16	4.23	52.4	14.04	149.3	51.4	217.2	43.31	392.8	75.6	8304
PD18-116 - 16	4	34	3.69	24.8	17.3	7.29	44.8	8.18	84.4	29.6	137	31.43	338.4	81	11960
PD18-116 - 18	8.1	61.2	8	52.8	37.9	16.9	97.3	15.3	123.8	37.4	161.5	37.37	377.4	84.9	11180
PD18-116 - 20	6.48	87.7	6.31	35.7	29.7	6.41	66.4	19.71	202.2	67.5	287	59.6	544	104.4	9840
PD18-116 - 22	49.4	300	48.7	261	176	34	272	69.2	537	123.4	438	81.3	697	128.9	6820
PD18-116 - 23	1.1	15.6	0.99	8.9	7.2	1.82	19.4	5.5	63.9	26.33	134	31.98	332	71.3	12100
PD18-116 - 25	2.25	40.9	2.17	19	14.8	7.09	42.4	10.8	100.7	32.6	132.1	28.5	284	60	9350
PD18-116 - 26	1.51	36.7	1.69	11.7	10.2	2.69	27.7	7.59	80.1	28.7	132.1	30.05	305.4	66.2	9160
PD18-116 - 28	3.93	58.1	3.97	26.4	19.2	6.21	47.8	11.68	104.7	34.13	148.6	31.26	316.4	69.1	7690
PD18-116 - 29	1.29	17.62	0.97	9.02	7.89	3.26	25	6.63	64.2	21.7	86.9	17.31	156.4	30	7450
PD18-116 - 31	1.16	36.2	1.25	9.8	8.2	2.65	30.2	8.56	95.7	35.1	159	34.4	325	68.3	9390
PD18-116 - 34	0.288	15.3	0.343	4.14	7.66	1.06	54.1	19.69	256	104	473	96.3	861	166.2	10980
PD18-116 - 35	25.5	183	25.9	145	106.2	21.6	167	41.2	306	74.8	265	50.4	459	97.1	7950
PD18-116 - 38	22.3	168	21.9	129	91.5	22.4	171	37.6	286	69.6	245	46.5	425	83.9	9830
PD18-118 - 1	0.016	10.1	0.378	7.23	17.7	5.16	121.4	42.47	508	191.5	821	160.9	1444	276.1	10300
PD18-118 - 2	0.142	8.78	0.331	6.07	15.51	4.31	101.4	35.3	424	157.4	672	133.3	1165	217.8	10050
PD18-118 - 3	1.06	12.34	0.906	10.81	22.4	5.69	138.8	46.8	552	204.1	868	168.8	1499	286	10980
PD18-118 - 4	0.152	10.65	0.91	14.2	30.5	7.44	177	59.7	695	256	1096	221	1990	383	10900
PD18-118 - 5	1.13	9.79	0.91	8	10.96	2.87	61.6	22.18	275.7	107.2	483	101	948	189.2	11330

PD18-118 - 6	0.185	6.69	0.344	5.84	12.6	3.87	81	28.1	333	125.8	545	110.4	996	194.7	10790
PD18-118 - 7	0.091	9.89	0.348	6.76	17.61	4.99	125.6	43	512	192.3	807	159.2	1391	264.4	10460
PD18-118 - 8	0.03	10.04	0.457	8.88	20.5	5.47	127.9	43.2	501	183.6	767	149.5	1301	246.5	10100
PD18-118 - 9	0.0154	8.83	0.294	6.69	17.1	4.51	112.9	39.6	466	175.3	759	149.6	1330	254.6	10190
PD18-118 - 10	0.02	10.11	0.351	7.28	19.17	4.68	122.3	41.47	474	174.2	720	142.1	1233	230.8	10660
PD18-118 - 14	Below LOD	6.06	0.125	2.78	8.64	2.38	72.3	27	346	137.1	613	127.4	1180	232.8	10900
PD18-118 - 15	0.0094	7.64	0.096	2.9	10.25	2.36	80.9	31.6	401	159.4	719	146.9	1351	265.3	11100
PD18-118 - 16	0.186	10.4	1.21	17.9	32.6	7.8	164	52	589	214	886	174	1520	288	10690
PD18-118 - 17	0.017	7.46	0.157	3.91	11.04	3.08	92.5	35.12	445	174.9	779	160.3	1477	290	11180
PD18-118 - 18	0.089	9.31	0.55	8.3	16.9	4.89	106.7	39.3	472	179.7	789	160.2	1445	279.8	10830
PD18-118 - 19	0.0091	5.28	0.086	1.86	6.51	2.05	55.1	20.74	271.2	110.4	501	104.9	966	190.7	10950
PD18-118 - 20	0.0156	10.3	0.457	8.8	22	5.54	144.2	49.6	583	213	904	176.7	1529	287.4	10640
PD18-118 - 21	0.014	6.54	0.169	4.07	10.72	3.3	76.5	26.71	325.1	123.4	532.5	107.2	970	186.9	10730
PD18-118 - 22	0.54	9.9	0.487	6.98	14.05	4.08	91.8	32.38	392	149.4	650.1	129.3	1166	224.6	10380
PD18-118 - 23	0.043	7.29	0.265	4.95	12.51	4.04	86.8	30	363	136	591	119.2	1063	205.1	10790
PD18-118 - 24	Below LOD	4.88	0.071	1.76	6.11	1.68	50.4	19.34	250.2	99.8	458.6	97	928	187.6	11070
PD18-118 - 26	0.528	9.19	0.529	7.03	13.2	4.34	86.3	29.4	354	133.8	581	116.8	1043	200.2	10610
PD18-118 - 27	0.0142	7.29	0.24	4.79	13.15	3.71	88.8	31.6	378.9	142.7	610	123.2	1110	212.4	10650
PD18-118 - 30	0.018	4.13	0.107	1.97	6.02	1.64	43.1	17.3	222	87.9	412	88.7	848	173	9110
PD18-118 - 31	0.084	8.15	0.229	4.6	12.49	3.4	88.6	32.25	398.8	151.1	667	136	1231	240.1	10340
PD18-118 - 32	0.354	5.35	0.251	2.78	5.98	1.91	45.2	16.26	204.6	81.4	366.7	77.5	738	152.3	10810
PD18-118 - 33	0.019	9.51	0.246	6.45	18.68	4.86	128.7	46.2	560	210.7	895	175.4	1540	295	10850
PD18-118 - 34	0.0171	6.85	0.143	3.04	10.14	2.8	76.5	28.1	357	138.4	617	127.4	1156	227	10680
PD18-118 - 35	Below LOD	7.94	0.163	4.35	12.8	3.69	93.2	32.8	401	153.1	658	132.1	1179	226	11020
PD18-118 - 37	Below LOD	8.76	0.17	4.06	13.53	3.49	108.5	40.4	514	198.8	869	175.4	1567	302.1	10940
PD18-118 - 38	Below LOD	7.1	0.175	3.7	10.44	2.96	76.4	27.68	343.4	130.8	572.4	115.9	1039	203.7	10960
PD17-21-186	10.9	116.7	4.4	27.3	23.8	8.2	93.6	32.1	383	149.3	683	151	1450	285	12040
PD17-21-187	14.8	81	5.5	28.3	18.1	4	62.3	19.89	237	87.9	407	85.4	798	156.7	11060
PD17-21-188	3.99	58.8	1.5	13.4	15.4	3.83	67.9	21.6	243	87.3	381	76.9	693	132.5	10190

PD17-21-189	50.9	157.7	12.94	75.7	22.2	8.78	51.7	15.86	189.3	73.1	337	74.5	717	150.9	13460
PD17-21-190	15.1	93.2	5.46	27.1	13	3.57	52	17.05	201	76.9	351.4	74.6	688	137.3	11340
PD17-21-191	12.6	95.6	5.26	31.2	14.8	3.64	56.1	19.2	234.7	92.6	418.8	91	838	160.5	11200
PD17-21-192	19.7	96	8.5	44.7	16.9	3.6	50.8	15.82	189.8	74.5	351	78.5	751	156.4	10950
PD17-21-193	7.79	66	3.76	25.6	16.5	5.3	56.4	18.43	218.2	84.2	386	83	762	147.4	11180
PD17-21-196	22.9	92	6.01	26.8	11.87	2.99	42.7	15.02	192.4	79.7	387.2	88.4	883	184.1	13000
PD17-21-197	29.4	131	15.7	79.3	24.1	9.7	50.7	13.44	139.7	52	238.9	53.4	530	119.8	12980
PD17-21-206	13.5	74.9	4.82	25.7	13.29	2.89	47.7	14.6	180.5	69.7	317.1	67.9	637	126.3	10680
PD17-21-207	24	77.2	5.03	23.6	10	2.97	37.1	13.02	167	67.8	331	76.4	794	176.2	13810
PD17-21-209	75	231	22	128	37.4	11.03	66.5	18.05	204.2	78.4	368	80.4	766	153.8	11410
PD17-21-211	3.24	33.7	1.41	8.2	5.27	2.39	23.2	8.34	110.5	46.3	241.9	57.2	608	139.7	12380
PD17-21-212	108	252	23.1	87.6	30	6.87	65.7	18.25	196.4	72	345	78.6	835	181.5	13620
PD17-21-213	4.81	53.4	1.67	10.5	10.48	2.69	52.4	18.56	235.2	92.3	437	92.9	859	171.2	11520
PD17-21-215	10	60.8	2.96	17.3	11.4	3.09	43.8	13.75	157	58.3	264	55.4	508	98.6	10790
PD17-21-216	29.5	123.6	11.25	71.7	17.8	4.31	48.8	14.06	160.7	60.5	267.9	58.9	583	129.7	14240
PD17-21-217	5.3	55.1	2.12	12.4	10.67	2.43	49.6	16.69	204.1	79.2	363	77.7	736	146.7	10790
PD17-21-218	18.27	84.4	4.43	29.5	14.8	8.49	54.4	16.27	185.6	68.8	300	62.9	579	111.7	10660
PD17-21-227	11.9	61.5	3.99	21.1	11.2	2.6	42.1	13.99	163.9	63.5	295	64.7	635	131.5	13020
PD17-21-228	3.61	57.7	1.53	9.91	9.81	2.31	42.4	14.66	180.1	72.4	340.6	73.7	703	143	11500
PD17-21-229	9.5	79.1	5.32	38.4	11.02	6.17	19.9	5.99	84	42.2	266.6	80.4	1061	293.5	20960
PD17-21-230	35.1	126	8.4	41.2	14.9	3.24	49.4	16.55	202.2	77.4	356	77.3	722	138.2	10580
PD17-21-232	6.83	61.3	2.12	12.78	12.9	3.87	55.5	17.1	199.4	77.8	363.5	79.6	776	160.7	10580
PD17-21-233	2.74	37.5	1.51	8.92	8.07	2.12	38.2	13.2	166.9	67.2	319	69.6	657	131.9	12560
PD17-21-235	27.3	91.9	5.54	25	9.87	2.22	33.1	11.24	138.3	53	255.4	56.1	545.6	117.3	12040
PD17-21-236	13	81	4.3	21	9.06	1.84	32	10.88	133.6	51.8	241.2	51.7	491	96.4	11250
PD18-108-70	95.7	1228	119.1	676	327	53.1	342	56.6	351	84.8	291.2	54.7	463	86.2	12960
PD18-108-72	261	2360	210	1235	472	75.7	484	70	383	78.7	250	47.2	454	94.6	11960
PD18-108-73	24	161	21.3	133	43.8	25.1	52.4	9.1	83.7	28.4	123.4	27.9	259	55.9	11340
PD18-108-75	11.07	98.9	12.9	79.5	30	10.95	38.9	7.77	65.5	21.3	90.2	20.21	191.2	38.9	10870

PD18-108-76	10.9	120	12.8	78	41.5	10.9	56.6	10.7	87	27.9	115.1	23.45	214.9	43	8520
PD18-108-77	3.13	21	3.3	18.8	6.7	1.11	11.3	3.02	35.7	15.08	72.3	16.27	154.9	32.1	11270
PD18-108-78	143	759	81.4	530	279	82.3	363	45.1	265	64.6	226.4	43.5	390	75.7	12240
PD18-108-79	9.13	92.6	7.98	46.7	21.9	11.11	49.2	12.49	129	44.2	191.7	40.3	383	77.1	9250
PD18-108-80	14	55	5.7	27.3	5.42	5.9	21.5	6.25	64.2	22.6	97.5	20.2	182	37.9	8380
PD18-108-81	3.2	30.3	1.92	11.8	7.84	2.28	34.5	12.81	149.1	55.7	246.3	51.3	454	84.4	11940
PD18-108-83	6.41	64.5	6.41	41.1	20.9	3.96	37.1	8.55	85.9	32.5	147	33.7	333	76.5	10920
PD18-108-84	84.3	824	80.7	446	171.2	58.1	179.4	30.5	189.5	42.3	146.3	28.2	254	47.8	11670
PD18-108-92	96	971	94.3	500	161	33.4	155	20.7	140	44.7	219.9	55.8	615	142	12080
PD18-108-93	48.9	390	45.8	265	96	21.2	118	24.1	210	61.2	250	49.6	456	86.3	11860
PD18-108-94	10.94	92.5	9.67	55	18.5	9.05	32.1	7.42	73.4	26.6	107.8	22.21	201	37.9	12240
PD18-108-96	1.79	36.7	2.06	19	16.3	7.09	63.6	16.83	164.2	54	214.4	41.6	368	71.6	8320
PD18-108-98	7.6	63.3	5.87	38.2	21.5	3.88	62	15.9	166	53.9	222	44.7	399	72.7	11600
PD18-108-99	7.81	71.3	7.92	39	22.5	10.53	51.4	13.07	123.2	40.7	163.4	32.8	284	54.7	8820
PD18-108-100	14.8	127	12.2	69.9	34.3	5.87	59	14.77	146.9	52.2	223.3	48.3	456	91.2	10170
PD18-108-101	14.8	105.4	12.4	74.2	26.6	8.39	48	12.82	139.6	51.3	224.2	46.9	438	82.9	11620
PD18-108-102	94.8	531	67.6	353	94.7	32.5	97.2	17	147.7	48	209	45.3	431	85.1	10180
PD18-108-103	187.9	1279	88.3	418	146	57.7	161	27.6	207.5	58.3	235.7	47.9	438	82.8	14360
PD18-108-104	32.8	266	31	179	49.6	14.4	43.7	6.95	53.1	17.26	78.4	18.13	195.6	42.2	12070
PD18-108-105	11.1	58.7	6.03	33	15.6	4.71	34.7	8.88	95.4	34	145	30.2	280.9	57.1	9510
PD18-108-106	6.73	52.9	6.15	38.6	18.3	7.65	19.6	4.27	34.7	11.6	50.9	10.79	108.4	22.32	10720
PD18-108-114	101	627	78.1	482	107.5	41.1	115.6	21.71	186.2	59.9	241.9	49.1	457	89	12230
PD18-108-115	143.8	1178	156.8	897	446	64.2	520	88.9	564	120.2	372	63.2	503	91.3	13190
PD18-108-116	109.3	1008	107.1	656	262	41.1	298	48	332	79.8	284	52.6	450	81.4	12540
PD18-108-117	34.2	236	26.1	140.2	48.1	16.8	61.9	11.62	103	33.7	141	29.1	273	53.7	11050
PD18-108-118	4.54	60.1	3.91	21.5	11.5	4.15	28.1	7.87	91.6	35.5	158.4	34.8	328	65.3	11630
PD18-34-147	7.8	31.3	2.56	35	41.9	6.48	42.9	6.39	55.2	19.53	94	20.86	215.1	45.8	11450
PD18-34-148	0.056	19.7	0.164	2.82	4.86	1.26	23.1	6.72	72.6	26.3	117.1	24.2	236	50.2	10780
PD18-34-149	101.9	273	32.1	221	86.1	13.54	136	26.7	230	56.7	190.6	32.98	297.1	59.6	10660

PD18-34-150	257	792	101	499	125	60	446	83.1	458	84.4	288	52.3	474	92.1	11600
PD18-34-151	750	2660	415	2960	1105	98.8	1212	261	2500	616	1890	264	1720	252	11650
PD18-34-152	136	209	17.9	108	50.5	43	67.2	14.3	143	51.9	246.5	54.6	550	103.2	11950
PD18-34-153	163.9	396	38.7	235	162.5	80.4	312	52.9	412	111.3	435	79.6	706	128	11510
PD18-34-154	28.3	65.7	8.3	77.5	25.9	12.23	26.8	8.09	118.4	52.67	295.9	74.2	843	186.7	13950
PD18-34-155	278	994	143.7	764	261	62	566	131.4	1344	439	1800	338	2780	464	12990
PD18-34-156	1398	2930	209.1	1418	1127	298.5	1326	133.1	804	201.8	770	145.3	1324	242.3	12880
PD18-34-157	523	825	90.7	356	64.3	37.9	80.8	17.89	188.2	63.2	294.7	65	663	142.2	11920
PD18-34-158	11.81	124	1.29	13.02	22.3	2.61	121.6	40.9	505	181.8	823	161.7	1460	267.6	9090
PD18-34-159	10.8	55.2	4.76	30.3	18.4	2.16	65.8	23.94	315	118.5	539	105.7	933	168.5	13490
PD18-34-160	146.5	480	67.7	531	136	72.5	145.3	21.95	236.6	84.5	387	77.7	711	132.8	12460
PD18-34-161	16.7	63.6	6.93	47.5	18.41	5.46	38.8	10.13	121.8	43.87	196.5	38.02	346.4	66.2	10180
PD18-34-169	94	400	50.1	264	70.5	70.8	231	92	1090	310	962	147	1099	165.5	10190
PD18-34-170	30.2	113	6.68	34.5	18	2.43	63	18.7	235	83	382	76.4	712	132	10890
PD18-34-171	327	327	41.6	186	33.8	7.41	66	18.2	216	82.3	393	82.7	782	143.8	13880
PD18-34-172	393	1222	168.3	1313	334	172.9	298	37.3	378	138.2	636	129.1	1179	214.6	13480
PD18-34-173	36	132.6	17.1	137.4	57.2	6.91	86.3	16.28	168.8	57.4	243	44.9	405	75.9	11190
PD18-34-174	390	1270	153	904	283	28.3	400	93.2	933	228	679	99.9	759	125.4	10300
PD18-34-175	1389	1604	129.4	568	240.2	140.7	673	129.3	955	206.8	655	114.5	1097	200.6	15920
PD18-34-176	21.8	126.7	13.8	88	33	7.83	96.2	28.4	344	119.6	521	100.1	904	167.7	10330
PD18-34-177	21.6	81.5	8.77	52.3	15.5	8.12	41.5	12.05	141	52.3	246	50.6	487	97.2	10290
PD18-34-178	506	2350	317	1731	402	133.2	1144	337	3340	793	2315	314	2049	283.3	10780
PD18-34-179	179	600	93	550	184	20.9	264	54.5	498	143	549	100.3	890	159.2	12560
PD18-34-180	79.4	134	10	46.5	10	2	18.5	5.44	69.7	28.62	157.4	38.45	418	89.1	12960
PD18-34-181	60.5	142.9	11.12	59.3	49.5	20.9	118.8	18.16	128.9	31.14	116	22.5	210.1	42	10290
PD18-34-182	6.5	40.4	2.17	14.9	9.71	1.74	43.3	14.46	171.5	64.1	291	58.3	541	103.2	10240
PD18-34-183	0.059	27.99	0.144	1.86	3.7	0.762	21.94	7.99	102.4	39.85	191.5	40.44	381.2	75.5	10730
PD18-34-192	18.6	136.6	11.16	65.8	25.1	2.05	44	10.66	116	42.6	205.6	42.8	413	83.1	11510
PD18-34-193	118.4	387	35.3	156	38.2	8.86	58.5	14.54	172.9	62.2	292	59.5	565	103.6	11830

PD18-37-194	42.2	124	8.83	56.4	34.4	7.6	90.3	19.8	175	47.1	172	27.9	211	34.2	9610
PD18-37-195	12.59	78.2	4.41	36.7	25.7	9.47	70.4	15.54	134.5	36.1	139	23.5	199	35.6	7730
PD18-37-196	18.7	103.3	5.07	38.9	28.2	15.4	92.4	14.2	112.1	30.7	115.7	19.7	171	30.8	7680
PD18-37-197	6.44	29.7	1.74	12.4	5.57	1.57	11.1	2.3	22.3	6.74	27.4	5.18	51.3	10.58	12180
PD18-37-198	72.5	234	16.34	156.7	69	24.2	87.1	14.67	118.6	31.9	116	19.3	160.5	28.7	9890
PD18-37-199	6.6	43.1	2.76	20.7	8.4	3.31	21	4.41	41.2	11.7	46.6	8.33	74.1	14.62	10890
PD18-37-200	5.4	90.8	2.53	29.4	28.2	10.81	80	17.41	154.1	42.6	162	28.1	242.3	43.1	8040
PD18-37-201	7.7	43.9	3.05	21.3	15.4	3.11	34.1	6.6	51.8	14.1	51.1	8.77	74.7	14.8	10690
PD18-37-202	39	78.5	4.19	21.3	11.8	3.65	32.1	7.04	64.2	20.05	86.5	17.95	180.5	36.2	14770
PD18-37-203	5.11	56.5	1.85	14.76	15.37	5.46	45.8	10	88.9	25.54	97.2	17.36	149.2	26.6	8620
PD18-37-204	10.51	107.6	7.29	37.4	14.89	6.41	30.9	6.35	54.5	15.23	58.1	10.08	87.8	16.21	11020
PD18-37-205	30.8	160.2	7.7	34.9	16.81	7.89	56.9	13.13	123.1	35.96	135.4	23.62	200.5	35.5	8010
PD18-37-213	848	1104	77.7	760	205.5	57.8	239.4	38.6	301.2	77.9	272.6	44.6	359.1	59.8	8910
PD18-37-214	15.8	58.6	5.11	38.1	13.3	3.76	20.2	3.94	33.6	9.24	34	5.82	53.7	10.64	12270
PD18-37-215	3.06	58.8	1.18	14.88	18.86	7.52	60.2	13.05	116.9	33.01	125	22.2	187.1	33.28	8200
PD18-37-216	7.28	53	2.9	45.4	14.1	5.48	20.3	4.22	37.7	11.5	50.1	10.4	107.8	22.9	13850
PD18-37-217	13.2	84.7	3.39	19.8	17.8	7.51	54.9	12.11	107.8	30.94	117.9	20.8	179.8	32.23	7780
PD18-37-218	20.4	115.2	8.61	84.1	42	18.56	70.8	12.98	107.2	29.7	109.8	18.8	165	29.7	8060
PD18-37-219	0.127	41.6	0.489	9.7	8.2	2.86	25.8	5.77	53.4	15.7	64.9	12.2	106.6	20.8	10830
PD18-37-221	30.4	221	14.1	109	43.9	13.3	92	17.9	150	39.9	148	26.2	226	42.1	11670
PD18-37-222	356	812	83.2	528	279	51.6	363	55.3	361	73.9	213.1	30.1	201.9	31.1	10010
PD18-37-223	307	622	67	495	343	70.5	641	118.3	836	175	535	82.4	594	89.7	11720
PD18-37-224	319	549	35.8	138	40.7	13.6	87.5	19.18	172.6	50.3	200.1	36.6	318	58.1	10350
PD18-37-225	16.1	182	7.72	81.4	71.8	20.89	166.5	32.95	266.1	69.6	253.7	42.8	353.6	60.9	8150
PD18-37-226	39.4	129.1	15.76	106.2	51.6	9.07	91.5	17.31	136.5	35.3	124.7	20.25	168.7	29.61	7550
PD18-37-227	8.4	200	1.56	21.9	33.4	11.5	104	24	217	62.6	239	41.5	350	61.1	8360
PD18-37-235	20.1	116.1	6.08	63.8	23.6	4.89	62.9	15.21	150.1	45.6	181.7	31.3	270.3	46.5	10180
PD18-37-236	0.241	33.2	0.51	6.4	4.8	2	11.7	2.84	28.9	10.1	51.8	12.4	140	33.3	7470
PD18-37-237	5.17	81.8	2.99	28.5	24.9	9.31	73.8	14.51	129.2	35.71	136.1	22.85	194.9	33.98	7700

PD18-54-240	188	1350	120	1010	361	72	336	45.6	273	58.5	220	47.7	551	121.1	13990
PD18-54-241	316	1178	114	588	195	31	230	37.5	261.7	64.2	270	61.9	701	145.4	12340
PD18-54-242	32.1	125	12.2	54.5	17.7	5.78	23.2	3.76	33.7	12.7	88.9	30.5	418	101.4	13200
PD18-54-243	195	1420	131	950	299	55.2	314	49.6	323	67.3	244	50.7	553	114.9	12400
PD18-54-244	133	967	88.5	677	274	52.4	287	40.9	266	58.4	205	40	393	77.5	12270
PD18-54-245	150.3	868	113.4	766	193	40.9	213	31.2	220	53	214	46.9	519	110.3	12600
PD18-54-246	642	7410	547	4570	1355	304	1357	166.4	908	159.1	466	78.4	765	154.9	12330
PD18-54-247	187	1410	94.6	595	269	43.5	339	57.7	408	91.7	318	58.9	584	115	11870
PD18-54-248	137.2	839	81.6	536	148.5	29.7	177	28.1	204.9	52.5	215.1	46	496	105.4	10610
PD18-54-249	336	2210	212	1600	454	95	453	61.6	357	70.3	234	49.7	554	117.8	12510
PD18-54-250	270.8	1142	141.7	974	233	48	252	34.3	244	65.4	263.7	54.7	570	115	11340
PD18-54-251	23.2	161	18.5	133	43.3	9.52	67.4	14.3	141.9	44.7	199	41.7	438	90.4	12370
PD18-54-252	95	200	34.2	176	63.8	11.6	109.7	25.8	255	82.6	359.7	68.5	649	126	9690
PD18-54-260	272	990	121	760	177	33.5	190	30.3	234	62.2	251	52	544	111.7	12190
PD18-54-261	218.4	777	91.2	635	181	49.5	181	21.5	134.8	35.8	167.6	46.3	594	126.1	12300
PD18-54-262	78	364	51	302	75.7	16.9	84.1	14.5	107.2	27.1	124.5	31.5	395	87.8	13230
PD18-54-263	216	827	118.7	676	150	28.1	157.9	27.2	231	64.3	270	54.5	549	107.9	13100
PD18-54-264	1177	3480	457	2570	781	126	830	118.6	769	161.7	519	86.6	706	124.5	11970
PD18-54-265	194	930	81	400	163	32	202	34	237	53.4	208	45.6	521	113.6	13710
PD18-54-266	308.7	1113	110.4	629	213	37.1	225	33.7	220	51.2	213.1	50.6	598	126.5	13910
PD18-54-267	169	1110	91	510	183	32.5	223	39.2	290	71.1	277	55	552	109.7	12940
PD18-54-268	217	761	89.1	592	368	52.3	523	60.9	412	106	399	72.9	692	124.5	12010
PD18-54-269	252	730	76	441	198	43.7	207	26.4	182	48.9	228	54.4	653	132.5	13000
PD18-54-270	383	2680	226	1332	434	84.1	515	79.9	519	110.2	371	66.9	661	127	12740
PD18-54-271	61	393	26.5	143	51.9	12.3	101.4	24.1	225.8	71.2	296.5	56.5	513	97.4	9580
PD18-54-272	87.2	479	50.8	340	164	39.9	247	31.6	217	55.9	213.4	39.8	371.7	69.4	11550
PD18-54-273	179.5	464	85.1	546	128.7	28.4	150.7	28.5	263	81.9	359	69.3	657	124.6	11830
PD18-54-274	491	394	175	840	182	26.1	191	27.5	238	80.6	397	87.1	893	179.8	20940
PD18-54-275	361	2980	263	1611	508	92.2	596	81.8	486	87.3	280	54.8	597	127.3	12630
PD18-54-276	353	4850	425	3670	1281	278	1354	180.9	1118	219	652	97.8	753	128.8	12800

PD18-54-284	74.4	414	46.7	277	93.1	18.9	109.7	19.7	168	50.3	227	47	495	99.9	10550
PD18-54-285	147	783	100.7	777	277	54.9	286.6	35.27	223.3	50.2	180.6	35.09	356.8	73.4	12010
PD18-54-286	72	62.9	23.4	107.6	36.4	6.2	53.7	11.35	109.3	34.2	146.8	29.2	295	57.9	13380
PD18-54-287	12.6	17.25	5.14	25.5	9.24	2.46	23.8	6.44	78.1	29.2	144.5	30.2	306	64.6	10470
PD18-45-320	89	305	29.6	239	49.7	14.8	64.1	14.6	172	60.7	277	55.6	519	98.1	11710
PD18-45-328	22.9	88.5	7.4	50.7	20.1	71.1	41.4	9.82	106	37.6	180	37.9	369	70.6	12160
PD18-45-330	64.6	307	22.9	162	21	8.22	56.1	16.15	190.8	69.2	314	62.4	596	109.1	11480
PD18-45-332	6.9	75.6	2.21	21.2	19.1	3.72	83.7	25.61	308.1	109.3	482	91	819	149.9	10410
PD18-45-333	3.83	22.7	0.58	2.78	1.12	0.114	5.19	1.82	28.6	12.31	65.5	14.97	162.2	34.23	12470
PD18-45-334	39	97	7.8	48	14.7	1.79	39.6	11.09	132.8	48.1	229.8	45.6	417	80.3	11660
PD18-45-335	74	217	23.4	99	20.4	2.89	42.2	10.55	117.7	42.1	195.4	39.3	367	71.9	10860
PD18-45-336	13.69	73.8	4.47	37	9.19	4.79	23.1	7.09	88.9	33.9	163.2	34.1	335.3	64.4	10700
PD18-45-337	51.5	162.3	9.03	63	10.11	8.91	33.4	10.35	135.8	50.5	240.9	48.6	466	88.4	10950
PD18-45-338	88.3	561	50.3	442	112.6	15.4	104.2	19.28	194.7	66.8	304	57.4	534	99.4	11280
PD18-45-339	225	304	20.9	160	31.8	5.85	68.4	17.38	203.9	73.7	341.7	65.5	614	114.7	9340
PD18-45-340	84.5	151.3	10.01	65.2	9.43	2.38	27.1	8.24	103.3	38.1	185	37.1	357	68.6	11620
PD18-45-341	66.9	235.8	17.1	90.3	19.7	6.75	60.2	16.93	206.3	73.3	337	69.3	619	117.9	11800
PD18-45-342	59.1	127.4	9.72	57.7	13.2	3.32	34.9	9.53	111.9	39.2	185.8	36.5	342	66.2	9700
PD18-45-350	14	70	2.49	12.2	7.2	0.86	37.1	11.8	150.2	56	265	53.1	496	96.1	11210
PD18-45-351	19.8	74.6	3.55	22.5	7.02	2.19	37.1	11.4	144	52.2	247	48.2	455	86.8	13100
PD18-45-352	0.65	31.5	0.399	4.04	4.69	0.436	24.3	8.14	104.7	39.1	193	39.4	383	73.4	12530
PD18-45-353	80.1	170	11.3	106	16.9	3.65	41.8	12.3	149	54.4	254	48.8	464	87.3	11600
PD18-45-354	58.9	197	10.73	119.8	27.3	26.9	36.3	7.2	75.5	27.4	137.3	29.25	296.5	60.3	12630
PD18-45-357	45.1	198	19	143	31.7	6.43	52	12.61	144.3	50.3	226.3	44.3	420	79.8	11990
PD18-45-358	37.7	99.7	4.93	39.8	16.9	2.85	63.4	18.55	231.9	83.8	383.6	76.5	706	130.2	11770
PD18-45-359	70.7	169.7	13.01	74.4	14.9	3.3	44	12.3	156	55	267	52.5	490	93	13390
PD18-45-360	27.4	84.8	3.93	40.3	11.47	3.64	34.4	10.75	134.4	49.6	242	48.2	471	91.4	11270
PD18-45-362	119.3	295	25.7	229	29.4	11.88	35.1	5.75	64.6	24.44	123.4	26.92	273.4	55.1	13900
PD18-45-365	54.1	133.4	9.75	70.5	12.4	3.18	25	7.11	86.2	33.58	164.4	34.19	337	65.6	11760

PD18-47-288	12.3	66.9	5.97	41	18.8	7.53	68.4	18.6	186	53.5	198.3	32.3	264	43	11790
PD18-47-289	8.2	21.76	1.115	6.17	5.07	2.4	26.6	7.61	90.7	32.1	141.7	26.8	256.1	49	11770
PD18-47-290	15.8	41	2.55	15.8	9.8	3.65	33.7	8.91	98.4	32.4	138.7	26	239	43.8	11710
PD18-47-291	12.1	56.3	3.33	27	23.9	9.1	72.8	16.31	163	50.5	211	39.2	347	63.9	10080
PD18-47-292	6.52	22.87	1.62	10.63	5.89	1.68	18.2	3.96	32.6	8.11	26.9	4.46	37.2	6.64	10870
PD18-47-293	1.17	14.8	0.456	5.4	7.7	2.95	32.5	9.22	100.3	32.2	134.6	24.6	220	40.5	12190
PD18-47-294	41.5	100	7.84	91.6	35	12.79	60.1	11.8	114.8	31.9	119.1	20.48	174.9	29.12	12540
PD18-47-295	7.79	69.2	4.97	24.7	10.7	9.77	34.2	8.63	94.4	32.2	140	27	243	45.5	12060
PD18-47-296	3.78	14.7	0.64	4.16	4.07	1.95	17.8	5.6	57.9	18.08	77.8	15.04	136.3	25.9	12040
PD18-47-297	19.9	82	7.41	40.3	20.7	6.6	60.6	15.71	156	45.9	190.3	34.7	307.5	56.5	10240
PD18-47-298	4230	9370	958	3690	673	48.4	567	79.5	460	76.9	206.3	28.65	220.7	35.27	8600
PD18-47-306	3.67	29.4	1.17	7.52	6.57	2.78	30.6	9.32	106	35.15	153.9	29.09	261.4	49.05	9570
PD18-47-307	13.5	51.4	4.57	29.6	17.6	5.02	48.5	10.71	109	32	133.1	24.3	227.6	40.7	13380
PD18-47-308	18.77	117.6	15.78	107.6	54.1	22.2	113.3	23.65	202.5	53.3	196.8	34.67	297.1	52.1	12540
PD18-47-309	38.3	118	10.9	46.8	10.4	2.86	38	13.76	181	61.5	255	46.1	392	67.9	13230
PD18-47-310	11.03	52.9	4.97	37.8	15.2	15.4	38.7	9.5	107.8	35.5	150.9	27.64	247	42	16750
PD18-47-311	10.83	53.1	2.9	28.9	19.1	10.25	49.5	11.1	114.4	34.3	139.7	24.57	221.7	39.9	10280
PD18-47-312	9.34	39.9	3.98	24.1	9.28	3.77	27.9	6.96	79.1	26.7	119.7	24.2	243.2	50.4	13830
PD18-47-313	2.98	16	0.798	6.6	6.74	2.62	24.6	6.11	67.9	22.3	100.1	20.3	194	36.4	12710
PD18-47-314	88	89.2	12.76	39.5	4.29	1.21	3.63	1.23	23.9	13.47	96.7	27.7	361	93.7	33200
PD18-47-315	11.8	69	3.57	20.2	13.43	4.91	45.9	11.48	117.7	36.3	148.1	26.34	234.8	43.3	9200
PD18-47-318	31.6	106	12.5	63.4	28.7	8.82	65.2	15.03	145.1	43.8	174.9	31.81	289.4	53.2	10680
PD18-27-101	12.03	43.5	5.83	36.4	14.5	2.28	29.2	8.32	102	35.39	169.2	35.68	324.4	58.5	12310
PD18-27-102	14	61.3	4.49	47.7	63.6	23.3	99.3	11.85	97.2	30.9	129.8	26.84	263	49	11480
PD18-27-103	382	1320	217	1320	461	45.8	579	90.6	550	107.7	303	49.1	386	67.3	12120
PD18-27-104	311	1108	143.2	857	324	60	691	183.1	1345	255.2	548	60.4	406.3	63.8	12520
PD18-27-105	57.5	229.7	28.4	189.1	30	31.3	72.9	16.4	149	41.2	160.5	32	304.1	56.4	13450
PD18-27-106	62.9	257	29.3	103.7	15.47	8.76	25.7	6.75	78.4	29.1	143.1	32.9	337	65.3	12460

PD18-27-107	18	62.6	5.44	56.3	64.7	28.9	104.7	16.92	146	43.6	169	32.53	291.5	51.9	12770
PD18-27-108	217	769	98.7	704	289	48.7	456	93.5	727	154.5	418	61.1	418	66.5	10690
PD18-27-109	281	873	124.5	782	195	63.9	295	69.1	621	142.9	359	43.7	294.3	45.8	12720
PD18-27-110	51.5	169	21.9	137	51	10.8	81.7	16.5	149	45.1	180.2	35.1	316	56.7	13280
PD18-27-111	217.2	1082	125.3	800	341	87.4	341	45	345	96.9	387	74.4	629	116.3	13150
PD18-27-112	25.2	110	12.5	75	22.3	10.8	40.9	8.57	86.5	30.2	139.6	30.9	306	58.2	11250
PD18-27-113	7	16	0.671	4.35	6.88	2.65	39.1	12.02	130.6	41.6	164	29.6	254.7	45	12640
PD18-27-114	106.9	402	61.3	426	80.1	44.3	123.3	25.7	216	52.1	179.7	32.5	297.8	54.3	12750
PD18-27-115	364	1289	141.1	1324	430	131.6	337	38.1	207.3	46.1	174.1	36.2	357.8	67.9	12680
PD18-27-124	49.9	201	29.1	170.6	39.2	15.45	102.9	28.1	267	67.1	216.9	35.3	296.8	52.6	11700
PD18-27-125	15.8	58.2	4.85	26.8	8.6	5.65	25.6	5.88	60.5	20.36	99.1	24.14	275.8	59	11970
PD18-27-126	379	1398	182.1	1188	394	130.6	737	160.3	1273	265.9	627	69.5	419	56.3	10610
PD18-27-127	441	2092	259.2	1857	740	101.7	1034	224.8	1800	370	844	92.6	557	78.8	9930
PD18-27-128	79	187	25.2	134	51.5	7.66	92	26.4	241	62.2	223	41.9	369	65.4	11960
PD18-27-129	617	1417	147	1186	438	172.5	411	37.8	207	47.6	170.9	31.65	298	55.2	12500
PD18-27-130	307	1330	179	1190	350	83.7	488	81.6	525	100.2	257	38.9	317.9	54.5	11410
PD18-27-131	29.5	154	19.7	99.9	20.5	19.23	45.6	10.32	103.5	31	129.4	28	287.7	54.7	12840
PD18-27-132	170	498	63	373	151	30.7	245	54.2	458	108.6	306	40.1	307	51.1	10060
PD18-27-133	191	808	128.4	936	258	50.5	319	59.4	456	102.8	274	40.5	344.4	62.2	11540
PD18-27-134	19.2	44.5	4.04	18.4	11.2	2.74	44.5	12.77	135.1	43.1	174.7	32.21	275.4	49.3	12080
PD18-27-135	23.7	53.1	5.39	29.1	17.79	5.68	61.1	15.8	157	45.1	180	33.1	284	51	12170
PD18-27-136	247.3	1177	154.3	1242	590	136.4	771	172.9	1557	354	946	115.8	682	79.7	11130
PD18-27-137	298	634	94.9	660	237.9	51.8	257.9	34	192.4	40.7	138.1	27.21	277	52.2	13210
PD18-27-138	121	441	60.8	428	127	42.9	189	32.4	246	59	206.4	38.2	325.6	60.3	11410
PD18-44-373	49	79.6	5.53	26.6	10.3	0.87	41.1	12.28	154.3	55.8	250.5	48.3	442	81.1	12540
PD18-44-374	6.3	62.5	2.58	20.7	18.2	2.06	81.3	23.4	278	100.8	462	86.2	758	133.1	12200
PD18-44-375	4.01	71.1	3.31	25.8	17.9	1.61	48.8	11.93	127	42.9	187	36.04	333	63.6	10590
PD18-44-376	14.3	55.6	4.39	24.2	8.85	1.81	25.4	7.14	82.9	29.76	136	26.69	253.1	47.9	10780
PD18-44-377	22	91.6	5.64	27.8	13.3	1.56	55.1	18.07	229.1	85.8	429	88.6	834	156.3	12720

PD18-44-378	68.1	204	19.5	115	47.3	6.29	91	19.4	200.9	68.4	314	63.9	626	121.6	14510
PD18-44-379	9.26	87.7	6.09	62.1	34.2	10.01	63.7	12.55	140.8	48.5	220.1	42.6	391.6	71.9	10060
PD18-44-380	10.5	64	5.82	56.6	29.6	8.9	65.6	15.28	164.8	53.6	228.5	41.5	370	67.6	9970
PD18-44-381	139	457	41.3	292	98	47.6	180	27	262	82.4	357	67.8	609	112.5	10850
PD18-44-382	1.16	32	0.76	7.27	8.56	1.24	42.5	13.13	158.3	56.1	255.3	48.6	450	84.4	9870
PD18-44-384	9.23	89.9	6.86	66.4	32	3.94	41.8	8.32	83.9	29.2	135.6	27.8	272.7	55	14750
PD18-44-385	7.5	49.4	4.22	33	10.6	2.76	25.2	6.13	70.1	23.8	112	22.79	228	47.7	13490
PD18-44-386	41	238	26.5	240	112.9	22.3	171.9	21.23	167	50.2	217	42	408	81	11080
PD18-44-387	145.2	409	47.4	380	73.5	33.2	81.3	13.98	140.4	50.5	240	49.8	479	91.9	14220
PD18-44-396	25.3	183	17.6	139	92	6.5	138	22.4	202	63.4	274	51.5	472	88.1	10660
PD18-44-397	133	342	34.7	161	35.4	5.66	77.4	18.67	209.1	70.2	309	57.6	529	95.1	10380
PD18-44-398	28.4	145	14.2	107	23	9	36.8	7.36	74.1	24.9	118.2	25.2	265	59.8	14990
PD18-44-399	7.4	71.9	4.09	37.8	14.4	1.7	29.4	8.36	96.1	34.28	159.5	31.87	300.5	56.8	11510
PD18-44-401	36.3	170.7	13.64	93.1	22.4	7.53	63.3	17.17	200.1	69.4	311.8	58.9	539	96	11040
PD18-44-402	28.5	112	9.1	48.7	20	1.44	61.9	17.56	210.7	73	333	62	561	102.4	12570
PD18-44-403	52	167	20.2	132	44.4	7.66	64.8	10.71	89.9	27.8	120	23.17	220.5	43.8	11620
PD18-44-404	75.4	247	26	232	65.6	14.87	64.9	10.96	102.9	32.6	141.8	26.99	258	49.7	10370
PD18-44-405	30.1	101.2	8.01	57.4	20	7.24	55.9	15.46	175.1	61.9	271.6	51.8	461	85.6	11620
PD18-44-406	134	820	95.9	887	158	44.1	129	17	120.9	32.9	135.6	26.6	271	55.7	12370
PD18-44-407	46	133	11	66.4	21.9	6.35	48.6	11.99	134.6	47.4	216.8	42.4	397	73.9	11480
PD18-44-408	148	715	58.4	452	138	125	213	45.8	452	140.6	608	111.7	984	177.6	11180
PD18-44-409	93.1	509	41.4	240	47.7	23.8	92.5	26.8	351	133.9	633	128.5	1227	231	11420
PD18-39-425	38	305	23.7	168	114.3	15.5	136.9	23.17	220.8	70.9	328.3	68.1	689	137.3	9980
PD18-39-426	87.2	586	66.7	408	136.4	22.5	177	36.6	351	106.2	453	85.2	805	153.1	11520
PD18-39-427	71.2	560	41.6	237	105.1	21.9	151	33.7	309	94.6	416	86.3	831	157.2	12150
PD18-39-428	27.3	169.2	16.7	104.3	38.2	7.03	65.2	15.13	161.1	52.6	240.7	49.3	488	96.1	11620
PD18-39-429	11.09	74.3	7.07	44.4	15.9	3.12	29.4	7.02	79.8	27.5	126.2	26	263	53	12370
PD18-39-430	109	501	52.6	305	120.9	23.2	181	39.9	371	109.7	436	80.6	745	137.5	12250
PD18-39-431	625	4040	368	2000	741	148.6	1022	192.6	1541	378	1339	221.2	1828	284.1	13300

PD18-39-432	8.9	42.6	3.72	24.6	12.2	2.7	24	6.16	71	26.6	134.3	30.5	327	68.1	12250
PD18-39-433	227	1720	164	982	450	85.4	603	114.8	964	247	944	166	1426	229.6	11440
PD18-39-434	1.72	17.3	0.99	5.8	2.96	0.7	9.75	3.45	45.3	17.94	94.8	21.51	228.5	47.6	13610
PD18-39-435	32.4	494	19	105.7	45.9	10.43	73.1	16.2	148.5	42.1	178.6	34	324	59	12670
PD18-39-436	259	2070	153.9	907	340	66.8	477	93.6	825	226.5	856	151	1348	242.5	11000
PD18-39-437	20.7	259	12.8	68	34.2	8.29	59.8	16.1	153	46.6	196	38.1	355	67.7	8300
PD18-39-438	17.1	118.2	12.88	80.1	36.5	5.69	54.5	10.75	106.3	36.7	172	36.6	377	77.3	13360
PD18-39-439	20.8	187.9	17.95	123.1	53	9.04	76.7	15.44	140.3	40.8	172	33.2	320	61.5	10460
PD18-39-448	267	1350	148	828	307	56.1	387	74.8	605	157.6	593	107.9	963	164.5	13220
PD18-39-449	31.6	69	7.3	37.5	12.1	2.09	20.2	4.76	52.3	18.67	90.3	18.39	190.5	39.9	8180
PD18-39-450	52.8	324	38.6	218	83.3	15.4	116	25.2	254	79.8	356.5	74.5	741	142.2	11570
PD18-39-451	810	6110	461	2776	1076	192.7	1242	207.4	1470	337	1181	215.9	1962	351.1	13130
PD18-39-452	104.6	764	66.9	410	178	33.9	244	47.3	395	107.6	415	76.9	714	131.5	15440
PD18-39-453	35.4	151	12.5	70	31.9	5.75	64.7	16.21	174.7	59.8	277.1	57.5	574	116.1	9500
PD18-39-454	125.4	1031	95.4	536	231	43.4	311	64.3	578	156.9	610	113.5	1033	174.9	12350
PD18-39-455	67.2	577	45.4	357	130.3	23.35	144.5	24.74	220.1	67.8	301.1	61.6	610	119.4	10550
PD18-39-456	629	3350	432	2530	1038	210.4	1365	252	1942	454	1572	265	2160	335	11290
PD18-39-457	90.2	487	57.5	351	120.7	21	164.3	32.3	306	93.2	377	70.5	657	121.3	12860
PD18-39-458	96.8	725	78.7	485	158	26.4	197	39.9	342	92.3	345	63.2	544	93.6	12920
PD18-39-459	1.27	39.7	1.51	10.2	5.32	1.37	20.2	6.31	78.8	28.4	133.3	27.2	273.4	55.3	10890
PD18-39-460	50.2	610	36.4	232	104.5	19.7	154	31.7	278	77.1	308	57.3	527	97	12470
PD18-39-461	18.38	135.7	9.75	63.4	30.6	5.58	49.1	11.36	114.3	37.91	167.7	33.37	311.5	60.2	10940
PD18-39-462	82.6	449	48.5	272	101.5	18.9	152	31.6	311	92.8	377	69.5	621	111.7	9610
PD18-01-10	11.08	123.9	6.77	37.6	11.99	5.89	46	13.18	148.9	54.5	245.8	52.9	507	98.8	8980
PD18-01-12	230	898	108	656	187	58.1	151.9	21.33	172.3	56.6	261.8	59.8	615	135	11310
PD18-01-13	1.78	77.6	6.9	50	8.5	2.81	24.2	7.5	94.8	38.8	191	45.2	465	100	12140
PD18-01-14	26.6	114.9	14.8	103	22.4	6.51	26.5	5.4	53.6	19.6	92	21.9	230	50.6	11860
PD18-01-15	73	221	27.1	154	47.7	15	65.3	14.73	147.9	51.7	232	48.4	463	96.2	11060
PD18-01-16	39.6	253	23.6	123	29.1	8.3	53.5	14.21	163.4	62.3	282	60.3	574	118.5	10630

PD18-01-21	944	4290	542	2730	550	137.8	470	69.9	479	125.2	476	97.5	917	183.3	8820
PD18-01-22	0.41	26.1	0.336	4.47	6.42	2.35	28.2	8.26	93.9	33.5	149.7	32.7	322	67.2	10180
PD18-01-25	18.4	117	9.1	60.4	16.2	7.14	30.9	7.88	82.3	30.6	143.5	30.8	300	65	10570
PD18-01-26	1.85	15.4	0.83	3.74	2.51	1.03	11.95	3.96	42	15.58	70.4	15.8	156.6	32.72	10780
PD18-01-36	83.8	823	103.8	704	144	71.5	143.4	25.2	232	91.7	514	131.1	1409	296	11630
PD18-01-38	22.3	99.9	11.3	61.9	17.4	6.06	58.5	17.7	203	73.8	330	68.4	611	120.4	10180
PD18-01-39	10.8	105.5	7.31	40.8	10.57	4.65	36.6	10.37	114.3	42.1	189.7	40.6	393	82.6	9950
PD18-01-40	16.8	67	8.15	59.5	14.2	3.71	36.1	10.53	122.4	44.8	205.5	43.1	422	85.2	8970
PD18-01-41	18.5	158.7	23.8	209	45.7	9.18	45.7	9.58	106.7	40	191.1	43.4	447	94.5	11760
PD18-01-43	101.1	389	51	270	72.9	25	90.6	15.71	137.3	44.1	188.4	40.7	397	83.5	12570
PD18-01-44	27.3	138	15.5	118	22.5	6.15	40	11.13	128.4	50	232	51.9	514	108.8	10930
PD18-01-45	6.95	61.9	3.72	28.1	11.08	7.25	26.4	6.92	77.7	30.54	147.5	34.4	350.6	78.4	11100
PD18-01-46	24.3	149	13.3	69.7	18.2	7.58	27.2	6.22	70.3	28.63	145.7	34.05	352.6	81	8990
PD18-01-47	100	374	55.1	267	63	16.6	77.1	13.95	130.7	45.9	213.9	48.6	505	112.9	12380
PD17-1-10	1.12	22.9	0.428	2.89	3.14	0.99	14.9	6.23	88.8	42.4	243.3	69.6	777	172.5	14020
PD17-1-11	0.089	35	0.47	7.3	8.8	3.02	30.3	8.55	97.9	38.9	202.5	56.74	648	144.2	13040
PD17-1-13	1.77	65	1.29	14.6	16.4	5.22	47.4	11.5	114.7	41.7	202.8	54.4	606	135.6	14050
PD17-1-14	1.32	60	0.575	6.81	10.39	3.93	43.7	12.21	130.5	48.2	222.4	53.9	544	118.4	12080
PD17-1-15	2.43	60	0.78	6.7	8.9	3.04	36.3	10.7	112	40.5	189.4	47.4	500	109.7	12050
PD17-1-16	11.8	84.3	4.35	25.6	16.4	1.5	71.1	24.73	292.5	112.7	485.3	99.3	855	164.1	10130
PD17-1-17	1.38	31.9	1.75	15.2	10.4	1.56	26.9	8.9	103	42.5	240.3	68.9	795	186.6	14170
PD17-1-18	3.59	47.4	1.47	14.2	13.1	4.4	36.8	10.44	124.4	50.9	272.3	76.7	838	186.1	14140
PD17-1-20	40.1	100	9.4	47.3	13	37	26.8	9	125	55.1	298	77	808	178	13950
PD17-1-21	28.2	92	13	66	22	2.66	37	10.8	130	53.8	300	88.3	1071	241	19150
PD17-1-31	7.3	86.1	1.87	14	19.7	3.71	95.1	34	397	151	661	137.9	1232	238.2	11160
PD17-1-32	3.46	31.3	0.891	5.09	4.97	1.66	24.6	9.58	129.3	56.5	314	88.1	999	216.7	14200
PD17-1-33	2.54	10.9	1.13	6.3	1.79	0.432	7.6	3.41	51.7	24.5	136.7	34.8	365	83.6	12650
PD17-1-34	3.9	23.9	0.78	4.5	2.79	1.28	14.39	6.6	100.7	47	264	75.4	839	189.6	15360
PD17-1-35	31.5	160	13.2	73	23.8	25.5	63.1	18	188	68	295.8	69.3	687	143.3	14070

PD17-1-37	1.24	30.3	0.619	5.43	6.54	2.17	25.8	8.21	99.7	41.5	219.8	57.5	623	138.3	13190
PD17-1-38	2.32	26.5	0.668	4.88	4.7	1.52	17.8	6.67	93.5	42.54	240.8	67.2	755	168.4	14260
PD17-1-39	22.8	70.8	7.27	36.3	10.5	7.4	18.2	5.65	76.6	35.8	209.7	60	687	155.2	14000
PD17-1-41	4	84.6	2.62	22.5	20.8	6.22	54.9	12.8	122.8	44.2	211.5	52.6	561	122.9	12380
PD17-1-42	0.52	12.4	0.126	0.76	0.39	0.169	5.27	3.21	57.5	31.34	195.2	58.2	676	158.9	14630
PD17-1-51	0.92	34.1	0.335	3.43	6.04	2.81	31.7	11.04	132.1	51.9	252	62.9	653	137.9	13880
PD17-1-52	0.36	13.91	0.146	0.75	0.91	0.106	7.26	4.26	76.5	38.5	237	67.7	764	166.3	14040
PD17-1-53	0.69	39.1	0.94	11.5	12.4	3.82	37.2	9.96	112.5	43.55	224.5	58.5	650	139.6	12700
PD17-1-54	620	910	65	253	46.4	8.2	73.2	17.88	177.5	63.7	311	80.7	861	181.6	13850
PD17-1-55	2.04	16.1	0.4	1.87	1.46	0.42	9.5	4.81	72.3	33.2	175	44.6	470	102.9	14010
PD17-1-56	0.707	11.38	0.096	0.77	1.29	0.163	13.9	9.12	153.9	74.8	425	117.8	1315	278.5	17610
PD17-1-58	5.07	24.7	1.59	8.7	1.9	0.55	5.97	2.98	51.7	27.03	164.6	47.5	530	116.7	13700
PD17-1-59	17.04	27.3	0.92	4.96	4.9	1.51	20.3	6.88	81.3	30.9	155.7	39.3	435	96.5	14040
PD17-1-60	0.076	11.75	0.019	0.099	0.47	0.076	4.92	2.86	53.6	28.9	180.4	52.9	630	141.9	14750
PD17-1-61	11.2	152.6	3.36	22.4	28.6	4.32	147.8	51.9	606	228.1	991	203.8	1782	327	9330
PD17-5-70	63.7	269.7	38.7	166.6	40.3	6.08	47.6	8.85	76.1	24.7	111.8	25.55	254.7	58.1	14030
PD17-5-71	149	437	43.2	221	52.2	12.16	66.6	11.13	91.8	29.68	127.3	27.81	279.8	63.8	14290
PD17-5-73	15.21	105.4	9.68	62.2	23.3	5.58	43	10.74	111.1	40.9	184.2	40.9	405	86.8	12430
PD17-5-76	13.4	93	10.9	65	37.2	7.6	71	17.2	157	50.2	207	41.4	376	73.4	11720
PD17-5-77	50.6	248	31.7	182	78	16.6	144	29.9	270	85.5	339	66.3	600	117	12170
PD17-5-78	8.2	97.8	9.9	72.2	38.6	7.91	81.1	18.32	172.4	58.5	241.1	50.3	463	93.3	12230
PD17-5-81	11.33	105.4	9.16	58.9	37.3	6.71	92.7	22.7	216	72.7	299	61.3	555	112.8	12450
PD17-5-91	33.9	184	26.8	167	75.9	10.81	107.9	18.8	150.8	46.1	195.1	41.9	419	93	14450
PD17-5-92	7.59	65.6	7.28	46.8	26.8	8.26	59.6	14.08	126.8	40.4	163.6	33.4	306	62.5	11820
PD17-5-93	13.6	76.4	9.69	60.2	30.2	5.53	54.9	11.97	106.3	34.6	149.1	32.3	322	69.1	13440
PD17-5-94	28.2	167.3	11.61	71.7	31.1	5.06	60.5	13.91	145.1	51.7	242	53.8	531	113.6	14160
PD17-5-98	6.88	60.7	7.91	59.8	38	7.56	75.7	17.1	160	53.5	230	49.5	487	102.9	9690
PD17-5-99	18.4	110	12.2	71	31.5	4.51	54.9	13	125	41.4	175	37.9	368	81	14120
PD17-5-110	12.4	107.5	11.4	75.1	36.7	7.99	59.2	11.99	107.7	35.8	158.4	34.3	342	72.8	12610

PD17-5-111	12	61	7.01	34.7	10.9	1.87	24.3	7.03	83.2	31.95	156	35.92	363	82.3	12300
PD17-5-113	47	177	24.3	133	55.3	9.6	77.9	16.6	142.3	46.3	200.3	43.8	434	98.2	14240
PD17-5-114	26.8	189	22.4	134	63.4	13.7	116.1	26.4	245	80.3	324	65.3	572	113.5	9960
PD17-5-115	18.3	82.2	9.03	52.3	23.4	3.77	55.4	15.48	169.4	62.2	275	57.7	534	107.7	12940
PD17-5-117	3.99	36.1	3.32	20.1	10.6	1.65	17.9	4.66	49	17.75	85.9	20.64	217.5	49.7	13860
PD17-5-118	7.3	66.4	3.77	26.5	17.4	4.18	53.1	15.07	161.8	56.8	238.1	47.9	417	81.5	9550
PD17-48-475	83	300	21.6	105	50.3	16.5	114	29.3	239	52	144	23.4	192.9	34.95	13110
PD17-48-476	127.4	413	32.6	153	62.5	22.6	162	43	372	86.7	244	37.5	279	46.4	12760
PD17-48-477	31.8	101.2	8.1	43.7	27.7	10.9	86.2	22	192	46.5	146.2	24.3	197.5	32.13	13690
PD17-48-478	8.6	48.5	2.18	13.71	17.7	9.2	80.6	22.09	199.3	52.7	166	26.83	199	32.79	12090
PD17-48-479	39.6	152	10.1	48.8	22.1	7.7	60	16.4	151	38.8	129	24	209.4	38.18	12850
PD17-48-480	0.98	30.9	0.56	6.34	12.7	6.49	63.3	16.85	147.5	39.2	125.1	20.02	152.2	25.4	10240
PD17-48-481	90	313	22.4	106.1	41.2	13.8	92	23	196	46.3	141	24	197.3	35.55	13100
PD17-48-482	241	868	68	359	163	55.3	321	74.7	617	125.7	330	45.3	306	48	13030
PD17-48-491	54.8	151.1	12.62	64.3	34.9	13	102.1	25.6	218	50.6	152.6	24.7	200	34.21	13020
PD17-48-492	50.1	162.3	12.57	64.4	34.2	12.9	101.3	24.9	214	51	145.6	21.7	158.5	25.2	11220
PD17-48-493	29.6	101	9.2	37.9	12.3	4.19	25	7.64	79.1	25.1	110.4	25.24	249.4	46	12750
PD17-48-494	73.4	223	19.31	94	45.2	15.6	106.3	26.3	218	49.3	141.8	23.17	187.1	32.84	13230
PD17-48-495	42.3	103.5	8.86	42.1	24.5	9.3	80	21.3	186	45.3	146.4	25.9	218.6	37.5	13210
PD17-48-496	47.2	177	13.1	69.2	34.5	15.4	85	21.3	175	40.7	118	19.6	170.5	34.99	15010
PD17-48-497	36.9	197	14.55	72.5	24.9	13.2	43.8	10.7	89.5	23	81.2	16.25	168.1	41	15160
PD17-48-498	49.7	135.4	12.22	58.6	24.7	8.93	66.9	18.66	172.8	45.2	150.1	27.42	238.9	41.94	13480
PD17-48-499	1.26	11.4	0.54	3.11	4.4	1.8	18.8	5.93	62.6	20.8	90.3	20.23	195.7	37	13450
PD17-48-500	66	196	21	124.4	52.8	88.1	120.2	26.6	215	53.5	160.5	27	221.1	39.2	13760
PD17-48-501	37.1	92.4	8.94	50	24.4	15.1	61	14.9	136	37.3	129	24.3	215	39.1	12550
PD17-48-502	96	456	28.7	147	52	18.4	87.6	20.9	172	40.5	126	21.5	191	36.3	13440
PD17-48-503	52.8	159.5	12.85	64.9	36.9	13.63	109.2	27.9	234	54.1	159.3	25.66	206.5	36.66	13140
PD17-48-512	36	106	6.4	24.5	10	3.69	33.8	9.1	84	24.6	91.9	19.2	183.4	36.11	13760
PD17-48-513	4.19	62.1	1.8	21.7	36.4	17.08	155.2	36.7	284	65.4	181	26.34	180.7	27.16	10270

PD17-48-514	6.29	45.8	2.13	15.9	20	10	95.3	24.47	203.1	48.74	140	21.66	157.7	25.48	12590
PD17-48-515	53.3	420	15.5	80	44.2	18	142	35.7	302	75.7	227	33.7	237	38.4	11870
PD17-48-516	64	244	17.8	94	37.1	14.8	103	27.2	240	56.8	177.3	29.5	244	42.3	12200
PD17-48-517	59.4	151	14.3	64.9	31.7	11.8	95	23.8	196	46.4	139	22.3	182.7	31.2	13320
PD17-48-518	60.5	203	15.7	75.3	26.6	8.48	51.7	13.4	117.1	27.1	81.8	15.01	140.1	29.5	14480
PD17-48-521	54.3	521	20.1	117	56.7	32.3	101.2	20.5	146	31.3	90.5	15.31	133.6	24.83	13990
PD17-48-522	15.3	71	4.37	25.9	18.2	7.92	71.6	20.4	191	52.5	179	31.9	270	45.9	13000
PD17-49-531	14.5	87	10.8	84	54.5	20	95.1	18.9	162.1	48.1	201.9	45.2	447	88.2	13320
PD17-49-532	92	432	50.8	311	202	62.2	452	101	718	156	462	75.3	623	114.3	13880
PD17-49-533	58.9	298	37	230	133.1	33.4	262	57.4	412	93.5	321	62.9	585	113.8	12880
PD17-49-534	41.8	186	19.9	136	70.4	22.9	145	32.6	297	93.7	382	77.9	705	134.3	12060
PD17-49-535	25.5	144	16.2	109	68	18.6	132	31.5	259	69.2	267	57.1	561	111.2	12230
PD17-49-536	31.2	159	15.6	101	63	16.9	151	36.8	322	93.9	371	75.6	694	129.7	13660
PD17-49-537	20.5	119.8	10.44	61	47	14.7	134.1	37.3	334	99	375	71.3	630	116.1	12070
PD17-49-538	46.4	235	23.2	150	91.6	34.5	204	49.3	415	114	418	77.3	665	119.3	12190
PD17-49-539	109	199	18.2	78.7	28.1	6.59	66.2	18.8	200	67.3	305.4	67.4	645	126.2	14520
PD17-49-540	22.3	158.4	14.1	79.7	44.8	10.19	95.5	23.8	223	73.7	309	64	602	124.8	12060
PD17-49-541	185	820	107	633	409	103	900	200	1400	311	915	148.7	1171	200.1	14170
PD17-49-542	84	408	51	311	217	57.5	482	125	920	182	493	71.8	532	91.9	12570
PD17-49-551	150	573	86	443	311	87	690	219	1730	368	1050	154	1109	176	12660
PD17-49-552	6	24.7	3.49	26.5	13.3	3.8	26.5	8.9	104	37.6	186	45.9	478	94.7	14210
PD17-49-553	45	210	26.6	141	98	28.6	219	64.8	552	136	476	83.8	690	124.2	11750
PD17-49-554	176.3	976	118.1	769	546	148	1179	222.1	1326	247.9	649	101.1	822	149.6	14300
PD17-49-555	830	1230	118	487	164	34.4	272	53.8	412	108.7	391	73	645	119.5	11830
PD17-49-556	24.9	146.6	16.4	106.2	61.5	26.3	138.9	33.4	281	79	300.8	59.3	552	107.4	13040
PD17-49-557	72	181	16.1	92.8	50.3	19.7	113.7	28.5	266	78.9	318	66	626	120.7	13490
PD17-49-558	71.8	355	41.3	266	169	44.9	367	82.6	606	142	470	85.3	767	142.7	12960
PD17-49-559	173	701	111.7	565	390	104.9	808	261	2040	408	1135	165.6	1138	178.7	12570
PD17-49-560	16.8	87.6	7.09	35.4	24	7.28	74.7	23.97	253.2	85.8	361.2	72.5	659	122.9	11360

PD17-49-561	42.8	172	18.3	101	61	24.4	155	41.7	375	107.6	417	83.7	755	145.3	11980
PD17-49-562	24.6	125	14.7	87	52.9	13.4	127	32.9	289	80.1	300.7	58.3	517.6	97.3	12930
PD17-49-571	16.2	102.4	10.8	70.1	45.5	16.5	120.6	36.1	338	100.7	399	77.4	691	129.7	12550
PD17-49-572	154	778	109.2	655	448	116	938	211	1453	293	776	113.1	866	147.7	15080
PD17-49-573	66.8	298	34.9	204	140.2	34.3	327	87.6	695	164.8	532	89.9	757	135.6	12710
PD17-49-574	5.56	47.7	3.19	23	22.7	8.17	80.4	22.3	199.9	54.3	181.4	29.26	227.3	38.3	9510
PD17-49-575	36.2	132.5	15.55	77.7	41.6	12.97	99.2	28.6	248	69.3	274.6	57.5	558	106.9	14480
PD17-49-576	46.1	176	14.96	78.1	44.6	14.6	123.3	34.2	315	92.3	355	68.3	590	112.2	12740
PD17-49-577	32	147	19.9	116	73	16.7	147	36.9	287	68.7	254	51.4	465	92.2	13170
PD17-49-578	13.5	75	8.37	48.5	35.3	10.09	97.2	25.4	236	70.7	294	62.1	596	118.2	11930
PD17-49-579	12.6	69.5	6.79	39.1	30.1	8.02	87.6	24.9	233	68.5	279	59.2	572	111.2	13030
PD17-49-580	74.8	375	42.6	253	173	43	407	96.5	745	175.5	566	96.3	795	141.9	11570
PD17-49-581	123	435	43.4	201	91.9	23.6	193	48.9	404	104.3	388	76.2	683	130.9	14750
PD18-120 - 1	102.3	184.5	22	90.5	41.6	9.65	92.6	29.9	316.3	108.2	445	90	792	142.8	14560
PD18-120 - 2	6.7	57.3	7.5	43.6	29.8	7.92	88.9	30.1	330	113.2	473	94.5	823	145.5	11850
PD18-120 - 3	0.013	25.19	0.028	1.08	5.72	4.13	51.2	20.13	244.1	89.9	379.9	74.9	652	116.6	9640
PD18-120 - 4	0.51	28.38	0.069	0.87	7.28	5.07	80.8	34.92	447.2	167.5	712	138.7	1162	192.9	12810
PD18-120 - 5	3.24	54.2	3.48	24.3	22.8	8.25	73	19.41	166.8	45.2	151	25.37	198.9	33.09	7360
PD18-120 - 6	7.91	60.3	6.7	41.4	27	12.29	90.4	36.1	430	160	683	133.5	1119	188.9	13130
PD18-120 - 7	0.017	2.49	Below LOD	Below LOD	0.27	0.203	3.56	1.86	29.1	14.4	91.7	25.9	334	89.5	15130
PD18-120 - 8	3.74	18.9	2.57	14.9	10.4	2.26	15.9	4.26	41.7	15.05	79.6	21.5	266	65.8	14370
PD18-120 - 10	65.7	427	86.3	512	287	38.5	327	57.2	444	125	474	94.2	836	154.9	15840
PD18-120 - 12	2.15	18.3	1.56	8.8	8.6	3.1	48.3	21.4	279	108.6	486	98.7	852	156	13710
PD18-120 - 14	4.33	52.6	6.18	40.6	31.6	7.89	65.8	17.1	147	44	180	36	332	71.1	11100
PD18-120 - 15	0.61	6.2	0.47	2.81	1.63	0.52	9.5	3.2	43	17.6	94	23.3	262	61.9	13230
PD18-120 - 16	5.7	77.9	6.4	42	32	9	92.7	27.8	290.4	99.7	406.4	78.2	670	117.9	8580
PD18-120 - 17	7.69	60.8	6.89	41.8	31	10.19	74.6	17.55	144.5	37.2	128.1	23.23	190.1	33.6	9190
PD18-120 - 18	7.37	63.1	6.42	35.8	31	8.34	96.7	33.5	369	127.2	532	105.1	922	167.8	11210
PD18-120 - 19	13.3	76.9	13.9	89	57	11.7	93	24.2	274	98.7	439	92.8	827	156.8	19350

PD18-120 - 20	0.177	27.3	0.495	7.6	15.8	8.4	75.8	20.7	191	57	212	39.5	322	57	8760
PD18-120 - 21	73.6	416	75.9	470	290	53.7	445	107.9	769	171.5	525	89.8	708	116.4	13890
PD18-120 - 22	50	304	59	345	233	43.3	329	71	504	122.4	385	65.3	509	85.4	12430
PD18-120 - 23	1.71	29.73	1.29	8.59	9.67	4.27	48.3	17.91	206	72.6	305	60.9	529	95.4	10150
PD18-120 - 24	13.78	45	4.99	22	11.2	4.19	40.6	14.08	160.2	57.1	248.3	47.5	433	75.1	10500
PD18-120 - 25	6.01	38.5	3.9	22.9	17.9	5.4	58.6	22.14	264.5	100	427	86.5	733	132.1	11410
PD18-120 - 27	9.3	75.2	9.2	56.3	40.5	11.2	104.9	32.3	343.9	115.3	469	88.8	747	128.5	10180
PD18-120 - 28	3.19	26.1	3.18	20.1	15.8	3.37	51.6	21.18	259.6	97.7	440.9	91.5	830	152.7	15510
PD18-120 - 29	3.07	18.97	2.17	12.94	10.22	2.24	29	10.67	127.2	46.17	203.6	45.9	458	95	11400
PD18-120 - 30	1.57	25.63	1.24	6.5	6.19	3.08	33.6	11.94	138.2	51.7	223.2	44.1	388.2	70.1	8790
PD18-120 - 31	5.3	28.8	2.54	13.3	11.3	4.09	64.3	27.28	341.4	129.8	572	117.1	1026	177.8	15110
PD18-120 - 32	4.2	13.5	0.9	3.9	2	1.63	20	9.1	118	48.6	230	51.3	499	103.7	12960
PD18-120 - 33	6.51	45.5	5.41	32.5	24.9	6.82	100.2	42	536	196.7	855	169.6	1442	239.2	15810
PD18-120 - 34	15.1	75.1	12.25	75.3	59.4	12	118.2	32.4	263	69.6	253.9	52.3	456	83	13150
PD18-120 - 35	1.85	41.9	2.33	20.1	25.5	3.06	76	25.3	298	111	540	114	1050	198	15200
PD18-120 - 36	5.15	40	4.33	25.4	18.9	4.99	52.3	16.15	168.6	57.5	241.2	48.5	430	81.3	9440
PD18-110-119	374	750	92.7	449	172	11.9	251	63.2	626	214.5	900	190.7	1658	312	12430
PD18-110-121	112	291	25.6	112	50.9	13.05	112.9	25.9	226	61.6	224	41	329	58.4	8920
PD18-110-122	16.95	81.9	8.27	43.5	16.7	4.39	40.9	12.6	141.1	48.8	212	44.3	415	77	12490
PD18-110-123	3.87	27.7	2.76	18.1	13.1	4.65	36.9	9.32	83.8	24.65	91.5	18.21	157.6	31.04	8910
PD18-110-124	6.29	26	1.99	10.1	7.5	2.18	27.8	8.55	84.8	27.2	110.1	22.4	197	36.6	10700
PD18-110-126	89.4	280	25.1	80.9	16.4	4.1	34.1	9.75	96.7	31.7	131.6	27.7	256	47.8	11380
PD18-110-127	36.7	545	41.5	391	239	30.9	262	28.6	164	39.1	153	33.1	351	78.7	12960
PD18-110-133	16.1	86	6.24	28.6	10.8	7.47	28.6	8.18	81.6	26.6	106.5	21.4	183.7	32.4	12000
PD18-110-137	10.99	36.4	2.61	16.3	11.8	5.28	50.9	14.87	143.4	45.6	181.8	37.3	338.9	63	11030
PD18-110-138	0.8	9.75	0.345	2.47	3.14	1.1	15.7	5.02	56.5	18.7	77	14.5	130	23.7	10410
PD18-110-139	124	559	72.4	400	179	29.5	266	58.2	435	101	345	60	500	82.7	11490
PD18-110-140	460	1027	47.1	122.7	21.9	6.02	53.6	17.15	184.2	63.5	273	56.9	524	88.3	15150
PD18-110-142	51.1	306	44.3	293	84	26.8	94.5	17.41	146.3	44	177.3	36	324	61.4	10160

PD18-110-143	77	1180	70	395	209	42.3	277	43.3	293	75.3	280	56.9	582	115	13400
PD18-110-144	104.9	306	88.1	418	209	62.4	274	63.7	511	128.3	491	99.4	931	158.7	11760
PD18-110-145	11.4	57.4	6.27	36.4	23.1	4.28	58.8	15.99	155.3	47.3	184	36.8	316.1	57.6	10980
PD18-110-146	44.9	179.4	19.9	114	36.8	12.1	71.6	19.2	195.8	59.3	222	41.5	347	58.3	10650
PD18-110-147	6.74	25.3	0.85	6.06	8.4	2.73	42.7	11.5	121	36.6	144	28.7	264	49.8	10460
PD18-110-148	18.4	138.8	13.74	100.4	83.1	15.64	197	46.3	378	94.6	314	52.7	424	71.5	9260
PD18-110-149	12.9	51	4.9	28	9.3	7	26.6	7.04	74.1	25.05	109.9	24.76	247.5	49	11310
PD18-110-150	41.5	136	17	98	55.5	20	113	27.8	233	59.9	214	38.8	314	54.7	10450
PD18-110-158	852	4200	419	1877	513	80.6	576	120.8	783	153.1	485	90.9	806	136.5	17410
PD18-110-159	2.3	32	0.65	4.3	6.78	2.28	45.7	16.5	182.8	60.9	247.7	48.2	416	73.5	13890
PD18-110-160	2.65	46.1	1.61	11.5	16.4	4.61	70.5	19.8	201	62	237	44	372	64.8	10780
PD18-110-161	8.91	52.3	4.69	31.9	25.9	7.71	73.9	17.53	157.3	46.5	175.5	34.3	314.5	60.2	10310
PD18-110-162	0.052	11.84	0.139	1.94	4.04	1.67	20	6.02	66.5	22.98	95.1	18.66	173.3	32.3	8650
PD18-110-163	71.6	416	55.7	442	283	48.2	266	36.7	216	43.7	135.6	24.7	216	36.3	10140
PD18-110-164	50.1	224	23	152	65	26.8	104	19.1	157	43.6	168	34	329	62.8	11030
PD18-110-165	13.02	25.8	1.81	11.2	9.3	3.83	35.5	9.3	98.4	29.7	123.5	24.6	226	42	10530
PD18-110-166	38.3	172	15.7	75.5	25.1	7.42	56.3	14.39	125.3	36.2	125.3	24.2	199	34.8	11030
PD18-104-395	74.3	262	26.8	149	78.7	9.9	116.5	22.7	185.7	55	230.1	47.1	444	88.6	9830
PD18-104-397	110	678	67.9	357	172.4	21.9	230	43.6	306	76.6	267	49.8	443	87.9	10220
PD18-104-398	3.69	29	2.39	17.3	9.6	1.31	17.1	3.3	26.7	8.35	39.9	9.6	103.6	23.8	11300
PD18-104-399	58.5	515	35.2	177	82.8	9.11	119.6	28.1	231	62.4	249	46.8	428	84.6	9630
PD18-104-400	325	4410	186	877	307	39.9	330	63.2	449	109.2	381	71.2	628	122.4	10410
PD18-104-401	15.5	100	9.34	55.9	35.5	4.83	73.4	17.9	165	52.6	204	38.5	333	66.8	8790
PD18-104-402	78	830	52.1	275	124	15.7	160	27.5	192	48.1	173	32.3	295	56.8	9600
PD18-104-403	11.2	75	8.5	64	23.3	2.97	37.9	8.57	83.6	31	143.8	33.2	336	72.9	10150
PD18-104-404	36.1	203	23.6	140.1	60.3	7.63	94.3	19.1	169	51.8	220	45	418	85.5	10060
PD18-104-406	199.2	2670	117.3	569	195.7	22	204.5	40.2	269	61.4	216.7	41.1	384	78.8	10600
PD18-104-407	78	167	16.2	81.8	28.7	4.04	44.7	10	97	35.5	159	36.9	394	82.2	10220
PD18-104-408	24.7	196	18.4	114.3	60.2	7.31	84.6	14	107.6	28.1	109.5	22	218	45	9490

PD18-104-411	42.4	311	38.4	247	85.7	10.17	115	21.73	183.8	55.3	230.5	46.1	432	88.5	8890
PD18-104-419	13.2	130	9.5	50	25.1	2.96	41.3	10	100	34.7	168	36.7	394	81	10710
PD18-104-420	278	1570	154	830	408	48.1	559	111.5	762	175	553	104.5	852	154	11450
PD18-104-421	44	291	28	148	70.8	7.81	91.8	21.4	164	44.3	176	36.5	350	77.7	11210
PD18-104-423	448	3430	183	919	289	32.8	332	55.6	401	97.7	352	66	592	109.9	11470
PD18-104-424	95.2	929	58.9	299	120.8	14.46	141.1	28.8	228	62.7	248	50.8	479	97.7	11640
PD18-104-425	7.33	102.1	3.5	18.2	12	2.11	50.1	14.7	157	57.2	242	46.7	423	81.9	9350
PD18-104-426	63.7	1040	35.7	165	59.7	7.82	80.3	18.7	166	53.2	225	47	456	95.9	9980
PD18-104-427	16.9	91.6	8.64	48.5	27.1	3.28	49.6	11.83	113.9	38.9	181.2	38.5	394	80.5	11470
PD18-104-428	1.31	37.4	0.88	7.92	8.34	1.54	43	13.11	150.7	53.5	227	45	406	77.8	8890
PD18-104-429	20.5	124	11.9	76.7	35	4.54	57.2	12.67	123.7	42.8	193	42	412	84	10240
PD18-104-430	92.7	1378	54.6	307	129.6	18.3	179.9	33	253	70.1	271	55.2	511	103.1	10610
PD18-104-431	32.4	231	23.2	130.7	56	6.55	79.8	15.39	136.7	45.6	199.5	42.7	411	85.4	10850
PD18-104-432	205	2510	120.4	606	210	26.8	242	44.6	318	79.1	291	56.3	519	100.8	10560
PD18-104-434	221	1810	132	672	258	31.4	308	56.6	403	102.3	377	73.7	683	131.1	11140
PD18-104-442	10.4	58.5	5.52	34	13.6	1.57	23.7	5.98	61.9	23.3	110	24.2	260	54.7	9870
PD18-104-443	26.1	195	18.9	115	64	7.8	101	18.8	151	42.9	167	32.4	299	62.2	10160
PD18-104-444	89	427	44.4	248	132	15.6	182	34.1	248	64.7	241	48.4	447	90.9	12220
PD18-104-445	109.6	546	66.9	342	170.2	22.3	224.2	47.5	333	76.7	261.6	48.8	457	88	10100
PD18-104-447	9	55.8	5.74	38.6	22.3	2.79	38.2	8.83	79	28.4	126.5	29.1	291	58.6	10360
PD17-14-128	11.6	88.6	6.2	37.1	17.7	4.28	60.6	16.93	187.4	69.8	307.4	64.2	576	116.7	10940
PD17-14-129	35.6	179	15.7	99	23.6	6.91	54.1	16.43	194.2	75.4	351.5	75	699	143.9	11740
PD17-14-130	5.34	65.8	1.8	10.4	9.22	2.81	41	13.67	164.5	65.1	297	63.3	591	120.4	10620
PD17-14-131	14.1	57.2	4.21	24.2	12	3.01	33.1	10.73	124.4	49.9	237	51.9	497	102.8	12300
PD17-14-132	23.8	157	16.1	96.8	60.6	14.1	143.4	33.4	292	88.1	346.8	68.2	597	119.5	10550
PD17-14-133	9	58.8	4.5	19	7.89	1.9	21.7	6.81	82.7	34.5	172.2	40.3	401	90.1	11520
PD17-14-134	290	590	55.8	228	55.8	10.7	80.9	16.45	145.2	45.8	187.2	36.5	322	65.6	6670
PD17-14-135	299	503	47.4	190	36.4	6.19	49.7	10.87	114.3	41.5	183.9	38.36	347.8	72.9	9110
PD17-14-136	60.6	317	42.5	250	99.4	20.97	146.6	33.8	273.5	77.4	298.5	58.3	513	105.6	10160

PD17-14-137	8.55	62	3.31	18.9	10.68	2.34	39.5	12.76	148.1	56.6	255	55.4	531	114.6	13250
PD17-14-139	347	595	63.8	268	58.2	9.49	51.6	8.52	57.7	13.65	56	12.52	142.9	39.5	14980
PD17-14-148	11	170.1	6.85	49.2	31.6	7.65	93.3	25.5	265	91.1	386	78.1	696	138.3	11060
PD17-14-149	134	531	59.3	347	170.1	40.6	276	57.3	464	132.8	488	89.8	766	145.9	9170
PD17-14-150	29.8	178	12.7	63.7	29.2	5.72	72.7	20.1	222	77.8	341.9	71	644	121.6	10630
PD17-14-151	31.8	148.5	17.1	101	36.8	10.55	66.6	14.83	142.2	50	212.1	43.45	394.4	81.7	9040
PD17-14-153	206	383	36.4	161	36.5	6.82	50.8	11.1	106.9	37.7	170.3	37.4	365	79.5	11510
PD17-14-154	39	198.3	27.8	155.2	56.5	12.93	68.9	14.51	121.1	36.8	168	38.9	415.2	98.3	13180
PD17-14-155	15.8	78	12	58	22.3	4.32	26.4	6.4	54.5	16.5	72	17.3	191.8	51.8	12280
PD17-14-156	273	637	75.4	363	111.2	18.8	155.2	36.2	336	107	434.3	84.8	738	142.1	11590
PD17-14-157	95.4	483	62.4	341	148.6	29.2	207.7	47.2	377	105.1	402	79	728	148	11680
PD17-14-158	6.52	106.3	4.94	33.1	20.3	5.13	60.6	17.4	184	63.5	265	53.3	474	92.2	9350
PD17-14-159	34.7	196.5	22.7	154.5	58.8	10.54	85.5	22.2	220	73.8	315	64.6	582	111.6	12880
PD17-14-168	48.8	282	29.2	145	45.2	10.64	73.6	16.49	158.7	54.3	232.6	47.6	442	88.3	9180
PD17-14-169	375	650	68.6	276	51.6	8.31	48.5	7.4	54.6	16.1	73	16.5	190	49.8	14220
PD17-14-170	31.1	219	22.6	157	76.2	22.6	109.7	21.26	178.1	54.1	218.7	44.14	408	84.2	13500
PD17-14-171	7.57	43.3	3.46	20.1	11.6	3.09	36.9	9.86	103	35.9	156.8	32.8	303	61.5	11130
PD17-14-172	1080	1910	182	762	155	24.6	176	35	318	104.8	441	88.7	802	156.8	10210
PD17-14-173	100.1	480	70	425	163	30.4	212	42.5	294	71.3	251	50.6	484	112.3	14070
PD17-14-174	590	1330	159	869	291	58	376	71.5	484	121.2	404	72	634	125.7	12250
PD17-14-175	53.5	376	44.8	271.6	117.7	22.33	149.8	28.48	218.6	57.9	228	46.5	436	93.9	12450
PD17-14-176	78.5	270	30.1	162	48	10.5	71.4	15.6	126	38.6	155	31.6	309	70.3	13100
PD17-14-177	180	629	78.7	397	164	32.9	222	51.4	424	118	457	89.6	796	159	11980
PD17-56-590	4.98	38.5	2.34	17	15.9	5.06	56.5	17.8	205	74.3	330	70.1	670	142.6	10840
PD17-56-591	0.68	4.2	0.424	2.16	1.4	0.51	3.88	1.61	26.4	14.76	103.2	32.9	458	154.4	12890
PD17-56-592	0.09	14.75	0.288	5.11	10.5	4.04	66.5	22.87	278.3	106.8	467.9	92.5	815	161.1	10150
PD17-56-594	9.91	53	5.7	34.9	19.5	7.06	49.4	13.77	135.7	45.3	203.7	44.4	471.1	120.6	12740
PD17-56-595	1.62	18.8	0.98	7.8	10.19	3.64	52.1	17.84	216.7	83.7	369	75.7	694	137.8	9820
PD17-56-596	2.45	17.9	1.4	8.4	8.61	3.23	37.9	13.24	159.7	61	276.3	56.9	536	109.3	10620

PD17-56-597	15.6	67.1	8.9	52.2	28.5	9.3	63.3	16.4	158	52.3	236	50.5	520	134.8	12110
PD17-56-598	8.2	32.9	4.8	28.4	17.6	5.6	34.3	9.5	92.3	31.8	171	45.2	548	160.7	13690
PD17-56-599	3.35	26.9	1.87	11.8	8.32	2.35	28.2	9.68	112	44.4	218.8	50.7	524.1	122.6	11470
PD17-56-600	0.0114	12.88	0.152	2.97	7.4	2.78	46.4	16.58	211.2	82.5	372.8	75.1	677	135.4	10210
PD17-56-601	0.057	76.6	0.467	9.07	23.29	6.8	173.8	62	776	294.6	1273	248.2	2147	407.1	9760
PD17-56-610	0.55	16.62	0.51	5.84	10.01	4.06	62.9	21.54	269.3	105	466.5	92.3	827	163.8	9790
PD17-56-611	1.49	33.6	0.777	6.94	9.91	3.13	56.1	20.09	252.5	98	433	87.4	793	153.8	10760
PD17-56-612	0.074	11.18	0.129	2.47	5.97	2.29	41.2	14.88	185.4	72	323.8	65.3	600	120.5	10100
PD17-56-613	4.99	35	2.85	18.3	16.44	5.93	64.2	20.4	239	91.1	421	89.1	870	194.6	12000
PD17-56-615	4.6	30.5	3.07	21.5	18.3	5.58	68.9	22.14	258.9	95.2	431	86.2	782	157.3	10830
PD17-56-616	4.49	38	2.56	20.7	22.8	7.67	114.5	37.9	453	171.6	761	147.2	1335	256.6	10120
PD17-56-617	55	199	23.4	135	88.2	28.4	251	73.6	764	251	1028	195	1655	307	8810
PD17-56-618	82.8	176.1	17.02	82.1	31.1	14	85.7	22.7	232.2	81	347	70.2	638	135	11030
PD17-56-619	6.69	36.4	3.45	23.2	15.74	5.96	55.8	16.51	187	70.9	327	70.1	690	152.2	11310
PD17-56-620	0.502	38.9	0.764	11.65	26.1	8.68	173.4	59.2	735	272.3	1196	230.3	2012	380	9670
PD17-56-621	2.17	25.86	1.582	13.18	15.88	5.83	86.6	30.6	364	138.4	615	121.3	1118	229.2	10460
PD17-56-630	0.443	26.2	0.531	7.16	14	4.52	93	32.4	404	155	682	136	1230	244	10900
PD17-56-631	1.18	47.5	0.842	9.69	21.6	8.39	165	57.7	686	250	1057	203	1760	336	9280
PD17-56-632	2.01	12.16	0.968	6.38	5.31	1.99	20.67	7.34	88.5	34.4	162.5	36.2	359.7	82.9	12090
PD17-56-633	1.51	23.87	0.701	6.09	9.43	3.63	63.1	22.49	281.8	108.4	490	97.9	877	172.9	10310
PD17-56-634	11.1	50.1	3.77	22	17.1	5.16	66.4	21.42	253.4	95.7	435.2	91.7	849	173.6	10350
PD17-56-635	66	86	6.2	22.8	6.99	2.69	28	9.62	121.1	48.4	222.7	46.6	442	89.9	10350
PD17-56-636	70	124	9.6	40.1	17.3	5.68	83.9	27.5	336	130.3	579	113.5	1016	199.6	9620
PD17-56-637	0.51	21.49	0.552	6.67	11.27	4.34	82.6	28.82	363.3	141.7	626	125.3	1116	221.6	9850
PD17-56-639	121	240	28.1	145	52.5	13.08	137.6	38.65	442.7	164.6	713	136.8	1191	228.2	9740
PD17-56-640	1.47	21.66	0.998	10.4	15.5	5.39	83	29.12	354.9	136	596	116.6	1019	199.1	10030
PD17-56-641	1.72	15.39	0.94	6.63	7.04	2.89	37	13	159.9	62.8	288.8	60.2	570	121.7	10810
PD17-56-642	0.042	18.9	0.175	3.31	8.14	3.07	55.2	20.93	261.3	102.4	461.7	92.4	845	166.7	9680
PD17-56-651	11	85.6	5.78	36.3	26.8	9.93	80.1	24.54	270.4	95.3	435	92.4	900	192	11520
PD17-56-652	63.5	149	16.9	86.4	30.2	9.7	80.8	24.66	291.6	111.9	492	99.1	908	181.6	10500

PD17-56-653	2.98	51.6	1.92	17.37	26.5	8.88	157	54.3	650	242.4	1048	203.7	1769	336	9370
PD18-101-351	12.9	43.7	3.6	23.4	6.1	1.41	10.6	2.6	29.3	12.42	63.8	15.12	164.8	37.5	12100
PD18-101-352	5.81	30	2.21	19.1	3.98	1.68	7.74	2.25	28	11.37	59.9	14.32	157.2	35.4	12160
PD18-101-353	62.8	253	24.5	157	24.7	7.59	41.6	9.72	103.1	36.9	166.3	36.1	351	75.6	11400
PD18-101-354	30.9	132.5	11.22	93.5	37.9	13.75	61.1	12.56	127.6	43.4	183	35.3	321	61.9	9240
PD18-101-355	34.5	157	17.9	125	27.5	6.37	33.7	6.38	62.7	21.7	100.6	22.1	225	49.2	11450
PD18-101-356	12	36.7	0.9	4.86	2.82	0.88	13.11	4.84	63.6	27.41	145.2	35.8	395	94.7	11920
PD18-101-357	45.7	162	19.1	124.6	17.4	4.19	22.2	3.88	39.9	15.9	78.4	18.8	215	55.2	11980
PD18-101-358	63.2	181	13.8	70	22.3	5.55	42.1	9.45	103	37.6	172.1	38.7	383	82.1	11290
PD18-101-359	16	51	4.2	28.3	8.3	2.49	11.5	2.6	28.8	12.4	58.9	14.44	160	35.2	12710
PD18-101-360	620	1060	92	367	52.8	9.86	53.7	11.17	125.3	49.8	236	54.2	506	105.5	9080
PD18-101-362	618	1043	78.5	241	35.9	8.62	40.9	6.64	63.9	23.4	110.6	25.2	267	57.9	11770
PD18-101-363	188	461	51.3	245	55.5	17.7	77.9	13.52	122.7	43.1	194.3	41.3	404	86.3	10230
PD18-101-364	167	558	59.5	324	46.1	10.13	52.5	9.21	91.1	33.5	154.5	34.7	353	76.3	11550
PD18-101-365	42	144	11.7	69	27.2	6.4	70.8	18.6	196	72.2	320	68.7	646	130.4	10150
PD18-101-373	44.3	119.9	9.87	45.3	16.5	3.33	37.4	10.13	111.4	42.3	196.9	43.6	444	95.4	11380
PD18-101-374	18.8	75	4.92	27.2	14.3	5.75	48.7	12.55	124.6	40	159.3	31	289	56.6	10660
PD18-101-375	4.9	25.3	1.78	10.1	3.65	0.89	8.5	2.67	34	14.47	75.8	18.62	200.2	46.8	12270
PD18-101-377	10.2	34.6	3.01	15.1	4.34	1.17	9.6	3	36.1	15.22	79.8	20.22	216.2	51.3	11420
PD18-101-378	1710	1410	87	176	14.2	5.1	27	6.56	68.1	25.5	119.7	25.9	259.5	56	10470
PD18-101-379	18.3	96.6	6.3	51.7	27.4	9.23	86.7	21.7	224	73.9	297	57.9	536	99.2	10240
PD18-101-380	3.01	24.4	1.33	5.3	2.26	0.8	9.16	3.24	40	16.8	86.8	20.9	218	48.6	12330
PD18-101-381	1370	1920	147	420	28.5	4.35	43.9	12.3	138	51	229	51.9	509	102.9	10710
PD18-101-382	5.9	96.5	2.45	19.7	17.83	5.37	68.4	19.2	203	73	314	63.4	575	112.3	9050
PD18-101-383	780	1340	127	599	77	14.9	71	10.31	96.2	34.7	163	36	358	76.8	12980
PD18-101-384	10.8	47.1	3.83	20.9	4.95	1.14	11.12	3.51	42.6	18.3	93	22.8	245	58.1	11790
PD18-101-385	8.4	44.6	3.33	17.2	3.1	1.05	10.4	3.5	43.6	18.5	94.6	22.5	244	55.7	12670
PD18-101-386	47.5	215	18.4	100.2	19.4	7.57	28.6	7.06	82.9	32.8	153.9	32.7	339	68.7	10290
PD18-101-387	0.012	16.35	0.062	1.4	3.22	0.96	18.6	6.45	74.6	30	134.5	30.2	291	62.7	10810

PD18-105-449	16.7	82.5	6.47	25.5	14.9	1.31	82.2	31.1	399	155.1	698	145	1366	247	11210
PD18-105-450	15.3	84.7	5.04	26.5	16.9	1.29	97.9	35.7	455	177.6	807	164.1	1460	280.7	10470
PD18-105-451	95.9	359	42.1	193	51.1	3.33	119.2	38	382	130.7	565	115.2	1080	206.3	13730
PD18-105-452	21	104	11.1	75.5	76.9	3.32	241	63.1	587	190.4	774	150	1338	244.1	8610
PD18-105-453	0.542	32.6	0.245	4.75	15.54	1.26	111.1	40.8	524	203.9	931	189	1663	309	11060
PD18-105-454	15.9	84.5	6.49	41.7	34	2.36	130.4	41.1	416	142.5	580	113.7	1016	186	8740
PD18-105-455	12.74	58.2	7.14	40.7	37.1	1.04	131.8	43.1	416	121.5	467	90.9	829	156.4	13460
PD18-105-456	7.76	82.4	8.46	73.8	37.4	7.69	102.2	28.44	298	98.6	420	81.8	718	138.5	9140
PD18-105-457	65.2	196	23.9	155	96.2	24.5	279	55.1	508	162.7	688	142.1	1269	241	10700
PD18-105-459	5.35	45.9	1.55	11.79	17.9	1.03	90.9	33.71	393	147.5	657	132.5	1208	227.6	10050
PD18-105-460	87.1	177	16.5	58.7	25.7	1.1	92.4	32.4	359	129.4	556	113	1016	196.9	11620
PD18-105-461	74.4	352	40.4	281	196	28.2	440	101.7	900	261	1028	199.5	1711	321	9310
PD18-105-469	12.1	64.7	5.42	36.1	28.5	1.13	119.1	39.8	425	143.8	593	120.7	1026	197.9	10800
PD18-105-470	21.4	112	12.2	74.3	56.6	2.54	183.4	57.8	625	206.8	846	165.4	1480	271	10690
PD18-105-471	76	819	106	490	119.7	8.38	214	55.9	486	142	559	114	1083	214	11030
PD18-105-472	106.2	160	25.4	83.2	30.4	1.52	121.4	44.9	500	182.3	777	160.3	1410	271.6	9830
PD18-105-473	133	1710	69.8	368	210	4.45	380	85.9	737	215.9	848	168.7	1430	269.3	11190
PD18-105-474	160	385	51.6	217	111	3.29	208	57.9	526	168.3	693	136.2	1228	224.4	10880
PD18-105-475	76.5	375	52.2	297	138	42.3	197	44.5	358	90.8	333	63.7	570	97.9	9850
PD18-105-476	5.17	72.5	5.63	38.8	19.1	1.4	70.7	23.9	281.1	109.8	490	99.6	899	171.5	10300
PD18-105-477	10.83	91.4	6.77	37.1	27.5	1.93	126.4	43.1	473	166.1	706	140	1233	231.7	10300
PD18-105-478	96.8	232	18.01	68.7	41.5	6.04	164	51.5	598	218.4	928	181.3	1562	288.5	9570
PD18-105-479	217	786	107.3	540	352	10.16	1130	364	3190	698	2140	345	2540	393	10160
PD18-105-480	394	731	69.1	252	55.5	1.56	105.2	33.9	388	143.5	621	125.3	1108	211.8	10840
PD18-105-481	17.9	102.3	11.5	68.5	52.3	1.82	159.3	50.1	457	134.8	528	104.1	940	180.6	11000
PD18-105-482	32	115	15.1	71	29.2	1.03	98.2	31.8	381	142.8	621	128.4	1128	214.1	10750
PD18-105-483	27	116	16.3	67	44.7	3.1	126	33.1	333	109.8	456	89	780	144.6	9010
PD18-105-493	1059	489	76.6	231	40.2	4.48	137.9	45.3	509	181.1	796	162.8	1421	274	9980
PD18-105-494	99.4	283.4	26.65	101.5	40.7	1.78	111.9	34.9	356	118.9	513	107.6	962	191.5	11900

PD18-105-495	21.61	197.5	22.1	154.4	60	7.46	121.4	34.2	323	102.3	429	85.7	750	148.4	11110
PD18-105-496	95	303.7	34.3	171	90.8	4.62	246.3	70.9	718	222.9	896	175.7	1483	275.1	10600
PD18-105-497	41.9	79.6	3.13	17.5	22.3	2.52	125.3	43.1	521	201.7	908	187.8	1663	319.3	9810
PD18-105-498	44.8	78.5	8.37	40.7	29.8	1.64	124.6	40.3	432	143.1	574	112.2	1001	191.2	14430
PD18-105-499	0.743	9.96	0.682	6.74	10.95	1.79	64	21.4	242.4	90.2	389.8	76.5	661	127.7	8140
PD18-105-500	250	600	58.5	219	66.4	7.66	119.1	34.7	360	127.7	568	122.4	1156	224.2	13570
PD18-105-501	8.7	33.5	2.88	21.7	15.7	0.95	53.9	17.9	213	77.1	345	73.5	679	123.2	10230
PD18-105-503	18.4	83.9	6.71	38	34.5	2.62	147	48	550	198	846	164	1434	262	9920
PD18-111-167	229.3	3120	248.8	1498	562	113.4	730	121.4	871	231.8	882	179.1	1609	304	13710
PD18-111-168	19	144	14.17	102.5	60.2	13.14	105.3	21.7	183.4	60.7	259	55.2	527	111.2	9920
PD18-111-169	14.1	152.9	13.95	85.2	39.6	9.11	73.2	14.91	130.2	41.9	190.3	40.5	396	82.5	12060
PD18-111-170	6.65	53.4	4.14	28	24	4.74	64.3	15.2	159	59.6	283	61.5	618	128.2	12650
PD18-111-171	13.2	167	15.7	124.3	86.4	17.6	150	22	166.7	46.9	196.6	40.8	409	83.8	10920
PD18-111-172	61.7	503	47.1	285	152	35.4	216	36.3	267	79.3	321	67.5	649	131.5	12420
PD18-111-180	2.84	25.7	2.35	15.9	12.2	3.19	36	9.76	116.2	46.1	226.9	51.7	510	111.2	11010
PD18-111-181	75.5	1370	82.7	512	201	44.8	236	40.4	298	83.8	335	71.1	682	137.5	13380
PD18-111-182	5.63	49.1	4	29.2	17.4	3.89	35	7.66	69.4	24.8	118.6	27.6	295	65.3	11500
PD18-111-184	98.8	1094	99	555	231	47.1	265	44.1	305	79.2	318	70.9	729	155.3	16860
PD18-111-185	5.75	40.9	6.87	50	28.6	5.56	43.9	7.13	63.1	23.44	114.6	26.09	263.5	58.3	11770
PD18-111-186	7.01	65	5.1	43.9	21.5	4.2	37	8.43	86.5	31.6	151	33.6	337	74.6	8150
PD18-111-187	9.26	134.1	9.44	77	72.7	12.2	122.1	18.82	163.1	57.3	258.9	56	528	105.2	8330
PD18-111-188	8.7	66.6	7.2	44.6	22.7	5.02	40.7	8.58	75.3	25.02	115.9	26.5	264.3	58.2	7880
PD18-111-189	7.01	81.7	6.03	39.6	18.1	4.15	32.4	7.13	67.4	24.47	119.2	26.51	273.2	60	8990
PD18-111-190	10	64.7	5.3	31.1	17.6	3.27	33.3	7.4	72.9	26.7	124.1	29.6	295	64.7	9600
PD18-111-191	9.61	110.1	7.79	43.5	21.4	5.49	39.4	8.96	80.7	27.7	129.8	29.1	292.1	65.6	9140
PD18-111-192	11.1	96.6	8.49	70.6	52.1	11.15	78.2	13.43	111.9	36.2	167.8	37.8	366	81.1	8990
PD18-111-193	28.6	471	24.5	133.6	65.1	16.6	100.3	17.55	142	46.6	203	44.1	422	86.9	9100
PD18-111-194	50.1	268	27.8	139.2	46.6	8.38	82.3	20.87	236.6	94.7	453	100.4	947	195.6	10960
PD18-111-202	24.9	254	20.9	110	56.5	13.8	110.8	31.1	329	122.8	547	116.2	1073	205.8	10570

<i>PD18-111-203</i>	19.1	198	19.3	182	82.8	14.2	114.8	21.4	194.7	68.3	303	63.9	606	122.7	10460
<i>PD18-111-204</i>	7.84	60.2	5.57	37.2	18	3.9	40.2	9.29	90	33.16	154.3	35.5	359.3	78.9	9560
<i>PD18-111-205</i>	4.7	43.5	3.74	30.3	22	4.14	47.4	12.08	128.2	49.3	231.5	52.7	511	106.8	10060
<i>PD18-111-206</i>	19.1	230	20.6	200	120	22.6	141	21.9	167.3	49.1	209	44.7	432	91.5	11140
<i>PD18-111-207</i>	71.3	628	58.9	422	108.3	21.5	150.2	28.1	245	83.1	353	76.3	719	140.7	11930
<i>PD18-111-208</i>	8.5	80	8.3	61	41.1	8.83	79.9	15.7	144.1	50.1	213.5	43.9	404	79.9	10870

Appendix 2.3 Zircon Lu–Hf isotopic data – Granitoids of the Dharwar Craton

Analysis N	Hf176/ Hf177	2 S.E.	Lu176/ Hf177	U/Pb AGE (grain)	2 S.E.	Age rock	2 S.E. rock	Hf Chur (t)	Hf DM (t)	Hf NC(t)	Hf _i	eHf	2SE	TDMc	TNCc	Above DM line?
PD17-1-16	0.280992	4.99E-05	0.001564	2618	19	2562	11	0.281104	0.281329	0.281267	0.280913	-6.77	1.764941	3.49	3.360889	No
PD17-1-20	0.281123	4.44E-05	0.002242	2593	22	2562	11	0.281120	0.281347	0.281285	0.281012	-3.87	1.568781	3.30	3.16965	No
PD17-1-33	0.280752	2.55E-05	0.001009	3323	25	3323	25	0.280637	0.280795	0.280741	0.280688	1.82	0.902255	3.54	3.433734	No
PD17-1-42	0.281067	3.5E-05	0.001308	2472	19	2562	11	0.281200	0.281438	0.281375	0.281006	-6.90	1.238859	3.38	3.250921	No
PD17-1-51	0.281091	3.94E-05	0.001725	2553	19	2562	11	0.281146	0.281377	0.281315	0.281007	-4.97	1.392693	3.33	3.202564	No
PD17-1-55	0.281073	3.26E-05	0.001451	2529	22	2562	11	0.281162	0.281395	0.281332	0.281003	-5.68	1.151457	3.36	3.224915	No
PD17-1-58	0.281063	3.27E-05	0.001134	2542	26	2562	11	0.281154	0.281386	0.281323	0.281008	-5.19	1.155469	3.34	3.206534	No
PD17-1-60	0.281096	2.92E-05	0.001675	2525	19	2562	11	0.281165	0.281398	0.281335	0.281015	-5.33	1.031285	3.33	3.201124	No
PD17-21-206	0.280966	3.13E-05	0.002177	3031	24	2991	13	0.280831	0.281017	0.280960	0.280839	0.30	1.105245	3.40	3.282359	No
PD17-21-227	0.280934	3.42E-05	0.001911	2973	20	2991	13	0.280869	0.281061	0.281003	0.280825	-1.57	1.210061	3.46	3.343988	No
PD17-21-215	0.280936	4.65E-05	0.001485	2960	22	2991	13	0.280878	0.281071	0.281013	0.280852	-0.94	1.644495	3.42	3.296263	No

PD17-21-218	0.280989	4.35E-05	0.001682	2960	27	2991	13	0.280878	0.281071	0.281013	0.280893	0.54	1.538686	3.33	3.209911	No
PD17-21-213	0.280967	7.13E-05	0.00233	2952	21	2991	13	0.280883	0.281077	0.281019	0.280835	-1.72	2.519772	3.46	3.335714	No
PD17-21-236	0.280914	4.02E-05	0.00103	2905	23	2991	13	0.280914	0.281112	0.281054	0.280857	-2.04	1.420201	3.44	3.315933	No
PD17-27-471	0.280981	3.34E-05	0.001762	2989	37	3000	14	0.280859	0.281049	0.280991	0.280880	0.77	1.181034	3.34	3.21997	No
PD17-27-451	0.280966	3.91E-05	0.001618	2988	33	3000	14	0.280859	0.281049	0.280992	0.280873	0.50	1.381661	3.36	3.235221	No
PD17-27-435	0.280925	6.32E-05	0.001897	2985	42	3000	14	0.280861	0.281052	0.280994	0.280817	-1.59	2.234034	3.47	3.355113	No
PD17-27-436	0.280878	3.74E-05	0.00112	2977	41	3000	14	0.280867	0.281058	0.281000	0.280814	-1.87	1.321301	3.48	3.364485	No
PD17-27-438	0.280963	5.28E-05	0.00201	2975	33	3000	14	0.280868	0.281059	0.281001	0.280848	-0.72	1.868046	3.42	3.295655	No
PD17-32-249	0.281188	3.88E-05	0.002444	3214	25	3217	10	0.280709	0.280878	0.280823	0.281037	11.67	1.371862	2.88	2.766858	Yes
PD17-32-277	0.280976	4.67E-05	0.002413	3214	20	3217	10	0.280709	0.280878	0.280823	0.280827	4.19	1.649712	3.32	3.205722	No
PD17-32-266	0.280912	2.94E-05	0.001451	3200	26	3217	10	0.280719	0.280889	0.280833	0.280823	3.70	1.039244	3.34	3.222545	No
PD17-32-288	0.281038	5.38E-05	0.002294	3195	19	3217	10	0.280722	0.280892	0.280837	0.280897	6.23	1.900918	3.19	3.070289	Yes
PD17-32-276	0.280954	4.1E-05	0.002452	3187	22	3217	10	0.280727	0.280898	0.280843	0.280804	2.74	1.448914	3.38	3.268018	No
PD17-32-267	0.280896	2.61E-05	0.001428	3170	29	3217	10	0.280739	0.280911	0.280856	0.280809	2.50	0.923748	3.38	3.267652	No
PD17-32-252	0.280929	2.8E-05	0.00208	3041	27	3217	10	0.280824	0.281009	0.280952	0.280808	-0.59	0.99157	3.46	3.342157	No
PD17-38-354	0.280843	3.15E-05	0.000855	3170	19	3170	19	0.280739	0.280911	0.280856	0.280791	1.85	1.114698	3.42	3.305655	No
PD17-38-335	0.280784	4.05E-05	0.001042	3138	21	3138	21	0.280760	0.280936	0.280880	0.280721	-1.39	1.43066	3.58	3.468524	No
PD17-38-330	0.280873	3.28E-05	0.001039	3129	17	3129	17	0.280766	0.280942	0.280887	0.280810	1.58	1.160422	3.40	3.28807	No
PD17-38-334	0.280836	1.94E-05	0.000949	3112	18	3112	18	0.280777	0.280955	0.280899	0.280779	0.06	0.687367	3.48	3.362593	No
PD17-38-333	0.280886	3.9E-05	0.001417	3058	28	3058	28	0.280813	0.280996	0.280940	0.280803	-0.35	1.379488	3.46	3.342477	No
PD17-38-312	0.280895	3.91E-05	0.001404	3056	20	3056	20	0.280814	0.280998	0.280941	0.280812	-0.07	1.380911	3.44	3.324113	No
PD17-38-307	0.280867	3.02E-05	0.000963	3052	20	3052	20	0.280817	0.281001	0.280944	0.280810	-0.24	1.067211	3.45	3.330697	No
PD17-44-392	0.280855	4.58E-05	0.002315	3200	19	3190	21	0.280719	0.280889	0.280833	0.280712	-0.23	1.618006	3.57	3.451649	No
PD17-44-414	0.280797	4.62E-05	0.001369	3198	21	3190	21	0.280720	0.280890	0.280835	0.280713	-0.25	1.633265	3.57	3.451261	No

PD17-44-385	0.280844	3.62E-05	0.002009	3176	23	3190	21	0.280735	0.280907	0.280851	0.280722	-0.47	1.281791	3.56	3.445701	No
PD17-44-369	0.280778	2.4E-05	0.000697	3162	17	3190	21	0.280744	0.280917	0.280862	0.280736	-0.29	0.849042	3.54	3.424211	No
PD17-44-405	0.280820	4.09E-05	0.001428	3145	19	3190	21	0.280755	0.280930	0.280875	0.280734	-0.77	1.44582	3.55	3.437917	No
PD17-44-423	0.280831	4.78E-05	0.002063	3123	22	3190	21	0.280770	0.280947	0.280891	0.280707	-2.25	1.690467	3.62	3.505912	No
PD17-48-514	0.280757	3.44E-05	0.000333	3178	29	3174	11	0.280733	0.280905	0.280850	0.280737	0.13	1.217051	3.53	3.41243	No
PD17-48-478	0.280800	3.5E-05	0.000451	3172	28	3174	11	0.280737	0.280910	0.280854	0.280772	1.25	1.236355	3.46	3.342512	No
PD17-48-480	0.280743	4.12E-05	0.00054	3171	31	3174	11	0.280738	0.280911	0.280855	0.280710	-1.00	1.45783	3.59	3.472709	No
PD17-48-513	0.280790	3.75E-05	0.000326	3171	30	3174	11	0.280738	0.280911	0.280855	0.280770	1.13	1.32521	3.46	3.348749	No
PD17-48-498	0.280762	4.17E-05	0.000525	3160	29	3174	11	0.280745	0.280919	0.280863	0.280730	-0.54	1.473931	3.55	3.437056	No
PD17-48-499	0.280767	3.45E-05	0.000539	3152	30	3174	11	0.280751	0.280925	0.280869	0.280735	-0.56	1.220052	3.55	3.43163	No
PD17-48-479	0.280756	4.11E-05	0.000495	3151	29	3174	11	0.280751	0.280926	0.280870	0.280726	-0.90	1.452597	3.57	3.450224	No
PD17-49-574	0.280752	3.05E-05	0.000459	3254	32	3191	17	0.280683	0.280847	0.280793	0.280723	1.43	1.077636	3.51	3.399547	No
PD17-49-560	0.280832	3.58E-05	0.001138	3159	31	3191	17	0.280746	0.280920	0.280864	0.280763	0.59	1.265908	3.49	3.370171	No
PD17-49-579	0.280831	4.97E-05	0.001032	3143	31	3191	17	0.280757	0.280932	0.280876	0.280769	0.45	1.757909	3.48	3.365495	No
PD17-49-577	0.280740	0.000425	0.001218	3116	44	3191	17	0.280775	0.280952	0.280896	0.280667	-3.84	15.03684	3.71	3.592756	No
PD17-56-601	0.281011	6.74E-05	0.005719	3337	30	3302	12	0.280627	0.280784	0.280731	0.280644	0.57	2.382965	3.63	3.517538	No
PD17-56-620	0.280882	3.62E-05	0.002266	3334	37	3302	12	0.280629	0.280787	0.280733	0.280737	3.82	1.279131	3.44	3.326695	No
PD17-56-635	0.280800	3.67E-05	0.001846	3315	47	3302	12	0.280642	0.280801	0.280747	0.280682	1.42	1.29682	3.56	3.450516	No
PD17-56-592	0.280784	3.7E-05	0.001974	3309	37	3302	12	0.280646	0.280806	0.280752	0.280658	0.43	1.307813	3.61	3.502701	No
PD17-56-642	0.280841	3.96E-05	0.002353	3286	39	3302	12	0.280661	0.280823	0.280769	0.280692	1.09	1.400498	3.56	3.445439	No
PD17-56-630	0.280986	7.06E-05	0.004922	3267	33	3302	12	0.280674	0.280838	0.280783	0.280676	0.08	2.498263	3.60	3.48845	No
PD17-56-641	0.280868	5.08E-05	0.001729	3198	38	3302	12	0.280720	0.280890	0.280835	0.280762	1.50	1.795948	3.46	3.349526	No
PD17-56-641-2	0.281229	7.52E-05	0.002184	3198	38	3302	12	0.280720	0.280890	0.280835	0.281094	13.33	2.657565	2.77	2.655254	Yes

PD18-01-16	0.281186	3.28E-05	0.001333	2685	21	2613	24	0.281060	0.281278	0.281217	0.281118	2.08	1.158428	3.02	2.893708	No
PD18-01-47	0.281186	3.09E-05	0.001335	2628	19	2613	24	0.281097	0.281321	0.281259	0.281119	0.79	1.091339	3.05	2.923035	No
PD18-01-22	0.281246	4.76E-05	0.001195	2589	24	2613	24	0.281123	0.281350	0.281288	0.281186	2.26	1.683139	2.94	2.80392	No
PD18-01-45	0.281192	2.5E-05	0.000922	2551	22	2613	24	0.281148	0.281379	0.281316	0.281147	-0.03	0.882346	3.04	2.908677	No
PD18-101-354	0.281003	3.2E-05	0.000888	2578	36	2545	16	0.281130	0.281359	0.281296	0.280959	-6.08	1.133155	3.42	3.287791	No
PD18-101-359	0.281010	2.76E-05	0.000522	2540	37	2545	16	0.281155	0.281387	0.281324	0.280985	-6.06	0.974645	3.39	3.256321	No
PD18-101-375	0.280999	2.76E-05	0.000686	2538	34	2545	16	0.281156	0.281389	0.281326	0.280966	-6.78	0.974319	3.43	3.296793	No
PD18-101-374	0.281000	2.45E-05	0.000649	2514	40	2545	16	0.281172	0.281407	0.281344	0.280968	-7.24	0.866044	3.44	3.30484	No
PD18-101-352	0.281045	2.88E-05	0.000693	2499	36	2545	16	0.281182	0.281418	0.281355	0.281012	-6.03	1.020028	3.35	3.221534	No
PD18-104-425	0.280784	3.64E-05	0.001163	3342	33	3301	22	0.280624	0.280780	0.280727	0.280709	3.04	1.287794	3.49	3.378667	No
PD18-104-447	0.280788	2.26E-05	0.001039	3310	36	3301	22	0.280645	0.280805	0.280751	0.280722	2.72	0.79881	3.48	3.370358	No
PD18-104-427	0.280761	3.49E-05	0.00101	3306	31	3301	22	0.280648	0.280808	0.280754	0.280696	1.72	1.233466	3.54	3.425538	No
PD18-104-428	0.280794	3.36E-05	0.00127	3303	32	3301	22	0.280650	0.280810	0.280756	0.280714	2.26	1.189358	3.50	3.39133	No
PD18-104-403	0.280775	2.84E-05	0.001058	3297	35	3301	22	0.280654	0.280815	0.280761	0.280708	1.92	1.005512	3.52	3.406187	No

PD18-105-503	0.281226	4.53E-05	0.002619	2689	34	2600	18	0.281057	0.281275	0.281214	0.281092	1.23	1.600601	3.08	2.947134	No
PD18-105-453	0.281257	4.03E-05	0.001898	2624	33	2600	18	0.281100	0.281324	0.281262	0.281162	2.20	1.424681	2.97	2.836618	No
PD18-105-497	0.281367	4.35E-05	0.00394	2583	29	2600	18	0.281127	0.281355	0.281292	0.281172	1.61	1.536833	2.97	2.837571	No
PD18-105-460	0.281247	6.39E-05	0.003216	2550	33	2600	18	0.281148	0.281380	0.281317	0.281090	-2.06	2.259596	3.16	3.028232	No
PD18-105-459	0.281285	9.4E-05	0.002755	2526	38	2600	18	0.281164	0.281398	0.281335	0.281152	-0.42	3.322894	3.04	2.911803	No
PD18-108-83	0.280782	3.17E-05	0.001234	3285	49	3232	32	0.280662	0.280824	0.280770	0.280704	1.51	1.119526	3.53	3.42049	No
PD18-108-76	0.280845	2.77E-05	0.000789	3266	50	3232	32	0.280675	0.280838	0.280784	0.280795	4.29	0.978815	3.36	3.242679	No
PD18-108-99	0.280851	4.88E-05	0.000959	3256	49	3232	32	0.280681	0.280846	0.280791	0.280791	3.92	1.725815	3.37	3.256041	No
PD18-108-106	0.280790	3.34E-05	0.000645	3228	49	3232	32	0.280700	0.280867	0.280812	0.280750	1.76	1.182046	3.47	3.358625	No
PD18-108-96	0.280888	5.97E-05	0.001254	3205	50	3232	32	0.280715	0.280885	0.280830	0.280811	3.40	2.109726	3.36	3.24425	No
PD18-108-77	0.280818	2.13E-05	0.000446	3169	53	3232	32	0.280739	0.280912	0.280857	0.280791	1.85	0.752502	3.42	3.305193	No
PD18-110-138	0.280892	3.84E-05	0.000533	3197	46	3197	46	0.280721	0.280891	0.280836	0.280859	4.94	1.35727	3.26	3.147472	Yes
PD18-110-160	0.280834	3.88E-05	0.000988	3089	49	3079	22	0.280792	0.280973	0.280916	0.280776	-0.60	1.371531	3.50	3.382138	No
PD18-110-162	0.280863	3.05E-05	0.000725	3215	50	3215	50	0.280709	0.280877	0.280822	0.280818	3.91	1.07813	3.34	3.222957	No

PD18-110-165	0.280823	3.5E-05	0.000716	3049	48	3079	22	0.280819	0.281003	0.280946	0.280781	-1.36	1.23805	3.51	3.393744	No
PD18-111-172	0.280870	3.31E-05	0.001455	3250	48	3221	16	0.280685	0.280850	0.280796	0.280779	3.33	1.170218	3.40	3.285574	No
PD18-111-191	0.280846	3.75E-05	0.001246	3221	48	3221	16	0.280705	0.280873	0.280818	0.280769	2.29	1.324847	3.44	3.321971	No
PD18-111-190	0.280857	3.06E-05	0.001259	3219	50	3221	16	0.280706	0.280874	0.280819	0.280779	2.61	1.080911	3.42	3.30199	No
PD18-111-186	0.280890	4.07E-05	0.001568	3209	50	3221	16	0.280713	0.280882	0.280827	0.280794	2.89	1.439877	3.39	3.277525	No
PD18-111-206	0.280823	2.41E-05	0.000822	3181	50	3221	16	0.280731	0.280903	0.280848	0.280773	1.48	0.853764	3.45	3.3362	No
PD18-111-188	0.280846	2.64E-05	0.000713	3177	54	3221	16	0.280734	0.280906	0.280851	0.280802	2.42	0.933829	3.39	3.278198	No
PD18-116-15	0.280866	3.02E-05	0.001163	3209	26	3211	11	0.280713	0.280882	0.280827	0.280795	2.92	1.067944	3.39	3.275494	No
PD18-116-22	0.280892	3.31E-05	0.001179	3199	16	3211	11	0.280719	0.280889	0.280834	0.280820	3.58	1.168874	3.34	3.228964	No
PD18-116-5	0.280845	2.48E-05	0.000638	3199	21	3211	11	0.280719	0.280889	0.280834	0.280806	3.08	0.878005	3.37	3.25817	No
PD18-116-20	0.280885	3.19E-05	0.001627	3186	16	3211	11	0.280728	0.280899	0.280844	0.280785	2.04	1.128044	3.42	3.308093	No
PD18-116-1	0.280889	3.45E-05	0.001233	3174	14	3211	11	0.280736	0.280908	0.280853	0.280814	2.77	1.21968	3.37	3.255242	No
PD18-116-12	0.280885	4.49E-05	0.001679	3171	20	3211	11	0.280738	0.280911	0.280855	0.280782	1.58	1.58633	3.44	3.322145	No
PD18-116-7	0.280890	5.11E-05	0.00136	3127	26	3211	11	0.280767	0.280944	0.280888	0.280808	1.47	1.807275	3.41	3.292654	No
PD18-116-17	0.280836	2.86E-05	0.001071	3125	17	3211	11	0.280769	0.280945	0.280890	0.280772	0.12	1.011494	3.49	3.369968	No
PD18-118-25	0.280953	3.79E-05	0.002948	3329	56	3284	10	0.280633	0.280790	0.280737	0.280764	4.68	1.338907	3.38	3.272145	Yes
PD18-118-3	0.280895	3.63E-05	0.002375	3304	36	3284	10	0.280649	0.280809	0.280756	0.280744	3.38	1.282791	3.44	3.327056	No

PD18-118-18	0.281032	5.61E-05	0.004142	3303	51	3284	10	0.280650	0.280810	0.280756	0.280768	4.21	1.984767	3.39	3.277858	No
PD18-118-20	0.280966	4.47E-05	0.003378	3294	48	3284	10	0.280656	0.280817	0.280763	0.280752	3.41	1.579465	3.43	3.317129	No
PD18-118-26	0.280938	4.17E-05	0.002947	3287	64	3284	10	0.280661	0.280822	0.280768	0.280752	3.25	1.474729	3.43	3.320696	No
PD18-118-9	0.280954	4.95E-05	0.003113	3276	52	3284	10	0.280668	0.280831	0.280777	0.280757	3.18	1.749684	3.43	3.31572	No
PD18-118-14	0.280981	4.54E-05	0.003811	3264	53	3284	10	0.280676	0.280840	0.280785	0.280742	2.33	1.605941	3.47	3.355128	No
PD18-120-29	0.280873	2.6E-05	0.00098	3169	14	3153.7	9	0.280739	0.280912	0.280857	0.280814	2.65	0.920109	3.37	3.258148	No
PD18-120-5	0.280876	2.45E-05	0.001103	3160	13	3153.7	9	0.280745	0.280919	0.280863	0.280809	2.26	0.868029	3.39	3.273446	No
PD18-120-20	0.280858	4.73E-05	0.00112	3155	13	3153.7	9	0.280749	0.280923	0.280867	0.280790	1.48	1.671751	3.43	3.315164	No
PD18-120-14	0.280858	3.44E-05	0.001001	3149	11	3153.7	9	0.280753	0.280927	0.280872	0.280797	1.58	1.216939	3.42	3.304079	No
PD18-120-27	0.280879	4.23E-05	0.001125	3149	8	3153.7	9	0.280753	0.280927	0.280872	0.280810	2.06	1.497155	3.39	3.276164	No
PD18-120-23	0.280898	3.39E-05	0.001445	3144	11	3153.7	9	0.280756	0.280931	0.280875	0.280811	1.94	1.198757	3.39	3.278902	No
PD18-126-35	0.280791	2.88E-05	0.000946	3083	45	3087	25	0.280796	0.280977	0.280921	0.280735	-2.18	1.019247	3.59	3.469143	No
PD18-126-19	0.280829	4.27E-05	0.000867	3066	23	3087	25	0.280808	0.280990	0.280934	0.280778	-1.05	1.508485	3.51	3.389346	No
PD18-126-11	0.280816	3.05E-05	0.000518	3046	38	3087	25	0.280821	0.281005	0.280948	0.280786	-1.24	1.077302	3.50	3.384264	No
PD18-126-9	0.280788	4.98E-05	0.000895	3027	15	3087	25	0.280834	0.281020	0.280963	0.280736	-3.46	1.760028	3.62	3.498197	No
PD18-126-5	0.280799	5.78E-05	0.001077	2983	14	3087	25	0.280863	0.281053	0.280995	0.280738	-4.46	2.044396	3.64	3.520506	No
PD18-126-14	0.280801	6.11E-05	0.00087	2949	22	3087	25	0.280885	0.281079	0.281021	0.280752	-4.75	2.160845	3.63	3.51008	No
PD18-27-113	0.281053	7.4E-05	0.000683	2717	13	2722	20	0.281039	0.281254	0.281193	0.281018	-0.73	2.615795	3.21	3.085917	No
PD18-27-134	0.281064	3.19E-05	0.000545	2691	16	2722	20	0.281056	0.281274	0.281213	0.281036	-0.69	1.126864	3.19	3.062299	No
PD18-34-183	0.280886	3.38E-05	0.001779	2996	23	2972	50	0.280854	0.281043	0.280986	0.280783	-2.52	1.194084	3.54	3.418027	No
PD18-34-182	0.280931	4.03E-05	0.001802	2995	24	2972	50	0.280855	0.281044	0.280987	0.280828	-0.97	1.424082	3.45	3.326888	No
PD18-34-192	0.280944	3.5E-05	0.001102	2925	21	2972	50	0.280901	0.281097	0.281039	0.280882	-0.68	1.23913	3.37	3.252623	No
PD18-37-205	0.281042	2.96E-05	0.000559	2747	20	2747	20	0.281019	0.281231	0.281171	0.281012	-0.23	1.046252	3.21	3.080552	No

PD18-37-236	0.281133	3.03E-05	0.000567	2584	23	2566	16	0.281126	0.281354	0.281292	0.281105	-0.76	1.071947	3.11	2.979061	No
PD18-37-203	0.281055	3.29E-05	0.000581	2573	24	2566	16	0.281133	0.281362	0.281300	0.281026	-3.80	1.164597	3.28	3.149581	No
PD18-37-215	0.281062	2.94E-05	0.000615	2564	25	2566	16	0.281139	0.281369	0.281307	0.281032	-3.81	1.040248	3.27	3.142738	No
PD18-37-199	0.281053	2E-05	0.000176	2536	24	2566	16	0.281158	0.281390	0.281327	0.281045	-4.01	0.708678	3.26	3.132163	No
PD18-37-200	0.281104	4.92E-05	0.000775	2525	22	2566	16	0.281165	0.281398	0.281335	0.281067	-3.50	1.740489	3.23	3.092896	No
PD18-37-196	0.281077	2.62E-05	0.000325	2524	19	2566	16	0.281166	0.281399	0.281336	0.281061	-3.71	0.927093	3.24	3.104746	No
PD18-39-432	0.281072	6.71E-05	0.002178	2679	36	2682	29	0.281064	0.281283	0.281221	0.280961	-3.66	2.373373	3.36	3.227376	No
PD18-39-461	0.281066	3.53E-05	0.00136	2678	25	2682	29	0.281064	0.281283	0.281222	0.280996	-2.43	1.248901	3.28	3.154192	No
PD18-39-434	0.281069	3.59E-05	0.00095	2666	23	2682	29	0.281072	0.281292	0.281231	0.281021	-1.83	1.270213	3.24	3.109192	No
PD18-44-376	0.280942	2.86E-05	0.000847	2689	34	2665	22	0.281057	0.281275	0.281214	0.280898	-5.66	1.012551	3.48	3.352526	No
PD18-44-402	0.280964	2.73E-05	0.000828	2668	35	2665	22	0.281071	0.281291	0.281230	0.280921	-5.32	0.96508	3.44	3.315759	No
PD18-44-382	0.280943	3.44E-05	0.001076	2656	21	2665	22	0.281079	0.281300	0.281238	0.280888	-6.79	1.215145	3.52	3.392138	No
PD18-44-373	0.280966	3.94E-05	0.001513	2647	52	2665	22	0.281085	0.281307	0.281245	0.280889	-6.96	1.392341	3.52	3.395304	No
PD18-44-374	0.280953	3.03E-05	0.001157	2640	44	2665	22	0.281089	0.281312	0.281250	0.280895	-6.91	1.072665	3.52	3.386607	No
PD18-45-334	0.281017	2.71E-05	0.001114	2662	25	2676	17	0.281075	0.281295	0.281234	0.280960	-4.08	0.957274	3.37	3.238429	No
PD18-45-352	0.281030	3.04E-05	0.000887	2653	20	2676	17	0.281081	0.281302	0.281241	0.280985	-3.39	1.075016	3.32	3.190215	No
PD18-45-332	0.281013	3.76E-05	0.001695	2645	17	2676	17	0.281086	0.281308	0.281247	0.280928	-5.63	1.328692	3.44	3.315649	No
PD18-45-336	0.281029	2.97E-05	0.001058	2637	20	2676	17	0.281091	0.281314	0.281253	0.280976	-4.11	1.05055	3.35	3.219471	No
PD18-45-333	0.280990	2.47E-05	0.001047	2625	26	2676	17	0.281099	0.281323	0.281261	0.280937	-5.76	0.875087	3.44	3.307195	No
PD18-47-292	0.281206	2.33E-05	0.000113	2627	38	2620	23	0.281098	0.281322	0.281260	0.281201	3.66	0.823657	2.88	2.752016	No
PD18-47-295	0.281231	7.3E-05	0.000728	2563	28	2620	23	0.281140	0.281370	0.281307	0.281195	1.97	2.582347	2.93	2.79977	No
PD18-47-306	0.281236	5.87E-05	0.000794	2548	29	2620	23	0.281150	0.281381	0.281318	0.281198	1.70	2.074982	2.94	2.803858	No
PD18-47-293	0.281263	3.86E-05	0.000885	2503	22	2620	23	0.281179	0.281415	0.281352	0.281220	1.46	1.363561	2.92	2.781394	No

PD18-54-271	0.281274	3.54E-05	0.001225	2646	18	2627	20	0.281085	0.281308	0.281246	0.281212	4.50	1.253516	2.85	2.717853	No
PD18-54-287	0.281258	3.13E-05	0.000844	2628	19	2627	20	0.281097	0.281321	0.281259	0.281215	4.21	1.106105	2.85	2.720457	No
PD18-54-242	0.281249	5.22E-05	0.001086	2596	16	2627	20	0.281118	0.281345	0.281283	0.281195	2.75	1.846356	2.91	2.780832	No

Appendix 3.1 Detrital Zircon U–Pb data – Detrital Record of the Dharwar Craton

Comments	²⁰⁷ Pb/ ²³⁵ U	2σ	²⁰⁶ Pb/ ²³⁸ U	2σ	Error Correlation (ρ)	²⁰⁷ Pb/ ²³⁵ U Age (Ma)	Age Error 2σ	²⁰⁶ Pb/ ²³⁸ U Age (Ma)	Age Error 2σ	²⁰⁷ Pb/ ²⁰⁶ Pb Age (Ma)	Age 2σ	Final_U_Th_Ratio	Th/U	Discordance
PD17-42-654	7.28	0.24	0.277	0.0085	0.9108	2144	31	1575	43	2732	34	3.067	0.326	42.350
PD17-42-655	18.55	0.48	0.566	0.014	0.7147	3017	25	2888	58	3095	38	1.894	0.528	6.688
PD17-42-656	24.06	0.62	0.656	0.014	0.7836	3269	25	3250	56	3271	33	3.56	0.281	0.642
PD17-42-657	20.5	1.3	0.519	0.025	0.8686	3099	60	2690	110	3360	40	1.716	0.583	19.940
PD17-42-658	14.64	0.38	0.498	0.012	0.8561	2791	25	2604	51	2919	33	2.116	0.473	10.791
PD17-42-659	24.17	0.66	0.653	0.015	0.6323	3273	27	3236	59	3285	39	1.563	0.640	1.492
PD17-42-660	22.45	0.62	0.646	0.015	0.6555	3201	27	3209	57	3185	38	2.477	0.404	-0.754
PD17-42-661	27.58	0.85	0.684	0.021	0.6241	3402	30	3355	79	3434	39	5.32	0.188	2.301
PD17-42-662	10.08	0.35	0.3419	0.0095	0.8230	2439	32	1894	46	2921	38	2.29	0.437	35.159
PD17-42-663	20.09	0.61	0.588	0.015	0.8736	3093	30	2978	61	3161	32	2.25	0.444	5.789
PD17-42-672	12.47	0.38	0.413	0.01	0.8042	2638	28	2228	47	2960	38	1.61	0.621	24.730
PD17-42-673	26.07	0.63	0.6542	0.0083	0.7707	3348	24	3244	32	3405	30	2.319	0.431	4.728
PD17-42-674	14.84	0.44	0.433	0.01	0.5707	2804	29	2318	45	3322	43	3.57	0.280	30.223
PD17-42-674-2	10.14	0.44	0.377	0.016	0.7924	2443	40	2058	74	2773	50	2.52	0.397	25.784

PD17-42-675	14.13	0.57	0.455	0.016	0.8750	2756	39	2417	72	3007	40	2.47	0.405	19.621
PD17-42-676	19.06	0.55	0.519	0.01	0.6641	3043	28	2695	42	3270	36	2.007	0.498	17.584
PD17-42-677	11	0.75	0.326	0.019	0.9641	2507	65	1813	94	3137	38	0.651	1.536	42.206
PD17-42-678	20.82	0.52	0.5473	0.0083	0.8259	3128	24	2812	35	3328	29	4.54	0.220	15.505
PD17-42-679	8.59	0.21	0.3488	0.0059	0.7887	2294	22	1928	28	2627	32	2.987	0.335	26.608
PD17-42-680	17.78	0.57	0.479	0.011	0.7888	2974	32	2519	50	3288	39	2.447	0.409	23.388
PD17-42-681	7.9	0.19	0.2641	0.005	0.5649	2219	22	1510	25	2954	34	0.783	1.277	48.883
PD17-42-682	20.41	0.51	0.5738	0.0087	0.6743	3109	24	2922	36	3220	32	2.86	0.350	9.255
PD17-42-683	21.3	0.54	0.5677	0.009	0.4884	3155	27	2897	37	3310	38	8.19	0.122	12.477
PD17-42-692	20.81	0.89	0.569	0.021	0.8009	3125	41	2900	86	3269	46	1.213	0.824	11.288
PD17-42-693	27.83	0.73	0.688	0.014	0.5294	3410	26	3372	53	3419	39	1.42	0.704	1.375
PD17-42-694	14.89	0.4	0.4668	0.0084	0.8330	2807	26	2468	37	3048	33	8.06	0.124	19.029
PD17-42-695	13.03	0.39	0.3636	0.0088	0.8512	2677	29	1997	41	3231	32	1.504	0.665	38.193
PD17-42-695- 2	11.59	0.35	0.3153	0.0077	0.7883	2570	29	1766	38	3272	35	1.253	0.798	46.027
PD17-42-696	14.44	0.52	0.369	0.01	0.6899	2777	34	2023	49	3373	46	1.282	0.780	40.024
PD17-42-697	16.59	0.42	0.478	0.0087	0.7719	2909	24	2516	38	3185	32	1.829	0.547	21.005
PD17-42-698	10.94	0.38	0.341	0.01	0.8057	2515	34	1890	50	3056	38	1.185	0.844	38.154
PD17-42-699	9.06	0.25	0.3288	0.0063	0.7103	2343	25	1832	30	2816	37	1.701	0.588	34.943
PD17-42-699- 2	23.26	0.66	0.643	0.015	0.7818	3237	28	3197	59	3249	35	4.66	0.215	1.600
PD17-42-700	25.46	0.77	0.671	0.018	0.6913	3325	29	3310	69	3325	41	2.93	0.341	0.451
PD17-42-701	12.85	0.33	0.3789	0.0064	0.7413	2667	24	2070	30	3145	34	0.978	1.022	34.181
PD17-42-702	12.75	0.37	0.398	0.011	0.7753	2659	28	2159	53	3056	40	1.405	0.712	29.352
PD17-42-703	12.18	0.31	0.3803	0.0069	0.8207	2616	24	2076	32	3052	31	3.63	0.275	31.979
PD17-42-712	24.47	0.57	0.667	0.0093	0.8157	3288	22	3293	36	3270	29	3.566	0.280	-0.703
PD17-42-713	10.26	0.25	0.3202	0.0055	0.6132	2457	23	1790	27	3055	35	0.822	1.217	41.408
PD17-42-714	16.18	0.4	0.4777	0.0091	0.7487	2887	24	2516	39	3144	34	1.32	0.758	19.975
PD17-42-715	27.95	0.67	0.697	0.011	0.5738	3416	24	3406	40	3407	32	1.082	0.924	0.029
PD17-42-716	19.92	0.51	0.565	0.01	0.8251	3086	25	2886	42	3206	31	3.18	0.314	9.981
PD17-42-717	18	0.57	0.54	0.011	0.5282	2987	31	2780	46	3118	42	1.972	0.507	10.840

PD17-42-718	21.93	0.6	0.635	0.011	0.5622	3179	26	3166	45	3168	39	2.237	0.447	0.063
PD17-42-719	19.6	0.55	0.535	0.011	0.8331	3071	27	2763	45	3264	32	5.84	0.171	15.349
PD17-42-720	15.43	0.64	0.433	0.016	0.8280	2840	40	2316	72	3229	41	1.86	0.538	28.275
PD17-42-722	27.62	0.69	0.688	0.01	0.6466	3404	24	3373	39	3410	32	1.815	0.551	1.085
PD17-42-723	14.57	0.39	0.4478	0.0088	0.6370	2787	26	2385	39	3079	37	2.63	0.380	22.540
PD17-42-732	22.4	0.55	0.5987	0.0078	0.5623	3200	24	3024	31	3299	33	7.75	0.129	8.336
PD17-42-733	19.44	0.6	0.564	0.015	0.6806	3062	30	2883	63	3171	43	1.805	0.554	9.082
PD17-42-734	12.83	0.35	0.4386	0.0099	0.7606	2666	26	2343	45	2915	35	2.474	0.404	19.623
PD17-42-735	25.1	0.82	0.662	0.017	0.3558	3308	32	3268	68	3330	54	1.424	0.702	1.862
PD17-42-736	12.99	0.46	0.3284	0.0086	0.8055	2675	33	1829	42	3386	38	2.683	0.373	45.983
PD17-42-737	5.82	0.22	0.2515	0.0081	0.8681	1944	33	1445	42	2676	39	3.09	0.324	46.001
PD17-42-738	17.14	0.42	0.5075	0.0092	0.8089	2940	24	2644	39	3141	31	2.78	0.360	15.823
PD17-42-739	16.02	0.55	0.465	0.015	0.9305	2876	33	2462	64	3174	33	1.75	0.571	22.432
PD17-42-740	7.74	0.31	0.272	0.011	0.8549	2197	36	1548	53	2866	43	1.333	0.750	45.987
PD17-42-741	11.21	0.3	0.3973	0.0074	0.7248	2539	25	2156	34	2849	34	3.007	0.333	24.324
PD17-42-742	5.17	0.27	0.1994	0.0064	0.4819	1840	49	1171	35	2894	41	1.891	0.529	59.537
PD17-42-743	7.42	0.2	0.3252	0.0084	0.8146	2161	25	1822	38	2734	35	1.82	0.549	33.358
PD17-42-752	10.94	0.34	0.3842	0.0094	0.6702	2515	29	2094	44	2862	37	2.675	0.374	26.834
PD17-42-753	19.1	0.7	0.54	0.014	0.7301	3044	35	2784	58	3210	42	1.578	0.634	13.271
PD17-42-754	16.5	0.5	0.464	0.011	0.8474	2904	30	2457	47	3220	33	0.977	1.024	23.696
PD17-42-755	22.88	0.55	0.605	0.01	0.6117	3220	23	3046	40	3321	32	1.243	0.805	8.281
PD17-42-757	19.48	0.56	0.551	0.012	0.7678	3064	28	2826	50	3215	36	2.093	0.478	12.100
PD17-42-757-2	9.64	0.32	0.3957	0.0074	0.6263	2398	30	2149	34	2607	44	16.2	0.062	17.568
PD17-42-758	24.08	0.82	0.634	0.018	0.8292	3269	34	3162	72	3326	38	2.12	0.472	4.931
PD17-42-759	19.8	0.66	0.574	0.013	0.7671	3079	32	2923	55	3175	39	2.184	0.458	7.937
PD17-42-760	15.26	0.35	0.5285	0.0088	0.6437	2832	22	2735	37	2888	37	9.36	0.107	5.298
PD17-42-761	22.5	0.53	0.6445	0.0087	0.5044	3205	23	3206	34	3191	33	1.917	0.522	-0.470
PD17-42-762	6.9	0.26	0.2196	0.0058	0.9217	2092	33	1278	31	3019	34	1.152	0.868	57.668
PD17-42-763	19.36	0.6	0.565	0.013	0.7306	3058	30	2900	48	3162	37	2.35	0.426	8.286

PD17-42-772	25.3	0.6	0.6668	0.0097	0.6059	3321	22	3292	38	3323	32	2.15	0.465	0.933
PD17-42-773	17.1	0.48	0.517	0.011	0.8801	2937	27	2683	45	3107	31	2.99	0.334	13.647
PD17-42-774	23.33	0.63	0.613	0.011	0.5503	3238	26	3081	43	3326	39	1.351	0.740	7.366
PD17-42-775	14.04	0.67	0.459	0.019	0.9305	2748	44	2430	82	3126	36	5.36	0.187	22.265
PD17-42-776	15.77	0.62	0.474	0.014	0.8104	2860	38	2500	59	3115	41	1.431	0.699	19.743
PD17-42-777	19.26	0.54	0.582	0.011	0.5367	3054	27	2954	47	3108	41	1.273	0.786	4.955
PD17-42-778	16.36	0.42	0.494	0.01	0.7840	2896	24	2585	44	3108	33	1.697	0.589	16.828
PD17-42-779	15.74	0.39	0.4452	0.0086	0.5291	2860	24	2373	38	3219	39	1.512	0.661	26.281
PD17-42-780	19.7	0.46	0.527	0.0091	0.7745	3076	23	2728	39	3299	32	2.074	0.482	17.308
PD17-42-781	19.19	0.64	0.562	0.015	0.8320	3049	33	2874	61	3157	37	0.592	1.689	8.964
PD17-42-782	15.36	0.73	0.43	0.016	0.9195	2831	45	2303	73	3225	38	1.399	0.715	28.589
PD17-42-783	15.09	0.49	0.4462	0.0082	0.6403	2818	31	2377	36	3136	43	1.401	0.714	24.203
PD17-42-792	15.5	0.34	0.5419	0.007	0.6311	2846	21	2795	28	2874	32	5.13	0.195	2.749
PD17-42-793	15.74	0.45	0.505	0.011	0.9213	2858	27	2632	46	3011	31	3.42	0.292	12.587
PD17-42-794	13.81	0.52	0.527	0.017	0.5672	2735	35	2727	72	2737	54	27.3	0.037	0.365
PD17-42-795	19.33	0.55	0.569	0.012	0.7250	3056	27	2902	49	3147	35	1.646	0.608	7.785
PD17-42-796	16.89	0.44	0.5144	0.0093	0.8484	2927	25	2674	40	3093	30	2.163	0.462	13.547
PD17-42-797	23.06	0.57	0.643	0.011	0.5160	3229	24	3199	43	3235	36	1.274	0.785	1.113
PD17-42-798	21.01	0.56	0.612	0.013	0.7731	3138	26	3077	53	3165	34	2.337	0.428	2.780
PD17-42-799	20.42	0.5	0.5971	0.0096	0.7308	3110	24	3016	39	3159	32	1.906	0.525	4.527
PD17-42-800	29.21	0.66	0.7016	0.0085	0.6354	3460	22	3425	32	3464	30	2.405	0.416	1.126
PD17-42-801	17.26	0.4	0.5081	0.0084	0.7695	2948	22	2647	36	3150	32	3.1	0.323	15.968
PD17-42-802	19.97	0.52	0.596	0.011	0.7639	3088	25	3014	45	3124	33	2.393	0.418	3.521
PD17-42-803	21.74	0.53	0.6123	0.0093	0.5108	3170	24	3077	37	3219	35	2.69	0.372	4.411
PD17-42-812	8.76	0.22	0.3214	0.005	0.6576	2311	23	1796	24	2791	36	2.842	0.352	35.650
PD17-42-813	26.49	0.63	0.665	0.013	0.7006	3363	23	3282	52	3401	32	1.825	0.548	3.499
PD17-42-814	18.93	0.62	0.502	0.014	0.7795	3036	31	2622	59	3302	33	2.214	0.452	20.594
PD17-42-815	22.58	0.51	0.6228	0.0084	0.7098	3208	22	3119	34	3252	30	1.293	0.773	4.090
PD17-42-816	20.31	0.64	0.534	0.016	0.5479	3103	31	2755	67	3333	39	0.779	1.284	17.342
PD17-42-817	19.31	0.68	0.561	0.019	0.8566	3053	34	2867	77	3171	38	2.093	0.478	9.587

PD17-42-818	24.95	0.64	0.662	0.012	0.5850	3305	25	3271	48	3315	33	2.778	0.360	1.327
PD17-42-819	18.39	0.68	0.514	0.018	0.8960	3007	35	2673	79	3235	37	1.138	0.879	17.372
PD17-42-820	20.17	0.51	0.59	0.01	0.8161	3098	24	2989	42	3157	31	1.874	0.534	5.322
PD17-42-821	21.62	0.8	0.617	0.022	0.7956	3164	36	3095	88	3202	45	1.679	0.596	3.342
PD17-42-822	17.76	0.49	0.507	0.011	0.7959	2976	26	2642	47	3200	36	7.46	0.134	17.438
PD17-42-823	16.1	0.56	0.497	0.018	0.8619	2879	33	2597	79	3080	41	7.7	0.130	15.682
PD17-42-823-2	13.59	0.38	0.4413	0.0099	0.8116	2720	26	2355	44	2987	33	4.38	0.228	21.158
PD17-42-832	21.18	0.51	0.624	0.01	0.7126	3148	25	3125	41	3151	34	2.478	0.404	0.825
PD17-42-833	18.42	0.63	0.562	0.017	0.8831	3009	33	2870	69	3090	34	1.645	0.608	7.120
PD17-42-834	16.1	0.77	0.485	0.019	0.7570	2878	45	2548	84	3107	54	2.34	0.427	17.992
PD17-42-835	8.31	0.24	0.2982	0.0078	0.8016	2264	26	1681	38	2828	40	1.494	0.669	40.559
PD17-61-1000	20.59	0.58	0.5397	0.0099	0.6296	3118	28	2781	42	3331	37	2.25	0.444	16.512
PD17-61-1001	20.76	0.6	0.5671	0.0099	0.7749	3132	24	2895	41	3264	34	5.11	0.196	11.305
PD17-61-1001-2	17.65	0.44	0.4821	0.0083	0.7161	2970	24	2536	36	3266	33	5.46	0.183	22.352
PD17-61-1002	16.48	0.5	0.45	0.011	0.7920	2904	29	2392	49	3276	37	2.78	0.360	26.984
PD17-61-1003	26.09	0.61	0.646	0.0093	0.6898	3349	23	3211	37	3421	30	2.32	0.431	6.139
PD17-61-1003-2	24.9	0.78	0.642	0.012	0.7225	3303	31	3194	49	3361	37	44	0.023	4.969
PD17-61-1004	19.95	0.68	0.527	0.017	0.9033	3085	34	2726	71	3319	32	8.83	0.113	17.867
PD17-61-1013	13.99	0.38	0.4102	0.009	0.8305	2747	26	2214	41	3159	31	0.881	1.135	29.915
PD17-61-1014	13.54	0.46	0.402	0.0099	0.8945	2716	33	2177	46	3131	34	2.8	0.357	30.469
PD17-61-1015	27.8	0.74	0.688	0.016	0.6837	3413	28	3372	60	3420	34	1.71	0.585	1.404
PD17-61-1016	14.25	0.47	0.405	0.012	0.8408	2764	31	2192	54	3202	39	1.369	0.730	31.543
PD17-61-1017	22.56	0.9	0.628	0.023	0.8363	3203	39	3137	91	3247	36	1.392	0.718	3.388
PD17-61-1018	24.67	0.72	0.633	0.013	0.7626	3293	29	3158	52	3368	35	1.975	0.506	6.235
PD17-61-1019	23.09	0.6	0.5989	0.0099	0.6733	3229	25	3023	40	3340	35	1.893	0.528	9.491
PD17-61-1020	17.89	0.53	0.5	0.013	0.8375	2980	29	2612	57	3230	34	1.556	0.643	19.133
PD17-61-1021	29.15	0.71	0.694	0.011	0.7795	3457	24	3397	44	3475	29	1.298	0.770	2.245
PD17-61-1022	30.36	0.72	0.693	0.012	0.7421	3500	22	3394	45	3544	30	1.841	0.543	4.233

PD17-61-1023	24.63	0.61	0.647	0.012	0.7440	3293	24	3213	48	3328	32	2.816	0.355	3.456
PD17-61-1024	22.32	0.64	0.579	0.011	0.8027	3196	27	2944	47	3343	33	1.874	0.534	11.935
PD17-61-1025	25.21	0.72	0.626	0.015	0.7758	3314	28	3133	59	3416	35	4.05	0.247	8.285
PD17-61-1026	9.83	0.34	0.322	0.01	0.7091	2417	32	1800	49	2973	45	3.04	0.329	39.455
PD17-61-1027	14.7	0.39	0.4106	0.0081	0.8390	2794	25	2216	37	3228	30	1.605	0.623	31.351
PD17-61-1028	20.95	0.53	0.584	0.011	0.7503	3134	25	2963	44	3235	32	0.891	1.122	8.408
PD17-61-837	14.56	0.4	0.462	0.012	0.7564	2786	26	2449	53	3194	38	4.97	0.201	23.325
PD17-61-838	9.98	0.34	0.322	0.01	0.9086	2429	33	1798	51	3002	36	1.57	0.637	40.107
PD17-61-839	26.91	0.71	0.681	0.013	0.8550	3378	26	3344	51	3387	30	17.87	0.056	1.270
PD17-61-840	18.82	0.59	0.52	0.012	0.8715	3031	30	2699	52	3245	35	2.505	0.399	16.826
PD17-61-841	17.16	0.52	0.473	0.013	0.8647	2941	30	2496	56	3252	33	2.121	0.471	23.247
PD17-61-842	21.64	0.54	0.5608	0.0099	0.7531	3166	25	2868	41	3344	31	2.91	0.344	14.234
PD17-61-843	25.23	0.74	0.665	0.016	0.8202	3315	28	3282	61	3323	34	2.169	0.461	1.234
PD17-61-852	26.81	0.66	0.673	0.013	0.7150	3375	24	3315	48	3398	33	1.846	0.542	2.443
PD17-61-853	12.5	0.32	0.3464	0.0062	0.8485	2641	24	1916	30	3244	30	4.75	0.211	40.937
PD17-61-854	21.27	0.54	0.563	0.014	0.6056	3150	25	2876	58	3323	39	2.33	0.429	13.452
PD17-61-854-2	23.55	0.65	0.598	0.015	0.6400	3248	27	3018	59	3390	34	2.729	0.366	10.973
PD17-61-855	10.99	0.34	0.353	0.011	0.8880	2519	29	1948	52	3006	34	1.757	0.569	35.196
PD17-61-856	18.37	0.52	0.491	0.013	0.8365	3007	27	2573	57	3301	35	2.98	0.336	22.054
PD17-61-857	28.73	0.71	0.68	0.013	0.7617	3443	24	3342	51	3490	32	3.34	0.299	4.241
PD17-61-858	24.22	0.62	0.629	0.012	0.7143	3276	25	3145	45	3346	33	3.7	0.270	6.007
PD17-61-859	10.82	0.41	0.353	0.012	0.8608	2504	35	1949	59	2983	39	3.56	0.281	34.663
PD17-61-860	17.03	0.48	0.474	0.011	0.8109	2933	27	2498	48	3238	34	1.315	0.760	22.854
PD17-61-861	12.74	0.4	0.402	0.012	0.8809	2656	30	2173	55	3041	35	6.46	0.155	28.543
PD17-61-862	10.94	0.33	0.3024	0.008	0.8959	2514	28	1701	40	3248	32	3.61	0.277	47.629
PD17-61-863	11.03	0.32	0.3761	0.009	0.7956	2522	27	2056	42	2914	39	6.01	0.166	29.444
PD17-61-872	14.67	0.41	0.415	0.011	0.8300	2792	27	2236	48	3212	35	0.717	1.395	30.386
PD17-61-873	12	0.31	0.3822	0.0083	0.7405	2602	24	2084	39	3021	35	1.435	0.697	31.016
PD17-61-874	23.25	0.85	0.617	0.023	0.8799	3233	36	3093	91	3312	38	7.48	0.134	6.612

PD17-61-875	30.33	0.76	0.722	0.012	0.7325	3495	25	3500	46	3483	31	1.989	0.503	-0.488
PD17-61-876	30.12	0.82	0.733	0.016	0.7706	3491	26	3542	60	3447	34	3.072	0.326	-2.756
PD17-61-877	25.82	0.76	0.646	0.017	0.8524	3336	29	3207	66	3405	33	1.324	0.755	5.815
PD17-61-878	25.16	0.63	0.65	0.013	0.6804	3314	25	3225	53	3354	37	4.6	0.217	3.846
PD17-61-879	21.51	0.57	0.566	0.011	0.6488	3161	25	2889	45	3327	35	5.22	0.192	13.165
PD17-61-880	13.02	0.44	0.381	0.012	0.8954	2678	33	2077	58	3160	35	1.389	0.720	34.272
PD17-61-881	14.17	0.49	0.402	0.015	0.8344	2758	33	2176	71	3207	44	0.823	1.215	32.148
PD17-61-882	20.87	0.67	0.553	0.016	0.8555	3129	32	2832	67	3316	35	1.226	0.816	14.596
PD17-61-883	14.27	0.47	0.421	0.013	0.9158	2764	32	2262	60	3146	33	9.23	0.108	28.099
PD17-61-884	25.32	0.81	0.6	0.017	0.8430	3317	31	3025	68	3492	36	1.527	0.655	13.373
PD17-61-892	15.48	0.58	0.436	0.015	0.8625	2842	36	2330	69	3217	39	0.44	2.273	27.572
PD17-61-893	15.46	0.48	0.438	0.013	0.8045	2845	28	2338	60	3210	38	1.045	0.957	27.165
PD17-61-894	18.53	0.53	0.454	0.01	0.8399	3016	28	2412	45	3435	32	1.269	0.788	29.782
PD17-61-895	15.03	0.48	0.431	0.012	0.8798	2813	31	2305	56	3191	33	1.499	0.667	27.766
PD17-61-896	26.02	0.67	0.67	0.013	0.8327	3345	25	3303	52	3356	30	1.55	0.645	1.579
PD17-61-897	24.06	0.64	0.601	0.013	0.8149	3269	26	3032	52	3407	32	1.319	0.758	11.007
PD17-61-898	18.72	0.55	0.495	0.013	0.8536	3024	29	2588	54	3319	33	1.253	0.798	22.025
PD17-61-899	17.48	0.42	0.5079	0.0081	0.3574	2961	23	2647	35	3311	37	0.958	1.044	20.054
PD17-61-900	13.56	0.37	0.419	0.0085	0.8398	2717	27	2254	39	3299	31	1.035	0.966	31.676
PD17-61-901	24.43	1.1	0.666	0.025	0.8674	3283	43	3289	97	3270	42	1.171	0.854	-0.581
PD17-61-902	31.58	0.82	0.722	0.017	0.8018	3536	26	3501	62	3536	33	2.357	0.424	0.990
PD17-61-903	5.73	0.24	0.2028	0.008	0.9516	1933	36	1189	43	2855	35	3.76	0.266	58.354
PD17-61-912	19.01	0.7	0.508	0.015	0.7684	3038	37	2644	65	3299	44	1.71	0.585	19.855
PD17-61-913	22.21	0.66	0.587	0.018	0.8120	3191	29	2973	72	3322	38	2.55	0.392	10.506
PD17-61-914	13.33	0.39	0.411	0.0096	0.8727	2699	28	2217	44	3076	32	1.128	0.887	27.926
PD17-61-915	18.98	0.66	0.546	0.018	0.8241	3035	34	2803	75	3184	39	1.205	0.830	11.966
PD17-61-916	25.89	0.66	0.674	0.012	0.7966	3340	25	3319	48	3338	30	1.625	0.615	0.569
PD17-61-917	9.2	0.29	0.2838	0.0081	0.8500	2355	29	1609	41	3075	36	0.767	1.304	47.675
PD17-61-918	24.63	0.69	0.607	0.013	0.8472	3290	28	3053	52	3429	31	2.319	0.431	10.965
PD17-61-919	16.21	0.47	0.466	0.012	0.8425	2887	28	2464	53	3185	33	1.223	0.818	22.637

PD17-61-920	27.6	0.89	0.647	0.02	0.8728	3402	32	3213	78	3504	34	13.53	0.074	8.305
PD17-61-921	19.42	0.76	0.553	0.019	0.8431	3059	39	2833	80	3200	40	0.99	1.010	11.469
PD17-61-922	21.7	0.65	0.581	0.013	0.8189	3167	29	2959	56	3286	33	0.663	1.508	9.951
PD17-61-923	22.02	0.59	0.56	0.012	0.7805	3183	26	2863	50	3382	32	1.112	0.899	15.346
PD17-61-932	11.06	0.29	0.3288	0.0072	0.8625	2526	24	1831	35	3128	31	0.936	1.068	41.464
PD17-61-933	17.28	0.5	0.455	0.01	0.8631	2946	28	2416	46	3318	32	1.29	0.775	27.185
PD17-61-934	27.05	0.88	0.649	0.017	0.6496	3383	32	3220	67	3467	42	1.86	0.538	7.124
PD17-61-935	10.04	0.35	0.341	0.01	0.7787	2434	32	1891	48	3077	39	1.045	0.957	38.544
PD17-61-936	18.68	0.69	0.53	0.018	0.8761	3022	37	2740	76	3204	39	1.411	0.709	14.482
PD17-61-937	9.57	0.32	0.2847	0.0082	0.7982	2390	32	1613	41	3130	38	2.245	0.445	48.466
PD17-61-938	21.07	0.6	0.53	0.014	0.8382	3138	28	2737	57	3397	33	1.113	0.898	19.429
PD17-61-940	18.07	0.52	0.538	0.014	0.8440	2990	28	2768	60	3361	34	12.9	0.078	17.644
PD17-61-941	27.09	0.76	0.684	0.016	0.8024	3384	28	3354	62	3390	34	2.329	0.429	1.062
PD17-61-942	22.45	0.6	0.5763	0.0099	0.6503	3202	26	2933	40	3349	30	1.905	0.525	12.422
PD17-61-943	19.06	0.54	0.519	0.015	0.8465	3042	28	2692	64	3274	37	2.152	0.465	17.776
PD17-61-952	21.37	1	0.607	0.032	0.7782	3149	46	3050	130	3205	54	1.818	0.550	4.836
PD17-61-955	19.94	0.48	0.582	0.01	0.8018	3087	24	2952	42	3317	30	3	0.333	11.004
PD17-61-956	27.61	0.83	0.681	0.019	0.7654	3405	31	3340	71	3430	37	2.143	0.467	2.624
PD17-61-957	24.31	0.59	0.63	0.01	0.8851	3280	23	3149	39	3347	30	1.275	0.784	5.916
PD17-61-958	16.52	0.57	0.476	0.015	0.7983	2902	34	2507	65	3180	39	1.004	0.996	21.164
PD17-61-959	18	0.67	0.511	0.018	0.8582	2987	36	2656	79	3347	38	1.808	0.553	20.645
PD17-61-960	27.5	0.74	0.668	0.017	0.7622	3399	26	3293	67	3452	36	1.113	0.898	4.606
PD17-61-961	25.41	0.64	0.659	0.014	0.8106	3322	25	3261	53	3354	32	2.71	0.369	2.773
PD17-61-962	25.71	0.92	0.635	0.021	0.7984	3331	36	3163	85	3424	40	2.026	0.494	7.623
PD17-61-963	13.27	0.39	0.3844	0.0098	0.8090	2697	28	2095	46	3175	35	7.39	0.135	34.016
PD17-61-964	24.43	0.82	0.623	0.018	0.8307	3282	33	3116	72	3374	36	3.817	0.262	7.647
PD17-61-973	21.06	0.64	0.538	0.015	0.8762	3137	30	2768	62	3374	33	2.387	0.419	17.961
PD17-61-974	13.17	0.44	0.429	0.013	0.8737	2688	32	2299	60	3178	35	1.027	0.974	27.659
PD17-61-975	12.25	0.48	0.413	0.018	0.8511	2621	38	2226	81	3170	46	1.03	0.971	29.779
PD17-61-976	18.91	0.47	0.5198	0.0093	0.7986	3036	24	2697	39	3250	31	1.565	0.639	17.015

PD17-61-977	23.2	0.54	0.636	0.01	0.7748	3234	23	3171	41	3262	30	1.683	0.594	2.790
PD17-61-978	21.54	0.59	0.591	0.016	0.8786	3161	27	2988	64	3422	33	1.737	0.576	12.683
PD17-61-979	19.28	0.55	0.528	0.014	0.8212	3053	28	2729	58	3263	34	1.106	0.904	16.365
PD17-61-980	15.03	0.45	0.442	0.011	0.8799	2820	27	2359	50	3148	34	1.825	0.548	25.064
PD17-61-981	22	0.95	0.639	0.032	0.9029	3180	42	3180	130	3174	46	0.841	1.189	-0.189
PD17-61-982	17.38	0.47	0.4311	0.0087	0.6812	2955	26	2310	39	3415	35	1.01	0.990	32.357
PD17-61-983	15.7	0.42	0.4523	0.0088	0.8200	2855	26	2410	41	3177	32	2.594	0.386	24.142
PD17-61-984	11.59	0.27	0.3561	0.0057	0.7503	2574	24	1963	27	3086	31	3.72	0.269	36.390
PD17-61-993	23.76	0.73	0.646	0.016	0.8493	3255	30	3208	65	3273	34	1.228	0.814	1.986
PD17-61-994	27.15	0.79	0.6567	0.0085	0.7326	3387	28	3253	33	3456	35	2.293	0.436	5.874
PD17-61-994-2	21.5	0.89	0.581	0.025	0.7138	3157	41	2950	100	3286	50	3.51	0.285	10.225
PD17-61-995	23.39	0.69	0.6	0.017	0.7650	3240	29	3023	68	3367	38	1.884	0.531	10.217
PD17-61-996	27.1	0.69	0.672	0.013	0.7482	3385	25	3308	51	3424	31	1.93	0.518	3.388
PD17-61-997	22.7	0.66	0.587	0.014	0.8295	3211	28	2984	59	3340	32	1.503	0.665	10.659
PD17-61-998	18.26	0.49	0.491	0.011	0.5273	3003	26	2575	48	3297	40	2.688	0.372	21.899
PD17-61-999	18.31	0.53	0.498	0.011	0.8361	3005	29	2604	47	3276	34	4.88	0.205	20.513
PD18-117-10	7.57	0.26	0.2459	0.0084	0.7046	2181	15	1417	22	3004	21	1.013	0.987	52.830
PD18-117-100	6.78	0.22	0.2248	0.007	0.6562	2083	14	1307	18	2971	22	1.23	0.813	56.008
PD18-117-102	17.5	0.49	0.5832	0.013	0.5452	2963	14	2962	27	2963	20	2.097	0.477	0.034
PD18-117-103	17.44	0.51	0.577	0.015	0.7309	2959	14	2936	31	2975	17	2.055	0.487	1.311
PD18-117-104	10.62	0.4	0.3075	0.011	0.7392	2490	18	1728	27	3188	21	1.513	0.661	45.797
PD18-117-105	6.86	0.28	0.1921	0.012	0.7073	2094	18	1133	32	3241	35	0.497	2.012	65.042
PD18-117-106	9.51	0.28	0.35	0.0088	0.7902	2389	14	1935	21	2802	15	3.86	0.259	30.942
PD18-117-107	23.28	1.1	0.561	0.025	0.7839	3239	23	2871	52	3475	24	1.269	0.788	17.381
PD18-117-108	20.85	0.67	0.561	0.015	0.6540	3132	16	2871	31	3303	20	1.732	0.577	13.079
PD18-117-109	20.15	0.67	0.564	0.017	0.7821	3099	16	2883	35	3241	17	1.524	0.656	11.046
PD18-117-11	9.13	0.38	0.2695	0.011	0.6508	2351	19	1538	28	3157	28	1.115	0.897	51.283
PD18-117-119	5.194	0.14	0.1685	0.0036	0.3836	1852	12	1004	10	3007	22	0.895	1.117	66.611

PD18-117-12	9.56	0.29	0.3198	0.0079	0.4151	2393	14	1789	19	2957	25	1.81	0.552	39.499
PD18-117-120	17.25	0.49	0.588	0.016	0.5169	2949	14	2981	33	2927	22	1.008	0.992	-1.845
PD18-117-121	7.74	1	0.2278	0.024	0.6333	2201	58	1323	63	3162	82	0.521	1.919	58.159
PD18-117-122	7.41	0.32	0.2514	0.0097	0.5230	2162	19	1446	25	2934	33	1.502	0.666	50.716
PD18-117-123	8.94	0.43	0.2753	0.012	0.7874	2332	22	1568	30	3090	24	0.83	1.205	49.256
PD18-117-124	10.67	0.34	0.3244	0.0089	0.6949	2495	15	1811	22	3110	19	1.326	0.754	41.768
PD18-117-125	5.242	0.13	0.2108	0.0046	0.5987	1859	11	1233	12	2656	18	2.749	0.364	53.577
PD18-117-126	22.26	0.69	0.626	0.019	0.6336	3195	15	3134	38	3234	21	1.85	0.541	3.092
PD18-117-127	10.07	0.36	0.3013	0.011	0.7159	2441	17	1698	27	3136	22	0.801	1.248	45.855
PD18-117-13	7.6	0.6	0.2249	0.017	0.8822	2185	35	1308	45	3153	30	1.13	0.885	58.516
PD18-117-135	18.47	0.54	0.487	0.014	0.6636	3015	14	2558	30	3335	19	1.006	0.994	23.298
PD18-117-136	9.6	0.32	0.2933	0.0088	0.5166	2397	15	1658	22	3103	25	1.36	0.735	46.568
PD18-117-137	9.77	0.28	0.3002	0.0082	0.7491	2413	13	1692	20	3093	16	1.493	0.670	45.296
PD18-117-138	20.14	0.61	0.623	0.017	0.5964	3098	15	3122	34	3083	21	2.38	0.420	-1.265
PD18-117-139	9.73	0.39	0.3004	0.011	0.4731	2410	19	1693	27	3086	32	0.844	1.185	45.139
PD18-117-14	9.05	0.34	0.302	0.011	0.7691	2343	17	1701	27	2961	21	1.222	0.818	42.553
PD18-117-140	21.02	0.58	0.5959	0.014	0.6398	3140	14	3013	28	3221	18	1.954	0.512	6.458
PD18-117-142	19.44	0.53	0.5674	0.013	0.4462	3064	13	2897	27	3175	21	2.223	0.450	8.756
PD18-117-143	3.195	0.27	0.1327	0.0068	0.2036	1456	33	803	19	2602	75	2.837	0.352	69.139
PD18-117-144	13.02	0.5	0.442	0.016	0.7305	2681	18	2360	36	2933	22	1.348	0.742	19.536
PD18-117-145	17.47	0.79	0.497	0.022	0.7966	2961	22	2601	47	3216	23	0.696	1.437	19.123
PD18-117-15	7.22	0.41	0.2321	0.013	0.5905	2139	25	1345	34	3021	41	0.833	1.200	55.478
PD18-117-153	15.45	0.88	0.441	0.024	0.5350	2843	27	2355	54	3210	43	0.972	1.029	26.636
PD18-117-154	18.48	0.62	0.599	0.016	0.4640	3015	16	3026	32	3008	26	2.467	0.405	-0.598
PD18-117-155	19.3	0.78	0.556	0.022	0.5142	3057	20	2850	46	3196	31	2.75	0.364	10.826
PD18-117-156	9.9	0.34	0.314	0.011	0.6365	2426	16	1760	27	3043	24	1.56	0.641	42.162
PD18-117-157	18.11	0.52	0.49	0.012	0.4836	2996	14	2571	26	3295	22	2.104	0.475	21.973
PD18-117-158	11.78	0.42	0.3835	0.013	0.7109	2587	17	2093	30	3001	22	2.109	0.474	30.257
PD18-117-16	8.01	0.32	0.2444	0.0097	0.6249	2232	18	1410	25	3105	28	0.684	1.462	54.589
PD18-117-160	11.56	0.46	0.3471	0.013	0.5288	2569	19	1921	31	3130	30	2.23	0.448	38.626

PD18-117-161	12.58	0.41	0.3906	0.011	0.6075	2649	15	2126	26	3077	22	1.027	0.974	30.907
PD18-117-162	7.57	0.45	0.2363	0.012	0.8390	2181	27	1367	31	3068	26	0.598	1.672	55.443
PD18-117-17	25.07	0.62	0.5904	0.014	0.8711	3311	12	2991	28	3511	10	2.166	0.462	14.811
PD18-117-18	17.78	0.57	0.574	0.015	0.5968	2978	16	2924	31	3014	22	1.138	0.879	2.986
PD18-117-19	9.78	0.54	0.3274	0.013	0.6056	2414	25	1826	32	2956	36	2.024	0.494	38.227
PD18-117-27	5.19	0.25	0.1614	0.0056	0.6387	1851	21	965	16	3074	30	0.972	1.029	68.608
PD18-117-28	5.38	0.16	0.206	0.005	0.6804	1882	13	1207	13	2737	19	1.516	0.660	55.901
PD18-117-29	10.08	0.29	0.3133	0.0093	0.6832	2442	13	1757	23	3075	19	1.091	0.917	42.862
PD18-117-30	10.87	1.4	0.3368	0.028	0.6812	2512	60	1871	68	3080	75	0.953	1.049	39.253
PD18-117-31	11.18	0.55	0.3217	0.015	0.4631	2538	23	1798	37	3198	39	0.917	1.091	43.777
PD18-117-32	9.68	0.41	0.318	0.013	0.8286	2405	20	1780	32	2986	20	1.174	0.852	40.388
PD18-117-33	7.32	0.31	0.2583	0.01	0.5099	2151	19	1481	26	2871	33	1.712	0.584	48.415
PD18-117-34	8.08	0.31	0.2474	0.008	0.7496	2240	17	1425	21	3099	21	0.758	1.319	54.017
PD18-117-35	14.46	0.49	0.4179	0.012	0.7026	2780	16	2251	27	3191	20	0.655	1.527	29.458
PD18-117-36	6.56	0.44	0.2004	0.012	0.7639	2054	30	1177	32	3103	35	0.816	1.225	62.069
PD18-117-37	12.65	0.61	0.3826	0.017	0.8790	2654	23	2088	40	3119	19	1.111	0.900	33.055
PD18-117-45	22.8	1	0.613	0.026	0.7769	3218	21	3082	52	3305	23	0.812	1.232	6.747
PD18-117-47	23.83	0.66	0.636	0.016	0.5689	3261	14	3173	32	3316	20	15	0.067	4.312
PD18-117-48	24.06	0.68	0.664	0.018	0.5333	3271	14	3283	35	3264	21	1.226	0.816	-0.582
PD18-117-49	18.5	0.44	0.5945	0.013	0.4707	3016	12	3008	26	3022	19	2.067	0.484	0.463
PD18-117-50	14.7	0.43	0.4135	0.011	0.5057	2796	14	2231	25	3234	22	1.107	0.903	31.014
PD18-117-51	18.82	0.55	0.605	0.014	0.6796	3033	14	3050	28	3021	18	1.48	0.676	-0.960
PD18-117-52	9.16	0.27	0.2432	0.0064	0.6182	2354	14	1403	17	3324	20	0.924	1.082	57.792
PD18-117-53	5.2	0.2	0.1699	0.0061	0.5551	1853	16	1012	17	2995	28	0.687	1.456	66.210
PD18-117-54	6.19	0.2	0.2134	0.0054	0.4628	2003	14	1247	14	2908	25	0.985	1.015	57.118
PD18-117-55	9.39	0.65	0.2658	0.018	0.7102	2377	32	1519	46	3224	41	0.692	1.445	52.885
PD18-117-63	11.09	0.4	0.3885	0.012	0.6808	2531	17	2116	28	2882	22	1.069	0.935	26.579
PD18-117-64	14.06	0.76	0.452	0.023	0.8649	2754	26	2404	51	3021	22	2.97	0.337	20.424
PD18-117-65	20.13	0.55	0.607	0.016	0.4909	3098	13	3058	32	3123	22	1.184	0.845	2.081
PD18-117-66	13.07	0.4	0.3625	0.01	0.6917	2685	15	1994	24	3256	18	1.268	0.789	38.759

PD18-117-67	8.55	0.22	0.2427	0.0061	0.6998	2291	12	1401	16	3219	16	0.575	1.739	56.477
PD18-117-68	17.5	0.56	0.584	0.018	0.7370	2963	15	2965	37	2961	19	2.631	0.380	-0.135
PD18-117-69	5.38	0.17	0.2202	0.0055	0.7251	1882	14	1283	15	2627	18	1.248	0.801	51.161
PD18-117-70	8.45	4	0.29	0.068	0.6052	2281	215	1642	170	2916	308	0.927	1.079	43.690
PD18-117-71	8.53	0.6	0.2596	0.0099	0.8693	2289	32	1488	25	3109	33	0.938	1.066	52.139
PD18-117-72	12.69	0.73	0.349	0.018	0.5518	2657	27	1930	43	3269	41	1.649	0.606	40.961
PD18-117-73	17.69	0.55	0.591	0.016	0.5742	2973	15	2993	32	2959	22	2.222	0.450	-1.149
PD18-117-81	23.35	0.71	0.657	0.017	0.7227	3242	15	3255	33	3233	17	0.816	1.225	-0.680
PD18-117-82	21.51	0.76	0.562	0.019	0.7118	3162	17	2875	39	3349	21	1.104	0.906	14.153
PD18-117-83	19.84	0.58	0.61	0.017	0.4067	3084	14	3070	34	3092	25	2.078	0.481	0.712
PD18-117-84	15.21	0.63	0.491	0.015	0.5579	2828	20	2575	32	3014	28	0.812	1.232	14.565
PD18-117-85	13.21	0.4	0.3686	0.01	0.6616	2695	14	2023	24	3246	19	0.773	1.294	37.677
PD18-117-86	11.06	0.33	0.3204	0.0082	0.7256	2528	14	1792	20	3187	17	1.384	0.723	43.772
PD18-117-87	18.56	0.55	0.607	0.014	0.5401	3019	14	3058	28	2994	21	1.874	0.534	-2.138
PD18-117-88	8.9	0.3	0.295	0.0089	0.7305	2328	15	1666	22	2972	19	1.635	0.612	43.943
PD18-117-89	14.26	0.58	0.4463	0.015	0.6881	2767	19	2379	33	3064	24	1.969	0.508	22.356
PD18-117-9	8.97	0.28	0.2822	0.0079	0.6225	2335	14	1602	20	3056	21	1.106	0.904	47.579
PD18-117-90	4.6	0.15	0.1679	0.0046	0.7891	1749	14	1001	13	2816	17	1.173	0.853	64.453
PD18-117-91	9.92	0.53	0.25	0.013	0.8932	2427	25	1438	34	3406	19	1.88	0.532	57.780
PD18-117-99	18.05	0.61	0.585	0.019	0.6096	2992	16	2969	39	3008	24	2.227	0.449	1.297
PD18-125-170	15.07	0.83	0.438	0.02	0.6158	2820	26	2342	45	3182	36	4.85	0.206	26.398
PD18-125-171	17.24	0.5	0.456	0.011	0.5179	2948	14	2422	24	3330	21	0.802	1.247	27.267
PD18-125-172	14.47	0.61	0.429	0.014	0.7373	2781	20	2301	32	3150	23	1.45	0.690	26.952
PD18-125-173	14.53	0.41	0.4283	0.013	0.5777	2785	14	2298	29	3160	22	1.116	0.896	27.278
PD18-125-174	15.68	0.42	0.514	0.011	0.3535	2858	13	2674	23	2990	23	1.146	0.873	10.569
PD18-125-175	19.25	0.6	0.563	0.018	0.5267	3054	15	2879	37	3172	25	2.171	0.461	9.237
PD18-125-176	19.29	0.48	0.6239	0.013	0.3829	3056	12	3125	26	3011	21	4.302	0.232	-3.786
PD18-125-177	13.88	0.49	0.3791	0.01	0.6864	2742	17	2072	23	3280	21	0.725	1.379	36.829
PD18-125-178	13.76	0.41	0.389	0.012	0.8033	2733	14	2118	28	3226	15	2.53	0.395	34.346

PD18-125-179	19.75	0.49	0.539	0.013	0.7343	3079	12	2779	27	3281	15	1.8	0.556	15.300
PD18-125-180	18.79	0.55	0.54	0.015	0.6476	3031	14	2783	31	3200	19	1.024	0.977	13.031
PD18-125-181	21.42	0.79	0.586	0.02	0.6647	3158	18	2973	41	3277	23	1.338	0.747	9.277
PD18-125-182	19.09	0.52	0.467	0.013	0.6747	3046	13	2470	29	3452	18	1.86	0.538	28.447
PD18-125-183	18.24	0.82	0.5	0.022	0.7267	3002	22	2614	47	3274	26	1.516	0.660	20.159
PD18-125-192	11.05	0.61	0.339	0.017	0.8005	2527	26	1882	41	3096	27	1.258	0.795	39.212
PD18-125-193	17.18	0.44	0.466	0.014	0.5872	2945	12	2466	31	3291	20	0.93	1.075	25.068
PD18-125-194	15.87	0.61	0.447	0.015	0.9397	2869	18	2382	33	3231	11	0.858	1.166	26.277
PD18-125-195	24.23	0.67	0.668	0.016	0.3501	3278	14	3298	31	3265	24	2.13	0.469	-1.011
PD18-125-197	20	0.69	0.578	0.019	0.6909	3091	17	2941	39	3191	21	1.529	0.654	7.835
PD18-125-198	17.75	0.8	0.547	0.02	0.4718	2976	22	2813	42	3089	34	2.13	0.469	8.935
PD18-125-199	21.27	0.6	0.57	0.015	0.8287	3151	14	2908	31	3310	13	1.648	0.607	12.145
PD18-125-200	19.19	0.54	0.477	0.014	0.7524	3051	14	2514	31	3427	16	0.775	1.290	26.641
PD18-125-201	14.01	0.48	0.396	0.012	0.6853	2750	16	2151	28	3226	21	0.726	1.377	33.323
PD18-125-202	21.61	0.86	0.612	0.024	0.6780	3166	19	3078	48	3223	25	1.129	0.886	4.499
PD18-125-203	17.05	0.44	0.524	0.013	0.5978	2938	13	2716	28	3093	18	2.436	0.411	12.189
PD18-125-206	22.37	0.63	0.627	0.019	0.8348	3200	14	3138	38	3239	14	0.908	1.101	3.118
PD18-125-214	18.57	0.54	0.488	0.014	0.7636	3020	14	2562	30	3340	16	0.97	1.031	23.293
PD18-125-215	22.49	0.65	0.635	0.015	0.7466	3205	14	3169	30	3228	16	1.683	0.594	1.828
PD18-125-216	10.32	0.65	0.2806	0.022	0.3050	2464	29	1594	55	3287	66	1.416	0.706	51.506
PD18-125-217	18.7	0.62	0.5541	0.018	0.8051	3026	16	2842	37	3151	17	1.8	0.556	9.806
PD18-125-218	21.11	0.73	0.61	0.019	0.7279	3144	17	3070	38	3191	20	19.3	0.052	3.792
PD18-125-219	12.57	0.52	0.3798	0.018	0.3699	2648	20	2075	42	3120	40	0.844	1.185	33.494
PD18-125-220	13.21	0.41	0.4275	0.011	0.4407	2695	15	2294	25	3010	25	1.158	0.864	23.787
PD18-125-221	22.31	0.59	0.635	0.014	0.4039	3197	13	3169	28	3215	21	1.79	0.559	1.431
PD18-125-222	24.99	0.61	0.688	0.015	0.4149	3308	12	3375	29	3267	20	1.964	0.509	-3.306
PD18-125-223	9.22	0.28	0.2703	0.0078	0.7839	2360	14	1542	20	3168	16	1.036	0.965	51.326
PD18-125-224	21.63	0.53	0.564	0.013	0.6606	3167	12	2883	27	3353	16	1.855	0.539	14.017
PD18-125-225	18.32	0.45	0.605	0.014	0.8000	3007	12	3050	28	2978	13	2.928	0.342	-2.418
PD18-125-226	24.02	0.66	0.661	0.015	0.5431	3269	14	3271	29	3268	20	1.107	0.903	-0.092

PD18-125-227	21.25	0.62	0.602	0.016	0.4072	3150	14	3038	32	3222	24	1.301	0.769	5.711
PD18-125-228	14.24	0.65	0.383	0.017	0.7152	2766	22	2090	40	3304	27	1.134	0.882	36.743
PD18-125-239	6.96	0.22	0.2095	0.0059	0.4960	2106	14	1226	16	3126	24	1.632	0.613	60.781
PD18-125-240	21.57	1.1	0.561	0.03	0.6676	3165	25	2871	62	3357	34	1.233	0.811	14.477
PD18-125-241	17.8	0.58	0.4564	0.016	0.5276	2979	16	2424	35	3379	26	1.302	0.768	28.263
PD18-125-242	8.4	0.57	0.2576	0.013	0.3369	2275	31	1478	33	3097	56	3.33	0.300	52.276
PD18-125-243	19.75	0.51	0.532	0.012	0.5229	3079	13	2750	25	3302	19	1.266	0.790	16.717
PD18-125-244	19.77	0.57	0.545	0.012	0.5724	3080	14	2804	25	3265	19	2.7	0.370	14.119
PD18-125-246	23.66	0.62	0.631	0.014	0.6518	3254	13	3154	28	3317	17	1.255	0.797	4.914
PD18-125-247	14.78	0.89	0.409	0.025	0.2440	2801	29	2210	57	3259	59	1.644	0.608	32.188
PD18-125-248	16.47	0.67	0.473	0.017	0.6872	2904	20	2497	37	3201	24	3.15	0.317	21.993
PD18-125-249	12.54	0.53	0.3625	0.013	0.5784	2646	20	1994	31	3190	29	1.225	0.816	37.492
PD18-125-250	21.63	0.54	0.6056	0.013	0.4649	3167	12	3052	26	3241	19	2.166	0.462	5.832
PD18-125-251	20.96	1.1	0.569	0.028	0.4292	3137	26	2904	58	3289	43	2.67	0.375	11.706
PD18-125-252	21.82	0.59	0.619	0.015	0.5827	3176	13	3106	30	3220	19	1.401	0.714	3.540
PD18-125-253	14.09	0.6	0.3829	0.016	0.6362	2756	20	2090	37	3288	29	0.722	1.385	36.436
PD18-125-261	16.7	0.42	0.4059	0.0096	0.5618	2918	12	2196	22	3462	18	0.964	1.037	36.568
PD18-125-262	21.77	0.56	0.633	0.015	0.3732	3174	13	3161	30	3181	22	1.393	0.718	0.629
PD18-125-263	21.32	0.56	0.593	0.015	0.8603	3153	13	3002	30	3251	11	1.948	0.513	7.659
PD18-125-264	17.04	0.65	0.477	0.021	0.5361	2937	18	2514	46	3241	32	1.261	0.793	22.431
PD18-125-265	16.93	0.44	0.4421	0.0094	0.5078	2931	13	2360	21	3350	19	0.773	1.294	29.552
PD18-125-266	10.26	0.39	0.3411	0.011	0.7883	2459	18	1892	26	2967	19	2.4	0.417	36.232
PD18-125-267	18.68	0.72	0.527	0.018	0.7970	3025	19	2729	38	3229	19	1.058	0.945	15.485
PD18-125-268	14.03	0.44	0.386	0.013	0.5919	2752	15	2104	30	3268	23	0.831	1.203	35.618
PD18-125-269	24.07	0.8	0.6387	0.017	0.5439	3271	16	3184	33	3325	23	9.44	0.106	4.241
PD18-125-270	12.59	0.49	0.361	0.012	0.6193	2649	18	1987	28	3203	25	0.653	1.531	37.964
PD18-125-273	17.04	0.69	0.444	0.017	0.5836	2937	20	2369	38	3354	28	1.442	0.693	29.368
PD18-125-275	11.27	0.27	0.3459	0.0084	0.6096	2546	11	1915	20	3095	17	2.534	0.395	38.126
PD18-125-283	5.72	0.2	0.1974	0.0065	0.6529	1934	15	1161	18	2907	23	2.76	0.362	60.062
PD18-125-284	5.02	0.15	0.1983	0.0051	0.6381	1823	13	1166	14	2686	20	1.601	0.625	56.590

PD18-125-285	9.57	0.34	0.2185	0.0081	0.4303	2394	16	1274	21	3559	30	1.188	0.842	64.203
PD18-125-286	20.56	0.52	0.583	0.012	0.5016	3118	12	2961	24	3221	19	1.074	0.931	8.072
PD18-125-287	10.33	0.33	0.3364	0.0098	0.6466	2465	15	1869	24	3000	21	2.02	0.495	37.700
PD18-125-288	19.55	0.93	0.542	0.028	0.7677	3069	23	2792	59	3256	27	1.39	0.719	14.251
PD18-125-289	23.09	0.56	0.6362	0.014	0.3622	3231	12	3174	28	3266	21	1.47	0.680	2.817
PD18-125-290	13.47	0.42	0.3637	0.011	0.7286	2713	15	2000	26	3298	18	0.878	1.139	39.357
PD18-125-291	22.43	0.63	0.606	0.015	0.6677	3203	14	3054	30	3297	17	1.47	0.680	7.370
PD18-125-292	22.96	0.83	0.609	0.022	0.7316	3225	18	3066	44	3326	21	1.249	0.801	7.817
PD18-125-293	14.77	0.42	0.43	0.01	0.7763	2801	14	2306	23	3179	15	0.938	1.066	27.461
PD18-125-294	13.42	0.37	0.3642	0.009	0.5955	2710	13	2002	21	3290	19	1.332	0.751	39.149
PD18-125-296	9.97	0.27	0.3135	0.0072	0.6833	2432	13	1758	18	3057	17	1.41	0.709	42.493
PD18-125-297	7.53	0.25	0.239	0.0083	0.8102	2177	15	1381	22	3042	17	0.614	1.629	54.602
PD18-125-305	18.25	0.98	0.547	0.03	0.6012	3003	26	2813	63	3133	39	1.473	0.679	10.214
PD18-125-306	19.07	0.53	0.5195	0.013	0.6848	3045	14	2697	28	3284	17	1.202	0.832	17.875
PD18-125-307	20.45	0.92	0.56	0.026	0.3405	3113	22	2867	54	3276	41	1.51	0.662	12.485
PD18-125-308	18.44	1.1	0.591	0.018	0.2941	3013	29	2993	37	3026	47	2.11	0.474	1.091
PD18-125-310	21.91	0.55	0.532	0.013	0.6044	3180	12	2750	27	3463	18	0.598	1.672	20.589
PD18-125-311	17.75	0.64	0.44	0.016	0.7759	2976	17	2351	36	3431	19	1.59	0.629	31.478
PD18-125-312	17.25	2.1	0.521	0.021	0.7824	2949	58	2703	45	3121	75	0.855	1.170	13.393
PD18-125-313	22.95	0.62	0.609	0.015	0.7719	3225	13	3066	30	3325	14	1.15	0.870	7.789
PD18-125-314	14.3	0.46	0.489	0.015	0.8056	2770	15	2566	32	2922	16	1.631	0.613	12.183
PD18-125-315	21.97	0.59	0.626	0.017	0.4575	3182	13	3134	34	3213	23	1.027	0.974	2.459
PD18-125-316	23.73	0.6	0.663	0.016	0.4919	3257	13	3279	31	3244	20	2.099	0.476	-1.079
PD18-125-317	14.76	0.54	0.471	0.014	0.3510	2800	17	2488	31	3033	31	1.343	0.745	17.969
PD18-125-318	19.11	0.63	0.545	0.02	0.3072	3047	16	2804	42	3212	33	2.66	0.376	12.702
PD18-125-319	15.37	0.48	0.472	0.014	0.6195	2838	15	2492	31	3094	22	1.141	0.876	19.457
PD18-125-327	20.86	0.56	0.572	0.016	0.6204	3132	13	2916	33	3274	19	1.63	0.613	10.935
PD18-125-328	17.56	0.49	0.5312	0.012	0.4612	2966	14	2747	25	3118	21	1.843	0.543	11.899
PD18-125-329	19.07	0.52	0.484	0.012	0.3360	3045	13	2545	26	3395	24	0.81	1.235	25.037
PD18-125-330	21.18	0.71	0.602	0.018	0.6643	3147	16	3038	36	3217	21	1.702	0.588	5.564

PD18-125-331	18.95	0.54	0.5975	0.014	0.4600	3039	14	3020	28	3052	22	1.407	0.711	1.048
PD18-125-332	13.3	0.55	0.3719	0.014	0.7783	2701	20	2038	33	3243	21	1.538	0.650	37.157
PD18-125-333	19.3	0.81	0.5113	0.013	0.7929	3057	20	2662	28	3328	21	0.869	1.151	20.012
PD18-125-334	17	0.42	0.4481	0.013	0.4555	2935	12	2387	29	3336	22	1.157	0.864	28.447
PD18-125-335	22.06	0.6	0.629	0.017	0.7170	3186	13	3146	34	3212	17	1.933	0.517	2.055
PD18-125-336	17.19	0.5	0.486	0.013	0.6531	2945	14	2553	28	3226	19	1.146	0.873	20.862
PD18-125-337	17.4	0.84	0.477	0.027	0.9014	2957	23	2514	59	3274	20	1.299	0.770	23.213
PD18-125-338	25.82	0.71	0.689	0.017	0.5180	3340	14	3379	32	3316	21	1.717	0.582	-1.900
PD18-125-339	6.84	0.78	0.2158	0.02	0.6807	2091	51	1260	53	3051	68	1.397	0.716	58.702
PD18-125-340	20.08	0.51	0.559	0.013	0.7524	3095	12	2862	27	3250	14	1.029	0.972	11.938
PD18-125-342	23.59	0.57	0.6562	0.014	0.4100	3252	12	3252	27	3251	20	2.178	0.459	-0.031
PD18-125-343	18.7	0.73	0.524	0.016	0.8471	3026	19	2716	34	3240	17	2.72	0.368	16.173
PD18-51-1286	3.127	0.098	0.0988	0.0031	0.5171	1438	27	607.5	19	3043	26	0.4063	2.461	80.036
PD18-51-1287	32.08	0.69	0.706	0.013	0.9035	3550	22	3443	50	3604	23	1.99	0.503	4.467
PD18-51-1288	23.37	0.41	0.593	0.0091	0.5597	3242	18	2999	37	3389	25	1.12	0.893	11.508
PD18-51-1289	7.42	0.92	0.251	0.017	0.8190	2177	73	1467	84	2928	50	18.67	0.054	49.898
PD18-51-1290	23.63	0.38	0.6529	0.0097	0.4323	3252	16	3238	38	3249	24	5.161	0.194	0.339
PD18-51-1291	31.71	0.68	0.713	0.014	0.4525	3540	23	3469	53	3578	21	3.819	0.262	3.046
PD18-51-1292	10.15	0.47	0.3192	0.011	0.7274	2446	37	1785	54	3038	28	11.16	0.090	41.244
PD18-51-1293	24.78	0.44	0.6523	0.01	0.8632	3298	21	3236	40	3330	24	1.99	0.503	2.823
PD18-51-1294	21.84	0.38	0.6327	0.0084	0.3707	3175	17	3159	33	3180	28	1.724	0.580	0.660
PD18-51-1295	29.61	1.3	0.701	0.026	0.6976	3477	55	3421	110	3508	30	0.786	1.272	2.480
PD18-51-1296	7.65	0.28	0.2463	0.0068	0.4748	2190	39	1419	35	3004	35	2.568	0.389	52.763
PD18-51-1297	21.11	0.44	0.5706	0.011	0.5517	3142	20	2909	44	3286	25	2.494	0.401	11.473
PD18-51-1305	32.86	0.65	0.748	0.014	0.3950	3574	19	3598	51	3555	29	1.274	0.785	-1.210
PD18-51-1306	13.26	0.6	0.3899	0.015	0.7206	2697	36	2122	65	3156	25	0.609	1.642	32.763
PD18-51-1307	21.31	0.36	0.6224	0.01	0.5843	3152	16	3118	41	3166	28	2.225	0.449	1.516
PD18-51-1308	2.247	0.05	0.1268	0.003	0.1687	1195	16	770	17	2073	38	12.43	0.080	62.856

PD18-51-1309	32.72	0.86	0.722	0.017	0.2509	3570	28	3501	64	3610	25	1.484	0.674	3.019
PD18-51-1310	33.2	0.44	0.7533	0.0097	0.6832	3586.1	13	3618	36	3559	22	1.46	0.685	-1.658
PD18-51-1311	24.98	1.2	0.574	0.022	0.8734	3306	60	2923	97	3535	30	1.469	0.681	17.313
PD18-51-1312	11.3	0.87	0.293	0.016	0.8223	2514	98	1650	81	3311	84	3.817	0.262	50.166
PD18-51-1313	30.43	0.66	0.692	0.015	0.7463	3500	23	3397	57	3555	22	2.77	0.361	4.444
PD18-51-1314	26.7	0.71	0.666	0.014	0.6432	3375	28	3289	54	3408	28	1.292	0.774	3.492
PD18-51-1315	27.62	0.47	0.6875	0.012	0.3466	3405	17	3372	46	3425	25	1.454	0.688	1.547
PD18-51-1316	10.76	0.46	0.3172	0.011	0.7898	2501	38	1776	53	3150	26	3.59	0.279	43.619
PD18-51-1317	25.9	0.63	0.637	0.015	0.6946	3342	26	3176	60	3441	22	1.646	0.608	7.701
PD18-51-1318	18.08	0.32	0.5362	0.0088	0.7336	2992	17	2766	37	3141	24	1.406	0.711	11.939
PD18-51-1319	21.27	0.35	0.6232	0.0089	0.5269	3150	16	3121	35	3157	25	1.525	0.656	1.140
PD18-51-1320	18.74	0.74	0.5301	0.018	0.6592	3027	48	2741	83	3220	24	1.69	0.592	14.876
PD18-51-1321	26.81	0.75	0.671	0.017	0.5120	3371	28	3304	63	3411	39	0.0751	13.31 6	3.137
PD18-51-1322	6.66	0.25	0.2135	0.0066	0.4955	2066	30	1247	34	3014	30	1.49	0.671	58.626
PD18-51-1329	19.57	0.47	0.4921	0.012	0.7836	3068	24	2578	53	3404	23	1.382	0.724	24.266
PD18-51-1330	4.579 4	0.09	0.1853	0.0032	0.6774	1744	17	1096	17	2627	28	8.11	0.123	58.279
PD18-51-1331	18.03	1.3	0.5005	0.029	0.8400	2990	100	2615	140	3250	55	1.5	0.667	19.538
PD18-51-1332	21.99	0.32	0.6264	0.0096	0.7543	3182.3	14	3134	38	3207	25	1.941	0.515	2.276
PD18-51-1341	28.49	0.78	0.6283	0.015	0.5146	3435	31	3142	62	3607	23	1.352	0.740	12.892
PD18-51-1343	24.09	0.38	0.6545	0.01	0.5032	3271	16	3251	42	3281	26	1.589	0.629	0.914
PD18-51-1344	33.61	0.52	0.7194	0.01	0.5345	3597	15	3492	38	3649	23	1.541	0.649	4.303
PD18-51-1345	16.49	0.4	0.437	0.0098	0.6864	2904	22	2334	43	3341	27	0.37	2.703	30.141
PD18-51-1346	26.93	0.45	0.6841	0.012	0.5828	3380	16	3358	45	3391	23	1.931	0.518	0.973
PD18-51-1347	23.31	0.51	0.627	0.012	0.4311	3238	21	3136	50	3297	29	1.16	0.862	4.883
PD18-51-1348	20.79	0.47	0.5494	0.011	0.4503	3127	23	2822	46	3321	26	2.79	0.358	15.026
PD18-51-1349	28.13	0.49	0.68	0.01	0.4901	3422	17	3343	40	3457	29	10.8	0.093	3.298
PD18-51-1350	30.86	0.5	0.7137	0.012	0.5861	3513	16	3470	44	3530	23	1.337	0.748	1.700
PD18-51-1351	26.46	0.57	0.583	0.0096	0.8326	3362	23	2959	40	3592	24	1.854	0.539	17.622
PD18-51-1352	18.85	0.37	0.5021	0.0097	0.5818	3033	18	2621	41	3309	24	4.31	0.232	20.792

PD18-51-1353	30.13	0.68	0.679	0.013	0.4605	3488	22	3339	50	3566	34	3.98	0.251	6.366
PD18-51-1361	25.9	0.63	0.606	0.013	0.7563	3339	24	3053	54	3521	24	0.813	1.230	13.292
PD18-51-1362	25.83	0.45	0.6649	0.0098	0.8826	3339	17	3285	38	3363	24	1.101	0.908	2.319
PD18-51-1363	32.24	0.53	0.7403	0.011	0.7373	3556	16	3570	40	3544	21	1.492	0.670	-0.734
PD18-51-1364	26.19	0.42	0.689	0.0092	0.5845	3352	16	3378	35	3329	23	17.73	0.056	-1.472
PD18-51-1365	20.7	1.1	0.522	0.025	0.5704	3122	70	2707	120	3398	33	0.55	1.818	20.335
PD18-51-1366	27.87	0.63	0.693	0.014	0.5665	3411	22	3390	55	3411	33	1.748	0.572	0.616
PD18-51-1367	32.1	0.5	0.7269	0.01	0.6184	3552	15	3521	38	3562	22	4.548	0.220	1.151
PD18-51-1368	19.63	0.5	0.477	0.011	0.9144	3072	23	2511	50	3445	22	1.768	0.566	27.112
PD18-51-1369	23.27	0.35	0.6478	0.0088	0.3785	3237	15	3219	34	3244	23	3.217	0.311	0.771
PD18-51-1370	21.21	0.45	0.565	0.011	0.5138	3147	22	2887	47	3304	23	1.176	0.850	12.621
PD18-51-1371	10.4	0.4	0.2996	0.01	0.8105	2467	41	1688	51	3195	32	3.28	0.305	47.167
PD18-51-1372	26.87	0.52	0.6604	0.011	0.4289	3377	19	3267	41	3433	29	1.622	0.617	4.835
PD18-51-1373	29.15	0.53	0.703	0.011	0.6993	3456	18	3430	40	3466	23	1.014	0.986	1.039
PD18-51-1374	20.04	0.58	0.505	0.013	0.7792	3091	27	2634	52	3400	23	7.85	0.127	22.529
PD18-51-1375	20.32	2.2	0.527	0.055	0.8173	3105	110	2729	200	3356	34	4.3	0.233	18.683
PD18-51-1376	23.96	0.36	0.6601	0.009	0.4593	3266	15	3267	35	3253	25	5.24	0.191	-0.430
PD18-51-1377	21.3	0.39	0.632	0.011	0.6751	3150	18	3154	45	3141	30	1.504	0.665	-0.414
PD18-51-1385	24.65	0.54	0.6062	0.011	0.4062	3292	22	3053	47	3430	34	1.409	0.710	10.991
PD18-51-1386	21.25	0.61	0.628	0.016	0.6635	3148	30	3136	66	3143	28	1.048	0.954	0.223
PD18-51-1387	22.25	0.33	0.5751	0.0078	0.5808	3194	14	2928	32	3357	22	6.6	0.152	12.779
PD18-51-1388	21.7	0.39	0.6281	0.0089	0.6792	3169	17	3141	35	3173	25	2.175	0.460	1.009
PD18-51-1389	18.48	0.84	0.508	0.021	0.5588	3019	50	2646	92	3265	28	1.632	0.613	18.959
PD18-51-1390	29.64	0.65	0.715	0.013	0.3746	3475	22	3475	47	3467	35	1.918	0.521	-0.231
PD18-51-1391	21.72	0.45	0.6284	0.01	0.4057	3169	21	3142	40	3179	32	1.886	0.530	1.164
PD18-51-1392	21.25	0.8	0.525	0.015	0.9411	3148	42	2718	68	3419	27	1.695	0.590	20.503
PD18-51-1393	25.64	0.54	0.66	0.013	0.8086	3330	21	3265	49	3363	30	1.666	0.600	2.914
PD18-51-1394	11.53	0.53	0.356	0.012	0.8101	2565	39	1963	57	3091	27	17.02	0.059	36.493
PD18-51-1395	7.1	0.75	0.282	0.025	0.9720	2129	83	1600	120	2692	30	5.44	0.184	40.565
PD18-51-1396	21.34	0.39	0.6205	0.01	0.4703	3152	18	3110	40	3171	29	1.738	0.575	1.924

PD18-51-1398	12.13	0.34	0.3321	0.0073	0.8885	2613	29	1848	36	3273	27	3.55	0.282	43.538
PD18-51-1399	30.08	0.57	0.705	0.014	0.6477	3487	19	3436	54	3509	29	3.275	0.305	2.080
PD18-51-1400	23.8	1.6	0.614	0.034	0.8663	3258	75	3085	150	3363	30	0.74	1.351	8.266
PD18-51-1401	22.33	0.5	0.582	0.013	0.6910	3197	22	2954	54	3357	22	1.357	0.737	12.005
PD18-51-1409	23	0.46	0.5894	0.011	0.6987	3225	20	2985	41	3375	28	3.34	0.299	11.556
PD18-51-1410	26.2	1.2	0.628	0.025	0.9365	3353	61	3138	110	3474	29	1.319	0.758	9.672
PD18-51-1411	29.27	0.66	0.6477	0.01	0.3037	3462	22	3219	40	3602	25	2.013	0.497	10.633
PD18-51-1412	29.68	0.51	0.6489	0.0098	0.4219	3475	17	3223	39	3619	22	1.005	0.995	10.942
PD18-51-1413	12.04	0.84	0.378	0.022	0.3819	2606	91	2065	110	3055	49	2.295	0.436	32.406
PD18-51-1414	20.52	0.33	0.6047	0.0084	0.5426	3115	16	3048	34	3152	25	3.809	0.263	3.299
PD18-51-1415	28.48	0.74	0.682	0.014	0.7115	3433	27	3350	56	3476	23	1.212	0.825	3.625
PD18-51-1416	17.82	0.89	0.521	0.023	0.5886	2979	66	2703	110	3154	30	1.507	0.664	14.299
PD18-51-1417	13.82	0.68	0.428	0.02	0.8790	2736	53	2297	91	3074	23	2.189	0.457	25.277
PD18-51-1418	25.24	0.47	0.6449	0.013	0.5516	3316	18	3207	52	3377	26	1.52	0.658	5.034
PD18-51-1419	17.77	1.2	0.543	0.033	0.9443	2975	78	2796	140	3089	25	3.79	0.264	9.485
PD18-51-1420	7.49	0.27	0.2471	0.0088	0.8666	2171	29	1423	44	2977	24	0.946	1.057	52.200
PD18-51-1421	28.93	0.89	0.6622	0.019	0.7764	3450	33	3274	78	3544	21	1.416	0.706	7.619
PD18-51-1422	23.69	1.2	0.629	0.03	0.5298	3246	53	3135	120	3319	63	1.472	0.679	5.544
PD18-51-1423	17.95	0.5	0.4776	0.011	0.3495	2986	25	2516	48	3316	26	0.917	1.091	24.125
PD18-51-1424	1.119	0.16	0.05829	0.0066	0.8188	761	58	365.2	39	2217	36	1.964	0.509	83.527
PD18-51-1425	25.96	0.47	0.6551	0.01	0.5739	3343	18	3247	40	3396	24	1.221	0.819	4.388
PD18-51-1426	19.61	0.98	0.565	0.025	0.8578	3070	56	2883	110	3185	40	0.812	1.232	9.482
PD18-51-1427	22.71	0.35	0.6305	0.0086	0.8162	3214	15	3151	34	3245	24	3.044	0.329	2.897

Appendix 3.2 Detrital Zircon Lu–Hf data. – Detrital record of the Dharwar Craton

<i>Analysis N</i>	<i>Hf176/Hf177</i>	<i>2 S.E.</i>	<i>Lu176/Hf177</i>	<i>U/Pb AGE (grain)</i>	<i>2 S.E.</i>	<i>Hf Chur (t)</i>	<i>Hf DM (t)</i>	<i>Hf NC(t)</i>	<i>Hfi</i>	<i>eHf</i>	<i>2SE</i>	<i>TDMc</i>	<i>TNCc</i>	<i>Above DM line?</i>
<i>PD17-61-952</i>	0.280702	0.000044	0.000927	3205	54	0.280715	0.280885	0.28083	0.280645	-2.51074	1.555952	3.701774	3.588163	No
<i>PD17-61-1017</i>	0.280606	0.000056	0.001306	3247	36	0.280687	0.280853	0.280798	0.280524	-5.80577	1.980303	3.925079	3.813019	No
<i>PD17-61-977</i>	0.280711	0.000059	0.001342	3262	30	0.280677	0.280841	0.280787	0.280627	-1.80346	2.086391	3.705879	3.593746	No
<i>PD17-61-901</i>	0.280597	0.000051	0.000755	3270	42	0.280672	0.280835	0.280781	0.28055	-4.36778	1.80349	3.860266	3.748661	No
<i>PD17-61-993</i>	0.280738	0.00004	0.002357	3273	34	0.28067	0.280833	0.280779	0.28059	-2.86716	1.414502	3.776039	3.664335	No
<i>PD17-61-857</i>	0.280642	0.000044	0.000844	3490	32	0.280525	0.280667	0.280616	0.280585	2.137231	1.555952	3.659425	3.553071	No
<i>PD17-61-879</i>	0.280641	0.000051	0.000869	3327	35	0.280634	0.280792	0.280738	0.280585	-1.73741	1.80349	3.753477	3.643117	No
<i>PD17-61-1023</i>	0.280724	0.000038	0.000754	3328	32	0.280633	0.280791	0.280738	0.280676	1.505725	1.343777	3.566716	3.455996	No
<i>PD17-61-916</i>	0.280757	0.000066	0.000895	3338	30	0.280627	0.280783	0.28073	0.2807	2.591256	2.333929	3.511776	3.401201	No
<i>PD17-61-858</i>	0.280521	0.000048	0.001187	3346	33	0.280621	0.280777	0.280724	0.280445	-6.30355	1.697403	4.031336	3.922034	No
<i>PD17-61-957</i>	0.280737	0.00005	0.00124	3347	30	0.280621	0.280777	0.280723	0.280657	1.29493	1.768128	3.594056	3.483883	No
<i>PD17-61-961</i>	0.280837	0.000053	0.001887	3354	32	0.280616	0.280771	0.280718	0.280715	3.530504	1.874215	3.470087	3.35984	No
<i>PD17-61-896</i>	0.2807	0.00005	0.000434	3356	30	0.280615	0.28077	0.280717	0.280672	2.037656	1.768128	3.558222	3.448208	No
<i>PD17-61-839</i>	0.280949	0.000057	0.00179	3387	30	0.280594	0.280746	0.280693	0.280832	8.488438	2.015666	3.208345	3.098415	Yes
<i>PD17-61-941</i>	0.280753	0.000066	0.001353	3390	34	0.280592	0.280744	0.280691	0.280665	2.587286	2.333929	3.553532	3.444387	No
<i>PD17-61-877</i>	0.280639	0.000048	0.000632	3405	33	0.280582	0.280732	0.28068	0.280598	0.551685	1.697403	3.683195	3.574699	No
<i>PD17-61-1015</i>	0.280723	0.000038	0.001474	3420	34	0.280572	0.280721	0.280668	0.280626	1.919404	1.343777	3.616122	3.507877	No
<i>PD17-61-1003</i>	0.280706	0.000037	0.001543	3421	30	0.280571	0.28072	0.280668	0.280604	1.174245	1.308415	3.659978	3.551848	No
<i>PD17-61-996</i>	0.280659	0.000055	0.00092	3424	31	0.280569	0.280718	0.280665	0.280598	1.031429	1.944941	3.670616	3.562584	No
<i>PD17-61-956</i>	0.280891	0.000047	0.001141	3430	37	0.280565	0.280713	0.280661	0.280816	8.919053	1.66204	3.218043	3.109251	Yes
<i>PD17-61-876</i>	0.280744	0.000053	0.000473	3447	34	0.280554	0.2807	0.280648	0.280713	5.651827	1.874215	3.421632	3.313692	Yes
<i>PD17-61-960</i>	0.280662	0.000045	0.0005	3452	36	0.280551	0.280697	0.280644	0.280629	2.782499	1.591315	3.591786	3.484318	No
<i>PD17-61-994</i>	0.2809	0.00016	0.00219	3454	35	0.280549	0.280695	0.280643	0.280754	7.304674	5.658009	3.331333	3.223393	Yes
<i>PD17-61-1022</i>	0.280787	0.000044	0.000783	3475	30	0.280535	0.280679	0.280627	0.280735	7.10287	1.555952	3.359995	3.252657	Yes
<i>PD17-61-875</i>	0.280656	0.000046	0.001929	3483	31	0.28053	0.280673	0.280621	0.280527	-0.12219	1.626678	3.784088	3.677802	No

PD17-61-1021	0.280655	0.00005	0.000536	3544	29	0.280489	0.280626	0.280575	0.280618	4.607127	1.768128	3.560062	3.454905	Yes
PD17-42-794	0.281055	0.000087	0.01109	2737	54	0.281025	0.281239	0.281178	0.280474	-19.6119	3.076542	4.326914	4.20268	No
PD17-42-792	0.280728	0.000051	0.000727	2874	32	0.280935	0.281136	0.281077	0.280688	-8.78948	1.80349	3.806545	3.684631	No
PD17-42-717	0.280712	0.000048	0.000809	3118	42	0.280773	0.280951	0.280895	0.280664	-3.90523	1.697403	3.713999	3.598171	No
PD17-42-802	0.280682	0.000039	0.000998	3124	33	0.280769	0.280946	0.28089	0.280622	-5.23911	1.37914	3.795924	3.680427	No
PD17-42-832	0.280747	0.000054	0.00072	3151	34	0.280751	0.280926	0.28087	0.280703	-1.7049	1.909578	3.612441	3.497245	No
PD17-42-718	0.280839	0.000037	0.001471	3168	39	0.28074	0.280913	0.280857	0.280749	0.337801	1.308415	3.507284	3.392302	No
PD17-42-660	0.280794	0.000043	0.000763	3185	38	0.280729	0.2809	0.280845	0.280747	0.663315	1.52059	3.501861	3.387307	No
PD17-42-761	0.280864	0.000046	0.001904	3191	33	0.280725	0.280895	0.28084	0.280747	0.803496	1.626678	3.49848	3.384075	No
PD17-42-803	0.280847	0.000036	0.001092	3219	35	0.280706	0.280874	0.280819	0.280779	2.613701	1.273052	3.415513	3.301656	No
PD17-42-797	0.280719	0.000066	0.001414	3235	36	0.280695	0.280862	0.280807	0.280631	-2.29269	2.333929	3.71284	3.600025	No
PD17-42-699	0.280676	0.000038	0.000438	3249	35	0.280686	0.280851	0.280797	0.280649	-1.33456	1.343777	3.668466	3.555919	No
PD17-42-712	0.280757	0.000059	0.0014	3270	29	0.280672	0.280835	0.280781	0.280669	-0.11227	2.086391	3.614332	3.502214	No
PD17-42-656	0.280766	0.000045	0.001572	3271	33	0.280671	0.280835	0.28078	0.280667	-0.15435	1.591315	3.617563	3.505477	No
PD17-42-659	0.280777	0.000036	0.001229	3285	39	0.280662	0.280824	0.28077	0.280699	1.326451	1.273052	3.542868	3.430988	No
PD17-42-818	0.280755	0.000048	0.000954	3315	33	0.280642	0.280801	0.280747	0.280694	1.853894	1.697403	3.53618	3.425061	No
PD17-42-772	0.280865	0.000037	0.001698	3323	32	0.280637	0.280795	0.280741	0.280756	4.263252	1.308415	3.402724	3.291535	No
PD17-42-700	0.281034	0.000056	0.00508	3325	41	0.280635	0.280793	0.28074	0.280709	2.620747	1.980303	3.499687	3.388751	No
PD17-42-735	0.280748	0.000049	0.0014	3330	54	0.280632	0.28079	0.280736	0.280658	0.93246	1.732765	3.601507	3.490911	No
PD17-42-813	0.280755	0.000041	0.000919	3401	32	0.280585	0.280735	0.280683	0.280695	3.9227	1.449865	3.484969	3.375968	No
PD17-42-715	0.280723	0.000037	0.000604	3407	32	0.280581	0.280731	0.280678	0.280683	3.657647	1.308415	3.505134	3.396329	No
PD17-42-693	0.28085	0.00011	0.0074	3419	39	0.280573	0.280722	0.280669	0.280363	-7.48328	3.889881	4.156156	4.048972	No
PD17-42-661	0.280741	0.000055	0.001377	3434	39	0.280563	0.28071	0.280658	0.28065	3.108408	1.944941	3.558542	3.450543	No
PD17-42-800	0.280759	0.000046	0.000488	3464	30	0.280543	0.280687	0.280635	0.280726	6.550351	1.626678	3.383191	3.275615	Yes

Appendix 3.3 Detrital Zircon REE (ppm) – Detrital record of the Dharwar Craton

Comments	La139	Ce140	Pr141	Nd146	Sm147	Eu153	Gd157	Tb159	Dy163	Ho165	Er166	Tm169	Yb172	Lu175	Hf178
PD18-51-1286	25.54	1738	199.4	2000	1119	355.6	1474	308.6	2386	511	1720	303.7	2597	387.3	13580
PD18-51-1287	18.9	84.2	9.08	41.8	13.8	5.57	33.2	8.78	91.9	27.92	121.1	22.57	219.1	39.9	11680
PD18-51-1288	6.9	83.9	5.98	36.3	17.2	6.6	41.6	11.39	124.6	44	213.1	43.7	464	91.3	11660
PD18-51-1289	7.4	15.9	1.82	9.3	5.7	4.9	27.9	8.13	74.6	21.3	87.5	16.66	150.8	28.4	12270
PD18-51-1290	0.16	3.51	0.054	0.46	1.02	0.269	8.31	2.86	39.9	16.09	83.2	17.72	186.7	38.2	11370
PD18-51-1291	0.371	12.92	0.34	2.69	3.52	1.04	22	8.22	119.7	48.4	246.2	52.4	526	102.1	13990
PD18-51-1292	5.1	24.6	2.58	13.9	5.14	4.27	15.3	4.66	58.7	21.83	110.1	24.2	261.5	54	13510
PD18-51-1293	3.59	44	2.67	16.9	10.14	3.77	35.4	10.27	122.1	41.8	192.6	36.7	349	64.2	10150
PD18-51-1294	0.65	17.93	0.89	7.39	5.96	0.9	22.4	6.74	86.2	31.9	153.4	31	295	55.3	11590
PD18-51-1295	4.23	50.8	7.82	56.1	35.8	8.67	66	16.12	181.7	63.2	286.2	54.8	525	97	9900
PD18-51-1296	11	64	6.61	34	13.7	4.82	25	7.02	77.5	26.51	128	28.2	295	57.1	12130
PD18-51-1297	28.1	385	21.3	118.4	42.4	12.21	58	11.88	110.9	34.17	154.7	31.22	312	60.2	12120
PD18-51-1305	0.025	5.95	0.221	5.07	10.94	1.75	70.3	21.77	271.5	95.3	419.7	76.6	685	120.6	10370
PD18-51-1306	35.8	222	24.7	131	49.3	14.1	78.3	16.7	166	52.3	237	50.2	533	112.9	13900
PD18-51-1307	0.264	14.21	0.162	1.51	1.8	0.216	11.09	4.19	57	22.28	107.9	21.59	212	39.6	12360
PD18-51-1308	22.8	81	10	51.3	20.2	10.3	33.4	8.21	89.4	28.2	145.7	34.6	371	71.7	13240
PD18-51-1309	Below LOD	10.46	0.144	2.55	6.96	1.58	45	15.49	198.9	74.2	341.3	65.2	599	108.9	9190
PD18-51-1310	0.232	7.73	0.523	6.28	8.52	2.39	45.7	13.77	162.7	55.9	259.1	51	490.6	92.9	8350
PD18-51-1311	8.56	69.6	7.44	51.7	31.6	7.93	86.1	22.5	238.8	75.7	317.5	56.9	507	91.5	11640
PD18-51-1312	51.5	162	23.2	121	53.2	32.9	132.1	32.1	281	77.3	318	62.1	603	111.1	13610
PD18-51-1313	9.7	48	4.6	24	8.6	2.76	24	6.93	80	28.3	137	28.6	299	62.4	12250
PD18-51-1314	1.39	28.8	1.31	8.7	5.77	2.24	20.8	5.17	60.9	21.1	102.4	21.6	227.7	48.5	10650
PD18-51-1315	3.31	40.9	3.68	28.2	24.8	6.6	114.2	36.47	460.4	162.2	724	128.1	1129	202.8	9950
PD18-51-1316	19.3	112.9	14.7	82.9	44	16.8	70.5	14.32	121.1	29.6	113.4	22.88	246.4	54.4	12580
PD18-51-1317	8.3	110	7.46	47.2	25.8	6.48	58.4	15.77	183.9	67.1	326.1	64.9	629	120.3	10630
PD18-51-1318	65	134	15.6	79.3	29.1	5.14	45	9.95	97.5	30.31	138.2	27.64	267.8	50.02	11140
PD18-51-1319	122	269	32.4	144	36.7	3.32	50.8	10.76	105.8	33.61	150.5	29.02	272.7	49.4	10820

PD18-51-1320	2.01	44.7	0.78	6.4	8.9	4.65	52.7	18.4	236.6	90.8	449	90.1	887	173.1	9490
PD18-51-1321	0.345	8.97	0.332	2.77	2.54	0.52	14.04	5.02	72.2	29.21	151.1	31.9	318.8	61.4	16150
PD18-51-1322	226	1120	99	562	231	70.3	295	50.3	375	94.4	387	75.5	745	144.4	11850
PD18-51-1329	56.9	769	53.5	358	196	46.9	250	40.8	277	67.8	274.1	52.5	510	94.1	9540
PD18-51-1330	34.5	226	17.39	89.2	28.7	20.2	50.7	10.98	96.2	25.71	108	22.4	221	45	12500
PD18-51-1331	8.5	51.8	4.25	22.1	11.6	6.41	40.7	10.46	106.1	30.1	124.9	22.77	215.5	40.4	10590
PD18-51-1332	Below LOD	12.92	0.054	1.52	4.52	0.69	31.4	10.85	149.7	56.5	264.9	50.2	471	86	10370
PD18-51-1341	0.551	20.78	0.235	2.54	4.76	1.56	26.8	8.46	101.8	36	163.2	31.7	288.2	52.9	10190
PD18-51-1343	0.062	23.56	0.124	2.26	4.91	1.74	26.8	8.38	107	40.81	210.5	43.69	447.9	89.1	9930
PD18-51-1344	2.93	29	2.16	11.5	5.91	1.52	19.4	5.37	61.7	20.96	94.9	18.66	181.4	34.29	10320
PD18-51-1345	56	168	20.8	114	60.3	11.52	174	38.6	363	102.6	472	96.3	918	164.6	17900
PD18-51-1346	1.93	20.1	0.75	4.2	3.67	1.3	16.1	4.44	51.6	18.05	88	18.99	201.4	41.8	10590
PD18-51-1347	9.6	41	3.6	26.6	8	2.87	26.6	7.2	83.9	28.4	134.8	26.68	260.1	52.7	8790
PD18-51-1348	15.4	48.6	5.05	27.9	11.7	3.73	23.1	6.34	67.5	21.1	96.6	19.71	202.1	40.4	11180
PD18-51-1349	0.398	6.6	0.481	3.24	1.53	0.572	3.55	0.873	9.93	3.38	18.11	4.07	48.5	11.27	12180
PD18-51-1350	1.55	11.44	1.83	13.3	7.85	1.84	10.55	2.08	16.73	4.74	21.59	4.68	50.4	10.83	7290
PD18-51-1351	7.3	63.4	5.75	36.4	21.8	5.72	41.4	9.75	96.4	30.6	139.9	29.4	292	55.5	11820
PD18-51-1352	8.48	41.7	5.2	35.8	18.7	4.51	34.3	7.96	84.3	28.4	137.5	30	320	62.9	12780
PD18-51-1353	3.69	20.34	2.52	13.46	3.09	1.5	4.79	1.202	14.92	6.73	42.1	10.49	141.9	40.4	11860
PD18-51-1361	33.7	154	14.3	104.6	146.9	81.2	696	156.3	1196	237.9	639	80.6	564	80.1	11830
PD18-51-1362	1.184	36.5	1.466	11.55	8.29	2.28	19.69	5.25	57.5	20.2	99.8	20.88	215.4	42.4	10160
PD18-51-1363	0.264	12.97	0.436	4.96	7.46	0.99	40.9	12.44	155.2	55.5	251	47.1	443	81	9260
PD18-51-1364	0.34	4.69	0.147	1.15	1.21	1.04	13.12	6.64	108.1	43.95	245.1	61.2	700	139.8	13980
PD18-51-1365	5.11	51.6	3.41	22.8	13.2	3.83	22.6	4.74	44.8	13.86	64.4	13.36	137	28.74	8770
PD18-51-1366	Below LOD	11.41	0.034	0.78	2.13	0.422	14.58	5.16	70.5	27.55	131.6	26.9	261.4	50.6	11400
PD18-51-1367	1.71	12.69	1.91	11.78	7.45	2.42	16.92	4.96	59	21.54	105.7	21.42	211.3	40.35	14100
PD18-51-1368	17.6	214	14.8	80.1	33.1	10.94	52.5	11.99	108.8	30.1	126.5	25.73	271.8	55.4	11970
PD18-51-1369	4.3	22.5	1.51	9.1	6.6	1.68	16.8	4.32	46.3	15.52	71.1	14.22	141.4	28.56	9920
PD18-51-1370	10.9	46.2	5.1	35.2	26.1	5.23	100.8	31	360	122.6	549	98.7	896	161.1	9500

PD18-51-1371	24.7	110	13.8	71	24.8	21.7	57.2	14.2	123.9	36.8	174.4	37.5	420	92.7	8760
PD18-51-1372	3.15	20.67	1.66	10.41	8.75	2.27	42.4	14.17	185.2	66.8	310.5	57.9	533.6	95.1	10520
PD18-51-1373	0.4	14.73	0.245	2.92	4.38	1.55	26.1	8	105.8	41	206.5	43.1	445	91.9	9330
PD18-51-1374	14.2	35	4.69	24.9	8.41	6.1	18	4.16	39.4	10.7	48.4	9.99	110.9	23.73	11710
PD18-51-1375	5.1	29.7	3.22	17	7.1	3.29	19.2	4.86	47.1	13.9	62	12.7	131.5	29.5	12710
PD18-51-1376	Below LOD	4.55	0.0079	0.43	1.46	0.742	10.12	3.95	55	21.72	110.1	23.22	233.8	47.2	9790
PD18-51-1377	Below LOD	14.57	0.017	0.59	1.58	0.195	10.19	3.78	49.5	19.14	93.4	19.21	184.7	34.58	10740
PD18-51-1385	4.29	41.4	2.87	17.3	9.27	2.76	41.2	13.8	174	61.8	285	53.5	486	88.3	9800
PD18-51-1386	190	428	52.3	209	41.2	2	47.4	8.73	90.5	30.1	141	27.98	272.5	52.2	11490
PD18-51-1387	11.4	56.6	8.31	55.7	29.9	7.45	55.6	11.7	96	24.6	102	20.77	221.6	46.9	12230
PD18-51-1388	Below LOD	9.88	0.04	0.71	2.04	0.108	11.82	4.06	55.8	21.7	108.5	22.2	219	41.3	11780
PD18-51-1389	11.4	75.2	6.88	40.5	19.8	7.2	67.2	18.03	206.3	69.9	325	65.5	618	118.3	11200
PD18-51-1390	Below LOD	11.35	0.066	1.34	2.21	1.14	12.39	3.65	44.6	16.42	80.8	17.31	182.5	38.7	9110
PD18-51-1391	0.082	7.96	0.145	1.32	2.8	0.333	17.47	5.62	72.3	26.18	122.7	23.88	224.6	41.99	9510
PD18-51-1392	71	164	18.6	86	28.6	11	81.1	21.2	227	67.3	275	50.2	446	80.2	10280
PD18-51-1393	0.784	6.2	0.542	4.03	2.02	0.991	6.36	1.54	17.21	6.42	32.3	7.33	84.4	18.72	7600
PD18-51-1394	2.42	4.89	0.359	1.61	1.67	1.34	10.1	4.02	61.2	25.3	139.3	31.6	334	67.3	11250
PD18-51-1395	187	577	85	387	106.8	61.7	147	33.2	303	88.6	435	97.6	1030	205.3	13430
PD18-51-1396	0.006	8.97	0.104	2.08	4.25	0.252	24.8	7.96	100.8	35.1	160.3	29.7	271.7	48.7	9830
PD18-51-1397	101	192	22.7	133	269	167	1730	511	4430	912	2700	315	1840	229	10510
PD18-51-1398	9.89	55.8	6.97	43.2	26.6	10.36	44.7	9.37	78.7	21.83	96.8	19.49	198.1	41.2	11740
PD18-51-1399	0.015	2.19	0.043	0.37	0.87	0.432	5.6	1.83	25.7	10.71	56.8	12.5	141.1	30.2	8840
PD18-51-1400	3.95	61	1.29	11	9.6	4.91	46.1	13.85	164.9	61.1	296	61.8	627	121.2	8870
PD18-51-1401	1.68	55.3	2.12	12.7	7.8	2.39	23	6.14	77.9	29.7	163	37.8	403	84	12380
PD18-51-1409	1.48	18.09	1.158	7.62	3.22	1.09	7.34	1.81	19.3	6.19	29.7	6.31	76.2	18.33	10800
PD18-51-1410	4.78	54	4.18	28.7	21.2	6.6	61.5	17	202.5	62.5	292	52.8	504	96.6	10010
PD18-51-1411	1.53	22.2	1.4	9.3	4.22	2.21	12	3.2	36.1	13.24	68.5	16.73	194.5	47.2	11780
PD18-51-1412	106	1340	87.2	481	165	36.1	189	33.9	295	86.2	347	62	552	94.9	8320

PD18-51-1413	10.1	64.6	5.04	25	9.6	3.97	29.3	8.43	109.1	41.2	202	40.4	390	75.3	11980
PD18-51-1414	1.29	8.42	0.763	5.45	2.79	0.825	6.03	1.76	21.82	8.42	46.5	10.86	120.1	25.91	10600
PD18-51-1415	0.241	24	0.221	2.05	2.63	1.13	13.5	3.97	47.9	16.31	80.4	17.85	194.5	42.5	11350
PD18-51-1416	9.11	111.1	7.68	43.7	20.4	5.46	45.4	12.28	135.8	43.6	197	38.6	368	67.1	12290
PD18-51-1417	4.21	33.9	2.37	14.8	8.4	3.09	30.7	9.86	121.5	44.6	209.4	40.5	383.7	70.4	12530
PD18-51-1418	6.95	68.9	7.98	56.2	29.4	6.05	46.7	9.06	82.6	24.3	111	22.6	233	47.5	10580
PD18-51-1419	47.4	153.4	19.1	100.8	59.2	53.2	315	77.3	668	157.3	556	92.1	781	136.1	13430
PD18-51-1420	30.3	116.8	12.58	67.8	29.2	16.9	97.7	28.2	312	96.4	409	75.5	687	118.5	10890
PD18-51-1421	26.1	102.4	10.77	54	17	4.74	37.6	9.67	105.3	34.29	153	29.39	273.8	50.4	9840
PD18-51-1422	0.213	8.69	0.27	1.88	2.02	0.83	8.57	2.53	32.6	12.04	59.9	12.4	129.1	26.75	9080
PD18-51-1423	8.28	85.7	4.65	26.4	12.71	5.75	48.4	14.32	172.6	59.3	283.3	55.9	546	104.5	10680
PD18-51-1424	1191	2962	437	2030	457	286.7	698	138.8	1093	263	1038	197	1892	335	12090
PD18-51-1425	0.76	26.4	0.94	7.1	5.47	1.52	16.22	4.4	51.6	18.97	94	20.38	214.2	44.16	9920
PD18-51-1426	9.9	70.3	5.78	35.6	24.8	6.01	69.6	20	228	77	340	63.9	600	104.9	11070
PD18-51-1427	0.82	6.46	0.343	2.32	2.64	0.96	14.13	4.26	50.7	17.68	83.6	16.81	164.7	31.32	10430
PD17-42-654	40.3	228	44.9	389	755	416	3340	836	6660	1610	5120	820	6190	918	14230
PD17-42-655	5	19.1	1.91	17.5	97.9	53.8	947	244	1679	347	949	138.6	977	151.2	11760
PD17-42-656	0.172	15.82	0.194	1.88	3.41	1.41	27.4	11.55	148.8	59	295	66.5	663	140.1	13270
PD17-42-657	5.11	33.9	3.44	17.3	9.6	2.64	24	7.13	80.1	29.1	132.5	29	284	59.9	11000
PD17-42-658	3.63	53.5	5.37	56.1	95	48.9	477	122	1100	311	1120	191	1481	242	8950
PD17-42-659	0	12.85	0.034	0.48	1.53	0.581	8.75	2.87	32	12.11	57.8	12.4	120.3	26.12	11410
PD17-42-660	0.098	6.81	0.055	0.88	2.29	0.214	15	6.04	81.2	33.9	162.8	34.6	323	63.4	12280
PD17-42-661	0.76	9.12	0.76	3.8	1.72	0.47	7.83	2.77	35.6	15.13	80.4	19.4	219	51.8	13800
PD17-42-662	62	299	38.4	247	338	194	1460	393	3130	720	2210	365	2740	435	17900
PD17-42-663	3.11	49.7	3.07	18.1	10.6	3.88	27.9	8.48	88.8	32	151.7	34.65	361.3	82.7	12380
PD17-42-672	810	1450	153	600	184	68	428	121	1030	242	770	127	980	155	8310
PD17-42-673	2.76	28	1.92	11.75	15.11	5.99	74.7	25.21	290.5	106.7	484	100.9	932	187.4	11950
PD17-42-674	24.6	150.3	18.2	95.7	36.6	11.34	62.4	17.5	149.6	37.5	130.6	24.7	220	42.1	14030
PD17-42-674-2	35	200	23.7	117	38.5	9.9	49	11.5	109.1	38.5	183	44.4	478	99.8	14790
PD17-42-675	11.4	66.7	7.45	38.1	17.1	3.59	36.8	11.45	139.6	54.1	244.4	51.9	473	94.1	12070

PD17-42-676	7.21	49.6	4.78	26.8	11.6	2.83	24.1	7.11	80.5	28.52	133.1	29.05	274.2	55.8	11110
PD17-42-677	46.9	331	35.9	189	69.7	19.5	96.2	20.4	165	50	209.2	43.5	424	86.6	10850
PD17-42-678	2.09	14.16	2.13	13.24	13.8	6.97	60.5	14.15	115.2	29.4	100.6	18.11	149	27.15	11670
PD17-42-679	36.4	204	37.2	303	451	223	1860	523	4670	1180	3800	609	4590	688	13190
PD17-42-680	2.54	17.9	2.03	11.9	6.36	2.7	19.6	5.9	68.4	25.5	121.9	28.1	296	69.1	7800
PD17-42-681	91.9	601	58.8	294.4	118.5	34.7	179	41.3	321	75.6	274	54.3	505	100	15400
PD17-42-682	1.305	15.25	1.111	7.17	6.21	2.91	29.6	8.01	78.6	26.7	116	24.7	241	51	11950
PD17-42-683	2	11.58	1.77	10.9	5.67	2.84	17.9	5.47	60.2	22.2	108.6	24.24	244.5	52.8	11820
PD17-42-692	1.32	46.5	1.58	11.4	9.3	3.71	29.4	8	76.1	24.02	103.2	21.5	214.5	44.8	10090
PD17-42-693	0.0103	11.61	0.032	0.79	1.47	0.657	6.15	1.69	17.57	6.45	30.33	7.09	75.5	17.87	9820
PD17-42-694	7.05	32.3	6.62	69.9	169	87.5	843	215	1700	403	1166	180	1278	196	13280
PD17-42-695	8.24	49.9	5.47	31.8	41.4	21	170	36.3	307	86.7	329	61.5	535	100.9	13150
PD17-42-695-2	11.32	105.9	9.38	50.1	24	7	47.5	12.75	123.9	39.5	169.3	36.17	353	73.4	10100
PD17-42-696	5.75	64.7	4.45	24.4	13.7	4.37	32.2	9.46	99.1	32.7	144.3	30.1	295	62.5	9270
PD17-42-697	1.71	32.05	1.427	8.6	6.37	1.98	20.32	5.98	61.9	21.51	93.4	20.19	193.6	40.44	11910
PD17-42-698	22.71	135.3	14.75	80.3	46.8	24.7	145	40.5	346	93	305	52.5	443	79	10730
PD17-42-699	41.6	253	30.4	174	132	57.6	407	109	930	243	780	141	1150	198	14760
PD17-42-699-2	0.52	9.92	0.557	6.05	17.2	9.77	105	31.2	280	75.4	276	54.1	495	94.3	13560
PD17-42-700	0.93	14.8	0.69	6.4	16.5	7.97	85	23.6	218	65.4	258	49.9	456	88.5	11620
PD17-42-701	23.9	152.5	16.6	89.4	35.4	9	50.3	12.93	134.4	42.5	194.2	41.4	404	82.7	11470
PD17-42-702	42.3	313	26.9	128.8	51.9	13.34	93.2	25.8	274	97.3	431	90.1	821	156.8	15440
PD17-42-703	15.73	104.6	12.92	68.2	39.8	16.3	111	29.3	259	67.9	239	45	381	68.2	13150
PD17-42-712	0.509	13.67	0.335	2.37	2.72	0.936	15.16	5.05	57.1	20.68	91.7	19.92	198.9	42.44	12150
PD17-42-713	65.4	390	43.7	241.1	154.8	66.3	460	119.3	1041	259	882	152.7	1225	203	14600
PD17-42-714	20.26	149	13.51	72.8	30.5	8.93	49.1	12.83	130.9	44.6	198.6	44.4	451	94.2	12970
PD17-42-715	0.0169	22.9	0.119	2.4	3.56	1.54	15.04	4.34	45.5	16.83	78.2	17.06	175.2	39.11	8570
PD17-42-716	15	65.1	7.44	44.6	24.6	7.12	63.2	16.1	160	52.2	218	45.6	434	91.1	11920
PD17-42-717	2.76	18.5	2.11	12.2	6.8	2.15	29.3	9.86	125.1	46.1	211.7	43.4	396.4	78	10580
PD17-42-718	0.52	8.3	0.404	3.55	5.61	1.26	32.4	11.07	142.8	56	245.3	48.6	426	83.5	10270
PD17-42-719	5.5	39.9	4.78	30.9	23.3	12.29	106.1	39.9	345	93.3	357	71	667	128.4	15410
PD17-42-720	9.4	52.5	6.65	39.4	15.7	5.42	25.8	7.26	63.5	19.66	91.7	22.91	260	62.8	11710

PD17-42-722	1.11	13.29	0.487	2.94	2.97	0.86	14.52	4.92	62.1	24.9	120.9	25.8	259.2	56.1	9040
PD17-42-723	2.01	34	1.28	10.6	20.3	11	102	29.7	258	75.4	299	62.2	574	111.3	12510
PD17-42-732	2.34	16.2	2.11	12.2	9.77	5.61	48.2	20.8	189	49.6	192	39.9	410	86.2	14230
PD17-42-733	3.1	37.3	2.04	12.7	13	2.16	71.1	24.82	300.1	114.3	495	95.4	835	155.6	11260
PD17-42-734	12.6	87	16.8	171	313	163	1670	463	4020	1040	3400	548	4050	646	10770
PD17-42-735	0.81	13.68	0.361	2.85	3.51	1.62	25.4	9.08	121.8	49.7	233.1	48.72	459.9	94.3	10450
PD17-42-736	3.29	24.27	3.34	21.8	20	7.41	75.7	21.1	178	46.5	167.1	30	256.1	49.3	10320
PD17-42-737	42.3	264	61	620	1530	1040	7500	1850	14400	3440	10100	1660	12100	1660	14220
PD17-42-738	5.65	51.8	4.47	29.5	68	38.8	351	68	500	122	405	73.4	633	116.6	13370
PD17-42-739	15.6	88	11.1	65.6	53.3	22.5	189	55.4	490	139.7	551	106.3	955	181.8	12340
PD17-42-740	53.8	346	42.5	260	261	130	1010	274	2340	587	1870	308	2400	365	13380
PD17-42-741	12.5	82.1	10.3	75	110	56.2	468	117	1050	262	890	136	1100	182	10790
PD17-42-742	32.9	176.1	25.5	168	212	99	1010	278	2380	528	1600	257	1900	293	11540
PD17-42-743	100.9	685	103.9	852	1084	485	4240	1311	11930	3110	10060	1653	12230	1808	20970
PD17-42-752	27.7	157.6	20.8	119.1	80	35.3	242	70	590	149	542	92	790	134	11640
PD17-42-753	11.8	52.3	4.03	19.1	8.59	2.8	20.9	6.03	62.4	22	100.8	21.2	221.1	49.5	10910
PD17-42-754	24.6	214	16.9	92.2	56.1	21.9	160	42.4	368	102	399	73.9	679	131.1	10390
PD17-42-755	2.03	26.3	1.079	6.53	4.44	1.59	18.1	5.93	70.6	27.7	133	29.9	305	68	10570
PD17-42-756	0.227	20.25	0.38	3.54	4.91	1.95	23.8	7.55	85	31.25	141.3	30.31	297.2	63.2	9350
PD17-42-757	9.4	70.2	7.8	45.1	24.7	8.7	73	24	231	69.2	280	57.8	556	112.3	12560
PD17-42-757-2	4.91	26	3.54	18.6	13.2	5.6	39	11.8	121	41.8	205	54.6	644	143.5	15970
PD17-42-758	2.31	35.2	1.72	11.5	13.2	4.58	64.8	22.9	294	115.7	560	121.1	1146	225.4	13380
PD17-42-759	1.15	15.8	1.15	7.31	7.08	1.38	32.9	12.47	161.2	62.7	293.9	60.1	538	104.6	12620
PD17-42-760	3.77	31.4	5.8	63	92	48	390	119	1190	332	1160	207	1690	283	17100
PD17-42-761	0.036	20.56	0.22	4	10.36	0.52	66.4	25.06	322.9	127	562	108.3	916	172.5	10890
PD17-42-762	61.9	428	45.6	246	136	54.6	376	85	670	171	588	101.8	839	147.7	10540
PD17-42-763	6.15	45.1	4.76	28.8	15.4	5.33	40.2	11.6	108	34.6	139	27.1	245	49.9	10620
PD17-42-772	0.121	20.44	0.146	0.9	1.2	0.329	3.79	1.406	16.88	7.04	37	9.4	103.9	23.38	11430
PD17-42-773	7.93	51.6	5.43	30.3	19.5	8.37	80.5	31.2	290	78.3	260	49.3	426	72.8	13140
PD17-42-774	0.817	24.37	1.16	8.16	5.7	2.11	21.31	6.1	69	25.48	121	27.44	284.2	63.4	9990
PD17-42-775	1.88	12.28	1.28	7.8	9.3	7.2	46	10.9	100	29.3	115.8	24.7	226	46.1	14030

PD17-42-776	15.8	122	12.8	74	37.4	11.9	77.6	19.8	177	49.3	187.7	36.3	339	67.9	10130
PD17-42-777	1.82	38.4	1.21	9.6	10.37	3.91	39.8	11.88	115.7	37.5	155.6	31.1	287.1	55.7	8370
PD17-42-778	22.5	99	9.9	51.4	31.3	11.88	111.2	32.9	295	82.7	308	56.3	470	85.5	9940
PD17-42-779	20.2	117.2	14.5	77.3	37.3	11.48	98.4	27.1	276	92	386	75.1	691	141	10030
PD17-42-780	9.71	59.4	5.91	32.2	22.9	8.29	75	20.4	182	58.4	242	50.3	470	92.2	12290
PD17-42-781	6.46	151.1	5.51	39.4	34.7	10.25	112	29.7	290	93.6	380	75.9	667	127.1	8780
PD17-42-782	5.49	49.1	4.48	24.9	15.8	5.9	50.8	15.5	151.3	40.1	149.9	29.1	247.3	46.1	11020
PD17-42-783	8.55	67.9	6.9	37.5	17.7	4.89	30.6	7.79	75.8	22.8	95.7	20.7	203	41.8	11960
PD17-42-792	0.308	17.6	0.378	3.71	12.2	6.58	65.9	21.5	194	55.5	226.8	51.2	534	116.3	14440
PD17-42-793	5.71	59	4.5	30.1	36.6	17.93	146.2	46.7	396	100.6	350	65.9	594	112.6	13550
PD17-42-794	3.77	19.5	2.41	13.4	6.7	3.19	23.8	9.7	103	35.1	176.9	48.8	578	128.9	15510
PD17-42-794-2	1.04	14.23	1.12	8	9.6	2.92	38.2	13.98	146.8	48	206.9	41.5	371	72.2	9380
PD17-42-795	48	131	18.9	84	24	3.15	51.7	15.17	179.6	66.2	290.5	57.9	516	99.2	11340
PD17-42-796	14.4	86.6	7.92	40.1	25.7	10.06	92	29.2	289	93	395	82.1	777	160.8	11200
PD17-42-797	50	113	12	53.1	15.4	5.02	24.9	5.32	46.5	15.43	65.8	14.6	152.8	36.95	10000
PD17-42-798	4.23	62.9	2.47	12.5	7.16	2.47	30.6	9.52	104.8	38.1	175.4	39.5	388.9	78.7	10990
PD17-42-799	3.48	46.3	2.41	13.6	7.83	2.79	28.1	9.21	108	41	199	46.2	477	105.6	11550
PD17-42-800	0.218	8.37	0.128	1.3	2.48	0.553	14.26	5.3	66.3	27.77	136.2	30.45	297.9	63.5	10590
PD17-42-801	70	168	20.1	92	71.1	36.2	315	84.6	716	188	669	120.1	1007	176.8	14130
PD17-42-802	1.99	23.2	1.79	9.3	5.34	1.22	22.2	8.14	102.2	40.9	195.7	41.8	389.4	75.4	12450
PD17-42-803	0.065	9.07	0.084	0.94	1.68	0.541	8.57	3.08	37	14.9	72.8	15.7	156	33.6	10970
PD17-42-812	57.9	360	57.1	472	880	524	4110	980	7800	1830	5540	840	5970	870	13940
PD17-42-813	0.473	17.93	0.286	2.51	3.05	0.829	14.7	4.87	59.6	23.4	113	24.5	248.6	54.8	11080
PD17-42-814	13.6	83.1	8.32	47.8	44.2	28.1	190	44.9	350	87	336	62.9	540	99.9	11260
PD17-42-815	0.346	24.51	0.509	5.74	9.68	2.28	50.8	17.11	206.3	78.5	359.1	75.5	695.3	139	9730
PD17-42-816	4.77	46.6	3.03	17	9.21	2.57	24.1	7.4	76.2	27.3	116.2	23.17	216.4	43.1	10140
PD17-42-817	1.03	15.12	1.07	6.56	5.65	0.96	32.7	11.96	156.7	63	294	59.2	529	103.3	12530
PD17-42-818	0.585	9.3	0.5	3.03	3.53	1.29	12.24	3.94	45.5	17.07	79.5	17.8	176.4	39.1	10440
PD17-42-819	8.4	107.7	7.8	46.9	30.6	10.42	90.7	25.5	253	83.7	333	63.5	547	102.8	10060
PD17-42-820	172	380	41	164	37.6	2.44	79.4	23.2	269.9	100.3	443.7	86.5	754	143.2	11770
PD17-42-821	0.93	17.8	1.08	9	10.9	2.44	59.3	19.17	229.8	83.8	362.6	70.9	621	119.8	11170

PD17-42-822	6.62	42	5.87	33.5	27.4	10.58	90.5	32	305	82	324	66.6	652	129.9	15280
PD17-42-823	4.29	20.6	3.89	28.1	55.3	30.3	265	72.9	656	168	621	122	1184	244	28100
PD17-42-823-2	9.91	46	8.49	64.7	110	56	531	135	1140	278	960	176	1530	308	25500
PD17-42-832	0.41	23.92	0.261	1.63	2.93	1.21	16.04	5.58	64.7	24.73	119.7	27.26	273.7	59.2	10870
PD17-42-833	3.33	60.3	2.94	16.6	15.9	7.3	73	25.3	242	72.2	296	62.5	600	129.8	11210
PD17-42-834	3.59	31.2	4.17	27.1	13.6	4.24	53.3	17.7	200	72.5	316	60.4	538	106.3	9470
PD17-42-835	320	790	80	377	231	105	790	197	1610	380	1210	204	1580	254	15540
PD17-61-837	68	503	53.2	301	152	47.2	260	52.1	377	99.8	374	71.2	641	126	10160
PD17-61-838	185	970	106	577	225	66	310	45.6	320	93.4	393	82	789	160.4	12410
PD17-61-839	6.26	36.7	4.52	27.6	13.9	3.77	22.8	3.46	25	7.72	37.2	9.98	124.9	33.4	13750
PD17-61-840	101.6	750	64.2	377	211	52.2	284	44.6	252	59.3	194.6	36	311	59.3	14280
PD17-61-841	24.07	146.4	17.53	103.7	49.6	12.63	87.7	18.58	161	51.5	221.4	46.4	437	87.8	11550
PD17-61-842	33.8	250	24.6	145.9	74.6	16.23	121.3	22.01	169.5	47	185.1	35.4	312.4	59.5	11680
PD17-61-843	65	416	44.7	253	103	26.3	167	32	274	83.1	334	63.3	556	103.9	9420
PD17-61-852	2.26	31.5	1.59	9.9	7.78	1.86	36.9	12.47	157.6	65.6	304.6	64.5	601	120.3	11990
PD17-61-853	416	3180	258.7	1428	579	130.3	748	96.9	492	105.2	350	65.7	637	134.2	13910
PD17-61-854	42.5	334	27.7	167	95	24.5	158	30.4	228	68.6	289	60.1	576	120	13340
PD17-61-854-2	11.3	92.6	8.37	53.1	30.9	7.51	66	13.49	120.9	40.7	179.2	38.3	376	83	11880
PD17-61-855	251	1370	152	885	403	116.2	592	93.1	594	149.4	546	101.7	902	177.2	10410
PD17-61-856	474	2730	272	1474	584	127.4	744	85.5	401	86.1	285	53	497	95.8	13490
PD17-61-857	7.94	68.9	7.23	49.4	33.9	7.13	57.5	11.07	87.2	26.52	109.3	23.04	218.9	44.35	12260
PD17-61-858	6.62	44.2	4.47	27.2	15.3	4.79	31.4	7.79	78.1	26.77	120	25.36	243.7	49.7	12160
PD17-61-859	368	2610	257	1451	690	189.4	900	129.9	725	158.8	551	105.6	981	201.5	11720
PD17-61-860	153	1016	110.7	679	408	90.2	576	91	541	129.9	467	90.3	811	153.5	11750
PD17-61-861	268	1800	182.5	1040	457	181.3	644	103.7	664	161.5	573	113.2	1063	206.3	11140
PD17-61-862	544	3740	340	1780	619	153.6	824	111.9	610	133.3	415	70.2	581	106.5	12130
PD17-61-863	170	1070	118	728	788	420	4370	1230	10900	2800	8550	1230	8530	1240	12770
PD17-61-872	567	2003	276	1601	690	170.3	892	115.2	628	141.1	468	83.2	713	128.5	12190
PD17-61-873	583	3930	337.2	1862	1023	304	2520	554	4490	1270	4060	634	4720	699	12100
PD17-61-874	8.9	76.5	5.06	28.7	17.5	5.18	35.5	9.23	92.5	34	152.7	32.4	306	59.1	14720

PD17-61-875	9	78	11.2	73	30.3	2.94	74.3	19.24	201.2	70.7	296.6	56.7	489.1	91.1	9400
PD17-61-876	0.75	8.3	0.474	3.03	2.27	0.69	12.43	4.28	55	23.47	117.1	27.2	278.2	61.5	8860
PD17-61-877	7.7	53.7	6.04	40.1	25.7	6.56	69.1	18.34	195.3	71.5	318	64.7	586	116	9310
PD17-61-878	9.1	102	8.1	49.2	27.4	7.09	47.3	9.63	76	23.64	103.7	22.43	225.6	48	12130
PD17-61-879	43.6	271	25.3	133	51	14.8	75	14	111	34.5	148	31.4	311	69.1	12600
PD17-61-880	620	3640	375	2090	858	199	1109	138.6	709	160.2	521	93.1	813	152	12270
PD17-61-881	802	5260	509	2820	1192	246	1409	168.4	807	173.5	567	101.2	889	166.7	10390
PD17-61-882	279	2040	202	1049	417	94.2	583	93	667	194.3	755	141.2	1210	218.3	9430
PD17-61-883	252	1583	149.1	799	352	86	460	66.3	368	86.8	331	72.1	744	164.1	17080
PD17-61-884	253	1370	138	704	256	64.4	356	49.3	323	91	368	76.1	733	148.9	10550
PD17-61-892	328	1150	132	701	333	79	458	67.5	395	92.8	309	57.7	461	85.5	10240
PD17-61-893	412	2032	223	1137	393	95.1	542	78.4	491	121.7	414	72.6	611	108.1	8780
PD17-61-894	218	793	101	499	173	40.5	241	33.3	209.9	56.1	209.8	40.7	384	78.9	9780
PD17-61-895	516	4900	349	1979	999	271	1376	224	1364	295	920	157.9	1292	205	11730
PD17-61-896	37.3	369	25.6	154	96	24.4	155	25.8	167	45.2	190	42.3	449	100.6	11120
PD17-61-897	158	784	110	735	435	100	634	86	456	94.5	301	51.1	435	80.4	11160
PD17-61-898	33.3	205	24.2	148	74.6	21.8	130	23.8	196	54.9	205	38.9	333	59.7	9930
PD17-61-899	102.6	607	55.6	290	109.2	26	172	27.3	203	66.2	285	61.8	622	135.4	11750
PD17-61-900	567	2520	260	1355	586	128.5	743	102.9	565	128.5	457	88.2	820	169.5	9780
PD17-61-901	3.27	47.1	2.93	21.4	18.9	4.15	66.8	18.4	195.8	70.4	301	58.2	515	97.1	9080
PD17-61-902	33.9	193	20.2	107	43.7	11.3	74	13.9	117	37.8	162.1	33.6	313	61	11430
PD17-61-903	380	2840	314	1990	1174	242	1593	229	1210	232.6	696	123.1	1105	221	14960
PD17-61-912	151	1510	99.9	563	303	64.7	426	70.2	435	102.8	368	67.9	596	110.8	12760
PD17-61-913	25.6	203	17.1	96	49.3	12.5	85	16.9	129	37.3	153	30.8	287	53.2	12140
PD17-61-914	190	1223	125.2	730	342	93.3	481	70.7	414	96.6	340	63.4	582	115.4	9920
PD17-61-915	1570	1724	378	1820	576	141	698	105.2	662	160	581	107.3	960	181.9	10610
PD17-61-916	39	59.4	9.6	47	18.8	3.45	38.2	9.33	96.7	34.55	155.7	31.39	288.4	56.1	11020
PD17-61-917	524	3900	349	1810	724	194	972	157.6	1001	232.5	796	142.8	1250	236.6	10500
PD17-61-918	12.54	108.4	10.55	62.7	31.5	8.38	53.6	10.87	94.6	30.8	133.3	28.48	279	58.8	10470
PD17-61-919	245	1536	140.1	746	331	76	454	72	484	130.2	484	88.7	765	146.7	9490
PD17-61-920	107	494	58	319	122.9	31.5	147	19.1	118.6	35.9	165.2	45.9	574	142.5	17360

PD17-61-921	159	980	95	547	254	53.7	356	51.3	304	70.4	247	43.3	383	71.1	10040
PD17-61-922	170	551	81.6	501	240	61.7	340	50.4	321	82.6	319	63	587	115.7	11220
PD17-61-923	96.6	1035	78.5	482	317	77.1	476	76.1	436	94.9	314.5	57.2	493	93	10720
PD17-61-932	647	3310	320	1652	659	151.6	878	131.1	815	212.7	801	158.3	1462	288.8	11040
PD17-61-933	291	1410	169	1010	505	128	691	103.1	595	133.9	448	79.4	696	131.9	10130
PD17-61-934	15.4	110	9.5	54.4	30.4	7.68	53.9	11.03	94	30.2	131.4	27.7	260.2	54.2	9800
PD17-61-935	697	3720	378	2034	828	202.1	1096	147.2	902	232.6	834	153.8	1330	246.6	10680
PD17-61-936	43.8	252	30.1	177	90	21.5	139	27.3	228	72.2	308	64.9	594	115.1	11990
PD17-61-937	384	2680	331	2010	929	221	1212	172.6	929	185.1	534	83.5	654	113	10880
PD17-61-938	396	2240	226.5	1185	418	90.8	545	69.3	409	106.2	407	81.7	772	162.5	10960
PD17-61-939	178	821	106	627	328	92	508	82.5	549	140	486	86.5	712	130.1	9240
PD17-61-940	55	344	38.2	220	113	26.1	152	21.1	121	28.5	110.1	22.6	219	43.7	11820
PD17-61-941	14.6	106.8	10.51	67.6	42.1	9.93	78	16.62	145.2	48.1	208.5	45.7	445	91.5	11210
PD17-61-942	104.9	1111	66.1	395	242	57.6	347	55.9	339	80.2	292.7	55.1	470	92.6	11800
PD17-61-943	39.6	450	28	157	90	21.6	140	24	163	42.3	169.2	35.9	365	81.7	11300
PD17-61-952	860	600	156	720	223	44	230	28.3	160	38.4	144	29.9	283	57.5	12310
PD17-61-954	67.6	771	54.8	310	178	40.5	249	38.9	236	57.5	213	42.8	395	78.7	13060
PD17-61-955	19.5	143	14.1	87	52.4	13	89	16.9	131	39	162	33.6	309	59.2	12130
PD17-61-956	4.7	47.3	4.31	26.7	15.1	3.41	25.6	4.9	41.1	12.69	55.5	12.38	121.4	25.8	11540
PD17-61-957	19.7	131.9	13.87	88.9	56.7	13.28	105.8	21.51	183.8	59.8	252.6	51.2	482	98.4	10000
PD17-61-958	314	2360	230	1307	616	148	825	118.3	671	147.3	483	84.9	742	132.9	9810
PD17-61-959	41	307	34.1	211.7	121.6	24.2	198.4	34.3	248	70	269	53.5	497	102.4	11820
PD17-61-960	35	199	22.6	144	78.9	20.6	120.2	18.9	124.6	34.3	135.8	28.34	273.5	58.2	10250
PD17-61-961	10.1	81	7.7	47.2	22.1	5.63	41.9	8.95	84.3	28.9	124	24.9	228	45.2	11360
PD17-61-962	1280	1630	282	1410	434	82.1	498	63.2	420	121	474	89.4	784	143.4	12070
PD17-61-963	370	2041	203.7	1069	399	98.9	534	74.4	464	124.2	512	120.5	1359	300.5	37260
PD17-61-964	5.69	94	4.34	26.7	17.3	4.01	29.4	6.3	50.9	16.43	72	15.42	152.7	34	11000
PD17-61-973	417	2890	253	1416	811	208	1800	353	2510	576	1780	300	2360	410	16520
PD17-61-974	183.4	1943	125.1	688	339	75.8	438	65.2	389	92	316	55.3	469	86.2	10960
PD17-61-975	74	425	38.6	232	116	24.2	200	40.9	342	103.8	407	78.8	686	123.5	10520
PD17-61-976	480	2520	226	1180	499	126.7	654	94.8	567	130.1	427	75.4	605	108.4	11070

PD17-61-977	7.14	87.6	6.01	40.4	26.1	7.22	57.9	13.29	133.8	49.2	227.8	51	494	103.7	11740
PD17-61-978	55.9	440	38.7	238	152	41.7	256	44.6	317	86.6	326	63.9	571	108	11660
PD17-61-979	252	1300	146	821	351	69.3	449	58.5	364	100	398	79.6	770	156.1	9350
PD17-61-980	296	2356	214	1175	563	119.4	722	107.9	673	173.8	641	116.3	990	192.6	10530
PD17-61-981	540	650	104	470	161	28.7	199	36.6	317	105.2	424	87.9	772	140.9	11530
PD17-61-982	95	191.8	25.9	152	78.3	21.78	157.3	34.1	314.9	105.4	439	87.6	781	151.5	9470
PD17-61-983	367	2542	219	1184	497	109.3	617	76.7	382.6	82.4	278.6	54.5	532	115.9	11570
PD17-61-984	316	1701	197.4	1106	502	137.9	899	169	1172	280	924	162.7	1452	271	19010
PD17-61-993	16.5	147.4	11.39	73.5	47.8	11.08	84.6	15.51	115.4	33	133.5	27.2	262	53.7	10010
PD17-61-994	8.9	118	7.29	46	29.5	6.48	53.8	11.51	100	32.41	142.1	28.88	272.6	53.4	11840
PD17-61-994-2	24.8	420	20.1	115	71.4	15.9	99	18.3	120.2	32.1	125.6	26.2	247	52.3	11620
PD17-61-995	106	401	47.8	260	101.9	25.8	157	28.2	220	67.2	288	62.1	613	127.3	11810
PD17-61-996	1.87	28.9	1.68	11.19	7.68	2.14	23.6	6.67	71.6	25.54	114.4	23.34	217.2	42.5	12130
PD17-61-997	10.82	89	8.44	55	34.3	8.24	64.7	12.81	102.1	32	136.3	29.1	291	63.4	9690
PD17-61-998	106.2	489	64.9	408	216	59.2	302.8	49.5	323	78	274	51.5	469	92.4	12700
PD17-61-999	108.1	802	70.6	421	162	41.3	224	35.5	233	59.6	230	44.8	424	84.4	14480
PD17-61-1000	40.6	195	22.9	145	81.8	20.4	127.3	21.2	131	32.7	127.3	27.1	288	66.6	14680
PD17-61-1001	63.9	375	41.1	241	120.1	25.5	172	25.4	158.8	38.5	143.8	28.56	262.1	55	12860
PD17-61-1001-2	309	1896	210.3	1159	519	114	649	86.3	426	85.8	272.8	50.9	447	87	11580
PD17-61-1002	223	1710	151	810	345	84.1	442	67.4	386	85.1	287	49.8	416	77.2	13530
PD17-61-1003	22	204	20.1	126	71.9	14.8	109	19	140	41.4	170	35.5	340	69.2	11950
PD17-61-1003-2	13.5	68	7.6	40.9	14.7	3.67	20.8	3.57	36.7	15.3	80.7	23.7	315	83.9	15800
PD17-61-1004	226	1230	132.8	666	225	52.9	286	34.2	187	47	179.1	37.8	396	84.7	13540
PD17-61-1013	368	2100	202	1094	507	132	872	161	1310	376	1280	215	1600	280	11500
PD17-61-1014	31.5	205	24.2	144	78.7	19.7	131.6	27.3	200.5	55.5	215	40.8	368	69.4	11750
PD17-61-1015	12.2	139	9	58	37.8	10.24	71.1	13.96	109.9	32.9	132.7	27.3	261	52.6	10360
PD17-61-1016	220	1251	125.4	635	260	60.1	391	59	380	98	360.8	68.9	631	125.6	10960
PD17-61-1017	34.8	227	26.6	170	89	27.3	141	24.4	166	44.9	169	33.3	306	63.6	8380
PD17-61-1018	10.8	71	7.5	40	18.4	5	44.1	10.42	110.6	39.4	171	35.6	330.2	67.6	11600
PD17-61-1019	4.93	52.1	4.17	29	22.5	5.26	54.5	13.07	125.7	42.78	191.2	41.6	400.2	84.2	10380
PD17-61-1020	93	710	72	387	149	38	213	36.8	259	68.6	255	47.9	431	84.1	10570

PD17-61-1021	17.6	118.9	12.66	73.6	43	9.1	101.8	24.87	245.5	85.2	356.6	68.5	609	116.1	9270
PD17-61-1022	24.4	172	18.4	106	57.2	11.9	99.2	18.86	146.7	45.1	183.3	36.38	338.1	67.8	10790
PD17-61-1023	11	62.5	5.5	36.7	21.3	5.89	41	9.55	99.2	36.5	173.9	38.5	385	77	10500
PD17-61-1024	60.5	315	41	259	143	35.2	207	31.2	187	46.3	171.7	32.69	305.2	62	11880
PD17-61-1025	10.6	71.9	7.33	45.3	27.7	6.82	48.8	9.36	74	23.3	109.3	24.5	258	57.1	14250
PD17-61-1026	391	2238	244	1436	687	185.5	957	150	859	191.5	621	109.9	965	195.2	17090
PD17-61-1027	443.2	3450	261.1	1375	668	159	889	132.8	735	163.2	542	99.1	858	167.1	10670
PD17-61-1028	122.8	1336	83.1	495	338	92.6	533	89.4	535	123.5	433	80.5	711	134	10140
PD18-117-9	36.1	333	55.1	327	159.9	56.8	284.3	66.4	551	155.5	574	112.4	936	170.2	10650
PD18-117-10	41.8	464	70.8	438	215	78.7	348	76.2	535	125.9	407	72.9	633	117.2	7980
PD18-117-11	20.9	188.9	30	185.1	96	41	194.8	47.2	349	80.8	253	45.7	398	70.5	9220
PD18-117-12	19.8	217	31.2	197	190	91	620	139	990	227	690	113	900	154	13230
PD18-117-13	60	663	122	754	331	126	543	115	768	177	570	105.3	902	169.2	9720
PD18-117-14	26.5	162	28.5	174	84.2	24.7	171	39.5	354	104.5	399	73.1	611	113	9400
PD18-117-15	22.4	245	43.1	259	129	48.9	223	50	355	77.1	241	42.3	371	69.3	9160
PD18-117-16	49.3	497	85.8	488	240.5	100.9	410	87.9	566	110.9	301.7	49.6	401	68.3	10120
PD18-117-17	2.11	18.74	2.05	12.3	8.02	3.15	24.7	7.11	75.4	27.59	122.9	26.94	259.7	56.1	8220
PD18-117-18	0.013	20.3	0.066	1.1	2.1	0.571	10.4	3.06	33.4	11.86	53.2	11.1	105	21.14	9050
PD18-117-19	15.49	149.9	24	139.9	61.9	20.2	115.4	27.6	241.1	77.8	307	61.2	535	98.3	10570
PD18-117-27	90.8	571	108.2	612	273	114.7	514	114.2	811	176.3	534	91.2	741	127.7	11360
PD18-117-28	50.3	392	72.9	436	212	70.4	319	68.7	486	111	340	60.4	524	92	9040
PD18-117-29	30.1	252.2	44.9	267	122.7	49.6	215.1	48.7	365	90.8	321.1	60.8	539	99.9	10360
PD18-117-30	13.7	171	18.6	114	65.2	25.4	159	39.5	333	94	358	72.2	642	126.4	8440
PD18-117-31	18.5	236	37.6	237	109.4	51.9	213	47.3	421	130.6	571	128.9	1279	259	9980
PD18-117-32	20.9	250	39.5	242	109	39.5	198	50.3	397	119.5	456	86.4	752	141	10560
PD18-117-33	37.2	359	51.7	312	173.8	60.2	322	73.1	576	142.9	508	95.1	831	150.6	10230
PD18-117-34	36.9	404	47.8	274	144.5	52.8	280	71.4	527	122	389	69.3	585	103.6	8990
PD18-117-35	11.1	140	17.3	109	57.1	19.1	115	27.4	221	64.1	238	44.6	399	75	7800
PD18-117-36	49.5	507	94.9	536	267	92.9	429	94.1	689	174.6	612	119.8	1062	188.1	9550
PD18-117-37	17.3	192	32	182	93.2	37.7	171	37.9	287	73.7	255	47.3	403	77.1	9180

PD18-117-45	4.63	69.4	9.5	56.9	38.9	13	102.8	26.8	276	92.7	393	81.4	749	141	8510
PD18-117-47	0.164	3.47	0.187	1.46	0.92	0.506	3.47	1.139	11.26	4.06	18.87	4.23	44.9	9.63	2929
PD18-117-48	0	12.01	0.209	3.32	7.54	1.95	47.8	16.07	185.4	69.6	295	57.9	499	97.3	8730
PD18-117-49	0.017	13.14	0.217	4.23	9.45	1.06	53.9	18.31	224	85.8	369.4	70	585	108	8460
PD18-117-50	17	205	34.6	209	86.1	31.7	128	25.3	182	46.5	174.7	37.2	355	75.3	9890
PD18-117-51	4.8	33.5	2.56	15.4	6.68	1.72	19.7	5.93	65	23.83	107.6	23.38	218.8	43.85	9580
PD18-117-52	50.5	397	84	518	234	73.4	342.3	63	417	93.8	310	56.6	497	95.6	9510
PD18-117-53	124.1	1299	201.7	1228	793	369	2550	663	4820	1029	2830	417	2940	442	7220
PD18-117-54	69.6	772	117.7	703	332	141.4	597	124	849	192	596	99.1	795	135.2	10740
PD18-117-55	23.5	256	45.1	268	147.4	56.8	259	59.2	435	102.4	339	63.9	552	105.7	9230
PD18-117-63	10.7	105.8	10.53	60.5	29.1	9.33	55.6	12.38	103.3	31.6	131.4	28.1	272	57.2	9370
PD18-117-64	6.9	82.3	11.5	60.6	30	9.9	72.6	21.7	203.2	63	275	55.4	495	94	11000
PD18-117-65	0.35	28.7	0.7	7.91	10.84	4.39	51.1	15.82	167.1	58.4	246.8	49.6	447	85.7	9860
PD18-117-66	22.26	191.7	29.6	172.2	88.9	32.6	167.9	39.6	304	74.7	261	53.4	512	108.4	7910
PD18-117-67	44	506	94.5	587	282.3	110.1	454	90.1	591	119	358	62.6	539	102.8	8740
PD18-117-68	0.244	7.14	0.27	1.51	2.25	0.407	12.04	4.46	57.3	22.62	105.7	22.92	215.2	42.4	9950
PD18-117-69	44.7	306	44.2	260	139.4	59.5	264	59	419	93.2	283.2	47	370	61.3	11200
PD18-117-70	27.5	241	33.3	204	95.8	35.3	165	35.3	267	64.5	229	46.1	426	84	8410
PD18-117-71	46.3	188.9	32.6	223	129.4	39.6	227	45.5	327	82.3	285.9	56.5	535	113.1	10100
PD18-117-72	7.54	93.8	9.37	58.5	29.2	10.93	66.1	17.21	138.9	38.7	134.9	24.85	211.7	39.5	9020
PD18-117-73	0.0064	7.88	0.069	1.19	2.63	0.402	17.62	6.53	83.2	32.9	152.2	32.4	299.6	59	9320
PD18-117-81	0.465	73.7	2.31	35	45.9	21.7	127.8	25.8	192.4	48.5	157	26.2	203.1	34.9	7610
PD18-117-82	6.8	55	7.02	41.3	16.8	6.01	29.7	6.69	65.1	21.3	101.2	23.29	240	52.7	8680
PD18-117-83	0.072	5.51	0.31	2.86	6.15	1.55	32.6	10.54	126.3	45.8	196.7	38.5	343	65	8250
PD18-117-84	5.04	64.7	6.37	41.7	19.7	9.76	43.7	9.88	79.5	20.16	74.4	14.77	144.5	30.55	8760
PD18-117-85	30.3	348	62.3	357	153.4	54.3	235	46.1	334	81.7	299	60.4	573	115.1	8890
PD18-117-86	34.7	345	52.7	306.1	130.6	49.1	213.8	45.7	338	79.3	276.9	53.3	500	97	9180
PD18-117-87	0.028	14.62	0.229	3.99	8.17	0.85	50.9	16.7	209.5	76.9	332	64.5	562	105.4	8570
PD18-117-88	12.93	135.3	22.72	131.4	62	22.04	114.4	25.6	206.9	60.5	243.5	49.7	483	101.5	9180
PD18-117-89	4.93	46.6	5.9	38.6	22.1	7.62	55.7	15.4	147	43.2	173	34.7	316	58.7	10980
PD18-117-90	100.3	953	164.6	1017	446	165	691	134.9	877	198	622	115	972	173.5	10940

PD18-117-91	21.8	217	38.3	264	126	46.5	218	45.4	294	67.4	223	39.5	337	63	8610
PD18-117-99	0.099	12.59	0.39	3.88	6.39	1.18	40.5	13.19	168.1	62.6	277.9	53.6	456	85	8640
PD18-117-100	24.6	280	47.5	286	137	56.8	250	55.3	399	95.5	323	60.3	536	99	8320
PD18-117-102	13	37.5	3.93	20.5	9.34	1.42	37.4	12.19	142.5	54.3	235	45.4	401	75.6	8350
PD18-117-103	3.5	31.6	2.95	15.8	11.3	3.59	37.2	11.59	132.5	49	216	44.6	397	77.6	10680
PD18-117-104	16	178	21.4	119.6	69.4	25.1	158	42.6	344	92.2	333	63.8	548	106.9	7850
PD18-117-105	201.2	1254	223.8	1235	516	171.1	722	132.7	836	175	561	105.9	943	186.2	10330
PD18-117-106	7.39	93.3	14.5	87.8	49	20.8	110.1	27.9	244	65.3	250.1	46.8	407	73.1	9160
PD18-117-107	5.7	40.2	4.38	26.3	16.9	5.99	56.8	17.86	194.9	70.4	300.8	60.7	541	110.4	7930
PD18-117-108	2.29	26.9	2.86	17.3	11.7	3.39	33.6	10.48	113.9	41.6	185	39.1	367	71.8	8380
PD18-117-109	1.87	31.1	3.97	24.5	15.9	5.02	60	18.51	204.6	74.2	313	61.1	559	103.9	8670
PD18-117-119	89.4	698	139.7	841	404	121.8	580	106.2	661	136.3	405	70.4	620	120.2	11490
PD18-117-120	0.096	25.13	0.244	3.02	4.12	1.09	16.12	4.52	47.5	15.95	67.4	13.53	125.1	25.06	8650
PD18-117-121	49.2	537	92.2	556	288	130.3	527	115.9	810	180	562	98	836	154.1	9120
PD18-117-122	4.72	67.1	6.54	40.7	22	7.64	48.9	12.43	103.2	28.2	99.5	19.9	186	36	10730
PD18-117-123	29.5	377	53.3	323	152	53.9	255	53.6	393	103.7	378	74.9	701	138.4	8060
PD18-117-124	25.5	264	43.8	267	124.8	44.6	219	47.9	362	94.5	341	64.2	564	107.9	9730
PD18-117-125	43.8	276	44.5	256	136.8	66	256	58	433	103.2	352	62.5	509	90.8	11430
PD18-117-126	1.58	19.46	1.37	9.41	6.39	2.46	33	11.56	141.1	55.3	255.1	52.7	484	94	10460
PD18-117-127	38.7	450	79	467	208	77.8	333	66.1	446	101.8	342	64.8	580	112.5	9580
PD18-117-135	7.69	95.2	15.62	98.8	53.8	23.1	104.7	23.84	200.6	58.1	235.2	47.2	439	88.8	8890
PD18-117-136	49.6	466	84.4	486	243	91.8	376	84.4	614	143	530	108.7	1032	206.4	9690
PD18-117-137	24.13	225.7	40.9	239.4	113.8	44.2	188	39	265	60.5	197.2	37.7	336	66.9	12490
PD18-117-138	0.058	7.62	0.152	1.48	3.53	0.408	22.9	8.57	110.7	43.5	204.1	43.4	399	79.6	10940
PD18-117-139	36.2	295	48.3	282	113.1	40.5	182	37.1	254.1	62.2	226.5	44.4	422	83.9	9540
PD18-117-140	1.17	14.73	1.4	9.23	8.7	2.85	37.9	12.16	143.4	54.5	248.8	52.4	481	99.1	8420
PD18-117-142	2.33	12.1	1.38	9.68	9.71	3.3	44	14.29	168.6	63.4	282.1	57.4	500	93.9	8920
PD18-117-143	109.2	565	91.7	518	230	94.9	429	98.7	721	175.3	614	117.6	1035	198.1	11150
PD18-117-144	23.4	215	35.1	202	89.2	28.2	161	38.8	351	111.1	430	82.9	689	125.6	9400
PD18-117-145	13.7	165	24.7	155	81	32.8	167	40.9	372	115	450	91.1	830	164	7460
PD18-117-153	13.6	175	30.8	192	96	35.7	183	45.4	400	128.6	490	93.9	837	152	9270

PD18-117-154	0.78	9.28	0.175	1.41	1.79	0.285	12.62	4.66	57.7	23.81	109.2	23.19	214.4	42.5	9360
PD18-117-155	8.7	70.5	11.6	65.2	26.4	8.56	42	9.28	88.4	32.1	164	42.6	489	123.2	14720
PD18-117-156	27.8	268	44.9	262	115	45.6	217	49.3	388	108	397	82.6	731	140	11020
PD18-117-157	7.33	79.2	12.06	70	36.3	13.51	67.5	15.92	138	40.5	168	35.2	344	71.6	11070
PD18-117-158	3.23	46.6	5.55	36.1	18.9	6.36	34.6	7.8	71	20.6	87.3	19.57	197.8	44.3	10290
PD18-117-159	1.33	10.4	0.52	3.7	2.74	0.57	16.7	5.75	76.6	30	139.1	31.1	290	54.5	9350
PD18-117-160	27.7	284	56.5	315	129.2	47.6	196	39.4	301	86.8	352.6	85.2	934	204.6	11510
PD18-117-161	36.3	341	65	364	151	50.6	205	37.5	239	52.4	170.8	31.7	287	59.8	9840
PD18-117-162	57.9	658	115.9	695	336	133.2	575	119.4	815	182.7	581	104.1	915	164.9	10210
PD18-125-170	18.5	90.6	14.5	78.5	43.6	33.6	72.8	20.4	205.8	71.4	356	92.2	1088	256	15360
PD18-125-171	77.2	612	80.6	411	274	120.2	413	116.1	906	196	672	124.4	1000	146.5	10480
PD18-125-172	36.9	306	39	229	139	109	233	55.1	473	120.2	407	70.8	583	89	8280
PD18-125-173	13.09	114.8	11.22	64.6	42.6	22.49	81.9	21.7	186.6	50.4	177.4	31.8	278	48.9	11740
PD18-125-174	2.67	49.7	2.44	17.75	14.19	5.97	41.8	11.4	111.1	35.5	142.4	27.9	249.1	50	9780
PD18-125-175	3.27	45.9	2.89	19.1	11.9	5.73	22.2	5.55	46.7	14.47	57.3	11.98	115.4	23.1	11530
PD18-125-176	4.35	17.25	5.78	26.1	16.9	4.97	32.2	11.9	145.5	57.5	296	69.2	679	138.8	11480
PD18-125-177	54	404	53.8	300	185	82.4	304	80.7	655	160	540	99	803	124.1	9240
PD18-125-178	37.1	270	32.9	188	143.6	67.3	276	81	693	152.3	480	82.4	684	98.1	10910
PD18-125-179	10.9	98	12.2	72.2	46.6	17	94	27	257	77.2	304	59.2	521	95.4	8790
PD18-125-180	44.1	648	52.9	263	177	67.5	254	64.6	569	146	535	109.4	1055	176	8720
PD18-125-181	10.2	71.1	9.8	55.2	40.9	21.3	87.3	24.1	227	69	276	54.3	496	93.2	8940
PD18-125-182	53.6	900	56.8	309	214	96	343	90	750	167	556	102	850	126	11090
PD18-125-183	22.5	176	21.3	120	91	40.8	180	52.2	447	121	432	82.6	703	123.9	9410
PD18-125-192	61.1	482	54.9	308	215	149	406	114.2	948	225	768	141.8	1196	194.5	10050
PD18-125-193	35	284	32.6	182	124	57.3	228	65	552	131	439	84	690	111	11280
PD18-125-194	21.8	128	21.7	115	75	30.7	124	35.4	289	71	244	47.1	401	68.1	11320
PD18-125-195	7.1	55	8.7	43	26.5	20.4	55.4	15.44	148.8	43.4	171.8	34.6	302	55.3	11070
PD18-125-197	0.61	23.75	0.733	5.3	6.9	3.13	33.8	10.55	122.9	45.9	203.6	43	389	80	8910
PD18-125-198	10.48	98.3	10.05	58.5	43.3	19.5	87.2	23	197.3	53.7	188.4	35.2	297	52.6	10900
PD18-125-199	20.2	156	18.9	109.6	76.1	32.9	137.3	36.7	298	77.1	275	53.4	480	87.4	8110

PD18-125-200	73	630	70	382	254	113	450	124	1030	234	770	142	1150	179	9390
PD18-125-201	43.1	369	33.9	207	130.8	67.1	231	57.5	495	132.1	455	81.9	671	116.5	8940
PD18-125-202	1.55	15.23	2.54	15.3	13.2	3.4	51.6	18.96	246.4	99.7	460.9	93.1	834	159.5	7920
PD18-125-203	14.2	337	16.9	88	61	24.7	107	30.4	257	69.2	271	51.4	466	82.7	9890
PD18-125-206	22	130.7	25.4	129	91	38.8	182.1	53.5	533	172.3	686	127	1041	182	9650
PD18-125-214	39.6	351	35.7	211	135	82	253	70.6	561	131	434	78.2	627	99.8	11850
PD18-125-215	0.094	11.93	0.199	2.46	3.72	1.83	17.3	5.78	65.8	25.1	114.6	25.1	244.3	53	8530
PD18-125-216	8.28	93.3	8.71	61.4	40.6	34.5	79.2	19.93	179.5	51.1	186.5	33	283.7	48	9780
PD18-125-217	12.1	95.7	11.3	58.4	43.6	22.5	86.8	23.4	203	54.6	204	39.6	371	69.9	10750
PD18-125-218	4.68	30.5	4.01	23.1	15.2	8	28.3	7.79	69.3	19.6	72.6	15.04	149.6	33.9	8320
PD18-125-219	11	90.2	12.6	73.6	53.5	19	114.6	31.6	312	97.3	407	84.6	764	145	8370
PD18-125-220	0.84	17.88	0.848	5.75	6.5	2.57	23.8	6.99	75.3	25.93	113.2	23.31	222	45.5	9520
PD18-125-221	0.663	15.85	0.81	4.98	6.03	1.46	25.6	9.94	131.7	54.3	259.3	54.8	503	99.3	9560
PD18-125-222	0.461	13.48	0.532	4.53	5.18	1.52	19.68	7.24	90	36.6	176.4	39.38	380.3	81.6	8220
PD18-125-223	45.5	339	44	246	196	83.8	377	106.5	906	216	717	125.6	986	145.9	8890
PD18-125-224	6.91	47.6	8.67	45.9	31.7	11.4	91.5	30.56	357.2	131.9	567	112.1	979	187.5	9970
PD18-125-225	0	14.96	0.031	0.82	2.33	0.078	17.78	7.15	97.6	40.2	193.6	42.08	383	75.6	12360
PD18-125-226	0.31	10.9	0.46	4.31	10.11	0.82	71.4	26.92	317.9	115.8	482	88.7	717	122.5	10990
PD18-125-227	0.476	11.55	0.775	7.12	8.37	4.3	32.1	9.62	105.5	37.5	166.9	36.55	368.5	81	6760
PD18-125-228	41	445	41.5	256	159.2	68.9	286	72.6	642	175.7	640	118.2	1084	196.9	7990
PD18-125-239	203.4	2010	185.4	1087	634	384	973	225	1746	419	1385	270	2406	383	8800
PD18-125-240	30.5	213	25.8	146	99	49.9	200	56.6	493	132	486	93.5	819	142.5	9800
PD18-125-241	65.6	492	63.9	352	255	106.7	430	125.6	1026	243	822	144.9	1198	183.3	9580
PD18-125-242	136.8	842	127.1	739	419	426	630	138.4	1074	251	848	158.1	1377	225.3	17650
PD18-125-243	33.2	330	31.7	179	119	49.7	206	57.4	499	143	553	105.6	938	168.7	8410
PD18-125-244	20.01	110.2	19.2	103.2	59.9	40	104.8	26.9	243	69.9	266.9	52.2	470	86.6	11270
PD18-125-246	4.46	57.5	3.56	24.8	18.9	14	54.5	15.73	168.7	58.8	251.8	51.3	469	93.7	8640
PD18-125-247	2.63	35	2.64	18.4	12.6	7.23	29.2	8.09	79.1	26.2	109.7	22.7	232	47.1	10100
PD18-125-248	13.5	92	14	85.1	45.9	33.9	72.2	17.8	156	47	195	40.4	378	71.8	12380
PD18-125-249	45.4	426	43.7	262	167.1	80.5	312	81.7	678	181.3	635	111.8	938	151.9	8890
PD18-125-250	11.57	90.5	9.51	60.2	37.5	34.6	69.1	18.5	171.9	53.2	216.4	45.5	420	78.7	10990

PD18-125-251	7.04	50.5	6	37.3	23.2	12.8	47.6	11.9	102.5	27.8	96.2	18.1	161	31	11480
PD18-125-252	9.85	54.5	5.21	29.1	17.9	8.78	46.1	13.33	147.6	49.8	223.4	45.7	440	86.7	8280
PD18-125-253	48.6	391	44.9	253	193.1	89.4	388	113.4	949	232.7	784	141.2	1148	188.6	8250
PD18-125-261	64.4	537	64.2	367	279	126.5	548	162.2	1351	318.8	1088	193	1563	234.3	12590
PD18-125-262	1.34	25	1.25	8.8	8.02	2.74	25.5	7.9	83.6	29.68	130	28.18	268.5	54.9	9270
PD18-125-263	8.39	74	7.27	44.5	28.1	13.3	65.7	19.52	200.5	66.1	272.5	53.8	495	93	9510
PD18-125-264	47.3	268	48.1	257	181	73.7	322	94.2	810	212.5	768	153.4	1308	214	10060
PD18-125-265	61.4	518	57	312	214	101.4	391	108.6	890	203.8	656	114.7	901	131.5	11720
PD18-125-266	54.2	245	35.8	195.2	115	62	191.7	46.4	386	97	345	68.2	632	110.6	9700
PD18-125-267	11.11	72.8	11.31	59.5	39.5	18	63.1	18	169	50.2	211	41.4	386	75.5	10170
PD18-125-268	16.7	130	14.1	80	54.5	23.3	109	30.1	253	69	215	37.6	289	47.5	9470
PD18-125-269	1.22	8.82	1.25	5.93	4.8	1.92	17.9	7.45	99.6	38.3	199.4	49.6	542	113.6	11690
PD18-125-270	12.9	77.2	9.08	58.2	34.5	17.2	69.6	19.5	185	53.7	202	39	317	54.9	12160
PD18-125-273	122.7	309	171	776	404	125.9	357	85.6	643	145.1	506	103.7	937	147.8	13230
PD18-125-275	177	1292	170	907	586	320	912	253	1936	435	1395	264	2302	356	16180
PD18-125-283	114.4	624	114.6	597	387	250	640	175.4	1416	323	1081	198.6	1646	257.9	12960
PD18-125-284	173.5	961	139.3	782	484	329	845	193	1456	343.3	1170	223.4	1899	311.1	12790
PD18-125-285	226.9	2054	190.8	1018	645	292	1106	297	2395	562	1883	334	2747	415	10840
PD18-125-286	18.4	178	15.7	91	64.4	35.1	133	37.2	319	83	300	59.7	542	99.3	9150
PD18-125-287	115.2	599	91	539	254	167.8	390	81.3	655	164.2	566	102.5	882	158.7	10410
PD18-125-288	26.1	138	25.1	136	71.3	52.5	100	25.7	221	62.9	241	49	473	84	11250
PD18-125-289	2.32	27.4	2.5	16.2	14.6	7.29	43.5	13.69	150.2	52.2	220.3	46.4	436	88.7	8740
PD18-125-290	119.9	862	116.7	667	474	204	821	241	1840	430	1395	254	2030	305	10400
PD18-125-291	11.5	66	9.3	54	30.5	23.5	55.1	15.7	141	42.3	159	32.3	288	56.3	9650
PD18-125-292	11.09	77	8.18	44.5	27.5	15.39	58.4	16.32	157.8	51.8	212.1	44.9	432.4	85.7	8940
PD18-125-293	55.5	461	49	279	164.8	92.8	281	75.9	608	166.6	591	111.1	965	157.5	11930
PD18-125-294	7.5	77	6.6	43.9	30.1	11.4	79.3	22.3	217	67.3	259	49.2	419	75.5	9330
PD18-125-296	57.1	417	62.7	348	239	103.4	374	99.5	827	209	749	147.9	1310	222.9	9710
PD18-125-297	396	2540	254	1403	773	442	1203	317	2481	561	1829	322	2700	378	11260
PD18-125-305	28.8	131	14.7	80	51.8	27.1	98	28.2	249	68.6	262	50.5	452	79.6	9710
PD18-125-306	29	264	26.9	149	102	47.3	192	52.2	437	116	406	75.6	646	111.2	9410

PD18-125-307	8.5	81	7.5	47	34	15	60	17.3	146	37.2	134	26.3	225	36.7	11470
PD18-125-308	0.65	16.2	0.91	6.59	6.1	2.02	24.9	8.35	99.3	37.5	162.8	33.8	305	58.8	11160
PD18-125-310	66	289	95	453	246	109.8	278	69.4	558	136.8	486	94.2	854	141	9080
PD18-125-311	92.6	897	75.7	416	280	122.5	518	141.3	1161	279	933	173	1422	220	9040
PD18-125-312	3.44	52.7	3.51	25.3	23	7.93	68	18.3	175	55.6	216	41.8	377	73	8910
PD18-125-313	19.5	118	17.8	101	66.3	33.5	123	33.5	299	86.6	343	69.9	655	126.1	8960
PD18-125-314	17.2	139.3	16.4	93.6	62.7	27.3	116.8	29.3	246	59.3	205.4	39.5	349	63.6	10030
PD18-125-315	0.04	24.6	0.267	3.63	7.72	4.39	42.7	11.46	115.4	38.9	164	31.7	281	53.6	8300
PD18-125-316	2	17	1.94	11.9	8.2	3.91	21.2	6.37	66	24.9	115.4	25.53	252.3	54.2	9070
PD18-125-317	21.4	157	22.9	130	93.9	66.2	354	140	1780	730	2720	422	2880	376	9520
PD18-125-318	24.8	185	23.7	135	94	44.2	161	43.2	353	84	282	50.1	423	63.6	11600
PD18-125-319	13.8	122.1	10.35	64.9	49.4	37.7	150.2	42.1	407	129.9	495	95.4	826	150.6	8450
PD18-125-327	29.6	191	30.6	172	105	43.3	160	42.4	354	89	326	61.6	554	94.1	11750
PD18-125-328	11.3	118	10.5	64.2	49.5	27.2	112	28.5	241	65	252	56.2	550	121.5	9420
PD18-125-329	53.4	452	48.9	275	184	74.6	323	87.9	740	177	603	107.4	889	132	10050
PD18-125-330	5	46.9	6	29.3	18.9	7.09	53.7	18.65	227.5	86.4	397	84.7	790	156	11990
PD18-125-331	5.26	82.2	5.17	29.5	20.5	14.7	45.2	13.69	134.3	44.7	196.1	43.8	429	85.9	9300
PD18-125-332	82.2	569	68.4	368	251	150.4	451	122.6	1023	247	820	145.4	1221	186.7	12020
PD18-125-333	43.6	525	54.4	291	199	92.2	300	83.8	661	159	554	102	868	141.1	9200
PD18-125-334	46.3	277	38.4	216	155	69.8	301	82	708	178	583	106.1	867	132.7	9870
PD18-125-335	0.137	13.48	0.296	3.2	4.61	2.79	21.7	6.56	68.9	23.85	97.5	18.9	171.2	34.5	7690
PD18-125-336	40.1	189.3	30.2	169.1	107.9	65.5	181	49.6	418	118.8	448	88.3	813	154.3	8960
PD18-125-337	8.57	66.4	7.56	47.8	37.6	16.3	77.3	21.1	193	55.3	198	38.2	325	61.1	11430
PD18-125-338	0.407	19.3	0.496	5.28	8.92	1.08	50.4	17.04	208.8	80.9	352	70.4	614	115	10470
PD18-125-339	40.7	368	38.6	234	156	78.1	277	69.2	608	164	577	102.9	861	142.3	9970
PD18-125-340	24.4	128.7	27.3	142	81.2	30.5	112	30.8	270	71.2	271	51.6	439	75.4	9360
PD18-125-342	4.33	22.7	5.33	25.5	13.61	6.66	20.8	6.06	60.3	19.86	92.6	20.81	213.9	45.9	10950
PD18-125-343	51.5	158.6	62.3	296	163	62.8	176	42.4	340	80.5	282	54.8	529	85.9	13090

Appendix 4.1 Kaladgi-Badami Basin detrital zircon U–Pb data

Comments	²⁰⁷ Pb/ ²³⁵ U	2σ	²⁰⁶ Pb/ ²³⁸ U	2σ	Error Correlation (ρ)	²⁰⁷ Pb/ ²³⁵ U Age (Ma)	Age Error 2σ	²⁰⁶ Pb/ ²³⁸ U Age (Ma)	Age Error 2σ	²⁰⁷ Pb/ ²⁰⁶ Pb Age (Ma)	Age 2σ	U/Th ratio	Th/U	Concordance
PD18-10-470	11.41	0.4	0.4905	0.011	0.647	2554	33	2571	49	2532	59	1.687	0.593	101.540
PD18-10-471	2.377	0.098	0.0774	0.0032	0.822	1235	33	481	19	2985	53	0.739	1.353	16.114
PD18-10-472	9.44	0.3	0.3405	0.0069	0.659	2380	30	1888	33	2833	53	0.318	3.145	66.643
PD18-10-473	11.36	0.35	0.4647	0.0096	0.470	2552	29	2459	42	2625	54	1.539	0.650	93.676
PD18-10-474	9.3	0.31	0.353	0.0075	0.617	2371	28	1948	36	2755	52	0.327	3.058	70.708
PD18-10-475	1.875	0.088	0.0648	0.0024	0.870	1071	29	404.4	15	2896	51	1.442	0.693	13.964
PD18-10-476	0.951	0.11	0.02322	0.0032	0.843	678	45	148	20	3448	52	0.1567	6.382	4.292
PD18-10-477	11.29	0.36	0.484	0.011	0.580	2545	30	2542	48	2551	57	3.271	0.306	99.647
PD18-10-478	4.263	0.14	0.1279	0.003	0.668	1685	28	775	17	3125	49	0.2357	4.243	24.800
PD18-10-479	9.92	0.31	0.4005	0.0074	0.799	2426	29	2171	34	2645	52	4.53	0.221	82.079
PD18-10-480	9.49	0.32	0.3979	0.0084	0.663	2388	32	2158	39	2572	55	0.526	1.901	83.904
PD18-10-481	1.664	0.071	0.0443	0.0018	0.929	994	30	279.4	11	3308	49	0.1566	6.386	8.446
PD18-10-482	9.9	0.31	0.385	0.0085	0.354	2424	29	2098	40	2706	56	0.919	1.088	77.531
PD18-10-483	5.973	0.18	0.1912	0.0037	0.683	1971	27	1127	20	3016	50	0.542	1.845	37.367
PD18-10-484	4.391	0.26	0.1177	0.0046	0.539	1709	42	717	26	3299	60	0.547	1.828	21.734
PD18-10-492	2.672	0.1	0.0844	0.0026	0.558	1319	29	522	16	3044	55	0.1522	6.570	17.148
PD18-10-493	7.8	0.26	0.2482	0.0065	0.706	2207	32	1429	34	3046	50	2.53	0.395	46.914
PD18-10-494	1.984	0.12	0.0551	0.0046	0.854	1109	38	345.5	27	3242	57	0.1532	6.527	10.657
PD18-10-495	3.149	0.1	0.0885	0.0019	0.731	1443	26	547	11	3228	51	2.42	0.413	16.945
PD18-10-496	4.579	0.15	0.1502	0.0033	0.810	1744	28	902	19	2988	48	0.122	8.197	30.187
PD18-10-497	6.18	0.35	0.2645	0.011	0.932	1991	43	1512	57	2562	52	3.228	0.310	59.016
PD18-10-498	1.619	0.071	0.04424	0.0018	0.583	977.2	25	279.1	11	3275	52	0.3927	2.546	8.522
PD18-10-499	6.28	0.23	0.1705	0.0053	0.910	2015	35	1014	29	3282	50	0.805	1.242	30.896
PD18-10-500	1.21	0.038	0.0359	0.00078	0.784	804.9	18	227.3	4.9	3154	49	2.235	0.447	7.207
PD18-10-501	5.92	0.23	0.1815	0.0047	0.680	1963	36	1075	26	3094	54	0.454	2.203	34.745
PD18-10-502	10.15	0.35	0.4272	0.012	0.708	2447	35	2301	54	2567	54	0.606	1.650	89.638
PD18-10-503	5.146	0.51	0.1782	0.0075	0.289	1843	62	1057	40	2909	72	0.702	1.425	36.336
PD18-10-504	2.381	0.082	0.0674	0.0014	0.343	1235	25	420.3	8.2	3220	55	0.1384	7.225	13.053
PD18-10-505	4.453	0.17	0.1622	0.0054	0.575	1720	34	969	31	2826	49	0.813	1.230	34.289
PD18-10-506	8.61	0.27	0.327	0.0068	0.780	2296	28	1823	33	2745	51	1.384	0.723	66.412
PD18-10-507	9.11	0.3	0.361	0.008	0.657	2348	33	1986	38	2675	53	0.466	2.146	74.243
PD18-10-508	5.63	0.28	0.2008	0.0097	0.778	1919	52	1179	54	2837	54	0.01105	90.498	41.558
PD18-10-516	12.23	0.39	0.4751	0.01	0.800	2621	31	2505	45	2712	52	0.832	1.202	92.367
PD18-10-517	7.11	0.23	0.2444	0.0057	0.508	2123	30	1409	30	2896	52	1.162	0.861	48.653
PD18-10-518	3.462	0.14	0.0872	0.0032	0.774	1518	35	539	19	3416	49	0.774	1.292	15.779
PD18-10-519	12.37	0.39	0.5047	0.01	0.803	2631	30	2641	43	2620	52	8.3	0.120	100.802
PD18-10-520	6.913	0.21	0.2318	0.0044	0.645	2099	27	1344	23	2949	52	0.361	2.770	45.575

PD18-10-521	1.439	0.051	0.03901	0.001	0.782	904.9	23	246.7	6.4	3300	52	2.508	0.399	7.476
PD18-10-522	1.175	0.1	0.03438	0.0035	0.530	788	39	217.9	22	3301	55	0.18	5.556	6.601
PD18-10-523	3.6	0.23	0.1103	0.0072	0.854	1548	67	674	43	3081	53	0.668	1.497	21.876
PD18-10-524	2.922	0.15	0.0797	0.0041	0.804	1387	51	494	25	3291	53	0.467	2.141	15.011
PD18-10-525	5.185	0.17	0.1833	0.0043	0.628	1849	28	1085	23	2870	53	0.1183	8.453	37.805
PD18-10-526	4.52	0.19	0.1686	0.0072	0.727	1732	38	1004	41	2783	56	0.2297	4.354	36.076
PD18-10-527	9.57	0.69	0.4024	0.031	0.774	2392	98	2179	160	2556	67	1.277	0.783	85.250
PD18-10-528	5.7	0.24	0.1929	0.0077	0.731	1934	39	1137	43	2943	53	0.2144	4.664	38.634
PD18-10-529	4.33	0.18	0.1476	0.0043	0.819	1701	32	887	24	2932	53	2.952	0.339	30.252
PD18-10-530	3.61	0.15	0.1024	0.0034	0.744	1549	36	629	20	3204	52	0.4311	2.320	19.632
PD18-10-531	9.98	0.36	0.3672	0.01	0.731	2431	32	2015	47	2796	52	1.549	0.646	72.067
PD18-10-532	2.346	0.095	0.0648	0.0021	0.900	1224	29	405	13	3265	50	0.679	1.473	12.404
PD18-10-540	5.097	0.16	0.1702	0.0028	0.563	1834	27	1013.2	15	2955	51	0.38	2.632	34.288
PD18-10-541	2.039	0.11	0.0619	0.003	0.905	1126	42	386.8	18	3105	51	0.0583	17.153	12.457
PD18-10-542	2.668	0.14	0.0782	0.0037	0.501	1319	35	485.2	22	3171	50	0.2665	3.752	15.301
PD18-10-543	2.258	0.12	0.0692	0.0034	0.767	1202	32	431.1	20	3117	51	1.918	0.521	13.831
PD18-10-544	2.577	0.14	0.0833	0.0037	0.705	1293	35	516	22	3141	51	7.084	0.141	16.428
PD18-10-545	5.85	0.34	0.2376	0.013	0.679	1953	72	1374	75	2780	52	0.874	1.144	49.424
PD18-10-546	6.91	0.26	0.216	0.0062	0.821	2097	32	1260	32	3058	50	1.378	0.726	41.203
PD18-10-547	8.43	0.27	0.3245	0.0067	0.777	2277	29	1811	33	2722	51	0.631	1.585	66.532
PD18-10-548	1.339	0.054	0.03961	0.0011	0.766	862	22	250.4	6.6	3156	51	0.729	1.372	7.934
PD18-10-549	4.836	0.16	0.1621	0.0041	0.449	1790	30	968	23	2939	52	0.607	1.647	32.936
PD18-10-550	3.419	0.12	0.1024	0.0027	0.916	1508	29	628	16	3132	49	0.76	1.316	20.051
PD18-10-551	8.274	0.25	0.2872	0.0056	0.617	2261	27	1627	28	2890	52	1.55	0.645	56.298
PD18-10-552	10.31	0.4	0.3663	0.011	0.735	2461	36	2010	53	2855	54	0.1813	5.516	70.403
PD18-10-553	3.846	0.13	0.1186	0.0031	0.844	1600	28	722	18	3084	53	0.1574	6.353	23.411
PD18-10-554	7.05	0.39	0.3329	0.014	0.836	2116	43	1852	64	2529	52	3.85	0.260	73.231
PD18-10-555	7.72	0.26	0.288	0.0086	0.751	2197	30	1630	43	2777	54	0.349	2.865	58.696
PD18-10-556	1.142	0.043	0.03374	0.00093	0.594	773.1	19	213.9	5.8	3151	53	1.403	0.713	6.788
PD18-10-565	1.828	0.076	0.051	0.0022	0.631	1055	29	320.6	13	3233	51	0.2638	3.791	9.916
PD18-10-566	1.498	0.058	0.0495	0.0018	0.679	929	22	311.6	11	3112	53	0.4178	2.393	10.013
PD18-10-567	4.18	0.36	0.1517	0.015	0.797	1668	57	910	79	2807	56	0.471	2.123	32.419
PD18-10-568	1.288	0.059	0.03537	0.0018	0.817	839	25	224.1	11	3255	52	0.3841	2.603	6.885
PD18-10-569	6.33	0.19	0.1776	0.0036	0.634	2022	28	1054	20	3224	50	1.641	0.609	32.692
PD18-10-570	7.12	0.23	0.2577	0.0067	0.719	2125	30	1478	35	2834	51	0.656	1.524	52.152
PD18-10-571	2.977	0.098	0.097	0.0025	0.589	1401	26	596.6	15	2989	53	0.134	7.463	19.960
PD18-10-572	11.24	0.33	0.4869	0.0084	0.657	2542	28	2557	37	2533	52	1.385	0.722	100.947
PD18-10-573	7.353	0.23	0.2459	0.0054	0.566	2154	27	1417	28	2956	53	0.867	1.153	47.936
PD18-10-574	10.89	0.34	0.4505	0.0092	0.496	2512	29	2396	41	2606	57	0.913	1.095	91.942
PD18-10-575	18.64	1.7	0.569	0.029	0.970	3019	61	2900	110	3101	55	2.177	0.459	93.518
PD18-10-576	7.81	0.42	0.2461	0.0084	0.828	2208	45	1418	43	3049	61	1.195	0.837	46.507
PD18-10-577	9.14	0.51	0.31	0.018	0.847	2349	67	1738	96	2926	57	0.867	1.153	59.398

PD18-10-578	11.26	0.34	0.4881	0.008	0.549	2544	28	2562	35	2532	50	1.726	0.579	101.185
PD18-10-579	4.45	0.22	0.1328	0.0064	0.774	1721	53	804	38	3126	50	0.613	1.631	25.720
PD18-10-580	6.75	0.29	0.227	0.0081	0.839	2077	39	1318	42	2946	48	0.961	1.041	44.739
PD18-10-581	3.798	0.16	0.1209	0.0047	0.709	1591	37	736	28	3054	51	0.2238	4.468	24.100
PD18-10-589	8.76	0.27	0.2995	0.0065	0.640	2313	28	1688	32	2923	51	0.833	1.200	57.749
PD18-10-590	2.794	0.089	0.0851	0.0019	0.891	1353	25	526	12	3093	49	0.2561	3.905	17.006
PD18-10-591	8.35	0.32	0.3032	0.01	0.700	2268	39	1707	53	2826	51	0.684	1.462	60.403
PD18-10-592	6.39	0.25	0.1815	0.0065	0.703	2030	35	1075	36	3216	51	1.308	0.765	33.427
PD18-10-593	10.62	0.49	0.4583	0.023	0.423	2490	54	2431	110	2521	63	1.363	0.734	96.430
PD18-10-594	8.16	0.25	0.254	0.0051	0.616	2248	28	1458	26	3074	51	0.603	1.658	47.430
PD18-10-595	7.39	0.29	0.2618	0.011	0.760	2159	34	1498	56	2854	57	0.1448	6.906	52.488
PD18-10-597	7.94	0.27	0.2634	0.0064	0.861	2223	33	1507	33	2957	50	1.221	0.819	50.964
PD18-10-598	3.829	0.13	0.1214	0.0027	0.901	1597	28	738	16	3043	50	3.228	0.310	24.252
PD18-10-599	9.34	0.31	0.3713	0.0098	0.623	2370	32	2034	47	2663	55	0.557	1.795	76.380
PD18-10-600	4.67	0.16	0.1541	0.0045	0.929	1760	31	924	26	2971	52	0.932	1.073	31.101
PD18-10-601	10.95	0.5	0.455	0.018	0.315	2515	52	2414	86	2582	58	0.748	1.337	93.493
PD18-10-602	1.883	0.18	0.0559	0.0048	0.788	1074	50	350.4	29	3135	51	0.4813	2.078	11.177
PD18-10-603	8.93	0.33	0.35	0.0095	0.857	2328	35	1933	46	2690	52	0.522	1.916	71.859
PD18-05-611	6.16	0.22	0.2891	0.0079	0.74701	1996	33	1636	40	2540	54	1.03	0.971	64.40945
PD18-05-612	2.478	0.28	0.1154	0.012	0.8494	1270	63	703	65	2553	58	0.2007	4.983	27.53623
PD18-05-613	4.724	0.18	0.2099	0.006	0.72645	1770	34	1228	32	2474	53	0.735	1.361	49.63622
PD18-05-614	4.977	0.17	0.2291	0.0049	0.61669	1816	30	1329	26	2429	56	1.283	0.779	54.71387
PD18-05-615	8.73	0.31	0.3719	0.0091	0.79373	2308	35	2038	44	2541	53	1.064	0.940	80.20464
PD18-05-616	5.86	0.2	0.2609	0.0063	0.70173	1954	31	1494	32	2488	55	0.876	1.142	60.04823
PD18-05-617	11.83	0.39	0.5076	0.011	0.58836	2589	31	2645	46	2539	57	1.3	0.769	104.1749
PD18-05-618	5.53	0.29	0.2528	0.0091	0.71293	1903	41	1452	46	2576	56	0.476	2.101	56.36646
PD18-05-619	6.66	0.25	0.3189	0.0084	0.9089	2063	33	1783	41	2506	53	0.779	1.284	71.14924
PD18-05-620	11.58	0.37	0.4797	0.0099	0.24605	2569	31	2524	44	2592	58	0.6007	1.665	97.37654
PD18-05-621	1.376	0.058	0.0699	0.0025	0.76448	878	27	435.2	15	2277	55	1.081	0.925	19.11287
PD18-05-622	6.36	0.5	0.2722	0.019	0.87725	2026	89	1551	100	2562	57	0.811	1.233	60.53864
PD18-05-623	10.55	0.33	0.4451	0.0083	0.46333	2482	30	2372	37	2568	54	1.109	0.902	92.3676
PD18-05-624	5.9	0.33	0.2609	0.012	0.6923	1960	42	1494	57	2497	56	0.431	2.320	59.8318
PD18-05-625	9.33	0.3	0.3905	0.0089	0.54399	2369	30	2124	42	2591	54	0.849	1.178	81.97607
PD18-05-626	5.24	0.27	0.2263	0.01	0.53609	1856	52	1315	54	2510	59	0.338	2.959	52.39044
PD18-05-634	7.23	0.29	0.3224	0.0097	0.78982	2137	35	1800	47	2619	55	1.193	0.838	68.72852
PD18-05-635	8.9	0.48	0.3785	0.018	0.79227	2325	65	2068	90	2546	54	1.078	0.928	81.22545
PD18-05-636	7.33	0.23	0.3186	0.0065	0.5302	2152	30	1782	32	2503	55	0.974	1.027	71.19457
PD18-05-637	0.706	0.039	0.0364	0.0017	0.91875	541	23	230	10	2253	59	0.857	1.167	10.20861
PD18-05-638	1.15	0.077	0.0541	0.0037	0.8943	776	33	339.3	22	2396	57	0.1398	7.153	14.1611
PD18-05-639	11.78	0.43	0.5024	0.011	0.37235	2583	33	2622	47	2540	64	0.895	1.117	103.2283
PD18-05-640	9.41	0.3	0.4023	0.0073	0.60159	2377	29	2179	34	2548	54	0.787	1.271	85.51805

PD18-05-641	3.269	0.14	0.1515	0.0048	0.56103	1473	33	909	26	2418	55	0.492	2.033	37.59305
PD18-05-642	1.144	0.075	0.0565	0.0036	0.77758	773	44	354	23	2441	59	0.4159	2.404	14.50225
PD18-05-643	10.38	0.44	0.4379	0.015	0.40264	2466	45	2340	69	2561	57	1.3	0.769	91.37056
PD18-05-644	10.54	0.42	0.458	0.015	0.65903	2481	42	2430	69	2535	53	0.724	1.381	95.85799
PD18-05-645	10.33	0.34	0.4404	0.009	0.44711	2462	30	2351	40	2553	56	0.692	1.445	92.08774
PD18-05-646	6.62	0.27	0.2909	0.0082	0.88092	2057	39	1644	39	2498	56	3.87	0.258	65.81265
PD18-05-647	8.71	0.3	0.3413	0.0086	0.61479	2307	34	1892	42	2692	53	1.5	0.667	70.28232
PD18-05-648	12.18	0.38	0.5024	0.0092	0.57553	2617	29	2623	39	2608	56	1.82	0.549	100.5752
PD18-05-649	11.19	0.4	0.4814	0.012	0.29594	2536	33	2531	50	2544	68	0.732	1.366	99.48899
PD18-05-657	11.45	0.39	0.4719	0.01	0.39267	2558	31	2490	44	2604	59	4.1	0.244	95.62212
PD18-05-658	4.369	0.23	0.2165	0.0092	0.69498	1708	38	1263	47	2447	54	0.837	1.195	51.61422
PD18-05-659	4.64	0.19	0.2094	0.0058	0.92031	1754	32	1225	31	2449	54	0.3413	2.930	50.02042
PD18-05-660	2.75	0.27	0.1185	0.01	0.66021	1336	59	721	56	2545	64	0.78	1.282	28.33006
PD18-05-661	9.67	0.44	0.403	0.014	0.56314	2403	50	2182	69	2581	55	1.04	0.962	84.54088
PD18-05-662	6.61	0.21	0.2895	0.0054	0.5571	2059	29	1644	27	2493	54	0.366	2.732	65.94465
PD18-05-663	6.24	0.3	0.2494	0.0062	0.23139	2009	37	1435	31	2654	65	1.53	0.654	54.06933
PD18-05-664	6.77	0.3	0.241	0.0081	0.69539	2080	36	1392	41	2847	53	1.472	0.679	48.89357
PD18-05-665	7.87	0.38	0.3392	0.013	0.59488	2218	39	1881	60	2681	54	0.536	1.866	70.16039
PD18-05-666	5.82	0.28	0.2429	0.0095	0.45217	1948	50	1401	51	2598	55	1.572	0.636	53.9261
PD18-05-667	2.458	0.083	0.1127	0.0024	0.76102	1258	25	688	14	2422	54	1.018	0.982	28.40628
PD18-05-668	3.75	0.14	0.1698	0.0049	0.34526	1579	29	1010	27	2455	60	0.7	1.429	41.14053
PD18-05-669	9.37	0.32	0.4046	0.0092	0.70462	2372	31	2189	42	2532	55	0.837	1.195	86.4534
PD18-05-670	10.11	0.33	0.4156	0.0083	0.42174	2442	30	2239	38	2613	57	0.668	1.497	85.68695
PD18-05-671	10.07	0.37	0.4252	0.009	0.30849	2437	35	2283	40	2558	66	0.627	1.595	89.24941
PD18-05-672	4.953	0.21	0.2223	0.0072	0.68188	1810	41	1294	39	2475	54	1.517	0.659	52.28283
PD18-05-680	12.6	0.39	0.4547	0.0086	0.64667	2649	29	2415	38	2829	52	1.017	0.983	85.36585
PD18-05-681	1.245	0.047	0.0596	0.002	0.90236	820	22	373.3	12	2368	55	0.721	1.387	15.76436
PD18-05-682	13.68	0.46	0.516	0.011	0.42211	2725	32	2681	45	2754	54	1.519	0.658	97.34931
PD18-05-683	12.07	0.62	0.501	0.025	0.17043	2608	58	2614	110	2590	60	1.2	0.833	100.9266
PD18-05-684	1.499	0.053	0.0736	0.0018	0.84974	928	21	457.8	11	2311	55	0.922	1.085	19.80961
PD18-05-685	5.6	0.25	0.2475	0.0093	0.56692	1915	44	1425	50	2483	56	0.737	1.357	57.39025
PD18-05-686	11.95	0.42	0.483	0.01	0.69948	2598	33	2539	44	2640	60	1.506	0.664	96.17424
PD18-05-687	10.43	0.33	0.4471	0.0085	0.75938	2472	29	2381	38	2543	53	1.06	0.943	93.62957
PD18-05-688	10.49	0.33	0.4515	0.0079	0.51107	2483	31	2401	35	2542	55	1.207	0.829	94.45319
PD18-05-689	7.96	0.44	0.388	0.015	0.7243	2226	42	2113	67	2471	56	2.737	0.365	85.51194
PD18-05-690	5.54	0.26	0.2267	0.0079	0.93097	1903	37	1317	41	2609	52	0.906	1.104	50.47911
PD18-05-691	10.66	0.34	0.4683	0.009	0.60663	2492	30	2475	39	2507	53	1.014	0.986	98.72357
PD18-05-692	5.271	0.19	0.2411	0.0057	0.39218	1863	31	1392	29	2434	54	1.765	0.567	57.18981
PD18-05-693	3.98	0.21	0.1761	0.0077	0.82225	1632	38	1045	42	2494	54	0.548	1.825	41.90056
PD18-05-694	7.51	0.47	0.312	0.016	0.30365	2169	70	1748	81	2570	63	0.3644	2.744	68.01556
PD18-05-695	4.89	0.19	0.2144	0.0067	0.72596	1798	37	1252	36	2506	55	0.788	1.269	49.9601
PD18-05-703	9.44	0.33	0.4067	0.0099	0.49306	2384	33	2199	46	2534	56	0.758	1.319	86.77979

PD18-05-704	2.204	0.23	0.1168	0.0088	0.89816	1180	56	712	49	2331	57	0.983	1.017	30.54483
PD18-05-705	11.83	0.4	0.5064	0.01	0.56279	2588	31	2640	43	2546	56	1.675	0.597	103.6921
PD18-05-706	12.26	0.49	0.4832	0.017	0.53306	2623	43	2540	80	2674	55	3.52	0.284	94.98878
PD18-05-707	10.14	0.37	0.429	0.013	0.69632	2446	37	2299	59	2585	54	1.168	0.856	88.93617
PD18-05-708	11.11	0.37	0.474	0.01	0.54619	2530	31	2499	45	2552	55	0.977	1.024	97.9232
PD18-05-709	10.85	0.5	0.471	0.014	0.39212	2511	47	2487	61	2533	68	0.861	1.161	98.18397
PD18-05-710	9.51	0.31	0.4048	0.0083	0.80736	2388	29	2190	38	2550	57	0.419	2.387	85.88235
PD18-05-711	8.18	0.32	0.3455	0.01	0.70369	2250	40	1912	52	2558	54	1.006	0.994	74.7459
PD18-05-712	10.92	0.36	0.4645	0.011	0.61122	2514	31	2457	49	2559	56	0.871	1.148	96.01407
PD18-05-713	9.93	0.4	0.4701	0.016	0.6554	2427	42	2483	71	2520	54	1.056	0.947	98.53175
PD18-05-714	11.1	0.35	0.4738	0.0091	0.48419	2530	29	2499	40	2553	56	1.461	0.684	97.88484
PD18-05-715	9.94	0.38	0.4185	0.011	0.66668	2427	38	2252	52	2565	57	0.738	1.355	87.79727
PD18-05-716	7.96	0.25	0.3497	0.0069	0.49559	2225	30	1933	33	2499	54	1.559	0.641	77.35094
PD18-05-717	10.12	0.46	0.419	0.017	0.49075	2443	50	2254	78	2582	58	0.53	1.887	87.29667
PD18-05-718	5.72	0.43	0.2515	0.017	0.93056	1928	90	1445	94	2486	57	0.665	1.504	58.1255
PD18-05-726	8.7	1	0.396	0.03	0.84296	2301	140	2150	150	2580	91	0.732	1.366	83.33333
PD18-05-727	5.52	0.29	0.2689	0.012	0.73514	1901	47	1535	60	2487	56	0.817	1.224	61.72095
PD18-05-728	10.73	0.36	0.4753	0.0099	0.41596	2498	32	2505	41	2634	57	2.001	0.500	95.10251
PD18-05-729	10.51	0.36	0.4536	0.01	0.38423	2478	32	2410	45	2531	62	1.02	0.980	95.21928
PD18-05-730	2.132	0.15	0.098	0.0061	0.84606	1162	41	603	35	2424	53	1.142	0.876	24.87624
PD18-05-731	1.151	0.045	0.0551	0.0014	0.56176	777	21	345.5	8.6	2350	57	0.598	1.672	14.70213
PD18-05-732	10.8	0.37	0.4688	0.0096	0.31369	2503	32	2477	42	2529	57	2.188	0.457	97.94385
PD18-05-733	10.48	0.35	0.4463	0.0089	0.45167	2476	32	2378	42	2546	54	1.219	0.820	93.40141
PD18-05-734	12.07	0.42	0.44	0.011	0.78916	2608	35	2350	50	2795	56	0.937	1.067	84.07871
PD18-05-735	12.15	0.45	0.5125	0.012	0.17641	2618	34	2666	50	2563	64	1.212	0.825	104.0187
PD18-05-736	6.77	0.54	0.297	0.023	0.87108	2076	100	1673	120	2516	55	0.515	1.942	66.49444
PD18-05-737	2.836	0.31	0.1307	0.013	0.78378	1363	61	798	69	2420	55	0.442	2.262	32.97521
PD18-05-738	7.73	0.37	0.3339	0.012	0.65503	2199	38	1856	57	2522	54	0.782	1.279	73.59239
PD18-05-739	0.519	0.027	0.02777	0.0012	0.67927	424.4	17	176.5	7.4	2161	58	0.2917	3.428	8.167515
PD18-05-740	9.78	0.34	0.4174	0.0097	0.77687	2412	32	2247	44	2552	52	0.847	1.181	88.04859
PD18-05-741	9.42	0.37	0.397	0.013	0.73956	2378	41	2155	60	2560	54	1.025	0.976	84.17969
PD18-05-749	11.88	0.41	0.4974	0.01	0.10663	2593	33	2601	45	2578	60	1.178	0.849	100.8922
PD18-05-750	2.248	0.51	0.103	0.021	0.77061	1194	94	632	110	2419	59	1.399	0.715	26.1265
PD18-05-751	4.113	0.18	0.1985	0.0067	0.62126	1655	40	1167	37	2484	55	0.526	1.901	46.98068
PD18-05-752	7.77	0.28	0.3334	0.0088	0.71885	2203	32	1854	42	2532	52	1.312	0.762	73.22275
PD18-05-753	9.99	0.36	0.4221	0.012	0.4767	2432	37	2269	54	2568	53	0.537	1.862	88.3567
PD18-05-754	9.89	0.31	0.4238	0.0083	0.48992	2423	28	2276	37	2543	55	0.912	1.096	89.50059
PD18-05-755	4.63	0.26	0.1975	0.0096	0.6248	1752	40	1162	50	2534	55	0.253	3.953	45.85635
PD18-05-756	6.878	0.21	0.2977	0.0055	0.47813	2095	27	1679	27	2526	53	0.4889	2.045	66.46873
PD18-05-757	10.5	0.51	0.46	0.018	0.54613	2485	54	2437	85	2533	63	1.483	0.674	96.21003
PD18-05-758	10.87	0.35	0.4546	0.0088	0.55612	2511	30	2415	39	2587	55	0.487	2.053	93.35137
PD18-05-759	1.882	0.15	0.0873	0.0059	0.84353	1072	43	539	34	2407	55	0.444	2.252	22.39302

PD18-05-760	11.97	0.45	0.4892	0.01	0.30101	2597	35	2566	44	2618	64	1.804	0.554	98.01375
PD18-05-761	8.98	0.3	0.3886	0.0087	0.61133	2334	30	2120	41	2524	56	0.492	2.033	83.99366
PD18-05-762	2.661	0.13	0.1211	0.005	0.78785	1317	40	737	29	2431	53	0.2641	3.786	30.31674
PD18-05-763	12.89	0.44	0.482	0.011	0.73966	2669	32	2533	48	2782	54	1.497	0.668	91.0496
PD18-05-764	7.52	0.25	0.3606	0.0074	0.63025	2174	29	1984	35	2503	56	0.512	1.953	79.26488
KL18-8-772	6.46	0.22	0.2696	0.0062	0.77955	2038	29	1538	31	2590	53	1.665	0.601	59.38224
KL18-8-773	7.34	0.25	0.2991	0.0074	0.70751	2153	34	1686	37	2628	54	0.4721	2.118	64.15525
KL18-8-774	10.08	0.4	0.4101	0.011	0.59997	2439	39	2214	53	2613	52	1.179	0.848	84.7302
KL18-8-775	2.68	0.12	0.1162	0.0047	0.60289	1321	36	709	27	2663	56	0.586	1.706	26.62411
KL18-8-776	9.66	0.37	0.402	0.0092	0.18547	2397	35	2177	42	2602	66	1.493	0.670	83.66641
KL18-8-777	8.79	6.9	0.3447	0.087	0.67516	2314	220	1909	320	2688	160	1.121	0.892	71.01935
KL18-8-778	6.65	0.28	0.2853	0.0084	0.75062	2059	37	1616	42	2547	60	1.216	0.822	63.44719
KL18-8-779	7.76	0.37	0.3288	0.014	0.45239	2202	54	1832	73	2577	56	0.762	1.312	71.09042
KL18-8-780	6.52	0.25	0.2731	0.0082	0.85518	2044	34	1554	41	2584	55	1.38	0.725	60.13932
KL18-8-781	3.232	0.16	0.1341	0.0061	0.70496	1462	44	811	35	2601	55	1.129	0.886	31.18032
KL18-8-782	7.43	0.24	0.3161	0.0074	0.5127	2163	28	1770	36	2558	56	1.279	0.782	69.19468
KL18-8-783	5.43	0.17	0.2328	0.0051	0.7577	1888	28	1348	27	2546	53	0.979	1.021	52.9458
KL18-8-784	18.29	0.84	0.58	0.017	0.66821	3000	48	2944	70	3027	75	0.713	1.403	97.25801
KL18-8-785	7.61	1.1	0.321	0.02	0.75845	2184	95	1794	95	2558	88	1.056	0.947	70.13292
KL18-8-786	5.38	0.18	0.221	0.0051	0.80459	1880	30	1286	27	2626	54	1.626	0.615	48.97182
KL18-8-787	10.33	0.4	0.444	0.015	0.6358	2461	40	2368	68	2525	58	1.303	0.767	93.78218
KL18-8-795	6.99	0.29	0.2871	0.01	0.52502	2108	43	1626	53	2600	60	1.255	0.797	62.53846
KL18-8-796	10.37	0.33	0.4335	0.0082	0.5683	2469	30	2320	37	2590	57	0.803	1.245	89.57529
KL18-8-797	10.85	0.35	0.4484	0.0094	0.57302	2511	31	2387	41	2604	52	1.437	0.696	91.66667
KL18-8-798	5.69	0.23	0.2451	0.0091	0.88054	1924	35	1410	47	2681	56	1.097	0.912	52.59232
KL18-8-799	7.76	0.27	0.32	0.0086	0.76659	2201	31	1788	42	2611	55	1.033	0.968	68.47951
KL18-8-800	4.95	0.72	0.1986	0.022	0.73598	1809	94	1167	110	2645	71	1.215	0.823	44.12098
KL18-8-801	10.06	0.61	0.399	0.023	0.67792	2439	77	2163	110	2662	56	3.79	0.264	81.2547
KL18-8-802	3.47	0.13	0.1429	0.0041	0.87944	1518	30	861	23	2602	53	2.539	0.394	33.08993
KL18-8-803	7.84	4.1	0.317	0.058	0.69638	2207	170	1772	230	2627	130	1.009	0.991	67.45337
KL18-8-804	8.17	2	0.334	0.027	0.6775	2248	130	1854	120	2616	120	1.05	0.952	70.87156
KL18-8-805	6.12	0.29	0.2636	0.01	0.52233	1990	47	1507	54	2520	59	1.168	0.856	59.80159
KL18-8-806	8.77	0.31	0.3574	0.0096	0.71262	2312	34	1968	46	2622	54	1.653	0.605	75.05721
KL18-8-807	9.87	0.41	0.406	0.017	0.68779	2420	44	2197	83	2598	56	1.982	0.505	84.56505
KL18-8-808	8.32	0.27	0.3936	0.0075	0.51465	2265	29	2139	35	2513	55	0.7705	1.298	85.11739
KL18-8-809	5.43	4.7	0.226	0.038	0.3735	1889	180	1313	170	2587	170	1.07	0.935	50.75377
KL18-8-810	11.69	0.37	0.4926	0.01	0.355	2581	31	2580	43	2578	57	6.33	0.158	100.0776
KL18-8-818	11.74	0.42	0.492	0.012	0.54166	2580	34	2575	51	2582	61	25.2	0.040	99.72889
KL18-8-819	5.36	0.19	0.2273	0.006	0.70533	1878	32	1320	32	2580	52	0.998	1.002	51.16279
KL18-8-820	10.32	0.67	0.4341	0.027	0.65128	2467	88	2323	130	2565	55	1.231	0.812	90.5653
KL18-8-821	8.31	0.41	0.339	0.014	0.8261	2261	53	1882	72	2611	55	1.233	0.811	72.07966

KL18-8-822	7.005	0.22	0.2804	0.0057	0.45438	2111	28	1593	29	2654	54	1.341	0.746	60.02261
KL18-8-823	7.25	0.33	0.3006	0.012	0.58578	2141	48	1693	60	2586	56	1.328	0.753	65.4679
KL18-8-824	3.81	0.27	0.1569	0.0053	0.82992	1592	52	939	30	2613	82	1.159	0.863	35.93571
KL18-8-825	12.24	0.4	0.5039	0.0094	0.4956	2620	31	2629	40	2610	56	1.191	0.840	100.728
KL18-8-826	7.06	0.24	0.3012	0.0071	0.80611	2121	34	1696	36	2552	54	2.068	0.484	66.45768
KL18-8-827	4.19	0.18	0.1751	0.0066	0.90101	1668	35	1039	36	2588	53	0.941	1.063	40.14683
KL18-8-828	2.79	8.2	0.111	0.091	0.88653	1334	310	678	360	2690	190	0.813	1.230	25.20446
KL18-8-829	6.93	0.24	0.294	0.0073	0.74534	2100	30	1660	36	2558	54	1.337	0.748	64.89445
KL18-8-830	6.66	0.24	0.2874	0.0086	0.69185	2070	36	1627	43	2552	56	1.419	0.705	63.75392
KL18-8-831	11.32	0.42	0.4845	0.011	0.23087	2546	35	2545	48	2547	63	0.81	1.235	99.92148
KL18-8-832	6.49	0.39	0.254	0.015	0.74943	2042	75	1459	83	2682	57	1.304	0.767	54.3997
KL18-8-833	4.64	0.34	0.1931	0.014	0.54098	1755	49	1138	72	2610	56	1.52	0.658	43.60153
KL18-8-841	7.14	0.33	0.296	0.011	0.60961	2126	47	1670	57	2588	54	0.405	2.469	64.52859
KL18-8-842	9.6	0.34	0.4076	0.01	0.71286	2395	34	2203	47	2550	55	0.997	1.003	86.39216
KL18-8-843	8.56	0.27	0.3668	0.0073	0.60765	2290	29	2014	34	2547	54	1.003	0.997	79.07342
KL18-8-844	6.82	0.33	0.2868	0.013	0.67407	2087	53	1625	66	2561	56	1.028	0.973	63.45178
KL18-8-845	9.69	0.31	0.4064	0.0079	0.78865	2404	30	2197	36	2587	56	1.475	0.678	84.92462
KL18-8-846	5.03	0.22	0.2021	0.006	0.37446	1821	36	1185	32	2640	78	1.435	0.697	44.88636
KL18-8-847	9.26	0.31	0.3904	0.0079	0.59929	2365	32	2123	37	2561	54	0.816	1.225	82.89731
KL18-8-848	6.25	0.28	0.2619	0.01	0.58594	2010	47	1499	54	2571	55	1.448	0.691	58.30416
KL18-8-849	7.63	0.35	0.327	0.013	0.58905	2187	39	1823	61	2532	54	1.182	0.846	71.99842
KL18-8-850	10.19	0.32	0.4314	0.0077	0.55738	2450	29	2311	35	2568	55	0.8718	1.147	89.99221
KL18-8-851	8.18	0.33	0.3373	0.011	0.73551	2249	40	1873	55	2599	52	1.242	0.805	72.06618
KL18-8-852	1.769	0.072	0.0664	0.0027	0.68394	1034	30	414.2	17	2763	57	1.432	0.698	14.99095
KL18-8-853	17.05	1.4	0.3901	0.019	0.69042	2936	61	2122	85	3539	57	1.407	0.711	59.96044
KL18-8-854	7.105	0.22	0.3131	0.0061	0.57134	2123	29	1756	30	2502	54	4.76	0.210	70.18385
KL18-8-855	8.56	0.27	0.3496	0.007	0.70347	2291	29	1932	33	2623	55	1.287	0.777	73.65612
KL18-8-856	6.56	0.21	0.2742	0.006	0.56931	2053	28	1561	31	2577	55	0.164	6.098	60.57431
KL18-8-857	6.92	0.25	0.292	0.008	0.7329	2097	32	1650	40	2562	58	0.746	1.340	64.40281
KL18-8-858	5.73	0.25	0.2382	0.0083	0.74815	1929	39	1376	44	2607	63	0.719	1.391	52.78097
KL18-8-866	7.17	0.23	0.305	0.006	0.49863	2132	28	1715	30	2558	55	0.87	1.149	67.04457
KL18-8-867	3.06	0.12	0.1222	0.0043	0.84607	1420	34	743	25	2659	54	2.378	0.421	27.94284
KL18-8-868	1.036	0.038	0.02539	0.0012	0.71326	722	20	161.6	7.8	3457	68	0.763	1.311	4.674573
KL18-8-869	1.369	0.069	0.0348	0.0021	0.80984	875	34	220.2	13	3377	72	6.42	0.156	6.52058
KL18-8-870	9.02	0.42	0.367	0.015	0.64358	2334	57	2013	77	2615	54	2.67	0.375	76.97897
KL18-8-871	7.189	0.23	0.2994	0.0069	0.57067	2134	30	1688	35	2594	54	1.28	0.781	65.07325
KL18-8-872	9.58	0.51	0.4036	0.0085	0.72102	2393	43	2185	40	2572	84	0.81	1.235	84.95334
KL18-8-873	8.52	0.45	0.367	0.02	0.75884	2285	72	2014	110	2527	57	1.93	0.518	79.69925
KL18-8-874	2.009	0.19	0.0768	0.0075	0.7246	1117	50	477	44	2722	54	3.117	0.321	17.52388
KL18-8-875	8.33	0.28	0.342	0.0086	0.40178	2265	31	1896	42	2628	56	1.479	0.676	72.14612
KL18-8-876	8.69	0.32	0.3639	0.0097	0.66633	2303	35	1999	46	2576	58	0.2724	3.671	77.60093
KL18-8-877	6.61	0.23	0.2761	0.0061	0.48701	2058	29	1571	31	2590	59	0.664	1.506	60.65637

KL18-8-878	7.97	0.44	0.3391	0.017	0.28494	2224	64	1881	89	2539	57	0.436	2.294	74.08429
KL18-8-879	11.26	0.36	0.4831	0.0089	0.5236	2543	30	2540	39	2540	57	0.903	1.107	100
KL18-8-880	6.27	0.24	0.2494	0.0092	0.30581	2014	39	1435	49	2655	55	2.146	0.466	54.04896
KL18-8-881	7.94	0.34	0.3422	0.0073	0.12356	2227	38	1896	35	2562	74	0.84	1.190	74.00468
KL18-8-882	7.47	0.28	0.3	0.0069	0.73428	2164	34	1690	34	2655	60	0.722	1.385	63.65348
KL18-8-890	11.13	0.36	0.4636	0.0095	0.59569	2532	30	2454	42	2597	56	1.571	0.637	94.49365
KL18-8-891	5.26	0.19	0.1996	0.0071	0.76307	1861	34	1173	39	2738	57	1.267	0.789	42.84149
KL18-8-892	11.41	0.41	0.4645	0.011	0.27106	2553	33	2457	47	2618	62	2.411	0.415	93.85027
KL18-8-893	11.35	0.36	0.4911	0.0098	0.41259	2551	29	2574	42	2528	57	1.683	0.594	101.8196
KL18-8-894	4.47	0.18	0.2045	0.0075	0.70307	1722	33	1199	40	2573	56	1.281	0.781	46.5993
KL18-8-895	8.12	0.33	0.3417	0.011	0.52184	2243	37	1894	57	2569	55	0.426	2.347	73.72518
KL18-8-896	4.67	6.6	0.217	0.1	0.94268	1753	250	1264	390	2544	160	1.429	0.700	49.68553
KL18-8-897	8.56	0.33	0.37	0.011	0.76683	2289	36	2025	50	2527	58	0.916	1.092	80.13455
KL18-8-898	6.56	0.23	0.2889	0.0071	0.82791	2055	30	1641	36	2498	53	0.758	1.319	65.69255
KL18-8-899	6.12	0.25	0.2731	0.01	0.52431	1992	42	1556	54	2511	53	1.164	0.859	61.96734
KL18-8-900	9.96	0.36	0.419	0.011	0.46139	2429	36	2255	51	2583	57	2.2	0.455	87.30159
KL18-8-901	12.07	0.41	0.492	0.012	0.63822	2608	35	2578	54	2615	52	2.1	0.476	98.58509
KL18-8-902	10.05	0.34	0.43	0.0086	0.63488	2436	31	2304	39	2542	59	1.183	0.845	90.63729
KL18-8-903	2.869	0.14	0.1304	0.006	0.59856	1373	39	790	34	2588	55	1.205	0.830	30.5255
KL18-8-904	2.59	0.19	0.0981	0.0037	0.49053	1297	56	603	22	2744	94	1.389	0.720	21.97522
KL18-8-905	9.39	0.33	0.402	0.0096	0.53088	2374	32	2176	44	2553	61	0.971	1.030	85.23306
PD18-12-921	5.84	0.2	0.1417	0.0043	0.58681	1951	29	854	24	3469	49	0.418	2.392	24.61805
PD18-12-922	8.04	0.28	0.3477	0.012	0.5348	2234	37	1923	62	2537	29	1.126	0.888	75.79819
PD18-12-923	11.86	1.3	0.476	0.013	0.40957	2584	76	2509	54	2630	100	0.757	1.321	95.39924
PD18-12-924	12.69	0.25	0.504	0.0082	0.33494	2655	19	2630	35	2680	32	1.134	0.882	98.13433
PD18-12-925	10.59	0.28	0.4454	0.01	0.54969	2485	24	2374	46	2576	30	0.76	1.316	92.15839
PD18-12-926	9.67	0.2	0.4068	0.0073	0.48852	2402	19	2205	33	2568	35	0.7062	1.416	85.86449
PD18-12-928	5.29	0.23	0.2144	0.0097	0.82618	1864	35	1252	51	2644	30	0.669	1.495	47.3525
PD18-12-929	7.96	0.17	0.3251	0.0066	0.5622	2224	19	1813	32	2626	32	0.853	1.172	69.04037
PD18-12-930	12.35	0.37	0.5017	0.011	0.70606	2625	28	2619	45	2626	45	1.218	0.821	99.73343
PD18-12-931	3.698	0.099	0.1424	0.0037	0.78118	1574	22	858	21	2730	25	0.771	1.297	31.42857
PD18-12-932	5.35	0.32	0.209	0.013	0.65588	1873	43	1223	66	2708	32	1.084	0.923	45.16248
PD18-12-933	5.51	0.25	0.2062	0.0087	0.85525	1900	36	1208	46	2758	29	0.472	2.119	43.79985
PD18-12-934	10.87	0.32	0.4695	0.011	0.41256	2507	28	2479	47	2528	45	1.163	0.860	98.06171
PD18-12-935	5.08	0.2	0.1975	0.0079	0.55766	1831	39	1161	44	2714	30	0.366	2.732	42.77819
PD18-12-936	6.37	0.2	0.2144	0.0067	0.72313	2027	30	1252	36	2951	26	0.615	1.626	42.4263
PD18-12-944	6.7	0.37	0.266	0.015	0.65554	2069	65	1517	81	2667	28	0.608	1.645	56.88039
PD18-12-945	10.54	0.27	0.4149	0.0096	0.76235	2479	24	2235	44	2688	36	0.525	1.905	83.14732
PD18-12-946	4.3	0.12	0.1691	0.005	0.65904	1689	24	1011	28	2691	39	0.569	1.757	37.56968
PD18-12-947	2.034	0.17	0.0641	0.0055	0.79838	1126	47	400.4	33	3044	23	0.321	3.115	13.15375
PD18-12-948	3.806	0.065	0.1378	0.0023	0.64956	1593	14	832	13	2832	28	0.728	1.374	29.37853

PD18-12-949	0.644	0.017	0.01683	0.00043	0.71314	504	10	107.6	2.7	3342	32	0.2078	4.812	3.219629
PD18-12-950	1.858	0.14	0.0654	0.0058	0.88202	1064	43	408	34	2869	26	0.2331	4.290	14.22098
PD18-12-951	7.3	0.17	0.2847	0.007	0.77719	2146	21	1613	35	2701	25	0.941	1.063	59.71862
PD18-12-952	11.61	0.48	0.3083	0.013	0.81806	2572	36	1731	64	3321	25	0.856	1.168	52.12285
PD18-12-953	9.16	0.29	0.379	0.011	0.52131	2348	31	2067	51	2599	40	0.509	1.965	79.53059
PD18-12-954	3.02	0.12	0.1007	0.0041	0.78755	1411	34	618	24	2966	25	0.332	3.012	20.83614
PD18-12-955	2.918	0.082	0.1047	0.0032	0.87622	1386	20	642	18	2847	25	0.3376	2.962	22.55005
PD18-12-956	2.061	0.1	0.0696	0.0038	0.73458	1134	37	434	23	2942	31	0.2104	4.753	14.75187
PD18-12-957	5.14	0.15	0.2028	0.0065	0.63706	1842	29	1190	36	2674	26	0.71	1.408	44.50262
PD18-12-958	10.24	0.53	0.439	0.013	0.47273	2453	41	2344	59	2524	64	0.6	1.667	92.86846
PD18-12-959	6.72	0.27	0.2815	0.012	0.7721	2073	43	1598	61	2577	28	1.956	0.511	62.01009
PD18-12-960	7.2	0.3	0.296	0.013	0.73903	2132	44	1668	65	2609	34	1.293	0.773	63.93254
PD18-12-968	6.56	0.18	0.2565	0.007	0.58238	2051	26	1471	36	2709	28	0.611	1.637	54.30048
PD18-12-969	4.18	0.14	0.162	0.006	0.77204	1668	31	968	34	2714	30	1.094	0.914	35.66691
PD18-12-970	10.38	0.22	0.4493	0.0086	0.57203	2467	19	2391	38	2527	31	1.127	0.887	94.61812
PD18-12-971	10.51	0.27	0.4286	0.0088	0.58865	2478	26	2298	40	2627	35	0.591	1.692	87.47621
PD18-12-972	10.88	0.23	0.4558	0.009	0.44718	2514	19	2419	40	2590	36	0.732	1.366	93.39768
PD18-12-973	4.259	0.12	0.1574	0.0045	0.68284	1684	22	942	25	2794	26	0.741	1.350	33.7151
PD18-12-974	3.4	0.22	0.11	0.0074	0.86148	1503	52	673	43	3009	24	0.432	2.315	22.36623
PD18-12-975	5.862	0.16	0.22	0.0058	0.43794	1955	21	1282	30	2778	24	0.564	1.773	46.14831
PD18-12-976	5.8	1.3	0.1663	0.037	0.84231	1945	110	991	180	3206	25	1.131	0.884	30.91079
PD18-12-977	5.448	0.1	0.2249	0.0039	0.62535	1891	16	1307	20	2616	25	1.275	0.784	49.96177
PD18-12-978	10.55	0.19	0.4506	0.008	0.66689	2483	17	2397	36	2555	31	0.898	1.114	93.81605
PD18-12-979	11.64	0.53	0.461	0.02	0.48852	2572	52	2443	95	2669	35	1.148	0.871	91.53241
PD18-12-980	7.12	1.9	0.27	0.027	0.92085	2113	120	1536	130	2741	99	0.776	1.289	56.03794
PD18-12-981	9	0.26	0.3649	0.0086	0.6584	2332	28	2003	41	2634	43	0.397	2.519	76.04404
PD18-12-982	10.9	0.45	0.428	0.018	0.87357	2511	46	2294	88	2685	25	1.1	0.909	85.43762
PD18-12-983	11.64	0.25	0.4886	0.01	0.7106	2573	20	2562	45	2581	31	1.047	0.955	99.26385
PD18-12-984	9.4	0.19	0.3992	0.0084	0.61002	2376	19	2164	39	2558	30	0.7333	1.364	84.59734
PD18-12-992	3.2	0.16	0.1248	0.0064	0.9085	1454	46	758	38	2711	26	0.596	1.678	27.96016
PD18-12-993	3.788	0.15	0.2455	0.0096	0.81458	1588	37	1415	51	1816	25	1.85	0.541	77.9185
PD18-12-994	0.836	0.068	0.02279	0.0028	0.84934	616	32	145.2	18	3271	45	0.2446	4.088	4.439009
PD18-12-995	6.13	0.36	0.2321	0.014	0.71455	1993	70	1344	77	2748	26	1.157	0.864	48.9083
PD18-12-996	26.11	0.5	0.681	0.012	0.5662	3348	19	3351	46	3350	28	2.881	0.347	100.0299
PD18-12-997	9	0.2	0.2554	0.005	0.77742	2337	21	1466	26	3222	24	0.829	1.206	45.49969
PD18-12-998	3.593	0.16	0.1305	0.0062	0.93135	1546	37	790	35	2822	24	0.4136	2.418	27.99433
PD18-12-999	6.63	0.15	0.2731	0.0057	0.71362	2064	20	1555	29	2616	29	0.595	1.681	59.4419
PD18-12-1000	8.31	0.17	0.3234	0.0062	0.62603	2264	19	1806	31	2712	26	0.674	1.484	66.59292
PD18-12-1001	10.62	0.31	0.4655	0.0098	0.29746	2485	27	2462	43	2502	50	0.76	1.316	98.40128
PD18-12-1002	2.83	0.37	0.068	0.0071	0.62163	1363	70	423.9	41	3483	34	0.2306	4.337	12.17054
PD18-12-1003	10.87	0.31	0.44	0.011	0.75804	2512	25	2346	51	2647	34	0.86	1.163	88.62864
PD18-12-1004	0.529	0.021	0.01111	0.00069	0.61715	431	13	71.2	4.4	3679	39	0.2504	3.994	1.935309

PD18-12-1005	7.31	0.15	0.2995	0.0055	0.57466	2148	18	1688	27	2621	31	0.859	1.164	64.4029
PD18-12-1006	4.73	0.12	0.1925	0.0048	0.63049	1771	21	1134	26	2642	28	0.864	1.157	42.92203
PD18-12-1007	7.13	0.19	0.2049	0.0059	0.75952	2126	24	1201	31	3198	25	0.3247	3.080	37.55472
PD18-12-1008	8.82	0.22	0.357	0.0097	0.71142	2317	24	1967	47	2646	28	1.069	0.935	74.33862
PD18-12-1016	5.67	0.16	0.2321	0.0073	0.85711	1924	30	1345	39	2617	28	0.705	1.418	51.39473
PD18-12-1017	11.72	0.57	0.478	0.012	0.80359	2578	41	2515	51	2618	47	2.176	0.460	96.0657
PD18-12-1018	2.664	0.16	0.0826	0.0055	0.72903	1317	57	511	33	3081	40	0.2203	4.539	16.58552
PD18-12-1019	0.4336	0.043	0.00766	0.0015	0.61876	365.5	27	49.2	9.6	3947	72	0.2282	4.382	1.246516
PD18-12-1020	6.7	0.24	0.241	0.0086	0.9164	2064	32	1389	44	2836	29	0.68	1.471	48.97743
PD18-12-1021	0.47	0.016	0.00949	0.0004	0.52564	391	11	60.9	2.6	3747	34	0.3265	3.063	1.6253
PD18-12-1022	7.73	0.44	0.33	0.02	0.66434	2199	71	1837	100	2551	32	0.718	1.393	72.01098
PD18-12-1023	6.84	0.29	0.2909	0.013	0.57979	2089	33	1645	64	2575	40	1.039	0.962	63.8835
PD18-12-1024	1.045	0.11	0.0355	0.0041	0.82827	726	44	225.1	25	2916	30	0.61	1.639	7.719479
PD18-12-1025	4.84	0.18	0.1902	0.0076	0.93108	1789	31	1121	41	2695	24	0.572	1.748	41.59555
PD18-12-1026	11.16	0.31	0.477	0.012	0.43179	2532	26	2511	52	2548	47	0.769	1.300	98.54788
PD18-12-1027	4.437	0.24	0.1368	0.007	0.56425	1718	40	827	39	3075	26	0.3106	3.220	26.89431
PD18-12-1028	3.68	0.11	0.1324	0.0043	0.76379	1566	26	801	25	2830	27	0.614	1.629	28.30389
PD18-12-1029	6.46	0.14	0.2682	0.0067	0.53186	2039	18	1531	33	2601	28	0.768	1.302	58.86198
PD18-12-1030	1.133	0.23	0.03492	0.0099	0.6339	769	75	221.3	59	3086	42	0.21	4.762	7.171095
PD18-12-1031	11.22	0.33	0.443	0.012	0.46926	2538	29	2360	56	2688	39	1.071	0.934	87.79762
PD18-12-1032	16.71	0.34	0.5379	0.0095	0.67517	2919	21	2773	40	3014	26	0.556	1.799	92.00398
PD18-12-1040	4.24	0.12	0.1604	0.0045	0.78908	1680	24	959	25	2753	25	0.481	2.079	34.83473
PD18-12-1041	2.158	0.1	0.1245	0.007	0.86213	1165	38	756	41	2039	42	1.381	0.724	37.077
PD18-12-1042	1.204	0.072	0.03441	0.0026	0.84498	802	29	218	16	3198	31	0.2296	4.355	6.81676
PD18-12-1043	8.9	0.22	0.3841	0.009	0.5621	2329	22	2094	41	2538	31	0.574	1.742	82.50591
PD18-12-1044	16.03	0.38	0.533	0.012	0.4967	2875	22	2752	50	2954	39	0.646	1.548	93.16181
PD18-12-1045	0.518	0.029	0.01274	0.0013	0.78095	426	18	81.6	8.2	3444	55	0.392	2.551	2.369338
PD18-12-1046	5.736	0.11	0.2365	0.0044	0.7554	1935	17	1368	23	2616	27	0.911	1.098	52.29358
PD18-12-1047	6.68	0.13	0.2721	0.0043	0.68877	2069	18	1551	24	2620	26	0.714	1.401	59.19847
PD18-12-1048	10.65	0.2	0.4686	0.0093	0.27266	2492	18	2477	43	2498	31	1.935	0.517	99.15933
PD18-12-1049	6.49	0.15	0.2634	0.0068	0.58637	2042	23	1506	35	2632	34	0.608	1.645	57.21884
PD18-12-1050	4.59	0.61	0.115	0.0063	0.13087	1747	73	701	36	3425	81	0.2163	4.623	20.46715
PD18-12-1051	8.25	0.16	0.3409	0.0059	0.71129	2257	18	1890	29	2605	27	0.72	1.389	72.55278
PD18-12-1052	5.553	0.11	0.22	0.0045	0.70069	1907	18	1282	24	2674	26	0.867	1.153	47.94316
PD18-12-1053	5.21	0.17	0.1972	0.0071	0.86056	1852	31	1160	37	2753	26	0.449	2.227	42.13585
PD18-12-1054	4.92	0.16	0.1833	0.0051	0.73873	1804	30	1084	28	2769	25	0.659	1.517	39.14771
PD18-12-1055	1.121	0.047	0.0373	0.0018	0.86371	768	23	235.8	11	2961	37	0.287	3.484	7.963526
PD18-12-1063	7.58	0.34	0.3055	0.015	0.75183	2179	48	1717	76	2641	33	1.463	0.684	65.01325
PD18-12-1064	9.74	0.43	0.425	0.02	0.62924	2408	49	2282	96	2520	37	0.545	1.835	90.55556
PD18-12-1065	4.955	0.17	0.1989	0.0067	0.44	1811	26	1169	35	2657	29	0.486	2.058	43.99699
PD18-12-1066	4.85	0.1	0.3162	0.007	0.77624	1792	18	1770	35	1811	25	2.76	0.362	97.73606
PD18-12-1067	8.52	0.32	0.2493	0.0049	0.53772	2286	40	1434	26	3169	57	0.3189	3.136	45.25087

PD18-12-1068	3.787	0.15	0.1446	0.0062	0.81826	1589	36	870	36	2743	27	0.3269	3.059	31.7171
PD18-12-1069	11.28	0.48	0.33	0.013	0.58522	2545	58	1838	67	3150	27	1.082	0.924	58.34921
PD18-12-1070	11.3	0.56	0.45	0.011	0.43191	2542	40	2395	47	2663	56	1.09	0.917	89.93616
PD18-12-1071	4.09	0.27	0.1587	0.011	0.76942	1659	64	949	65	2698	34	0.482	2.075	35.1742
PD18-13-1072	3.49	0.13	0.1224	0.0048	0.78682	1523	29	744	27	2877	27	0.414	2.415	25.86027
PD18-13-1073	7.12	0.23	0.2289	0.0074	0.8493	2125	33	1328	40	3021	24	0.578	1.730	43.95895
PD18-13-1074	6.86	0.25	0.2594	0.012	0.62548	2091	34	1486	61	2744	34	0.378	2.646	54.15452
PD18-13-1075	8.33	0.54	0.33	0.024	0.86314	2265	82	1836	120	2670	41	0.492	2.033	68.76404
PD18-13-1076	3.887	0.34	0.1421	0.012	0.67031	1610	54	857	64	2792	27	0.5905	1.693	30.69484
PD18-13-1077	3.89	0.1	0.1342	0.0031	0.61974	1609	22	811	18	2890	29	0.404	2.475	28.06228
PD18-13-1078	0.595	0.015	0.01032	0.00053	0.48527	473.6	9	66.2	3.4	3975	43	0.5057	1.977	1.665409
PD18-13-1079	0.924	0.031	0.02032	0.00099	0.55265	664.3	15	129.7	6.2	3617	32	0.3001	3.332	3.585845
PD18-13-1087	5.81	0.17	0.2222	0.0071	0.78113	1947	28	1293	38	2730	27	0.58	1.724	47.36264
PD18-13-1088	2.654	0.089	0.0863	0.0037	0.79737	1315	22	534	22	3003	26	0.2793	3.580	17.78222
PD18-13-1089	2.824	0.11	0.0961	0.0044	0.7767	1361	35	592	26	2905	30	0.2961	3.377	20.37866
PD18-13-1090	9.64	0.23	0.2673	0.006	0.81884	2402	22	1526	30	3256	25	1.185	0.844	46.86732
PD18-13-1091	1.854	0.17	0.0598	0.0068	0.86429	1063	50	374	40	3011	37	0.376	2.660	12.42112
PD18-13-1092	17.93	0.85	0.5121	0.018	0.7634	2985	35	2664	71	3200	23	3.88	0.258	83.25
PD18-13-1093	6.29	0.25	0.2413	0.0099	0.70372	2012	38	1392	53	2722	30	1.23	0.813	51.13887
PD18-13-1094	5.7	0.25	0.1895	0.0093	0.77892	1928	44	1118	52	2955	37	1.005	0.995	37.83418
PD18-13-1095	6.18	0.53	0.1924	0.015	0.73479	1999	59	1134	76	3049	24	0.46	2.174	37.19252
PD18-13-1096	9.06	0.37	0.3453	0.01	0.60835	2340	41	1911	49	2739	46	0.983	1.017	69.76999
PD18-13-1097	6.27	0.3	0.1903	0.0093	0.79632	2012	57	1122	53	3108	40	0.505	1.980	36.10039
PD18-13-1098	5.07	0.19	0.1744	0.0069	0.44179	1830	32	1036	38	2909	37	0.579	1.727	35.61361
PD18-13-1099	7.11	0.16	0.2858	0.0061	0.72194	2123	22	1620	31	2655	27	0.477	2.096	61.01695
PD18-13-1100	7.6	0.4	0.321	0.019	0.77194	2183	67	1795	98	2575	34	1.029	0.972	69.70874
PD18-13-1101	2.335	0.11	0.0824	0.0035	0.90366	1222	27	510	21	2876	25	0.44	2.273	17.73296
PD18-13-1102	6.99	0.32	0.2789	0.015	0.69412	2107	45	1584	75	2648	39	0.529	1.890	59.81873
PD18-13-1103	5.54	0.32	0.2184	0.013	0.82315	1905	66	1273	75	2680	29	0.973	1.028	47.5
PD18-13-1111	3.29	0.26	0.1117	0.0099	0.83008	1485	92	682	60	2953	100	0.3402	2.939	23.09516
PD18-13-1112	6.66	0.28	0.2803	0.013	0.70023	2063	45	1591	66	2569	36	0.632	1.582	61.93071
PD18-13-1113	5.361	0.12	0.212	0.0049	0.59638	1877	19	1239	27	2677	26	0.74	1.351	46.28315
PD18-13-1114	7.84	0.23	0.2286	0.0068	0.81905	2211	28	1327	36	3163	24	0.549	1.821	41.95384
PD18-13-1115	2.619	0.36	0.0672	0.011	0.65828	1305	71	419	62	3376	30	0.263	3.802	12.41114
PD18-13-1116	7.65	0.31	0.2635	0.011	0.86584	2188	45	1507	60	2907	27	1.1	0.909	51.84039
PD18-13-1117	0.648	0.021	0.0115	0.00066	0.40784	507.3	13	73.7	4.2	3942	46	0.3427	2.918	1.869609
PD18-13-1118	6.37	0.13	0.248	0.0046	0.7582	2026	17	1428	24	2703	25	0.577	1.733	52.83019
PD18-13-1119	4.65	0.21	0.1808	0.0094	0.74851	1756	32	1071	49	2710	28	1.089	0.918	39.5203
PD18-13-1120	8.5	0.26	0.2624	0.0081	0.82516	2284	30	1501	42	3077	25	1.429	0.700	48.78128
PD18-13-1121	7.54	0.31	0.2386	0.0094	0.71222	2176	45	1379	51	3046	31	0.622	1.608	45.27249
PD18-13-1122	5.42	0.23	0.2096	0.0095	0.74143	1888	40	1226	52	2723	28	0.789	1.267	45.02387

PD18-13-1123	1.284	0.24	0.0359	0.0087	0.69194	837	69	227	52	3265	44	0.1991	5.023	6.952527
PD18-13-1124	22.24	0.46	0.603	0.013	0.82066	3198	20	3039	51	3293	24	1.995	0.501	92.28667
PD18-13-1125	4.16	0.2	0.1606	0.0079	0.56052	1661	35	959	43	2721	40	0.53	1.887	35.2444
PD18-13-1126	5.18	0.15	0.2142	0.0068	0.57273	1846	26	1251	37	2604	34	0.4171	2.398	48.04147
PD18-13-1127	6.23	0.15	0.2486	0.0055	0.73284	2006	22	1431	28	2665	30	1.029	0.972	53.69606
PD18-13-1135	9.15	0.27	0.2663	0.0069	0.69664	2351	31	1522	36	3179	25	1.251	0.799	47.87669
PD18-13-1136	4.083	0.073	0.1531	0.0027	0.77353	1650	15	918	15	2775	23	0.62	1.613	33.08108
PD18-13-1137	7.48	0.35	0.24	0.013	0.76165	2166	55	1383	70	2995	88	0.764	1.309	46.17696
PD18-13-1138	4.789	0.11	0.1888	0.0045	0.68283	1781	19	1114	24	2688	29	0.558	1.792	41.44345
PD18-13-1139	16.77	0.69	0.4458	0.016	0.67265	2920	44	2376	73	3321	28	1.016	0.984	71.54472
PD18-13-1140	4.756	0.13	0.1887	0.0055	0.73977	1776	26	1114	30	2675	27	0.882	1.134	41.64486
PD18-13-1141	7.11	0.41	0.275	0.012	0.48482	2122	55	1563	59	2707	93	0.546	1.832	57.73919
PD18-13-1142	0.996	0.087	0.0229	0.003	0.66283	700	39	145.8	19	3545	48	0.2596	3.852	4.112835
PD18-13-1143	6.08	0.15	0.2319	0.0057	0.73854	1986	25	1344	30	2724	27	0.597	1.675	49.33921
PD18-13-1144	6.02	0.23	0.2374	0.009	0.78024	1975	38	1372	48	2674	31	0.812	1.232	51.3089
PD18-13-1145	11.87	0.3	0.456	0.01	0.38566	2591	25	2420	47	2728	38	1.728	0.579	88.70968
PD18-13-1146	6.8	0.14	0.272	0.0053	0.64794	2084	18	1550	27	2662	28	0.595	1.681	58.2269
PD18-13-1147	6.09	0.2	0.2378	0.0075	0.52862	1986	33	1375	40	2689	33	0.872	1.147	51.13425
PD18-13-1148	2.473	0.13	0.0848	0.005	0.84444	1263	37	525	30	2915	23	0.3407	2.935	18.01029
PD18-13-1149	9.22	0.18	0.3088	0.0052	0.33103	2359	19	1734	26	2950	29	0.83	1.205	58.77966
PD18-13-1150	9.41	0.31	0.389	0.013	0.83762	2375	33	2115	62	2596	30	0.619	1.616	81.47149
PD18-13-1151	0.45	0.018	0.00735	0.00058	0.74996	377.1	12	47.2	3.7	4090	55	0.406	2.463	1.154034
PD18-13-1152	5.49	0.28	0.2186	0.011	0.75187	1899	54	1274	61	2664	40	0.39	2.564	47.82282
PD18-13-1153	7.47	0.22	0.3113	0.0091	0.86826	2172	28	1745	45	2591	26	0.798	1.253	67.34851
PD18-13-1161	2.576	0.096	0.0856	0.0038	0.76369	1293	26	529.6	22	2965	26	0.3619	2.763	17.86172
PD18-13-1162	7.19	0.34	0.288	0.015	0.78583	2142	55	1629	78	2648	33	2.58	0.388	61.51813
PD18-13-1163	3.752	0.19	0.1422	0.008	0.75568	1580	51	857	47	2755	32	0.499	2.004	31.10708
PD18-13-1164	2.636	0.15	0.0854	0.0057	0.70537	1308	36	528	33	2971	27	0.593	1.686	17.77179
PD18-13-1165	4.108	0.091	0.1527	0.0031	0.61088	1655	18	916	17	2782	26	0.3054	3.274	32.92595
PD18-13-1166	5.687	0.2	0.2275	0.0083	0.56599	1928	34	1321	45	2659	28	1.077	0.929	49.68033
PD18-13-1167	5.8	0.13	0.2222	0.0057	0.44374	1945	20	1293	30	2734	25	0.633	1.580	47.29334
PD18-13-1168	4.91	0.095	0.1762	0.0026	0.66755	1802	16	1046	14	2831	27	0.579	1.727	36.94807
PD18-13-1169	4.176	0.34	0.1434	0.012	0.64699	1668	50	864	64	2913	26	0.44	2.273	29.66014
PD18-13-1170	2.765	0.21	0.0792	0.0039	0.77261	1345	46	491	23	3183	42	0.3267	3.061	15.4257
PD18-13-1172	8.53	0.28	0.269	0.0088	0.76571	2287	28	1533	44	3057	23	1.67	0.599	50.1472
PD18-13-1173	2.488	0.25	0.0692	0.0081	0.85609	1273	66	431	47	3261	35	0.3293	3.037	13.2168
PD18-13-1174	3.681	0.087	0.1333	0.0027	0.458	1569	19	806	15	2821	27	1.086	0.921	28.57143
PD18-13-1175	3.141	0.19	0.1053	0.006	0.87268	1441	41	645	34	2952	24	0.4452	2.246	21.84959
PD18-13-1176	0.646	0.028	0.01117	0.00088	0.71812	506	16	71.6	5.6	4002	55	0.2713	3.686	1.789105
PD18-13-1177	3.98	0.24	0.141	0.0094	0.5809	1629	67	850	56	2862	44	0.357	2.801	29.69951
PD18-13-1185	4.316	0.098	0.1894	0.0045	0.66354	1695	21	1118	25	2514	30	0.462	2.165	44.47096
PD18-13-1186	5.29	0.18	0.1961	0.0073	0.85799	1864	31	1153	40	2777	27	1.701	0.588	41.51963

PD18-13-1187	1.426	0.14	0.05826	0.0057	0.56675	899.5	46	365	33	2623	25	1.136	0.880	13.91536
PD18-13-1188	4.127	0.21	0.1506	0.0086	0.26361	1659	53	904	50	2815	34	0.475	2.105	32.11368
PD18-13-1189	6.67	0.2	0.2724	0.008	0.69965	2066	29	1552	42	2624	30	0.747	1.339	59.14634
PD18-13-1190	1.115	0.024	0.02294	0.00068	0.53961	760.1	12	146.2	4.3	3716	42	0.2421	4.131	3.934338
PD18-13-1191	8.33	0.25	0.3191	0.0084	0.72421	2264	29	1784	42	2724	29	0.851	1.175	65.49192
PD18-13-1192	7.05	0.74	0.2368	0.024	0.78088	2115	68	1369	110	2949	29	0.596	1.678	46.42252
PD18-13-1193	11.11	0.25	0.4798	0.0089	0.3259	2529	21	2525	39	2522	40	1.426	0.701	100.119
PD18-13-1194	9.17	0.52	0.385	0.024	0.71196	2353	72	2096	120	2587	34	1.215	0.823	81.02049
PD18-13-1195	8.43	0.28	0.3437	0.01	0.64718	2275	33	1903	51	2622	35	0.396	2.525	72.57818
PD18-13-1196	6.719	0.11	0.2706	0.0047	0.54168	2074	15	1543	24	2648	28	0.806	1.241	58.27039
PD18-13-1197	5.3	0.16	0.2153	0.0072	0.82074	1870	24	1256	38	2639	29	0.831	1.203	47.59379
PD18-14-1198	17.34	0.63	0.478	0.016	0.73252	2952	38	2518	71	3263	24	66.4	0.015	77.16825
PD18-14-1199	9.24	0.21	0.3781	0.0084	0.61758	2364	21	2066	39	2621	32	0.739	1.353	78.82488
PD18-14-1200	10.86	0.49	0.36	0.012	0.68347	2510	45	1981	61	2959	63	0.851	1.175	66.94829
PD18-14-1201	1.004	0.16	0.0244	0.0072	0.75026	704	60	155.6	46	3461	75	0.1622	6.165	4.49581
PD18-14-1209	14.31	0.5	0.5905	0.018	0.72534	2770	40	2990	79	2612	26	1.195	0.837	114.4717
PD18-14-1210	3.013	0.41	0.1144	0.019	0.33255	1410	83	698	100	2737	41	0.3107	3.219	25.50237
PD18-14-1211	9.52	0.27	0.274	0.0065	0.74376	2386	24	1560	33	3182	26	0.534	1.873	49.02577
PD18-14-1212	8.49	0.33	0.2291	0.008	0.91858	2282	43	1329	43	3284	24	0.566	1.767	40.46894
PD18-14-1213	7.51	0.45	0.329	0.02	0.83873	2173	67	1833	100	2516	29	1.231	0.812	72.85374
PD18-14-1214	4.768	0.092	0.1945	0.003	0.78303	1778	16	1145	16	2621	28	1.61	0.621	43.68562
PD18-14-1215	4.68	0.16	0.1885	0.0061	0.76508	1763	31	1113	34	2643	26	0.672	1.488	42.11124
PD18-14-1216	10.82	0.24	0.4668	0.0083	0.48934	2508	19	2468	37	2536	33	1.167	0.857	97.31861
PD18-14-1217	1.267	0.1	0.03511	0.0035	0.75843	829	46	222.4	22	3266	47	0.1778	5.624	6.809553
PD18-14-1218	2.607	0.24	0.0924	0.0095	0.42937	1302	51	569	54	2862	35	0.3163	3.162	19.8812
PD18-14-1219	7.36	0.25	0.2376	0.0076	0.44581	2155	34	1374	41	3013	25	0.691	1.447	45.60239
PD18-14-1220	4.82	0.11	0.1942	0.0048	0.58923	1788	19	1144	26	2650	24	0.499	2.004	43.16981
PD18-14-1221	2.859	0.12	0.1118	0.0051	0.76403	1369	28	683	29	2699	29	1.182	0.846	25.30567
PD18-14-1222	8.01	0.27	0.3313	0.012	0.72295	2231	36	1844	61	2608	28	1.001	0.999	70.70552
PD18-14-1223	11.23	0.23	0.4736	0.0079	0.69525	2540	19	2498	35	2566	35	1.133	0.883	97.34996
PD18-14-1224	0.682	0.094	0.0151	0.0039	0.84654	527	44	96.6	24	3602	66	0.2185	4.577	2.681843
PD18-14-1225	6.3	0.36	0.2647	0.016	0.84879	2016	66	1512	87	2578	31	1.367	0.732	58.65012
PD18-14-1233	1.436	0.059	0.0423	0.0021	0.62371	907	22	267.1	13	3158	30	0.204	4.902	8.457885
PD18-14-1234	4.78	0.087	0.178	0.0032	0.76601	1780	15	1056	18	2776	27	0.747	1.339	38.04035
PD18-14-1235	8.75	0.42	0.2732	0.011	0.54862	2311	39	1557	52	3065	27	0.798	1.253	50.79935
PD18-14-1236	11.37	0.23	0.4675	0.0073	0.22018	2552	19	2472	32	2608	35	1.179	0.848	94.78528
PD18-14-1237	13.85	0.57	0.4024	0.014	0.63814	2743	50	2179	70	3181	30	1.071	0.934	68.50047
PD18-14-1238	12.73	0.29	0.5116	0.0078	0.25521	2657	21	2662	33	2644	39	1.107	0.903	100.6808
PD18-14-1239	1.437	0.2	0.0445	0.0074	0.81652	903	60	280.7	44	3079	33	0.283	3.534	9.116596
PD18-14-1240	5.26	0.18	0.1897	0.0069	0.82143	1860	34	1119	38	2828	26	0.364	2.747	39.5686
PD18-14-1241	2.643	0.098	0.0936	0.0043	0.62978	1311	25	576	25	2864	29	1.006	0.994	20.11173

PD18-14-1242	9.18	0.34	0.2393	0.0088	0.82717	2377	30	1382	44	3378	24	0.441	2.268	40.91178
PD18-14-1243	11.16	0.36	0.391	0.013	0.80859	2535	35	2126	61	2867	24	0.876	1.142	74.15417
PD18-14-1244	1.542	0.12	0.0512	0.0042	0.90467	946	39	322	25	2968	32	0.2545	3.929	10.84906
PD18-14-1245	7.04	0.39	0.2337	0.0081	0.18535	2116	47	1354	43	2960	45	1.93	0.518	45.74324
PD18-14-1246	5.09	0.25	0.1602	0.0094	0.83787	1833	45	958	53	3051	28	0.39	2.564	31.39954
PD18-14-1247	8.47	0.34	0.3668	0.011	0.59852	2279	32	2013	52	2527	31	1.272	0.786	79.65968
PD18-14-1248	6.15	0.63	0.0674	0.005	0.33775	1995	130	421	30	4649	110	0.2263	4.419	9.055711
PD18-14-1249	6.29	0.18	0.2605	0.0063	0.67976	2012	25	1491	32	2595	35	0.862	1.160	57.45665
PD18-14-1257	3.628	0.072	0.1499	0.0028	0.82354	1555	16	900	16	2602	23	4.96	0.202	34.58878
PD18-14-1258	4.6	0.21	0.187	0.0091	0.83817	1747	46	1104	51	2636	28	0.394	2.538	41.88164
PD18-14-1259	3.79	0.51	0.1435	0.022	0.70686	1588	72	872	110	2717	32	1.514	0.661	32.09422
PD18-14-1260	3.681	0.11	0.1361	0.0041	0.64268	1565	27	822	23	2789	29	1.303	0.767	29.47293
PD18-14-1261	15.76	0.3	0.4748	0.008	0.60455	2861	18	2504	35	3115	25	1.047	0.955	80.38523
PD18-14-1262	3.237	0.17	0.1233	0.0068	0.26453	1465	34	750	38	2742	28	0.652	1.534	27.3523
PD18-14-1263	1.312	0.26	0.02247	0.013	0.58254	850	96	143.2	75	3974	120	0.1293	7.734	3.603422
PD18-14-1264	5.649	0.16	0.2221	0.0056	0.72458	1923	25	1293	30	2689	25	0.782	1.279	48.08479
PD18-14-1265	1.304	0.12	0.03096	0.0018	0.60432	845	44	196.5	11	3499	51	0.2051	4.876	5.61589
PD18-14-1266	10.28	0.2	0.3306	0.0062	0.47993	2459	19	1841	30	3018	23	1.513	0.661	61.00066
PD18-14-1267	3.37	0.11	0.1292	0.0044	0.85002	1495	27	783	25	2722	31	0.312	3.205	28.76561
PD18-14-1268	5.96	0.23	0.1728	0.0067	0.86298	1969	29	1027	35	3167	24	0.392	2.551	32.42817
PD18-14-1269	9.66	0.27	0.3859	0.011	0.63089	2400	27	2102	51	2663	31	3.39	0.295	78.93353
PD18-14-1270	0.5794	0.011	0.00817	0.00016	0.47801	463.7	7.1	52.46	1	4267	28	0.2634	3.797	1.229435
PD18-14-1271	9.1	0.54	0.375	0.023	0.7411	2344	79	2049	120	2601	34	0.679	1.473	78.77739
PD18-14-1272	9.07	0.26	0.387	0.017	0.63882	2342	27	2108	84	2557	94	0.53	1.887	82.44036
PD18-14-1273	11.83	0.27	0.4839	0.0089	0.49016	2588	22	2543	39	2616	37	0.978	1.022	97.20948
PD18-14-1281	4.36	0.15	0.172	0.0056	0.58357	1703	27	1023	31	2683	28	0.752	1.330	38.12896
PD18-14-1282	7.14	0.49	0.28	0.02	0.73766	2126	100	1590	110	2696	37	0.501	1.996	58.97626
PD18-14-1283	1.921	0.085	0.0719	0.0037	0.64075	1087	26	447	22	2762	31	1.669	0.599	16.18392
PD18-14-1284	5.54	0.53	0.2257	0.022	0.80983	1904	62	1311	110	2624	37	0.737	1.357	49.96189
PD18-14-1285	3.219	0.19	0.098	0.0056	0.86272	1460	44	602	33	3108	24	0.3731	2.680	19.36937

Appendix 4.2 Kaladgi-Badami Basin detrital zircon REE (ppm)

Comments	La	Ce	Pr	Nd	Sm	Eu	Gd	Tb	Dy	Ho	Er	Tm	Yb	Lu	Hf
PD18-10-470	0.0073	11.48	0.069	1.52	3.59	0.222	22.15	6.96	81.2	28.25	126.7	23.87	224.7	41.2	10170
PD18-10-471	69.2	1467	125.3	1062	1339	552	4220	1022	9130	2156	6930	1038	7980	1163	13360
PD18-10-472	17.99	199.8	22.03	149.4	148.3	54.2	382	86.8	691	158.1	544	92.5	781	129.1	11700
PD18-10-473	0.46	19.2	0.687	8.49	12.54	4.46	43.1	11.3	116.5	35.5	150	27.7	253.9	48.9	9370

PD18-10-474	13.08	168.5	15.44	115.3	123.7	42.8	288	61.5	469	111.8	394	68	603	106.6	10880
PD18-10-475	75	2557	172.5	1418	1609	596	4500	946	7260	1549	4520	583	4074	572	16270
PD18-10-476	150	3280	294.8	2606	3100	1204	8470	2032	16330	3640	11700	1840	14350	2191	22050
PD18-10-477	0.031	8.83	0.078	1.63	1.86	0.349	7.97	2.82	36.8	13.81	67.8	14.11	140.2	27.26	14090
PD18-10-478	208.6	2130	282.2	1784	1411	472	3160	618	4460	896	2713	411	3170	460	11700
PD18-10-479	2.71	37	4.12	33.8	29.2	11	86	19	188	51.5	217	40	365	64.5	14340
PD18-10-480	2.79	101.9	4.79	40.3	46.8	17.88	146.7	35.4	310	80	276.5	46.9	399	64.8	10510
PD18-10-481	147.6	2940	250.6	1888	2221	826	5980	1470	12140	2800	9140	1389	10790	1556	18050
PD18-10-482	1.49	60.5	2.42	18.5	23.1	9.1	99	27.5	273	77.1	294	51.4	447	79.4	11060
PD18-10-483	46.2	479.4	52.1	385.7	448.6	174.8	1274	311.5	2592	620	2030	321	2490	370.1	12550
PD18-10-484	129.1	1230	155.5	1160	1257	490	3900	869	7280	1640	4990	686	4910	697	12050
PD18-10-492	107.5	1693	164.7	1460	1797	690	4750	1057	8770	1911	5920	863	6760	958	13950
PD18-10-493	57.6	243	35.6	190	143	43.7	271	56.6	424	103.3	377.1	69.4	649	119.5	13230
PD18-10-494	153.1	2133	203.5	1690	2091	830	5930	1427	11920	2745	8830	1339	10550	1531	17070
PD18-10-495	169.5	1492	198.9	1494	1435	528	2750	618	4730	970	2970	470	3660	501	19240
PD18-10-496	113	1230	140.2	868	804	267.3	2030	419	3095	673	2096	323	2523	373.9	14980
PD18-10-497	34.8	298.3	29.9	210	151.5	59.8	431	105.3	888	217.8	799	148.3	1376	244.5	15020
PD18-10-498	125	2824	260.7	2215	2443	919	7060	1594	12950	2995	9510	1450	11070	1631	19880
PD18-10-499	125.1	990	111.8	723	688	235	1430	312	2310	497	1630	267	2170	339	12500
PD18-10-500	70.8	2492	146.3	1368	1832	713	5920	1500	12010	2635	7870	1121	8460	1219	16200
PD18-10-501	218.9	2282	327	1735	796	211.6	1550	264	1804	378	1158	174.3	1307	200	10360
PD18-10-502	1.63	51.2	3.64	36.4	58.2	23.1	182	45.6	402	103.2	371	61.7	516	87.1	11760
PD18-10-503	110.1	764	115	710	492	177.8	1213	257	2050	452	1420	217	1685	245.6	12970
PD18-10-504	113.3	2144	190.1	1568	1907	754	5460	1355	11450	2617	8370	1248	9570	1346	15120
PD18-10-505	61.1	816	88.7	589	548	199	1452	304	2381	519	1625	242.4	1874	280	11620
PD18-10-506	16.3	177	21.1	133.3	103.9	35.3	272	54.9	416	95.1	325	55.6	506	91.6	10590
PD18-10-507	3.81	97.8	6.3	54.9	72.1	27.5	210.1	52.9	443	108.5	376	61.2	502	81.4	11730
PD18-10-508	40	774	71.1	745	1122	512	2840	743	6390	1347	4330	674	5450	680	11950
PD18-10-516	0.534	68.2	2.06	28.6	38.3	14.1	100.3	22.5	196	53.8	217	39.8	363	66.7	10810
PD18-10-517	26.8	305.7	30.3	223.7	255	90.5	600	141.1	1153	269	907	151.3	1242	197.9	12610

PD18-10-518	162.8	2670	247.3	1670	1622	570	3770	818	6650	1470	4580	658	4880	680	11930
PD18-10-519	11.28	20.5	1.63	7.56	4.18	0.541	18.3	6.74	86.6	32.72	153.5	31.3	300	55.3	13380
PD18-10-520	65.1	447	60.6	406	407	147.2	861	195	1556	342	1134	190	1556	228.8	14920
PD18-10-521	95.6	3220	211.5	1681	1944	744	5530	1394	11330	2563	8000	1249	9670	1413	18620
PD18-10-522	75.2	2283	161.8	1639	2251	928	6760	1727	14830	3480	11230	1724	12840	1905	15000
PD18-10-523	107.9	1473	153	1151	1240	484	3490	773	6060	1378	4270	606	4530	654	12200
PD18-10-524	143.5	2190	199	1597	2000	763	5140	1249	9800	2140	6790	1022	7760	1144	17810
PD18-10-525	38.1	732	68	587	808	299	1909	451	3340	680	2026	315	2366	342	11700
PD18-10-526	48.8	620	69.5	477	479	160.6	1218	269	2010	454	1483	229	1778	264	12320
PD18-10-527	2.31	79.9	4.33	38.7	48	18.9	140.2	35.5	315	79.8	281.6	47.8	397	63.5	13260
PD18-10-528	110.7	1304	133.1	864	756	245	1698	360	2570	563	1695	272	2060	306	12240
PD18-10-529	183.9	1489	169.5	1083	719	190.5	1346	182.9	1003	186.4	551	86.1	748	128.5	13090
PD18-10-530	99.7	1652	146.1	1169	1386	525	3940	916	7810	1793	5700	822	6430	920	14900
PD18-10-531	16.8	85.7	11.38	76.9	65.4	27.1	198	46.1	407	99.4	357	62.9	561	97.7	11480
PD18-10-532	112.8	1997	170.8	1430	1839	745	5420	1325	10980	2484	7600	1118	8460	1147	14840
PD18-10-540	46.7	716	67.7	533	611	233.2	1736	410.5	3393	786	2549	390.1	3031	452	13580
PD18-10-541	156.6	2061	238.6	2126	2663	1034	7080	1692	13120	2787	8660	1277	10090	1358	15410
PD18-10-542	108.6	1653	175.9	1869	2298	892	6180	1335	10900	2490	7810	1106	8530	1181	13010
PD18-10-543	163	2529	266.6	1979	2016	755	5850	1253	10020	2240	6740	948	7350	1020	18660
PD18-10-544	139.4	1533	146.2	1059	1237	450	3463	774	6220	1337	4070	563	4140	586	14890
PD18-10-545	16.7	238	22.8	180	212	86.7	575	141.8	1200	280	928	153	1272	194	14980
PD18-10-546	23.39	118.3	13.63	135.3	128.4	45	320	69.2	618	167	637	112.4	978	161.7	12400
PD18-10-547	5.79	111.9	8.57	68.7	85.1	33.7	240	60.4	517	129.3	437	76.4	631	101.9	14870
PD18-10-548	107.9	2367	209.4	1955	2387	929	6630	1631	13320	2983	9120	1320	10010	1375	15110
PD18-10-549	34.7	544	49.5	373	447	171	1156	282.4	2285	513	1654	264.1	2125	316.3	12590
PD18-10-550	264.9	2131	305	1922	1542	539	4210	829	6510	1383	4336	614	4640	679	19350
PD18-10-551	21.1	154.4	16.8	109	113.2	37.8	264	65	535	136.4	490	88.8	778	131.9	11090
PD18-10-552	38.4	234	30	182	146	47.9	338	73	575	137	456	76	639	100.6	8660
PD18-10-553	115	1686	162.9	1441	1960	690	4410	1041	7850	1552	4590	644	4680	641	15080
PD18-10-554	17.68	29.9	9.9	65.2	40.7	9.17	106	25.2	254	81.8	370	75.9	694	122.5	13440

PD18-10-555	14.3	244	21.5	176	209	79.4	542	120	963	218	724	117.7	969	151	10640
PD18-10-556	93.8	3141	188.9	1614	1983	777	6150	1565	13030	2942	9190	1364	10250	1425	17320
PD18-10-565	129.9	2137	211	2091	2822	1251	8940	2016	15890	3610	11190	1653	12150	1773	14280
PD18-10-566	76.1	2128	158.2	1581	2235	925	6750	1675	13870	3210	10080	1492	11290	1629	14110
PD18-10-567	31.9	633	56.9	500	612	247	1870	403	3540	811	2760	411	3120	468	14800
PD18-10-568	96.2	2526	191.8	1782	2340	944	7270	1796	15230	3560	11490	1734	12910	1870	18410
PD18-10-569	123.8	1188	123.9	757	680	221.3	1403	274	1825	359	1062	158.9	1198	176.1	14030
PD18-10-570	49.2	582	54.3	375	359	110.1	777	150.2	1094	236	734	110.1	888	138.5	10650
PD18-10-571	81.8	1661	142	1255	1808	666	4456	1078	8790	1787	5470	784	6010	818	14940
PD18-10-572	1.94	22.9	0.741	4.89	2.93	0.627	9.11	2.67	33.2	13.27	72.8	17.38	203.7	47.8	11060
PD18-10-573	42.1	271	30	189	183	68.1	471	110	864	206.5	700	110.8	905	137.4	10870
PD18-10-574	1.7	28	2.04	18.2	22.3	4.43	79.7	20.58	209.2	65.3	266.3	46.6	403	72.1	9700
PD18-10-575	40.7	35.2	7.27	63.6	230	75.9	456	81	580	136	467	77.4	641	108.6	15220
PD18-10-576	54.4	465	59.7	370	263	74	566	116.4	842	195	630	106.6	844	138.2	11730
PD18-10-577	26.3	190	20.7	139	143	52.6	366	90.3	782	189	683	115.1	970	157.5	13590
PD18-10-578	0.136	25.9	0.24	2.44	2.98	0.75	12.36	3.65	39.3	13.09	60.4	12.58	125.1	24.28	11080
PD18-10-579	153.1	1992	225.9	1684	1689	583	4126	892	6900	1449	4380	600	4370	608	14580
PD18-10-580	53.6	445	47	294	226	73.3	548	116.6	870	199	656	106.8	870	135.2	11660
PD18-10-581	112	1113	123.3	939	1061	396	2910	655	5350	1218	3770	578	4400	646	13650
PD18-10-589	11.83	133	8.94	55.9	36	8.26	99.1	19.96	185.2	56.7	240.5	47.57	452.5	85	10480
PD18-10-590	91.6	1846	148	1206	1456	590	4290	1012	8770	2019	6510	955	7560	1051	16050
PD18-10-591	45.2	467	51	329	306	91.4	660	132.4	940	198	625	102.4	852	147.2	10600
PD18-10-592	133.1	653	90.1	503	422	134.7	940	195.9	1488	329	1083	173	1354	203.5	13060
PD18-10-593	0.43	25.9	1.5	16.9	21.8	10	64	15.9	145	37.5	148	26.9	245	43.4	14520
PD18-10-594	45.2	325	32.8	207	203	68.9	497	111.8	896	219	761	127.1	1051	171.6	9700
PD18-10-595	67.8	740	78.6	443	376	123	855	180	1350	280	908	153	1238	193	13760
PD18-10-597	66.1	114.1	48.9	329	259	96.9	770	171	1444	354	1179	187	1492	241.9	12350
PD18-10-598	278.6	1223	190.2	1161	589	164.7	1144	162.4	1015	209.7	654	106.7	897	148.5	14500
PD18-10-599	6.8	90.8	7.39	51.1	58.1	21.4	145	35.8	273	67.3	256	45.8	425	84.2	12830
PD18-10-600	64.9	992	97.5	782	938	326	2326	496	3649	799	2471	370	2874	422	13740

PD18-10-601	0.356	36.7	0.85	11.8	16.9	7.1	60	13.8	129	35.5	144	23.9	215	38.5	10840
PD18-10-602	77.4	3044	188.8	1737	2288	870	6270	1530	11560	2403	6920	940	7060	900	19510
PD18-10-603	23.9	149.6	19.2	116.4	95.7	30	229	47.9	376	92.8	323	56.7	459	76.2	11840
PD18-05-611	6.86	174	14.1	104.4	90.9	40.2	254	58.7	473	111.4	383	63	535	89.2	10630
PD18-05-612	28.7	572	55.2	385	315	144	800	181	1405	317	1032	169	1356	214.3	10630
PD18-05-613	31.4	656	64.8	416	268.5	112.2	575	120.1	888	195.4	647	110.5	978	167.7	11470
PD18-05-614	14.57	262.5	26.4	174.1	125.8	51.1	272.1	55.3	419	96.5	344.9	62.5	594	112.9	14870
PD18-05-615	3.47	91.8	4.84	33	27	12.31	65.3	16.36	128.7	33.1	127.8	25.06	242.7	48.1	11390
PD18-05-616	43.7	521	59.5	306	177.4	71.8	334	67.3	505	105.2	347.1	59.4	517	84.2	12280
PD18-05-617	0.129	23.82	0.61	4.78	6.38	2.23	26.7	7.28	82.9	29.74	141.1	29.59	309.4	63.3	9930
PD18-05-618	9.7	277	18.8	125	99	45.7	245	55.4	440	98.9	333	55.9	482	79	12110
PD18-05-619	13.8	229	22.1	135	106	45.5	222	48.3	372	87.6	331	61.5	591	110.5	11630
PD18-05-620	0.202	50	0.347	3.41	4.4	1.94	18.42	4.91	53.8	19.34	95.7	21.68	235	49.2	9690
PD18-05-621	134.7	3070	292	1910	1287	563	2854	612	4480	892	2860	444	3620	538	18820
PD18-05-622	30.1	537	59.9	354	249	95.8	524	93.8	735	143.9	445	71.9	563	82	15810
PD18-05-623	1.93	74.3	3.08	24.7	25.7	11.99	79.6	18.66	164.5	47.3	193.8	36.8	345.1	67.4	9510
PD18-05-624	35.7	1004	74.2	489	310	126.6	622	124.8	886	195	619	99.6	783	122.7	9880
PD18-05-625	4.92	66.7	6.31	39.4	29.3	11.8	81.1	19.4	178	47.7	186	33.8	309	56	10200
PD18-05-626	5.39	118.2	8.55	63.3	59.7	28.5	177	40.4	324	74.9	261	43.9	395	65.3	11140
PD18-05-634	6.49	74.8	8.43	61.7	56.7	24.8	144	31.7	241	54.9	186.5	31.2	277	48.5	11880
PD18-05-635	6.8	92	9.6	63	50	21.6	116	24.5	200	47.6	180	33.9	328	64.6	12870
PD18-05-636	8.53	213.3	16.7	113.2	85.4	39.6	211.8	49.6	396	92.3	318	55.8	509	90.5	13160
PD18-05-637	184.4	4210	439	2840	1864	795	4200	846	6300	1275	3920	574	4610	665	12670
PD18-05-638	142.7	2220	240	1629	1294	568	3110	697	5340	1065	3340	518	4350	639	15530
PD18-05-639	0.0157	56.9	0.208	4.46	7.58	1.62	33.2	10.02	110.8	38.2	177	34.5	324	61.5	10680
PD18-05-640	2.47	49.7	4.17	30.2	25.1	11.03	73	18.43	168.2	48.7	211	41.1	403	80	11430
PD18-05-641	45.7	1007	105.7	643	410	172.9	901	189.5	1394	316	1032	175.6	1496	246	11050
PD18-05-642	96.6	1765	176.9	1190	932	423	2270	538	3970	848	2700	441	3510	517	12550
PD18-05-643	1.29	37.9	1.82	13.8	13.7	6.58	39.9	10	89.2	22.5	87.9	17.42	171.6	32.04	12870

PD18-05-644	64	214	18	77	24.5	7.1	49.1	10.3	82.7	23.4	99.9	19.4	181.8	34.5	11090
PD18-05-645	1.69	47.4	2.51	18.7	18.8	7.3	54.8	13.45	122	33.9	136.4	25.3	237.2	45.3	11610
PD18-05-646	8.1	172	17.4	109	59	24.3	122	24.1	190	52.9	230	47	497	104.1	12350
PD18-05-647	13.7	374	33.2	226	121.7	51	251	53.2	387	85.7	293	49.8	436	74.1	13370
PD18-05-648	0.168	12.9	0.324	2.97	4.15	1.41	16.5	5.08	59.4	21.29	101.9	20.75	203.3	39.61	11180
PD18-05-649	0.027	32.5	0.425	6.86	8.86	2.86	30.1	8.11	83.3	27.7	124	24.39	231	45.2	8950
PD18-05-657	0.089	62	0.66	10.1	15.7	5.9	56	13.1	130	38.7	156	28.7	268	50	11020
PD18-05-658	37.5	711	68.4	427	317	144.5	719	152	1152	249.1	823	135.2	1144	190.4	10890
PD18-05-659	56	833	93.8	555	347	141.3	675	132.5	930	192.3	634	107.1	953	161.3	11530
PD18-05-660	5.83	113.4	10.37	71.5	63.8	29.9	172	41.7	340	77.8	270	46.8	393	66.6	9250
PD18-05-661	0.87	49	1.53	14.5	18.1	6.75	64.3	18.09	191	61.5	281.9	57	580	117.6	9730
PD18-05-662	35.6	234	24.9	145	95.8	38.1	242	57.7	512	142.6	558	98.9	869	150.2	11330
PD18-05-663	18.3	168	15.9	120	69.2	3.81	121	20	168.7	48.5	207	39.5	377	71.3	11180
PD18-05-664	6.29	127.2	10.95	78	65.8	28.9	162.9	38.3	292	69.3	244	43.3	397	70.6	11060
PD18-05-665	4.51	171	10.74	76.7	59.1	26	147.6	34.7	276	67	233	38.5	323	52.3	13560
PD18-05-666	9.15	187.1	16.28	120	91.8	36.3	223.4	54.2	470	125.1	489	85.3	765	132.2	11540
PD18-05-667	53	1023	97	654	515	233.4	1294	301	2377	530	1763	290	2384	366	14730
PD18-05-668	29.7	611	59	400	291	132	714	160.4	1225	263	845	136.9	1135	181.1	11920
PD18-05-669	2.05	50.4	3.25	23.9	24.9	11.02	65.2	16.3	131.6	32.4	122.4	22.88	215	40.8	10570
PD18-05-670	1.13	36.1	1.72	14.8	21.1	9.88	76.1	18	155.9	40.9	155.5	27.62	244.1	45.1	9500
PD18-05-671	0.41	73.3	0.7	7.83	13.19	6.56	51.4	12.46	108.5	29.11	112.3	20.05	181.8	33.03	10570
PD18-05-672	20.8	591	54.9	381	232	97.7	508	107.7	833	178	604	90.5	749	117.2	13370
PD18-05-680	1.96	49.5	3.9	26.7	24	10.81	74.6	18.65	168.7	46	182.7	33.15	296.2	54.9	9090
PD18-05-681	105.5	3410	243.2	1717	1307	564	2979	639	4720	956	2986	461	3600	530	13690
PD18-05-682	0.25	14.7	0.57	5.47	7.43	3.37	33.4	9.29	94	29.1	121.2	22.54	210.4	39.5	9820
PD18-05-683	0.57	22.2	1.19	9	10.4	3.99	45.3	12.77	144.9	49.3	230	45.8	458	92.3	10560
PD18-05-684	128.6	1829	199.9	1293	942	438	2177	522	3989	871	2838	458	3721	554	10000
PD18-05-685	20.6	649	58.1	377	202	79.7	416	77	573	128	435	74.1	667	123.9	11330
PD18-05-686	0.085	7.75	0.229	2.4	4.29	1.89	25.9	8.4	106.8	39.2	190.9	38.8	381	78.3	8030
PD18-05-687	0.787	43.2	1.23	10.01	11.05	4.97	40.5	10.19	101.7	31.37	143.6	28.92	299	60.8	11140

PD18-05-688	1.77	30.9	1.66	10.34	7.4	3.09	20	4.56	46.9	14.83	70.5	15.39	166.7	36.4	11470
PD18-05-689	4.31	53.3	0.47	3.06	2.38	1.24	13.44	4.43	62.1	27.2	164	40.6	476	109.4	10300
PD18-05-690	60.5	927	102.3	620	394	169.7	876	181.6	1319	276	862	133.9	1065	161.1	12690
PD18-05-691	0.281	33.11	0.593	6.78	10.5	2.53	45.3	12.12	127.9	41	176.1	32.8	300	54.4	10220
PD18-05-692	31.3	649	67.4	397	221.3	95.1	471	91.9	685	152.9	534	94.1	854	153.6	11860
PD18-05-693	28	514	53	334	238	103.4	556	123.3	936	210.5	703	117.7	991	165.5	11180
PD18-05-694	5.24	93.4	9.88	85.4	80.4	21.7	250.8	52.2	418	99.1	326.8	51.1	413	72.9	11780
PD18-05-695	20.4	415	40.8	269	205	89.7	506	112.8	946	226	759	130.9	1131	182.9	12720
PD18-05-703	2	53.1	3.05	20.8	19.8	9.11	53.1	13.28	117.3	33.7	143.3	29.47	310.8	66	11170
PD18-05-704	57	786	85.2	578	449	195	1012	220	1610	342	1127	188	1630	264	11760
PD18-05-705	0.026	10.45	0.117	2.14	3.89	1.23	21.8	7.03	86.4	32.4	158.5	32.8	321	65.1	10360
PD18-05-706	3.14	15.1	0.52	2.17	1	0.217	6.7	2.09	30.8	12.5	66.4	15.9	174	39.9	14500
PD18-05-707	2.65	44.1	3.35	28.5	28.4	9.8	79	18.5	165	41.3	172	31.6	304	58	8640
PD18-05-708	0.68	28.6	0.75	6.5	8	2.58	26.1	7.2	73.4	24	107.8	20.97	204.9	39.7	9740
PD18-05-709	0.226	53.5	0.63	8	10.8	3.85	40.9	11.27	109.1	34.4	146.6	27.82	255.3	46.7	8790
PD18-05-710	8.3	125.8	6.25	42.1	33.4	12.2	96.6	23.5	210.1	58.5	232.8	41.8	386	68.8	10000
PD18-05-711	8.89	110.6	9.52	63.1	46.8	21.6	109.5	24.9	194	46.2	176	33.6	330	66	12710
PD18-05-712	1.67	47	2.43	18.2	19.3	7.37	53.9	13.41	122.9	34.8	144.7	28	264.8	49.9	10660
PD18-05-713	2.18	59	3.83	23.4	12.7	4.72	32.3	7.86	81.6	27.1	132.4	29.1	309	67.3	11240
PD18-05-714	0.623	37.9	1.89	12	7.74	3.2	22.6	5.5	57.3	19.8	99.6	21.95	243.4	55.1	11470
PD18-05-715	1.387	47.4	2.12	16.6	16.4	6.96	50.1	12	105.8	29.8	118.5	23.1	212	39.9	14180
PD18-05-716	10.44	147.3	15.49	87.8	52.1	21.7	108.4	21.7	173	41.7	160.1	31.5	321	67.5	13390
PD18-05-717	0.676	21.28	1.178	10.01	12.13	4.45	37.9	9.17	80	20.02	74.6	12.75	110.1	19.65	13610
PD18-05-718	11.6	436	25.1	180	124.7	58.8	329	75.8	601	159	661	126.8	1218	216.3	8400
PD18-05-726	0.291	43.2	1	14.2	14.8	4.78	58.9	14.7	139.3	45.3	184.1	34.9	313	56.7	10440
PD18-05-727	22.9	529	53.2	343	197	77.7	384	76.6	538	117.1	387	64.9	583	100.8	13480
PD18-05-728	0.0178	6.44	0.046	0.75	1.4	0.413	10.02	3.57	46.4	17.81	84.3	17.32	166.2	32.6	11000
PD18-05-729	0.369	33	0.82	8.3	9.7	3.43	30.2	7.35	73.4	21.9	96	18.8	186	37.4	12010
PD18-05-730	68.8	1866	140.8	976	720	319	1706	361	2651	553	1755	281.6	2341	359	13290
PD18-05-731	98.3	1710	170	1189	917	406	2340	526	4190	902	2910	464	3710	568	14430

PD18-05-732	0.144	19.67	0.231	2.49	3.32	0.76	14.99	4.58	55.1	20.59	102.2	21.38	215.8	41.5	11660
PD18-05-733	0.66	28.9	1.24	10.2	11.7	5.1	39.6	10.15	94	26.7	111	22.17	213.6	40.4	13520
PD18-05-734	2.91	35.1	4.09	29	28.2	11.5	69.7	16.1	135.8	35.4	138.4	25.78	242.8	46.3	12390
PD18-05-735	0.67	16.65	0.442	3.11	3.48	0.856	13.11	3.42	38.7	13	59.9	11.79	116.3	23.1	7060
PD18-05-736	7.34	154	12.4	80	68.3	31.1	161	39.2	289	68.1	217	35.3	305	51.3	11970
PD18-05-737	64.3	1337	112.3	732	565	245	1220	255	1850	390	1231	203	1759	288	11690
PD18-05-738	12.8	157.6	12.18	80.1	63.4	26.8	161.9	37.1	328	87.3	349	66.4	655	124.5	12530
PD18-05-739	234.3	5170	486	3458	2536	1088	5790	1238	9290	1850	5640	803	6310	889	20410
PD18-05-740	1.17	53.3	2.18	20.4	26.6	12.16	89.8	21.2	187	48.3	177.7	31.1	268	48.2	10230
PD18-05-741	2.42	82.7	3.51	27.5	28.1	12	77.1	19.69	182.5	52.9	230.3	47.1	487	100.3	13230
PD18-05-749	1.37	28.5	0.89	6.22	5.21	1.64	19.5	5.64	62.7	20.74	97.5	20.07	205.7	41.4	11540
PD18-05-750	44.5	927	92.5	625	495	214	1100	230	1720	382	1280	213	1790	299	12010
PD18-05-751	17.2	370	35.3	227	169	76.3	419	92.5	693	155	520	87.6	763	123	12850
PD18-05-752	15	309	28.2	178	100.4	43.4	205	38.4	271	60	212.4	39.2	385	77.4	13270
PD18-05-753	1.98	52.4	3.07	23.3	22	9.85	63	15.57	144.8	42.2	181	37	379.2	77.9	11090
PD18-05-754	1.61	62.3	3.42	25.7	22.1	9.6	58.9	14.5	131.2	38.2	164.5	33.15	340.7	71.8	11760
PD18-05-755	16.61	393	28.7	202	178	84	507	115	873	189.9	633	105.1	889	147.7	11480
PD18-05-756	18.09	468.4	41.4	269.7	181	77.8	383.3	81	588	122.6	398	64.6	551	89	12290
PD18-05-757	1.15	25.7	1.39	10	7.1	2.66	20.7	4.78	49.5	14.8	70.5	15.64	168.1	36.7	9570
PD18-05-758	2.61	54.4	2.7	17.8	17	6.52	51.4	12.9	120.9	35.7	148.2	28.3	262.5	49.5	11190
PD18-05-759	79.8	1686	158.1	1095	818	344	1864	426	3290	701	2228	352	2790	427	11250
PD18-05-760	0.012	2.42	0.032	0.46	1.01	0.543	7.87	2.75	38.6	15.61	81.4	17.45	178.1	37.16	8160
PD18-05-761	6.6	61.4	5.79	40.9	32.6	13.46	86.5	22.33	199.2	55.2	226.4	44.3	410	78.9	11320
PD18-05-762	79.8	1222	121.4	788	623	291.5	1512	352	2620	545	1761	277	2229	339	8110
PD18-05-763	1.77	35.4	2.58	24.7	27.8	11.6	79	18.2	154.8	40.2	142.5	24.34	206.2	35.2	11210
PD18-05-764	2.23	138.7	4.11	37	43.2	14.32	148.3	36.5	354	103.8	418	77.5	695	123.9	11440
KL18-8-772	23.68	408	45.3	328.5	178.3	73.9	311	61.2	480	111.1	379.3	65.1	564	96.5	12800
KL18-8-773	28.8	336	46.5	280	207	86	353	95.5	828	185.9	660	117.7	1028	151.6	9310
KL18-8-774	6.1	67.8	7.12	48.8	39.6	17.9	85.7	21.3	191	45.3	174.7	34.2	331	64.9	12100

KL18-8-775	54.4	600	65.7	469	337	164.5	711	146.3	918	186	556	83.4	710	118.4	11040
KL18-8-776	0.766	10.84	0.625	5.54	6.18	2.7	22.1	6.15	70.1	24.53	115.4	23.27	231	48.2	10250
KL18-8-777	7.42	85.9	9.82	97	97	49.4	260	53.8	425	96.2	327	54.5	482	92.9	11600
KL18-8-778	8.29	87.9	8.82	79.4	90.9	51.9	322	66	502	109.6	329	48.9	383	67.9	13630
KL18-8-779	4.12	71.9	4.14	37.9	37	18.3	104.9	25.7	225	58.1	226	40.3	374	69.6	10050
KL18-8-780	9.59	157	18.3	159	139	66	303	53.2	372	80.5	277	49	453	88.7	11410
KL18-8-781	45.9	584	68.5	538	344	165.1	713	135.1	971	190	584	91	747	121.5	13290
KL18-8-782	6.72	86.1	7.66	66.3	64.1	36.7	197.9	46.3	364	86	285	47.9	420	79.7	11430
KL18-8-783	17.3	225	24.3	189	148.9	71.2	332	69.7	533	116.7	403	68.5	629	111.3	10990
KL18-8-784	1.35	31.2	1.07	11.1	9.24	2.8	29.1	6.95	73.3	22.9	96.3	18.17	166.3	30.5	10240
KL18-8-785	9.93	150	12.3	85.7	65.3	31.8	130	29.7	250	65.6	264	52.2	510	100.1	12960
KL18-8-786	14.8	194	29.6	260	180	76.5	324	59.7	412	87.1	275.6	46.2	398	69	11830
KL18-8-787	0.76	26.5	0.94	8.3	8.2	3.82	24.4	5.88	56.3	17.38	81.2	17.27	180	41.3	12160
KL18-8-795	6.56	95.9	7.94	60.9	48.2	22.9	123.9	28.2	234	55.7	196.3	33.9	298.1	52.9	11680
KL18-8-796	1.36	47.1	1.22	11.56	13.3	4.69	42.3	10.95	107.3	32.6	139	26.64	258.8	48.2	11770
KL18-8-797	4.8	59.1	3.78	23.4	13.1	5.16	28.6	6.01	53.5	16.9	78.4	16.71	176.4	38.5	11430
KL18-8-798	11.9	122.7	23.5	212	169	80.3	411	74.5	529	111.3	359	54.5	440	72.7	10060
KL18-8-799	6.51	126.5	12.67	109.6	90	40.2	211.1	40	309	77.2	283.9	50.5	443.2	78.5	11810
KL18-8-800	15.1	209	22.4	161	124	58.1	277	54	391	85.3	282	46.9	416	66.6	12510
KL18-8-801	3.68	43	3.98	30.8	24.8	13.7	59.3	13	112.8	29	123	25.3	237	46	11740
KL18-8-802	83.8	1281	161.7	1169	655	286.6	1181	223.6	1584	321.9	969	145.5	1186	185.9	13880
KL18-8-803	4.05	46.6	3.81	30.2	26.5	14	68	15.1	125.8	27.8	96.8	17.5	164.7	31.5	11940
KL18-8-804	5.5	76.8	6.54	53.1	39.7	19.4	97.5	21.4	186	50.6	215	43.7	439	87.6	13010
KL18-8-805	5.26	94.4	7.09	54.1	44.1	19.09	97.5	24.4	211.2	53.5	200.9	36	327	58.8	11980
KL18-8-806	5.3	50.8	7.56	65.5	66.2	35.1	198.6	42.7	344	81.7	282.7	45.8	391.3	70	10830
KL18-8-807	1.72	24	2.68	19.4	16.4	8.7	46.1	9.5	77.9	23.4	103.6	21.6	233	51.8	11560
KL18-8-808	1.69	75.7	2.37	27.4	33.1	10.93	118.4	30.2	305.4	91.6	371	66.5	591	104.9	10490
KL18-8-809	16.5	237	21	153.6	110.3	61.4	295	65	499	111.9	362	61.6	528	88.6	11630
KL18-8-810	0.017	4.57	0.023	0.159	0.255	0.179	1.79	0.636	10.39	5.38	35.1	9.69	134.6	38.93	14050
KL18-8-818	0	0.688	0.0078	0.056	0.097	0.137	1.54	0.612	10.49	4.82	29.1	7.34	90.4	22.6	11950

KL18-8-819	27.3	375	43.4	325	173.4	73.6	321	62.9	479	111.7	397	70.3	669	127	12310
KL18-8-820	1.52	38.3	1.94	15.5	13.6	6.84	36.4	9.62	93.5	29.2	131.8	27.1	289.8	60	12950
KL18-8-821	5.37	72.3	5.82	46.5	40.9	19.5	98.6	22.7	187	46	183.3	34.5	344	66.8	12400
KL18-8-822	8.77	86	14.02	124.3	111.7	54.1	310	59.3	439	96.2	308	48.8	409	66.6	12420
KL18-8-823	6.44	78.4	7.01	57.5	44.5	20.28	86.9	18.29	137.1	32.9	125.4	23.92	239.9	49	12590
KL18-8-824	35.3	394	37.3	298	273	147.5	684	151.1	1084	233.2	707	112.6	947	154.2	11920
KL18-8-825	0	17.24	0.094	2.04	5.02	0.834	32.9	10.05	121.3	42.1	198.5	38.9	379	75	11610
KL18-8-826	11.37	130	13.1	105.1	95.1	51.6	264	58.4	464	97.6	309	46.6	375	62.8	12530
KL18-8-827	66	1036	137.4	932	416	176.6	644	122.4	874	187.4	614	104.4	945	171.9	10970
KL18-8-828	21.9	249	26.2	231	225	131	730	154	1200	244	716	105	749	115	10060
KL18-8-829	8.29	102.4	10.22	83.1	66.8	34.2	165	33.1	260	64.5	251	47.2	475	95.7	11840
KL18-8-830	15.4	207	25	164	80.1	33.4	196	40.3	338	82.2	307	53.2	458	80.9	10940
KL18-8-831	0.078	46.6	0.56	8.97	11.53	4.34	41.6	10.79	112.4	35	152.6	29	273	51.1	10110
KL18-8-832	16.1	163	25.5	202	147	70.7	345	67.8	519	119.2	420	71.1	661	118.6	13010
KL18-8-833	27.7	359	41.3	313	203.1	87	348	76.5	609	138	504	92	833	148.9	12520
KL18-8-841	11.65	138.9	13.53	109.6	100.2	54.4	256	53	380	78.3	255	41.56	363	66.7	13950
KL18-8-842	1.195	62.7	1.44	13.54	15.39	5.41	51	12.79	128.7	38.8	165.5	31.11	289.3	54.1	10940
KL18-8-843	7.81	91.8	7.42	49.4	43.7	24.7	85.7	16.4	113.1	26.2	111.8	23.9	270	64	13070
KL18-8-844	11.78	188	21.7	174	114.2	46.8	191	40.2	317.3	76.7	279	51.4	475	92.7	11200
KL18-8-845	2.63	44.5	3.18	27.2	26.1	13.58	77.6	17.39	145.1	36.1	135.9	25.27	247	51.2	11100
KL18-8-846	2.49	23.39	3.46	40.4	51.7	31.5	195.2	41.7	323	71.8	208.1	29.02	216.5	33.88	10330
KL18-8-847	3.06	54.9	3.14	22.12	20.9	9.36	43.9	11.12	99.9	28.43	127.4	26.72	290.7	64.1	11400
KL18-8-848	9.64	143.8	15.2	119.1	95	43.8	217	43.8	330	75.3	267.3	46.9	447	85	12010
KL18-8-849	4.87	77.9	6.4	46.9	32	13.1	64.1	15.5	135	36.7	160.1	32.1	335	67.5	11450
KL18-8-850	1.84	46.6	2.07	20.6	22.2	10.05	74.6	17.68	161.7	44.9	177.7	31.77	290.1	53.8	10490
KL18-8-851	6.22	107.9	10.8	91.3	62.3	29.1	137	23.8	176	44.7	182.5	36.6	388.5	87.9	11590
KL18-8-852	143.8	1731	154.8	1191	867	459	1849	390	2995	644	2165	352	2910	446	14700
KL18-8-853	40.8	223.2	29.3	216	126.1	54.8	245	45.5	356	83.5	302	53.6	503	92	11830
KL18-8-854	1.31	30.5	1.54	10.4	10.5	4.9	26.3	6.68	73.4	27.49	144.8	33.07	376.1	85	12660
KL18-8-855	6.36	74.9	9.63	84.4	68.7	35.2	179	33	251	60.1	226.2	43	435	92.6	12410

KL18-8-856	19.59	184.2	21.36	192.8	188	103	470	101.3	763	173	556	88.3	761	126.8	11870
KL18-8-857	5.94	95.5	7.23	62.6	71.2	38.2	226	50.4	400	92.7	282	45.5	355	57.6	10120
KL18-8-858	4.98	47	5.32	47.7	56.6	33.3	189	38.6	305	60.8	178	26.3	214	36	12150
KL18-8-866	9.61	142.4	11.66	96.1	86.8	44	202	41.6	339	80.9	303	53.9	521	106.8	12140
KL18-8-867	53	640	67.4	510	310	145.5	590	114.8	797	162.8	489	72.4	648	120.2	13980
KL18-8-868	324	3760	374	2870	2433	1310	5260	1272	9670	1971	5930	840	6780	902	11710
KL18-8-869	340	3500	338	2590	2046	1079	4290	878	6720	1366	4230	636	5100	769	18730
KL18-8-870	2.48	20.2	3.24	40.4	60.3	36	258	47	408	91	268	38.3	281	43.4	13660
KL18-8-871	11.54	216	21.4	168.6	118.3	55.4	275	56.7	436	103.2	363	63.4	580	104.7	11810
KL18-8-872	3.67	54.9	3.95	33.2	32.5	16.95	93.8	20.65	172.5	43.3	164.5	31.3	313	64.2	11170
KL18-8-873	4.62	59.7	4.63	34.4	34.5	17.6	89	19.8	165	40.8	158	30.6	345	78.9	16840
KL18-8-874	194.9	2970	330	2470	1420	653	2810	536	3680	744	2240	368	3040	498	19460
KL18-8-875	4.5	76.9	6.77	59.1	55.1	25.3	130.5	25.2	186	48.1	181.3	33.7	307	56.4	11100
KL18-8-876	4.94	70	5.99	57.8	64.5	35	203.6	44.2	346	76	244.2	39.3	322.5	52.5	10410
KL18-8-877	5.97	100.6	8.36	74.5	71.6	35.8	189.8	46.8	375	81.9	273.4	43.9	367	58.7	11510
KL18-8-878	2.68	36.7	3.64	36.8	48.3	27.4	172.3	39.2	306	72.5	245.7	39.6	332	60.8	10520
KL18-8-879	0.141	26.66	0.384	6.2	8.61	1.83	33.9	8.8	95.9	31.3	139.6	26.73	252.7	48.5	11140
KL18-8-880	16	100.2	27.1	231	178	87	476	97	740	170	574	92	759	119.1	12870
KL18-8-881	3.26	63.3	4.06	34.9	31.8	12.87	96.8	23.12	215.6	60.6	243.6	44.1	411	72.3	9840
KL18-8-882	13.69	169	15.4	119.1	105.5	56.7	306	72.7	553	126.1	426	69.9	612	110.2	11500
KL18-8-890	0.141	18.42	0.253	2.58	3.41	1.23	12.8	3.44	39	14.09	67	14.14	148.3	30.21	12110
KL18-8-891	30.7	402	43.2	325	191	82.9	351	64.9	516	124.3	477	87.4	814	150	12670
KL18-8-892	0.243	6.71	0.363	4.04	5.09	1.87	20.3	6.2	77.2	28.5	136.2	27.1	267	54.5	9900
KL18-8-893	0.18	30.6	0.43	4.01	5.77	0.9	26.2	7.85	92.3	31.13	142.8	27.7	260	47.8	11350
KL18-8-894	20.82	375	39.1	330	268	123	502	94.8	650	135.2	438	71.1	606	103.2	10410
KL18-8-895	7.49	86.7	10.05	89.7	88.3	47.3	259	57	439.5	97.5	316.7	50.7	441	80.8	11930
KL18-8-896	33.2	520	59	420	215	97	443	92	704	164	546	91	804	145	12210
KL18-8-897	3.32	92.6	3.92	31	29	11.94	86.8	21.4	212	61.2	260	49.2	458	84.3	11420
KL18-8-898	10.7	179	15.9	113	77.1	32.5	146	33	286	72.7	295	56.2	549	109.2	11350
KL18-8-899	16.3	258	25.5	195	103.9	47.4	200	41	317	76.5	316	61.7	584	117.6	9970

KL18-8-900	1.8	18.5	1.65	13.5	12.9	6.29	35.2	8.37	76	20.92	87.1	16.74	164.6	31.8	12190
KL18-8-901	0.268	9.07	0.42	3.98	4.76	1.32	26.8	9.49	136.8	53.5	263	52.5	505	97.3	13880
KL18-8-902	0.92	25.46	1.36	13.7	13.63	5.22	44.8	10.99	110.2	35.3	158	30.5	291	56.9	11480
KL18-8-903	44.9	652	72.5	608	505	243	967	169	1102	209.4	594	92.6	769	119.7	12140
KL18-8-904	43.7	480	63.6	558	594	339	2080	417	3100	656	1811	251	1760	243	11620
KL18-8-905	1.11	39.3	1.67	16.63	26.2	13.5	95.1	19.4	158	40.3	153.8	27.91	260.1	48.28	9660
PD18-12-921	308	840	119.7	839	506	217.1	790	168.8	1316	290.7	1018	171.8	1484	228.3	11060
PD18-12-922	1.96	63	6.55	58.4	45.5	16.1	119.6	30.1	296.9	90.2	359.4	63.2	539	96.5	8130
PD18-12-923	1.6	37	0.71	7.68	9.08	1.74	33.2	8.65	92.7	29.8	125.5	23.2	206	37.1	9160
PD18-12-924	104	261	28	138	30.2	2.13	39.3	7.95	80.7	27	123.6	23.82	222.7	42.23	10780
PD18-12-925	0.375	24.87	1.22	12.39	10.21	4.6	28.7	6.77	67	20.4	88.2	17	165.2	31.98	9910
PD18-12-926	0.632	44.7	2.62	25.3	20	6.76	43.2	9.72	89.7	25.39	102	18.71	171.1	31.99	9190
PD18-12-928	19.7	381	66.6	574	368	154.7	506	105.4	810	174.2	604	104.5	883	134.8	9380
PD18-12-929	2.86	98.3	11.54	125.5	94.2	43	129.9	25.4	180.3	42.7	141.6	23.5	213	35.9	11660
PD18-12-930	0.024	18.8	0.071	1.11	1.66	0.74	8.5	2.4	31	12.1	62.9	14.2	153	34.5	10020
PD18-12-931	24.3	404	76.4	642	408	168.7	566	116.2	853	183	603	103.2	879	130.6	10540
PD18-12-932	6.4	146.5	26.3	222	148.8	63.3	208.1	44.7	353	82.9	308	57.9	530	88.1	13080
PD18-12-933	9.3	241.8	36.7	325	235	105.6	343	70.7	568	125.2	464	83	776	134.8	8440
PD18-12-934	1.13	20.2	0.43	3.9	4.8	1.04	21.4	6.14	67	22.31	96.3	18.95	174.6	32.67	9420
PD18-12-935	7.22	219	30.4	293	210	98	288	58.8	440	98.8	328	57.2	517	85.7	11980
PD18-12-936	12.6	340	46.4	455	311	144.4	445	93.4	721	172.8	649	119.8	1057	172.4	11700
PD18-12-944	6.1	189	24.8	226	171	73.3	245	53.8	409	103.8	384	67.2	581	96.6	9930
PD18-12-945	1.193	48.6	4.52	39.6	28.5	12.12	60.6	14.79	143.6	43.35	190	38.37	376.8	72.1	10160
PD18-12-946	9.57	233.8	36.7	332	232	99.3	347	74.1	586	141.1	509	90.4	802	120.5	10470
PD18-12-947	74.8	1843	292.7	2850	2014	934	2855	583	4376	880	2908	484	4124	613	11630
PD18-12-948	26.27	421	86.1	715	457	185.5	629	134.4	1058	236.4	834	148.8	1287	201.3	10330
PD18-12-949	155.1	2974	495.4	4443	3150	1432	4898	1078	8410	1733	5640	892	7900	1052	16500
PD18-12-950	64.9	1710	267	2570	1698	788	2510	521	3870	789	2580	416	3450	503	14990
PD18-12-951	8.34	167.8	24.8	214	139	56.6	221	52.4	442	114.1	476	86.9	815	142.2	11320

PD18-12-952	8.83	184.7	30.2	261.2	180.6	75.6	263.1	57.5	461	112.8	440	82.8	768	137.2	11120
PD18-12-953	0.81	31.7	2.9	24.1	18.6	7.51	38.5	9.85	96.6	27.5	115.1	22.7	209.7	36.4	10760
PD18-12-954	29.8	745	117.6	1124	768	363	1086	218	1630	337	1084	176	1460	210	4800
PD18-12-955	42.8	1355	193.3	2049	1419	673	1787	350	2442	504	1604	263.2	2141	314.9	8350
PD18-12-956	73.2	1832	266.3	2563	1796	840	2634	542	3980	835	2710	449	3721	537	9670
PD18-12-957	13.08	416	59.7	600	405	185.5	524	100.6	722	155.1	528	88	731	116.9	12610
PD18-12-958	0.304	37.1	0.96	10.1	11.2	3.94	37.9	9.91	105.8	33.1	144.7	27.3	255	48.4	10130
PD18-12-959	3.54	79.1	12.2	103.4	57.7	22.3	77.5	15.3	112.6	29.5	110	21.23	212	41.6	11750
PD18-12-960	2.99	59	7.78	60	37.9	14.37	54.3	11.83	101.9	30	129.9	27.4	303	60.7	11380
PD18-12-968	10.58	246	36.8	336	232	102.9	330	71.1	554	132.8	506	90.9	813	137.4	10020
PD18-12-969	20	347	58.4	483	330	133.6	493	103.4	825	194.6	720	134.9	1253	209.8	9510
PD18-12-970	0.78	39	2.21	20	15.51	5.87	35.1	8.97	91.7	27.74	119.7	23.24	216.3	39.1	10700
PD18-12-971	1.81	33.5	4.72	42.4	28.3	11.58	54.3	12.67	113.9	32	130.2	24.3	224	40.9	10470
PD18-12-972	0.197	27.4	0.791	8.4	8.36	2.72	23.9	5.73	57.5	17.42	73.2	13.94	133.2	25.39	9160
PD18-12-973	17.31	491	74.4	765	542	245	711	135.2	992	212.3	694	117.3	1015	155.7	10230
PD18-12-974	58.4	1637	233.3	2420	1677	803	2280	448	3250	671	2131	361	3010	448	12470
PD18-12-975	7.99	547	62.8	763	508	256	615	110.3	828	195	665	115.1	1016	167.1	10390
PD18-12-976	17.35	303.3	57.6	476	308	126.1	446	100.2	820	202.2	755	137.8	1215	199.6	11290
PD18-12-977	7.1	159.2	23.53	202	132	54	180.2	37.4	289.8	63.2	226.8	41.29	392.7	66.6	11340
PD18-12-978	0.394	36.6	1.35	11.7	9.27	3.52	20	4.85	44.9	12.76	51.1	9.9	95.4	18.36	9810
PD18-12-979	0.255	12.6	1.07	9.4	6.6	2.74	14.9	3.59	37	12.69	60.7	13.01	136.2	27.6	11310
PD18-12-980	5.59	149	21.7	187	125	51.4	197	41.1	356	95	382	71.8	672	118.1	9710
PD18-12-981	1.191	38.8	4.13	34.6	24.4	11.11	50.9	12.1	112.8	33.3	141.8	27.9	271.4	51.8	9690
PD18-12-982	2.58	143	14.1	158	129	59	181	38.6	343	97.9	411	80.3	762	132.8	14430
PD18-12-983	0.068	16.69	0.394	5.66	6.92	3.16	20.32	4.73	45.9	13.74	59	12	125.4	25.76	9090
PD18-12-984	2.05	80	7.44	61	42.1	17.7	73	15.8	128.4	32.7	121.2	22.2	198	33.7	10010
PD18-12-992	31.1	754	120.5	1140	809	376	1160	235	1720	370	1193	195	1650	247	13370
PD18-12-993	41	186	34.6	187	68.9	10.24	99	22.4	235	82.1	389	79.8	764	140.4	13710
PD18-12-994	125.9	2636	457	3990	2673	1261	4240	916	7150	1494	4850	755	6620	896	14280
PD18-12-995	8.83	186	34.6	296	191	81.2	280	61	487	115.6	447	79.2	716	120.8	10640

PD18-12-996	Below LOD	10.21	0.021	0.291	0.66	0.144	4.29	1.544	19.36	7.37	36.2	8.19	95.2	22.72	12920
PD18-12-997	11.14	514	68.3	788	517	248.5	649	116.7	821	171.1	546	91.9	768	120.4	11850
PD18-12-998	36.3	859	136.8	1251	882	417	1269	257.4	1911	396	1318	214	1750	254.8	12950
PD18-12-999	5.69	147.5	17.71	164.7	113.7	50.1	165.7	35.2	278.3	67.2	253.3	48.1	462	83.4	11580
PD18-12-1000	4.39	103.4	14.03	122.6	82.5	35.9	129.6	28.01	226.1	53.7	201.3	36.3	334.1	56.4	11020
PD18-12-1001	0.078	20.9	0.615	9.25	12.31	2.54	44.9	11.41	121.7	38.1	160.9	29.3	260.3	46	9590
PD18-12-1002	175	1503	239.5	2048	1402	640	2107	444	3374	717	2326	394	3270	480	10680
PD18-12-1003	1.01	32.5	3.06	27.5	19.2	7.51	49	13.7	146.6	49.7	224.8	43.8	415	72.1	11570
PD18-12-1004	154.1	2760	498	4315	2921	1361	4700	1047	8080	1659	5390	847	7380	1004	13400
PD18-12-1005	4.65	148.7	17.27	171.2	121.5	54.2	162.3	32.86	260.5	64.8	255	48.6	480	90.5	11820
PD18-12-1006	11.64	257.4	42.8	370	246	100.1	329	66.3	493	105.8	361	63	558	89.4	11090
PD18-12-1007	26.1	597	99.6	919	626	292	919	193.5	1479	316	1053	180.8	1563	237.1	13520
PD18-12-1008	1.56	146.4	10.57	142.8	122.3	58.6	160.9	29.1	227	57.7	221.8	42.9	417	84.4	11550
PD18-12-1016	9.44	277	36.1	330	232	103.6	323	65.6	488	107.5	374	67.1	611	104.6	11890
PD18-12-1017	0.038	7.46	0.186	2.03	2.97	0.458	14.87	4.74	58.7	21.42	103.3	20.32	195.2	35.8	11500
PD18-12-1018	64.8	1426	227.1	2030	1416	655	2209	475	3550	750	2481	414	3500	508	16490
PD18-12-1019	159.5	3043	510	4412	3051	1448	5060	1094	8550	1788	5780	902	7870	1052	16010
PD18-12-1020	9.45	211	32.6	291	207	89.4	317	69.1	580	148.3	569	101.5	911	150.3	12320
PD18-12-1021	157.6	2700	481.9	4121	2739	1313	4580	1015	8060	1683	5440	852	7340	1000	18450
PD18-12-1022	3.4	80.4	12.35	109.2	67.2	30.3	102.8	22.6	174	40.3	143.3	25.7	244	40.8	14440
PD18-12-1023	2.36	63.6	9.19	85.8	56.9	22.8	96.1	22.5	191.2	51.2	196.7	35.8	316.1	54.8	9720
PD18-12-1024	69.8	1946	279.4	2954	2820	1309	4010	777	5920	1218	4020	617	5320	761	19360
PD18-12-1025	18.6	661	89	909	616	289	800	154	1104	232	757	127.1	1086	165.2	13800
PD18-12-1026	3.43	27.3	1.1	9.03	7.64	1.81	29.7	8.1	87.2	28.6	122.3	23.14	210.7	38.11	9580
PD18-12-1027	31	722	116.3	1063	763	352	1133	236.2	1740	355	1144	193.6	1756	290.5	19170
PD18-12-1028	45.2	741	139	1111	649	281	927	192	1512	337	1187	208	1880	284	11600
PD18-12-1029	8.84	260	36	367	309	145	422	82.6	616	140.5	504	86.5	751	121.1	13520
PD18-12-1030	110.7	2390	383	3520	2340	1065	3640	783	5970	1237	3970	626	5150	739	15030
PD18-12-1031	0.93	26	2.44	26.1	15.9	7.13	35.6	8.76	89.1	29.1	129.4	25.67	246.5	48.8	9430
PD18-12-1032	1.071	60.3	3.04	30.7	25.2	9.46	58.8	14.55	152.2	47.81	209.9	40.03	374.5	69.3	10370

PD18-12-1040	22.08	914	121.6	1307	947	442	1188	221.1	1561	326.4	1051	175.5	1476	225.7	11390
PD18-12-1041	45.3	896	37.8	231	156	5.66	305	77.9	650	155	588	96.9	803	135.3	14470
PD18-12-1042	95.8	2623	408	3720	2651	1286	4110	876	6870	1427	4607	723	6440	877	16870
PD18-12-1043	1.67	66.6	6.62	60.1	40.2	19.17	75.1	18.75	164	43	172.1	32.07	294.1	49.6	11040
PD18-12-1044	0.47	31.4	1.44	16	16.8	4.5	62.5	18.7	217	73.5	330	64.6	588	104	10150
PD18-12-1045	149.1	2733	492	4290	3069	1420	4940	1063	8360	1679	5480	861	7480	995	13830
PD18-12-1046	9.25	199.2	30.15	256	169.3	70.8	241.3	49.4	376.1	84.4	297.4	54	497	83.4	11350
PD18-12-1047	8.77	201.5	28.53	247.4	167.2	74.1	232.8	48.2	362	79.8	284.7	50.8	460	79.2	11050
PD18-12-1048	2.68	28.1	1.8	15.1	13.4	4.14	37	9.25	95.5	29.9	129.2	24.1	228	44.1	10810
PD18-12-1049	7.86	122.6	24	207	142.9	61.8	206	43.4	332	72.6	256	46.2	413	65.9	14080
PD18-12-1050	76.3	1167	185	1670	1144	527	1640	339	2490	514	1680	272	2280	330	11090
PD18-12-1051	2.54	78.2	9.86	85.5	61.6	24.72	103.1	21.57	174.5	41.16	145.4	25.13	221.9	36.9	9820
PD18-12-1052	13.38	298.4	51.4	460	316	137.2	415	85.9	629	131.8	453.6	78.6	708	113.6	13090
PD18-12-1053	14.46	553	71.4	748	564	259	740	147.3	1154	265	957	167.1	1436	237.1	11970
PD18-12-1054	20.2	785	96.2	1024	808	369	980	178.1	1261	254	840	137.5	1165	171.1	13490
PD18-12-1055	114.7	2711	420	3986	2707	1284	3941	824	6420	1324	4320	686	5940	822	18050
PD18-12-1063	4.6	91.1	14.1	126	82.9	38.1	120	23.6	185	41.1	143.7	27.3	249	41.7	12160
PD18-12-1064	1.54	48.4	3.41	32.4	23.2	9.1	54.4	11.65	100	28.3	105.7	18.6	169	29.2	10000
PD18-12-1065	18.06	422	61.4	565	385	171	526	110.2	820	174	596	104.2	900	147	11650
PD18-12-1066	19.3	123.4	9.61	53.7	32.4	1.44	80.3	22.4	232	69.7	309.2	58	543	95.6	13330
PD18-12-1067	58.8	400	45.3	399	271	118.6	365	71.3	562	129.8	468.2	81.8	712	117.3	12000
PD18-12-1068	32.3	1053	142.9	1443	1030	487	1391	272	1937	403	1289	209.7	1759	258.5	13100
PD18-12-1069	9.55	188	31.1	278	188	77.9	259	53.6	409	91.6	317	57.9	543	85	13090
PD18-12-1070	3.46	24.6	1.72	12.6	7.09	3	23.3	6.46	68.8	22.11	99.3	18.76	174.4	31.9	9410
PD18-12-1071	20	726	99.3	1027	742	350	969	182	1367	292	936	158.1	1324	198	12700
PD18-13-1072	21.32	666	90.6	882	660	313	923	199.5	1483	307	1001	164	1347	199.9	15800
PD18-13-1073	9.87	336	45.6	447	329	150	462	103.2	802	183	655	113	1008	163.6	14080
PD18-13-1074	5.8	430	42	490	370	154	430	82	580	121	397	66.4	562	87	13480
PD18-13-1075	3.5	161	18.6	219	146	73	213	38.3	300	71	229	40.2	359	62.9	13190

PD18-13-1076	23.6	1263	145.3	1609	1198	551	1465	287	2112	423	1345	218.5	1767	264.3	18410
PD18-13-1077	14.23	356	52	457	332	154	510	113.6	909	197.6	679	120.4	1039	166	11770
PD18-13-1078	120.2	2340	355.2	2802	2012	1009	3911	970	7930	1669	5660	900	7930	1113	20910
PD18-13-1079	105.9	2394	369.2	3219	2344	1138	3808	872	6880	1408	4642	720	5990	864	16960
PD18-13-1087	13.05	543	65.6	657	492	223	612	130.4	955	199	646	108.4	900	139.8	10610
PD18-13-1088	49.7	1318	196.2	1788	1265	591	1828	413	3060	628	2019	335	2770	401	11480
PD18-13-1089	37.5	1197	164	1583	1212	570	1700	370.3	2753	563	1839	304.1	2485	362.2	7010
PD18-13-1090	6.74	188.4	28.7	242.2	171.7	72.3	246.4	54.7	438	102.3	371	65.4	575	94.8	10010
PD18-13-1091	61.1	1499	227.3	2051	1501	718	2250	507	3760	788	2575	416	3470	504	13960
PD18-13-1092	30.9	36	13.05	147.2	130.9	59.8	328	72.7	670	192.1	877	203.9	2248	426.2	19370
PD18-13-1093	4.04	117.5	14	119.9	82.9	34.9	124.8	27.3	226	52.9	206	36.7	337	58.1	12370
PD18-13-1094	17.08	1075	132.3	1455	989	469	1131	217	1521	308	970	157.6	1298	202.2	15980
PD18-13-1095	9.47	766	81.8	1021	912	441.5	1255	255.1	1858	400.1	1293	207.3	1671	262	10720
PD18-13-1096	4.1	84.4	7.53	73.8	55.6	23.4	88.3	19.2	161.6	39.7	141.8	25.6	216.3	36.2	9540
PD18-13-1097	13.4	405	58.3	539	420	186.8	613	128.8	1006	227	755	129.5	1100	173.6	14300
PD18-13-1098	13.32	408	57.4	550	400	178	556	126.6	943	208	705	120	1008	156.3	12360
PD18-13-1099	4.84	180.6	22.3	211.2	147.9	65.8	212.3	47.9	369	84.5	315	58.7	517	91.1	8770
PD18-13-1100	2.92	78	9.9	85	60	26.5	99	22.9	199	49.2	200	37.7	363	71.6	9410
PD18-13-1101	39.5	1796	213.2	2300	1796	839	2320	482	3480	730	2310	373	3060	444	10370
PD18-13-1102	3.4	141	15.6	161	116.3	50.9	194.3	44.4	379	95	348	59.8	511	85.8	10300
PD18-13-1103	6.24	207	29	291	228	109	312	64.2	481	102.8	349	60.3	509	81.1	12990
PD18-13-1111	19.9	414	63.3	539	370	183	588	145.2	1126	241	818	137.2	1145	175.6	14720
PD18-13-1112	2.96	101.3	12.03	109.3	90.8	36.6	141.2	32.3	272	65.3	239.9	42.4	372	60.5	9130
PD18-13-1113	9.89	378	46.8	451	337	155	434	88.4	675	138.5	465	79.8	695	114.2	13170
PD18-13-1114	13.43	517	64.5	667	481	217.6	618	129.1	985	213	704	119	1034	164.7	12190
PD18-13-1115	55.2	1267	185.6	1681	1269	595	1940	453	3350	718	2351	394	3360	521	14490
PD18-13-1116	5.89	201	25.9	237	168.1	72.6	241	52.5	426	102.8	411	77.9	719	123.7	14710
PD18-13-1117	127.5	2557	424	3563	2579	1234	4250	1008	8030	1647	5440	839	7020	983	18020
PD18-13-1118	7.08	366.5	38.2	391	291.2	136.1	398	81.9	654	149.2	561	99.8	908	160.8	11130
PD18-13-1119	7.24	233.2	30	287	222	93.1	297	61.9	483	111	407	70.9	654	115	11860

PD18-13-1120	5.36	154.7	23.18	207.4	151.7	68.5	214	46.8	375	91	385	84.1	934	190.4	16690
PD18-13-1121	3.54	187	23.6	255	251	124.1	340	71.5	539	123.5	426	71.9	610	102.3	10400
PD18-13-1122	7.13	416	50.3	531	391	176	476	95.2	724	150	501	81.1	687	108.6	10990
PD18-13-1123	74	1820	280	2340	1632	756	2530	579	4510	932	2980	494	4130	578	13520
PD18-13-1124	1.78	18.86	0.856	9.19	10.64	2.17	47	14.91	188.2	67.3	321	66	624	109.7	13590
PD18-13-1125	12.9	305	39.9	340	233	105.2	333	74.3	603	136.4	490	87.9	790	138.9	11250
PD18-13-1126	2.51	90.9	10.07	87.9	68.3	30.2	126.3	30.69	262.4	64.9	245.9	43.03	374.1	62.1	10350
PD18-13-1127	4.79	135.5	15.6	137.6	93.9	39.7	131.5	27.9	223.9	54.9	206.3	39.2	381	71.1	11850
PD18-13-1135	6.31	267.3	32.7	319	256.7	109.5	335	68.1	538	115.6	391	69.2	589	94.5	11060
PD18-13-1136	19.63	898	119.2	1225	888	415.9	1108	228.5	1678	343.9	1124	185.6	1539	236.9	14460
PD18-13-1137	12	437	60	560	408	189	576	125.4	988	217	772	132.4	1156	189.5	13070
PD18-13-1138	9.85	305.3	43.3	392	286.3	127.2	398	86.5	653	139.5	468	80.8	706	113.6	17850
PD18-13-1139	1.45	76	6.94	80.7	71.2	31.7	127.2	29.2	300.7	92.5	405.3	77.3	722	134.8	11920
PD18-13-1140	11.57	400	47.9	460	342	152.7	466	97.6	738	162.4	563	96.4	859	146.7	12620
PD18-13-1141	6.7	224	26.8	257	185	85.2	251	57.5	470	111.6	419	75.7	668	121.2	11030
PD18-13-1142	106.7	2458	380	3338	2375	1136	3750	865	6980	1440	4660	721	6110	855	17150
PD18-13-1143	8.77	366	43.7	456	333	152.4	429	94	717	163.1	575	102.7	908	155	14470
PD18-13-1144	6.76	216	28.4	267	202	89	262	57	442	99.8	349	61.4	552	90	13230
PD18-13-1145	0.324	20.2	1.48	14.6	12.9	4.84	29.7	8.23	86.3	28.9	136.7	28.49	290.6	58.9	11590
PD18-13-1146	3.74	223.8	20.98	221.3	173.3	75.8	231.7	49.3	387.7	93.3	351.7	61.7	563	98.6	10390
PD18-13-1147	3.8	136.6	14.01	131.2	101.2	46.8	151	34.4	277	67.7	260	49.4	461	84.1	12300
PD18-13-1148	43.8	1128	164.8	1504	1140	530	1651	365	2870	581	1930	321	2659	391	13050
PD18-13-1149	2.84	104.6	8.74	89.3	125.4	62.9	222	40.3	323	85	352	67.9	684	136.4	10660
PD18-13-1150	1.49	66.8	5.71	54.9	39.8	18.8	60	14.1	106.9	25.9	96.5	17.7	153.1	26.52	11750
PD18-13-1151	146.4	2925	463	3812	2618	1180	4210	993	7960	1608	5350	850	6950	988	14840
PD18-13-1152	4.09	115.7	14.08	120.1	95.3	43.1	164.7	39.1	326.9	78.4	285.6	50.1	441	71.9	9890
PD18-13-1153	4.19	135	16.6	145	102.7	44.5	161	35.2	283	64.8	229	39.9	355	58.3	9790
PD18-13-1161	50.3	1591	208.3	2044	1561	727	2149	473	3474	720	2351	386	3208	467	15780
PD18-13-1162	1.57	42.3	5.84	50.3	34.5	14	52.3	12.01	102	26.6	106.6	19.22	191.3	34.5	10690
PD18-13-1163	18.1	694	90.1	900	671	309	874	184	1370	278	907	149	1260	187	15410

PD18-13-1164	28.24	1145	158.5	1562	1164	534	1514	322	2396	503	1737	289.6	2476	380.9	11370
PD18-13-1165	18.19	470	69.2	626	458	216.1	694	156.4	1186	252.5	849	144.3	1210	184.7	14150
PD18-13-1166	5.85	185	22.58	197.3	144.9	61.7	205.2	44.9	364	85.9	330.8	60.9	587	106.4	12050
PD18-13-1167	9.02	650	64.2	716	530	241	643	129	968	225	784	135.6	1184	193	11640
PD18-13-1168	17.66	681	88.4	890	639	292	829	173.6	1270	281	953	161.5	1392	223.5	12140
PD18-13-1169	16.87	641	82.1	826	645	295	883	192	1472	314	1074	179	1499	226	11100
PD18-13-1170	35.6	912	139	1272	949	444	1409	316	2439	509	1677	276.7	2339	357	14580
PD18-13-1172	4.1	108	14.4	130	97	40.6	143	37.9	373	106.7	484	103.8	1057	200	15760
PD18-13-1173	60.8	1513	219	2100	1633	749	2330	515	3820	788	2550	420	3400	497	14870
PD18-13-1174	20.3	564	91.9	789	567	250.3	766	164.8	1215	247.8	800	133.1	1117	163.1	14640
PD18-13-1175	40	1138	168.4	1619	1224	582	1706	373	2750	572	1935	328	2960	485	13140
PD18-13-1176	127.1	2516	414.4	3464	2429	1161	4053	973	7850	1599	5280	817	6710	957	17830
PD18-13-1177	27.8	928	133.5	1264	902	421	1199	262.8	1926	401	1325	220.6	1815	277	14200
PD18-13-1185	9.72	300	37.8	355	270	128	390	85.4	640	144.5	543	104.9	1044	203.3	13840
PD18-13-1186	9.94	264	44.6	375	261	114.7	380	83.7	662	153.8	566	107.5	1003	163.9	14830
PD18-13-1187	67.5	2860	209.6	2558	2359	1098	3300	650	4780	1034	3250	487	3740	560	16340
PD18-13-1188	24.7	807	113.8	1096	811	371	1081	229.7	1661	350	1127	184.9	1508	214.6	12660
PD18-13-1189	4.03	138.8	17.3	149.7	105.2	47.1	158.8	35.8	283.5	68.2	254.2	46.1	417	72.6	10920
PD18-13-1190	111.2	2508	395.8	3457	2483	1167	3882	901	7120	1436	4760	751	6190	883	14520
PD18-13-1191	3.32	100.1	11.98	104.3	71.7	31.6	115.9	26.2	213.1	51.1	195.1	35.2	323	57.6	12690
PD18-13-1192	6.14	194.9	24.8	241	189.3	86.9	284	65.3	513	121.7	454	81	704	117.9	14170
PD18-13-1193	0.108	15.98	0.241	2.7	2.99	1.32	12.09	3.61	44.3	17.05	85.6	18.91	203.7	44.4	11990
PD18-13-1194	0.96	42.8	3.71	34.2	23.2	10.3	38	9	79	22.4	91.4	18.8	187	35.6	14220
PD18-13-1195	2.22	71.2	5.96	52.2	39.7	17.6	92.2	22.53	203.6	54.1	210.8	39.1	353	62.2	11290
PD18-13-1196	4.12	175.8	17.1	163.4	125.6	56.6	181	39.3	309	71.7	262	47.6	440	77	11060
PD18-13-1197	6.61	242	27.8	253	193	80.2	284	64.4	527	127	483	84.5	732	118.8	10560
PD18-14-1198	1.31	28.2	3.24	11.9	2.31	0.87	12.5	6.5	108.2	45.2	258.7	69.9	857	179.9	14770
PD18-14-1199	0.97	46.8	3.88	37.9	30.6	8.55	71.2	19.6	217	73.9	342	68.2	661	126.2	11280
PD18-14-1200	2.26	181	20.1	205	106.9	33.2	139	29	235	57.8	218	40.8	379	66.1	15220

PD18-14-1201	62.2	2812	338	2893	1897	666	3064	702	5520	1160	3950	678	5870	834	13220
PD18-14-1209	0.13	50.5	0.238	2.5	3.35	1.31	17.2	4.59	54.3	19.9	102.1	22.54	249.4	53.9	11740
PD18-14-1210	13.54	494	64.1	548	343	124	526	120.5	933	203.8	699	124.1	1055	156.7	12750
PD18-14-1211	4.59	388	38.6	399	228	68	303	62.6	499	116.8	442	82.6	832	145.8	14910
PD18-14-1212	7.85	474	56.9	550	320	102.6	422	87.9	692	156.1	549	102.6	940	155.8	13340
PD18-14-1213	2.42	107	12	104	73	22.8	134	31.2	293	79.2	319	59.2	508	85.1	11590
PD18-14-1214	6.58	253.3	31.17	265.8	164.6	55.4	219.9	49.1	410	96.1	364.6	68.2	642	114.4	10300
PD18-14-1215	10.89	491	53.5	518	328	111	475	99	766	171.8	577	94.4	824	123.2	11490
PD18-14-1216	0.044	18.61	0.214	2.22	2.07	0.701	8.96	2.53	32.7	11.35	54	11.15	112.3	22.66	13640
PD18-14-1217	46	2130	258.9	2252	1469	507	2307	525	4090	867	2948	512	4390	626	15800
PD18-14-1218	21.6	1133	136.9	1290	816	274	1172	254	1976	433	1487	257.4	2182	324	10990
PD18-14-1219	7.33	673	71.3	742	387	118.7	470	96.8	744	158.3	539	93.4	822	127.9	13420
PD18-14-1220	8.8	485	55	512	309	100.7	439	93	744	163.9	569	100	881	139.6	11980
PD18-14-1221	13.28	489	64.8	560	365	130.1	508	115.5	944	213.4	773	140.5	1245	197.6	10960
PD18-14-1222	1.56	68.4	8.02	74.7	54.3	18.2	79.2	17.4	147	37.8	145.1	27	254	47.4	11490
PD18-14-1223	Below LOD	25.98	0.19	3.41	5.66	1.28	22.2	5.66	64	21.92	102.8	20.91	212.8	43.7	9520
PD18-14-1224	62.1	2730	350.6	3085	2120	749	3413	781	6180	1296	4490	753	6520	928	16630
PD18-14-1225	4.56	259	26.7	232	141	49.7	195	43.1	350	80	304	57.5	544	95.4	12760
PD18-14-1233	42.08	2486	279	2621	1679	580	2533	577	4460	958	3283	562	4770	691	13530
PD18-14-1234	9.58	537	61.7	579	342	112	450	98.7	792	178.5	677	124.2	1156	191.8	11610
PD18-14-1235	5.45	490	50.2	510	295	93.6	384	83.1	677	167.1	696	133.3	1307	216	15230
PD18-14-1236	0.134	17.38	0.645	7.09	5.91	1.8	16.66	4.48	47.9	16.33	77.2	16.22	166.7	32.85	11020
PD18-14-1237	1.79	96.8	10.91	105.6	63	20.5	114.5	26.5	267	78.7	342	64.8	613	112.9	10220
PD18-14-1238	0.0113	12.16	0.055	0.76	1.39	0.532	8.29	2.58	32.6	11.86	61.6	13.26	139.3	29.4	11370
PD18-14-1239	40.04	1897	241.2	2162	1449	489	2143	485	3780	815	2804	481	4110	607	17820
PD18-14-1240	10.94	1041	99	947	475	143.6	589	123.7	963	217	782	136.2	1194	188.3	9240
PD18-14-1241	29.6	1020	147.9	1189	706	248	1011	220.2	1751	362	1238	209.4	1806	251.4	10500
PD18-14-1242	6.76	341	36.3	319	216	72.6	305	68.7	561	125	454	84.6	733	116.8	9730
PD18-14-1243	5.21	406	28	215	99.6	36.2	130.2	27.3	230	58.3	238	47.1	468	89.7	12590
PD18-14-1244	38.9	2066	246.1	2253	1350	464	2014	451	3446	746	2574	439	3750	539	13250

PD18-14-1245	12.4	501	46.6	513	256	67.9	273	44.6	344	86.4	352	66.1	688	130.9	15870
PD18-14-1246	16.73	809	102.2	909	562	189.5	842	182.1	1413	314	1074	187.7	1648	251.8	15860
PD18-14-1247	1.12	59.5	5.21	49.7	38.6	10.8	91.7	23.7	237	68.2	283	51	448	77.9	9410
PD18-14-1248	708	3490	412	3013	1857	639	2788	632	4860	1034	3490	605	5200	737	11830
PD18-14-1249	4.28	155	14.9	127.1	82.7	28.7	129.4	28.8	238	55.8	207	37.1	329	56.3	10380
PD18-14-1257	144.5	502	67.4	337	89.2	14.75	102.8	19	171	58.4	318	77.2	867	176.6	15730
PD18-14-1258	6.7	315	36.1	347	216	76.4	324	75.7	603	130	464	84	746	119.8	12810
PD18-14-1259	9.83	325	40.6	332	204.8	71.8	278	60.3	467	101.7	368	66.5	604	101.2	13020
PD18-14-1260	14.29	522	70.8	588	369	127	489	107	837	182	639	114.7	995	151.2	13540
PD18-14-1261	1.13	59.6	5.69	51.7	34.9	11.6	63.8	16.62	173.8	54.1	249.8	50.2	488.2	91.3	12970
PD18-14-1262	12.52	502.5	68.9	612	412	144.7	591	137.5	1119	245.7	863	151.9	1301	194.9	8970
PD18-14-1263	110.7	3110	366	3180	2190	772	3410	798	6480	1381	4730	795	7220	975	14910
PD18-14-1264	6.21	848	83	909	447	120	485	90.1	658	138.9	468	80.2	701	110.7	13880
PD18-14-1265	57	2627	321	2860	1879	640	2742	612	4910	998	3540	574	5050	703	14310
PD18-14-1266	2.82	257.6	28.6	312	186.6	55.2	231.3	45.6	354	84.3	345	73.7	752	148.5	14340
PD18-14-1267	12.23	589	69.3	619	400	137.8	612	138.5	1127	248	851	150.3	1283	196.8	11880
PD18-14-1268	9.9	684	78.7	749	490	162	654	150	1134	253	888	163	1471	222	14200
PD18-14-1269	0.421	17.5	2.78	18.6	8.61	2.52	19.5	4.45	42.9	12.95	54.2	10.23	100.5	19.34	12890
PD18-14-1270	57.6	2265	307.8	2594	1810	664	3161	725	5900	1248	4302	733	6410	937	36990
PD18-14-1271	0.61	50.2	3.54	32.8	24.1	7.06	56.2	14.57	143.4	41.5	175.6	32.8	305	52.4	12210
PD18-14-1272	0.405	42.2	2.11	18.9	13.08	4.67	33	7.88	76	21.96	92.1	17.91	166.4	30.67	11060
PD18-14-1273	0.0111	13.36	0.108	1.99	4.4	1.29	23.36	6.87	80.2	27.87	126.7	23.84	228.9	43.04	10820
PD18-14-1281	9.64	271.1	37.9	317	189.9	66.9	264	58.1	459	98.3	344	62.3	538	82.4	14560
PD18-14-1282	1.66	86	8.5	81	55.3	17.8	111	32.1	377	125.1	573	108.4	1036	182.3	13790
PD18-14-1283	26.3	737	111.4	918	595	204.3	776	161.6	1243	247	821	136.4	1151	163.2	20100
PD18-14-1284	3.43	161	19.1	176	122	40.5	183	40.9	344	77.3	288	52.2	462	72.4	11510
PD18-14-1285	26.05	1544	193.5	1868	1077	345	1451	309.9	2394	496	1746	304	2722	416	18120

Appendix 5.1 Zircon U-Pb age data – Chapter 5

Zircon Grain	$^{207}\text{Pb}/^{235}\text{U}$	2 σ	$^{206}\text{Pb}/^{238}\text{U}$	2 σ	Error Correlation (ρ)	$^{207}\text{Pb}/^{235}\text{U}$ Age (Ma)	Age Error 2 σ	$^{206}\text{Pb}/^{238}\text{U}$ Age (Ma)	Age Error 2 σ	$^{207}\text{Pb}/^{206}\text{Pb}$ Age (Ma)	Age 2 σ	Age conc.	Age 2 σ	Concordance	Th/U
CO17-26Z-4	0.949	0.03	0.1071	0.0021	0.21349	678	16	656	12	750	71	663	11	87.41	0.22
CO17-26Z-7	0.947	0.056	0.1071	0.0022	0.14294	677	29	656	13	746	126	658	12	87.92	1.56
CO17-26Z-20	0.997	0.047	0.1082	0.003	0.4111	702	24	662	18	833	91	672	17	79.56	0.94
CO17-26Z-6	0.917	0.04	0.1085	0.0024	0.098707	661	21	664	14	650	101	663	12	102.15	0.88
CO17-26Z-19	0.938	0.051	0.1097	0.0026	0.12787	672	27	671	15	675	121	671	14	99.41	1.54
CO17-26Z-11	1.112	0.057	0.119	0.0025	0.30867	759	27	725	14	862	102	729	14	84.08	0.68
CO17-26Z-8	1.282	0.067	0.1228	0.0031	0.33909	838	30	747	18	1088	100	759	18	68.66	0.84
CO17-26Z-12	1.187	0.082	0.1257	0.0032	0.059535	795	38	763	18	883	149	769	17	86.44	0.93
CO17-26Z-16	1.148	0.04	0.1266	0.0022	0.30976	776	19	768	13	799	71	770	12	96.17	0.18
CO17-26Z-3	1.618	0.087	0.1271	0.0025	0.22675	977	34	771	14	1474	100	781	14	52.33	0.90
CO17-26Z-15	1.128	0.039	0.1271	0.0024	0.080105	767	19	771	14	754	80	770	11	102.34	0.20
CO17-26Z-1	1.355	0.067	0.1287	0.003	0.038227	870	29	780	17	1104	108	801	15	70.69	1.11
CO17-26Z-18	1.163	0.047	0.1288	0.002	0.04428	783	22	781	11	790	90	782	10	98.85	1.38
CO17-26Z-25	1.227	0.031	0.1296	0.002	0.19649	813	14	786	11	889	56	795	10	88.40	0.35
CO17-26Z-2	1.23	0.045	0.13	0.0022	0.067543	814	21	788	13	887	81	795	11	88.79	0.10
CO17-26Z-23	1.155	0.059	0.1303	0.0025	0.050723	780	28	790	14	751	113	788	13	105.14	1.22
CO17-26Z-22	1.175	0.045	0.1304	0.0022	0.032692	789	21	790	13	786	87	790	11	100.56	1.51
CO17-26Z-17	1.192	0.084	0.1306	0.0038	0.12275	797	39	791	22	813	152	792	20	97.33	0.92
CO17-26Z-27	1.315	0.089	0.1308	0.0039	0.12939	852	39	792	22	1012	143	804	21	78.30	0.97
CO17-26Z-29	1.222	0.049	0.1309	0.0026	0.084195	811	22	793	15	860	90	798	13	92.25	1.29
CO17-26Z-13	1.52	0.11	0.1313	0.0041	0.11968	939	44	795	23	1292	147	817	22	61.56	0.70
CO17-26Z-30	1.31	0.053	0.1318	0.0034	0.21704	850	23	798	19	988	88	817	17	80.75	0.75
CO17-26Z-28	1.301	0.07	0.1342	0.004	0.052258	846	31	812	23	937	123	823	19	86.64	1.14
CO17-26Z-14	1.244	0.027	0.1354	0.0019	0.38949	821	12	819	11	826	43	819	10	99.06	0.51

CO17-26Z-24	1.229	0.041	0.1357	0.002	0.15688	814	19	820	11	796	72	819	10	103.00	0.52
CO17-26Z-9	1.34	0.1	0.136	0.0049	0.13046	863	43	822	28	971	160	832	25	84.65	0.94
CO17-26Z-21	1.43	0.11	0.1362	0.0033	0.21727	902	46	823	19	1099	151	828	19	74.90	0.70
CO17-26Z-5	1.259	0.069	0.1389	0.0029	0.025475	828	31	838	16	798	122	836	15	105.06	0.88
CO17-26Z-26	1.844	0.065	0.1527	0.0033	0.11648	1061	23	916	19	1373	75	964	16	66.70	0.80
CO17-26Z-10	21.5	0.35	0.6044	0.0076	0.71591	3161	16	3048	31	3235	18	3184	15	94.22	0.50
CO17-55Z-1	23.44	0.47	0.6485	0.0086	0.78495	3245	20	3222	34	3260	20	3252	19	98.85	0.53
CO17-55Z-2	22.25	0.38	0.6328	0.0085	0.4857	3195	17	3161	34	3216	25	3194	17	98.27	0.70
CO17-55Z-3	23.34	0.3	0.6362	0.0073	0.7586	3241	13	3174	29	3283	13	3259	11	96.68	0.36
CO17-55Z-4	22.14	0.84	0.595	0.02	0.98612	3190	37	3010	81	3305	12	3322	9	91.06	0.06
CO17-55Z-5	25.56	0.38	0.6619	0.0081	0.40592	3330	15	3275	31	3363	23	3328	15	97.36	0.77
CO17-55Z-6	20.06	0.29	0.5822	0.0074	0.65661	3094	14	2958	30	3184	18	3114	14	92.89	0.55
CO17-55Z-7	26.29	0.41	0.6772	0.0091	0.74616	3357	15	3334	35	3372	16	3363	14	98.87	0.60
CO17-55Z-8	25.16	0.33	0.643	0.0067	0.3451	3314	13	3201	26	3384	21	3305	13	94.59	0.54
CO17-55Z-9	18.32	0.41	0.5271	0.009	0.88042	3007	22	2729	38	3198	17	3163	16	85.34	0.53
CO17-55Z-10	24.14	0.34	0.6454	0.0072	0.49582	3274	14	3210	28	3313	20	3274	14	96.89	0.40
CO17-55Z-11	25.48	0.35	0.6758	0.0069	0.4669	3327	13	3328	27	3326	20	3327	13	100.07	0.99
CO17-55Z-12	25.17	0.34	0.6791	0.0069	0.70605	3315	13	3341	27	3299	15	3310	13	101.27	0.34
CO17-55Z-13	21.61	0.65	0.59	0.016	0.93628	3166	29	2989	65	3281	17	3271	15	91.13	0.65
CO17-55Z-14	23.31	0.87	0.603	0.016	0.9835	3240	36	3042	64	3365	19	3440	10	90.40	0.42
CO17-55Z-15	28.15	0.39	0.7245	0.008	0.29378	3424	14	3513	30	3373	23	3431	13	104.15	0.65
CO17-55Z-16	20.84	0.33	0.5808	0.0082	0.76626	3131	15	2952	33	3248	16	3181	13	90.88	0.69
CO17-55Z-17	19.43	0.35	0.5297	0.0091	0.80717	3063	17	2740	38	3283	17	3174	14	83.47	0.27
CO17-55Z-18	23.41	0.34	0.6349	0.0076	0.36051	3244	14	3169	30	3291	24	3239	14	96.29	0.83
CO17-55Z-19	29.63	0.48	0.7139	0.0093	0.31231	3475	16	3473	35	3476	27	3475	16	99.93	0.32
CO17-55Z-20	19.19	0.39	0.5351	0.0098	0.83817	3051	20	2763	41	3247	18	3168	15	85.08	0.21
CO17-55Z-21	25.71	0.39	0.6659	0.0079	0.61391	3336	15	3290	31	3363	19	3340	15	97.83	0.47
CO17-55Z-22	24.59	0.44	0.665	0.013	0.88892	3292	18	3287	50	3295	14	3294	11	99.73	0.61
CO17-55Z-23	26.93	0.4	0.6928	0.0096	0.49561	3381	15	3393	37	3374	23	3380	14	100.58	0.94

CO17-55Z-24	23.83	0.33	0.6394	0.0073	0.70277	3262	14	3187	29	3308	16	3276	13	96.34	0.53
CO17-55Z-25	23.81	0.33	0.6399	0.0082	0.38212	3261	14	3189	32	3305	23	3259	14	96.47	0.70
CO17-55Z-26	24.5	0.34	0.631	0.0079	0.74887	3289	14	3154	31	3372	15	3323	12	93.53	0.17
CO17-55Z-27	26.09	0.35	0.6471	0.0071	0.81045	3350	13	3217	28	3431	12	3397	11	93.77	0.13
CO17-55Z-28	22.71	0.4	0.6307	0.0093	0.83198	3215	17	3152	37	3254	15	3239	14	96.89	1.06
CO17-55Z-29	25.69	0.38	0.6917	0.0088	0.42404	3335	15	3389	34	3302	23	3335	14	102.63	0.81
CO17-55Z-30	25.2	0.37	0.6595	0.0092	0.68354	3316	14	3265	36	3347	18	3325	13	97.56	1.17
CO17-55Z-31	19.57	0.37	0.5945	0.0082	0.71677	3070	18	3008	33	3112	21	3082	18	96.66	0.29
CO17-55Z-32	27.82	0.49	0.7051	0.011	0.62961	3413	17	3440	42	3397	22	3409	17	101.27	0.66
CO17-58Z-1	21.93	0.45	0.597	0.012	0.94745	3181	20	3018	48	3285	10	3270	9	91.86	0.07
CO17-58Z-2	21.8	0.49	0.6	0.014	0.96966	3175	22	3030	56	3268	9	3254	8	92.72	0.09
CO17-58Z-3	18.41	0.44	0.5341	0.0073	0.82056	3011	23	2759	31	3185	24	3048	27	86.62	0.09
CO17-58Z-4	29.61	0.45	0.7432	0.01	0.79226	3474	15	3582	37	3412	15	3442	13	104.99	2.27
CO17-58Z-5	22.78	0.37	0.6313	0.0085	0.86974	3218	16	3155	34	3257	13	3247	12	96.86	0.24
CO17-58Z-6	24.59	0.48	0.6634	0.011	0.95655	3292	19	3280	43	3299	10	3300	9	99.43	0.08
CO17-58Z-7	20.4	0.48	0.548	0.012	0.96559	3111	23	2817	50	3306	10	3303	8	85.20	0.23
CO17-58Z-8	20	0.27	0.6093	0.0065	0.44932	3091	13	3067	26	3107	21	3091	13	98.72	0.41
CO17-58Z-9	19.88	0.29	0.5892	0.0072	0.58481	3086	14	2986	29	3151	20	3093	14	94.77	0.45
CO17-58Z-10	27.86	0.37	0.7073	0.008	0.88127	3414	13	3448	30	3394	10	3399	10	101.59	0.20
CO17-58Z-11	22.85	0.34	0.6298	0.0079	0.90171	3221	15	3149	31	3266	10	3259	10	96.42	0.55
CO17-58Z-12	15.54	0.3	0.4369	0.0071	0.94076	2849	18	2337	32	3234	11	3239	7	72.25	0.38
CO17-58Z-13	24.79	0.35	0.6513	0.0078	0.70186	3300	14	3233	30	3341	16	3313	13	96.78	0.14
CO17-58Z-14	25.37	0.33	0.6449	0.0071	0.74812	3323	13	3208	28	3392	14	3352	12	94.57	0.34
CO17-58Z-15	21	0.31	0.5959	0.0073	0.89041	3139	14	3013	30	3220	11	3205	10	93.59	0.17
CO17-58Z-16	25.45	0.35	0.665	0.0076	0.77331	3326	13	3287	29	3349	14	3337	12	98.12	0.10
CO17-58Z-17	24.99	0.38	0.6673	0.0096	0.85748	3308	15	3295	37	3315	12	3313	11	99.40	0.10
CO17-58Z-18	16.03	0.3	0.4414	0.0087	0.9357	2879	18	2357	39	3267	11	3175	7	72.14	0.17
CO17-58Z-19	14.96	0.28	0.5194	0.0066	0.65231	2813	18	2697	28	2897	23	2813	19	93.08	0.17
CO17-58Z-20	22.2	0.45	0.5542	0.011	0.82596	3193	20	2843	46	3420	18	3318	15	83.11	0.31

CO17-58Z-21	19.69	0.33	0.5444	0.0084	0.9079	3076	16	2802	35	3261	11	3223	9	85.93	0.08
CO17-58Z-22	21.99	0.28	0.6259	0.0067	0.7786	3183	12	3133	27	3215	13	3198	11	97.46	0.06
CO17-58Z-23	24.38	0.73	0.639	0.018	0.97652	3284	29	3185	71	3345	10	3345	10	95.23	0.15
CO17-58Z-24	24.97	0.33	0.6529	0.0072	0.71604	3307	13	3240	28	3348	15	3322	12	96.75	0.09
CO17-58Z-25	25.98	0.34	0.6864	0.0077	0.66644	3346	13	3369	29	3332	16	3342	12	101.11	0.10
CO17-58Z-26	23.27	0.33	0.618	0.0069	0.66268	3238	14	3102	28	3324	17	3257	14	93.32	0.26
CO17-58Z-27	16.7	0.32	0.5152	0.0091	0.90433	2918	18	2679	39	3087	13	3048	11	86.78	0.04
CO17-58Z-28	25.51	0.36	0.6723	0.0087	0.4954	3328	14	3315	34	3336	21	3329	14	99.36	0.22
CO17-58Z-30	25.01	0.39	0.6282	0.0098	0.90863	3309	15	3143	39	3411	10	3384	9	92.13	0.10
CO17-58Z-31	16.38	0.29	0.4795	0.0073	0.90937	2899	17	2525	32	3171	12	3131	10	79.64	0.10
CO17-58Z-32	22.41	0.3	0.6181	0.0071	0.8188	3202	13	3102	28	3265	12	3238	11	95.03	0.24
CO17-58Z-33	27.1	0.36	0.7006	0.0079	0.44708	3387	13	3423	30	3366	20	3387	13	101.69	0.10
I16-07Z-2	18.43	0.3	0.6078	0.0093	0.58458	3013	16	3061	37	2980	23	3008	15	102.72	0.81
I16-07Z-16	18.65	0.3	0.6	0.0074	0.53312	3024	16	3030	30	3020	23	3024	16	100.33	1.02
I16-07Z-8	15.56	0.3	0.5226	0.0099	0.81475	2850	18	2710	42	2951	19	2899	15	91.85	0.42
I16-07Z-5	13.19	0.41	0.451	0.015	0.89842	2693	29	2400	67	2922	24	2837	17	82.13	0.79
I16-07Z-4	14.86	0.34	0.4522	0.0093	0.94054	2806	22	2405	41	3109	13	3087	10	77.36	0.34
I16-07Z-9	12.04	0.27	0.4074	0.0088	0.78907	2608	21	2203	40	2939	23	2738	18	74.97	0.19
I16-07Z-12	9.78	0.29	0.3602	0.0098	0.97023	2414	27	1983	46	2801	12	2804	8	70.80	1.49
I16-07Z-17	7.15	0.14	0.2841	0.0049	0.82849	2130	17	1612	25	2676	18	2302	20	60.24	0.79
I16-07Z-6	8.15	0.26	0.2908	0.0082	0.95387	2248	29	1646	41	2853	16	439	21	57.68	0.47
I16-07Z-11	5.854	0.1	0.237	0.0044	0.38898	1954	15	1371	23	2645	33	1768	19	51.84	0.43
I16-07Z-15	4.802	0.092	0.2078	0.0039	0.8648	1785	16	1217	21	2534	17	530	21	48.03	0.69
I16-07Z-1	3.435	0.1	0.1701	0.0052	0.74378	1512	23	1013	29	2305	37	1094	54	43.93	0.09
I16-07Z-14	4.41	0.15	0.1882	0.0055	0.97771	1714	28	1112	30	2557	14	278	10	43.47	0.24
I16-07Z-7	4.55	0.4	0.189	0.012	0.99504	1740	73	1116	65	2602	43	433	10	42.89	0.48
I16-07Z-13	3.229	0.048	0.1515	0.0022	0.73612	1464	12	909	12	2397	18	710	15	37.94	0.27
I16-07Z-3	1.445	0.039	0.0836	0.0021	0.97347	908	16	518	13	2034	11	98	5	25.45	0.63
I16-07Z-10	2.312	0.05	0.0966	0.0019	0.97641	1216	15	595	11	2593	8	103	4	22.93	1.32

I16-17Z-10	21.99	0.32	0.6365	0.0073	0.78366	3183	14	3175	29	3188	14	3186	13	99.59	0.63
I16-17Z-8	22.16	0.34	0.6274	0.0081	0.66385	3191	15	3139	32	3223	19	3199	14	97.39	0.30
I16-17Z-7	20.55	0.32	0.6036	0.009	0.63504	3118	15	3044	36	3165	21	3128	15	96.18	0.55
I16-17Z-11	20.45	0.33	0.5904	0.011	0.62904	3113	16	2991	45	3192	24	3130	15	93.69	0.44
I16-17Z-14	21.31	0.42	0.5909	0.011	0.81592	3153	19	2993	45	3256	18	3208	15	91.92	0.44
I16-17Z-2	21.01	0.44	0.586	0.015	0.81073	3139	20	2973	61	3247	24	3185	15	91.57	0.39
I16-17Z-5	17.86	0.61	0.538	0.012	0.79575	2982	33	2775	50	3125	34	3034	33	88.80	0.40
I16-17Z-9	15.96	0.28	0.479	0.0061	0.67281	2874	17	2523	27	3131	21	2878	19	80.58	0.35
I16-17Z-1	13.63	0.25	0.4354	0.0085	0.88362	2724	17	2330	38	3031	15	2911	11	76.86	0.65
I16-17Z-12	13.6	0.23	0.4225	0.0077	0.87309	2722	16	2272	35	3076	14	2927	10	73.86	0.45
I16-17Z-13	8.52	0.25	0.2713	0.0085	0.96712	2288	27	1547	43	3036	13	0	18	50.96	0.33
I16-17Z-6	4.675	0.1	0.1729	0.0036	0.8806	1763	18	1028	20	2794	17	316	15	36.80	0.28
I16-17Z-15	1.663	0.045	0.047	0.0016	0.97276	995	17	296	10	3226	16	0	3	9.18	0.17
I16-18Z-27	22.21	0.35	0.7021	0.0088	0.86237	3193	15	3429	33	3048	13	3089	13	112.48	0.87
I16-18Z-23	17.46	0.23	0.5765	0.007	0.49028	2961	13	2935	29	2978	21	2961	13	98.53	0.79
I16-18Z-2	20.06	0.36	0.6081	0.0083	0.64705	3094	17	3062	33	3115	22	3098	17	98.31	0.70
I16-18Z-28	16.97	0.24	0.5601	0.0064	0.6478	2933	14	2867	26	2979	18	2941	13	96.25	0.51
I16-18Z-26	16.73	0.36	0.5562	0.01	0.96007	2920	21	2851	41	2967	11	2972	10	96.08	0.56
I16-18Z-13	15.82	0.25	0.5249	0.0062	0.87174	2866	15	2720	26	2970	13	2944	12	91.57	0.69
I16-18Z-29	11.46	0.19	0.4077	0.0054	0.83461	2561	16	2204	25	2857	15	2711	14	77.15	0.84
I16-18Z-6	11.404	0.16	0.4004	0.0052	0.81183	2557	13	2171	24	2879	14	2700	11	75.41	0.52
I16-18Z-14	10.83	0.16	0.3884	0.0047	0.84482	2509	14	2115	22	2844	13	2690	12	74.37	0.26
I16-18Z-21	11.05	0.22	0.3884	0.0078	0.94814	2527	19	2115	36	2877	11	2813	8	73.53	0.25
I16-18Z-31	12.538	0.16	0.398	0.0046	0.7429	2646	12	2160	21	3041	14	2750	12	71.01	0.50
I16-18Z-25	9.245	0.13	0.3296	0.0038	0.63021	2363	13	1836	18	2854	18	2219	19	64.35	0.07
I16-18Z-15	7.8	0.14	0.2994	0.0042	0.9036	2208	16	1688	21	2733	13	889	17	61.77	0.49
I16-18Z-16	6.184	0.085	0.2627	0.0028	0.69711	2002	12	1504	14	2565	17	1567	21	58.62	0.26
I16-18Z-8	6.551	0.11	0.2683	0.0043	0.67807	2053	15	1532	22	2626	22	1985	21	58.35	0.52

I16-18Z-10	8.66	0.17	0.2983	0.0048	0.83917	2303	18	1683	24	2910	17	1019	26	57.84	0.27
I16-18Z-7	5.993	0.11	0.2522	0.0027	0.55353	1975	16	1450	14	2581	26	1427	16	56.18	0.52
I16-18Z-5	5.372	0.08	0.237	0.0027	0.62531	1880	13	1371	14	2501	20	1423	18	54.81	0.44
I16-18Z-22	4.076	0.088	0.2023	0.0031	0.87178	1650	18	1188	17	2301	19	788	15	51.61	0.44
I16-18Z-12	4.211	0.068	0.2031	0.0025	0.90171	1676	13	1192	13	2350	13	664	10	50.72	0.59
I16-18Z-19	6.59	0.31	0.2446	0.0085	0.96037	2058	42	1411	44	2788	27	597	20	50.59	0.71
I16-18Z-18	3.781	0.082	0.1908	0.0044	0.90195	1589	17	1126	24	2273	17	1948	12	49.54	0.49
I16-18Z-4	3.289	0.087	0.1698	0.0034	0.91232	1479	21	1011	19	2233	20	544	13	45.27	0.55
I16-18Z-17	3.615	0.07	0.1749	0.0022	0.81762	1553	15	1039	12	2345	20	756	11	44.32	0.64
I16-18Z-1	3.001	0.045	0.1583	0.002	0.30258	1408	11	947	11	2196	29	1080	11	43.14	0.08
I16-18Z-3	5.18	0.12	0.1993	0.0033	0.86077	1849	20	1172	18	2729	20	685	14	42.93	0.25
I16-18Z-9	6.4	0.23	0.2143	0.0066	0.82269	2032	32	1252	35	2956	33	648	32	42.35	0.57
I16-18Z-30	2.93	0.1	0.1512	0.004	0.95901	1390	26	908	22	2234	20	377	11	40.63	0.12
I16-18Z-11	4.75	0.16	0.1606	0.0052	0.62207	1776	28	960	29	2940	46	751	33	32.66	0.21
I16-32Z-2	19.09	0.32	0.622	0.0077	0.82472	3046	16	3118	31	3000	15	3019	15	103.94	0.62
I16-32Z-21	25.03	0.32	0.6896	0.007	0.50786	3309	13	3381	27	3266	18	3307	12	103.52	0.54
I16-32Z-3	24.53	0.42	0.6732	0.0091	0.8267	3290	17	3318	35	3272	15	3279	14	101.40	0.66
I16-32Z-5	6.51	0.2	0.262	0.0056	0.86342	2047	27	1500	29	2655	27	990	26	56.51	0.95
I16-32Z-22	3.576	0.055	0.1996	0.0024	0.61718	1544	12	1173	13	2097	22	1260	15	55.94	0.57
I16-32Z-13	3.633	0.057	0.1946	0.0026	0.62506	1557	13	1146	14	2169	22	1264	17	52.84	0.66
I16-32Z-10	3.016	0.047	0.1716	0.0019	0.4695	1412	12	1021	11	2063	25	1077	11	49.48	0.71
I16-32Z-12	5.246	0.08	0.2169	0.0028	0.47239	1860	13	1266	15	2610	24	1418	17	48.49	0.57
I16-32Z-27	3.686	0.086	0.1846	0.0036	0.89479	1568	19	1092	20	2286	18	561	16	47.78	0.85
I16-32Z-14	4.35	0.12	0.1982	0.0056	0.9428	1703	23	1166	30	2447	16	160	18	47.63	0.66
I16-32Z-1	3.19	0.11	0.172	0.0036	0.96702	1455	27	1023	20	2158	27	614	8	47.42	0.66
I16-32Z-18	3.374	0.062	0.1764	0.0026	0.67802	1498	14	1047	14	2211	24	1004	18	47.36	0.73
I16-32Z-9	2.976	0.058	0.166	0.0021	0.84637	1402	15	990	12	2098	19	731	10	47.18	0.66
I16-32Z-26	3.1	0.11	0.1671	0.0035	0.88885	1433	27	996	19	2158	34	702	14	46.15	0.63
I16-32Z-7	4.01	0.13	0.1863	0.0036	0.8223	1636	26	1101	20	2414	34	818	17	45.62	0.66

I16-32Z-20	3.167	0.066	0.1651	0.0029	0.59645	1449	16	985	16	2216	30	1014	19	44.45	0.65
I16-32Z-6	5.65	0.15	0.2109	0.0057	0.8804	1924	23	1234	30	2779	22	350	25	44.39	0.89
I16-32Z-19	4.522	0.093	0.1924	0.0022	0.5744	1735	17	1134	12	2562	28	1037	13	44.27	0.59
I16-32Z-24	4.14	0.12	0.1839	0.0045	0.89473	1662	24	1088	25	2490	22	497	19	43.70	0.40
I16-32Z-15	3.979	0.1	0.1791	0.0051	0.44306	1630	20	1062	28	2468	48	1374	27	43.04	0.65
I16-32Z-8	4.15	0.11	0.1807	0.0045	0.88999	1664	22	1071	25	2523	20	398	20	42.43	0.60
I16-32Z-25	3.269	0.058	0.1601	0.0026	0.44137	1474	14	957	14	2324	31	1083	16	41.19	0.53
I16-32Z-4	3.97	0.12	0.1703	0.0034	0.9092	1628	25	1014	19	2549	25	580	12	39.78	0.62
I16-32Z-23	2.511	0.044	0.1383	0.0018	0.80257	1275	13	835	10	2121	18	608	10	39.38	1.33
I16-32Z-17	4.085	0.073	0.171	0.0021	0.6405	1651	15	1018	12	2589	23	863	12	39.30	0.81
I16-32Z-11	3.58	0.12	0.1602	0.0061	0.9037	1545	27	958	34	2477	28	116	26	38.67	0.52
I16-32Z-16	2.446	0.064	0.1174	0.0017	0.69359	1256	19	716	10	2359	33	581	9	30.34	0.42
I16-34Z-22	14.68	0.39	0.4541	0.01	0.66377	2795	25	2414	44	3083	33	2824	27	78.29	0.30
I16-34Z-20	20.91	0.42	0.603	0.012	0.75695	3134	20	3042	48	3194	22	3158	17	95.23	0.29
I16-34Z-18	21.3	0.37	0.5974	0.01	0.49695	3152	17	3019	40	3238	27	3158	17	93.25	0.49
I16-34Z-4	21.83	0.4	0.629	0.012	0.83664	3176	18	3146	48	3196	17	3187	14	98.44	0.32
I16-34Z-9	22.26	0.37	0.6234	0.0079	0.71095	3195	16	3123	31	3241	19	3209	16	96.39	0.47
I16-34Z-23	22.56	0.31	0.6214	0.0068	0.52668	3208	13	3116	27	3267	19	3210	14	95.37	0.56
I16-34Z-21	23.03	0.38	0.6313	0.0091	0.72872	3228	16	3155	36	3274	18	3245	15	96.35	0.62
I16-34Z-11	23.09	0.35	0.6391	0.0072	0.3966	3231	15	3186	28	3259	23	3227	15	97.74	0.43
I16-34Z-24	23.41	0.33	0.6511	0.0088	0.36608	3244	14	3233	34	3251	25	3244	14	99.42	0.31
I16-34Z-17	23.57	0.34	0.646	0.0079	0.42104	3251	14	3213	31	3274	23	3250	14	98.11	0.55
I16-34Z-8	23.72	0.33	0.6558	0.0066	0.49805	3257	14	3251	26	3261	20	3257	14	99.70	0.43
I16-34Z-14	23.73	0.38	0.6579	0.0086	0.51898	3257	16	3259	33	3256	23	3257	16	100.08	0.41
I16-34Z-28	23.73	0.34	0.6442	0.008	0.55864	3257	14	3206	31	3289	20	3261	14	97.45	0.48
I16-34Z-30	23.75	0.33	0.6513	0.0067	0.32846	3258	14	3233	26	3274	23	3256	13	98.77	0.62
I16-34Z-2	23.77	0.37	0.6585	0.0084	0.71615	3259	15	3261	33	3258	17	3259	14	100.11	0.58
I16-34Z-15	23.87	0.33	0.6611	0.0074	0.092661	3263	14	3271	29	3258	27	3264	13	100.41	0.70
I16-34Z-7	24.07	0.32	0.661	0.008	0.22512	3271	13	3271	31	3271	25	3271	13	99.99	0.38

I16-34Z-13	24.09	0.35	0.663	0.0078	0.46305	3272	14	3279	30	3268	22	3272	14	100.33	0.59
I16-34Z-10	24.25	0.4	0.6698	0.011	0.61912	3279	16	3305	43	3262	23	3275	15	101.31	0.55
I16-34Z-12	24.31	0.4	0.6684	0.0071	0.57368	3281	16	3300	27	3269	21	3281	16	100.93	0.38
I16-34Z-27	24.41	0.34	0.6697	0.008	0.50841	3285	14	3305	31	3273	20	3284	14	100.97	0.41
I16-34Z-1	24.6	0.38	0.6723	0.0093	0.34752	3293	15	3315	36	3279	26	3293	15	101.09	0.42
I16-34Z-16	24.6	0.39	0.6724	0.0081	0.38248	3293	16	3315	31	3279	25	3294	15	101.11	0.59
I16-34Z-6	24.64	0.37	0.6823	0.0089	0.50573	3294	15	3353	34	3258	22	3291	15	102.91	0.59
I16-34Z-29	24.8	0.31	0.6793	0.0076	0.65735	3300	12	3342	29	3275	16	3294	12	102.02	0.49
I16-34Z-5	25.09	0.37	0.6766	0.0081	0.49598	3312	14	3331	31	3300	21	3311	14	100.95	0.37
I16-34Z-25	25.31	0.35	0.6911	0.0077	0.37345	3320	14	3387	29	3280	22	3323	13	103.25	0.50
I16-34Z-19	25.65	0.42	0.7081	0.011	0.77557	3333	16	3451	42	3263	17	3301	14	105.77	0.53
I16-34Z-26	25.96	0.9	0.711	0.023	0.78319	3345	34	3462	87	3276	35	3312	29	105.70	0.37
I16-46Z-1	21.77	0.37	0.6216	0.0085	0.92957	3174	17	3116	34	3210	11	3211	10	97.08	0.14
I16-46Z-2	18.96	0.28	0.5685	0.0081	0.74134	3040	14	2902	33	3132	17	3074	13	92.64	0.18
I16-46Z-3	18.08	0.33	0.545	0.011	0.84857	2994	18	2804	46	3124	17	3062	12	89.77	0.24
I16-46Z-4	22.35	0.33	0.6302	0.0084	0.79929	3199	14	3150	33	3230	14	3215	12	97.54	0.38
I16-46Z-5	20.74	0.35	0.5841	0.0092	0.91249	3127	16	2966	37	3232	11	3210	10	91.77	1.85
I16-46Z-6	21.51	0.33	0.6243	0.0078	0.87511	3162	15	3127	31	3184	12	3179	11	98.21	0.18
I16-46Z-7	20.8	0.3	0.6241	0.0069	0.79649	3129	14	3126	27	3131	14	3130	13	99.84	0.45
I16-46Z-8	21.09	0.32	0.6002	0.0067	0.86069	3143	15	3031	27	3215	13	3197	12	94.26	0.15
I16-46Z-9	21.3	0.45	0.6055	0.011	0.93717	3152	21	3052	44	3217	12	3215	11	94.87	0.46
I16-46Z-10	21.1	0.25	0.6303	0.0073	0.66643	3143	12	3151	29	3138	15	3142	11	100.40	0.08
I16-46Z-11	21.86	0.3	0.6143	0.008	0.76294	3178	13	3087	32	3235	15	3202	12	95.43	0.31
I16-46Z-12	21.62	0.35	0.6271	0.008	0.8729	3167	16	3138	32	3185	13	3181	12	98.53	0.05
I16-46Z-13	19.52	0.28	0.6023	0.007	0.59698	3068	14	3039	28	3087	19	3070	14	98.45	0.11
I16-46Z-14	20.52	0.32	0.61	0.0071	0.71558	3116	15	3070	28	3146	17	3125	15	97.58	0.09
I16-46Z-15	21.96	0.33	0.63	0.0082	0.8331	3182	15	3150	32	3202	13	3194	12	98.35	0.15
I16-46Z-16	22.4	0.41	0.6462	0.0094	0.84534	3201	18	3213	37	3194	16	3196	15	100.61	0.21
I16-46Z-17	20.89	0.27	0.6173	0.0071	0.64079	3134	13	3099	28	3156	17	3138	12	98.21	0.15

I16-46Z-18	20.88	0.28	0.6	0.0063	0.79987	3133	13	3030	25	3200	13	3168	12	94.69	0.39
I16-46Z-19	22.07	0.27	0.6317	0.0067	0.42026	3187	12	3156	27	3206	20	3186	12	98.45	0.22
I16-46Z-20	22.68	0.29	0.6619	0.0073	0.73252	3213	12	3275	28	3175	14	3199	12	103.12	0.09
I16-46Z-21	13.04	0.56	0.416	0.016	0.97288	2683	41	2242	73	3033	17	3054	11	73.92	0.29
I16-46Z-22	24.86	0.42	0.7001	0.01	0.9063	3303	17	3421	38	3232	11	3242	12	105.86	0.14
I16-46Z-23	20.51	0.28	0.6003	0.0066	0.75002	3116	13	3031	27	3171	14	3137	12	95.59	0.29
I16-46Z-24	25.14	0.36	0.6782	0.0082	0.73835	3314	14	3337	32	3299	15	3308	13	101.15	1.08
I16-46Z-25	19.32	0.28	0.5902	0.008	0.58552	3058	14	2990	32	3103	20	3065	14	96.37	0.33
I16-46Z-26	18.92	0.31	0.5655	0.009	0.83475	3038	16	2889	37	3138	15	3093	12	92.09	0.21
I16-46Z-27	21.07	0.28	0.6049	0.0068	0.58355	3142	13	3050	27	3201	18	3149	13	95.26	0.15
I16-46Z-28	19.47	0.3	0.5742	0.0075	0.75109	3065	15	2925	31	3159	16	3101	14	92.60	0.14
I16-46Z-29	11.08	0.18	0.4201	0.0064	0.73464	2530	15	2261	29	2753	19	2590	14	82.12	0.14
I16-46Z-30	19.64	0.28	0.6005	0.0064	0.8953	3074	14	3032	26	3101	11	3098	11	97.76	0.15
I16-52Z-13	0.964	0.076	0.1048	0.0034	0.52561	685	39	643	20	829	141	641	20	77.50	0.47
I16-52Z-31	0.959	0.027	0.1079	0.0017	0.20317	683	14	661	10	757	62	667	9	87.28	1.01
I16-52Z-19	0.983	0.034	0.1115	0.0023	0.27172	695	17	682	13	740	74	686	12	92.13	0.46
I16-52Z-12	0.998	0.031	0.1127	0.0023	0.45276	703	16	688	13	749	60	693	12	91.90	0.64
I16-52Z-24	1.18	0.043	0.1247	0.0025	0.37625	791	20	758	14	888	71	766	14	85.35	0.47
I16-52Z-29	1.124	0.038	0.1252	0.0024	0.10456	765	18	760	14	778	78	762	12	97.74	0.44
I16-52Z-4	1.184	0.029	0.1255	0.0022	0.57514	793	14	762	13	881	42	775	12	86.46	0.80
I16-52Z-20	1.204	0.036	0.1266	0.002	0.14707	802	17	768	11	898	65	778	10	85.57	0.55
I16-52Z-28	1.201	0.054	0.1275	0.0024	0.44323	801	25	774	14	878	83	775	14	88.09	0.53
I16-52Z-1	1.275	0.056	0.128	0.0022	0.091777	835	25	776	13	993	93	786	12	78.20	0.44
I16-52Z-18	1.182	0.06	0.1298	0.0035	0.20729	792	28	787	20	808	109	788	18	97.36	0.40
I16-52Z-27	1.199	0.038	0.1299	0.0019	0.05407	800	18	787	11	836	71	791	9	94.17	0.46
I16-52Z-10	1.189	0.038	0.1304	0.0018	0.007874	796	18	790	10	811	73	791	9	97.48	0.54
I16-52Z-11	1.254	0.032	0.1304	0.002	0.18943	825	14	790	11	921	56	802	10	85.80	0.53
I16-52Z-23	1.195	0.047	0.1312	0.0022	0.49487	798	22	795	13	808	72	795	13	98.33	0.51
I16-52Z-3	1.238	0.043	0.1312	0.0021	0.058756	818	20	795	12	882	77	801	11	90.12	0.43

I16-52Z-22	1.208	0.028	0.1314	0.0017	0.12909	804	13	796	10	828	52	799	8	96.15	0.52
I16-52Z-14	1.207	0.037	0.1318	0.0021	0.08566	804	17	798	12	820	70	800	10	97.38	0.42
I16-52Z-25	1.227	0.042	0.1319	0.0019	0.19654	813	19	799	11	852	72	801	10	93.71	0.41
I16-52Z-2	1.213	0.049	0.132	0.0022	0.22302	807	23	799	13	827	84	801	12	96.67	1.46
I16-52Z-16	1.262	0.048	0.1322	0.0024	0.19747	829	22	800	14	906	80	807	13	88.36	0.40
I16-52Z-34	1.243	0.044	0.1327	0.0021	0.055554	820	20	803	12	867	79	808	11	92.70	0.47
I16-52Z-6	1.24	0.037	0.1343	0.002	0.013051	819	17	812	11	837	69	814	9	97.08	0.45
I16-52Z-15	1.272	0.05	0.1371	0.0027	0.46802	833	22	828	15	847	72	829	15	97.80	0.46
I16-52Z-8	1.263	0.05	0.1374	0.0022	0.23655	829	22	830	13	827	81	830	12	100.30	0.53
I16-52Z-33	1.312	0.029	0.1401	0.0018	0.48339	851	13	845	10	866	40	847	10	97.59	0.70
I16-52Z-7	1.285	0.026	0.141	0.0016	0.43916	839	12	850	9	810	38	847	8	105.04	0.65
I16-52Z-17	10.58	0.2	0.3677	0.0053	0.27611	2487	18	2019	25	2895	33	2308	20	69.72	0.29
I16-52Z-32	12.74	0.23	0.4282	0.0051	0.78353	2661	17	2298	23	2950	19	2664	23	77.90	0.05
I16-52Z-26	16.89	0.51	0.51	0.013	0.96969	2929	29	2657	56	3121	13	3149	10	85.11	0.84
I16-52Z-5	17.04	0.82	0.512	0.02	0.9806	2937	46	2665	85	3129	20	3181	13	85.17	0.42
I16-52Z-21	23.01	0.29	0.6375	0.0066	0.53484	3227	12	3179	26	3257	18	3229	12	97.60	0.21
I16-52Z-9	22.83	0.6	0.6573	0.011	0.90467	3220	26	3257	43	3197	21	3195	21	101.87	0.31
I16-54Z-1	17.67	0.39	0.5129	0.0098	0.93457	2972	21	2669	42	3184	13	3173	11	83.83	0.03
I16-54Z-2	23.61	0.32	0.6689	0.0074	0.46762	3252	13	3302	29	3222	20	3252	13	102.46	0.41
I16-54Z-4	23.31	0.35	0.6564	0.0072	0.37318	3240	15	3253	28	3232	24	3241	14	100.66	0.31
I16-54Z-6	25.27	0.38	0.7265	0.0086	0.82148	3319	15	3520	32	3199	14	3246	13	110.04	0.72
I16-54Z-7	26.19	0.35	0.6809	0.0074	0.62172	3354	13	3348	28	3357	17	3354	13	99.72	0.10
I16-54Z-8	22.05	0.32	0.6346	0.0071	0.61679	3186	14	3168	28	3197	18	3188	14	99.07	0.10
I16-54Z-9	22.02	0.32	0.6424	0.0083	0.88637	3185	14	3198	33	3176	11	3178	10	100.71	0.02
I16-54Z-10	19.02	0.31	0.5493	0.0088	0.92062	3043	16	2822	37	3192	10	3158	9	88.42	0.01
I16-54Z-11	22.93	0.36	0.6541	0.0087	0.65164	3224	15	3244	34	3211	19	3221	15	101.02	0.59
I16-54Z-12	21.68	0.27	0.6329	0.0067	0.6659	3170	12	3161	27	3175	15	3171	12	99.56	0.18
I16-54Z-14	23.16	0.3	0.667	0.0073	0.75083	3234	13	3294	28	3196	14	3218	12	103.07	0.48
I16-54Z-15	22.37	0.37	0.6367	0.0096	0.80067	3200	16	3176	38	3215	16	3208	14	98.79	0.55

I16-54Z-16	22.73	0.29	0.6589	0.0076	0.72121	3216	12	3263	30	3186	15	3205	11	102.41	0.01
I16-54Z-17	22.84	0.31	0.6645	0.0075	0.75354	3220	13	3285	29	3180	14	3203	12	103.28	0.05
I16-54Z-18	19.82	0.31	0.6135	0.0089	0.91309	3083	15	3084	36	3082	10	3082	10	100.07	0.06
I16-54Z-19	19.79	0.29	0.5748	0.0071	0.85254	3081	14	2928	29	3183	12	3149	11	91.98	0.04
I16-54Z-20	21.06	0.31	0.6383	0.0074	0.83984	3141	14	3182	29	3115	13	3125	12	102.15	0.03
I16-54Z-21	17.08	0.3	0.5329	0.008	0.93991	2939	17	2754	34	3069	10	3067	9	89.73	0.01
I16-54Z-22	22.48	0.32	0.6547	0.0078	0.78452	3205	14	3247	30	3179	14	3192	12	102.14	0.08
I16-54Z-23	21.49	0.29	0.6373	0.0074	0.81732	3161	13	3178	29	3150	12	3155	11	100.90	0.02
I16-54Z-24	21.74	0.33	0.6284	0.0093	0.76865	3172	15	3143	37	3191	16	3180	13	98.52	0.02
I16-62Z-10	0.893	0.027	0.1066	0.0022	0.53814	648	15	653	13	631	56	651	12	103.55	0.55
I16-62Z-7	0.965	0.025	0.1103	0.0021	0.47697	686	13	675	12	723	50	680	11	93.24	0.05
I16-62Z-9	0.995	0.025	0.1118	0.002	0.46237	701	13	683	12	760	49	691	10	89.94	0.26
I16-62Z-28	1.022	0.029	0.1178	0.0022	0.35054	715	15	718	13	706	60	717	11	101.74	0.67
I16-62Z-21	1.165	0.031	0.1206	0.0019	0.23589	784	15	734	11	930	57	749	10	78.92	1.15
I16-62Z-24	1.125	0.034	0.1219	0.0022	0.36804	765	16	742	13	836	60	749	12	88.73	0.77
I16-62Z-6	1.159	0.042	0.122	0.0024	0.025795	782	20	742	14	896	84	754	12	82.84	0.75
I16-62Z-31	1.1	0.054	0.1221	0.0028	0.006263	753	26	743	16	785	114	746	14	94.60	1.41
I16-62Z-27	1.143	0.028	0.1227	0.0017	0.13636	774	13	746	10	855	55	755	8	87.25	0.10
I16-62Z-23	1.168	0.041	0.1256	0.002	0.19749	786	19	763	12	852	74	767	11	89.56	0.82
I16-62Z-25	1.076	0.035	0.126	0.0028	0.48187	742	17	765	16	672	63	755	14	113.86	0.16
I16-62Z-30	1.186	0.033	0.1267	0.0018	0.036052	794	15	769	10	865	64	777	9	88.88	1.19
I16-62Z-13	1.184	0.028	0.1268	0.0019	0.25793	793	13	770	11	860	51	778	9	89.48	0.18
I16-62Z-12	1.154	0.05	0.1275	0.0023	0.063637	779	24	774	13	795	96	775	12	97.31	0.54
I16-62Z-14	1.174	0.04	0.1275	0.0019	0.11394	789	19	774	11	831	74	777	10	93.09	0.95
I16-62Z-19	1.23	0.052	0.1275	0.0023	0.17879	814	24	774	13	927	88	781	12	83.42	0.43
I16-62Z-16	1.244	0.041	0.1276	0.0017	0.22771	821	19	774	10	949	67	781	9	81.58	1.07
I16-62Z-26	1.178	0.025	0.12816	0.0014	0.35418	790	12	777	8	827	42	780	8	93.96	0.32
I16-62Z-3	1.194	0.032	0.1282	0.0019	0.056524	798	15	778	11	855	62	784	9	90.98	0.61
I16-62Z-8	1.199	0.036	0.1286	0.0018	0.27933	800	17	780	10	857	61	784	10	91.01	1.08

I16-62Z-18	1.175	0.028	0.1297	0.0017	0.12616	789	13	786	10	797	54	787	8	98.64	0.77
I16-62Z-4	1.172	0.034	0.1299	0.0017	0.19074	788	16	787	10	788	62	787	9	99.86	1.35
I16-62Z-11	1.212	0.033	0.1299	0.002	0.039687	806	15	787	11	858	64	794	9	91.72	0.79
I16-62Z-32	1.181	0.026	0.1315	0.0018	0.05508	792	12	796	10	779	53	795	8	102.27	0.34
I16-62Z-17	1.247	0.044	0.1322	0.0023	0.2575	822	20	800	13	881	73	806	12	90.84	1.07
I16-62Z-15	1.231	0.063	0.1328	0.0028	0.21321	815	29	804	16	845	106	806	15	95.12	0.53
I16-62Z-1	1.329	0.064	0.1334	0.0022	0.33875	858	28	807	13	993	92	810	13	81.28	0.68
I16-62Z-5	1.233	0.042	0.1335	0.0022	0.26227	816	19	808	13	837	70	810	12	96.48	0.84
I16-62Z-2	1.27	0.038	0.1339	0.002	0.14527	832	17	810	11	892	65	816	10	90.78	0.89
I16-62Z-29	1.275	0.049	0.1341	0.0026	0.23867	835	22	811	15	898	80	817	14	90.38	0.57
I16-62Z-20	1.308	0.034	0.1377	0.0021	0.090059	849	15	832	12	896	60	838	10	92.86	0.88
I16-62Z-22	1.306	0.057	0.1417	0.0036	0.19055	848	25	854	20	833	96	852	17	102.56	0.73
GJ-1	0.82	0.022	0.09798	0.0013	0.20441	608	6	603	4	629	30	604	4	95.87	0.03
GJ-2	0.817	0.018	0.09686	0.0013	0.094243	606	5	596	4	645	27	600	3	92.40	0.03
GJ-3	0.822	0.021	0.09896	0.0012	0.26624	609	6	608	4	612	27	608	3	99.35	0.03
GJ-4	0.799	0.022	0.09791	0.0013	0.13873	596	6	602	4	574	31	601	3	104.88	0.03
GJ-5	0.821	0.019	0.0992	0.0013	0.12631	609	5	610	4	604	27	609	3	100.99	0.03
GJ-6	0.807	0.022	0.09757	0.0011	0.034058	601	6	600	3	603	32	600	3	99.50	0.03
GJ-7	0.812	0.019	0.0978	0.0013	0.015401	604	5	602	4	611	29	602	3	98.53	0.03
GJ-8	0.798	0.02	0.0972	0.0013	0.45064	596	6	598	4	587	24	598	4	101.87	0.03
GJ-9	0.828	0.023	0.09849	0.0012	0.03493	613	6	606	4	638	32	607	3	94.98	0.03
GJ-10	0.815	0.023	0.097	0.0012	0.089173	605	6	597	4	637	32	599	3	93.72	0.03
GJ-11	0.815	0.024	0.09735	0.0011	0.00062	605	7	599	3	629	34	600	3	95.23	0.03
GJ-12	0.81	0.023	0.09747	0.0013	0.022769	602	6	600	4	613	34	600	3	97.88	0.03
GJ-13	0.824	0.02	0.09743	0.0012	0.056875	610	6	599	4	651	29	602	3	92.01	0.03
GJ-14	0.827	0.023	0.09785	0.0012	0.012442	612	6	602	4	650	32	604	3	92.62	0.03
GJ-15	0.81	0.021	0.09792	0.0012	0.13811	602	6	602	4	603	29	602	3	99.83	0.03
GJ-16	0.809	0.022	0.09824	0.0012	0.043587	602	6	604	4	594	32	604	3	101.68	0.03
GJ-17	0.814	0.02	0.09817	0.0013	0.035801	605	6	604	4	609	30	604	3	99.18	0.03

GJ-18	0.83	0.023	0.09811	0.0011	0.22277	614	6	603	3	652	29	605	3	92.48	0.03
GJ-19	0.806	0.022	0.09736	0.0012	0.09875	600	6	599	4	605	31	599	3	99.01	0.03
GJ-20	0.82	0.019	0.09863	0.0013	0.051208	608	5	606	4	614	28	607	3	98.70	0.03
GJ-21	0.821	0.022	0.0986	0.0013	0.1974	609	6	606	4	618	30	607	4	98.06	0.03
GJ-22	0.826	0.021	0.09728	0.0012	0.12877	611	6	598	4	660	29	601	3	90.61	0.03
GJ-23	0.796	0.023	0.09843	0.0012	0.10352	595	7	605	4	554	33	603	3	109.21	0.03
GJ-24	0.823	0.022	0.09758	0.0012	0.018862	610	6	600	4	645	31	603	3	93.02	0.03
GJ-25	0.828	0.023	0.097	0.0013	0.23449	613	6	597	4	671	30	600	4	88.97	0.03
GJ-26	0.812	0.018	0.0978	0.0013	0.224	604	5	602	4	611	25	602	3	98.53	0.03
GJ-27	0.821	0.024	0.0983	0.0013	0.034457	609	7	604	4	624	34	605	3	96.79	0.03
GJ-28	0.811	0.024	0.09796	0.0012	0.14869	603	7	602	4	605	33	603	3	99.50	0.03
GJ-29	0.808	0.021	0.09888	0.0013	0.23398	601	6	608	4	577	29	606	4	105.37	0.03
GJ-30	0.802	0.022	0.0973	0.0013	0.15375	598	6	599	4	596	31	598	3	100.50	0.03
GJ-31	0.804	0.023	0.0976	0.0013	0.083732	599	6	600	4	594	33	600	3	101.01	0.03
GJ-32	0.816	0.019	0.0979	0.0014	0.024131	606	5	602	4	620	29	603	3	97.10	0.03
GJ-33	0.824	0.021	0.09846	0.0012	0.072465	610	6	605	4	629	30	607	3	96.18	0.03
GJ-34	0.808	0.023	0.09753	0.0012	0.2383	601	6	600	4	607	30	600	3	98.85	0.03
GJ-35	0.835	0.018	0.0977	0.0014	0.044279	616	5	601	4	674	27	607	3	89.17	0.03
GJ-36	0.79	0.022	0.0973	0.0012	0.010683	591	6	599	4	563	33	597	3	106.39	0.03
Plesovice-1	0.589	0.023	0.05424	0.00069	0.4667	470	7	341	2	1166	35	331	2	29.25	0.15
Plesovice-2	0.4282	0.0079	0.05398	0.00055	0.3184	362	3	339	2	512	20	343	2	66.21	0.13
Plesovice-3	0.477	0.013	0.05576	0.00065	0.049849	396	4	350	2	676	31	356	2	51.78	0.11
Plesovice-4	0.3921	0.0065	0.05361	0.00054	0.10537	336	2	337	2	331	21	336	1	101.81	0.14
Plesovice-5	0.4067	0.007	0.05475	0.00056	0.2559	346	3	344	2	366	20	344	2	93.99	0.14
Plesovice-6	0.4227	0.0071	0.05491	0.00055	0.27904	358	3	345	2	446	19	348	2	77.35	0.13
Plesovice-7	0.407	0.011	0.05381	0.00071	0.18596	347	4	338	2	406	31	339	2	83.25	0.09
Plesovice-8	0.4026	0.011	0.05474	0.00067	0.11333	344	4	344	2	343	32	344	2	100.29	0.09
Plesovice-9	0.3989	0.009	0.054	0.00065	0.2192	341	3	339	2	353	26	339	2	96.03	0.11
Plesovice-10	0.4029	0.0088	0.05437	0.00066	0.079797	344	3	341	2	360	27	342	2	94.72	0.10

Plesovice-11	0.4113	0.0091	0.05415	0.0007	0.19551	350	3	340	2	416	26	342	2	81.73	0.10
Plesovice-12	0.3911	0.0094	0.05333	0.0007	0.10108	335	3	335	2	337	30	335	2	99.41	0.10
Plesovice-13	0.4087	0.011	0.05474	0.00061	0.005898	348	4	344	2	377	33	344	2	91.25	0.10
Plesovice-14	0.415	0.0089	0.05449	0.00059	0.29668	352	3	342	2	422	23	344	2	81.04	0.11
Plesovice-15	0.397	0.0086	0.05386	0.0006	0.062902	339	3	338	2	348	27	338	2	97.13	0.11
Plesovice-16	0.3873	0.01	0.05336	0.00061	0.098469	332	4	335	2	313	31	335	2	107.03	0.09
Plesovice-17	0.4038	0.0093	0.05383	0.00062	0.090169	344	3	338	2	388	28	339	2	87.11	0.10
Plesovice-18	0.4028	0.01	0.05428	0.00058	0.053302	344	4	341	2	364	30	341	2	93.68	0.10
Plesovice-19	0.4183	0.01	0.05382	0.00061	0.3208	355	4	338	2	467	25	340	2	72.38	0.10
Plesovice-20	0.411	0.011	0.05385	0.0007	0.26145	350	4	338	2	427	30	340	2	79.16	0.10
Plesovice-21	0.4008	0.0084	0.05413	0.00062	0.080629	342	3	340	2	359	26	340	2	94.71	0.11
Plesovice-22	0.4039	0.0089	0.05443	0.00059	0.30383	344	3	342	2	363	24	342	2	94.21	0.11
Plesovice-23	0.441	0.012	0.05358	0.00068	0.12322	371	4	336	2	593	31	342	2	56.66	0.11
Plesovice-24	0.3967	0.0079	0.0545	0.00067	0.081524	339	3	342	2	320	26	341	2	106.88	0.11
Plesovice-25	0.405	0.012	0.05356	0.00066	0.042998	345	4	336	2	406	35	338	2	82.76	0.09
Plesovice-26	0.4019	0.01	0.05418	0.00069	0.043585	343	4	340	2	363	31	341	2	93.66	0.09
Plesovice-27	0.4121	0.0093	0.05454	0.00066	0.03208	350	3	342	2	404	28	344	2	84.65	0.10
Plesovice-28	0.4007	0.0093	0.0549	0.00063	0.046146	342	3	345	2	326	29	344	2	105.83	0.10
Plesovice-29	0.3988	0.01	0.05386	0.0007	0.26839	341	4	338	2	359	28	339	2	94.15	0.09
Plesovice-30	0.406	0.012	0.0552	0.00071	0.18151	346	4	346	2	343	34	346	2	100.87	0.09
Plesovice-31	0.4224	0.0087	0.05552	0.00065	0.22569	358	3	348	2	419	24	351	2	83.05	0.12
Plesovice-32	0.4493	0.0098	0.05508	0.0007	0.13372	377	3	346	2	573	26	353	2	60.38	0.10
Plesovice-33	0.4044	0.0087	0.0542	0.00061	0.011572	345	3	340	2	376	27	341	2	90.43	0.11
Plesovice-34	0.501	0.012	0.0533	0.00067	0.15796	412	4	335	2	874	26	346	2	38.33	0.10
Plesovice-35	0.418	0.008	0.05441	0.00061	0.19068	355	3	342	2	441	23	345	2	77.55	0.11
Plesovice-36	0.4582	0.011	0.05385	0.00067	0.2439	383	4	338	2	664	26	344	2	50.90	0.12
91500-1	1.866	0.057	0.1799	0.0023	0.13185	1069	10	1066	6	1075	32	1067	6	99.16	0.35
91500-2	1.89	0.06	0.1803	0.0029	0.03341	1078	11	1069	8	1096	35	1072	6	97.54	0.35
91500-3	1.912	0.065	0.1788	0.0029	0.10382	1085	11	1060	8	1136	36	1068	7	93.31	0.35

91500-4	1.832	0.055	0.1767	0.0026	0.18253	1057	10	1049	7	1074	31	1051	6	97.67	0.34
91500-5	1.882	0.066	0.1822	0.0025	0.004259	1075	12	1079	7	1066	38	1078	6	101.22	0.35
91500-6	1.892	0.063	0.1784	0.003	0.10092	1078	11	1058	8	1119	36	1065	7	94.55	0.35
91500-7	1.895	0.067	0.1812	0.0032	0.046806	1079	12	1074	9	1091	39	1076	7	98.44	0.35
91500-8	1.858	0.063	0.1783	0.0028	0.30608	1066	11	1058	8	1084	33	1060	7	97.60	0.35
91500-9	1.882	0.059	0.1789	0.0028	0.033741	1075	10	1061	8	1103	35	1066	6	96.19	0.36
91500-10	1.763	0.058	0.1773	0.0028	0.060745	1032	11	1052	8	989	36	1045	6	106.37	0.35
91500-11	1.905	0.05	0.1788	0.003	0.1184	1083	9	1060	8	1128	29	1071	6	93.97	0.35
91500-12	1.888	0.071	0.1794	0.0029	0.085817	1077	12	1064	8	1104	40	1067	7	96.38	0.34
91500-13	1.871	0.061	0.1776	0.0032	0.00311	1071	11	1054	9	1106	37	1061	7	95.30	0.35
91500-14	1.905	0.064	0.177	0.0032	0.25068	1083	11	1051	9	1148	34	1061	8	91.55	0.35
91500-15	1.846	0.064	0.1776	0.003	0.058082	1062	11	1054	8	1079	38	1057	7	97.68	0.34
91500-16	1.783	0.062	0.1784	0.0028	0.06665	1039	11	1058	8	1000	38	1052	6	105.80	0.34
91500-17	1.882	0.064	0.1795	0.0026	0.071191	1075	11	1064	7	1096	36	1067	6	97.08	0.35
91500-18	1.899	0.057	0.1789	0.0029	0.26716	1081	10	1061	8	1121	30	1068	7	94.65	0.35
91500-19	1.872	0.057	0.1772	0.0032	0.015907	1071	10	1052	9	1111	35	1060	7	94.69	0.34
91500-20	1.859	0.057	0.1797	0.0028	0.15288	1067	10	1065	8	1069	32	1066	7	99.63	0.35
91500-21	1.803	0.063	0.177	0.0031	0.071172	1047	11	1051	8	1038	38	1049	7	101.25	0.34
91500-22	1.846	0.063	0.175	0.0026	0.137	1062	11	1040	7	1108	35	1045	6	93.86	0.34
91500-23	1.835	0.057	0.1776	0.0028	0.055617	1058	10	1054	8	1067	34	1055	6	98.78	0.34
91500-24	1.855	0.053	0.1793	0.0026	0.079707	1065	9	1063	7	1069	31	1064	6	99.44	0.34
91500-25	1.864	0.059	0.1765	0.0029	0.12368	1068	10	1048	8	1111	34	1055	7	94.33	0.35
91500-26	1.872	0.065	0.1798	0.0029	0.11846	1071	11	1066	8	1082	37	1067	7	98.52	0.34
91500-27	1.883	0.054	0.181	0.0027	0.13503	1075	10	1072	7	1081	31	1073	6	99.17	0.34
91500-28	1.865	0.064	0.1766	0.003	0.11018	1069	11	1048	8	1111	37	1055	7	94.33	0.33
91500-29	1.849	0.072	0.1771	0.0029	0.069884	1063	13	1051	8	1088	41	1054	7	96.60	0.33
91500-30	1.825	0.069	0.1775	0.0031	0.11829	1054	12	1053	8	1057	40	1054	7	99.62	0.35
91500-31	1.852	0.061	0.1769	0.0028	0.035733	1064	11	1050	8	1093	36	1055	6	96.07	0.33
91500-32	1.844	0.063	0.1778	0.0027	0.12862	1061	11	1055	7	1074	36	1057	7	98.23	0.34
91500-33	1.782	0.065	0.1744	0.0029	0.21036	1039	12	1036	8	1044	37	1037	7	99.23	0.34

91500-34	1.902	0.064	0.1771	0.0028	0.36749	1082	11	1051	8	1144	31	1058	7	91.87	0.35
91500-35	1.896	0.069	0.1768	0.0028	0.19863	1080	12	1049	8	1141	36	1056	7	91.94	0.35
91500-36	1.825	0.06	0.1792	0.0029	0.048623	1054	11	1063	8	1038	36	1060	7	102.41	0.35

Appendix 5.2 Chapter 5 Zircon REE concentrations (ppm)

Zircon Grain	Y	Nb	La	Ce	Pr	Nd	Sm	Eu	Gd	Tb	Dy	Ho	Er	Tm	Yb	Lu	Hf	Th	U
CO17-26Z-5	868	4.16	0	29.83	0.226	3.65	4.99	2.33	25.2	7.58	84.1	28.35	123	24.7	216.3	43.4	8510	29.28	34.9
CO17-26Z-23	1257	4.14	0.022	39.3	0.533	8.8	11.54	4.56	42.1	11.69	125.1	43.5	177.5	34.3	300.3	58.2	7930	44.7	38.4
CO17-26Z-24	1056	5.54	0.082	21.8	0.274	3.85	6.43	2.8	32.3	10.09	101.9	34.7	142.1	27.52	246.3	46.3	9950	38	79.4
CO17-26Z-15	637	9.45	0	13.81	0.049	0.88	2.27	1.1	12.69	4.26	55.1	20.82	94.5	20.79	193.2	38.32	12040	13.67	72.7
CO17-26Z-6	1055	5.98	0	41.5	0.176	4.24	5.99	2.63	25.6	8.17	90.6	33.09	154.6	32.2	305.5	62.7	8300	38	45.9
CO17-26Z-22	1746	6.27	0.461	46.21	1.151	13.52	15.29	7.27	64.4	18.5	185.6	60.8	240.1	44.7	387	71.1	7170	74.8	52.2
CO17-26Z-19	1729	5.68	0.129	42.5	0.866	11.82	14.98	7.05	65.4	18.6	187.7	61.2	234.3	43.9	371	69.3	7010	70.2	47.4
CO17-26Z-14	5270	76	6.32	55.1	3.13	20.2	21.6	8.88	104.5	39.1	476	172	717	137	1170	205	13680	251	548
CO17-26Z-18	1535	6.98	0.071	46.4	0.689	9.82	12.59	6.48	54.1	15.85	162.3	52.8	206.9	39.25	334.3	62.8	7620	64.4	50.6
CO17-26Z-17	752	2.86	0.225	28	0.392	5.73	5.48	3.41	23.5	6.99	74	25.2	105.2	21.3	192	37.3	7330	20.5	22.3
CO17-26Z-16	949	18.84	0	11.7	0.151	1.98	2.57	1.3	15.4	5.95	78.6	30.93	144.6	30.41	280.7	54.2	14660	24.5	136.8
CO17-26Z-29	1559	5.67	0.042	50.5	0.662	9.63	12.5	5.92	49.9	15.4	161.3	54.5	218.9	41.6	369	69.9	7820	63.5	52.3
CO17-26Z-7	1790	6.66	0.143	47.6	0.754	10.23	13.6	6.62	61.4	18	185	62.3	246	46.4	394	73.2	7310	78.4	50.1
CO17-26Z-4	1022	16.84	2.62	18.5	1.48	10.26	8.51	3.89	27.9	8.6	94.5	33.9	150.1	31	278.3	54.3	13920	30.47	140.7
CO17-26Z-2	382.5	9.07	0	3.05	0	0	0	0.104	3.42	1.82	27.6	12.46	61.1	13.53	126.6	24.74	14060	7.02	72.7
CO17-26Z-25	1502	19.86	0.48	27.93	0.37	3.09	4.57	2.35	27.3	10.05	127.8	48.02	220.9	46.74	435.1	85.3	11960	46.59	139.8
CO17-26Z-10	1354	8.13	4.24	25.8	3.34	18.8	18.5	5.17	49.5	13.89	135.9	46.5	186.7	35.5	306.4	56.3	9830	120.4	256
CO17-26Z-12	679	3.13	0.094	27.42	0.199	2.88	4.07	1.91	19.8	6	65.4	22.28	97.3	19.9	180.1	34.4	8310	20.62	23.27
CO17-26Z-28	818	2.84	0.027	26.4	0.345	6.44	7.19	3.68	30.6	8.37	88	28.7	111.6	21.49	186.3	35.3	7770	26.6	24.9
CO17-26Z-11	1112	7.33	1.83	47.1	1.27	11.28	10.63	4.96	35.9	10.24	106.4	37.74	157.8	32.1	290.3	58.54	8530	36.45	56.1
CO17-26Z-9	787	3.4	0	26.8	0.152	3.43	5.53	2.66	24.2	7.38	77.5	26.5	109.2	21.65	190.8	37.6	8400	24.31	26.4

CO17-26Z-20	1184	5.54	0	44.5	0.16	3.21	6.66	2.96	30.4	9.65	108.9	39	165.7	33.6	303	58.2	7910	38.6	42.8
CO17-26Z-30	1058	6.13	0.89	30.7	0.582	5.37	7.62	3.13	28.8	9.25	98.5	34.7	153	30.8	286	56.6	9790	42.9	57.2
CO17-26Z-27	460	1.7	0	18.38	0.063	1.67	2.98	1.43	12.77	4.08	44.4	15.07	65.5	13.11	117.6	23.99	7940	17.51	18.84
CO17-26Z-21	700	3.84	0.85	27.4	0.404	3.99	5.06	2.44	20.2	6.25	67.2	23.15	95.2	19.47	172.9	34.8	7890	18.7	28
CO17-26Z-1	919	3.43	0.038	28.5	0.255	5.57	8.4	3.36	30.6	9.09	95.6	32.2	127	24.72	218.8	41.4	7640	28.7	26.99
CO17-26Z-8	895	3.52	1.75	36.3	1.21	8.27	9.7	4.18	30.7	8.82	90.1	30.83	125.6	25.06	219.3	43	7920	28.1	35
CO17-26Z-26	1280	8.07	6.28	72.1	3.37	23.1	20.1	8.36	54.7	13.68	130.7	42.98	175.1	34.14	311	61.35	7760	37.73	49.2
CO17-26Z-13	960	6.7	1.01	35.6	1	8.03	8.18	4.06	29.1	8.48	89.8	32.2	132.4	27.5	251	48.8	9050	27.4	41.2
CO17-26Z-3	1500	9.5	3.78	53.3	2.1	15.35	15.2	6.28	54	14.3	151	51.9	203	38.7	348	64.8	8310	66.1	74.7
CO17-55Z-15	360	1.1	0.02	12.07	0.047	0.82	1.06	0.243	6.52	2.2	28.2	11.43	55.8	12.87	127.2	28.31	8130	47.2	75.2
CO17-55Z-29	576	1.23	0	9.23	0.059	0.85	2.3	0.612	12.3	4.1	48.8	19.1	86.3	18.51	171.5	34.84	8110	58.9	74.5
CO17-55Z-32	446.9	0.94	0	7.62	0	0.26	1.25	0.23	7.54	2.7	34.5	13.83	70.4	14.47	142.9	30.19	8600	52.5	83.6
CO17-55Z-12	480	1.82	0.405	14.74	0.255	1.69	1.51	0.441	7.55	2.65	35.2	14.83	75.5	16.73	173.3	37.89	10380	89.2	269
CO17-55Z-23	1611	1.87	0	15.09	0.29	4.72	8.2	3.04	40	12.36	143.8	54.3	239.8	51	477	97.4	6390	114.9	127.8
CO17-55Z-11	997	1.41	0.2	20.73	0.346	4.44	6.13	1.93	25.5	7.35	84.9	33.4	150.5	33.2	320	65.2	8410	135.7	139.8
CO17-55Z-19	440.1	8.05	0.48	6.61	0.051	0.22	0.33	0.099	5.76	2.15	32.5	14.96	74	17.16	170.2	37	7890	22.41	72.6
CO17-55Z-22	1030	3.99	1.04	27.3	0.74	5.16	3.49	1.01	21.1	7.09	86	33.5	149	31.8	295	56.9	11440	206	303
CO17-55Z-7	986	1.19	0	9.42	0.136	2.82	4.56	1.64	24.5	7.45	88.6	33	151	32.1	301	63.1	8630	80.3	140
CO17-55Z-1	921	1.7	0.099	9.28	0.112	1.56	2.62	1.07	14.8	5.78	72.7	30.15	144.6	32.04	310.4	65.9	7050	69.5	134.5
CO17-55Z-2	401	1.02	0.096	12.68	0.108	0.81	0.97	0.195	7.19	2.42	31.4	12.81	61	13.07	127.6	25.77	8930	32.8	49
CO17-55Z-21	441	1.83	4.3	23.5	0.86	4.4	2.22	0.35	8.1	2.57	36.2	14.93	69.9	14.84	147.3	28.6	8980	66.6	149.3
CO17-55Z-30	2450	2.93	0.097	20.5	0.51	8.7	16.3	5.82	72.4	21.1	232	85.3	364	74.1	677	132	6900	210	178
CO17-55Z-5	955	0.7	0	5.8	0.114	2.23	3.88	1.33	22.4	7.48	87.7	32.7	145.1	30.3	278	55.5	7180	56.4	76.6
CO17-55Z-28	2635	2.4	0.077	21.07	0.58	10.4	14.8	5.6	69.3	21.45	233	86.8	387	80.6	765	151	6530	313	307.8
CO17-55Z-10	295.9	0.83	0.164	11.51	0.075	0.52	0.79	0.161	4.93	1.7	22.4	9.22	46.3	10.53	103	22.53	9320	61.7	161.1
CO17-55Z-3	767	5.64	0.705	17.82	0.571	3.14	1.95	0.68	9.29	4	55	24.1	118.8	26.7	264	55.7	10750	160.1	469
CO17-55Z-31	251.1	1.04	17.4	50	4.3	18.6	3.52	0.68	5.11	1.69	19.52	7.64	39.5	9.27	94.2	21.02	8580	30.73	109.2
CO17-55Z-25	780	1.53	0.09	13.4	0.172	1.84	2.72	1	16.2	5.8	69	25.1	120	25	227	50.3	10160	107	146
CO17-55Z-24	1540	3.35	5	30.6	3.24	22	8.2	3.12	28.1	8.8	119	49.3	236	51	501	104	9150	200	352

CO17-55Z-18	1438	2.29	0.356	13.59	0.339	3.84	7.43	2.05	37.1	11.61	134.1	50.4	219	43	402	78.5	6700	129.8	162.8
CO17-55Z-8	336.6	1.35	0.258	13.86	0.256	1.75	1.44	0.42	5.98	2.05	24.76	10.6	52.9	12.07	118	25.99	9720	73.1	135.2
CO17-55Z-27	1063	8.15	0.289	9.76	0.206	0.93	1.19	0.193	10.13	5.04	73.4	34.21	172.1	39.61	409.1	84.6	10540	128.2	998
CO17-55Z-26	253.8	0.89	0.146	5.69	0.145	0.99	0.9	0.225	3.26	1.27	16.94	7.21	39.5	9.51	105.4	23.81	9890	77.9	470.2
CO17-55Z-6	296.1	0.88	0.065	13.66	0.091	0.69	1.06	0.393	4.82	1.78	22.9	8.96	44.6	10.37	108	24.07	9240	65.52	124.7
CO17-55Z-13	577	1.21	0.145	14.18	0.109	1.57	2.53	0.54	12	4	48.9	19	83.4	18.5	173	35.2	8710	69.4	124
CO17-55Z-4	407	3.27	2.96	15.4	1.97	9.7	3.34	1.41	5.71	1.93	28.3	12.22	66.4	16.36	181.4	41.5	10760	44	670
CO17-55Z-16	1325	2.48	0.129	32.5	0.196	2.8	4.92	2.09	27.1	9.07	105.9	41.5	193	42.2	415	86.4	8890	187.1	281
CO17-55Z-14	1520	6.78	1.16	19.6	0.777	4.81	4.29	1.27	27.4	10.3	128	50.9	234	46.9	425	82	9700	223	520
CO17-55Z-9	763	2.78	1.31	20.1	0.9	5	2.29	1.03	11.6	4.25	56.8	24.2	115	26.8	264	57.3	9730	128	257
CO17-55Z-20	479	2.28	1.81	13.67	1.3	7.3	3.2	1.3	8	2.68	36.2	15.2	78.2	18.3	191	40.3	11810	56.1	295
CO17-55Z-17	458.5	1.45	0.195	9.37	0.156	1.41	0.94	0.332	7.91	2.77	35.4	14.73	71.1	16.23	163.1	34.03	10360	39.6	150.5
CO17-58Z-1	1121	5.9	17.7	63.5	8.74	54.2	24.4	7.43	35.3	7.09	82.6	34.5	192.5	47.3	475	101.2	12190	39.8	574
CO17-58Z-2	1014	6.7	57	196	27.5	153	54.6	7.61	62.6	8.75	83.9	32.7	161.1	36.9	359	74.5	12650	54.5	663
CO17-58Z-4	1328	5.09	4.80E+03	8.20E+03	770	2750	460	12.5	325	36.3	181	46.7	189.8	42.14	403.5	85.8	12200	2000	454
CO17-58Z-33	1177	5.35	24.6	91	15.16	103.2	43.3	5	55	8.43	92	37.1	198.4	46.2	455	95.5	11960	33.1	369
CO17-58Z-10	2258	8.28	27.8	107	13.8	88	24.7	7	52.2	14.91	189.9	75.6	359	76.5	679	130.7	12070	255	1322
CO17-58Z-25	973	8.41	12.9	47.2	7.16	45.5	14	2.92	22.9	5.22	69.1	31.4	162.6	38	376	76.7	12740	99.4	1079
CO17-58Z-6	3720	10.72	478	1736	321	2195	872	94.3	871	87.9	506	128.5	488	101.3	916	172.5	13590	98.5	1233
CO17-58Z-17	2048	9.96	46.4	136.5	17.89	118	33.4	4.55	46.9	12.36	155	66.8	330.7	74.6	707	135	13570	124.7	1330
CO17-58Z-28	1334	3.32	11.5	29.9	3.17	22.2	10.3	1.68	26.2	8.12	108	43.6	215.8	47.9	452	95.4	11500	143.3	678
CO17-58Z-8	627	4.7	0.342	10.33	0.216	1.7	1.8	0.125	11.23	4.2	53.7	21.29	97.3	21.12	187.9	37.24	11230	60.2	152.7
CO17-58Z-16	1640	7.07	71	180	22.7	132	39.5	5.28	51.4	11.3	137	55.6	268	59	559	108	13960	133	1080
CO17-58Z-22	1304	5.02	32.9	114	16.3	88	29.9	4.9	38.3	8.17	96.4	40.9	218	55.2	602	132	16310	94.2	1650
CO17-58Z-5	3620	10.11	147	373	45.7	268	99.9	21.3	141.9	26.7	297	118.2	583	125	1116	220	10500	227	999
CO17-58Z-13	593	3.93	15.1	54.8	7.9	49.7	17	2.41	24.6	4.72	50.7	19.81	94.9	21.7	209	43.3	12410	51.7	369
CO17-58Z-24	1191	5.46	23.2	72.8	9.88	70.4	25.2	3.68	34.9	6.82	83.7	36.4	202.3	51.2	522	110.2	13620	49.2	568
CO17-58Z-11	3900	7.15	72	249	39.4	265	102	10.7	157	34.4	366	133.8	593	119.2	1059	206.8	9550	385	734
CO17-58Z-23	1089	6.44	48.6	172	23.9	139	40.4	12	45.1	8.1	86.7	34.8	175.7	40.5	407	82.6	11760	102	688

CO17-58Z-32	2160	6.66	205	810	148	1050	406	53.8	423	43.4	265	71.6	286	59.4	568	116.9	9800	120.5	514
CO17-58Z-9	1185	4.69	24.1	97.1	12.47	89.5	39	7.46	56.8	11.19	108	40	172.9	35	317.7	63.3	11790	147.9	344
CO17-58Z-14	2667	9.19	79.1	253	32.8	202	67.2	18.4	100.9	21.9	235.6	88.8	405	82.8	744	138.6	10220	313.8	955
CO17-58Z-15	1513	11.9	127	304	39	228	71.7	9.21	87.2	12.85	123.3	46.8	233	53.3	532	114.4	12130	184	1027
CO17-58Z-26	809	6.02	54.1	193	35.8	236	106	11.1	125	13.7	91	27.2	113.2	23.8	231	45.2	11500	83.6	336
CO17-58Z-19	1347	4.58	29.1	111	18.5	107	39.8	4.95	52.6	10.7	114.7	44.9	214	47	444	87.1	11240	101	618
CO17-58Z-30	1410	13.9	111.8	334	47.1	262	100	12.5	120	14	108.5	38.8	195.9	48.9	563	125.9	15290	149.5	1464
CO17-58Z-27	1276	23.4	78.8	203	25.5	142.1	35.9	12.3	42.3	7.79	93.7	39.27	202.5	47.6	495	103.8	27390	70.6	1582
CO17-58Z-3	1364	23	178.7	486	70	400	152.9	27.3	160.2	20.02	141.7	40.8	158.1	33.27	338.1	64.6	3.31E+04	78.8	884
CO17-58Z-21	1903	9.23	168	444	63.6	406	160	18.2	171	21.3	178.5	60.4	280.6	65	672	129	15000	154	1931
CO17-58Z-7	1930	5.32	148	365	58	362	172	16.9	198	24.8	194	64	273	57.9	530	104	11780	142	608
CO17-58Z-20	492	1.44	10.51	33.2	4.31	28.8	15	3.02	25.6	4.65	45.4	15.38	71.4	15.57	154.6	34	11580	50.1	171
CO17-58Z-31	1430	6.26	72	282	38.3	207	57.2	12.8	61	10.9	115.3	46.1	223	52.6	506	103.5	14890	94.3	970
CO17-58Z-12	3424	8.92	243.2	797	116.3	622	167.7	33.9	200	34.2	325	114.7	505	106.9	964	176.6	9880	607	1609
CO17-58Z-18	2540	11.7	396	750	93.8	513	157	17.9	193	27.7	234	82.8	379	83	762	149.3	12410	267	1478
I16-07Z-2	762	1.33	0.023	13.39	0.038	1.24	3.22	1.01	16.5	5.38	66	24.9	112.1	24.12	217.4	45.2	7320	71.5	93.5
I16-07Z-16	1837	4.38	1.08	39.4	0.75	5.3	7.03	1.51	39.8	14.01	161.8	62.4	280.1	55	501	97.1	8670	213.1	218.8
I16-07Z-8	809	3.71	0.69	18.6	0.45	5.9	4.88	1.32	17.7	5.86	70.4	26.6	119.6	24.5	234	45.4	9870	93.7	233
I16-07Z-5	1442	4.09	1.3	46.8	1.62	15.9	11.9	2.53	42.5	11.65	126.9	50.3	214	41.4	376	71.8	7620	255	340
I16-07Z-4	1128	1.77	6.38	59.4	5.26	36	23.9	9.65	57.6	13.2	118.5	35.87	146.5	30.49	268.1	50.5	10910	140.9	426
I16-07Z-9	1150	6.9	0.39	16.3	0.51	2.29	1.44	0.36	14.4	6.3	89	38.6	186	42.5	409	79	13710	151	666
I16-07Z-12	2633	14.05	5.94	99.3	3.1	19.8	15.2	4.76	68.3	21.92	249	90.4	382	75	650	121.3	8640	845	595
I16-07Z-17	2359	9.67	2.51	60.8	1.28	9.7	9.5	2.41	49.5	16.94	205.2	79.4	349	70.9	621	116.7	10030	473	628
I16-07Z-6	3102	20.8	3.83	40.1	0.48	4.1	5.4	1.08	43.2	18.3	250.7	99.9	469	101.7	899	171.4	10060	739	1658
I16-07Z-11	2511	14.8	23.5	73.3	5.35	28.2	10.4	2.52	43.2	15.92	205.4	79.8	374	76.9	679	125.2	10940	362	893
I16-07Z-15	2977	13.16	4.15	76.5	4.11	33.1	21.8	3.5	70	21.79	256.1	97.7	438	88	777	144.1	10170	646	993
I16-07Z-1	1710	14.2	3.54	42.5	4.03	25	9	2.73	25.7	8	119	53.1	275	63.7	624	130.6	14260	183	1201
I16-07Z-14	2382	27	8.7	49.6	3.73	23.6	7.18	1.64	31.9	13.16	184	78.3	376.3	84.8	782	151.4	12740	297.4	1308
I16-07Z-7	3400	15.6	10.6	101.8	8.61	59.2	34.1	4.97	84.3	24.43	287	110.6	491	100.1	847	158.9	11720	498	1180

I16-07Z-13	2448	21.28	18.8	94	7.77	47.1	17.2	4.78	45.3	15.03	192.5	79.2	372	80.2	726	140.2	14260	387	1488
I16-07Z-3	4470	30.7	85	259	19.6	74.2	28.2	9.16	83.7	28.8	359	146.5	692	146	1360	261.1	10290	1690	2451
I16-07Z-10	4870	19.6	35.2	234.9	23.7	144.4	68.8	23.2	166.1	43.3	457	160	650	128.8	1101	198	10210	2595	2005
I16-17Z-10	1171	2.05	3.18	53.9	2.61	17.8	13.4	4.47	41.6	11.43	113.1	38.8	161.3	32.71	283.9	55.7	9350	211.9	351.4
I16-17Z-8	501	1.06	1.83	18.6	1.32	8.3	5.7	2.92	15.4	5.11	48.5	17.3	71.9	15.4	138	26.9	11920	46.4	162
I16-17Z-7	816	1.39	45.4	155	17.9	90	22.7	5	36.9	8.65	83.6	27	118.7	23.6	216	40.8	9110	163.2	306.9
I16-17Z-11	966	1	2.25	30.2	2.51	18.1	15.6	7.81	38.9	11.25	103	32.3	132.1	27.2	235.9	47	7960	64.9	154.3
I16-17Z-14	742	0.6	1.48	19.7	1.16	9.3	9.3	3.98	25.5	8.05	76.6	24.7	103.3	21.8	192.8	39.5	8290	62.6	143.6
I16-17Z-2	900	0.68	12.3	85	11.2	59	45	14.1	79	16	114	28.8	101	19.3	169	32.3	9310	60.1	143.4
I16-17Z-5	951	1.19	3.55	36.5	4.18	25.4	18.7	8	43.4	11.3	108	30.4	126.1	24.5	223	41.7	8900	86.3	227
I16-17Z-9	1152	2.94	5.63	50.3	4.69	30.1	16.8	7.36	44.4	12.33	120.4	38.9	155.9	29.9	258.3	45.9	10490	140.7	419.1
I16-17Z-1	1658	1.8	7.08	75.3	8.38	52	49.7	22.3	103.6	27	222.9	58.6	211.3	38.3	331	56	8260	239.3	380.7
I16-17Z-12	1118	1.35	4.35	53.2	4.81	32.4	33.2	14.5	73	14.9	128	36.6	147.5	28.9	253	48	9710	126.6	289
I16-17Z-13	3170	5.7	56	298	39	232	179	67.4	290	70.4	525	115.9	376	65.6	508	79.2	10150	271	857
I16-17Z-6	3360	6.92	45.4	414	54.4	344	191	68	271	62.8	489	120.4	391	72.3	606	93	10720	317.2	1180
I16-17Z-15	16750	19.7	203.8	1336	183	1157	892	307	1521	371	2750	584	1805	298	2160	307	17480	492	3140
I16-18Z-27	3840	15.5	0	66.5	0.12	3.08	8.86	1.69	63.5	23.97	321	131.2	603	129.1	1182	235.3	8620	568	681
I16-18Z-23	2816	10.07	0.7	44.3	0.286	2.55	6.4	1.44	42.4	16.47	225.9	91.5	439.2	95.4	920	185.7	7810	212	283.3
I16-18Z-2	974	0.71	0	11.69	0.086	1.62	3.99	1.68	22.7	7.31	86.5	33	149.7	31.26	295.2	60.5	7430	38	56.3
I16-18Z-28	2877	11.49	15.36	61.8	3.85	17.4	10.3	1.58	46.9	18.39	238.6	97.2	456	99.2	957	191.7	8970	236.7	483.3
I16-18Z-26	5470	29.4	9.3	67.6	2.76	13.6	12	2.16	75.6	33.3	446	182	856	179.1	1688	321.6	9000	678	1276
I16-18Z-13	6550	24.7	1.4	51.5	0.58	5.6	10.5	1.9	89.5	37.6	521	211.1	1003	209.5	1937	368.7	9300	827	1216
I16-18Z-29	9010	56.8	0.91	121.7	0.54	8.6	20.1	3.13	138.3	57.1	744	300	1349	288	2590	497	8820	1743	2230
I16-18Z-6	5830	38.9	1.28	43.3	0.96	5.7	7.72	1.39	68.1	33.2	457.5	191.9	916	196.4	1827	350.9	9880	802	1626
I16-18Z-14	3000	30.66	12.4	40	3.06	14.4	8.8	1.25	39.8	17.8	245	100.1	485	114.1	1185	243.1	2.04E+04	322	1294
I16-18Z-21	5430	62	19.3	106.3	9.11	55.1	44	7.57	153	48.4	531	179.9	768	170.5	1574	303.4	11390	637	2634
I16-18Z-31	5470	61.3	6.61	69.2	1.67	9.6	10.4	1.67	72.7	32.2	450	185.3	863	187.9	1732	332	9460	888	1835
I16-18Z-25	2971	44.2	62.1	130.4	10.84	56.3	26.9	6.2	75.8	24	275.5	97.6	443	108.4	1215	251	25850	141	1811

I16-18Z-15	6880	29.9	26.6	69.9	3.77	17.2	10.72	2.16	81.4	37.3	532	224.3	1073	232.8	2128	406.1	9700	820	1749
I16-18Z-16	3320	18.55	7.69	55	3.58	21.1	12.4	3.04	58.4	21.06	278	108.7	515	117.1	1146	234.5	11930	317	1229
I16-18Z-8	4180	17.2	2	48	0.99	8.9	11.9	2.32	64.5	26.4	352	138.8	648	137.4	1259	243.3	8650	372	747
I16-18Z-10	2311	14.53	33.5	122.2	13.77	72.1	23.1	4.53	53.3	17.8	202.1	73.5	341.6	71.1	681	133.5	9970	194.1	740
I16-18Z-7	3798	37.6	28.2	108.1	8.53	46	17.8	3.37	72.7	26.37	335	127.3	587	124.1	1139	218	10560	643	1291
I16-18Z-5	4860	64	27.3	113	11.6	63	32	2.53	93.9	32.74	411.3	160.2	755	163.4	1499	286.8	13380	885	2111
I16-18Z-22	5210	45	147	265	20.9	87.1	25	4.02	81.9	31.62	420.6	171	796	177.9	1645	320.5	13510	766	1832
I16-18Z-12	7100	29.9	5.51	61.3	1.94	11.4	12.5	2.48	92	38.82	548	229.6	1074	228.4	2045	393.2	10870	724	1288
I16-18Z-19	3070	42.3	20.8	166.4	8.41	47.5	24.4	4.22	89.3	27.8	302	103.4	439	87.7	778	148.4	8790	623	915
I16-18Z-18	4913	43.2	50.5	181.6	14.45	70.3	27.2	5.54	95.3	33.2	432.6	169.7	761	159.5	1489	286.5	10160	655	1402
I16-18Z-4	5625	47.9	27.7	109.2	7.34	35.2	16.6	3.39	82.7	34.02	459.6	188.6	868	187.7	1754	341.5	10680	885	1688
I16-18Z-17	7020	69.2	90.1	295	31.8	158	71	9.59	186	56.7	634	233.2	1040	210.5	1915	366.2	9080	1175	1900
I16-18Z-1	2530	34.17	3.47	23.2	1.4	7.5	4.54	1.33	28.5	12.51	185.7	81.9	410	97.9	1009	206.9	10840	102	1229
I16-18Z-3	3766	77.3	35.6	219.3	21.4	123.3	56.1	7.59	145.8	41.2	417	128	461.4	77.7	627	104.5	11920	315	1356
I16-18Z-9	1462	39.5	21.7	125	10.79	68.6	27.9	7.25	78.9	21.4	177	52.1	170	29.4	223	35.9	2040	184.6	328
I16-18Z-30	4470	77.9	68.6	179	18	80.1	36.4	17.9	125.3	36.4	393	133.8	590	133.7	1459	291.4	21800	229.7	2002
I16-18Z-11	5220	34.7	30.7	79	7.41	34.4	21.9	2.87	88.7	34.1	437	168.5	773	162.7	1514	292.6	9980	484	2430
I16-32Z-2	2531	4.95	0	22.23	0.086	1.35	4.9	1.16	42.1	15.75	210.5	86.3	379	81.1	745	148	9240	146.9	249.5
I16-32Z-21	1420	2.15	0.127	10.95	0.158	1.86	3.16	0.553	22.9	8.53	113.9	46.9	224	48.7	463	95.2	8810	99.3	190.2
I16-32Z-3	1628	2.58	0.67	9.6	0.34	3.62	5.17	0.6	29.9	10.5	138.4	56.2	254.8	52	487	95.9	8034	73.1	117.2
I16-32Z-5	4500	23.6	54.2	127.9	9.8	44	24.9	6.51	100.9	32.5	395	145.7	640	134.5	1233	232.8	9080	576	640
I16-32Z-22	3886	39.5	11.4	96.5	3.76	22.9	13.3	2.95	68.1	24.21	330.1	128.9	599.8	131.9	1225	234.2	8980	748	1365
I16-32Z-13	4304	39.4	53.9	145.6	11.2	50.1	26.9	7.62	90.2	31	377	144.5	660	144.6	1323	259.3	9040	677.4	1076
I16-32Z-10	5280	49.6	140.1	315.7	30.4	148	68.3	16.37	154.8	43.1	459	168.6	740	157.1	1444	276.7	8940	802	1188
I16-32Z-12	6870	87.7	79.3	237	30.2	136	63.8	17.8	158	49	553	200	932	199.4	1869	344	9810	1027	1900
I16-32Z-27	7660	188.4	188.5	945	121.8	709	356	69.8	389	81.2	726	229.3	960	202.6	1925	363	9380	939	1152
I16-32Z-14	10550	93.7	233.2	499	48.1	239.9	108.8	29.5	285	78.3	848	301	1295	268.9	2457	452	9960	1640	2605
I16-32Z-1	5250	44	157	349	37.3	135.9	40.3	21.4	109.5	34.6	420	160.6	744	163.7	1539	298.7	10280	779	1217
I16-32Z-18	5040	62.5	194	570	62.1	261	65	14.7	127.4	37.6	419	156.4	737	161.5	1477	288.6	8630	833	1201

I16-32Z-9	8270	81.5	379	1034	135	568	166	51.1	249.2	68	722	243.5	1045	212.6	1916	349.3	9210	870	1390
I16-32Z-26	7730	86.8	121.3	425	45.8	193	71	24.1	166.5	49.9	571	209.4	945	204.8	1885	350.8	9680	810	1328
I16-32Z-7	6780	49.4	104.2	443	50.1	243.6	83.7	26.51	150.1	43.9	479.5	165.2	724	161	1573	297.4	9020	741	1157
I16-32Z-20	7310	212	93.4	445	45.7	255	88.8	34.9	174.3	49.3	520	184.1	809	174.6	1615	301.3	9480	863	1386
I16-32Z-6	12580	149.5	183	552	72.7	327	157.7	36.8	352	99.1	1017	326	1429	316.2	2980	540	8470	1333	1575
I16-32Z-19	5900	88.4	210	873	99.2	410	99.4	16.7	140.8	40.7	472.3	178.3	838	181.3	1702	327.8	8960	676	1204
I16-32Z-24	6770	74.7	174.3	482	56.8	291.1	150.4	37.3	247.4	58.6	547	174.3	772	181.5	1873	389.1	10070	539.5	1417
I16-32Z-15	6500	84	373	600	51.6	195	62	48	140	41.5	493	184	852	184	1710	340	10440	783	1258
I16-32Z-8	5770	69	262.1	633	68.5	282.3	82.4	19.51	131.9	39.8	442	159.4	766	180.6	1873	375.1	10320	1087	1858
I16-32Z-25	5190	40.7	149.9	359	41.5	167.7	55.5	24.1	131.5	37.5	407	149.2	691	150.5	1434	287.1	9180	640	1266
I16-32Z-4	7910	62.8	178.4	824	74.3	344	118.8	38.1	231.8	63.5	639	210.6	926	198.6	1785	344.1	9230	846	1433
I16-32Z-23	6850	96.2	143.3	531	50.2	210.4	90.6	28.4	199.9	49.9	527	187.6	863	186.8	1796	351.8	9210	2020	1590
I16-32Z-17	5450	127	188.7	602	68.2	312	93.3	17.27	146.9	38.4	429.8	168.2	807	184.2	1792	357	9190	1147	1487
I16-32Z-11	5860	89	168	197	42	175	63.6	18.1	148	46.4	506	175	803	181.6	1756	337	11500	615.7	1248
I16-32Z-16	7630	107.4	126.5	312.8	38.4	164.7	66.4	23.5	162.6	50.2	564	203.7	934	220.4	2224	455.5	14020	799	1994
I16-34Z-19	1047	3.99	0.99	12.82	0.702	5.5	3.33	0.72	17.3	6.22	84.7	34.5	162.8	34.4	320.7	68	7990	70.2	137.7
I16-34Z-26	520	0.93	0	2.8	0.035	0.3	0.95	0.083	7.2	2.81	40	17.2	88	19.1	204	47	10690	23.7	60
I16-34Z-25	1219	2.33	16.6	68.6	9.27	50.3	16.9	2.55	33.1	9.33	102.1	39.7	187.2	41.1	387.6	77.1	8750	75.2	156.4
I16-34Z-6	1506	1.83	0	9.24	0.052	1.17	3.3	0.52	25.2	9.77	126.9	50.1	240.8	49.6	472.1	95.1	7865	90.3	161
I16-34Z-29	1397	1.18	0	8.42	0.044	0.83	2.89	0.439	22.8	8.12	111.4	45.7	219.8	47.3	462.8	97.2	9060	89	190.4
I16-34Z-10	1471	1.72	0.71	13.49	0.316	4.21	4.71	0.74	28.6	10.06	124.5	49.6	230.4	48.2	446	89.9	9020	80.7	150.9
I16-34Z-16	1141	2.17	0	6.99	0.053	0.86	1.96	0.296	17.8	6.79	89.7	37.79	179.3	40.27	367.7	77.7	7780	68	121.6
I16-34Z-1	1100	1.69	0	6.26	0.022	0.42	2.22	0.35	17	6.61	86.2	35.85	176.5	38.96	365.2	78.6	7990	51	128.6
I16-34Z-27	1127	1.8	0.013	8.87	0.068	1.63	2.56	0.333	16.9	6.2	87.3	37.2	179.9	40.9	406	86	8870	64.8	163.3
I16-34Z-5	977	1.28	0.028	5.28	0.052	0.35	1.41	0.31	12	5.13	74.6	31.51	156.8	35.07	347.8	71.5	8400	37.09	103.9
I16-34Z-12	1190	1.76	0	6.57	0.023	0.58	2.23	0.407	16	6.38	89.5	38.9	195.5	43.33	422.4	88.7	8120	50	137.1
I16-34Z-15	2133	1.42	0	9.96	0.117	3.24	6.33	1.01	38.7	14.18	181.5	72.8	332.7	68	621	125.7	7820	129.4	195
I16-34Z-13	1624	1.31	0.073	9.23	0.09	2.2	3.9	0.64	30.4	10.58	135.4	54.5	252.4	53.3	506.6	102.6	8590	112.2	198
I16-34Z-2	1597	1.32	0.521	14.54	0.325	3.58	4.69	0.68	27.9	9.85	127.6	52.8	249	55	512	106.7	9630	117.6	218

I16-34Z-14	854	1.43	0.503	6.65	0.352	2.49	3.02	0.47	15.8	5.24	69.6	27.95	133.7	29.32	289	62.1	9850	47.6	121.3
I16-34Z-7	1062	1.61	0.106	5.85	0.092	1.35	2.45	0.53	13.9	5.82	84.1	33.98	165.7	37.38	375	77.7	7990	41.3	114.6
I16-34Z-8	1178	2.27	0	7.64	0.055	0.61	2.44	0.315	17.3	6.86	90.4	38.95	194.1	42.08	415	87.2	7800	58.62	140.7
I16-34Z-24	1057	2.63	8.2	29.5	2.98	17.5	4.5	1.98	18.5	6.39	81.8	35.12	174.6	38.83	390.5	84.9	8310	46.13	154.9
I16-34Z-30	1868	1.45	0.126	10.35	0.21	3.11	6.09	0.87	34.1	12.94	162	62.4	289.9	59.7	553	112.1	8450	118.2	199.5
I16-34Z-4	1183	0.97	0.124	7.25	0.092	1.32	2.36	0.467	19.9	7.46	94.2	40.5	188.9	41.6	400	84	9320	66.9	211.9
I16-34Z-17	1098	1.85	0.101	9.84	0.063	1.24	2.51	0.4	16.2	6.76	89.6	37	176.3	38.54	367.5	76.4	7990	99.9	190.5
I16-34Z-11	973	1.43	0.79	9.73	0.375	3.55	2.23	0.57	14.3	5.52	73.7	31	150.5	35	354	75.3	10110	67.7	159
I16-34Z-28	1369	2.73	0.01	9.2	0.041	0.93	2.62	0.46	21.7	7.91	109.9	44.77	222.6	48.6	470.4	101.7	7760	77.3	165.5
I16-34Z-9	1182	2.82	1.43	12.9	0.82	7	6.26	1.32	26.2	8.03	99.9	40.2	182	38.5	364	76	7980	84.2	172.5
I16-34Z-21	1677	7.76	1.11	16.04	0.587	6.02	5.29	1.34	27.9	10.88	140.6	56.7	262.5	54.61	510	105.3	8440	121.2	205.7
I16-34Z-23	1429	2.37	0.523	11.95	0.298	2.87	3.84	0.58	22.1	8.22	110.9	46.9	226.6	51	501	106.8	9790	142.3	265.5
I16-34Z-20	929	1.49	0.067	6.56	0.11	1.03	1.6	0.33	12.9	5.14	70.7	30.4	149.2	34	331	72.1	8310	42.6	155
I16-34Z-18	687	2.05	4.89	22.7	1.74	9.5	4	0.6	13.5	3.57	47.1	20.11	101.4	27.6	306.1	73.2	11470	140.3	301.4
I16-34Z-22	631	3.32	6.44	32.9	3.2	21	9.8	2.66	23.6	4.75	47.1	17.55	91.9	21.9	260	69.9	19640	59.1	208.1
I16-46Z-22	1376	43.6	1.41	6.14	0.435	3.64	2.95	0.85	14.3	5.43	85.1	41.7	250	72.9	892	189.1	9820	82.6	595
I16-46Z-20	2904	39.2	0.057	8.03	0.042	0.9	4.97	0.264	50.3	23.36	303.8	101.5	380.9	65.1	480.8	79.5	12530	67.2	825.1
I16-46Z-24	4600	651	58	252	18.6	82.6	33.3	6.8	106	35.7	413	141.3	586	112	878	117.4	11240	686	665
I16-46Z-16	1234	38.4	3.7	12.3	0.99	4.3	2.75	0.49	12.6	5.66	85.7	40	222.5	55.8	550	101.1	9790	132	641
I16-46Z-10	759	10.02	0.792	5.04	0.258	2.03	2.13	0.214	9.6	3.8	59.6	26.2	128.6	29	276.7	54.5	9100	23.1	316.6
I16-46Z-7	2091	29.1	1540	2900	281	1090	203	8.9	222	35	256	70.9	292	57.8	540	101.9	10070	273	593
I16-46Z-12	844	23.6	0.54	2.89	0.106	0.94	1.17	0.276	8.85	4.41	65.2	28.2	151.3	40.1	445.2	91.1	12070	28.8	547
I16-46Z-13	1259	6.36	203	257	21.6	76.4	10	1.26	20	7.34	99.8	42.3	199.9	39.3	342	61.7	11340	35.06	332.4
I16-46Z-19	1866	78.3	68	150	19	88	19	1.62	32	7.9	111.6	56.1	357	95.1	933	169.9	8900	147	669
I16-46Z-15	1127	21.3	0.42	4.77	0.171	2.32	1.19	0.46	9.4	4.81	76.1	35.1	193.3	53.3	591	113.7	10550	96.8	654.8
I16-46Z-17	1093	9.96	0	5.64	0	0.26	1.58	0.032	20.2	8.77	107.8	37.8	149.8	26.45	207.5	36.4	10490	43.2	302.5
I16-46Z-6	1252	29.9	1020	2030	230	920	191	4.6	160	21.7	135	41.2	200.9	50.9	518	97.4	8870	315	624.9
I16-46Z-30	1290	19	5.86	15.6	2.14	15	9.1	2.78	38	10.76	116.9	42.7	182.4	36.9	350	60.3	13410	86.2	541
I16-46Z-14	2301	11.02	0.103	6.43	0	0.39	1.54	0.109	24.8	14.44	210.2	79.3	333.2	61.1	488.5	81.8	11430	47.47	559.4

I16-46Z-4	1807	34.3	18.2	56.4	7.49	54.9	27.4	8.88	82.1	16.26	150.1	51.6	264.1	64.6	605	104	7940	299.2	801
I16-46Z-1	2039	75.5	6.9	21.8	2.11	13.7	10.4	2.29	38.7	13.1	159.8	70.4	366	85	738	117.8	6590	118.6	867
I16-46Z-25	1395	21.9	7.62	18.2	2.12	13.5	9.3	1.97	30	8.02	107	43.6	221	50.2	506	95.6	9940	154	462
I16-46Z-23	2620	25.6	65.4	136	19.8	132	97	26.6	274	51.1	354	85.9	303	60.4	595	118	9120	198.1	682
I16-46Z-11	1572	68.7	13.8	30.5	3.28	24.8	14.2	3.84	39.5	9.92	113.3	49.4	265.5	64.7	616	112.5	8770	227.1	751.5
I16-46Z-27	1612	46.7	0.202	5.61	0.106	1.35	1.79	0.191	13.3	5.52	87.5	43.5	267.1	69	622	98.6	8970	98.2	670
I16-46Z-9	1492	47.5	9.7	33.9	3.07	16.9	5.4	0.77	19.1	8.24	115.9	48.4	236.2	51.9	486	87.1	10570	228.8	516.5
I16-46Z-18	1390	131	111	223	24.2	100.2	36.9	6.87	70.2	14.07	118.2	43.9	212	51.8	512	84.9	8000	221.8	603
I16-46Z-8	2009	59.8	2.83	10.5	0.83	4.89	5.38	1.68	24.9	9.01	134.8	62.5	369	101.2	1059	198.4	9830	120.2	778
I16-46Z-2	1343	46	2.5	9.9	0.73	7	5.7	1.44	25.9	9	108.6	44.5	235.4	58	579	113.1	10520	96	472
I16-46Z-28	1635	38	19.9	58.1	8.2	58.4	23.1	4.84	52.8	11.07	128	52.6	276	67.8	687	135.4	11770	97.8	732
I16-46Z-26	890	12.4	12.4	30.3	3.7	30.8	13.2	3.7	43	9.2	79	27.5	122	26.5	257	48.1	10640	86	317
I16-46Z-5	7630	517	63.8	217	19.3	125	101	32	311	78.9	727	208	736	118.5	775	90.9	8810	1279	728
I16-46Z-3	1770	17.9	28.7	67	9.5	59	37.3	9.3	112	23.2	201	59.3	235	50.1	472	88.1	11290	190	560
I16-46Z-29	802	6.88	59	65	5.7	18.2	4.9	1.78	15.3	4.42	58.6	25.5	132.1	33	348	69.3	10890	52.7	357
I16-46Z-21	2150	46.9	12.1	34.5	4.12	29.2	18.4	4.78	55.5	14.2	163	64.6	342	88.6	988	197.2	13070	217	734
I16-52Z-33	1570	18.5	3.5	42.3	3.3	28.2	16.6	3.57	47.6	13.7	149	51.1	228	46.6	428	79.6	8820	325	468
I16-52Z-26	1684	8.93	18.3	131	15.7	115	58.3	14.5	110	23.3	193	57.8	225.4	42.7	375.1	69.1	9730	344	398
I16-52Z-23	1318	3.08	0.039	15.49	0.113	2.21	3.38	1.93	24.2	8.6	110	44.4	197.2	43	397	84.1	7030	70	144.9
I16-52Z-10	1023	1.43	0.289	13.02	0.596	6	7.1	2.81	28.8	8.28	92.1	34.14	150.8	33.07	308.8	65.2	6770	52.5	102.9
I16-52Z-5	1848	11.47	2.09	26.7	3.15	32.7	27	4.7	69.3	18.1	188.8	65.9	292	60.5	546	108.7	7720	85.3	211.4
I16-52Z-24	1289	2.98	0.53	19.02	0.78	9	8	3.24	31.5	9.47	109.1	42.9	195.1	40.8	387	79.2	6900	65.3	143.8
I16-52Z-9	560	0.74	0	11.4	0.06	1.79	3.76	1.87	22.3	6.2	56.9	17.9	68	13.46	126.2	25.7	8490	78.9	247
I16-52Z-27	945	1.68	0	10.7	0.103	1.38	2.65	1.56	18.4	6.14	77.8	31.33	146	31.33	306.6	64.5	6680	45	101
I16-52Z-7	1367	7.58	0.213	20.38	0.39	3.63	6.07	1.67	29.6	9.85	120.9	42.9	201.6	43.1	396.9	75.9	7580	277.5	445.6
I16-52Z-14	944	1.88	0	10.89	0.036	1.25	2.94	1.5	17.1	5.94	80.9	31.11	147.8	31.85	311.2	66.87	6870	43.81	109.3
I16-52Z-19	923	1.43	0.565	12.51	0.587	5.33	6.19	2.1	24.8	7.44	82.9	30.8	137.6	29.8	288	60.3	6800	42.8	92.6
I16-52Z-16	608	1.05	0	7.27	0.05	0.91	1.97	1.16	12.83	3.9	49.6	20.46	96	21.15	209.4	45.5	6740	24.29	63.4
I16-52Z-15	629	1.78	0.295	7.68	0.094	1.29	2.9	0.96	12	4.07	51.8	20.2	98.7	21.7	214.5	47.9	6760	31.9	74.5

I16-52Z-11	1224	2.71	0.058	14.68	0.138	2.38	3.56	2.12	25.5	8.37	105.1	40.28	186.3	39.73	377.1	77.5	6660	68.6	135.5
I16-52Z-17	1085	2.34	0	8.53	0.086	1.14	2.63	1.76	19.2	7.25	92.4	37.2	173.6	37.4	384	80.5	8140	37.5	131.4
I16-52Z-3	949	2.02	2.6	18.5	0.94	5.4	3.25	1.65	16.95	5.84	77.1	30.5	148.9	31.27	314	65.5	6700	43	103.3
I16-52Z-4	1273	14.2	10.9	90.4	12	91.8	60.8	11.3	94.9	18.8	145.7	42.1	165.7	33.9	314.1	63.1	6920	295	296
I16-52Z-20	1205	2.81	0.16	17.6	0.275	3.33	4.97	2.43	26.7	9.15	105.6	39.7	182.9	37.6	362.7	74.1	6970	84.1	144.8
I16-52Z-34	967	1.77	0	11.7	0.09	1.43	3	1.54	18.07	6.37	79	31.19	149	32.12	315.2	65	6960	45.93	102.4
I16-52Z-18	470	0.63	0	4.71	0.028	0.61	1.85	0.98	9.7	3.29	39.1	15.76	72.8	15.76	163.8	36.69	6910	15.74	41.5
I16-52Z-1	777	1	0	8.43	0.104	1.48	2.93	1.4	15.23	5.11	63.9	25.57	120.5	26	257.3	55.8	6960	32.64	77.7
I16-52Z-12	1467	2.92	2.16	24.6	0.77	5.7	5.27	2.68	32.4	10.96	132.7	49.7	222	45.9	427	86.2	6770	107.3	168
I16-52Z-22	1385	2.98	0.071	16.73	0.185	2.55	4.75	2.36	26.8	9.12	117.1	46.28	211.9	44.72	422.5	87.9	6830	77.86	157.5
I16-52Z-8	1064	2.55	0.15	13.15	0.294	3.57	5.06	2.26	25.3	7.76	93	36.15	159.8	34.31	321.5	66.6	7080	62.3	123.8
I16-52Z-13	263	1.64	0.187	4.01	0.25	3.17	4.62	0.73	13.1	3.28	29.8	8.4	32.6	6.54	62	10.9	7580	30.6	68.2
I16-52Z-21	1140	2.36	0.067	8.38	0.126	0.79	1.78	0.69	12.75	6.23	87.6	38.3	194.7	48	511	110.6	12110	44.8	219.7
I16-52Z-6	997	2.07	0.087	12.01	0.167	2.68	3.52	1.8	20.8	6.52	81.3	32.16	152.4	33.02	320.5	68.7	6810	47.39	110.5
I16-52Z-2	809	4.19	0.041	41.1	0.454	6.42	7.89	3.6	26.5	7.85	85.7	27.42	104.7	19.68	166.4	30.5	5290	86.7	62.3
I16-52Z-25	966	2.09	0	11.17	0.047	1.47	3.31	1.5	17.5	6.07	77.3	30.67	148.3	32.2	312.3	66.9	6930	41.8	107.7
I16-52Z-32	25.4	0.43	0.232	1.99	0.4	2.74	4.03	0.61	9.6	1.31	5.27	0.74	1.75	0.277	1.68	0.39	11600	19.7	442.8
I16-52Z-31	1215	3.42	10.2	50	4.3	27.2	18.2	5.41	52	13.35	127.4	42.4	169	33.2	301	59.4	6890	203	176
I16-52Z-29	784	1.86	0.723	13.99	1.38	15.2	13.3	3.56	27.7	6.57	67.5	25.5	117.1	25.1	247.6	53.6	6870	33.5	78.9
I16-52Z-28	1141	1.72	1.01	20.12	2.24	19.7	18.4	4.95	41.7	9.56	104.3	38.7	168.3	36.4	340	71.3	6980	57.9	112.9
I16-54Z-6	2158	4.07	0.195	68.9	0.71	8.35	17.8	11.37	88.3	25.2	235	69.2	258	46.1	389	74.6	6623	389	576
I16-54Z-17	998	22	0.44	23.69	0.151	2.14	1.53	0.74	11.7	4.93	62	25.24	139	35.6	409	90.4	10160	91.2	1957
I16-54Z-14	1573	2.34	0	28.74	0.041	1.55	6	4.09	40.1	13.22	137.5	47.5	200.7	38.88	346.1	68.1	7270	227.8	494.4
I16-54Z-2	682	0.77	0	12.21	0.029	1.01	3.54	2.08	19.6	6.19	62.6	21	86.9	17	153	29.3	7320	78.1	200.6
I16-54Z-16	1127	31.6	0.079	6.09	0.028	0	0.12	0.296	6.4	3.17	61	29.6	183.5	53.4	642	146	9210	28.9	2880
I16-54Z-20	1330	9.9	11.56	47.6	3.03	13.8	4.22	2.1	10.8	4.43	66.9	35.64	227.9	65.4	756	166.8	11100	57	2177
I16-54Z-22	2044	23.1	0.014	23.3	0.017	0.32	2.08	0.58	17.1	8.83	137.3	59.8	316	76.2	784	151.5	9440	194	2566
I16-54Z-11	947	1.9	0.367	23.4	0.336	5.22	6.09	3.43	34	9.35	92.9	28.8	113	21	182.8	35.4	7100	124.3	221
I16-54Z-23	1375	20.1	0.052	30.3	0	0.43	2.49	0.96	16.3	6.79	84.5	34.4	181.3	47.4	540.5	119.8	9480	40.96	2391

I16-54Z-9	1419	44.1	0.049	10.15	0.033	0.35	0.36	0.81	8.83	4.49	75.9	39.6	234	67	755	161.8	9620	57.8	3640
I16-54Z-4	694	0.85	0	10.6	0.063	0.66	3.35	1.84	18.2	5.8	64.8	22.1	90.3	17.3	154.4	30.4	8280	67.8	222
I16-54Z-18	819	19.6	0.31	13.01	0.54	2.32	2.11	0.49	7.83	3.6	51.6	21.9	127.8	33.72	368.7	74.3	9200	63.4	1041
I16-54Z-7	842	6.74	0.054	3.57	0.045	0.4	0.94	0.186	8.96	4.16	62	28.41	146.8	37.3	408.4	89.5	10260	31.1	328.1
I16-54Z-12	1432	9.43	3.6	39.9	1.19	7.2	5.2	2.72	22.9	8.49	109.1	42.15	202	43.3	422.8	81	8720	206.8	1199
I16-54Z-8	800	9.49	4.9	39.9	2.16	12.2	5.7	7.1	15.8	5.01	58.2	23.2	112.7	25.8	254.1	52.1	12570	76	830
I16-54Z-15	1147	1.81	0.108	43.4	0.147	1.93	6.5	4.19	33.6	10.16	105.9	33.4	136.2	26	218	40.1	5870	123	229
I16-54Z-24	393	4.91	5.5	26.7	2.61	12.3	4.24	2.39	9.99	2.13	25.9	10.47	53.9	13.71	195	57.1	8740	8.83	463
I16-54Z-19	1931	35.9	20.7	102	9.7	62	18.7	23.8	39.8	9.74	119.6	51.9	293.2	74.2	801	161.2	9820	123.1	3080
I16-54Z-21	966	27.6	18	82.4	7.71	45.7	12	10.4	20.7	4.1	49.1	23.51	145.7	44.12	559	145.3	9400	16.8	2375
I16-54Z-10	1332	51.7	1.36	5.69	0.234	1.95	0.55	0.39	4.4	2.83	52.9	31.5	232.8	77.1	1009	267	1.58E+04	22.18	4379
I16-54Z-1	1267	10.69	17.5	117.4	15.6	124.1	56.4	20.2	90	15.4	116.1	31	120.4	25.6	267	63.9	8460	29.2	961
I16-62Z-1	783	1.08	159	350	31	125	20.1	3.2	26.2	6.77	70.2	26.7	119.3	25	241	49.7	8290	43.6	63.9
I16-62Z-25	780	0.72	2.7	11.7	0.83	5.7	4.82	1.64	19.8	6.28	72	26.9	117.7	23.7	226	45.4	9450	36	233
I16-62Z-10	1666	2.14	0.28	10.41	0.345	4.25	6.51	3.92	37.9	12.8	151.7	57.1	259	53.7	509	104.4	8060	130	237.9
I16-62Z-22	786	1.1	0.7	12.1	0.42	3.6	3.66	1.41	19.5	6	70.9	26.9	118.3	25.1	225	45.4	8420	35.9	52.4
I16-62Z-32	2010	1.59	0.034	11.9	0.309	5.59	10.4	3.89	61	18.3	204	72.2	298	59.3	520	100.9	7730	106	181
I16-62Z-28	2088	1.33	0.323	11.8	0.481	5.7	11.1	3.67	57.1	18.84	208.6	74.5	309	60.8	533.3	101.9	9090	114.4	177
I16-62Z-4	3420	2.38	0.044	23.11	0.539	10.14	22.1	7.11	105.4	32.6	357.8	120.7	507	94.2	813	151.5	7200	213	165.5
I16-62Z-18	2179	1.56	0.043	11.58	0.288	5.43	10.33	3.59	60.3	19.17	219.8	78.3	330	62.8	557	104.8	8350	117.1	163.8
I16-62Z-12	854	1.29	0.065	7.89	0.084	1.37	2.68	0.99	16.85	5.73	72.4	28.43	132.8	28.6	268.8	54.5	7980	29.88	57.9
I16-62Z-5	1640	0.99	0	10.4	0.215	4.56	8.9	2.99	45.8	14.5	162	58.1	246	48.6	426	81.3	8490	82.7	96.5
I16-62Z-15	800	0.69	0	7.16	0.062	1.48	3.15	1.14	20.2	6.24	72.3	27.9	121.1	24.5	223	43.6	8570	33.7	60
I16-62Z-31	3206	2.47	6.1	46	4.5	33.4	27.9	8.47	113.8	31.7	343	115.5	478	89.8	756	145.6	6710	177.6	133.7
I16-62Z-26	2370	2.29	1.62	20.4	1.16	10.5	14.2	5.13	74	21.6	239	85.1	350	67.6	600	117.1	8510	171	456
I16-62Z-7	599	0.76	0.277	4.76	0.172	1.6	2.25	1.02	13.3	4.56	52.1	20.4	91	19.2	189	40.1	10400	24	321
I16-62Z-14	1750	1.24	0.145	10.61	0.31	4.6	8.97	2.82	46.3	15	170	61.7	257	50.9	458	88.6	8550	88.5	98.6
I16-62Z-20	1440	1.37	0.57	11.05	0.53	4.39	7.9	2.77	40.8	12.9	149	52.1	208	40.9	361	68.9	9950	108.8	134.1
I16-62Z-11	1306	1.2	0	8.45	0.179	3	7.08	2.52	36.4	11.44	128.3	46.4	197.8	40.4	349.3	70.8	7810	75.1	102.6

I16-62Z-8	2508	1.33	0.058	12.13	0.445	6.34	12.44	4.82	69	22.48	251.7	89.5	374.2	70.1	613	114.1	7580	125.7	123.6
I16-62Z-3	1430	1.09	1.62	16.7	1.34	11.3	10.5	3.48	41.6	12.8	138	50	211	42.4	375	73.1	8430	74.3	111.7
I16-62Z-9	1644	1.22	0.81	12.5	0.64	6.9	7.63	2.71	42.7	13.39	159	57.2	246	48.6	437	84.8	9170	82	333
I16-62Z-17	1819	0.98	0	10.49	0.362	5.74	11.32	3.95	55	16.99	186.3	64.6	267.8	52.1	454.3	84.7	7470	72	70.1
I16-62Z-2	1990	1.28	0.077	10.87	0.357	6.97	11.9	4.06	60.6	18.4	196	70.5	299	56.5	498	95.3	7410	93.1	103.6
I16-62Z-29	700	0.74	0	6.32	0.102	1.71	3.5	1.41	16.1	5.5	64	23	101	21.2	202	41.5	10060	42.6	69.8
I16-62Z-23	1413	0.89	0	9.87	0.158	3.57	7.23	2.46	36.9	11.86	136.7	49.6	207.6	41.87	369.9	70.8	8650	67.2	86.3
I16-62Z-13	920	1.02	0.031	6.21	0.106	1.53	3.4	1.38	20.9	7.1	83	31.6	138	28.7	273	55.3	9070	45.7	200.3
I16-62Z-24	2059	1.33	0.053	10.23	0.319	5.55	10.63	4.1	56.4	18.67	207.7	73.2	309.4	60.2	524.6	100.9	8080	97.6	134.3
I16-62Z-30	2872	1.77	0.419	18.91	0.529	8.43	17.08	5.53	84.9	27.03	296.4	102.7	425.3	81.8	706	130.1	7210	158.4	137.7
I16-62Z-27	930	0.69	0	5.7	0.12	2.04	4.6	1.44	24.3	7.3	88	29.9	133	26.8	243	46.9	8740	35.9	186
I16-62Z-19	234.8	0.485	0	4.35	0.021	0.23	0.46	0.255	3.21	1.28	16.98	7.1	37.4	8.98	96.5	21.41	10740	18.45	44
I16-62Z-6	897	0.96	0.016	9.31	0.093	2.14	3.74	1.29	21.2	7.38	84.1	31.1	135	27.6	249	48.3	8243	40.8	56.4
I16-62Z-16	2060	1.61	0.135	15.67	0.363	5.78	11.59	3.62	59.2	18.19	199.5	71.9	302	59.8	517	98.7	8450	130.8	128.5
I16-62Z-21	3026	2.13	0.138	14.71	0.454	6.74	16.15	5.55	87.3	27.34	308.6	109.1	444.6	86.3	748	144.1	7630	157.9	144.8

Appendix 5.3 Apatite U–Pb age data. Reported ages are isochron corrected in IsoplotR.

Apatite Grain	²⁰⁷ Pb/ ²³⁵ U	2σ	²⁰⁶ Pb/ ²³⁸ U	2σ	Error Correlation (ρ)	²⁰⁷ Pb/ ²³⁵ U Age (Ma)	Age 2σ	²⁰⁶ Pb/ ²³⁸ U Age (Ma)	Age 2σ	²⁰⁷ Pb/ ²⁰⁶ Pb Age (Ma)	Age 2σ	Age conc.	Age 2σ
I16-17A-1	56.2	3.3	0.898	0.035	0.76067	2799	45	2799	27	2799	73	2799	26
I16-17A-2	54.1	3.2	0.9	0.037	0.67775	2925	44	2925	31	2925	72	2925	28
I16-17A-3	28.3	2	0.716	0.038	0.80892	3481	34	3481	71	3481	31	3481	29
I16-17A-4	26.3	1.6	0.665	0.022	0.72173	3008	33	3008	36	3008	45	3008	31

I16-17A-5	50.4	3.6	0.868	0.035	0.75733	2927	51	2927	31	2927	78	2927	31
I16-17A-6	23.56	1.1	0.639	0.016	0.75985	2988	25	2988	28	2988	31	2988	24
I16-17A-7	45.1	3.7	0.855	0.039	0.70872	3390	46	3390	49	3390	62	3390	42
I16-17A-8	44.2	2.6	0.891	0.035	0.5672	4107	26	4107	60	4107	29	4107	24
I16-17A-9	32.9	1.8	0.736	0.019	0.63896	3169	31	3169	28	3169	45	3169	26
I16-17A-10	33.2	2.8	0.748	0.047	0.58893	3600	41	3600	87	3600	53	3600	41
I16-17A-11	30.78	1.4	0.73	0.019	0.52777	3533	22	3533	35	3533	29	3533	22
I16-17A-12	28.5	1.4	0.703	0.019	0.77092	3333	25	3333	34	3333	28	3333	25
I16-17A-13	53.9	4.5	0.95	0.047	0.84072	4305	37	4305	78	4305	29	4305	29
I16-17A-14	36.6	1.8	0.772	0.026	0.78603	3215	26	3215	36	3215	33	3215	26
I16-17A-15	40	2.2	0.783	0.02	0.63277	2978	38	2978	23	2978	59	2978	22
I16-17A-16	28.89	1.4	0.69	0.02	0.54727	3032	28	3032	31	3032	44	3032	24
I16-17A-17	34.3	1.9	0.765	0.022	0.66002	3663	27	3663	40	3663	31	3663	27
I16-17A-18	30.09	1.3	0.707	0.019	0.71916	3112	23	3112	29	3112	31	3112	23
I16-17A-19	41.6	2.6	0.814	0.027	0.60092	3164	40	3164	32	3164	60	3164	29
I16-17A-20	38.1	2.4	0.794	0.026	0.6802	3768	30	3768	47	3768	34	3768	30
I16-17A-21	33.39	1.6	0.726	0.021	0.54355	2991	31	2991	28	2991	49	2991	24
I16-17A-23	42.2	2.5	0.802	0.025	0.7302	2975	40	2975	27	2975	59	2975	27
I16-17A-24	28.3	1.4	0.661	0.019	0.52868	2810	33	2810	27	2810	54	2810	24
I16-17A-25	30.75	1.5	0.73	0.019	0.67274	3533	24	3533	35	3533	28	3533	24
I16-17A-26	33.3	1.8	0.742	0.02	0.73796	3211	30	3211	30	3211	39	3211	27
I16-17A-27	31.38	1.4	0.724	0.02	0.56881	3198	25	3198	31	3198	36	3198	23
I16-17A-28	27.44	1.2	0.672	0.017	0.54716	2975	26	2975	26	2975	40	2975	22
I16-17A-29	37.4	2.1	0.777	0.021	0.66397	3176	34	3176	28	3176	48	3176	26
I16-17A-30	35.1	2.5	0.782	0.029	0.65421	3724	33	3724	52	3724	38	3724	33
I16-07A-10	26.4	1.2	0.66	0.018	0.60514	3030	25	3030	30	3030	37	3030	23
I16-07A-11	30	1.6	0.688	0.02	0.74334	3028	31	3028	31	3028	42	3028	28
I16-07A-13	36.2	1.9	0.718	0.021	0.60524	2886	38	2886	27	2886	60	2886	25
I16-07A-15	34.4	4.3	0.72	0.077	0.72373	3007	71	3007	106	3007	109	3007	69
I16-07A-16	24.93	1.1	0.647	0.016	0.47402	3016	25	3016	27	3016	39	3016	21
I16-07A-17	26	1.6	0.646	0.034	0.69053	2934	33	2934	55	2934	50	2934	33

I16-07A-18	28.71	1.4	0.681	0.021	0.62471	3058	28	3058	33	3058	40	3058	26
I16-07A-19	28.02	1.3	0.665	0.021	0.65344	2962	27	2962	33	2962	40	2962	25
I16-07A-2	26.16	1.3	0.664	0.019	0.44431	3090	28	3090	33	3090	44	3090	24
I16-07A-20	30.49	1.6	0.69	0.021	0.40117	3012	34	3012	32	3012	56	3012	25
I16-07A-21	25.67	1.1	0.66	0.016	0.54605	3089	23	3089	28	3089	34	3089	21
I16-07A-22	30.8	1.7	0.704	0.019	0.69417	3124	32	3124	30	3124	43	3124	27
I16-07A-23	30.55	1.5	0.687	0.019	0.6779	2982	30	2982	28	2982	43	2982	25
I16-07A-24	30.8	1.6	0.686	0.02	0.59247	2957	33	2957	29	2957	51	2957	26
I16-07A-25	27.4	1.5	0.676	0.018	0.68279	3113	30	3113	30	3113	41	3113	27
I16-07A-26	31.4	1.6	0.702	0.021	0.53542	3056	31	3056	31	3056	49	3056	26
I16-07A-28	21.83	1.2	0.604	0.02	0.48674	2853	31	2853	35	2853	51	2853	27
I16-07A-29	24.56	1.6	0.65	0.027	0.70112	3076	34	3076	48	3076	44	3076	34
I16-07A-3	28.11	1.4	0.687	0.019	0.59295	3176	27	3176	32	3176	38	3176	25
I16-07A-30	26.3	1.4	0.672	0.025	0.53502	3169	28	3169	44	3169	42	3169	27
I16-07A-31	47.2	2.5	0.82	0.033	0.80146	3006	33	3006	35	3006	48	3006	29
I16-07A-32	29.17	1.3	0.68	0.02	0.6532	3015	26	3015	31	3015	38	3015	24
I16-07A-33	34.6	1.9	0.714	0.024	0.59657	2946	37	2946	32	2946	58	2946	28
I16-07A-34	26.11	1.3	0.655	0.016	0.62379	3005	28	3005	27	3005	41	3005	24
I16-07A-4	25.5	1.2	0.651	0.016	0.53014	3012	27	3012	27	3012	41	3012	23
I16-07A-5	24.36	1.1	0.638	0.015	0.55002	2975	25	2975	26	2975	38	2975	22
I16-07A-6	25.12	1.2	0.652	0.018	0.73842	3051	25	3051	31	3051	32	3051	25
I16-07A-7	23.2	2.1	0.619	0.044	0.59641	2889	50	2889	76	2889	79	2889	48
I16-07A-8	26.47	1.2	0.657	0.017	0.68572	2998	25	2998	28	2998	35	2998	23
I16-07A-9	23.15	1.1	0.621	0.016	0.62412	2909	27	2909	28	2909	39	2909	24
I16-18A-1	16.85	0.91	0.5625	0.014	0.58474	2776	28	2776	27	2776	41	2776	24
I16-18A-10	17.62	1	0.5695	0.013	0.66046	2770	30	2770	24	2770	43	2770	23
I16-18A-11	27.37	1.3	0.654	0.017	0.49781	2674	33	2674	22	2674	57	2674	20
I16-18A-12	28.86	1.4	0.7	0.023	0.75011	2985	26	2985	33	2985	35	2985	25
I16-18A-13	16.18	0.68	0.5544	0.0097	0.36581	2760	22	2760	19	2760	35	2760	16
I16-18A-15	19.18	1.2	0.594	0.016	0.58806	2873	33	2873	30	2873	48	2873	27
I16-18A-16	20.5	1.3	0.6057	0.014	0.64933	2854	35	2854	25	2854	51	2854	24

I16-18A-17	28.8	1.9	0.724	0.026	0.52737	3511	31	3511	49	3511	41	3511	31
I16-18A-18	22.02	1.1	0.611	0.013	0.57351	2752	30	2752	21	2752	47	2752	20
I16-18A-19	20.14	1.2	0.589	0.014	0.81184	2719	33	2719	23	2719	46	2719	23
I16-18A-2	24.1	1.2	0.646	0.017	0.58076	2906	28	2906	27	2906	42	2906	23
I16-18A-20	25.99	1.1	0.66	0.016	0.59771	2849	25	2849	23	2849	39	2849	20
I16-18A-21	25.6	1.1	0.666	0.015	0.66822	2971	24	2971	24	2971	33	2971	21
I16-18A-22	26.68	1.3	0.656	0.019	0.65255	2745	30	2745	26	2745	47	2745	24
I16-18A-23	20.58	1.1	0.622	0.018	0.88819	3111	26	3111	36	3111	25	3111	24
I16-18A-24	25.36	1.1	0.646	0.014	0.51658	2772	27	2772	20	2772	45	2772	19
I16-18A-25	32.8	2.6	0.71	0.032	0.73831	2698	53	2698	36	2698	82	2698	36
I16-18A-26	27.16	1.2	0.656	0.016	0.54636	2705	30	2705	21	2705	49	2705	20
I16-18A-27	22.87	1.3	0.615	0.019	0.72707	2713	33	2713	29	2713	48	2713	27
I16-18A-28	27.62	1.3	0.671	0.018	0.63705	2796	29	2796	25	2796	45	2796	22
I16-18A-29	27.56	1.2	0.668	0.017	0.45914	2774	29	2774	23	2774	49	2774	20
I16-18A-3	17.36	2.1	0.5653	0.022	0.32748	2753	66	2753	41	2753	109	2753	39
I16-18A-30	26.4	1.8	0.714	0.025	0.75296	3474	31	3474	47	3474	33	3474	31
I16-18A-31	19.04	0.77	0.5945	0.011	0.42386	2897	21	2897	21	2897	33	2897	17
I16-18A-32	18.32	0.94	0.597	0.013	0.89976	3063	24	3063	27	3063	25	3063	24
I16-18A-33	31.9	2.3	0.779	0.031	0.65632	3713	32	3713	56	3713	35	3713	32
I16-18A-34	29.3	1.6	0.67	0.017	0.53257	2654	40	2654	21	2654	68	2654	20
I16-18A-35	19.48	1.4	0.594	0.016	0.36994	2837	39	2837	29	2837	64	2837	26
I16-18A-36	16.11	0.63	0.5637	0.0093	0.14873	2879	19	2879	19	2879	33	2879	14
I16-18A-37	26.7	1.5	0.661	0.019	0.63548	2788	35	2788	27	2788	54	2788	25
I16-18A-38	30.1	1.7	0.693	0.024	0.56139	2774	38	2774	30	2774	62	2774	27
I16-18A-4	25.68	1.1	0.646	0.015	0.55349	2743	27	2743	21	2743	44	2743	19
I16-18A-5	17.57	1.1	0.56	0.016	0.56686	2682	34	2682	29	2682	53	2682	27
I16-18A-6	21.87	1.2	0.611	0.015	0.40597	2766	33	2766	24	2766	55	2766	22
I16-18A-7	20.7	0.96	0.6097	0.011	0.51508	2879	25	2879	19	2879	39	2879	18
I16-18A-8	25.82	1.1	0.652	0.016	0.60928	2785	26	2785	23	2785	41	2785	20
I16-18A-9	30.3	1.5	0.714	0.021	0.7676	2977	28	2977	29	2977	37	2977	25
I16-32A-1	809	110	6.82	0.92	0.96946	5689	17	5689	53	5689	14	5689	14

I16-32A-2	1059	120	9.8	1.1	0.91341	5659	15	5659	30	5659	19	5659	15
I16-32A-3	685.8	27	11.81	0.23	0.97049	5331	5	5331	4	5331	6	5331	3
I16-32A-5	926	77	7.43	0.52	0.96833	5735	12	5735	26	5735	10	5735	10
I16-32A-6	94.7	49	1.136	0.41	0.92837	4656	240	4656	558	4656	149	4656	142
I16-32A-7	196	28	2.44	0.36	0.85956	5177	37	5177	133	5177	33	5177	28
CO17-58A-1	11.5	0.55	0.457	0.013	0.6159	2182	26	2182	23	2182	44	2182	21
CO17-58A-10	11.65	0.55	0.459	0.011	0.084041	2181	29	2181	19	2181	60	2181	15
CO17-58A-11	11.74	0.72	0.4519	0.013	0.29003	2112	38	2112	22	2112	75	2112	20
CO17-58A-12	16.8	0.75	0.5967	0.014	0.67348	3017	20	3017	28	3017	25	3017	20
CO17-58A-13	14.1	0.68	0.491	0.015	0.48685	2166	30	2166	23	2166	57	2166	20
CO17-58A-14	13.11	0.6	0.493	0.013	0.38109	2307	26	2307	22	2307	49	2307	18
CO17-58A-15	13.71	0.95	0.462	0.018	0.6362	1996	44	1996	26	1996	84	1996	26
CO17-58A-16	12.81	1	0.466	0.013	0.54054	2109	49	2109	21	2109	90	2109	21
CO17-58A-17	10.95	0.51	0.4676	0.011	0.46389	2368	23	2368	22	2368	39	2368	19
CO17-58A-18	14.4	0.68	0.4839	0.012	0.5376	2083	31	2083	17	2083	59	2083	17
CO17-58A-19	11.84	0.6	0.463	0.013	0.49473	2193	28	2193	23	2193	52	2193	20
CO17-58A-2	15.51	0.93	0.511	0.017	0.68012	2171	36	2171	24	2171	63	2171	23
CO17-58A-20	17.02	1.1	0.524	0.021	0.60897	2116	43	2116	27	2116	81	2116	25
CO17-58A-21	14.78	0.73	0.484	0.014	0.54789	2048	33	2048	20	2048	64	2048	19
CO17-58A-22	10.36	0.53	0.462	0.014	0.47269	2405	24	2405	30	2405	40	2405	22
CO17-58A-23	11.45	0.52	0.468	0.011	0.60515	2293	23	2293	21	2293	38	2293	19
CO17-58A-24	12.71	0.64	0.491	0.014	0.63328	2347	26	2347	25	2347	42	2347	22
CO17-58A-25	14.71	0.72	0.502	0.014	0.35998	2187	32	2187	21	2187	63	2187	18
CO17-58A-26	13.75	0.63	0.491	0.011	0.55191	2206	27	2206	17	2206	49	2206	17
CO17-58A-27	11.35	0.5	0.482	0.012	0.73569	2486	21	2486	25	2486	27	2486	21
CO17-58A-28	14.07	0.71	0.4821	0.012	0.42571	2102	34	2102	18	2102	65	2102	17
CO17-58A-29	11.49	0.61	0.458	0.012	0.55553	2192	29	2192	22	2192	51	2192	20
CO17-58A-3	13.66	0.67	0.478	0.012	0.43495	2113	32	2113	18	2113	61	2113	17
CO17-58A-30	10.99	0.54	0.46	0.013	0.39237	2277	26	2277	25	2277	48	2277	20
CO17-58A-4	10.19	0.53	0.4404	0.011	0.43706	2195	27	2195	21	2195	50	2195	19
CO17-58A-5	14.1	0.69	0.4786	0.012	0.50114	2074	32	2074	18	2074	62	2074	17

CO17-58A-6	11.66	0.57	0.4697	0.011	0.40243	2280	26	2280	20	2280	48	2280	18
CO17-58A-7	14.88	0.77	0.483	0.014	0.53534	2033	35	2033	19	2033	69	2033	19
CO17-58A-8	10.31	0.62	0.446	0.016	0.33027	2233	31	2233	31	2233	61	2233	24
CO17-58A-9	11.53	0.5	0.4614	0.01	0.43829	2217	24	2217	18	2217	44	2217	16
CO17-26A-1	90.9	7.5	0.847	0.062	0.79862	681	156	681	3	681	671	681	3
CO17-26A-10	16.8	1.3	0.2484	0.011	0.71113	703	111	703	7	703	461	703	7
CO17-26A-11	14.79	1	0.2238	0.011	0.31043	679	132	679	8	679	578	679	7
CO17-26A-12	13.55	0.78	0.2201	0.0065	0.66986	700	80	700	5	700	331	700	5
CO17-26A-13	8.53	0.54	0.1773	0.0055	0.43554	697	80	697	7	697	339	697	7
CO17-26A-14	9.46	0.42	0.1937	0.0047	0.36221	732	61	732	5	732	248	732	5
CO17-26A-15	12.98	0.69	0.2252	0.0059	0.53221	734	77	734	5	734	313	734	5
CO17-26A-16	9.03	0.43	0.1859	0.005	0.40361	715	63	715	6	715	262	715	6
CO17-26A-17	6.92	0.9	0.165	0.0087	0.33424	703	150	703	12	703	633	703	12
CO17-26A-18	7.96	0.35	0.1728	0.004	0.094324	698	63	698	5	698	271	698	5
CO17-26A-19	16.54	0.8	0.25	0.0085	0.60908	715	75	715	5	715	312	715	5
CO17-26A-2	11.03	0.51	0.1983	0.0049	0.45642	698	67	698	5	698	283	698	5
CO17-26A-20	22.16	1.1	0.2986	0.0093	0.44659	716	98	716	4	716	410	716	4
CO17-26A-21	17.46	0.88	0.2584	0.0081	0.40789	716	93	716	5	716	389	716	5
CO17-26A-22	14.35	0.7	0.2355	0.0077	0.31661	728	88	728	6	728	364	728	5
CO17-26A-23	13.09	0.69	0.222	0.007	0.48046	720	81	720	6	720	334	720	6
CO17-26A-24	14.55	0.76	0.2322	0.0076	0.48583	712	85	712	6	712	354	712	5
CO17-26A-25	15.21	0.9	0.242	0.0081	0.54107	725	93	725	6	725	379	725	6
CO17-26A-26	14.69	0.7	0.2406	0.0081	0.41405	735	81	735	6	735	335	735	6
CO17-26A-27	10.71	0.77	0.1915	0.0075	0.77945	682	80	682	7	682	335	682	7
CO17-26A-28	17.65	0.85	0.2667	0.0085	0.50739	735	82	735	5	735	336	735	5
CO17-26A-29	11.49	2.9	0.1964	0.023	0.68491	677	330	677	21	677	1404	677	20
CO17-26A-3	23.8	1.9	0.308	0.017	0.69248	705	130	705	7	705	546	705	7
CO17-26A-30	15.75	0.71	0.2489	0.0071	0.33923	732	82	732	5	732	339	732	5
CO17-26A-4	16.39	0.78	0.2467	0.0083	0.52692	708	80	708	5	708	336	708	5
CO17-26A-5	18.1	1.3	0.256	0.011	0.75173	694	101	694	6	694	425	694	6
CO17-26A-6	12.42	1	0.2089	0.008	0.47999	694	122	694	7	694	519	694	7

CO17-26A-7	20.6	1.6	0.276	0.013	0.7737	692	112	692	6	692	470	692	6
CO17-26A-8	11.32	0.57	0.2009	0.0059	0.54797	698	69	698	6	698	293	698	6
CO17-26A-9	10.45	0.62	0.2043	0.0067	0.66979	739	69	739	7	739	274	739	7
I16-62A-1	25.2	1.5	0.317	0.015	0.36372	642	136	642	5	642	620	642	4
I16-62A-10	13.25	0.87	0.1999	0.009	0.36416	601	116	601	6	601	562	601	6
I16-62A-11	17.1	1.7	0.222	0.018	0.41068	576	203	576	9	576	1017	576	9
I16-62A-13	29.3	2.1	0.335	0.022	0.69485	608	129	608	6	608	615	608	5
I16-62A-14	12.07	0.73	0.2018	0.0095	0.38803	640	100	640	7	640	463	640	7
I16-62A-15	36.4	2.7	0.382	0.023	0.709	589	136	589	4	589	665	589	4
I16-62A-16	14.17	0.86	0.2139	0.0099	0.3638	621	112	621	6	621	527	621	6
I16-62A-17	14.56	0.86	0.2171	0.01	0.38188	621	109	621	6	621	516	621	6
I16-62A-18	14.98	1.1	0.22	0.012	0.53354	619	120	619	7	619	564	619	7
I16-62A-19	17.07	1.1	0.2386	0.0096	0.70494	621	92	621	5	621	426	621	5
I16-62A-2	15.51	1.1	0.238	0.012	0.6652	658	98	658	7	658	437	658	7
I16-62A-20	24.4	2.1	0.286	0.023	0.67002	590	156	590	8	590	763	590	7
I16-62A-21	11.9	0.71	0.1977	0.0099	0.41053	631	99	631	8	631	465	631	7
I16-62A-22	11.09	0.82	0.1835	0.0078	0.31599	606	120	606	7	606	574	606	6
I16-62A-23	43.3	3.8	0.474	0.034	0.87169	640	112	640	5	640	505	640	5
I16-62A-24	14.49	1.3	0.212	0.014	0.52908	607	146	607	9	607	699	607	9
I16-62A-25	19.1	4.8	0.271	0.048	0.75818	660	333	660	22	660	1462	660	22
I16-62A-26	25	1.8	0.313	0.018	0.81022	637	95	637	6	637	432	637	6
I16-62A-27	18.9	1.3	0.26	0.011	0.25028	637	144	637	5	637	663	637	5
I16-62A-28	13.71	0.9	0.2092	0.0084	0.4394	618	109	618	6	618	510	618	6
I16-62A-3	12.35	0.7	0.2069	0.0068	0.12095	649	103	649	5	649	470	649	5
I16-62A-4	19.1	4.6	0.256	0.035	0.43588	622	454	622	16	622	2113	622	16
I16-62A-5	18.1	3.4	0.247	0.03	0.57948	621	313	621	15	621	1456	621	15
I16-62A-6	21.09	1.3	0.268	0.014	0.66673	610	102	610	6	610	484	610	5
I16-62A-7	17.13	1.1	0.2304	0.01	0.4553	598	119	598	5	598	575	598	5
I16-62A-8	10.44	0.81	0.179	0.011	0.44746	609	117	609	10	609	565	609	9
I16-62A-9	21.7	1.7	0.274	0.016	0.3967	612	167	612	6	612	792	612	6

CO17-55A-1	23.3	1.7	0.551	0.026	0.37621	2375	62	2375	38	2375	121	2375	32
CO17-55A-10	20.7	1.3	0.543	0.025	0.52773	2444	44	2444	40	2444	81	2444	32
CO17-55A-11	26.6	1.7	0.591	0.026	0.44506	2457	54	2457	35	2457	102	2457	30
CO17-55A-12	27.8	2	0.602	0.023	0.66449	2466	57	2466	30	2466	96	2466	30
CO17-55A-13	27.7	2.1	0.613	0.035	0.63944	2533	55	2533	47	2533	97	2533	40
CO17-55A-14	20.7	1.4	0.535	0.023	0.57207	2397	48	2397	36	2397	86	2397	32
CO17-55A-15	17.21	1	0.514	0.022	0.41986	2431	38	2431	39	2431	73	2431	29
CO17-55A-16	16.28	1	0.51	0.019	0.52443	2451	37	2451	34	2451	64	2451	29
CO17-55A-17	21.8	1.6	0.559	0.026	0.62228	2488	49	2488	40	2488	84	2488	36
CO17-55A-18	19.4	1.3	0.527	0.023	0.67761	2408	43	2408	38	2408	72	2408	34
CO17-55A-19	27.9	1.9	0.604	0.03	0.57143	2473	54	2473	39	2473	100	2473	34
CO17-55A-2	17.66	1.1	0.529	0.019	0.49394	2505	39	2505	33	2505	67	2505	29
CO17-55A-20	16.17	1	0.501	0.023	0.54932	2400	37	2400	41	2400	68	2400	31
CO17-55A-21	28.6	2	0.59	0.026	0.6297	2370	60	2370	33	2370	107	2370	31
CO17-55A-22	20.8	3.3	0.595	0.14	0.46317	2799	86	2799	244	2799	226	2799	82
CO17-55A-23	17	0.97	0.499	0.019	0.42713	2350	39	2350	33	2350	75	2350	27
CO17-55A-24	19.33	1.1	0.511	0.02	0.25162	2319	47	2319	32	2319	96	2319	25
CO17-55A-25	20	1.4	0.533	0.027	0.54017	2416	48	2416	44	2416	89	2416	35
CO17-55A-26	18	4.7	0.502	0.11	0.64642	2324	166	2324	185	2324	309	2324	139
CO17-55A-27	15.85	0.99	0.5	0.023	0.47585	2409	38	2409	42	2409	72	2409	31
CO17-55A-28	18.13	1	0.503	0.019	0.71693	2324	35	2324	32	2324	58	2324	28
CO17-55A-29	17.25	1	0.513	0.016	0.51954	2423	37	2423	28	2423	65	2423	26
CO17-55A-3	26.7	1.7	0.587	0.027	0.43781	2430	55	2430	36	2430	107	2430	30
CO17-55A-30	17.54	1.1	0.498	0.016	0.50098	2320	44	2320	27	2320	80	2320	26
CO17-55A-4	30.1	2.1	0.626	0.035	0.71618	2499	50	2499	44	2499	88	2499	37
CO17-55A-5	17.93	1.1	0.531	0.02	0.48036	2504	39	2504	35	2504	68	2504	29
CO17-55A-6	28.1	1.8	0.573	0.023	0.66563	2303	55	2303	29	2303	100	2303	28
CO17-55A-7	14.56	0.92	0.492	0.018	0.46026	2421	37	2421	34	2421	66	2421	29
CO17-55A-8	16.47	1.1	0.506	0.022	0.54123	2417	41	2417	39	2417	73	2417	33
CO17-55A-9	15.12	0.91	0.506	0.017	0.6161	2484	34	2484	32	2484	53	2484	28
I16-34A-1	22.44	1.2	0.648	0.02	0.66609	3341	25	3341	42	3341	29	3341	25

I16-34A-10	21.18	1.8	0.639	0.02	0.63669	3185	40	3185	39	3185	53	3185	36
I16-34A-11	44.6	3.7	0.891	0.045	0.75502	4107	37	4107	77	4107	33	4107	32
I16-34A-12	40.9	3.3	0.943	0.049	0.63878	4282	32	4282	81	4282	28	4282	26
I16-34A-13	40.7	2.9	0.848	0.039	0.45298	3959	32	3959	68	3959	41	3959	32
I16-34A-14	64.5	7.4	1.053	0.081	0.85855	4637	50	4637	127	4637	31	4637	30
I16-34A-15	36	2.4	0.812	0.038	0.74373	3832	31	3832	68	3832	29	3832	27
I16-34A-16	23.04	1.2	0.642	0.016	0.65281	3083	27	3083	29	3083	36	3083	25
I16-34A-17	18.9	0.79	0.6144	0.013	0.52656	3283	19	3283	29	3283	23	3283	19
I16-34A-18	80.4	6.5	1.156	0.094	0.81884	3085	48	3085	53	3085	84	3085	38
I16-34A-19	50.9	4.3	0.889	0.059	0.67197	3057	56	3057	55	3057	91	3057	44
I16-34A-2	24.54	1.3	0.677	0.018	0.56335	3333	25	3333	35	3333	33	3333	25
I16-34A-20	22.63	1.1	0.649	0.018	0.67411	3307	23	3307	37	3307	27	3307	23
I16-34A-21	23.25	1.1	0.663	0.016	0.54405	3279	22	3279	31	3279	30	3279	22
I16-34A-22	65.3	4.7	0.963	0.055	0.5948	2727	72	2727	35	2727	128	2727	31
I16-34A-23	108	14	1.26	0.091	0.70663	2528	166	2528	29	2528	293	2528	29
I16-34A-24	48.9	3.1	0.881	0.045	0.66971	3171	39	3171	46	3171	62	3171	34
I16-34A-25	22.03	1	0.641	0.016	0.60589	3230	22	3230	32	3230	28	3230	22
I16-34A-26	103.7	9.9	1.268	0.084	0.58869	2660	119	2660	29	2660	212	2660	28
I16-34A-27	19.74	0.83	0.6116	0.013	0.49454	3070	20	3070	26	3070	29	3070	19
I16-34A-28	71.9	5.2	1.052	0.064	0.74234	2894	56	2894	38	2894	94	2894	33
I16-34A-29	57.9	3.6	0.931	0.052	0.57045	2902	53	2902	40	2902	96	2902	30
I16-34A-3	18	0.69	0.6065	0.011	0.75578	3294	17	3294	26	3294	17	3294	17
I16-34A-30	19.57	3.8	0.616	0.068	0.86377	3170	92	3170	142	3170	84	3170	83
I16-34A-31	40.6	4.2	0.844	0.057	0.8614	3945	48	3945	100	3945	36	3945	36
I16-34A-32	39.5	2.5	0.85	0.033	0.86421	3966	29	3966	57	3966	22	3966	22
I16-34A-4	45.7	4.5	0.833	0.051	0.71751	2970	67	2970	51	2970	102	2970	48
I16-34A-5	57.8	4.2	0.966	0.057	0.71041	3239	44	3239	51	3239	68	3239	38
I16-34A-6	28.5	2	0.716	0.027	0.71646	3481	34	3481	51	3481	37	3481	33
I16-34A-7	19.66	0.94	0.609	0.013	0.66589	3044	23	3044	26	3044	30	3044	22
I16-34A-8	21.42	1.2	0.644	0.018	0.76387	3205	26	3205	35	3205	29	3205	26
I16-34A-9	62.2	5.6	0.994	0.059	0.70595	3095	63	3095	45	3095	98	3095	42

I16-52A-1	5.94	0.26	0.174	0.0034	0.52394	828	40	828	6	828	145	828	6
I16-52A-10	40.1	2.3	0.447	0.019	0.90406	834	74	834	5	834	266	834	5
I16-52A-11	46.6	2.9	0.489	0.023	0.80882	817	108	817	5	817	400	817	5
I16-52A-12	85.6	4.4	0.806	0.028	0.79884	831	104	831	2	831	379	831	2
I16-52A-13	77.1	3.7	0.746	0.026	0.73685	840	104	840	3	840	378	840	3
I16-52A-14	66.9	3.9	0.668	0.028	0.81602	845	106	845	3	845	384	845	3
I16-52A-15	72.1	3.9	0.7	0.03	0.79003	832	105	832	3	832	386	832	3
I16-52A-17	77.8	3.6	0.756	0.025	0.65596	845	111	845	2	845	405	845	2
I16-52A-18	53.5	2.4	0.543	0.016	0.62997	818	105	818	3	818	392	818	3
I16-52A-19	55.3	2.7	0.562	0.023	0.70619	825	106	825	4	825	393	825	4
I16-52A-2	45.2	20	0.496	0.14	0.39868	849	1178	849	32	849	4276	849	31
I16-52A-20	67	3.1	0.657	0.022	0.56958	829	121	829	3	829	447	829	3
I16-52A-21	78.7	4.1	0.756	0.025	0.71118	837	118	837	2	837	432	837	2
I16-52A-22	73.6	4.1	0.723	0.03	0.78079	846	110	846	3	846	398	846	3
I16-52A-23	53.5	2.5	0.558	0.017	0.67281	841	103	841	3	841	373	841	3
I16-52A-24	70.9	4.5	0.682	0.033	0.69126	822	147	822	4	822	546	822	4
I16-52A-25	23.89	2.1	0.322	0.017	0.62817	845	157	845	9	845	570	845	9
I16-52A-26	62.3	3.2	0.633	0.027	0.68317	847	116	847	4	847	422	847	4
I16-52A-27	99.3	22	0.893	0.17	0.91468	811	309	811	11	811	1153	811	11
I16-52A-28	53.4	2.7	0.561	0.021	0.61064	847	119	847	4	847	433	847	4
I16-52A-29	7.78	0.36	0.1913	0.0042	0.44375	841	52	841	6	841	190	841	6
I16-52A-3	8.31	0.42	0.1947	0.0042	0.74564	837	51	837	6	837	180	837	6
I16-52A-30	76.1	4.4	0.722	0.033	0.80491	821	111	821	3	821	412	821	3
I16-52A-31	67.1	4.4	0.682	0.033	0.79886	861	122	861	4	861	433	861	4
I16-52A-32	65	3.1	0.651	0.023	0.71132	842	103	842	3	842	375	842	3
I16-52A-33	77.3	3.9	0.754	0.03	0.7406	847	108	847	3	847	390	847	3
I16-52A-4	54.5	2.7	0.575	0.021	0.70861	855	103	855	4	855	370	855	4
I16-52A-5	64.8	3.1	0.642	0.022	0.67775	832	110	832	3	832	402	832	3
I16-52A-6	14.39	1	0.245	0.011	0.97613	843	56	843	10	843	181	843	6
I16-52A-7	70.8	3.5	0.687	0.023	0.74529	829	105	829	3	829	387	829	3
I16-52A-8	64.7	3.5	0.643	0.024	0.79967	835	103	835	3	835	375	835	3

I16-52A-9	15.07	0.74	0.2512	0.0067	0.67222	846	69	846	6	846	248	846	6
I16-54A-10	4.08	0.26	0.1961	0.0058	0.37269	652	35	652	5	652	157	652	5
I16-54A-12	5.18	0.6	0.218	0.012	0.57078	617	64	617	7	617	295	617	7
I16-54A-13	32.6	2.4	0.793	0.053	0.59734	483	63	483	2	483	367	483	1
I16-54A-14	12.7	1.1	0.365	0.019	0.64024	512	59	512	3	512	321	512	3
I16-54A-15	3.83	0.18	0.2026	0.0041	0.3032	719	25	719	4	719	104	719	4
I16-54A-16	5.52	0.71	0.1968	0.012	0.25483	513	90	513	6	513	495	513	6
I16-54A-17	9.3	0.56	0.3089	0.011	0.40169	567	45	567	3	567	227	567	3
I16-54A-18	3.75	0.19	0.203	0.0057	0.372	734	26	734	6	734	107	734	6
I16-54A-19	5.88	0.41	0.1792	0.0069	0.23129	435	53	435	3	435	341	435	3
I16-54A-2	3.59	0.21	0.1697	0.0047	0.10544	592	35	592	4	592	173	592	4
I16-54A-20	5.66	0.9	0.1689	0.0081	0.75173	418	98	418	4	418	625	418	3
I16-54A-23	5.1	0.38	0.241	0.014	0.36381	719	45	719	10	719	196	719	9
I16-54A-24	1.55	0.11	0.1262	0.0033	0.33472	662	24	662	7	662	104	662	7
I16-54A-25	9.04	0.61	0.302	0.012	0.73007	566	38	566	3	566	189	566	3
I16-54A-26	9.01	0.56	0.373	0.014	0.77334	760	31	760	5	760	117	760	4
I16-54A-28	2.91	0.2	0.1769	0.0073	0.66715	731	27	731	10	731	102	731	10
I16-54A-3	6.71	0.48	0.204	0.0075	0.74677	455	40	455	3	455	238	455	3
I16-54A-30	2.47	0.23	0.1405	0.0057	0.53901	593	39	593	8	593	183	593	8
I16-54A-31	12.06	0.56	0.438	0.012	0.53425	688	31	688	2	688	134	688	2
I16-54A-32	16.54	0.89	0.51	0.019	0.44744	593	44	593	2	593	213	593	2
I16-54A-33	18.5	2	0.549	0.038	0.72699	575	68	575	3	575	336	575	3
I16-54A-4	8.13	0.35	0.3562	0.0076	0.65415	797	24	797	3	797	88	797	3
I16-54A-5	2.499	0.12	0.1622	0.0037	0.19302	718	21	718	6	718	92	718	5
I16-54A-6	10	0.9	0.282	0.013	0.48018	471	68	471	3	471	398	471	3
I16-54A-7	2.08	0.17	0.1393	0.005	0.76238	649	29	649	8	649	112	649	8
I16-54A-8	29	2.1	0.507	0.028	0.47485	325	73	325	1	325	597	325	1
I16-54A-9	3.53	0.25	0.2061	0.005	0.77367	790	31	790	6	790	108	790	5
I16-46A-1	153	15	1.41	0.15	0.86723	805	176	805	4	805	666	805	3
I16-46A-10	9.17	0.29	0.1904	0.0047	0.10514	765	53	765	6	765	216	765	5

I16-46A-11	14.21	0.72	0.226	0.0084	0.40381	748	91	748	7	748	370	748	7
I16-46A-13	11.11	0.35	0.2014	0.0065	0.29825	747	59	747	7	747	249	747	5
I16-46A-14	9.26	0.45	0.1886	0.005	0.54061	754	60	754	6	754	239	754	6
I16-46A-15	96.1	7.7	0.859	0.065	0.87775	740	129	740	4	740	520	740	4
I16-46A-16	17.96	0.77	0.2616	0.0095	0.32869	767	93	767	6	767	374	767	6
I16-46A-17	54.6	2.7	0.581	0.028	0.58987	803	126	803	4	803	479	803	4
I16-46A-18	24.8	1.2	0.312	0.014	0.53843	756	105	756	6	756	424	756	6
I16-46A-19	129	12	1.16	0.11	0.83347	771	181	771	4	771	709	771	4
I16-46A-2	35	1.8	0.379	0.016	0.56086	728	121	728	5	728	498	728	4
I16-46A-20	36.7	3.3	0.374	0.019	0.53373	693	217	693	5	693	923	693	5
I16-46A-21	25.7	1.3	0.316	0.012	0.76945	748	79	748	5	748	314	748	5
I16-46A-22	76.9	4.8	0.756	0.051	0.81234	790	123	790	4	790	474	790	4
I16-46A-23	81.1	4.7	0.758	0.043	0.74264	756	131	756	3	756	523	756	3
I16-46A-24	120	10	1.024	0.083	0.88089	725	139	725	3	725	570	725	3
I16-46A-25	24.5	1.2	0.315	0.013	0.45773	769	110	769	6	769	435	769	5
I16-46A-26	21.4	1	0.279	0.011	0.38908	739	108	739	6	739	442	739	5
I16-46A-27	7.85	0.34	0.1781	0.0051	0.48907	757	50	757	7	757	201	757	7
I16-46A-28	14.94	0.76	0.234	0.012	0.42207	756	101	756	10	756	416	756	8
I16-46A-29	9.44	0.34	0.1941	0.0059	0.43622	771	50	771	7	771	204	771	6
I16-46A-3	6.65	0.43	0.1623	0.0069	0.36215	728	75	728	11	728	313	728	10
I16-46A-30	11.47	0.55	0.208	0.007	0.50632	762	69	762	7	762	277	762	7
I16-46A-4	82.8	5.2	0.782	0.054	0.68103	766	168	766	4	766	662	766	3
I16-46A-5	13.16	0.66	0.227	0.0079	0.52025	781	76	781	7	781	296	781	7
I16-46A-6	20	1.1	0.281	0.014	0.71362	776	85	776	8	776	333	776	8
I16-46A-7	35.3	1.9	0.383	0.019	0.64921	731	118	731	5	731	483	731	5
I16-46A-8	23.2	1	0.287	0.012	0.41181	723	108	723	6	723	451	723	5
I16-46A-9	10.25	0.39	0.1922	0.0059	0.31721	737	62	737	7	737	260	737	6
McClure-1	2.25	0.15	0.0977	0.003	0.21178	500	57	500	6	500	308	500	6
McClure-2	3.96	0.21	0.1173	0.0034	0.37951	513	68	513	5	513	363	513	5
McClure-3	2.143	0.12	0.0968	0.0028	0.037345	501	51	501	6	501	269	501	6
McClure-4	3.29	0.23	0.1097	0.0037	0.085413	507	79	507	6	507	421	507	6

McClure-5	3.77	0.26	0.116	0.0043	0.051796	512	87	512	6	512	458	512	6
McClure-6	2.52	0.16	0.1025	0.0033	0.14526	510	58	510	6	510	306	510	6
McClure-7	2.36	0.15	0.1045	0.0034	0.32676	527	55	527	7	527	284	527	7
McClure-8	2.56	0.19	0.104	0.0033	0.011778	514	68	514	6	514	362	514	6
McClure-9	2.5	0.16	0.1017	0.0032	0.4146	506	53	506	6	506	288	506	6
McClure-10	2.17	0.16	0.1018	0.0025	-0.030138	524	58	524	5	524	303	524	5
McClure-11	1.109	0.067	0.0911	0.0023	0.093203	529	30	529	6	529	149	529	6
McClure-12	3.62	0.26	0.1155	0.0037	0.33927	518	75	518	6	518	399	518	6
McClure-13	3.01	0.2	0.1093	0.0029	0.28035	520	64	520	5	520	342	520	5
McClure-14	3.57	0.25	0.1132	0.0037	0.42086	510	74	510	6	510	401	510	5
McClure-15	2.82	0.17	0.1067	0.0033	0.30934	516	58	516	6	516	305	516	6
McClure-16	2.94	0.15	0.1072	0.0025	-0.057056	513	58	513	4	513	305	513	4
McClure-17	2.24	0.14	0.0999	0.0029	0.55528	515	46	515	6	515	248	515	5
McClure-18	1.39	0.084	0.095	0.0023	0.19539	535	33	535	6	535	169	535	6
McClure-19	2.19	0.14	0.1009	0.0031	0.065958	519	55	519	6	519	285	519	6
OD306-1	80	24	1.53	0.39	0.999	4462	150	5984	497	3485	128	3498	37
OD306-2	3.41	0.18	0.2756	0.0051	0.20799	1507	21	1569	13	1662	60	1554	12
OD306-3	3.45	0.18	0.277	0.006	0.20432	1516	21	1576	15	1706	61	1556	13
OD306-4	3.5	0.18	0.2759	0.0057	0.095297	1527	20	1571	14	1736	61	1556	12
OD306-5	4.06	0.74	0.284	0.013	0.96484	1646	74	1611	33	1879	102	1589	14
OD306-6	3.49	0.18	0.2746	0.0057	0.41437	1525	20	1564	14	1746	59	1554	14
OD306-7	3.32	0.18	0.2737	0.0068	0.43279	1486	21	1560	17	1667	61	1533	15
OD306-8	3.41	0.17	0.272	0.0056	-0.019805	1507	20	1551	14	1734	61	1535	11
OD306-9	56	23	1.14	0.38	0.99939	4105	205	4904	572	3092	166	1580	55
OD306-10	3.39	0.17	0.2711	0.0063	0.19106	1502	20	1546	16	1729	61	1529	13
OD306-11	3.46	0.2	0.2718	0.0068	0.39711	1518	23	1550	17	1760	64	1541	16
OD306-12	3.3	0.18	0.2767	0.0063	0.17521	1481	21	1575	16	1625	63	1541	13
OD306-13	46	14	0.99	0.24	0.99828	3909	151	4436	389	3328	134	1502	58
OD306-14	3.29	0.17	0.2733	0.0059	0.093587	1479	20	1558	15	1676	62	1529	12
OD306-15	3.32	0.18	0.2773	0.0061	0.1735	1486	21	1578	15	1671	63	1546	13
OD306-16	3.45	0.17	0.2825	0.0057	0.11639	1516	19	1604	14	1710	61	1572	12

OD306-17	49	19	1.05	0.32	0.99895	3972	193	4627	503	3203	147	1682	64
OD306-18	3.64	0.19	0.2795	0.0059	0.34875	1558	21	1589	15	1825	60	1581	14
OD306-19	3.33	0.17	0.2803	0.0066	0.063301	1488	20	1593	17	1656	62	1548	13
OD306-20	3.44	0.2	0.2812	0.0068	0.20586	1514	23	1597	17	1733	67	1568	15
OD306-21	3.24	0.17	0.279	0.0057	0.37498	1467	20	1586	14	1601	60	1551	13
OD306-22	3.32	0.17	0.282	0.0057	0.42489	1486	20	1601	14	1627	58	1568	13
OD306-23	3.41	0.16	0.2815	0.0055	0.17029	1507	18	1599	14	1671	59	1566	12
OD306-24	3.37	0.17	0.2831	0.0057	0.40163	1497	20	1607	14	1636	58	1574	13
OD306-25	3.46	0.17	0.2789	0.0056	0.27889	1518	19	1586	14	1712	58	1564	12
OD306-26	3.35	0.16	0.2772	0.0053	0.26159	1493	19	1577	13	1655	58	1551	12
OD306-27	3.43	0.16	0.2797	0.0055	0.44141	1511	18	1590	14	1682	57	1566	13
OD306-28	3.4	0.17	0.277	0.0053	0.50671	1504	20	1576	13	1687	59	1562	13
OD306-29	3.32	0.17	0.2767	0.0056	0.16677	1486	20	1575	14	1651	61	1545	12
OD306-30	3.31	0.16	0.2785	0.0059	0.15436	1483	19	1584	15	1634	61	1544	12
OD306-31	3.81	0.17	0.2868	0.0055	0.41689	1595	18	1626	14	1823	55	1616	13
OD306-32	3.35	0.16	0.2795	0.0052	0.24463	1493	19	1589	13	1634	58	1559	11
OD306-33	3.26	0.17	0.2771	0.0056	0.30048	1472	20	1577	14	1593	62	1545	13
OD306-34	3.378	0.16	0.275	0.0055	0.16356	1499	19	1566	14	1669	58	1543	12
OD306-35	3.45	0.18	0.2779	0.0053	0.15915	1516	21	1581	13	1698	61	1562	12
OD306-36	3.33	0.16	0.2765	0.0056	0.2052	1488	19	1574	14	1644	59	1543	12
OD306-37	3.38	0.17	0.2789	0.0051	0.246	1500	20	1586	13	1678	60	1563	12
OD306-38	3.255	0.15	0.2819	0.0052	0.015568	1470	18	1601	13	1593	60	1552	10
401-1	0.654	0.087	0.087	0.0029	0.19862	511	27	538	9	701	151	537	9
401-2	0.703	0.085	0.0847	0.0025	-0.07143	541	25	524	7	916	134	526	7
401-3	0.668	0.072	0.0864	0.0027	-0.2148	519	22	534	8	799	131	532	7
401-4	0.67	0.076	0.085	0.0026	0.13703	521	23	526	8	812	130	526	8
401-5	0.71	0.073	0.0859	0.0031	0.096896	545	22	531	9	880	109	533	9
401-6	0.719	0.078	0.0858	0.0028	-0.14174	550	23	531	8	971	127	533	7
401-7	0.693	0.078	0.086	0.0026	0.085728	535	23	532	8	883	127	532	7
401-8	0.689	0.064	0.0844	0.0028	0.091246	532	19	522	8	910	108	524	8
401-9	0.69	0.064	0.0859	0.0033	-0.056118	533	19	531	10	898	112	532	9

401-10	0.703	0.069	0.0852	0.0026	-0.11785	541	21	527	8	942	116	529	7
401-11	0.714	0.084	0.0859	0.0032	0.1458	547	25	531	9	1010	132	533	9
401-12	0.678	0.07	0.0883	0.0029	-0.09258	526	21	545	9	799	121	542	8
401-13	0.67	0.062	0.0861	0.0027	0.23107	521	19	532	8	767	101	531	8
401-14	0.692	0.068	0.0835	0.0024	0.2005	534	20	517	7	951	107	518	7
401-15	0.647	0.067	0.088	0.0026	0.03582	507	21	544	8	717	121	539	7
401-16	0.648	0.07	0.0847	0.0024	-0.054181	507	22	524	7	802	124	522	7
401-17	0.651	0.073	0.083	0.0036	0.11724	509	22	514	11	764	117	513	10
401-18	0.731	0.073	0.0862	0.0027	-0.13213	557	21	533	8	1030	118	537	7
401-19	0.629	0.072	0.0862	0.0023	0.25861	495	22	533	7	683	125	532	7
401-20	0.68	0.065	0.0858	0.0031	0.071153	527	20	531	9	927	113	530	9
401-21	0.738	0.066	0.0847	0.0028	0.062001	561	19	524	8	1070	104	529	8
401-22	0.664	0.068	0.0851	0.0025	0.0060408	517	21	526	7	840	119	525	7
401-23	0.765	0.081	0.0858	0.0024	0.10691	577	23	531	7	1123	119	533	7
401-24	0.692	0.071	0.0872	0.0032	0.038566	534	21	539	9	868	119	538	9
401-25	0.676	0.08	0.0859	0.0028	-0.048643	524	24	531	8	898	139	530	8
401-26	0.675	0.076	0.0862	0.0028	-0.083838	524	23	533	8	837	129	532	8
401-27	0.748	0.068	0.0859	0.0031	0.12911	567	20	531	9	1051	103	536	9
401-28	0.701	0.067	0.0854	0.0028	-0.1516	539	20	528	8	945	115	530	7
401-29	0.646	0.072	0.0843	0.0029	0.11623	506	22	522	9	783	125	520	8
401-30	0.643	0.06	0.0855	0.0028	0.13618	504	19	529	8	747	109	526	8
401-31	0.668	0.063	0.0858	0.0028	0.19508	519	19	531	8	796	110	529	8
401-32	0.698	0.092	0.085	0.0027	0.097673	538	28	526	8	840	138	527	8
401-33	0.639	0.06	0.0857	0.0024	-0.11776	502	19	530	7	701	115	526	6
401-34	0.738	0.085	0.0856	0.0028	0.09711	561	25	529	8	996	126	532	8
401-35	0.677	0.08	0.0873	0.0026	0.15447	525	24	540	8	717	126	539	8
401-36	0.745	0.083	0.0877	0.0028	0.15955	565	24	542	8	965	119	543	8
401-37	0.693	0.082	0.0854	0.0026	-0.035262	535	25	528	8	898	132	529	7
401-38	0.693	0.068	0.0838	0.0026	0.017777	535	20	519	8	945	113	521	7

Appendix 5.4 Apatite REE concentrations (ppm) – Chapter 5.

<i>Apatite Grain</i>	<i>Sr</i>	<i>Y</i>	<i>Zr</i>	<i>La</i>	<i>Ce</i>	<i>Pr</i>	<i>Nd</i>	<i>Sm</i>	<i>Eu</i>	<i>Gd</i>	<i>Tb</i>	<i>Dy</i>	<i>Ho</i>	<i>Er</i>	<i>Tm</i>	<i>Yb</i>	<i>Lu</i>	<i>Th</i>	<i>U</i>
<i>McClure-1</i>	3523	206.1	3.42	1686	2825	258.2	873	98.9	40.93	65.8	7.4	39.25	7.13	19.23	2.56	14.65	1.994	50.51	17.6
<i>McClure-2</i>	3857	332.5	4.04	2409	3662	286.8	916	102.4	37.4	70.9	8.43	48.1	9.99	30.77	4.72	32.05	4.43	90.1	21.28
<i>McClure-3</i>	4076	228.7	4.22	1682	2825	266.5	934	113.4	36.86	77.9	8.38	45.4	8.11	21.23	2.67	15.57	2.19	51.5	18.97
<i>McClure-4</i>	4244	316	7.89	1613	3235	336.1	1284	173.9	41.88	117.1	13.32	69.4	11.84	28.99	3.48	18.29	2.3	22.63	9.22
<i>McClure-5</i>	3953	153.1	3.61	1231	2154	208.1	734	88.6	27.57	59.4	6.34	32.6	5.88	14.06	1.68	9.5	1.249	22.2	8.1
<i>McClure-6</i>	3991	305.3	11.88	2012	3857	366.1	1316	167.6	48.59	110.9	12.37	64	11.61	29.09	3.56	19.5	2.444	31.81	12.91
<i>McClure-7</i>	3817	182.8	5.66	1632	2700	245.2	835	95.2	33.7	62.7	6.73	36.7	6.47	17.05	2.18	12.49	1.74	46.9	14.35
<i>McClure-8</i>	3718	200.5	3.71	1693	2728	246.6	832	96	36.86	63.9	6.7	37.1	6.95	18.81	2.48	15.54	2.14	40.32	13.05
<i>McClure-9</i>	3592	163.2	2.9	1552	2540	228.7	761	85.6	37.49	54.7	5.91	31.79	5.8	15.27	1.87	10.88	1.59	43	14.54
<i>McClure-10</i>	3527	202.4	4.15	1628	2774	255.1	873	103.2	39.86	68.3	7.4	39.32	7.19	18.67	2.4	14	1.862	33.92	14.1
<i>McClure-11</i>	3163	273.3	3.66	2155	3777	335	1132	132.9	52	87	9.52	51.8	9.6	25.82	3.32	19.63	2.64	110.5	31.67
<i>McClure-12</i>	4136	251.8	2.82	1260	2381	253.6	993	135.8	32.11	96.5	10.7	54.7	9.67	23.28	2.64	13.6	1.8	24.61	9.7
<i>McClure-13</i>	3913	130.5	4.45	1517	2273	197.9	667	76	30.57	50.6	5.11	26.5	4.88	11.44	1.415	8.51	1.348	53	15.9
<i>McClure-14</i>	4656	235.9	4.79	1407	2626	266.6	992	128.4	34.44	87.7	9.77	50.2	8.64	22.03	2.63	13.75	1.717	23.19	9.11
<i>McClure-15</i>	3724	143	3.24	1667	2490	211.4	691.7	73.5	40	49.4	4.93	25.88	4.85	12.45	1.539	9.91	1.68	52.36	15.96
<i>McClure-16</i>	3965	299.7	6.17	2219	3767	326.2	1093	127.5	61.6	84.5	9.52	50.9	9.72	27.51	3.89	24.53	3.34	83.5	28.1
<i>McClure-17</i>	3797	82.9	3.3	1324	1781	139.4	429.8	41.3	20.29	26.9	2.81	14.18	2.74	7.54	0.932	5.9	1.024	43.5	14.08
<i>McClure-18</i>	3279	258.9	4.14	2275	4011	346	1165	134.3	68.9	84.5	9.31	49.5	8.9	23.75	3.09	17.75	2.52	82.1	27.68
<i>McClure-19</i>	3623	180.8	3.19	1496	2482	225.1	759.2	86.9	34.8	57.7	6.27	33.46	6.23	16.22	2.24	13.44	1.826	41.91	16.9
<i>OD306-1</i>	208.2	1230	0.6	2627	7370	757	2785	373.7	45.2	280.6	33.63	196.9	39.2	109.7	14.81	94	14.62	73.1	18.53
<i>OD306-2</i>	202	1178	0.171	2438	6934	714.9	2648	351.9	43.31	263.4	32.32	187.2	37.01	103.2	13.8	88.4	14.1	64.2	18.02
<i>OD306-3</i>	205.1	1416	0.211	2596	7390	780	2925	408.7	46.4	311.3	38.28	228	45.68	127.3	17.14	106.6	16.65	73.3	19.98
<i>OD306-4</i>	200.8	1484	0.28	2702	7655	804.7	3018	424.6	47.9	327.2	40.88	241	48.25	134.4	18	113.8	17.18	78.5	21.11
<i>OD306-5</i>	200.5	1320	0.145	2724	7610	790	2927	394.5	47.16	296.5	36.45	210.9	42.26	119	15.68	100.8	15.73	77	20.2

OD306-6	195.7	1200	0.182	2569	7256	753.8	2776	372.9	45.39	272	32.72	193.1	38.28	107.8	14.24	92.8	14.6	70.17	18.77
OD306-7	200.9	1319	0.34	2457	6991	734	2741	386	43.86	293.3	36.29	212	42.49	117.8	15.88	100.9	15.43	70.3	19.47
OD306-8	198	1420	0.36	2598	7418	780	2931	413.5	45.92	311.6	39.08	231.7	45.74	128.8	16.88	108.2	16.7	75.3	20.55
OD306-9	231	1191	0.254	2474	6900	723	2658	361	43.6	267.8	32.7	189.7	38.3	106.6	14.15	89.5	14.25	69.4	18.04
OD306-10	196.6	1228	0.235	2659	7436	764.7	2781	373.4	45.29	276.8	33.61	197.6	38.86	109.5	14.94	95.1	14.9	72.5	18.93
OD306-11	198.1	1215	0.167	2392	6805	713.2	2644	365.2	42.96	272.7	33.28	192.8	38.39	107.2	14.54	90.6	14.21	63.81	18.32
OD306-12	198.5	1393	0.199	2562	7327	770.8	2858	397.4	45.22	304.2	37.55	224.5	44.49	125.2	16.78	104.4	16.2	73.62	20.04
OD306-13	208.5	1110	0.62	2396	6740	700	2599	347.2	43	257.6	30.81	180.8	36.12	99.7	13.42	85.3	13.46	64.9	18.11
OD306-14	198.8	1305	0.208	2747	7727	798	2923	394	48.03	293.6	36.43	212.5	41.78	119.5	15.88	101.5	15.95	78.9	20.29
OD306-15	193.5	1190	0.149	2510	7124	733.9	2696	361.8	45.09	273.2	32.98	193.3	38.6	106.1	14	90.3	14.46	67.03	18.77
OD306-16	199.9	1354	0.22	2484	7140	748.3	2815	393.8	45.54	300.2	37.03	219.7	43.77	122	16.32	104.3	15.83	71.36	19.58
OD306-17	194.1	1096	1.69	2396	6780	699	2568	337.3	42.14	250.4	30.28	175.5	35.14	97.8	13.17	82.9	13.41	64.7	17.87
OD306-18	199.2	1299	0.246	2663	7576	778.4	2870	387.2	46.59	292.5	35.76	210.1	41.53	116.8	15.71	100	15.87	79.28	20.03
OD306-19	196.4	1229	0.3	2640	7394	767	2804	373.7	45.15	279.9	33.75	198.1	39.42	110.5	14.71	94.1	15.06	73.3	19.3
OD306-20	197.7	1230	0.37	2400	6855	716.2	2662	369.7	42.8	273.8	34.22	201.5	39.39	109.5	14.85	91.4	14.5	65.22	18.68
OD306-21	224.4	1601	0.62	3883	9890	998	3608	484.5	55.15	356.5	43.99	260.3	51.72	144.5	19.05	122.3	18.83	140.1	29.28
OD306-22	231.5	1612	0.47	3912	10060	1007	3646	487.9	55	361	45.13	261.6	52.78	146.7	19.75	122.5	19.19	140.8	29.77
OD306-23	233.5	1609	0.48	3893	9970	1000	3628	480.1	55.5	364	44.15	261.1	52.22	145.9	19.45	122.4	19.17	139.3	29.35
OD306-24	232.6	1618	0.5	3845	9950	1001	3619	484	55.35	359.5	44.58	260	51.73	144.6	19.29	120.5	19.19	139.7	29.39
OD306-25	231.3	1602	0.46	3818	9910	997	3620	482.1	55.1	353.1	44.32	256.5	51.72	143.2	19.25	120.2	18.91	139	29.4
OD306-26	228.5	1624	0.51	3884	10100	1006	3658	487.6	56.4	362.6	44.34	262.7	52.4	145.8	19.95	124.5	19.14	140.6	29.75
OD306-27	230.6	1613	0.43	3891	9980	1000	3632	484.8	55.6	363.8	44.46	262.6	52.6	145.4	19.97	122.3	19.12	140.1	29.37
OD306-28	230.6	1611	0.47	3840	9880	1001	3637	489.1	55.89	361.3	44.32	261.3	52.1	144.6	19.53	120.6	18.89	139.6	29.26
OD306-29	231.2	1595	0.6	3840	9890	991	3597	479.9	56.1	355.7	43.91	260.4	51.8	144.1	19.56	123.1	18.74	139.1	29.37
OD306-30	227.8	1569	0.43	3822	9790	984	3579	478.9	54.8	352.2	43.72	257	51.72	143.2	19.19	119.2	18.69	137.9	28.97
OD306-31	227.8	1595	0.86	3908	9910	994	3642	488	55.5	363.6	44.67	262	51.72	145	19.8	122.1	19.34	141.2	29.48
OD306-32	224.5	1579	0.5	3810	9730	977	3563	476.1	54.1	356.7	44.17	256.7	51.48	142.1	19.18	118.9	18.48	137.4	28.74
OD306-33	227.3	1597	0.61	3823	9820	985	3575	473.7	53.95	351.7	44.3	259.4	51.26	142.2	19.39	119.5	18.53	137.6	28.84
OD306-34	227.2	1590	0.47	3825	9780	983.1	3590	476.8	54.8	355.9	43.8	256.5	50.35	141	19.2	119.3	18.74	137.2	28.98
OD306-35	228.5	1583	0.37	3790	9750	976	3533	475	54.14	353.2	43.19	256.7	50.38	142	19	118	18.45	136.6	28.74

OD306-36	228.6	1626	0.36	3922	10050	1006	3660	490.9	56	365.9	44.39	265.9	52.32	147.1	20.02	123	19.24	141.2	29.7
OD306-37	229.3	1607	0.53	3864	9960	998	3615	482.2	55.4	358.3	44.07	258.8	52.4	145.4	19.59	121.8	19.09	139.8	29.45
OD306-38	231.4	1628	0.35	3866	9990	999	3623	489.4	55.8	359.7	44.72	259.7	52.27	143.9	19.82	118.7	18.83	139.3	29.16
401-1	457.1	1495	0.51	3807	9089	861.9	3068	440.3	42.66	354.8	44.05	254.7	48.61	129.9	16.14	87.7	10.48	112.8	14
401-2	452.8	1486	0.42	3797	9027	848.9	3047	440.6	43.36	353.5	43.76	250.4	48.27	127.6	16.04	88.4	10.36	112.8	13.98
401-3	461	1483	0.45	3842	9070	866	3086	448.8	43.85	355.2	44.47	255.9	48.33	131.4	16.11	88	10.46	115.1	14.3
401-4	458.6	1485	0.43	3807	9050	862	3089	445.3	43.58	363.5	44.56	256.2	49.2	131.7	16.44	89	10.55	114.3	14.27
401-5	455.2	1499	0.48	3819	9030	863	3067	447.5	43.41	359.6	44.33	255.5	49.46	130.2	16.27	88.9	10.75	114.7	14.17
401-6	452.9	1493	0.63	3814	8970	863	3072	443.6	43.4	354.5	43.83	254.1	48.67	128.8	16.12	88.8	10.58	115.1	14.05
401-7	450.6	1471	0.43	3732	8933	849.9	3049	444.7	42.39	351.9	44.15	252.4	48.41	128.4	15.82	87.1	10.46	113	13.82
401-8	449.9	1456	0.53	3741	8910	848.3	3027	440	42.59	350.8	43.72	249.9	48.29	130.1	15.97	86.7	10.55	113	14.1
401-9	452.3	1462	0.51	3738	8890	850	3022	440.6	42.9	352.9	43.24	250.3	48.57	127.4	15.85	86.2	10.33	113.5	13.77
401-10	452.8	1455	0.43	3743	8780	841	2986	435	42.82	352.2	43.53	248.6	47.86	128	16.01	86.4	10.25	114.7	13.94
401-11	447.8	1458	0.45	3723	8856	849	3009	439.1	42.22	351	43.34	250.2	48.56	128.4	15.87	87.2	10.48	116.5	13.91
401-12	452.9	1463	0.58	3696	8822	847.2	2991	437.7	42.3	346.4	43.28	251.1	48.04	128.4	15.83	86.3	10.24	116.5	14.19
401-13	460	1467	0.4	3825	9100	866	3083	451.1	43.83	361	44.5	258.1	48.74	131.1	16.19	87.6	10.54	120.3	14.45
401-14	465.8	1515	0.43	3878	9120	873.2	3112	446.5	44.14	364.7	44.81	260.4	50.16	133.4	16.63	90.6	10.97	122	14.9
401-15	454.5	1461	0.43	3711	8850	839.8	3013	439.6	42.07	351.7	43.6	249.8	48.41	129.3	15.72	87.4	10.41	117.3	14.13
401-16	454.3	1466	0.42	3735	8880	845.3	3040	442.6	43.4	353.7	43.75	254.3	48.8	129.7	16.15	88.8	10.35	118.1	14.51
401-17	450.9	1458	0.4	3691	8860	833	2999	440.4	42.38	348.6	42.77	251	47.95	127.5	15.89	85.7	10.26	117.6	14.56
401-18	452.5	1468	0.41	3733	8890	850	3014	435.1	42.09	352.1	43.07	251.6	48.15	128.5	16.01	86.9	10.67	117.3	14.09
401-19	455.8	1460	0.48	3697	8860	845	3000	437.4	42.61	350.4	43.43	251.1	48.77	127.7	16.16	87.9	10.21	116.4	14.17
401-20	454.2	1461	0.45	3729	8870	847	3025	435.2	42.64	353	43.52	253.9	48.56	129	16.22	89.5	10.54	116.4	14.24
401-21	451.9	1475	0.44	3683	8880	846	3029	437	41.33	348.5	44.13	252.4	48.77	129.8	16.35	85.9	10.5	117.5	14.27
401-22	444.5	1456	0.48	3596	8700	834	2976	435.4	41.7	349.7	43.28	250.8	47.77	127.2	16.39	85.8	10.38	115.2	13.97
401-23	454.1	1474	0.41	3717	8880	842.8	3006	438.9	43.03	353.8	43.65	250.5	48.71	128.4	16.15	86.4	10.25	117.4	14.13
401-24	453.6	1463	0.63	3699	8855	843.3	3006	431.5	42.72	349.7	43.32	250.1	48.25	129.4	15.85	87.3	10.56	116.1	14.11
401-25	456.5	1486	0.66	3759	8980	855.2	3059	441.4	42.68	354	44.12	253.7	48.38	128.4	16.25	87.6	10.75	117	14
401-26	459.1	1490	0.5	3795	8970	854	3047	439.4	42.9	354.4	44.29	254.2	48.75	130.8	16.06	88.1	10.66	117.4	14.2

401-27	452.6	1467	0.53	3721	8890	840	3007	434.9	41.73	349.9	43.97	251.6	48.55	127.3	16.22	87.9	10.42	116.7	14.09
401-28	445.5	1450	0.49	3647	8780	836	2982	430.7	42.27	349.7	43.05	246.7	47.84	128.3	15.95	85.2	10.32	115.7	13.96
401-29	450.1	1441	0.55	3670	8790	828	2971	429.3	42.3	348.7	43.39	248.8	47.76	126.7	15.66	86.2	10.18	115.5	14.21
401-30	451.2	1465	0.44	3675	8820	840	3001	437.9	41.93	345.1	43.93	248.5	48.12	127.6	15.8	86.9	10.58	116.4	14.14
401-31	454.8	1466	0.51	3762	8900	846	3023	437.5	43.06	355.5	44.02	250.9	48.25	128.3	15.94	87.2	10.58	117.9	14.32
401-32	448.1	1456	0.58	3645	8770	834	2982	435.3	41.41	347.7	43.16	249.1	47.61	127.5	15.87	86.3	10.27	115.7	14.04
401-33	462.4	1476	0.47	3772	8950	843	3020	437.1	42.8	351.1	43.69	250.8	48.52	127.9	16.26	87.2	10.44	116.4	14.1
401-34	458.3	1473	0.49	3751	8880	844	3008	438.1	42.51	349.9	43.56	251.6	48.78	129.3	15.95	85.6	10.51	117.1	14.11
401-35	454	1464	0.51	3702	8810	835	2982	437.9	42.17	345.2	43.62	247	48.15	127.9	15.55	85.4	10.48	115.1	13.9
401-36	447.5	1460	0.39	3648	8720	829.7	2977	430.3	42.31	344.6	43.02	247.2	47.42	126	15.69	85.5	10.62	113.8	13.85
401-37	456.5	1471	0.5	3713	8900	844	3003	439.2	42.2	348.5	43.61	249.1	48.23	127.3	15.88	85.6	10.46	115.6	14.11
401-38	452.2	1469	0.58	3716	8900	841	3004	432.2	42.24	345.7	43.1	248.7	48.27	127.2	15.74	87.8	10.34	115.6	14.07
I16-17A-19	289	1393	0.59	160	549	96.8	611	253.8	26.5	338	48.2	275.1	48.2	118.4	14.82	82.7	9.71	7.37	5.18
I16-17A-20	283.8	1541	0.149	143.1	491	88	566	247.6	28.34	347.2	51	301.2	53	131.4	16.53	92.8	10.95	9.25	5.8
I16-17A-21	286.2	1264	0.158	109.4	384	70.8	474	210.9	25.67	299.5	43.4	253.7	44.2	112	13.7	74.9	9.04	9.42	6.44
I16-17A-23	290.6	1261	145	102.2	358	65.1	432	197.3	24.43	283	42.15	249	43.76	110.8	13.62	75	8.89	7.32	4.24
I16-17A-24	258.5	805	0.37	11.82	38.23	7.5	57.7	48	26.68	117.9	21.16	145	28.05	73.3	8.79	47.1	6.15	5.06	5.22
I16-17A-25	297.2	1726	0.23	89.6	319	59.9	413	213	33	344	53.9	327	59.9	153.3	19.16	107.3	12.97	17.3	8.72
I16-17A-26	284.4	1570	0.23	203.8	700	122	762	310.4	30.69	390.9	54.9	316.3	53.3	131	16.5	91.6	11.2	12.52	7.34
I16-17A-27	286.4	1587	0.128	109.5	367.6	65.2	428	209.2	30.08	328.5	50.12	305	54.85	139.1	17.44	97.7	11.45	9.13	7.74
I16-17A-28	298.1	854	3.8	24.6	81.4	16	121	76.5	22.7	153.3	25.2	160	30.2	76.3	9.35	51.8	6.61	5.68	7.01
I16-17A-29	289.1	1457	0.207	101.2	334.2	59.5	399.9	198.9	27.52	309.2	47.13	282.4	50.1	127.1	16.07	88.9	10.54	8.68	5.87
I16-17A-30	303	1060	420	187	641	107.9	656	241	24.09	291	39.5	215.6	38.1	91	10.87	61.6	7.22	8.77	5.16
I16-07A-2	154.7	3255	0.068	178	640	111.3	677	303.2	22.5	467.5	87.3	611	118.8	316.1	39.15	210.8	24.65	7.49	9.04
I16-07A-3	165.6	3421	0	227.6	775.8	130.6	764	317.8	21.51	481.3	89.7	622.1	123.1	329.3	41.3	224.4	26.11	6.97	8.02
I16-07A-4	167.2	3548	0	316.7	1071	173.5	943	359.3	20.29	510.9	94	652.6	131.4	347.8	42.74	224.6	26.11	6.99	9.42
I16-07A-5	156	3433	0.081	175.2	608	102	609	277.2	25.7	460.9	87.8	622.5	125.4	329.9	40.86	219.7	25.18	6.86	9.28
I16-07A-6	160.3	3366	0.072	190.6	674	117.8	724	322.4	23.86	498	92.4	636	123.8	321.1	40.2	216.2	24.99	10.91	10.01

I16-07A-7	156.9	3151	410	174.9	615	106.1	657	296	24	470	85.3	591	118.5	308	37.9	204	23.1	9.91	10.9
I16-07A-8	155	3048	0	157.2	566.7	98.1	591	265.2	22.75	427.4	80.5	562.8	111.1	293.3	35.93	194	22.04	5.85	8
I16-07A-9	158.5	3185	0.055	148.2	526	90.7	557	263.2	23.32	439	83.5	594	115.8	308	38.3	202.4	22.94	7.7	9.84
I16-07A-10	160.6	3297	0.046	237.4	797	130.8	758	311	21.55	470.5	87.2	606	120.8	319.6	40.47	217.1	25.3	8.86	8.77
I16-07A-11	157.6	2781	0.089	168.8	564.6	93.4	552.2	241.5	20.71	394.9	73	511	101	265.2	32.46	175.5	20.32	4.7	6.64
I16-07A-12	46	800	0	0	0	0	0	0	0	0	1.8	40	12.9	52	7.8	73	6.8	0	0
I16-07A-13	262.1	2292	0.096	115.5	393	68	426.2	207.2	16.11	345.1	63.6	440.6	86.2	222.6	27.06	142.9	16.36	4.5	4.88
I16-07A-15	227.7	2252	0	113.5	390.3	65.9	404.7	195.8	17.51	325.9	60.8	422.6	81.9	214.7	25.84	139.5	16.3	4.24	5.8
I16-07A-16	166.9	3145	0.085	154.9	549.4	97.1	604	281.8	26.46	457	85.9	597	116.4	299.2	37.7	201.2	23.1	9.37	10.18
I16-07A-17	177.1	2724	0	155.1	559.3	97.4	585	260.6	21.42	413	76	530	100.8	261.8	31.87	167.7	19.13	10.09	8.01
I16-07A-18	154.8	2978	57	171	573.6	96.2	569	250.3	21.31	412.6	77.3	549	108.9	285.4	35.15	190.1	21.73	5.84	7.45
I16-07A-19	191.3	2894	0.094	267.9	940	154.7	868	326.5	19.09	463.2	82.8	557.6	109.1	282.3	34.29	180.2	20.62	7.56	7.99
I16-07A-20	152.3	2537	144	160.5	553.8	93.9	574.9	253.9	21.78	396.9	71.2	485.3	92.3	236.1	28.69	151.4	16.82	3.96	5.28
I16-07A-21	159.2	3424	0.201	285.6	962	159.2	908	360.6	22.98	521.5	95.4	653.7	127	333.7	41.41	222.9	26.24	14.52	10.21
I16-07A-22	174.9	3389	0	323.1	1065	169	917	350.4	19.52	496.5	90.5	632	125.2	331.9	40.99	218.1	25.27	8.89	9.03
I16-07A-23	168.6	3374	0.028	241.2	793	128.7	735	309.2	22.54	482.5	89.2	618.6	123.3	325.2	39.91	216.1	25.09	5.75	6.73
I16-07A-24	184.2	2629	70	97.8	373	68	434.5	217.1	20.98	379.1	71.9	496.6	96.8	251.1	30.41	162.5	18.34	4.89	5.42
I16-07A-25	148.6	3368	0	176.9	635	112.4	680	306	24.74	490	90.2	626	123.3	323.7	39.81	209	24.28	7.35	8.2
I16-07A-26	151.4	3178	0	124.2	476.1	86.5	543	258.8	21.5	432.9	81.8	578.1	116.3	309.1	37.37	195.5	22.72	4.34	5.45
I16-07A-28	162.1	3505	120	163.7	583	99.6	607	280.5	24.25	467	89.7	643	127.7	343.5	42.3	227	26.29	12.74	12.79
I16-07A-29	162.7	3017	61	159.2	598.5	109.2	694.2	312.8	23.81	471.3	86.3	584.7	112.4	290.7	35.85	188.5	21.29	6.81	9.45
I16-07A-30	161.3	2954	16	195.5	671	112.7	680	290.1	20.29	460	83	563	108.5	277.4	34.1	180.7	21.32	7.07	8.41
I16-07A-31	155.6	2492	0.01	220.2	876	150.6	833	321	18.59	420	75.5	504	94.2	238.2	29.61	157.7	18.45	2.22	3.03
I16-07A-32	154.7	2730	0	184	637.2	107.3	635.8	266.4	19.3	406.6	74.3	513.1	100.8	263.3	32.91	173.7	19.91	4.73	6.6
I16-07A-33	149.3	2372	0	101.9	365.1	63.57	398.2	194.4	19.68	345.3	64.17	445.3	87.6	222.6	26.75	138.3	15.69	3.47	4.34
I16-07A-34	170.4	3252	0.142	131	471	84.4	530	267.5	25.7	465	87.3	617	120	311.1	37.92	201.5	23.25	8.93	8.86
I16-18A-1	94.4	2960	0.075	274	995	165.1	897	454	60.1	638	120.7	734	117.4	281	36.3	215	25.8	27.1	42.1
I16-18A-2	101.2	2322	0	246.5	839	135	723	341.9	37.31	478	88.5	543	90.3	220.4	29.16	174.3	21.02	4.87	13.54
I16-18A-3	97.1	2500	0.128	290	1034	173.4	936	458	54.9	599	108.2	647	100.1	233.7	29.7	173.3	19.67	21	32.2

I16-18A-4	99.8	2134	0.008	251.7	841	133.7	706	334.8	35.53	458.7	83.1	501.2	81.6	200.9	25.98	152.5	18.29	3.34	10.36
I16-18A-5	110.4	3870	0.39	334.6	1226	202.7	1105	562	56.7	770	145.5	900	149.6	378	51.5	316	38.7	26	30.26
I16-18A-6	104.5	2419	0	271.5	946	150.6	808	386.8	42.1	519.9	96.3	576.9	93.5	226.8	30.11	179.9	21.27	8.2	16.99
I16-18A-7	102.2	3200	0.103	310.4	1091	176.3	922	453	45.3	637	119.5	747	124.8	308	42.5	256.6	31.7	11.45	22.7
I16-18A-8	101.7	2401	0.045	247	848	134.6	710	337.5	37.62	484.5	90.6	557.3	90.9	224	29.61	178.2	21.99	4.27	11.42
I16-18A-9	94.5	1626	0	219.1	728	115	615	287.3	32.78	388.7	68.9	401	63.2	150.4	18.83	105.5	12.94	2.6	6.38
I16-18A-10	95.6	2620	0.049	251.4	933	158.5	872	446	49.8	598	108.9	651	105.1	251	33.1	191.9	22.8	18.3	29.9
I16-18A-11	96.1	2008	0	193.9	704	115	615.2	297	32.84	421.7	78.1	474.7	76.8	186.6	23.73	139	17.16	2.82	8.15
I16-18A-12	96.8	1952	0.038	188.8	687	112.9	616	308.9	31.68	421	77.1	462	75	181	23.42	136.9	16.23	2.68	7.36
I16-18A-13	143.5	2310	0.3	200	748	125.4	691	357	37	495	93.3	574	94.2	230	30.1	177	22	17.7	26.5
I16-18A-15	100.7	3200	0.117	320.5	1111	180.6	958	465	44.7	637	120.4	745	124.1	312.4	41.1	248.7	30.75	17.2	27.8
I16-18A-16	99.8	3197	0.25	331.1	1159	187	976	485	45.2	652	121.8	741	123.5	304	41.3	250	31	14.2	21.4
I16-18A-17	98.9	1868	0	217	767	125.2	673	326	37	425	76.3	461	70.9	176	22.78	136	17.03	4.15	8.49
I16-18A-18	100.6	2398	0.145	240.8	844	136.4	732	357	41	496	92.7	568	94	229.5	30.01	181.3	22.22	8.12	18
I16-18A-19	98.1	2560	0	254.5	940	157.3	853	421	47.1	567	104.5	628	100.9	244	31.7	190	22.3	12.3	23.3
I16-18A-20	100	1996	0	233.9	815.3	133.5	713.1	335.2	35.52	447	80.7	487.3	77.6	185.9	23.79	139.2	16.65	3.63	9.76
I16-18A-21	100.7	2484	0	269.7	920	145.7	757	368.8	36.35	501.9	92.3	571.2	95.2	236.9	31.46	185.9	23.14	5.09	11.62
I16-18A-22	100.4	1882	0	196	692	112.9	611	293.2	30.97	409.1	73.9	443.2	72	175.8	22.31	129.5	15.91	2.84	8.67
I16-18A-23	98.4	4020	0.63	406	1447	233	1226	601	61.1	816	155.5	946	155	388	53.2	326	39.9	29.7	26.3
I16-18A-24	97.6	1990	0	249.1	846	134.7	711	336.3	35.38	427.8	75.4	459	75.6	186.7	24.83	148.1	17.99	4.6	10.79
I16-18A-25	93	1554	0	185.7	628	103.7	571	273.9	31.7	373.8	65.4	382.2	61.7	143.8	17.87	97.1	11.51	2.09	5.04
I16-18A-26	98.4	2136	0	268.4	920	146	771	358.2	35.47	473	85.4	513.1	83	200.9	26.79	158.7	19.71	3.95	9.79
I16-18A-27	114.3	1892	0	197.1	693	112.1	615	299.1	28.09	415	75.7	455	75.1	181.3	22.94	131.6	15.68	4.8	10.45
I16-18A-28	104.5	2237	0	237.1	817	129.9	690	334.2	33.65	463.5	84.9	521.7	85.3	209.9	28.42	169.8	21	3.79	10.29
I16-18A-29	102.8	2238	0	234.5	816	131.7	700.4	333.4	35.44	462.5	83.7	511.1	86.3	213.6	27.85	164	20.07	3.92	9.38
I16-18A-30	97.3	2000	0.053	233	819	135.6	720	350	36.6	472	85.1	498	78.6	183	23.8	133.1	15.8	5.4	13.3
I16-18A-31	97.5	2590	0.136	303	1062	173.2	914	435	49.9	581	106.8	639	102.2	243	31.8	189	22.3	13.37	25
I16-18A-32	96.2	3720	0.44	339	1240	204.1	1094	555	57.8	759	144.3	884	144.5	355	47.9	289	35.1	28.1	36.7
I16-18A-33	95	1677	0	223.6	739	118.9	629	299.7	32.8	394.6	70	409.4	65.5	153.8	19.08	108.5	13.04	2.34	6.94
I16-18A-34	95.6	1616	0.04	196.6	675	110.2	595	291.7	33.45	384.7	68.6	405	62.9	147.7	18.73	107.1	12.97	2.95	7.46

I16-18A-35	97.4	3036	0.124	289.1	1033	166.5	891	448.5	48.3	614.4	117.2	722	118.2	291.1	38.5	229.6	27.69	13.12	23.63
I16-18A-36	89.9	3170	0.306	268.8	1029	175	954	509	65	705	134	806	127.7	308	40.2	235	27.6	34.7	54.7
I16-18A-37	98.2	2205	0	252.2	862	135.6	708	332.5	33.8	458	85	521.1	85	209.1	27.43	163.2	20.52	4.21	10.07
I16-18A-38	112.5	1253	0	120.1	442.9	74.3	423.6	217.7	23.01	302.1	54.15	318	50.24	115.9	14.01	79.7	9.43	1.352	5.01
I16-32A-1	1004	667	0	12.94	40.71	8.65	63.6	49.3	10.6	107.1	19.27	123.1	22.52	57.3	7.5	44.1	5.5	0.827	0.322
I16-32A-2	683	2020	0	14.6	48.3	11.9	108.1	147	22.9	319	58.6	367	63.3	167	22.3	140	18.6	1.28	0.38
I16-32A-3	6.10E+03	5.50E+05	520	1.33E+05	6.80E+04	3.03E+04	1.30E+05	3.60E+04	5250	6.04E+04	1.19E+04	8.30E+04	1.91E+04	5.44E+04	8.70E+03	5.70E+04	8.00E+03	92	7.80E+04
I16-32A-4	no value	no value	no value	no value	no value	no value	no value	no value	no value	no value	no value	no value	no value	no value	no value	no value	no value	no value	no value
I16-32A-5	728	941	0	7.24	30.87	6.56	50	48.5	11.72	124.9	24.34	173.1	32.68	86.7	11.44	70.5	8.91	0.347	0.37
I16-32A-6	684	2590	1.06	50.7	214	48.2	380	294	21.87	468	83.1	521	91.5	237	32.4	203.8	26	17.3	4.63
I16-32A-7	356	2110	3.24	22	60.4	15.8	121	119	12.78	238	41.6	266	54.2	158	21.2	140	21.9	7.14	1.8
CO17-58A-1	281.4	1561	0.3	105	643	157.5	1170	489	24.41	577	71.2	372.2	61.8	136.4	14.81	73.7	9.16	3.89	14.44
CO17-58A-2	247	1578	0.242	1033	2659	346.3	1598	434.2	17.86	451	61.1	344.4	61.6	150.7	16.81	89.2	11.37	1.68	6.93
CO17-58A-3	264.1	1319	0	424.3	1357	227.7	1302	429.2	18.1	467.6	58.79	308.3	50.97	114	11.68	56.5	6.68	0.788	8.69
CO17-58A-4	198.5	1520	0.132	191.7	880	175.1	1114	413.2	18.18	477	63	342	58.5	137.5	15.25	79.8	10.12	0.217	9.75
CO17-58A-5	277.6	1265	0.117	360.9	1273	220.9	1294	438.2	20.61	478.7	58.4	299.3	49.3	109.6	12.05	60.9	7.76	1.287	8.9
CO17-58A-6	269.5	1499	0.3	121.8	703.6	160.1	1102	449.2	23.5	519.8	66.04	349.8	59.5	133.6	14.7	73	9.13	0.151	11.46
CO17-58A-7	269.7	1540	0.29	241.7	1173	214.4	1239	452	20.71	498	64	346.6	60.5	140.2	16.31	88.5	11.31	0.008	7.84
CO17-58A-8	225.4	2140	0.43	5.20E+03	1.12E+04	1280	5.30E+03	1130	37.9	920	104	514	85.6	195.4	21.84	114.9	15.19	9.6	15.9
CO17-58A-9	280	1551	0.2	98.6	643.3	156	1127	462	26.62	540.6	69.3	364.1	61	135.5	14.94	74.4	9.19	0.12	16.27
CO17-58A-10	252.8	1527	0.212	1032	2944	415.6	2048	563.7	18.28	563.8	69.2	361.7	59.5	135	14.73	74.3	9.47	3.5	11.68
CO17-58A-11	264.7	1432	1.56	1071	2943	414	2061	569	19.72	565	67	342.9	57.2	128.1	14.11	71.9	8.88	6.16	12.99
CO17-58A-12	299.1	3920	3.22	1.05E+05	1.96E+05	18680	6.26E+04	7400	138.1	3790	316	1231	167	311.2	30.42	139.5	16.88	8620	323
CO17-58A-13	266.7	1404	0.093	90.6	516.5	119.5	844	366.5	21.68	444.1	58.1	319.8	54.27	124.4	14.04	72	9.16	0.0306	8.78
CO17-58A-14	281.1	1458	0.4	189.5	902	184.4	1214	469	28.55	533	66.3	341.8	57.5	128.5	14.22	71.6	9.18	2.63	12.55
CO17-58A-15	265.3	1574	0.24	225.8	1092	195.5	1089	384	21.67	433	59.1	338	61.2	150.5	17.4	92.9	11.84	0.0167	8.4
CO17-58A-16	271.7	1955	0.191	1125	2938	387.1	1813	514	21.56	545	73.8	417.9	75.3	183	21.35	113	14.09	1.348	11.25

CO17-58A-17	246.4	1839	0.303	509	1936	325.2	1816	572	23.74	603.5	77	414.1	71.4	164.8	18.75	96.2	12.3	2.65	14.84
CO17-58A-18	297.6	1806	0.251	418.3	1695	281.5	1502	468.9	22.8	514.3	69	392.5	69.4	169.5	19.43	104.1	13.3	0.995	9.94
CO17-58A-19	221.4	1155	0.23	98.8	559	126.9	884	358.4	18.19	417.4	51.6	271.7	44.5	102	10.86	57.1	7.13	0.063	7.54
CO17-58A-20	246.6	1270	0.048	73	368.4	80.6	566.7	254.7	13.63	332.8	45.99	267.2	48.52	116.1	13.12	68.2	8.55	0.083	3.54
CO17-58A-21	303.1	1275	0.063	807	2361	344.1	1746	496.1	17.42	487.3	58.6	303	49.53	109.4	11.77	59.9	7.54	1.858	9.46
CO17-58A-22	202.5	1634	0.125	1200	3137	393.3	1775	469	16.14	472.2	62.6	353.3	62.7	154.1	17.81	96.6	12.16	0.538	9.8
CO17-58A-23	249.4	2071	0.38	143.4	798	173	1162	469.6	27.15	562.5	77.1	442.1	79	191.6	22.22	115.4	14.9	1.029	12.88
CO17-58A-24	266.1	1359	0.239	162.1	879	187.5	1245	464.6	25.52	519	63.6	325.8	53.2	116	12.42	62.4	7.72	2.57	12.13
CO17-58A-25	247.3	1283	0.093	1063	2728	358.4	1699	453.6	15.82	448.1	54.92	289.8	48.83	116.3	12.93	69.3	9.08	1.595	6.1
CO17-58A-26	318.8	1476	0.52	256.9	1085	207.8	1291	468.3	25.07	522.5	66.1	348.8	57.51	130.3	13.95	69.1	8.76	1.019	12.32
CO17-58A-27	296.9	1641	0.22	853	2559	374.9	1929	569	21.06	576.9	72.5	380.2	64.2	146.9	16.63	88.2	11.47	7.37	16.32
CO17-58A-28	279.2	1511	0.24	69.2	447	109.2	806	359.3	22.95	444.5	58.1	328	58.2	138.6	15.91	84.9	10.67	0.314	8.5
CO17-58A-29	236.7	1800	1.36	3.90E+03	9.30E+03	1120	4.70E+03	1020	21	820	90	433	70.3	148	15	73.6	8.91	6.9	11.5
CO17-58A-30	193	1719	0.144	993	2586	335.6	1563	444.3	14.88	476.1	65.8	375.5	67.6	162.8	18.5	98.8	12.16	0.82	8.36
CO17-26A-1	670	1234	0.052	33.74	85.1	12.79	71.8	34.9	60.8	98.6	23.11	193.8	44.13	123.3	15.35	88.8	12.13	0.16	1.93
CO17-26A-2	655.1	1978	266	29.29	96.5	16.63	101.1	59.9	63.4	168.5	38.84	322.3	71	195.3	25.42	150.5	20.21	2.74	16.26
CO17-26A-3	711	1353	0	24.68	75.5	12.57	78.6	46.1	50.2	131.1	29.1	230.5	49.8	135.7	16.27	96.1	12.78	0.673	7.01
CO17-26A-4	622	1524	0.026	24.23	81.6	14.12	86.3	48.8	42.53	132.6	29.49	243.8	55.2	151	19.43	114.3	15.58	1.383	9.94
CO17-26A-5	722	1710	0.047	34.64	113	18.95	111.6	59.5	70.9	159.9	35.5	288	63.1	170.3	22.09	128.8	17.08	1.72	11.27
CO17-26A-6	660	1911	340	36.6	109.1	18.1	111.9	63.5	61.1	175.8	38.69	312.9	70.3	192.3	24.28	143	19.94	2.1	13.68
CO17-26A-7	722	1357	10.7	32.31	94.3	15.16	86.1	46.2	56.4	123.5	27.15	223.5	49.6	135.8	17.25	99.3	13.19	0.866	8.77
CO17-26A-8	632.6	1892	2070	31.13	102.1	17.64	110.1	61.6	60.5	166.5	36.56	303.6	68.6	191.7	25.27	154.4	21.01	2.87	15.21
CO17-26A-9	588	1867	1320	32.4	98	17.95	109.7	61.8	51.2	170.9	37.5	306	66.8	185.4	23.67	143.4	20.28	2.69	14.55
CO17-26A-10	714	1606	62	32.04	98	15.44	85.9	41.4	61.6	106	26.35	235.7	56.2	161.3	21.13	124.2	16.59	1.086	10.14
CO17-26A-11	755	1914	54	25.4	82.4	14.48	94.9	56.3	44.4	157.5	35.19	294.2	66.7	186	24.21	149.5	20.59	1.82	12.37
CO17-26A-12	581	1657	0.032	26.2	89.6	15.81	103.1	60.6	42.5	156.2	34.3	269.1	58.8	161.7	20.74	126.1	17.46	1.25	10.66
CO17-26A-13	596.6	2236	0.76	32.49	115	21.16	139.4	81.3	57.5	212.2	46.1	370.1	79.5	219.3	28.16	171.1	23.3	2.89	17.73
CO17-26A-14	569.1	1940	0.044	36.53	131.5	24.44	177.7	98.1	44.77	228.3	45.14	337.9	69.6	183.4	23.68	138.6	19.3	1.709	15.23

CO17-26A-15	589.6	1810	350	36.64	127.7	24.06	172.9	99.7	45.9	223.9	43.85	315.6	65.36	169.1	21.01	124.1	16.85	2.01	10.79
CO17-26A-16	566.5	2276	0	31.61	104.3	17.55	112.6	69.6	62.6	194.3	44.64	364.2	80.8	222.9	29.07	177.6	24.07	2.237	16.01
CO17-26A-17	569.2	2714	0.18	42.3	142.3	25.71	169.6	103.1	71.1	274.8	58.8	457.2	97.4	263.5	34.45	209.8	28.98	4.65	21.47
CO17-26A-18	606	2185	0	34.91	116.6	20.07	120	65.4	71.6	169.3	39	335.2	77	222.8	29.61	186.6	25.87	3.24	22.28
CO17-26A-19	573	1661	0	27.1	94	16.45	103.2	54.4	41.9	143.3	31.4	264.1	58.2	162.9	21.11	130.4	18.22	1.44	8.58
CO17-26A-20	675	1147	410	24.46	76.76	12.9	75.2	37.5	40.07	89.1	21.13	174.9	40.5	116.7	15.16	89.5	11.91	1.016	7.42
CO17-26A-21	601	1501	61	26.72	85.5	14.38	87.1	49.5	48.56	127.2	28.72	237.9	53.7	150.6	19.96	119	16.71	1.046	8.67
CO17-26A-22	558.5	1796	0.021	27.23	90.4	16.41	106.6	64.6	49.5	172.3	37.01	292.7	63.9	176	22.51	136.6	18.89	0.837	8.8
CO17-26A-23	596.3	1766	370	28.86	94.4	16.38	99.1	53.5	52.6	142.9	33.17	279.3	63.2	176.8	23.43	142.7	19.63	1.571	10.93
CO17-26A-24	566.9	1792	0	24.06	81.7	14.61	99.2	59.6	47	162.3	36.62	293.3	64.29	174.2	22.34	132.7	18.4	0.962	9.79
CO17-26A-25	555.3	1736	0.29	30.53	103.3	18.05	121	69.8	43.5	181.7	38.13	290.9	63.1	166.7	21.58	127.2	17.66	0.921	8.52
CO17-26A-26	557.6	1628	0	35.34	117.8	20.13	125.1	62.9	43.4	149.6	31.94	257	57	161.8	21.13	129.8	18.25	0.965	8.8
CO17-26A-27	605	2063	8.3	27.82	93.6	16.57	98.7	59.9	53.2	183.2	41.7	342.5	75.7	204.8	26.32	155.3	21.38	2.58	15.61
CO17-26A-28	555.1	1677	12.1	29.94	101.3	17.56	111.3	63.2	42.72	166.7	35.96	279.8	59.89	163.2	21.1	125.7	17.4	0.695	7.36
CO17-26A-29	630	2260	0.121	38.2	115.3	18.65	116.2	69.3	65.3	196.1	44.9	368.5	80.8	224.2	28.7	171.9	23.17	2.86	16.52
CO17-26A-30	625	1631	860	23.66	78.2	13.27	85.1	49.8	45.6	137.8	31.44	260.1	58.1	161.5	20.5	124	16.99	1.64	10.21
I16-62A-1	329.9	533	0.99	570.7	1411	191.8	852	167.5	33.03	148.7	18.45	103.2	19.28	48.1	6.06	34.95	4.98	1.75	1.831
I16-62A-2	362.9	953	0.51	352.6	1100	174.6	890	212.2	88.4	215.9	29.01	173.1	33.47	92.2	12.89	83.2	12.78	5.36	3.88
I16-62A-3	362.9	1266	3	486	1511	242	1230	283.3	103.5	280.1	38.39	232	46.13	126.1	17.67	118.7	17.84	6.33	4.89
I16-62A-4	326	632	1.11	423.5	1314	188.4	900	185.3	37.22	169.8	21.36	122.6	23.11	59	7.42	45.3	6.61	1.295	2.49
I16-62A-5	362.1	1026	1.03	63.2	334	70.3	458	163.3	56	192.4	28.8	180.7	35.7	102.5	14.75	93.8	14	5.18	2.89
I16-62A-6	385.7	759	0.6	42.8	237.7	52	348.1	130.3	41.5	148.2	21.92	138.1	27.19	74.4	10.31	64	9.65	1.57	2.56
I16-62A-7	345.3	568	1.32	510	1433	195.3	909	172.6	48	156.8	19.49	110.2	20.66	53.1	6.89	41.3	5.86	5.81	3.05
I16-62A-8	308	690	0.228	113	642	121.9	677	172.5	42.53	172.5	23.3	132.6	24.82	64.9	8.17	45.8	6.68	0.473	3.17
I16-62A-9	316	620	0.23	295.8	1122	169.1	826	179	28.4	164.7	21.37	122.5	22.85	56.2	6.86	38.4	5.15	2.56	1.97
I16-62A-10	329.5	1065	0.85	498	1484	219.3	1113	266.7	45.8	269	36	211.2	38.96	100	12.59	69.9	9.51	3.87	3.83
I16-62A-11	335.2	708	0.94	23.7	158.5	39.6	295	108.5	40.1	133.6	19.04	123	24.82	70.3	9.85	65.9	10.11	0.401	2.62
I16-62A-12	0	0	0	0	370	0	0	0	0	0	0	0	0	0	0	0	0	0	0
I16-62A-13	337	504	0.51	135.8	479.6	81.7	448	110.1	30.12	113.4	15.39	95	18.28	49.2	6.29	38.9	5.76	0.357	1.451

I16-62A-14	348.8	1177	1.67	243.9	969	168.3	916	243.3	79.3	246.6	34.88	217.8	42.33	119.5	16.78	107	16	7.37	4.14
I16-62A-15	335.9	484.4	0.73	108.1	455.7	77.9	426	109.6	25.42	112	15.5	91.3	17.33	46.2	6.09	37.8	5.93	0.44	1.306
I16-62A-16	341.2	735	2.04	462	1561	227.8	1058	215.4	48.3	198.1	25.02	142.9	26.71	68	8.57	49.7	7	8.59	3.91
I16-62A-17	354.6	843	0.47	453.7	1357	197.9	960	204	58.3	186.7	25.61	154.4	30.09	82.8	11.52	71	10.79	5.92	3.5
I16-62A-18	364.7	1196	0.47	133.6	620.5	120.8	729	218.3	69.3	236.9	34.3	213.6	41.8	118.6	16.83	114.3	17.12	5.37	3.77
I16-62A-19	360	759	0.46	353.7	1176	178.8	912	203.2	49.8	192.1	25.33	146.9	27.68	69.8	8.76	54.3	8.09	7.13	3
I16-62A-20	336.4	601	0.31	281.5	994	149.9	749	159.9	29.99	146.7	18.97	112.8	21.64	58.2	7.97	48.2	6.98	1.25	1.87
I16-62A-21	339.4	928	0.34	659	1960	267	1262	261.3	30.6	238.6	30.87	177.8	33.41	84.9	10.69	60.7	8.1	7.04	3.79
I16-62A-22	384.8	947	0.85	502	1810	266.5	1268	267.3	45.6	239.8	30.93	180.4	34.14	91.8	11.84	71.2	10.23	9.72	4.57
I16-62A-23	357	442	0.28	255.7	926	134.9	644	130	20.7	115.6	15.06	84.8	15.68	41.3	5.16	30.5	4.2	0.852	1.158
I16-62A-24	300.1	534	1.06	380.6	1198	168	790	158.7	21.09	143.4	18.25	104.2	19.73	50.6	6.36	38.2	5.58	4.2	2.76
I16-62A-25	356.2	597	0.68	435	1473	203.5	931	180.3	38.6	158.4	19.95	115.7	21.46	54.9	7.22	42.3	6.28	3.15	2.79
I16-62A-26	347	612	0.28	155.8	565	97.5	518	129.2	41.9	129.6	18.25	113.2	21.76	59.6	8.07	50.4	7.43	2.36	1.99
I16-62A-27	330.3	640	0.94	296.3	1027	151.9	744	158.7	38.83	145	19.67	117.8	22.75	62.7	8.58	52.2	7.79	0.671	2.366
I16-62A-28	350.5	969	0.45	240.5	727	123.9	661	187	55.2	202.2	28.71	177.3	35.04	93.8	12.73	78.2	11.59	1.509	3.77
CO17-55A-1	229.9	616	0.36	2370	5.60E+03	580	2140	293	25.4	202	23	123	21.8	53.9	6.48	37	5.1	0.194	2.2
CO17-55A-2	208.8	515	0.62	574.1	1533	203.4	931	175.3	21	148.1	17.72	100.9	18.98	48.7	5.82	32.6	4.59	0.116	2.8
CO17-55A-3	253.4	362.2	0.46	195.2	785	125.6	614.3	118	21.78	99.3	12.25	68.8	12.55	32.81	4.18	24.4	3.57	0.071	2.093
CO17-55A-4	239.8	265.4	0.22	649.1	1624	183.7	719	106.6	11.76	82.6	9.86	52.3	9.71	24.85	3.03	17.33	2.45	0	1.704
CO17-55A-5	247.5	669	0.98	105.7	569.4	114.9	685	182.8	31.88	178.6	22.76	130.2	24.67	61.6	7.59	42.6	5.86	0.0341	4.02
CO17-55A-6	268.1	388.9	0.2	541.1	1513	195	837	140.8	21.15	110.4	13.1	71.5	13.57	36.1	4.57	26.87	4.07	0.101	2.11
CO17-55A-7	210.5	498.4	1.11	788	2060	257.1	1096	182.3	22.08	146.4	17.44	94.9	18.06	46.5	5.82	33.3	4.86	0.226	3.63
CO17-55A-8	239.2	512.5	1.37	176.5	812	141.7	746	158	33.7	137.2	17.03	97.2	17.84	47.29	5.95	34.21	4.93	0.04	3.5
CO17-55A-9	273	838	1.8	523.8	1624	234.8	1137	241.2	37.13	218.5	27.98	160.3	30.53	80.6	10.33	59.8	8.48	0.306	5.59
CO17-55A-10	252.8	412.8	0.75	791	2050	246.9	1014	160.8	22.48	124.6	14.77	79.8	14.85	38.28	4.52	26.73	3.76	0.246	2.89
CO17-55A-11	278.1	438	0.8	108.4	543	103.8	588	137	24.01	121.1	14.93	82.7	15.69	40.5	4.99	29.7	4.43	0.092	2.4
CO17-55A-12	250.7	433.2	1.05	98.3	471.7	87.8	509.9	121.4	27.2	115.4	14.31	82	15.51	40.7	4.94	28.3	4.15	0.061	2.179
CO17-55A-13	224.6	535	0.31	691.3	1928	257.2	1134	195.2	13.84	160.1	19.1	104.6	19.62	48.8	5.9	31.24	4.49	0.087	1.698

CO17-55A-14	209.7	537.7	0.67	692.1	1883	246.5	1102	195.7	17	161.9	19.25	107.9	19.58	50.3	6.24	35.17	4.94	0.136	2.464
CO17-55A-15	233.2	567	0.97	776	2131	268.3	1146	195.4	20.92	160.9	19.16	108.6	20.4	53.2	6.61	39.1	5.49	0.338	3.52
CO17-55A-16	237.3	805	1.03	33.93	232.8	47.5	375.3	175.7	32.36	194.1	26.08	155.8	30.06	78.5	9.44	55.8	8.04	0.0169	3.91
CO17-55A-17	239.7	411.4	0.46	522	1598	215.7	948	161.8	17.63	131.2	14.99	81.3	15.04	37.55	4.33	24.7	3.38	0.081	2.215
CO17-55A-18	221.8	581.1	0.43	259.3	888	143.2	753	171.8	24.07	156.9	19.72	111.8	21.01	54.2	6.65	36.5	5	0.0338	2.562
CO17-55A-19	271	246.3	0.219	404.7	1240	158.3	659.4	102.4	14.97	80.3	9.01	47.6	8.76	22.12	2.54	13.79	2.17	0.0371	1.885
CO17-55A-20	232.4	682.6	0.96	49.27	333.7	76.3	517.5	155.6	27.73	165.1	21.85	130.7	24.82	63.3	7.89	45.4	6.25	0.03	3.34
CO17-55A-21	257.1	410.3	0.81	116.9	504.3	90.8	511.3	121.6	27.66	113	14.08	78.4	14.61	37.6	4.63	25.98	3.8	0.0257	2.053
CO17-55A-22	238.2	339.2	0.8	566	1484	184.9	784	125.5	19.4	101.5	11.45	61.6	11.86	30.6	3.93	23.6	3.38	0.066	3.29
CO17-55A-23	235.2	286.8	0.54	805	1982	222.2	851	120.7	20.46	93.8	10.82	56.5	10.29	26.48	3.16	17.4	2.63	0.119	3.66
CO17-55A-24	250.7	562.3	1.15	497.6	1631	237.1	1112	209.8	24.93	178.7	21.08	113.6	20.55	49.8	5.89	32.7	4.65	0.089	3.14
CO17-55A-25	231	226.4	0.76	719.5	1709	192.3	742.7	103.9	17.53	72.2	8.2	42.7	7.82	20.23	2.59	14.78	2.22	0.091	2.48
CO17-55A-26	205.2	434.7	1	1045	2579	299.5	1169	168.1	18.3	126.3	14.81	82.2	14.99	39.11	5.17	30	4.23	0.199	3.22
CO17-55A-27	200.3	738	0.91	960	2770	379	1660	279	22.4	229	27.2	149.2	27.83	68.2	8.32	45.2	6.48	0.089	2.88
CO17-55A-28	222	482.6	0.167	720.2	1707	225.9	1005	171.8	20.91	150.3	17.64	95.4	18.08	45.9	5.54	32.57	4.34	0.182	2.896
CO17-55A-29	233.6	723	1.15	137.8	580.1	105.9	613.5	170.6	27.21	175.9	23.42	141.2	27.24	72.5	9.33	54.3	7.66	0.07	3.69
CO17-55A-30	244	391	0.56	844	2160	255	1032	161.6	23.39	123.3	14.13	75.7	13.79	34.99	4.3	24.04	3.46	0.126	3.52
I16-34A-1	147.2	321	0	49.3	141	21.3	122	37.9	9	54.5	8.05	51.7	11.3	32.2	4.12	26.2	4.19	1.29	10.6
I16-34A-2	144	351.5	0	27.17	103	19.03	121.7	42.6	8.91	60.6	8.69	56.4	12.28	35.7	4.85	31.14	5.24	0.473	7.02
I16-34A-3	142.9	1311	0.49	142.6	492	79.6	440	130.6	34.3	171	26.08	179.4	41.53	134.3	20.71	139.8	24.63	11.31	60.1
I16-34A-4	144	185.6	0	21.64	69.7	11.38	64.7	20.9	4.53	27.8	3.91	27.2	6.03	18.64	2.64	18.11	3.28	0.091	1.547
I16-34A-5	138.3	205.9	0	12.05	42.5	8.71	60.1	23.39	4.41	36.2	5.2	32.95	7.05	19.98	2.67	15.38	2.67	0.056	1.013
I16-34A-6	142.4	313	0.058	23.79	85.3	14.81	92.7	32.6	6.81	47.6	7.04	47.4	10.69	31.7	4.33	28.5	5.03	0.426	3.98
I16-34A-7	146.5	457	0	64.1	224	37.3	213	59.7	11.17	75.8	10.76	70.7	15.7	45.7	6.62	42.7	7.14	9.9	21.3
I16-34A-8	139.5	497	0.049	58.9	183	29.4	170	56.9	9.7	79.3	11.6	78.3	17.3	50	6.74	41.6	6.65	2.56	15
I16-34A-9	143.4	136.9	0	20.82	59.7	8.88	50	14.68	4.21	20.8	3.06	19.73	4.54	13.93	1.872	11.75	2.08	0.064	1.034
I16-34A-10	145.8	418	0.093	58.8	202	34.9	207	57.1	10	76	10.6	66.6	14.3	40.9	5.39	33.8	5.53	2.43	18.2
I16-34A-11	146	247	0	26.2	85	13.9	79.5	27	6.07	36.6	5.48	38.1	7.87	24.5	3.7	24.4	4.11	0.146	2.07
I16-34A-12	151.4	226.5	0	36.8	104.9	15.82	88.3	26.5	6.99	36.1	5.44	35.7	7.83	21.7	2.88	19.2	3.1	0.201	2.81

I16-34A-13	147.3	211.9	0	18.01	62.9	11.25	69.6	23.49	5.08	35	5.01	32.1	6.92	20.33	2.84	17.45	2.84	0.114	1.856
I16-34A-14	139.4	150.7	0	17.29	51.4	8.29	49.2	16.5	3.85	23.3	3.42	22.8	5.13	16	2.02	13.03	2.34	0.077	0.94
I16-34A-15	146	224.2	0	24.5	72.9	11.53	65.6	22.5	5.17	34.2	5.26	35.1	7.65	22.2	3.21	19.68	3.22	0.229	2.61
I16-34A-16	133.7	656	0.092	30.7	119.9	23.8	164	65.5	17.51	97.2	14.73	99.8	21.5	65.7	9.67	65	10.99	0.63	7.6
I16-34A-17	144.1	946	0.52	83.1	285	47.8	286	97.5	20.8	139.1	21.4	142.9	32.1	96	13.35	86.4	14.43	6.71	33.6
I16-34A-18	135.5	251.1	0	14.27	54.4	11	76.9	29.3	6.69	43	6.1	39.2	8.17	24.55	3.33	21.06	3.68	0.0331	0.761
I16-34A-19	141.5	79.9	0	20.35	55.2	7.18	33.5	7.39	4.75	9.88	1.35	9.11	2.28	7.93	1.21	9.89	2.14	0.112	1.213
I16-34A-20	144.9	586.2	0	32.5	115.3	20.96	135.1	52.4	11.48	81.9	12.84	87.7	19.74	59.7	8.36	53.5	9	0.717	8.75
I16-34A-21	142.3	422.3	0.068	59.5	171.1	23.77	119.8	35.4	11.74	53.2	8.38	56.3	13.2	43.6	6.72	47.3	8.92	0.666	8.19
I16-34A-22	145.7	211.7	0	21.38	69.5	11.95	73.8	23.97	5.17	33.8	4.94	32.1	7.06	20.85	2.91	18.48	3.12	0.06	0.953
I16-34A-23	140.3	213.8	0	15.06	55.6	10.65	73.9	25.1	4.04	35.5	5.19	32.7	7.05	19.99	2.58	15.7	2.61	0.038	0.494
I16-34A-24	145.5	296.3	0	26.37	84.7	14.53	90.6	31.57	5.46	44.4	6.78	44.8	10	29.5	4.21	26.58	4.51	0.169	1.322
I16-34A-25	148.8	451.5	0.117	60.6	188.3	28.89	160.9	49.5	14.36	68.4	10.15	67.8	15.11	44.7	6.44	43.3	7.23	0.911	10.77
I16-34A-26	141	107.9	0	18.75	52.7	8.07	48.7	13.92	5.29	20.9	2.78	16.32	3.59	10.39	1.367	8.92	1.68	0.052	0.495
I16-34A-27	143.5	721	0.24	78.3	266.6	44	249.4	76	26.88	101.9	15.61	103.6	23.39	72.9	10.71	75.2	13.48	2.33	18.6
I16-34A-28	143.1	148	0	24.76	70.9	10.62	58.3	16.32	4.87	22.3	3.1	20.76	4.77	14.27	1.96	13.44	2.4	0.055	0.817
I16-34A-29	141.3	272.3	0	22.54	81.7	15.49	103.6	36.3	6.6	49.4	7.02	43	9.03	26.7	3.54	23.1	3.98	0.096	1.099
I16-34A-30	135.2	850	0.28	71.5	237	37.5	218	76	16.2	118	18.3	130	29.1	92	13.4	88	15.6	5.02	28.7
I16-34A-31	143.5	319	0	26.5	90.8	15.6	96.1	31.8	6.02	46.6	6.92	46.9	10.29	31.5	4.36	27.6	4.87	0.274	2.51
I16-34A-32	145.3	214.8	0	28.51	85.6	13.52	78.2	23.62	5.1	35	5.05	33.04	7.15	21	2.77	16.85	2.81	0.177	2.24
I16-52A-1	1151	1169	0.23	84.7	345	61.8	377	124.1	24.78	184.8	31.07	204.3	39.59	105.2	14.13	82.7	10.39	8.26	45.19
I16-52A-2	1402	1340	1.44	249	766	115.6	615	176	28.08	217.3	35	235.2	45.9	123.5	16.4	97.1	11.59	7.32	4.5
I16-52A-3	1769	1021	2.78	1500	3830	429.9	1773	296.7	50.6	235.7	31.24	185.1	34.2	91.1	12.11	71.2	9.1	10.57	38
I16-52A-4	2336	969	2.28	681	1846	244.3	1127	218.3	35.07	198.8	28.38	174.7	32.1	84.5	11.62	68.7	8.71	11.84	4.79
I16-52A-5	1768	994	1.31	599.6	1633	222.6	1082	252.2	31.31	259.8	36.1	212.4	37.1	87.5	10.42	53.3	6.4	7.57	3.96
I16-52A-6	558	2178	1.33	445	1413	222.3	1197	404.3	33	477	73.5	454.4	82.3	201.2	23.09	119.1	13.52	8.6	20.26
I16-52A-7	2480	866	2.12	635	1679	220	993	186	31.97	167	23.62	148.7	28.25	75.9	10.44	62.9	7.77	7.64	3.75
I16-52A-8	2709	719	5.5	747	1966	251.7	1115	197.9	34.03	161.6	21.72	130.1	24.18	62.5	8.66	52.5	6.6	8.14	4.05
I16-52A-9	2061	1273	1.62	1035	2747	353	1585	323.3	34.72	297.2	41.2	245.7	44.9	113.4	14.62	86.6	10.45	34.35	20.02

I16-52A-10	933	1859	2.44	181	586	95.4	575	197	31.6	285	48	328.7	63.8	169.6	22.29	126.7	16.1	10.3	5.94
I16-52A-11	1201	1515	1.26	223	710	110	612	185	30.37	238.5	39.61	267.6	52	138	18.44	105.5	13.53	8.43	5.41
I16-52A-12	2784	899	1.84	745	1902	245.3	1106	215.8	31.09	189.4	26.8	164.5	30.21	80.3	10.7	64	8.05	7.09	3.16
I16-52A-13	2258	1070	2.35	699	1783	234.9	1089	230.9	31.86	213	30.46	186.1	34.6	89.4	12.25	71.8	8.98	8.23	3.55
I16-52A-14	2827	694	2.22	845	2159	276.6	1218	221	31.6	172.9	23.06	134.2	24.19	60.6	7.93	43.1	5.42	7.61	3.59
I16-52A-15	2933	728	2.13	868	2182	277.5	1205	218.8	32.52	175.7	23.66	135.2	24.49	63.2	8.26	49.1	6.07	7.49	3.58
I16-52A-17	2580	817	1.67	726	1834	237	1070	208.5	30.66	186	25.73	150.4	27.58	71.3	9.36	53.9	6.84	7.06	3.331
I16-52A-18	1654	1503	1.57	369	1073	157.1	808	208.6	29.36	239.1	38.86	258.6	50.3	136	18.38	110.1	13.71	8.4	4.57
I16-52A-19	2224	976	2.88	764	1992	259	1192	237.2	35.91	206.4	29.1	174.4	31.6	81.6	10.82	63.3	8.07	13.57	4.92
I16-52A-20	2640	901	2.01	763	1978	255.2	1166	221.4	32.36	191	26.04	159.2	29.8	78.3	10.62	65.1	7.84	8.11	4.01
I16-52A-21	2514	960	1.49	719	1843	239.3	1093	215.4	30.6	196.8	27.4	172.1	31.4	83.6	11.3	69.1	8.48	6.86	3.39
I16-52A-22	2415	986	1.92	686	1773	233.8	1072	212.1	30.84	194	28.18	173.1	32	85.8	11.58	69.9	8.54	7.65	3.68
I16-52A-23	1314	1464	1.47	308.8	913	134.7	711	196.2	31.02	235.8	38.8	256.1	48.8	130.1	17.3	100.8	12.73	8.24	4.63
I16-52A-24	1781	1177	1.75	481	1339	185	914	227.4	31.1	230.6	34.7	212.4	38.6	99.3	12.72	76.7	9.3	7.47	3.81
I16-52A-25	1127	1157	0.042	12.42	47.1	9.45	73.3	47.9	30.35	120.5	25.39	196.2	41.35	111	14.23	77.9	9.37	2.4	8.76
I16-52A-26	1898	775	2.3	798	2059	268.3	1217	240.3	31.01	202.2	26.73	155.9	26.85	64.5	7.89	41.35	4.9	8.17	3.74
I16-52A-27	1780	930	1.44	169.1	567	90.6	498	130.8	24.4	158.2	24.73	165.6	32.1	84.7	10.77	60.4	7.47	5.69	3.74
I16-52A-28	1091	1624	1.41	159.5	517	86	509	172.3	29.76	240.6	41.64	283.3	55.8	147.9	20.02	114.9	14.06	7.83	4.48
I16-52A-29	1308	1763	1.94	489.6	1445	210.3	1098	327.1	39.3	432	61.7	377.2	70.9	175.2	20.3	110.2	13.83	30.13	33.92
I16-52A-30	1454	1362	1.16	360	1020	148	772	209	27.5	245.9	37.99	249.2	46.6	121.6	15.99	93.2	11.45	6.8	3.49
I16-52A-31	2503	705	2.01	839	2147	273.6	1224	224.3	32.8	182.9	23.53	135.5	24.16	59.2	7.69	44.8	5.58	8.16	3.81
I16-52A-32	1541	1369	1.5	293.9	880	131.9	704	192.8	29.18	229.5	37.3	241.8	45.6	121.7	16.05	92.5	11.75	7.22	4
I16-52A-33	2286	1079	3.8	685	1778	233.1	1094	243.2	30.48	235.7	34.2	207.6	37.8	95.9	12.29	71.6	8.9	7.01	3.59
I16-54A-2	457.7	3635	0.55	9.27	51.9	16.06	173.3	165.2	48.2	386	71.3	500.5	102.7	291.9	39.3	227.2	28.97	6.99	28.98
I16-54A-3	510	1734	0.17	4.77	26.1	7.85	88.1	86.3	25.6	192.1	35.2	246.3	50.7	144.3	20.8	125.9	16.3	1.225	13.7
I16-54A-4	542.4	1910	0.105	10.81	103.3	34.25	320.4	205.1	118.5	309.4	48.8	300.7	57.6	158	22.05	134.2	18.6	0.665	25.29
I16-54A-5	458.4	3920	0.094	38.69	240.1	70.92	658	413.3	57	614	99.2	626	120.1	333.1	45.8	267.1	34.2	0.965	36
I16-54A-6	532	1210	0	5.3	40.6	11.29	108.1	79.9	23.29	151.2	26.5	178.6	35.6	100.5	14.21	84.8	11.5	0.153	10.7
I16-54A-7	531.9	2430	0.101	37.1	198.5	49.7	409	252	56.6	385	63.5	391	74.4	205	27.7	167	21.9	0.91	30.6

I16-54A-8	452.4	901	0	2.74	17.34	5.2	56	52.4	9.61	127.3	21.55	143.4	28.73	74.1	8.44	42.8	5.7	0.109	1.121
I16-54A-9	498.6	5089	0.49	14.56	107.8	35.48	376.4	309.5	56.7	607	106.5	723	147	432.9	61.8	377.7	49.7	16.22	99
I16-54A-10	522.4	1341	0.095	20.39	131.7	33.92	281.3	156.1	66	229.6	35.96	220.2	41.6	112.8	15.05	88.9	11.62	0.684	13.8
I16-54A-12	566	1206	0	29.4	176	43.1	327	165.6	39.8	214.6	32.2	191.7	36.2	95.6	12.87	75.6	9.97	0.061	11.2
I16-54A-13	463.6	1545	0	5.72	46.9	17.02	195.6	144.7	13.23	247.4	40.2	252.9	49.1	130.6	17.2	95.6	11.63	0.291	3.42
I16-54A-14	497.5	1104	3.9	2.63	14.57	3.99	40.5	43.1	20.29	114.9	22.1	156.8	33.17	96	13.47	79.5	10.46	0.022	3.9
I16-54A-15	520.1	2644	0.104	20.28	162.8	54.15	506.3	324.8	93.8	459.9	71.7	437	82.2	223.4	30.27	176	23.16	0.195	35.2
I16-54A-16	514	1986	0.14	7.01	46.5	16.34	180.2	142.6	44.9	267	45.4	294.2	58.8	158.6	20.9	120.6	15.68	1.89	14.43
I16-54A-17	475.3	2595	0.071	1.68	10.74	3.91	54.7	86.1	17.94	278.3	55.54	396.8	83.7	234.8	29.99	165.3	20.45	0.347	6.82
I16-54A-18	518.8	2856	0.051	15.52	63.9	14.9	147.1	138.7	36.72	317.9	59.3	416	85.3	244.1	34	199.7	26.1	1.55	20.41
I16-54A-19	443	1869	0.039	4.8	35.8	12.39	142	132.5	18.7	283	44.1	269.3	53.6	143.4	17.76	104.3	15.94	1.194	5.38
I16-54A-20	498.2	3362	0.14	7.01	43.3	13.87	166.1	176.2	46	403	73	496.6	100.4	274.7	37.76	210.9	27.02	0.83	15.63
I16-54A-23	481	7.00E+03	2.09	6.68	42.3	15	196	214	34.9	586	116	870	186	550	74	430	57	3.69	24.3
I16-54A-24	520.8	2105	0	27.56	176.2	50.38	446	271.9	57.6	378.7	58.3	349.6	64.4	173.8	23.05	135.6	17.57	0.303	17.88
I16-54A-25	548	2247	0.056	45.9	231.2	56.96	478.7	259.2	43.5	388.9	59.5	356.1	67.5	188.9	26.54	157	20.62	1.376	12.14
I16-54A-26	585	1739	0	42.1	191	45.6	371.8	215.7	48.6	301.3	47	283.7	52.3	145.1	19.12	115.1	15.06	0.227	11.61
I16-54A-28	550	2872	0.122	30.06	223.5	64.6	560	325.5	64.4	473	75.3	464	88.1	245.5	33.1	200	25.96	3.32	44
I16-54A-30	458.5	2310	0.062	4.02	18.17	5.25	59.5	72.4	16.93	224.3	43.2	316	66.6	193.5	26.9	157.2	20.4	1.047	11.16
I16-54A-31	566.7	1800	0.085	76.7	361.5	78.4	551.6	248.2	37.36	339.2	50.3	299.5	55.5	147.5	18.93	106.6	12.9	1.99	13.04
I16-54A-32	446.2	2051	0.027	63.3	264.1	55.6	409.9	221.8	35.1	350.8	55.9	346.4	65	172.2	21.94	117.1	13.72	0.76	4.9
I16-54A-33	461	1403	0	1.43	8.25	2.86	36	47.5	8.64	144.9	28.05	208.5	43.1	121.4	15.64	84.8	10.61	0.054	2.65
I16-46A-1	260.6	469	0	4.45	14	2.57	17.46	11.75	3.3	30.2	7.13	63.7	16.66	57	8.53	59.3	9.07	0.104	0.455
I16-46A-2	279.5	671	0	8.41	29.2	5.36	34.5	18.84	7.11	43.8	10.51	95.4	24.53	74.5	8.82	46.4	6.11	0.567	1.976
I16-46A-3	35.6	1660	42.7	30.6	165.3	37.6	230	118.4	148.5	185	37.7	280	57.5	163	23.2	152.5	20.3	2.09	12.78
I16-46A-4	303.2	340.6	0	2.91	11.15	2.23	16.1	10.39	3.81	27.8	6.11	52.7	13.05	38	4.54	23.64	3.34	0.111	0.842
I16-46A-5	270.7	2425	0.051	28.48	101.4	17.62	113	62.9	33.91	167	39.55	353.5	88.8	269.5	35.05	205.7	28.18	0.23	6.13
I16-46A-6	258.5	1549	19	18.18	67.3	12.77	83.3	48.4	18.59	112.8	24.91	214.5	55.3	182.4	27.62	182.9	26.99	0.554	4.01
I16-46A-7	327.1	1373	0.051	7.62	26.21	4.75	32.1	22.4	26.05	64.1	17.82	179.4	50.15	162.4	21.07	109.5	13.35	0.0307	2.05

<i>I16-46A-8</i>	294.9	1367	0	14.2	51.5	9.25	62.2	39.3	15.36	99.1	24.19	215.9	51.9	146.2	16.45	80.7	9.86	0.321	3.27
<i>I16-46A-9</i>	255.6	2529	0.125	25.71	91.6	16.43	109.7	66	26.98	169.9	39.6	350.9	91.2	297.8	44	290	42	0.542	7.77
<i>I16-46A-10</i>	268.5	2631	0.297	55.7	188.9	32.25	192.8	94.3	44.5	197.6	44.59	386.1	95.2	277.6	33.73	182.8	24.77	0.81	9.14
<i>I16-46A-11</i>	276	1793	29	28.03	102.4	18.36	117.9	64.2	26.18	139.8	32.16	273.3	66	190.8	23.3	125	16.3	0.726	5.66
<i>I16-46A-13</i>	283	1857	3.64	19.8	76.1	14.25	98.7	60.5	25.8	153.2	35.63	299.9	70.5	200.2	23.81	125.8	16.67	1.179	6.94
<i>I16-46A-14</i>	273.2	2882	0.3	61.1	213	37.03	221.6	108.3	46.6	218.9	49.86	424.1	103.2	301.7	37.41	201.4	27.65	0.375	9.37
<i>I16-46A-15</i>	282.9	510	0	1.61	5.68	1.096	8.76	8.67	3.39	32.8	8.32	74.3	18.65	54.1	6.14	29	3.45	0.051	0.726
<i>I16-46A-16</i>	265.9	1604	0	24.76	89.5	16.3	101.7	54.3	26.39	118.8	24.96	216.6	56.4	185.6	26.96	172.3	23.8	0.912	4.51
<i>I16-46A-17</i>	297.4	939	0	15.99	50.4	8.29	52.9	31	30.1	73.2	17.54	152	35.28	98.9	11.4	54.4	6.04	0.042	1.28
<i>I16-46A-18</i>	255.4	1334	0	10.78	41.82	8.45	60.8	40.7	13.6	104.5	22.93	192.7	48.65	157.4	23.23	152.9	22.53	0.424	2.85
<i>I16-46A-19</i>	291.2	359.4	0	2.62	10.26	1.97	13.29	8.82	3.06	23	5.48	48.7	12.85	40.2	5.15	32.1	4.95	0.119	0.562
<i>I16-46A-20</i>	267.5	816	0.037	3.6	14.07	2.83	20.3	14.8	4.99	43.7	11.32	103.8	29.12	103	15.66	110.3	18.4	0.398	1.92
<i>I16-46A-21</i>	266.2	1554	0.066	25.23	79.3	12.94	79.4	43.8	44.38	106.7	25.71	231.5	58.69	178	22.37	124	16.09	0.131	3.13
<i>I16-46A-22</i>	271.1	379	0	4.67	18.16	3.3	23.1	13.51	4.65	32.8	7.2	59.3	14	37.7	4.17	21.63	3.23	0.196	0.841
<i>I16-46A-23</i>	260.7	974	0.2	9.47	33.7	6.04	40.7	24.6	9.01	61.4	14.54	128.9	34.6	117.4	17.43	114.7	16.85	0.18	0.943
<i>I16-46A-24</i>	259.8	382.4	0	1.8	6.46	1.25	8.67	6.02	2.21	19.1	4.88	46	13.04	48.6	8.25	59.1	9.26	0.068	0.57
<i>I16-46A-25</i>	259	1491	0.009	19.56	64.6	11.08	68.2	36.6	18.3	86.6	20.55	191.5	52.48	180.1	26.8	173.9	25.3	0.493	3.32
<i>I16-46A-26</i>	281.4	1978	19	15.2	47.12	8.27	55.1	43.2	31.89	119.8	32.19	301.8	72.9	214.1	26.12	131.9	15.16	0.0323	3.68
<i>I16-46A-27</i>	253.6	2666	0.132	32.01	124.1	23.6	161.7	96.4	38.2	221.6	46.28	376.9	95	314.7	49.07	332.4	49.5	1.654	11.5
<i>I16-46A-28</i>	286.6	2500	17	28.6	102.4	18.82	121.5	71.6	31.4	177.5	43.6	383.8	93.8	269.2	31.39	158.7	19.48	0.44	5.57
<i>I16-46A-29</i>	255.7	3100	0.073	32.79	116.2	20.53	134.5	77.6	31.84	197	47.23	428.2	111.3	356.9	52.7	346.5	50.29	1.661	9.61
<i>I16-46A-30</i>	273.9	1898	0.075	35.6	120.2	20.74	129.6	68.2	31.92	152.9	35.07	293.2	69.3	197.8	23.85	126.2	16.47	0.303	6.89

Appendix 5.5 Monazite U–Pb age data – Chapter 5

Monazite Grain	$^{207}\text{Pb}/^{235}\text{U}$	2σ	$^{206}\text{Pb}/^{238}\text{U}$	2σ	Error Correlation (ρ)	Th/U	$^{207}\text{Pb}/^{235}\text{U}$ Age (Ma)	Age 2σ	$^{206}\text{Pb}/^{238}\text{U}$ Age (Ma)	Age 2σ	$^{207}\text{Pb}/^{206}\text{Pb}$ Age (Ma)	Age 2σ	Concordance
<i>I16-18M - 1</i>	16.5900	2.2000	0.5598	0.0140	0.8719	26.23	2911.4	63.5	2865.8	28.9	2943.1	90	97.37352
<i>I16-18M - 2</i>	17.6400	2.4000	0.5848	0.0130	0.5649	19.72	2970.3	65.4	2968.3	26.4	2972	101	99.8755

I16-18M - 3	17.3800	2.4000	0.5768	0.0130	0.8843	19.14	2956	66.3	2935.7	26.6	2969.9	95.6	98.84845
I16-18M - 4	17.2400	2.4000	0.5769	0.0130	0.8606	37.70	2948.3	66.8	2936.1	26.6	2956.6	97.1	99.30664
I16-18M - 5	17.4600	5.4000	0.5830	0.0910	0.7966	33.92	2960	149	2961	185	2960	167	100.0338
I16-18M - 6	17.5800	2.4000	0.5833	0.0130	0.7389	17.80	2967	65.6	2962.2	26.5	2970.3	97.5	99.7273
I16-18M - 7	17.6300	2.4000	0.5859	0.0130	0.7013	22.46	2969.8	65.4	2972.8	26.4	2967.7	98	100.1719
I16-18M - 8	18.0000	2.5000	0.5986	0.0130	0.6847	17.04	2989.7	66.8	3024.2	26.2	2967	101	101.9279
I16-18M - 9	17.4300	2.3000	0.5891	0.0290	0.8983	19.58	2958.8	63.4	2985.8	58.8	2940.5	73	101.5406
I16-18M - 10	17.6000	2.4000	0.5832	0.0130	0.7495	18.16	2968.1	65.5	2961.8	26.5	2972.4	97.1	99.64339
I16-18M - 11	17.5800	2.4000	0.5820	0.0130	0.7526	21.43	2967	65.6	2956.9	26.5	2973.9	97.2	99.42836
I16-18M - 12	17.5200	2.4000	0.5832	0.0130	0.7802	22.70	2963.8	65.8	2961.8	26.5	2965.1	97.1	99.88871
I16-18M - 13	17.0500	2.2000	0.5639	0.0180	0.8764	37.82	2937.7	61.9	2882.7	37.1	2975.5	82.3	96.8812
I16-18M - 14	17.5000	2.4000	0.5797	0.0130	0.8051	23.76	2962.7	65.9	2947.5	26.5	2972.9	96.5	99.14562
I16-18M - 15	17.5800	2.4000	0.5878	0.0130	0.7693	21.71	2967	65.6	2980.5	26.4	2957.9	97.1	100.7641
I16-18M - 16	17.4900	2.4000	0.5829	0.0130	0.7877	17.79	2962.1	65.9	2960.6	26.5	2963.1	97.1	99.91563
I16-18M - 17	17.5900	2.5000	0.5859	0.0140	0.8351	21.35	2967.6	68.3	2972.8	28.5	2964.1	99.1	100.2935
I16-18M - 18	16.6100	2.1000	0.5553	0.0170	0.8709	18.46	2912.6	60.5	2847.2	35.2	2958.1	81.4	96.25097
I16-18M - 19	17.5400	2.4000	0.5868	0.0130	0.7695	18.15	2964.8	65.7	2976.4	26.4	2957	97.3	100.6561
I16-18M - 20	17.8800	2.5000	0.5905	0.0130	0.6733	18.95	2983.3	67.2	2991.4	26.3	2978	102	100.45
I16-18M - 21	17.7100	2.4000	0.5912	0.0130	0.8359	28.60	2974.1	65.1	2994.3	26.3	2960.5	95	101.1417
I16-18M - 22	17.5200	2.4000	0.5839	0.0130	0.7032	20.87	2963.8	65.8	2964.6	26.5	2963.1	98.7	100.0506
I16-18M - 23	17.6500	2.4000	0.5880	0.0130	0.6219	20.45	2970.9	65.3	2981.3	26.4	2963.8	99.5	100.5905
I16-18M - 24	17.3400	2.3000	0.5784	0.0130	0.7890	28.74	2953.8	63.7	2942.2	26.5	2961.8	93.3	99.33824
I16-18M - 25	17.5400	2.4000	0.5883	0.0130	0.8558	17.49	2964.8	65.7	2982.5	26.4	2952.9	95.6	101.0024
I16-18M - 26	17.8300	2.5000	0.5958	0.0130	0.6941	23.07	2980.6	67.4	3012.9	26.3	2959	102	101.8216
I16-18M - 27	17.9000	2.5000	0.5978	0.0130	0.8181	15.99	2984.4	67.2	3021	26.2	2959.8	98.8	102.0677
I16-18M - 28	17.7000	2.4000	0.5898	0.0130	0.4313	21.81	2973.6	65.2	2988.6	26.4	2963	103	100.864
I16-18M - 29	17.8100	2.4000	0.5931	0.0130	0.6558	22.65	2979.5	64.8	3002	26.3	2964.4	98	101.2684
I16-18M - 30	17.8500	2.5000	0.5947	0.0130	0.6331	16.68	2981.7	67.3	3008.4	26.3	2964	103	101.498
I16-18M - 31	17.6700	2.4000	0.5947	0.0130	0.8061	17.30	2971.9	65.3	3008.4	26.3	2947.3	96	102.0731

CO17-58M - 1	20.4800	2.8000	0.6382	0.0150	0.6621	407.88	3114.3	66.2	3181.9	29.5	3071	97.8	103.6112
CO17-58M - 2	19.6700	2.7000	0.6220	0.0150	0.6521	214.78	3075.3	66.3	3117.9	29.8	3047.6	98.4	102.3067
CO17-58M - 3	19.4200	2.7000	0.6003	0.0140	0.6464	206.55	3062.9	67.1	3031	28.2	3083.9	99.9	98.28464
CO17-58M - 4	18.8600	2.6000	0.6008	0.0150	0.6675	536.49	3034.7	66.5	3033.1	30.2	3035.8	98.2	99.91106
CO17-58M - 5	19.2900	2.7000	0.6069	0.0140	0.6367	306.34	3056.4	67.6	3057.6	28.1	3056	101	100.0524
CO17-58M - 6	21.9800	3.1000	0.6390	0.0160	0.6271	551.01	3182.8	68.5	3185.1	31.5	3181	100	100.1289
CO17-58M - 7	20.9100	2.9000	0.6308	0.0140	0.5695	278.02	3134.4	67.2	3152.8	27.7	3123	101	100.9542
CO17-58M - 8	21.4800	2.9000	0.6495	0.0150	0.5645	429.13	3160.5	65.5	3226.3	29.3	3119	98.2	103.4402
CO17-58M - 9	21.9900	3.0000	0.6670	0.0160	0.5743	400.68	3183.3	66.2	3294.3	30.9	3114.1	98.9	105.7866
CO17-58M - 10	20.0000	2.8000	0.6227	0.0150	0.5698	467.20	3091.4	67.7	3120.7	29.8	3072	102	101.5853
CO17-58M - 11	20.8100	2.9000	0.6319	0.0160	0.6656	285.30	3129.8	67.5	3157.1	31.6	3112.3	98.7	101.4394
CO17-58M - 12	24.1000	3.1000	0.7370	0.0200	0.6683	407.45	3272.4	62.7	3559.4	37.1	3101	89.5	114.7823
CO17-58M - 13	20.2600	2.8000	0.6257	0.0150	0.6152	277.71	3103.9	66.9	3132.6	29.7	3085.3	99.7	101.5331
CO17-58M - 14	15.6900	2.2000	0.5500	0.0130	0.5273	242.06	2858.1	66.9	2825.2	27	2881	105	98.06317
CO17-58M - 15	20.1500	2.8000	0.6117	0.0160	0.5056	421.19	3098.6	67.2	3076.8	32	3113	102	98.83713
CO17-58M - 16	15.3200	2.0000	0.5506	0.0140	0.4131	378.96	2835.3	62.2	2827.7	29.1	2840.8	99.6	99.53886
CO17-58M - 17	21.8600	2.9000	0.6590	0.0160	0.5374	360.12	3177.5	64.4	3263.3	31.1	3123.8	96.5	104.4657
CO17-58M - 18	20.0900	2.8000	0.6383	0.0150	0.7210	321.55	3095.7	67.4	3182.3	29.5	3040	98.9	104.6809
CO17-58M - 19	22.0000	3.0000	0.6540	0.0160	0.6879	529.85	3183.7	66.2	3243.8	31.2	3146.1	96	103.1054
CO17-58M - 20	19.6600	2.6000	0.6120	0.0170	0.8215	461.78	3074.8	63.9	3078	34	3072.7	88.3	100.1725
CO17-58M - 21	20.3500	2.8000	0.6173	0.0150	0.5764	324.47	3108.1	66.6	3099.2	29.9	3113.9	99.7	99.52792
CO17-58M - 22	13.9900	5.0000	0.5140	0.0920	0.5926	91.04	2749	169	2674	196	2805	237	95.32977
CO17-58M - 23	17.6200	2.4000	0.5812	0.0140	0.6304	295.71	2969.2	65.4	2953.6	28.5	2979.8	98.6	99.12075
CO17-58M - 24	17.8400	2.4000	0.5810	0.0140	0.8078	165.78	2981.1	64.7	2952.8	28.5	3000.3	93.2	98.41682
CO17-58M - 25	16.2000	2.1000	0.5470	0.0150	0.5629	509.62	2888.7	62	2812.7	31.3	2942.1	94	95.60178
CO17-58M - 26	20.6600	2.9000	0.6208	0.0140	0.6379	207.73	3122.8	68	3113.1	27.8	3129	101	99.49185
CO17-58M - 27	17.3900	2.4000	0.5758	0.0140	0.5528	423.95	2956.6	66.3	2931.6	28.6	2974	102	98.57431
CO17-58M - 28	20.0600	2.7000	0.6228	0.0150	0.5332	376.47	3094.3	65.1	3121.1	29.8	3076.9	98.6	101.4365
CO17-58M - 29	20.9700	2.9000	0.6356	0.0160	0.4605	533.68	3137.2	67	3171.7	31.5	3115	102	101.8202
CO17-58M - 30	22.2700	3.1000	0.6550	0.0170	0.4456	903.50	3195.6	67.6	3247.7	33.1	3163	103	102.6778

CO17-58M - 31	18.6800	2.5000	0.5800	0.0150	0.7694	286.08	3025.4	64.5	2948.8	30.6	3076.8	91.9	95.83983
MADL - 1	0.6586	0.0910	0.0839	0.0019	0.3653	30.78	513.8	27.9	519.36	5.65	489	145	106.2086
MADL - 2	0.6547	0.0900	0.0832	0.0018	0.3627	29.81	511.4	27.6	515.19	5.36	494	145	104.2895
MADL - 3	0.6596	0.0910	0.0840	0.0018	0.3465	30.15	514.4	27.8	519.95	5.35	490	146	106.1122
MADL - 4	0.6613	0.0910	0.0841	0.0019	0.4987	30.36	515.4	27.8	520.55	5.65	493	141	105.5882
MADL - 5	0.6605	0.0910	0.0840	0.0018	0.4470	30.52	514.9	27.8	519.95	5.35	493	143	105.4665
MADL - 6	0.6600	0.0910	0.0831	0.0018	0.4097	30.49	514.6	27.8	514.6	5.36	515	143	99.92233
MADL - 7	0.6541	0.0900	0.0839	0.0018	0.2432	30.68	511	27.6	519.36	5.35	474	148	109.5696
MADL - 8	0.6593	0.0910	0.0842	0.0019	0.6568	30.86	514.2	27.8	521.14	5.65	483	137	107.8965
MADL - 9	0.6511	0.0900	0.0831	0.0018	0.6291	30.12	509.2	27.7	514.6	5.36	485	139	106.1031
MADL - 10	0.6616	0.0910	0.0838	0.0018	0.4265	31.06	515.6	27.8	518.76	5.35	502	143	103.3386
MADL - 11	0.6428	0.0890	0.0830	0.0019	0.5153	30.75	504	27.5	514	5.65	459	142	111.9826
MADL - 12	0.6590	0.0910	0.0840	0.0019	0.4823	30.93	514	27.8	519.95	5.65	488	142	106.5471
MADL - 13	0.8830	0.1500	0.0858	0.0021	0.7787	32.21	642.6	40.4	530.65	6.23	1059	153	50.10859
MADL - 14	0.6607	0.0910	0.0834	0.0019	0.5210	30.91	515	27.8	516.39	5.65	509	140	101.4519
MADL - 15	0.6621	0.0910	0.0835	0.0018	0.5681	31.26	515.9	27.8	516.98	5.35	511	139	101.1703
222 - 1	0.5587	0.0770	0.0720	0.0016	0.4614	16.71	450.7	25.1	448.19	4.81	463	143	96.8013
222 - 2	0.5586	0.0770	0.0720	0.0016	0.4860	16.49	450.6	25.1	448.19	4.81	463	142	96.8013
222 - 3	0.5623	0.0780	0.0723	0.0016	0.4822	15.98	453	25.3	450	4.81	468	143	96.15385
222 - 4	0.5585	0.0770	0.0722	0.0016	0.3989	16.42	450.5	25.1	449.4	4.81	456	145	98.55263
222 - 5	0.5664	0.0780	0.0734	0.0016	0.2822	18.54	455.7	25.3	456.61	4.8	451	148	101.2439
222 - 6	0.5602	0.0770	0.0728	0.0016	0.5282	17.19	451.7	25.1	453	4.81	445	141	101.7978
222 - 7	0.5577	0.0770	0.0729	0.0016	0.4249	17.00	450	25.1	453.6	4.81	432	145	105
222 - 8	0.5569	0.0770	0.0726	0.0016	0.3847	16.50	449.5	25.1	451.8	4.81	438	146	103.1507
222 - 9	0.5587	0.0770	0.0715	0.0016	0.6267	16.44	450.7	25.1	445.19	4.81	479	138	92.94154
222 - 10	0.5603	0.0770	0.0714	0.0016	0.2922	17.32	451.7	25.1	444.58	4.81	488	146	91.10246
Ambat - 1	0.6556	0.0910	0.0832	0.0018	0.2192	36.88	511.9	27.9	515.19	5.36	497	149	103.66

<i>Ambat - 2</i>	1.2860	0.1800	0.0888	0.0020	0.3836	37.02	839.5	40	548.44	5.92	1715	122	31.97901
<i>Ambat - 3</i>	0.6590	0.0910	0.0837	0.0019	0.3582	36.97	514	27.8	518.17	5.65	496	145	104.4698
<i>Ambat - 4</i>	0.6557	0.0910	0.0837	0.0018	0.4017	36.98	512	27.9	518.17	5.35	484	145	107.0599
<i>Ambat - 5</i>	0.9050	0.1500	0.0872	0.0020	0.6755	37.90	654.4	40	538.96	5.93	1076	152	50.08922
<i>Ambat - 6</i>	0.6544	0.0900	0.0837	0.0018	0.1438	37.92	511.2	27.6	518.17	5.35	480	150	107.9521
<i>Ambat - 7</i>	0.6559	0.0910	0.0838	0.0019	0.5287	38.07	512.1	27.9	518.76	5.65	482	142	107.6266
<i>Ambat - 8</i>	0.6621	0.0920	0.0843	0.0018	0.3489	37.52	515.9	28.1	521.74	5.35	490	147	106.4776
<i>Ambat - 9</i>	0.6860	0.0950	0.0829	0.0018	0.2335	38.02	530.4	28.6	513.41	5.36	604	146	85.00166
<i>Ambat - 10</i>	0.6547	0.0900	0.0824	0.0018	0.3233	37.83	511.4	27.6	510.43	5.36	516	145	98.92054

Appendix 5.6: Monazite REE concentrations (ppm) – Chapter 5

<i>Monazite Grain</i>	<i>Y</i>	<i>Zr</i>	<i>La</i>	<i>Pr</i>	<i>Nd</i>	<i>Sm</i>	<i>Eu</i>	<i>Gd</i>	<i>Tb</i>	<i>Dy</i>	<i>Ho</i>	<i>Er</i>	<i>Tm</i>	<i>Yb</i>	<i>Lu</i>	<i>Th</i>	<i>U</i>
<i>CO17-58M - 1</i>	3190	0.36	164000	29720	104560	12240	139	5885	431	1321	147	193.5	13.03	42.9	3.64	60040	147
<i>CO17-58M - 2</i>	2838	0.26	177000	28370	96350	10360	142	4754	349	1103	126	176.4	12.09	40.7	3.34	46370	216
<i>CO17-58M - 3</i>	4866	0.61	170000	28420	96800	11380	157	5899	496	1703	210	316.0	22.52	79.4	6.66	70000	339
<i>CO17-58M - 4</i>	4030	0.30	179000	29180	104000	14090	193	7369	560	1693	187	247.8	16.30	55.2	4.57	51020	95
<i>CO17-58M - 5</i>	3870	0.27	179000	28800	99780	12400	193	6279	489	1555	174	241.5	16.90	58.3	4.98	48310	158
<i>CO17-58M - 6</i>	3752	0.34	178000	29780	103000	13190	189	6677	509	1569	171	230.4	15.20	51.7	4.29	46340	84
<i>CO17-58M - 7</i>	4355	0.37	179000	29620	105000	14410	213	7710	578	1775	197	265.2	18.33	63.1	5.18	64500	232
<i>CO17-58M - 8</i>	4559	0.42	176000	30370	113000	15280	227	8260	604	1847	207	276.1	18.97	62.6	5.54	165000	385
<i>CO17-58M - 9</i>	4212	0.43	175000	29400	105000	14270	197	7460	567	1721	191	254.8	17.51	59.0	5.06	46800	117
<i>CO17-58M - 10</i>	3845	0.23	172000	29670	105000	13940	184	7183	547	1647	179	233.1	15.78	50.4	4.45	47000	101
<i>CO17-58M - 11</i>	3727	0.29	178000	28650	99100	12360	188	6176	483	1526	169	231.2	15.59	53.6	4.79	33380	117
<i>CO17-58M - 12</i>	3660	0.35	170000	29550	103000	11990	160	5936	452	1428	160	219.0	14.85	48.0	4.03	65600	161
<i>CO17-58M - 13</i>	3902	0.40	179000	28620	97800	11620	188	5819	462	1488	171	239.7	16.77	58.3	4.87	44600	161
<i>CO17-58M - 14</i>	3678	1.03	185000	28000	94900	11430	188	5704	448	1418	163	227.1	15.70	51.6	4.55	42240	175
<i>CO17-58M - 15</i>	3674	0.22	174000	29290	100000	12570	185	6331	487	1546	173	233.1	15.40	49.9	4.20	43130	102
<i>CO17-58M - 16</i>	3046	0.96	173000	29790	106000	12820	209	6151	437	1295	143	188.4	12.03	41.2	3.41	69350	183
<i>CO17-58M - 17</i>	2990	0.28	162000	30150	109000	12840	158	6082	431	1295	140	184.4	11.48	38.9	3.33	60140	167

CO17-58M - 18	4464	0.29	175000	29280	104000	13650	185	7122	556	1819	207	283.6	18.98	63.3	5.50	55500	173
CO17-58M - 19	3119	0.33	164000	30520	112000	14360	166	7077	492	1469	153	191.0	11.48	35.9	3.19	71000	134
CO17-58M - 20	2784	0.94	163000	30200	110000	13280	163	6327	431	1279	133	167.4	10.38	34.7	2.96	67050	145
CO17-58M - 21	4024	0.28	177000	28870	101000	12920	194	6532	509	1670	191	261.9	17.62	58.5	4.95	48800	150
CO17-58M - 22	49000	31.60	149000	28250	96000	17000	690	15200	1940	9500	1720	3500.0	410.00	2320.0	330.00	25400	279
CO17-58M - 23	3756	0.33	179000	28790	99200	12190	191	6055	469	1545	175	243.7	16.07	53.3	4.70	43410	147
CO17-58M - 24	3910	0.29	183000	28570	98720	11750	196	5962	460	1531	179	253.9	16.90	58.6	4.94	53250	321
CO17-58M - 25	2653	0.97	170000	29430	102000	11590	157	5380	385	1175	127	166.8	9.97	32.0	2.61	53000	104
CO17-58M - 26	5608	0.38	172000	28910	98400	11630	161	6304	539	1978	253	381.7	26.69	93.2	7.83	83300	401
CO17-58M - 27	4069	0.41	175000	29310	106000	13490	192	6940	519	1678	192	265.0	17.06	57.9	4.75	70800	167
CO17-58M - 28	4045	0.23	173000	29600	105000	13870	193	7159	545	1738	194	260.3	16.72	56.0	4.76	44160	117
CO17-58M - 29	3949	0.29	177000	29560	105000	14040	193	7333	546	1717	190	253.9	15.71	52.0	4.50	51820	97
CO17-58M - 30	2882	0.26	174000	29020	99900	11560	169	5548	407	1263	140	182.6	11.40	34.9	2.89	46530	52
CO17-58M - 31	4420	2000.00	174000	29200	102000	12770	185	6590	519	1743	205	297.0	19.44	68.4	5.99	55500	194
I16-18M - 1	26620	0.47	161000	31360	117000	24110	914	18570	2207	8937	1116	1812.0	163.20	697.0	60.70	56900	2169
I16-18M - 2	23060	0.60	164000	30460	110000	19550	821	14580	1802	7624	982	1609.0	142.30	605.7	52.41	32460	1646
I16-18M - 3	22200	7000.00	165000	29720	106000	18150	784	13100	1646	7110	938	1587.0	145.50	617.0	57.30	39700	2074
I16-18M - 4	25930	0.49	157000	32650	126000	28190	905	20180	2310	9020	1114	1797.0	161.40	695.0	61.40	115000	3050
I16-18M - 5	16600	145.00	165000	30380	110000	20930	832	14720	1654	6150	735	1160.0	105.00	449.0	39.20	52910	1560
I16-18M - 6	22860	0.43	162000	30140	107000	18790	815	13480	1709	7421	980	1617.0	143.70	612.3	53.06	45940	2581
I16-18M - 7	26910	0.53	160000	31630	117000	23780	927	18240	2220	9127	1144	1859.0	165.50	694.2	60.20	60300	2685
I16-18M - 8	19740	0.30	168000	29640	103000	16490	722	11430	1411	6190	839	1403.0	127.70	546.3	47.60	32890	1930
I16-18M - 9	19640	4.00	167000	29470	103000	15800	690	10600	1306	5890	828	1447.0	136.10	592.0	53.60	41900	2140
I16-18M - 10	23630	0.28	164000	30360	110000	19040	822	14090	1773	7622	1004	1672.0	153.60	659.6	58.49	30890	1701
I16-18M - 11	26070	1.54	160000	31210	115000	22100	890	16910	2093	8670	1113	1814.0	162.70	684.6	60.10	57600	2688
I16-18M - 12	21680	0.36	165000	30350	108000	19220	795	14080	1742	7200	918	1477.0	130.70	538.0	45.80	43700	1925
I16-18M - 13	22030	273.00	175000	31900	117000	23160	804	16230	1838	7240	912	1567.0	151.90	712.0	74.50	105000	2776
I16-18M - 14	25030	0.97	160000	31320	114000	22650	879	16930	2063	8310	1047	1699.0	150.50	634.0	54.60	59100	2487
I16-18M - 15	20710	0.61	163000	30040	106000	18540	777	13400	1652	6831	872	1409.0	123.90	507.6	43.59	41320	1903

I16-18M - 16	24470	0.48	159000	30650	109000	19130	837	14160	1805	7872	1012	1705.0	153.60	650.3	56.36	48820	2745
I16-18M - 17	19700	20.00	165000	30270	108000	18200	798	12920	1573	6480	813	1349.0	121.90	521.0	44.90	33410	1565
I16-18M - 18	22590	0.45	163000	30250	109000	18280	806	13170	1674	7300	943	1579.0	141.70	601.0	51.90	45420	2460
I16-18M - 19	22600	13.90	164000	30260	106000	17550	771	12440	1598	7067	936	1615.0	149.50	643.7	56.89	37000	2039
I16-18M - 20	22300	0.40	164000	30080	107000	17970	773	13260	1660	7180	928	1564.0	142.40	612.0	53.90	35150	1855
I16-18M - 21	27560	1.02	157000	32120	121000	25180	933	19100	2314	9400	1153	1891.0	169.50	722.0	62.20	85500	2990
I16-18M - 22	19470	0.68	166000	29870	104000	16900	734	11870	1464	6309	823	1371.0	123.30	515.4	44.73	38750	1857
I16-18M - 23	22160	0.42	164000	29970	106000	18160	775	13080	1642	7143	923	1561.0	140.60	594.8	53.11	41590	2034
I16-18M - 24	20390	3.80	169000	30460	110000	21010	760	15230	1774	7004	846	1381.0	121.80	514.2	44.44	74300	2585
I16-18M - 25	23030	0.55	162000	30400	108000	18370	805	13190	1682	7350	967	1639.0	148.00	633.0	55.10	47380	2709
I16-18M - 26	27090	1.53	162000	31320	114000	22030	875	16820	2087	8750	1112	1877.0	171.00	742.3	66.10	45880	1989
I16-18M - 27	25520	0.53	162000	29970	107000	18350	825	13330	1742	7880	1054	1816.0	166.70	716.00	63.40	48340	3023
I16-18M - 28	21770	0.60	161000	30090	108170	19010	792	13840	1716	7202	913	1512.0	131.20	548.50	47.18	47200	2164
I16-18M - 29	23070	0.39	163000	30370	109000	20150	809	14970	1846	7652	959	1582.0	139.90	587.40	51.48	45300	2000
I16-18M - 30	20180	0.35	166000	29730	103490	16470	736	11210	1391	6214	836	1434.0	130.00	551.80	47.20	39350	2359
I16-18M - 31	21770	0.45	165000	30060	106000	16830	749	11680	1477	6640	892	1540.0	144.00	610.70	53.70	43950	2541